

**N.V. PERELOMOVA**

**PROBLEMS IN  
CRYSTAL PHYSICS  
WITH SOLUTIONS**



**N.V. PERELOMOVA  
M.M. TAGIEVA**

**PROBLEMS IN  
CRYSTAL PHYSICS  
WITH SOLUTIONS**

## PREFACE TO THE ENGLISH EDITION

The English edition of the present problem book in crystal physics is a revised, enlarged, and supplemented version. The book comprises two new sections: § 13 "Optical Activity" and § 14 "Elastic Waves in Crystals"; § 4 "Physical Properties of Crystals Described by Tensors of Rank Two" and § 6 "Piezoelectric Properties of Crystals. Electrostriction", as well a number of tables in Appendix were revised and enlarged. This work was done by N. V. Perelomova. The authors hope that this problem book will prove useful to students in anglo-phone countries, who have a happy opportunity of excellent instruction with such classical textbooks as those written by J. Nye and W. Wooster. The impeccable style and lucid presentation of these textbooks are the features we always admired; they provided a strong stimulus for preparing the present problem book.

N.V. Perelomova  
M.M. Tagieva

## EDITOR'S FOREWORD

First published in 1972, this collection of problems in physical properties of crystals was the first such collection to appear on the book market. The momentous progress in crystal physics and in its applications during the last decade stimulated the writing and publication of a number of problem books; nevertheless, the present problem book meant for a profound study of the physics of crystals and physical crystallography courses by the students and for elaboration of solution techniques, remains unique as a practice-oriented manual. The book has survived a rigorous test of time and proved its merits for the lecturers and students at the Moscow Institute of Steel and Alloys. It has been revised with the view to take into account critical remarks of students, offered over a number of years, as well as the experience both of the editor and the authors and other lecturers at the Chair of Crystallography of the Institute. The authors and the editor will be grateful for any critical comments and advice.

M.P. Shaskol'skaya

## LIST OF SYMBOLS

The notation for point symmetry groups is given in Table 1.

The notation for symmetry elements is given in Table 2.

$X, Y, Z$ —axes of the crystallographic coordinate system

$X_1, X_2, X_3$ —axes of the crystallophysical coordinate system

$(C_{ij})$ —the matrix of transformation of the crystallophysical coordinate system (cosine matrix)

$\rho$ —density; specific rotation in optical activity

$c$ —heat capacity

$T_{\text{melt}}$ —melting point

$T_C$ —temperature of ferroelectric phase transition (Curie point)

$v$ —phase velocity;  $v_1, v_l$ —phase velocity of longitudinal and quasi-longitudinal waves, respectively;  $v_2, v_3, v_t$ —phase velocities of shear and quasishow waves, respectively

$S$ —group velocity

$\mathbf{n}$ —unit vector of wavefront normal

$\mathbf{u}$ —unit vector of displacement in the wave

$\mathbf{I}$ —energy flux vector

$\mathbf{E}$ —vector of electric field strength

$\mathbf{H}$ —vector of magnetic field strength

$\mathbf{D}$ —vector of electric induction

$\mathbf{j}$ —vector of electric current density

$\mathbf{P}$ —vector of electric polarization

$\gamma_i$ —pyroelectric coefficients

$[\varepsilon_{ij}]$ —dielectric permittivity tensor

$[\eta_{ij}]$ —tensor of dielectric impermeability, or tensor of polarization constants

$[\chi_{ij}]$ —tensor of polarizability coefficients

$[\rho_{ij}]$ —electric resistivity tensor

$[\sigma_{ij}]$ —electric conductivity tensor

$[r_{ij}]$ —tensor of infinitesimal strains

$[\omega_{ij}]$ —tensor of infinitesimal rotations

$[t_{ij}]$ —tensor of mechanical stress

$[\alpha_{ij}]$ —tensor of thermal expansion coefficients

$[\lambda_{ij}]$ —tensor of heat conduction coefficients

$[g_{ij}]$ —gyration tensor

$[\Lambda_{im}]$ —Green-Christoffel tensor

$\delta_{im}$ —Kronecker delta

$N_o$ ,  $N_e$ —refractive indices of ordinary and extraordinary waves in uniaxial crystals

$N_g$ ,  $N_m$ ,  $N_p$ , or  $n_1$ ,  $n_2$ ,  $n_3$ —refractive indices of biaxial crystals along principal axes

$n'_1$ ,  $n'_2$ —refractive indices for an arbitrary direction of light propagation

$n_r$ —refractive index for a circularly polarized wave with right-hand rotation

$n_l$ —refractive index for a circularly polarized wave with left-hand rotation

$[s_{ijkl}]$ —tensor of elastic compliances

$[c_{ijkl}]$ —tensor of stiffnesses

$[d_{ijkl}]$ —tensor of piezoelectric moduli

$[\Pi_{ijkl}]$ —tensor of piezoresistivity coefficients

$[\pi_{ijkl}]$ —tensor of piezooptic coefficients

$[P_{ijkl}]$ —tensor of elastooptic coefficients

$[r_{ijkl}]$ —tensor of coefficients of the linear electrooptic effect

$[\chi_{ijkl}]$ —tensor of nonlinear polarizability or quadratic susceptibility

$[Q_{ijkl}]$ —tensor of electrostriction coefficients

$[R_{ijkl}]$ —tensor of coefficients of the quadratic electrooptic effect

## CONTENTS

	<b>Preface to English Edition</b>	5
	<b>Editor's Foreword</b>	6
	<b>From the Preface</b>	
	<b>to the First Russian Edition</b>	7
	<b>Preface to the Second Russian Edition</b>	8
	<b>List of Symbols</b>	9
1.	Matrix Representation of Symmetry Operations and Symmetry Classes	13
2.	Symmetry Principle in Crystal Physics. Symmetry of Physical Phenomena and Properties of Crystals	22
3.	Physical Properties of Crystals Described by Tensors of Rank One	35
4.	Physical Properties of Crystals Described by Tensors of Rank Two	45
5.	Stress and Strain in Crystals. Analysis of Stressed State	69
6.	Piezoelectric Properties of Crystals. Electrostriction	87
7.	Elastic Properties of Crystals. Hook's law	115
8.	Piezoresistivity in Semiconductor Crystals	136
9.	Optical Properties of Crystals	151
10.	Piezooptical Properties of Crystals	170
11.	Electrooptical Properties of Crystals	181
12.	Generation of Optical Harmonics	208
13.	Rotation of Polarization Plane (Optical Activity)	225
14.	Elastic Waves in Crystals	231
15.	Thermodynamics of Crystals Answers to Problems References <b>Appendix</b>	274 290 295 296
Table 1.	Notation of 32 Symmetry Classes	296
Table 2.	Symbols of Symmetry Elements on Stereographic Projections	297
Table 3.	Rules for Setting of Crystals According to Symmetry System	298
Table 4.	Symmetry Elements and Rules for Choosing Axes for 32 Crystallographic Classes	298
Table 5.	Rules for Choosing Crystallophysical Axes	301
Table 6.	Matrices of Piezoelectric Moduli ( $d_{ij}$ ) and Piezoelectric Constants ( $g_{ij}$ )	302

<b>Table 7.</b>	Matrices of Piezoelectric Constants ( $h_{ij}$ ) and ( $e_{ij}$ ) for Crystals in Which These Matrices Differ from ( $d_{ij}$ ) and ( $g_{ij}$ )	304
<b>Table 8.</b>	Matrices of Piezoelectric Moduli ( $d_{ij}$ ) for Piezoelectric Textures	304
<b>Table 9.</b>	Matrices of Elastic Compliances ( $s_{ij}$ ) and Elastic Stiffnesses ( $c_{ij}$ )	304
<b>Table 10.</b>	Matrices of Piezoresistivity Constants ( $\Pi_{ij}$ )	308
<b>Table 11.</b>	Matrices of Piezooptical Constants ( $\pi_{kl}$ ) and Elasto-optical Constants ( $p_{kl}$ )	310
<b>Table 12.</b>	Matrices of Linear Electrooptical Effect Constants ( $r_{ij}$ )	314
<b>Table 13.</b>	Matrices of Quadratic Electrooptical Effect Constants ( $R_{ij}$ )	317
<b>Table 13.a</b>	Tensor [ $g_{ij}$ ]	319
<b>Table 14.</b>	Reference Data Required for Solving the Problems	321
<b>Table 15.</b>	Units of Physical Quantities and Conversion Factors for the Corresponding Units in the SI and CGSE Systems	331
<b>Table 16.</b>	Tensor of Physical Properties of Crystals Mentioned in the Book	336

# 1. MATRIX REPRESENTATION OF SYMMETRY OPERATIONS AND SYMMETRY CLASSES

The specific features of crystals are caused by the symmetry and anisotropy of the crystalline medium.

The symmetry of a crystal is defined as the property of the space the crystal occupies to coincide with itself as a result of certain transformations called symmetry operations.

Two types of such transformations can be distinguished: symmetry operations of the first kind (rotations) and symmetry operations of the second kind (reflections). The operations of the first kind transform the right-handed reference frame fixed to the crystal into the right-handed one, and the left-handed reference frame into the left-handed one, while the operations of the second kind transform a right-handed reference frame into the left-handed one (and vice versa).

The possible combinations of symmetry operations over crystal polyhedra form 32 point groups or 32 symmetry classes. These groups are called point groups because the symmetry transformations they comprise leave at least one point of the crystal-structured space fixed (the origin of the reference frame).

The notations of the 32 symmetry classes are listed in Table 1 (see Appendix); Table 2 lists the notations for symmetry elements on stereographic projections.

**Standard crystallographic and crystallophysical reference frames (coordinate systems).** Crystallographic coordinate axes used for unambiguous description of directions and planes in crystals are designated  $X$ ,  $Y$ ,  $Z$ ; the standard rules for their selection are given in Table 3. The description of the physical properties of crystals, as well as the analytical representation of their point symmetry groups are based on the orthogonal crystallophysical axes  $X_1$ ,  $X_2$ ,  $X_3$ ; the standard rules for orienting these axes with respect to the crystallographic axes are given in Tables 4 and 5. The crystallographic and crystallophysical coordinate systems are always chosen right-handed, with the angles between the positive directions of the corresponding crystallographic and crystallophysical axes being less than  $90^\circ$ . The positive direction of a crystallographic axis corresponds to the positive direction of the appropriate crystallophysical axis. The directions of axis in the crystallophysical and crystallographic coordinate systems coincide in the cubic, tetragonal, and rhombic crystal systems.

**Matrix representation of symmetry operations.** Symmetry operations can be described analytically as coordinate transformations. We take for the origin of the orthogonal crystallophysical coordinate system  $X_1, X_2, X_3$  the point of space which remains fixed under all symmetry operations of a point group. Any symmetry operation of the crystallographic class transforms the axes  $X_1, X_2, X_3$  into new axes  $X'_1, X'_2, X'_3$  (see Figs. 1.1-1.3).

The angles between the new ( $X'_1, X'_2, X'_3$ ) and original ( $X_1, X_2, X_3$ ) axes are given by the table of direction cosines:

Table 1.1

Axes	$X_1$	$X_2$	$X_3$
$X'_1$	$C_{11}$	$C_{12}$	$C_{13}$
$X'_2$	$C_{21}$	$C_{22}$	$C_{23}$
$X'_3$	$C_{31}$	$C_{32}$	$C_{33}$

The first subscript with the symbol  $C_{ij}$  ( $i, j = 1, 2, 3$ ) refers to the new axes, and the second to the original ones. Thus, for example,  $C_{23}$  is the cosine of the angle between axes  $X'_2$  and  $X_3$ .

Therefore, any symmetry transformation can be put in correspondence with the appropriate matrix of direction cosines  $C_{ij}$ , that is, can be written in the matrix representation. The angle of rotation is assumed positive if the rotation from the original axis to the new axis, observed from the positive end of the axis toward the origin, occurs in the counterclockwise direction.

The nine coefficients  $C_{ij}$  are not independent. As each row of the matrix  $(C_{ij})$  is composed of the direction cosines of a primed coordinate axis with respect to unprimed axes  $X_1, X_2, X_3$ , we have

$$C_{ik}C_{jk} = 1 \quad \text{for } i = j \quad (1.1)$$

As each pair of rows of the matrix  $(C_{ij})$  consists of direction cosines of two mutually perpendicular directions, we find

$$C_{ik}C_{jk} = 0 \quad \text{for } i \neq j \quad (1.2)$$

Equations (1.1) and (1.2) are called the *orthogonality relations* and can be written in a compact form

$$C_{ik}C_{jk} = \delta_{ij}$$

where  $\delta_{ij}$  is the Kronecker delta defined in the following manner:

$$\delta_{ij} = \begin{cases} 1 & \text{for } i = j \\ 0 & \text{for } i \neq j \end{cases}$$

The determinant of the direction cosines matrix,  $|C_{ij}|$ , is equal to  $+1$  for the transformations of the first kind, conserving the left-handedness and right-handedness of coordinate systems, and to  $-1$  for the transformations of the second kind.

**Crystallographic groups (symmetry classes).** The set of symmetry operations of an ideal crystal polyhedron, that is, the set of transformations under which this polyhedron coincides with itself, forms its point group of symmetry or a symmetry class constituting a mathematical group, that is, conforming to the following postulates:

1. A product of two symmetry operations  $A$  and  $B$  in a symmetry group is equivalent to a symmetry operation  $C$  in the same group:  $AB = C$ .

A product of symmetry transformations with respect to a coordinate system fixed to a crystal corresponds to the product of the corresponding matrices (in the sense of standard matrix multiplication).

The result of two consecutive symmetry transformations may depend on the order in which the operations are applied, so that one has to watch the order in which the corresponding matrices are written in the product.

2. Multiplication of operations is associative:

$$(AB)C = A(BC)$$

3. Among the symmetry operations there is one such identity operation  $E$  that  $AE = EA = A$  for any operation of the group. In this case operation  $E$  is called the *identity* operation.

The identity operation for symmetry transformations is the rotation by  $360^\circ$  around an arbitrary direction in a crystal, or the single-fold symmetry axis.

4. For each operation  $A$  there is an inverse operation  $A^{-1}$  belonging to the symmetry group and satisfying the relation

$$AA^{-1} = A^{-1}A = E$$

For example, if  $A$  is a clockwise rotation by an angle  $\varphi$ , then  $A^{-1}$  is the counterclockwise rotation by the same angle.

The set of matrices  $(C_{ij})$  constructed for all nonequivalent\* symmetry operations belonging to a specific point symmetry group, is called the *matrix representation of this group*, and the number of nonequivalent operations forming a symmetry group is called the *order of the group*.

If an operation transforms a crystal polyhedron into itself, then a repetition of this operation will again transform it into itself. The result of a sequence of symmetry operations is denoted as the

---

\* Symmetry operations are regarded as equivalent if they result in identical regrouping of parts of the figure. (For example, the operation of clockwise rotation by  $60^\circ$  and the operation of counterclockwise rotation by  $300^\circ$  are equivalent.)

power of this operation. For instance,  $6^1$ ,  $6^2$ ,  $6^3$  denote the rotations around the symmetry axis by  $60^\circ$ ,  $120^\circ$  and  $180^\circ$  respectively. Therefore, if an operation belongs to a group, all possible powers of this operation belong to the group.

The groups generated by a symmetry element, that is, consisting of powers of a single operation, are called *cyclic* and denoted by the symbols of symmetry elements generating them:  $1$ ,  $2$ ,  $3$ ,  $4$ ,  $6$ ,  $\bar{1}$ ,  $\bar{2} = m$ ,  $\bar{3}$ ,  $\bar{4}$ ,  $\bar{6}$ . A system of symmetry operations belonging to a given group is called the *system of generators* if these operations, multiplied in all possible combinations, generate all operations belonging to this group.

### Examples of Problems with Solutions

1.1. Write the matrix representation of all symmetry operations belonging to the point group  $mmm$ .

**Solution.** The point symmetry group  $mmm$  comprises eight symmetry operations: three mirror reflections in coordinate symmetry planes, three rotations by  $180^\circ$  around the coordinate axes, as well as the rotation by  $360^\circ$  and the inversion with respect to the origin  $O$ . The system of coordinate axes obtained from the original one by applying a symmetry operation will be denoted by  $X'_1$ ,  $X'_2$ ,  $X'_3$ .

The matrix representation of the reflection operation in plane  $X_1X_2$  (or, in compact form,  $m \perp X_3$ ) (Fig. 1.1) is written in the form

$$C_{ij} (m \perp X_3) = \begin{pmatrix} 1 & 0 & 0 \\ 0 & 1 & 0 \\ 0 & 0 & -1 \end{pmatrix}$$

Fig. 1.1. Transformation of the crystallophysical coordinate axes by a symmetry plane perpendicular to the axis  $X_3$ .

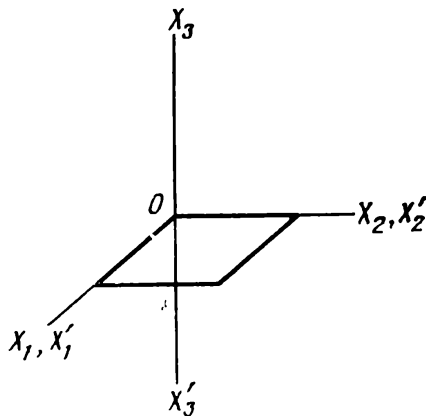
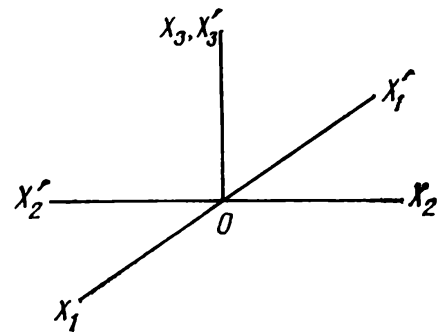


Fig. 1.2. Transformation of the crystallophysical coordinate axes by a two-fold symmetry axis parallel to  $X_3$ .



Similarly for  $(m \perp X_2)$  and  $(m \perp X_1)$  we find

$$C_{ij}(m \perp X_2) = \begin{pmatrix} 1 & 0 & 0 \\ 0 & -1 & 0 \\ 0 & 0 & 1 \end{pmatrix}, \quad C_{ij}(m \perp X_1) = \begin{pmatrix} -1 & 0 & 0 \\ 0 & 1 & 0 \\ 0 & 0 & 1 \end{pmatrix}$$

The determinant  $|C_{ij}(m \perp X_i)| = -1$ ; hence, the reflection with respect to a symmetry plane is an operation of the second kind.

The matrix representation of rotation by  $180^\circ$  around axis  $X_3$  ( $X_3, 180^\circ$ ; Fig. 1.2) is written in the form

$$C_{ij}(X_3, 180^\circ) = \begin{pmatrix} -1 & 0 & 0 \\ 0 & -1 & 0 \\ 0 & 0 & 1 \end{pmatrix}$$

Similarly, for  $(X_2, 180^\circ)$  and  $(X_1, 180^\circ)$  we find

$$C_{ij}(X_2, 180^\circ) = \begin{pmatrix} -1 & 0 & 0 \\ 0 & 1 & 0 \\ 0 & 0 & -1 \end{pmatrix}, \quad C_{ij}(X_1, 180^\circ) = \begin{pmatrix} 1 & 0 & 0 \\ 0 & -1 & 0 \\ 0 & 0 & -1 \end{pmatrix}$$

The matrix of rotation by  $360^\circ$  around any direction in a crystal, for instance, around axis  $X_3$  ( $X_3, 360^\circ$ ) has the form

$$C_{ij}(X_3, 360^\circ) = \begin{pmatrix} 1 & 0 & 0 \\ 0 & 1 & 0 \\ 0 & 0 & 1 \end{pmatrix}$$

The determinant  $|C_{ij}(X_j, 180^\circ)|$ , as well as the determinant  $|C_{ij}(X_i, 360^\circ)|$ , equals 1, that is, symmetry operations of rotation by  $180^\circ$  and  $360^\circ$  are operations of the first kind.

And finally, the matrix representation of the inversion  $(\bar{1})$  (Fig. 1.3) is

$$C_{ij}(\bar{1}) = \begin{pmatrix} -1 & 0 & 0 \\ 0 & -1 & 0 \\ 0 & 0 & -1 \end{pmatrix}$$

$|C_{ij}(\bar{1})| = -1$ , that is, this is an operation of the second kind.

1.2. Find the matrix representation and the order of the symmetry group for the low-temperature modification of quartz (all the crystal characteristics required for the solution of problems are listed in Table 14, p. 321).

**Solution.** In accord with the rule of selecting crystallophysical axes (see Tables 4 and 5), the axes  $X_1$ ,  $X_2$ ,  $X_3$  of the point symmetry group 32 are oriented as shown in Fig. 1.4.

The matrices corresponding to rotations around the axis  $X_3$  by  $120^\circ$ ,  $240^\circ$  and  $360^\circ$  (rotations by these angles are comprised in the

threefold symmetry axis), that is, rotations  $3^1$ ,  $3^2$ ,  $3^3$  are written in the following manner:

$$C_{ij}(X_3, 120^\circ) = \begin{pmatrix} -\frac{1}{2} & \frac{\sqrt{3}}{2} & 0 \\ -\frac{\sqrt{3}}{2} & -\frac{1}{2} & 0 \\ 0 & 0 & 1 \end{pmatrix}$$

$$C_{ij}(X_3, 240^\circ) = \begin{pmatrix} -\frac{1}{2} & -\frac{\sqrt{3}}{2} & 0 \\ \frac{\sqrt{3}}{2} & -\frac{1}{2} & 0 \\ 0 & 0 & 1 \end{pmatrix}$$

$$C_{ij}(X_3, 360^\circ) = \begin{pmatrix} 1 & 0 & 0 \\ 0 & 1 & 0 \\ 0 & 0 & 1 \end{pmatrix}$$

The matrices of rotations by  $180^\circ$  around twofold symmetry axes take the form

$$C_{ij}(2 \parallel X_1) = \begin{pmatrix} 1 & 0 & 0 \\ 0 & -1 & 0 \\ 0 & 0 & -1 \end{pmatrix}$$

$$C_{ij}(2 \text{ at an angle } 60^\circ \text{ to } X_1) = \begin{pmatrix} -\frac{1}{2} & -\frac{\sqrt{3}}{2} & 0 \\ -\frac{\sqrt{3}}{2} & \frac{1}{2} & 0 \\ 0 & 0 & -1 \end{pmatrix}$$

Fig. 1.3. Transformation of the crystallophysical coordinate axes by a center of inversion.

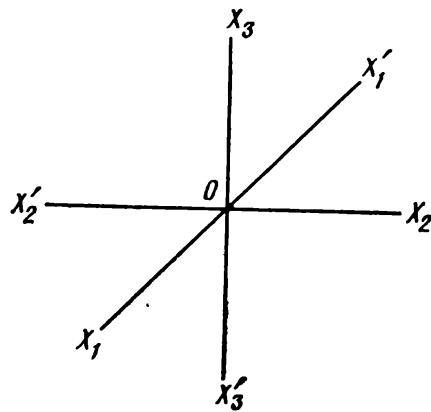
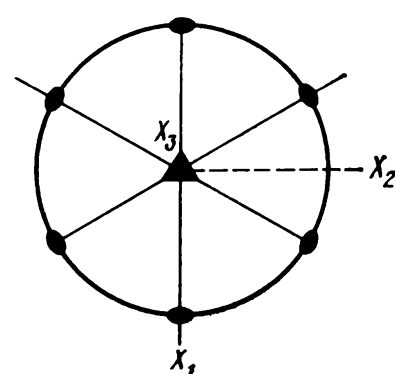


Fig. 1.4. Crystallophysical axes chosen for point symmetry group 32.



$$C_{ij} \text{ (2 at an angle } 30^\circ \text{ to } X_2) = \begin{pmatrix} -\frac{1}{2} & \frac{\sqrt{3}}{2} & 0 \\ \frac{\sqrt{3}}{2} & \frac{1}{2} & 0 \\ 0 & 0 & -1 \end{pmatrix}$$

The six nonequivalent matrices ( $C_{ij}$ ), corresponding to different symmetry operations included to the group 32, constitute the matrix representation of this symmetry group. The order of this group is six.

**1.3.** The Euler theorem states: the resultant of two intersecting symmetry axes is the third symmetry axis passing through the point of intersection of the first two. By using the matrix representation of symmetry elements, illustrate the Euler theorem taking the symmetry class 422 as an example.

**Solution.** We shall assume the fourfold symmetry axis and one twofold symmetry axis, perpendicular to the former, to be the initial symmetry elements. According to the rule of selecting the crystallophysical coordinate system, we direct the axis  $X_3$  along the fourfold axis, the axis  $X_1$  along the twofold axis, and add the axis  $X_2$  satisfying the condition of orthogonality of a coordinate system.

We can write the matrix representing a rotation by  $90^\circ$  around  $X_3$ :

$$C_{ij}(X_3, 90^\circ) = \begin{pmatrix} 0 & 1 & 0 \\ -1 & 0 & 0 \\ 0 & 0 & 1 \end{pmatrix}$$

The matrix corresponding to a rotation by  $180^\circ$  around  $X_1$

$$C_{ij}(X_1, 180^\circ) = \begin{pmatrix} 1 & 0 & 0 \\ 0 & -1 & 0 \\ 0 & 0 & -1 \end{pmatrix}$$

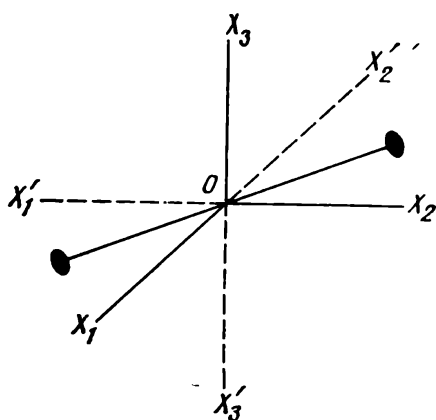


Fig. 1.5. Transformation of coordinate axes by a twofold symmetry axis aligned at  $45^\circ$  to the coordinate axes  $X_1$  and  $X_2$ .

Let  $(C_{ij}(X_3, 90^\circ)) = A$ ,  $(C_{ij}(X_1, 180^\circ)) = B$ . Using the first property of the group  $(AB = C)$ , we find the matrix representation of the element  $C$ :

$$C_{ij} = \begin{pmatrix} 0 & 1 & 0 \\ -1 & 0 & 0 \\ 0 & 0 & 1 \end{pmatrix} \begin{pmatrix} 1 & 0 & 0 \\ 0 & -1 & 0 \\ 0 & 0 & -1 \end{pmatrix} = \begin{pmatrix} 0 & -1 & 0 \\ -1 & 0 & 0 \\ 0 & 0 & -1 \end{pmatrix}$$

Obviously, the element  $C$  is a symmetry operation which transforms the axis  $X_1$  into  $-X_2$ ,  $X_2$  into  $-X_1$ , and  $X_3$  into  $-X_3$ .

The symmetry element realising this is the twofold axis at an angle  $45^\circ$  to the axes  $X_1$  and  $X_2$  and perpendicular to axis  $X_3$  (Fig. 1.5). Similarly, by taking successively the products of all matrices corresponding to rotations by  $90, 180, 270$ , and  $360^\circ$  around the axis  $X_3$  by the matrix corresponding to the rotation by  $180^\circ$  around  $X_1$  ( $2 \parallel X_1$ ), we obtain that four axes 2 are arranged perpendicularly to axis 4.

#### PROBLEMS

1.4. Write the matrix of the transformation of the coordinate system by a symmetry plane passing through the axis  $X_3$  at an arbitrary angle  $\varphi$  to the axis  $X_1$ .

1.5. Find the matrix of transformation of the coordinate system by a twofold symmetry axis lying in the coordinate plane  $X_1X_2$  at an arbitrary angle  $\varphi$  to the axis  $X_2$ .

1.6. A crystal is rotated by  $90^\circ$ , then reflected at the inversion center, and then rotated by  $180^\circ$  around the direction perpendicular to the axis of the initial rotation. Find the matrix representation of the symmetry operation producing the same result.

1.7. The crystal is rotated counterclockwise by  $120^\circ$  and then reflected at the inversion center. Find the matrix representation of the symmetry operation giving the same result. Indicate the symmetry element whose group includes this operation.

1.8. Use the matrix representation of symmetry elements and find a symmetry operation producing the same result as two two-fold axes intersecting at an angle of  $90^\circ$ .

1.9. Find the matrix representation of the symmetry operation producing the same result as twofold axes arranged at  $60^\circ$  angles to one another. Indicate the symmetry element whose group includes this operation.

1.10. Find the matrix representation and the order of the point symmetry group of potassium dihydrophosphate (KDP) for the conventional and unconventional ( $\bar{4}m2$ ) choice of crystallophysical coordinate axes.

1.11. Find the matrix representation of the point symmetry group 622.

1.12. Find the matrix representation and the order of the group  $\bar{6}$ .

1.13. Find the matrix representation of the group  $2/m$  when (i)  $2 \parallel X_2$  and (ii)  $2 \parallel X_3$ .

1.14. By using the matrix representation of symmetry operations, verify the validity of the Euler theorem for the point group 222.

1.15. By using the matrix representation of symmetry operations, verify the validity of the following theorem: a combination of an axis with even order and a plane perpendicular to it gives the symmetry center.

1.16. Verify the validity of the Euler theorem for twofold symmetry axes arranged at an angle of  $45^\circ$  to each other.

1.17. Determine the order of the following symmetry groups:  $mm$ , 222, 4mm, 422.

1.18. Write the system of generators for the group 4/mmm.

1.19. Check whether all group axioms are valid for the point symmetry group 2/m.

1.20. List the cyclic crystallographic groups of order 4.

1.21. What are the matrices describing the inverse rotations around the axis  $X_3$  by  $90^\circ$  by  $120^\circ$ ?

1.22. What is the order of cyclical groups 3 and  $\bar{3}$ ?

1.23. What matrices correspond to the threefold symmetry axes tilted at equal angles to the axes  $X_1$ ,  $X_2$ ,  $X_3$ ?

1.24. By using the matrix representation of symmetry operations, prove the equivalence of a rotation by  $180^\circ$  followed by inversion to the reflection in a plane perpendicular to the rotation axis.

1.25. Write the matrix representation of the reflection in the coordinate and diagonal symmetry planes in crystals belonging to the 4mm class.

1.26. List the cyclic groups of order 2.

1.27. Write the matrix representation of the symmetry operation  $3^1$  and of its inverse.

1.28. What matrix corresponds to the symmetry plane passing through the bisector of the internal angle between the coordinate planes  $X_1OX_3$  and  $X_2OX_3$ ?

## 2. SYMMETRY PRINCIPLE IN CRYSTAL PHYSICS. SYMMETRY OF PHYSICAL PHENOMENA AND PROPERTIES OF CRYSTALS

**Neumann's principle.** The symmetry of the physical properties of crystals (the symmetry of a physical property of a crystal is defined as a symmetry of the tensor surface which describes this property (see Sec. 4)) is determined by its point symmetry group. The appropriate relation is established by the fundamental law of the physics of crystals, as formulated in the works of Neumann and Minnigerode, known in the literature on the physics of crystals as *Neumann's principle*:

*The symmetry group of any physical property  
of a crystal comprises  
the point symmetry group of the crystal.*

This means that the crystal symmetry group either coincides with the symmetry group of its physical property or is a subgroup of the latter.

According to Neumann's principle, any physical property of the crystal must have all the symmetry elements that the crystal possesses. Among the symmetry groups describing the physical properties of crystals there are groups which comprise infinite-fold axes. These symmetry groups are called limiting (Curie) groups.

**Limiting point symmetry groups.** The limiting symmetry groups are easily memorizable with the help of the corresponding geometric figures (Fig. 2.1). By referring to the limiting symmetry groups, we can also describe the symmetry of textures, that is, polycrystalline aggregates with ordered arrangement of crystallites. For example, the symmetry of synthetic ferroelectric materials, such as barium titanite ceramics and rochelle salt (potassium sodium tartrate) are described by the groups  $\infty m$  and  $\infty 2$ , respectively.

Some of the limiting symmetry groups can be used to describe the symmetry of external physical factors. Thus, the symmetry of constant uniform electric field may be characterized by the group  $\infty m$ , that of the constant uniform magnetic field, by the group  $\infty/m$ , that of the uniaxial tensile or compressing mechanical stress, by the symmetry group  $\infty/mmm$ , that of the purely shear mechanical stress, by the group  $mmm$ , and that of the uniform compression, by the group  $\infty\infty m$ . The rotation of the optical polarization plane can be described by the limiting group  $\infty\infty$ .

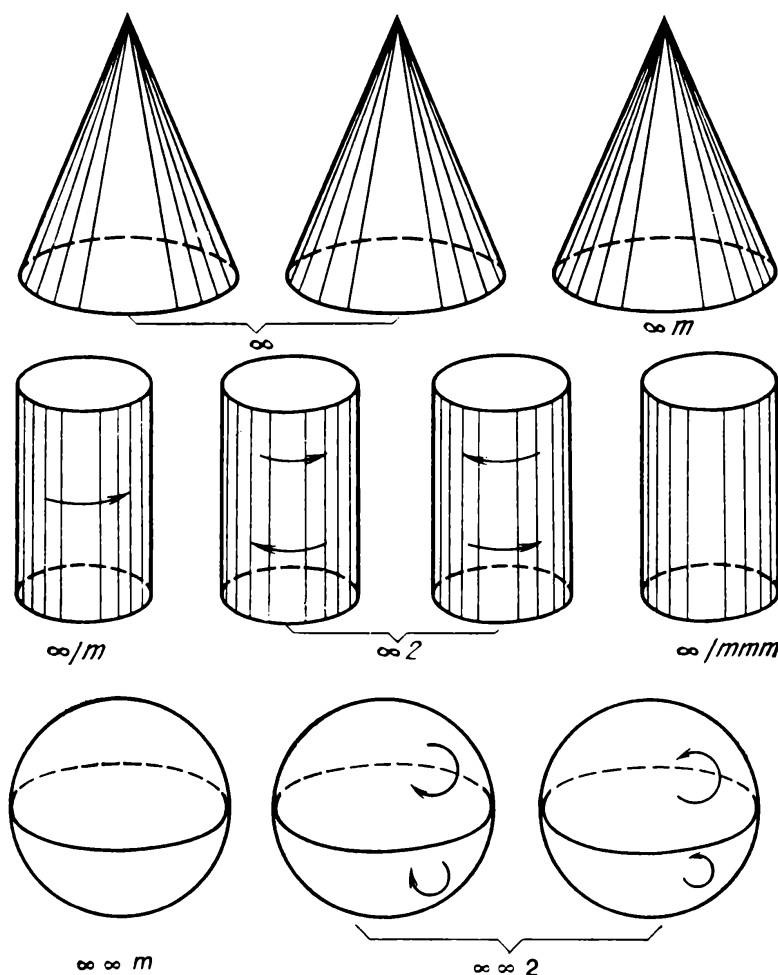
In accordance with the difference in symmetry, the strength of uniform magnetic and electric fields should be graphically represented as shown in Fig. 2.2.

Another corollary of Neumann's principle is that a crystal will have specific physical properties only when the point symmetry group of the crystal is a subgroup of the point symmetry group of the physical property involved.

**The Curie principle.** If an external physical factor (influence) is applied to a crystal with a known symmetry, the symmetry of this crystal in the field of the factor is modified and can be found by referring to the principle of symmetry superposition, called the *Curie principle*.

When several distinct natural phenomena are superposed to form a single system, their asymmetries add up (by Shubnikov's definition, asymmetry is the absence of a symmetry element). This leaves

Fig. 2.1. Patterns illustrating the limiting symmetry groups. Arrows indicate the directions of rotation or twisting of the patterns.



us with those symmetry elements which are common for all of the superposed individual phenomena.

It is assumed here that all symmetry elements of the interacting phenomena intersect at a single common point. This means that the crystal exposed to the external factor will have the symmetry elements which are common for the crystal not exposed to the factor, and for the external factor itself.

Elements decisive for the symmetry of the resultant effect are not only the symmetry of the interacting factors but also the mutual arrangement of their symmetry elements. In solving problems of this type it is convenient to use the stereographic projections of the point symmetry groups of crystals.

In order to illustrate the Curie principle, it is instructive to analyze the constraints imposed by the crystal symmetry on the possibility of generating the pyroelectric effect, piezoelectric effect, and the effect of polarization in the external electric field (see Secs. 3, 4, and 6). Let us compile the following table.

Table 2.1

Effect	Equation	Highest symmetry groups of crystals and textures before an external factor is applied	Symmetry of external factor	Symmetry of crystals evincing the effect
Pyroelectric	$P_i = \gamma_i \Delta T$	$\infty m$	$\infty \infty m$	Ten polar classes. The crystal itself generates dissymmetry necessary to result in $\mathbf{P}$
Piezoelectric	$P_i = d_{ijk} t_{ik}$	$\infty 2$ $\infty m$ , $\bar{4}3m$ , $\bar{6}m2$	$mmm$	Twenty classes without a center of symmetry. Dissymmetry of a crystal must cancel the central symmetry of the external factor
Polarization in an external field	$P_i = \chi_{ij} E_j$	$\infty \infty m$	$\infty m$	32 point symmetry groups. The necessary polar symmetry is provided by the dissymmetry of the external factor

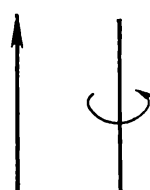


Fig. 2.2. Schematic representation of the vectors of strength of electric (left) and magnetic (right) fields.

The table shows that the crystal response may be identical to different physical fields with nonidentical symmetry.

According to Neumann's principle, the polarized crystal must have the symmetry of one of the ten polar classes, since only these classes have the single polar direction along which the polarization vector  $P$  is aligned.

A crystal may be polarized if as a result of the superposition of the external factor symmetry and the symmetry of the crystal, in accord with the Curie principle, the symmetry of one of the ten polar classes is retained, and it is immaterial whether this is achieved at the expense of the crystal symmetry at the highest symmetry of the external field (pyroelectric effect) or, contrarywise, at the expense of the polar symmetry of the applied field when the polarization can be generated in the crystal of arbitrary symmetry and even in an isotropic medium.

### Examples of Problems with Solutions

**2.1.** Quartz crystals are known to be ferroelectric, that is, are polarized by applied mechanical stress. By using the Curie and Neumann's principles, answer the following questions:

(i) Which of the oriented quartz plates: plates perpendicular to the axis 3 or axis 2, must be selected as sensitive elements of ferroelectric transducers of uniaxial pressure?

(ii) Is it possible to use quartz crystals as hydrostatic pressure transducers?

**Solution.** Quartz crystals belong to class 32.

(i) A uniaxial compression generates the polarization of a crystal if it gives rise to a singular direction which at the same time is a polar one (a *singular direction* is the direction which cannot be reproduced by the symmetry elements of the crystal; a polar direction is the direction in the crystal whose two ends cannot be superposed by any symmetry elements of a given class). In class 32 the threefold axis is the singular but not polar direction owing to the presence of twofold axes perpendicular to the threefold axes.

By applying to the quartz crystal along its threefold axis a compression with the symmetry group  $\infty/mmm$  (in our notation this is written in the form

$$32 \cap \infty/mmm$$

$\parallel 3$

where  $\cap$  is the symbol of intersection, or product, of the groups) we find that the crystal symmetry remains unaltered:

$$32 \cap \infty/mmm = 32$$

$\parallel 3$

Consequently, by compressing a quartz plate cut from a crystal with working faces perpendicular to axis 3 (Z-cut plate, Fig. 2.3), we observe no polarization.

Suppose we compress a quartz crystal along one of its axes 2:

$$32 \cap \infty/mmm = 2 \\ \parallel^2$$

This compression singles out a single direction among all polar directions lying in the plane perpendicular to axis 3. This direction becomes both singular and polar; hence, the piezoelectric polarization vector aligns with this direction.

Obviously, a quartz plate meant for generating ferroelectricity by applying uniaxial compression must be cut so that its faces be perpendicular to one of axes 2 (for example, an X-cut plate, Fig. 2.3).

(ii) Only crystals which have a singular polar direction in zero external field can be used as transducers hydrostatic pressure, whose symmetry is represented by the group  $\infty\infty m$ . Consequently, quartz crystals are not suitable for such measurements.

2.2. The following plates were cut out from rochelle salt (potassium sodium tartrate) crystals to study its physical properties at temperatures above 24°C: X-, Y-, Z-cuts (Fig. 2.3), and L-cuts (Fig. 2.4). Will the uniaxial compression perpendicular to the end faces polarize these plates?

**Solution.** At temperatures above 24°C rochelle salt crystals belong to class 222 in which all directions lying in coordinate planes are nonpolar.

A compression of X-, Y-, and Z-cut plates (see Fig. 2.3) perpendicular to their end faces means that a mechanical stress with symmetry  $\infty/mmm$  is alternately applied along crystallographic directions [100], [010], and [001]. The Curie principle indicates that the

Fig. 2.3. X-, Y-, and Z-cut plates.

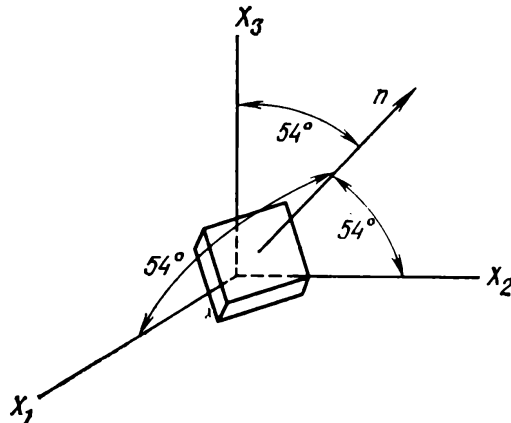
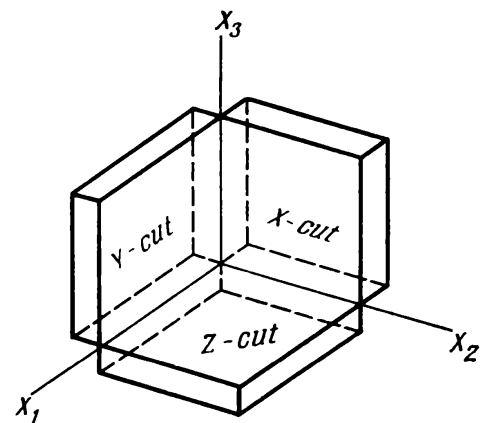


Fig. 2.4. L-cut plate.



crystal symmetry is not lowered by the uniaxial mechanical stress along the indicated directions.

Consequently, as follows from Neumann's principle, such plates cannot be polarized by uniaxial compressing stresses applied perpendicular to their end faces.

A uniaxial compressing stress acting on an *L*-cut plate tilted at equal angles to the twofold symmetry axes lowers the crystal symmetry to class 1; a specified polar direction, coinciding with the direction of stress, appears in the crystal, and the piezoelectric polarization vector can be aligned with this direction.

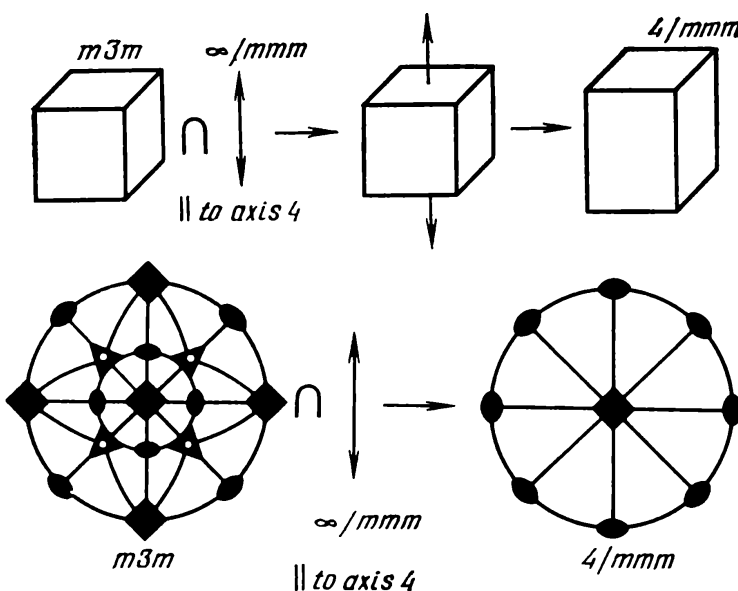
Such plates can be polarized by compression acting perpendicular to the working faces; this conclusion is borne out by experiments.

**2.3.** Uniaxial tensile stress is applied to a cubic crystal with symmetry  $m3m$ . What will be the symmetry of the crystal if the stress is applied along the directions (i) [001], (ii) [111], (iii) [110], (iv) [ $hk0$ ]?

**Solution.** (i) In this case tensile stress with symmetry  $\infty/mmm$  is applied to a crystal with symmetry  $m3m$  along [001], that is, along the fourfold symmetry axis. Consequently, the field of uniaxial stress with symmetry  $\infty/mmm$  interacts with a crystal whose symmetry is  $m3m$ .

As follows from the symmetry superposition principle, the symmetry group of the resultant effect (in this case, the crystal symmetry) must comprise one fourfold axis, four planes passing through it, and one plane perpendicular to it, an inversion center, and four

**Fig. 2.5.** Change in the symmetry of a crystal belonging to symmetry class  $m3m$ , induced by uniaxial mechanical stress along [100].



twofold axes. The crystal symmetry must be  $4/mmm$ , that is, be tetragonal (Fig. 2.5).

(ii) As a result of a tensile stress along [111], that is, along a threefold axis, the crystal retains the threefold axis along which the crystal is stretched, three symmetry planes, the inversion center, and three twofold axes.

In other words, this manner of applying a tensile stress generates a trigonal crystal with rhombohedral symmetry  $\bar{3}m$  (Fig. 2.6).

(iii) A cubic with symmetry  $m3m$  stretched along one of its two-fold symmetry axes retains only the set of symmetry elements  $mmm$  typical for rhombic crystals (Fig. 2.7).

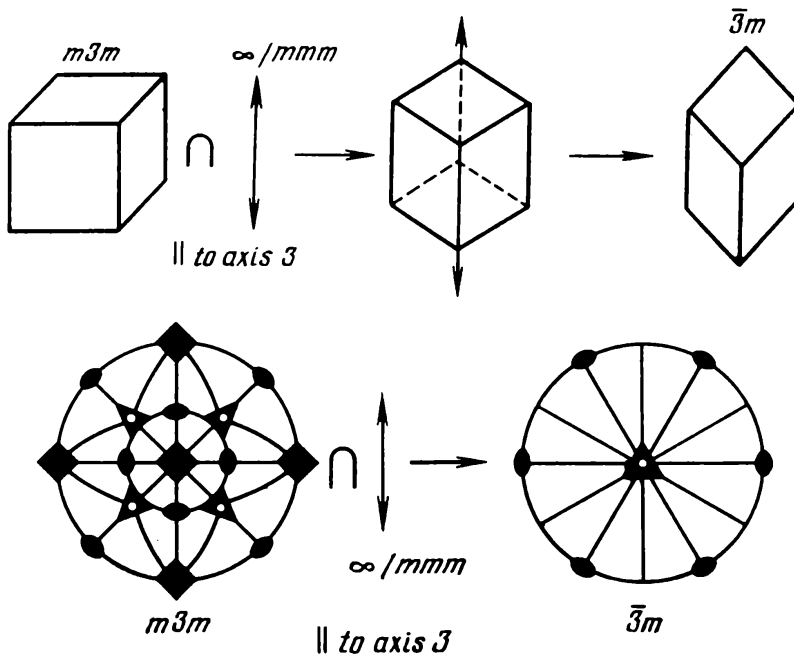
(iv) And finally, by applying a tensile stress along a direction  $[hk0]$ , that is along an arbitrary direction in one of symmetry planes, for instance, along  $AB$ , we find that the crystal will have symmetry  $2/m$  (the stretched crystal becomes monoclinic) (Fig. 2.8).

**2.4.** A Z-cut plate is prepared out of a sphalerite crystal (see Fig. 2.3).

Will such a plate be polarized by: (i) uniaxial compression stress applied to its working faces? (ii) purely shear stress acting in the plane of working faces and characterized by symmetry group  $mmm$ ?

**Solution.** (i) A compression of a Z-cut sphalerite plate signifies that the uniaxial mechanical stress with symmetry group  $\infty/mmm$  is acting on a crystal with symmetry  $\bar{4}3m$  in the direction [001].

**Fig. 2.6.** Change in the symmetry of a crystal belonging to symmetry class  $m3m$ , induced by uniaxial mechanical stress along [111].



This lowers crystal symmetry to class  $\bar{4}2m$ . As no polar direction is thereby singled out, no piezoelectric polarization is produced.

(ii) A purely shear stress with symmetry group  $mmm$  lowers crystal symmetry to class 2 in which the twofold axis is a singular polar

Fig. 2.7. Change in the symmetry of a crystal belonging to symmetry class  $m3m$ , induced by uniaxial mechanical stress along [110].

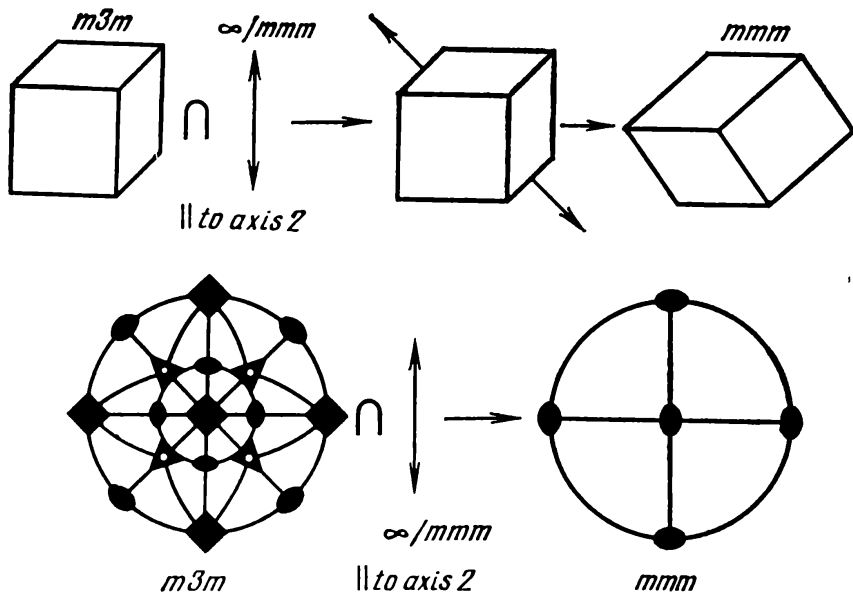
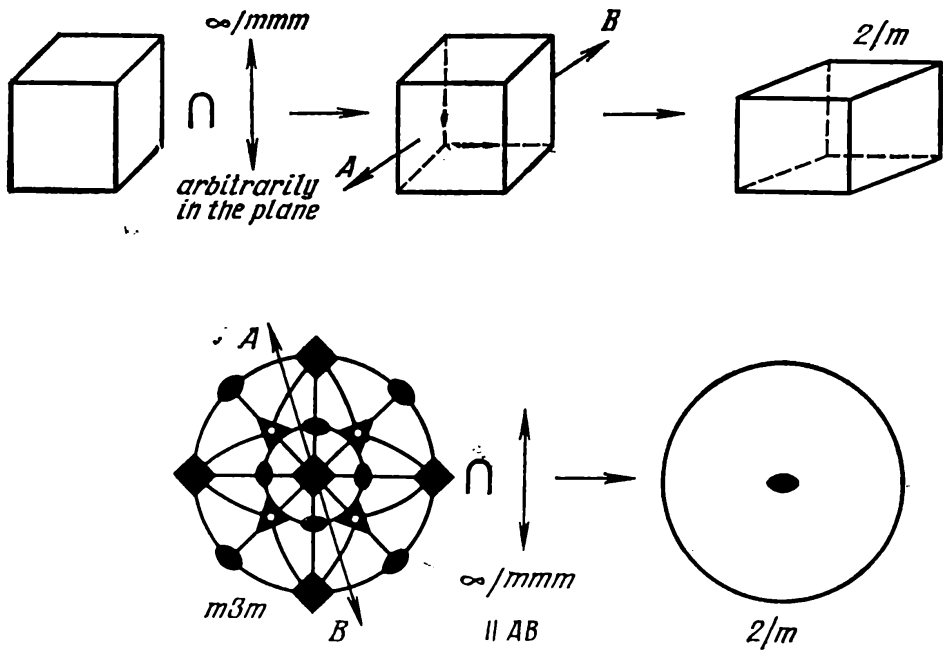


Fig. 2.8. Change in the symmetry of a crystal belonging to symmetry class  $m3m$ , induced by uniaxial mechanical stress along [hk0].



direction. In this case a Z-cut sphalerite plate can exhibit the piezoelectric effect, the conclusion borne out by experiments.

2.5. A single crystal cubic block of rock salt is placed in a uniform electric field in such manner that the electric field strength vector  $\mathbf{E}$  coincides alternately with the following crystallographic directions: (i) [001], (ii) [111], (iii) [110], and (iv) [hk0].

In general, the optical indicatrix (index ellipsoid) of a crystal may be a triaxial ellipsoid, an ellipsoid of revolution, or a sphere (see § 4); how will the indicatrix of a crystal change in each of the cases?

**Solution.** (i) The symmetry of the electric field is  $\infty m$ . If the direction of the electric field strength vector coincides with the crystallographic direction [001], that is, the field is in the direction of the fourfold axis, then the symmetry superposition principle yields that the cubic crystal symmetry  $m3m$  is lowered to tetragonal symmetry  $4mm$  (Fig. 2.9).

(ii) If the field is directed along [111], that is, along the threefold symmetry axis, the crystal symmetry is lowered to trigonal symmetry  $3m$  (Fig. 2.10).

In zero electric field the indicatrix of a cubic crystal is a sphere, and no birefringence is observed.

**Fig. 2.9.** Change in the symmetry of  $m3m$ , induced by electric field applied along [001].

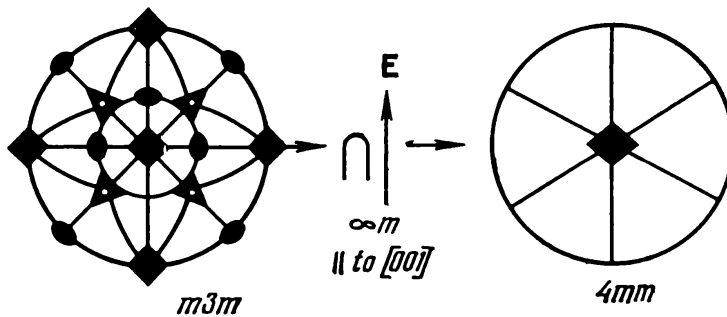
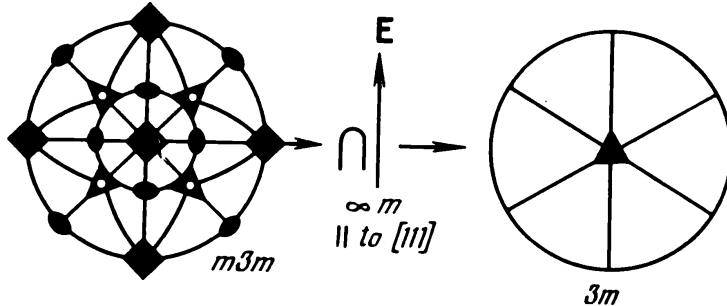


**Fig. 2.10.** Change in the symmetry of  $m3m$ , induced by electric field applied along [111].



The application of an electric field to the crystal deforms its indicatrix in cases (i) and (ii), transforming it into an ellipsoid of revolution. Birefringence is produced, and the crystal becomes optically uniaxial.

(iii) When the electric field is applied along [110], that is, along the twofold symmetry axis, the crystal symmetry is lowered to the rhombic  $mm$  symmetry (Fig. 2.11).

(iv) If the field is applied along directions of the type  $[hk0]$ , that is, along an arbitrary direction within the symmetry plane, the crystals become monoclinic with symmetry  $m$  (Fig. 2.12).

In the last two cases the indicatrix of the crystal is transformed into a triaxial ellipsoid, that is, the crystal becomes optically biaxial.

#### PROBLEMS

2.6. Two oriented plates were cut from a sphalerite crystal to study its physical properties. One of them is cut perpendicular to [100], and the second perpendicular to [111]. Which of these plates must be used to observe the piezoelectric effect caused by the uniaxial compression perpendicular to the working faces?

Fig. 2.11. Change in the symmetry of a crystal belonging to symmetry class  $m3m$ , induced by electric field applied along [110].

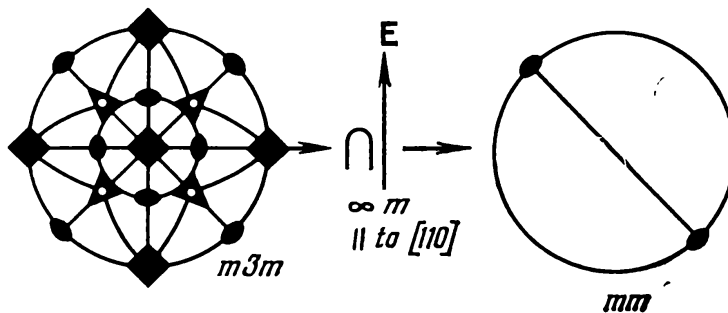
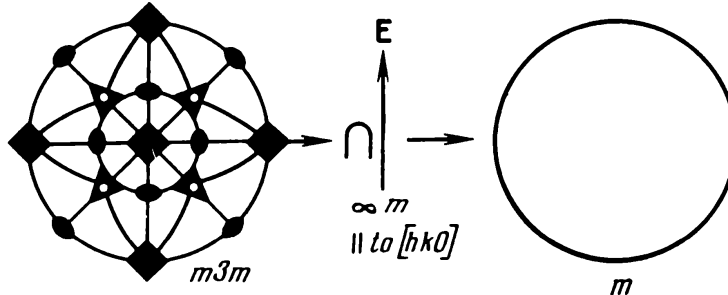


Fig. 2.12. Change in the symmetry of a crystal belonging to symmetry class  $m3m$ , induced by electric field applied along  $[hk0]$ .



2.7. A quartz crystal is stretched along (i)  $[0001]$  and (ii)  $[10\bar{1}0]$ . In which of the two cases can we observe a change in the crystal polarization as a result of heating?

2.8. An electric field is applied to a KDP (potassium dihydrogen phosphate) crystal along the direction (i)  $[001]$ ; (ii)  $[110]$ ; and (iii)  $[010]$ . Find the symmetry of the crystal in the field for each of the given directions of the electric field.

2.9. Is it possible to change a crystal with the initial symmetry  $432$  into a crystal with a polar symmetry group, by applying a uniaxial mechanical stress along  $[110]$ ? Can this transformation be effected by applying an electric field along this direction?

2.10. Find all possible changes in the point symmetry group of a ferroelectric crystal belonging to symmetry class  $222$ , if a ferroelectric phase transition takes place in the crystal (the symmetry of the ferroelectric phase is defined as the symmetry of one domain, see § 3, p. 37). Consider the following directions along which the spontaneous polarization vector may presumably align: (i)  $[100]$ , (ii)  $[010]$ , (iii)  $[001]$ , (iv)  $[hk0]$ , and (v)  $[hkl]$ .

2.11. A crystal with symmetry  $mm2$  is placed in an electric field so that the field direction is first along  $[001]$  and then along  $[010]$ . Find the crystal symmetry in each of the two cases.

2.12. Indicate the crystallographic directions in which the uniaxial tensile stress does not lead to a change of symmetry for crystals of medium symmetry classes.

2.13. Indicate symmetry classes and the corresponding directions along which an applied electric field does not change the crystal symmetry.

2.14. Indicate the crystallographic directions in which a hexagonal crystal with symmetry  $6/mmm$  must be stretched in order to lower its symmetry (i) to the rhombic, and (ii) to the monoclinic symmetry.

2.15. An electric field is applied to a crystal with symmetry  $\bar{6}$  along the directions (i)  $[0001]$ , and (ii)  $[10\bar{1}0]$ . Find the symmetry of the crystal in the field.

2.16. Find the crystallographic directions along which an electric field must be applied to a crystal with symmetry  $\bar{6}m2$  in order to lower its symmetry to (i) trigonal  $3m$ , (ii) rhombic  $mm2$ , and (iii) monoclinic symmetry  $m$ .

2.17. Find the crystal symmetry in the field of uniaxial mechanical stress applied along the crystallographic directions (i)  $[100]$ , (ii)  $[110]$ , (iii)  $[111]$ , (iv)  $[hk0]$ , and (v)  $[hkl]$ , if crystal symmetry at zero stress is  $432$ .

2.18. What must be the symmetry of crystals evincing the piezoelectric effect under uniform compression?

2.19. An electric field is applied along the directions (i)  $[100]$ , (ii)  $[111]$ , (iii)  $[110]$ , (iv)  $[hk0]$ , (v)  $[hkl]$ , and (vi)  $[h\bar{k}l]$  to a crystal

with symmetry 23. Find the symmetry of the crystal in the field for each of the indicated directions of the electric field.

2.20. What symmetry classes of medium-symmetry crystals have the symmetry of their index ellipsoids changed in the electric field applied along the highest-order symmetry axis?

2.21. What are the crystallographic directions along which an electric field must be applied to a crystal with symmetry 622 in order to lower it to the monoclinic symmetry? List all the crystallographic directions such that the application of the field  $\mathbf{E}$  along them gives the same results.

2.22. An electric field is applied to a crystal with symmetry 432 along the crystallographic directions indicated in Problem 2.19. Find the crystal symmetry in the field.

2.23. Find the symmetry of a sphalerite single crystal when an electric field is applied to it along the directions given in Problem 2.19.

2.24. A plate of lithium niobate is placed in an electric field such that the direction of the field strength vector  $\mathbf{E}$  is parallel to (i) the crystallographic direction  $[10\bar{1}0]$ , and then to (ii)  $[1\bar{1}20]$ . Find the crystal symmetry in this field. List the crystallographic directions for which the application of the field  $\mathbf{E}$  gives the same result.

2.25. Find the symmetry of a crystal subjected to uniaxial mechanical tension along the directions given in Problem 2.19, if the crystal symmetry in unstressed state is 23.

2.26. Find all possible changes in the point symmetry group of a ferroelectric crystal belonging to class  $2/m$ , if the crystal undergoes a ferroelectric phase transition. Consider the following crystallographic directions along which the spontaneous polarization vector may align: (i)  $[100]$ , (ii)  $[010]$ , (iii)  $[001]$ , and (iv)  $[h\bar{k}0]$ .

2.27. Find the symmetry of a barium titanite single crystal undergoing a ferroelectric phase transition, if the spontaneous polarization vector is aligned along (i)  $[100]$ , and (ii)  $[111]$ .

2.28. What will be the symmetry of a crystal undergoing a uniaxial mechanical tension along directions given in Problem 2.19, if its symmetry in the stressed state is  $m3$ ? Consider the case of a crystal with symmetry  $3m$  subjected to uniaxial tension along the directions given in Problem 2.24.

2.29. The symmetry of crystal faces is contained in the following ten classes: 1, 2, 3, 4, 6,  $m$ ,  $mm$ ,  $3m$ ,  $4mm$ ,  $6mm$ .

When the microhardness of a crystal is measured, a tetrahedral diamond pyramid is indented into a crystal face. The symmetry  $4mm$  is thereby superposed on the face symmetry. By using the Curie principle, determine the symmetry of the indentation made by the diamond indentor on faces with different symmetries.

2.30. What will be the symmetry of a homogeneous continuous isotropic medium (for instance, a melt) (i) in an electric field, and (ii) in a magnetic field?

**2.31.** Is it possible to use ADP plates oriented along the planes (100), (110), and (001), in order to achieve polarization along the uniaxial mechanical stress applied perpendicular to the working faces?

Before solving Problems 2.32 through 2.35, read § 3.

**2.32.** Is it possible to produce a single-domain ferroelectric by applying to it a mechanical stress? What kind of stress must this be (uniaxial tension, pure shear, uniform compression)? Is the orientation of the applied stress with respect to the direction of spontaneous polarization important for the effect?

**2.33.** How to explain, in terms of the Curie principle, the conservation in a ferroelectric crystal of the macroscopic symmetry corresponding to the group of the paraelectric phase, when the crystal is cooled below the Curie point?

**Comment:** The macroscopic symmetry of a ferroelectric crystal is defined as the symmetry of its domain arrangement.

**2.34.** Show how to explain the inevitable polarization of dielectric crystals in an external electric field, independent of their symmetry, in terms of symmetry relationships.

**2.35.** Is the macroscopic symmetry of a barium titanite crystal changed in phase transitions from the tetragonal to the trigonal and rhombic ferroelectric modifications?

**2.36.** Is it possible to alter the index ellipsoid of a crystal by placing it in a magnetic field?

**2.37.** A magnetic field is applied to a crystal with symmetry  $\bar{3}m$  in the direction (i)  $[000\bar{1}]$ , and (ii)  $[10\bar{1}0]$ . Find the symmetry of the crystal in a magnetic field.

**2.38.** Find the symmetry of the crystal in a magnetic field applied in the directions listed in Problem 2.37, for a crystal belonging to point group  $\bar{6}$ .

### 3. PHYSICAL PROPERTIES OF CRYSTALS DESCRIBED BY TENSORS OF RANK ONE

**Pyroelectric effect.** Dielectric crystals which have in the whole range of stability a non-zero vector of spontaneous polarization in zero external electric field are called *pyroelectrics*.

The crystals in which the direction of the spontaneous polarization vector cannot be changed by applying an external electric field even at field strength near to the breakdown point are called the *proper pyroelectric crystals*. Among such crystals are tourmaline, lithium sulphate, potassium tartrate, etc.

As a result of the spontaneous polarization, bound charge is formed at the opposite faces of a plate cut from a pyroelectric crystal. The charge density  $\sigma$  depends on the magnitude and direction of the spontaneous polarization vector with respect to the plate faces:

$$\sigma = (\mathbf{P}^s \cdot \mathbf{n}) = P_i^s n_i = |\mathbf{P}^s| \cos \alpha \quad (3.1)$$

where  $\mathbf{n}$  is a unit vector of the normal to the plate face, and  $\alpha$  is the angle between the vectors  $\mathbf{P}^s$  and  $\mathbf{n}$  (Fig. 3.1). (As a result of the compensation of the surface charge due to the electrical conduction of the real crystals,  $\sigma \neq |\mathbf{P}^s|$ .)

The maximum charge density will be observed on the faces of a plate cut perpendicular to the spontaneous polarization direction. However, it is not possible to detect the potential difference between the opposite faces of the plate because the bound charge is neutralized by the charge migrating from the air, and because the conduction of pyroelectric crystals is not exactly zero.

When the temperature of pyroelectrics is changed uniformly, the spontaneous polarization changes as well. This effect is called the *pyroelectric effect*.

If the temperature receives a small increment  $\Delta T$  identical in all points of the crystal (uniform heating), the increment in the

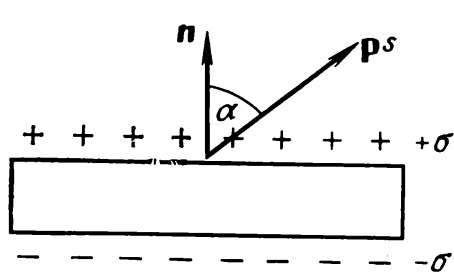


Fig. 3.1. Relationship between surface charge  $\sigma$  and spontaneous polarization  $\mathbf{P}^s$ .

spontaneous polarization vector  $\Delta\mathbf{P}^s$  is proportional to a change in temperature, that is,

$$\Delta\mathbf{P}^s = \gamma\Delta T \quad \text{or} \quad \Delta P_i^s = \gamma_i\Delta T \quad (3.2)$$

where  $\gamma$  ( $\gamma_1$ ,  $\gamma_2$ ,  $\gamma_3$ ) is the vector of pyroelectric coefficients (or, simply, the pyroelectric coefficient), which is defined analytically as

$$\gamma_i = \frac{dP_i^s}{dT} \quad (3.3)$$

The pyroelectric coefficient  $\gamma$  is assumed positive if the spontaneous polarization of a crystal increases with temperature.

**Constraints due to the crystal symmetry.** Owing to its symmetry  $\infty m$ , the electric polarization vector  $\mathbf{P}^s$  can align in the crystal only with the singular polar direction. Hence, according to Neumann's principle, only the crystals belonging to one of the ten polar symmetry classes, namely, 1, 2, 3, 4, 6,  $m$ ,  $mm$ ,  $3m$ ,  $4mm$ , and  $6mm$  constituting subgroups of the group  $\infty m$ , demonstrate the pyroelectric effect. In addition, the pyroelectric effect can be observed in textures with symmetries  $\infty$  and  $\infty m$ .

The orientation of the vectors  $\mathbf{P}^s$  and  $\gamma$  in a crystal is dictated by its symmetry. In the ten polar classes possessing only one singular polar direction, these vectors align precisely with this direction. Conventionally, the direction of the coordinate axis  $X_3$  is chosen in these symmetry classes along the singular polar direction, so that the vectors  $\mathbf{P}^s$  and  $\gamma$  lie along  $X_3$  and have a single nonzero component only along this coordinate axis. Thus, the singular polar direction in tourmaline crystals having symmetry  $3m$  is the symmetry axis 3. This gives, therefore, the direction of the spontaneous polarization vector  $\mathbf{P}^s$  and of the vector  $\gamma$ . In the crystallophysical coordinate system the symmetry axis 3 coincides with the coordinate axis  $X_3$ ; the vector  $\gamma$  is parallel to  $X_3$ , and its components are  $\gamma_1 = \gamma_2 = 0$ ,  $\gamma_3 \neq 0$ ; hence,  $\gamma$  has a single nonzero component.

If a crystal has more than one singular polar direction (classes 1 and  $m$ ), the direction of the vectors  $\mathbf{P}^s$  and  $\gamma$  is not predetermined by the crystal symmetry. In principle, these vectors may align with any of the singular polar directions. Moreover, in this case there is a certain freedom in the choice of the coordinate system, so that in symmetry class 1 the vector  $\gamma$  may have three nonzero components, while in the class  $m$  it may have two nonzero components, and the zero component along the coordinate axis perpendicular to the symmetry plane  $m$ .

**Electrocaloric effect.** As follows from thermodynamical arguments, there is an effect inverted with respect to the pyroelectric effect. It consists in a change in the pyroelectric's temperature when it is placed in an electric field; the effect is called the *electrocaloric effect*.

The equation of the electrocaloric effect is

$$\Delta T = \mathbf{q} \Delta \mathbf{E} \quad (3.4)$$

where  $\mathbf{q}$  is the electrocaloric coefficient  $\mathbf{q} = dT/d\mathbf{E}$ ;  $\mathbf{q}$  is related to the pyroelectric coefficient  $\gamma$  by the formula

$$\mathbf{q} = -\frac{\gamma T}{\rho c J} \quad (3.5)$$

where  $\rho$  and  $c$  stand for the density and specific heat of the crystal, respectively, and  $J$  is the mechanical equivalent of heat [formula (3.5) is derived in Problem 3.3].

By substituting  $\mathbf{q}$  from (3.5) into Eq. (3.4), we arrive at the following relation describing the electrocaloric effect:

$$\Delta T = -\frac{\gamma T}{\rho c J} \Delta \mathbf{E} \quad (3.6)$$

from which we find that when  $\gamma$  is positive and the electric fields strength vector  $\mathbf{E}$  lies along  $\mathbf{P}$ , the coefficient  $\mathbf{q}$  is negative (this means that an increase in the crystal's polarization by the applied electric field diminishes its temperature).

**Ferroelectric crystals.** Ferroelectric crystals, or ferroelectrics, are a subgroup of pyroelectrics and possess a number of specific features characterizing only this subgroup. The main difference between ferroelectrics and the proper pyroelectric crystals is that in the former the direction of the spontaneous polarization can be changed by an applied electric field.

At a temperature called the *Curie point* a ferroelectric crystal undergoes a phase transition modifying its structure. No spontaneous polarization exists above the Curie point, and the crystal is in the paraelectric phase. The crystal symmetry in the paraelectric phase is nonpolar. Below the Curie point the spontaneous polarization appears, and the crystal symmetry is lowered to the polar symmetry, that is, to the symmetry of one of the ten polar classes. The phase transition changes the symmetry owing to a spontaneous deformation of the unit cell configuration.

As follows from Neumann's principle, the crystal symmetry group in the ferroelectric phase must be a subgroup of the symmetry group of the paraelectric phase; moreover, this must be the maximum-order subgroup of the limiting symmetry group  $\infty m$  describing the spontaneous polarization, and of the point symmetry group of the crystal, for a specific arrangement of symmetry elements of these groups.

Below the Curie point the orientation of the spontaneous polarization is not uniform throughout the bulk of the crystal. Usually the crystal separates into the so-called domains, that is, macroscopic regions in which the spontaneous polarization vectors are antiparal-

lel, or the spontaneous polarization is aligned with the crystallographically equivalent directions, so that the multidomain crystal retains the symmetry of its paraelectric phase (here and below the term multidomain crystal means that a ferroelectric separates into domains producing depolarization of the crystal, that is, complete mutual compensation of spontaneous polarization of domains with different orientations of  $\mathbf{P}^s$ ). Both each individual domain and a single-domain crystal of a given ferroelectric will have a polar symmetry group.

Consequently, the separation into domains returns the ferroelectric crystal to the symmetry of its paraelectric phase. Therefore, its macroscopic properties (piezoelectric, optical, mechanical, etc.) are determined by the symmetry of the paraelectric phase.

### Examples of Problems with Solutions

**3.1.** What minimum temperature increment can be measured by a pyroelectric transducer consisting of a tourmaline plate 1 mm thick and a millivoltmeter with the sensitivity of  $10^{-3}$  V/div? How is the plate to be cut for this? How to describe the sensitivity of such a pyroelectric transducer? By what factor would the sensitivity of the transducer be increased if the tourmaline plate were substituted by a lithium sulphate plate of the same thickness, cut perpendicular to the polar axis?

**Solution.** The only nonzero pyroelectric coefficient of tourmaline,  $\gamma_3$ , is associated with the polar direction in the crystal, that is, axis 3. According to Eq. (3.1), the best way to orient a tourmaline plate is to cut it perpendicular to the axis 3, that is, parallel to the plane (0001). A temperature increment that such a plate "feels" can be found from Eq. (3.2), which in this case can be written in the form

$$\Delta P_3^s = \gamma_3 \Delta T \quad (3.7)$$

Obviously,  $\Delta P^s = |\Delta\sigma|$ ,  $\Delta V = \Delta Q/C \approx 10^{-3}$  V/div,  $\Delta Q = \Delta\sigma S$ ,  $C = \epsilon_{33} S/d$ , where  $S$  is the surface area of the plate,  $d$  is its thickness,  $\Delta Q$  is the total charge appearing due to the temperature increment, and  $C$  is the capacitance of the crystal capacitor. Equation (3.7) then yields that the minimum temperature increment measurable by a millivoltmeter and a tourmaline plate 1 mm thick is

$$\Delta T = \frac{\epsilon_{33} \Delta V \cdot 8.85 \cdot 10^{-12}}{d \cdot \gamma_3} \approx 10^{-5} \text{ K}$$

The sensitivity of a transducer of pyroelectric voltage can be characterized by the ratio

$$\frac{\Delta V}{\Delta T} = A \frac{\gamma_i}{\epsilon_{ii}}$$

where  $A$  is a constant,  $A = d/(8.85 \cdot 10^{-2})$ ;  $\gamma_i$  and  $\epsilon_{ii}$  are the pyroelectric coefficient and dielectric permittivity along the polar axis  $X_i$ . By using the values of  $\epsilon_{ii}$  and  $\gamma_i$  for tourmaline and lithium sulphate (choosing for lithium sulphate, as for all class 2 crystals, the axis  $X_2$  as the polar axis), we obtain that the sensitivity of the transducer with a lithium sulphate plate is larger than that with a tourmaline plate by a factor of approximately 27.

**3.2.** Find the equation of the representation surface of the pyroelectric effect (the *representation surface* of a physical property of a crystal is the surface whose radius vector magnitude is equal in each direction to the magnitude of the parameter in this direction). Determine the symmetry of this surface.

**Solution.** Let the pyroelectric effect along the polar direction  $OA$  be represented in the coordinate system  $X_1, X_2, X_3$  by a vector  $\mathbf{A} (A_1, A_2, A_3)$  (Fig. 3.2).

We choose a new direction and align with the axis  $X'_3$  of the new coordinate system. Then the pyroelectric effect along this direction is represented by  $A'_3$  for which we obtain the vector  $\mathbf{X} (x_1, x_2, x_3)$  such that

$$A'^2 = x_1^2 + x_2^2 + x_3^2 \quad (3.8)$$

Now we express  $A'_3$  in terms of the components of the original vector  $\mathbf{A} (A_1, A_2, A_3)$ :

$$A'_3 = C_{31}A_1 + C_{32}A_2 + C_{33}A_3 \quad (3.9)$$

Let us draw a plane  $P$  perpendicular to the vector  $\mathbf{A}$ . The projection of the vector  $\mathbf{A}$  onto  $OB$ ,  $A'_3$ , is positive for points  $(x_1, x_2, x_3)$  lying "above" the plane  $P$ , and negative for points  $(x_1, x_2, x_3)$  "below" the plane  $P$ . Then

$$C_{31} = \pm x_1/A'_3; \quad C_{32} = \pm x_2/A'_3; \quad C_{33} = \pm x_3/A'_3$$

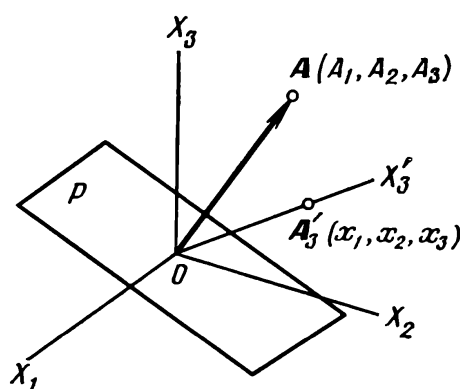


Fig. 3.2. Mutual arrangement of the polar direction  $OA$  and the axis  $X'_3$  of the primed coordinate system.

where the plus sign corresponds to the points  $(x_1, x_2, x_3)$  "above"  $P$ , and the minus sign to the points  $A'_3(x_1, x_2, x_3)$  "below"  $P$ . Therefore,

$$\left. \begin{aligned} A'_3 &= \pm \left( \frac{x_1}{A'_3} A_1 + \frac{x_2}{A'_3} A_2 + \frac{x_3}{A'_3} A_3 \right) \\ A'^2_3 &= \pm (x_1 A_1 + x_2 A_2 + x_3 A_3) \end{aligned} \right\} \quad (3.10)$$

By equating (3.8) and (3.10), we obtain

$$x_1^2 + x_2^2 + x_3^2 = x_1 A_1 + x_2 A_2 + x_3 A_3 \quad (3.11)$$

for the points  $A'_3(x_1, x_2, x_3)$  "above"  $P$ , and

$$x_1^2 + x_2^2 + x_3^2 = -x_1 A_1 - x_2 A_2 - x_3 A_3 \quad (3.12)$$

for the points  $A'_3(x_1, x_2, x_3)$  "below"  $P$ .

Equation (3.11) can be transformed to

$$\left( x_1 - \frac{A_1}{2} \right)^2 + \left( x_2 - \frac{A_2}{2} \right)^2 + \left( x_3 - \frac{A_3}{2} \right)^2 = \frac{A_1^2}{4} + \frac{A_2^2}{4} + \frac{A_3^2}{4} \quad (3.13)$$

and (3.12) to

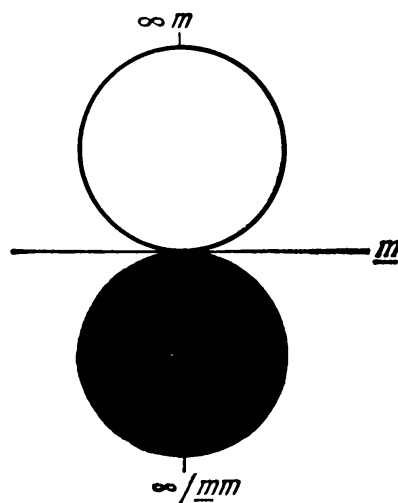
$$\left( x_1 + \frac{A_1}{2} \right)^2 + \left( x_2 + \frac{A_2}{2} \right)^2 + \left( x_3 + \frac{A_3}{2} \right)^2 = \frac{A_1^2}{4} + \frac{A_2^2}{4} + \frac{A_3^2}{4} \quad (3.14)$$

These equations describe two spheres contacting at the origin, and the center of the sphere described by Eq. (3.13) lies at the point  $+A/2$ , and that of the sphere described by Eq. (3.14) at the point  $-A/2$  (Fig. 3.3).

The surface drawn in Fig. 3.3 has symmetry  $\infty/mmm$ , if its shape only is taken into account. But if we also take account of the charge signs (here they are symbolized by the black and white colors), then an antisymmetry plane  $m$  exists between these two spheres.

Antisymmetry operations consist of the conventional symmetry operations combined with the operation of sign reversal. The phys-

Fig. 3.3. Magnitude surface of pyroelectric effect.



ical meaning of the sign reversal may vary: reversal of the charge sign (plus-minus), reversal of color (black-white), reversal of the direction of strain (tension-compression), and so on. The concept of antisymmetry introduced by A.V. Shubnikov\* is used in the physics of crystals to describe vector and tensor surfaces, to interpret the magnetic properties of crystals, etc. The antisymmetry operations are denoted by the symbol of the corresponding symmetry operations with an underbar.

In this notation, the antisymmetry of the characteristic surface of the pyroelectric effect is written as  $\infty/\bar{mm}$ .

**3.3.** Find the symmetry of a barium titanite single-domain crystal in the ferroelectric phase if its symmetry in the paraelectric phase is  $m3m$ , and the spontaneous polarization vector aligns with (i) [100], (ii) [111], (iii) [110].

**Solution.** If a spontaneous polarization with inherent symmetry  $\infty m$  appears in a crystal, the symmetry of a single-domain crystal in the ferroelectric phase will be the highest-order subgroup of the crystal symmetry group in the paraelectric phase and of group  $\infty m$ . For the directions of  $P^s$  listed in the problem these are groups (i)  $4mm$ , (ii)  $3m$ , (iii)  $mm$  (see Fig. 2.11).

**3.4.** It is required to monitor the accuracy of maintaining a constant temperature or to measure a small change in temperature in the room temperature range (22-24 °C). Which of the materials, tourmaline or rochelle salt, is preferable for this? What is advisable to use: ballistic galvanometer or millivoltmeter?

**Solution.** The indicated temperatures are close to the upper Curie point of rochelle salt. Consequently, the corresponding pyroelectric coefficient is large:  $\gamma_1 = 200$  CGSE units. However, the dielectric permittivity  $\epsilon_1$  also reaches the maximum value  $\epsilon_1 = 1000$ .

According to (3.2), for an  $X$ -cut rochelle salt plate

$$\Delta P_1^s = 200 \Delta T \text{ CGSE units}$$

Since  $E = P/\kappa$  and  $\epsilon = 1 + 4\pi\kappa$ ,

$$E_1 = \frac{12.8 \cdot 200}{1000} \Delta T = 2.56 \Delta T$$

For a  $Z$ -cut tourmaline plate

$$\Delta P_3^s = 1.2 \Delta T, \quad E_3 = \frac{12.8 \cdot 1.2}{7.5} \Delta T = 2.00 \Delta T$$

Obviously, if the coefficient  $\gamma_1$  is large, the potential difference between the opposite faces of a ferroelectric plate becomes approximately the same as in a linear dielectric, tourmaline, having a small

---

\* A.V. Shubnikov, *Symmetry and Antisymmetry of Finite Figures*, Izd. Nauk SSSR, Moscow, 1951.

pyroelectric coefficient. However, the charge on a face, proportional to  $\Delta P^s$ , in rochelle salt plates is larger than that of tourmaline by a factor of nearly 200. Therefore, it is advisable to use in the problem as stated a rochelle salt plate and a ballistic galvanometer.

**3.5.** Could a plate cut of a triglycin sulphate (TGS) crystal withstand a sharp drop in temperature from the Curie point,  $49^\circ\text{C}$ , down to  $39^\circ\text{C}$ ? Assume the electric strength of the crystal to be  $40 \text{ kV/cm}$ .

**Solution.** The TGS crystal symmetry is  $2/m$  in the paraelectric phase, and 2 in the ferroelectric phase. The direction of the axis 2 is chosen as the direction of the coordinate axis  $X_2$ . Consequently, the equation of the pyroelectric effect takes the form

$$\Delta P_2^s = \gamma_2 \Delta T$$

For  $\gamma_2$  close to the Curie point we assume a mean value of 500 CGSE units. This gives

$$\Delta P_2^s = 500 \cdot 10 = 5 \cdot 10^3 \text{ CGSE units}$$

The strength of the corresponding electric field is

$$E = \frac{4\pi \cdot \Delta P_2}{\epsilon_2} = \frac{12.8 \cdot 5 \cdot 10^3}{25} = 2600 \text{ CGSE units} \approx 10^6 \text{ V/cm}$$

This field exceeds the electric strength of the crystal, so that the crystal breaks down.

**3.6.** By how many degrees and to what temperatures can one "shift" the phase transition point of potassium dehydrophosphate (KDP) crystals by means of the electrocaloric effect, if the crystals are placed at the phase-transition point  $T_C = -150^\circ\text{C}$  into an electric field of  $20 \text{ kV/cm}^{-1}$ , applied in such a manner that the direction of the vector  $\mathbf{E}$  is (i) along  $\mathbf{P}^s$ ; (ii) opposite to  $\mathbf{P}^s$ ? (Assume  $c = 0.1 \text{ cal} \cdot \text{g}^{-1} \cdot \text{K}^{-1}$ ,  $\gamma_3 = 5000 \text{ CGSE units}$ .)

**Solution.** The value of the only nonzero electrocaloric coefficient of KDP crystals in the ferroelectric phase is found from relation (3.5):

$$q_3 = -\frac{\gamma_3 T}{\rho c J} = -0.06 \text{ CGSE units}$$

The applied electric field causes the temperature increment

$$\Delta T = q_3 \Delta E = -4 \text{ K}$$

Consequently, a field of  $20 \text{ V/cm}$ , parallel to the direction of spontaneous polarization, cools the crystal in the vicinity of the Curie point owing to the electrocaloric effect by approximately 4 K; this means that this field is capable of "shifting" the Curie point of KDP to higher temperatures by 4 K.

If this field is applied in the direction opposite to that of  $\mathbf{P}$ , the crystal will be heated by 4 K, and the Curie point will then shift to lower temperatures by the same amount.

## PROBLEMS

3.7. In a KDP crystal calculate the temperature increment plate caused by the spontaneous electrocaloric effect.

3.8. Find the density of surface charge formed on the opposite faces of a tourmaline plate uniformly heated by 30 K, if the plate is cut so that

- the normal to the plate is parallel to symmetry axis 3;
- the normal to the plate is at an angle of  $60^\circ$  to axis 3;
- the normal to the plate is perpendicular to axis 3.

3.9. What temperature increment is measurable with a lithium sulphate plate 1 mm thick and a millivoltmeter having a sensitivity of  $10^{-3}$  V/division? What is the best way to cut a plate for this purpose?

3.10. Find the electric field applied to a tourmaline crystal along [0001] which will produce the same polarization as a uniform temperature increment of 10 K.

3.11. Find the potential difference generated on a plate of potassium tartrate  $1 \times 1 \times 0.1$  cm<sup>3</sup> cut perpendicular to axis 2, when the plate is heated by 10 K. Calculate the charge generated on its faces.

3.12. Find the shift of the Curie points of rochelle salt crystal (see Table 14) placed in an electric field of 1000 V/cm. The field is applied in the direction of the electric axis of the crystal.

3.13. Calculate the pyroelectric coefficient of barium titanite at its upper Curie point ( $120^\circ\text{C}$ ), if the spontaneous electrocaloric effect is known to shift the Curie point by approximately 1 K.

3.14. Calculate the voltage generated between the plates of a capacitor formed by a Z-cut tourmaline plate 1 mm thick cooled from  $50^\circ\text{C}$  to room temperature.

3.15. Enumerate crystal symmetry classes in which the spontaneous polarization vector in a pyroelectric crystal changes, when heated, not only its magnitude but also its direction.

3.16. Estimate the temperature increment in a tourmaline plate placed in an electric field of 20 kV/cm.

3.17. Calculate the charge generated at the opposite faces of a lithium sulphate plate of  $1.2 \times 2 \times 0.2$  cm<sup>3</sup>, cut at an angle of  $60^\circ$  to axis 2, upon heating by 40 K.

3.18. By applying Neumann's principle, find the nonzero components of a vector property of a crystal belonging to class 6mm.

3.19. Will the pyroelectric effect be observed in crystals of (i) quartz, (ii) gallium arsenide, (iii) ADP crystals in paraelectric phase?

3.20. Can the pyroelectric effect be observed in a ferroelectric crystal separated into domains?

3.21. Calculate the electric charges generated on the opposite faces of a tourmaline plate 0.1 cm thick, with the area 1 cm<sup>2</sup>, cut

perpendicular to [0001], upon uniform heating by 10 K. What is the potential difference between the opposite faces?

3.22. Find the temperature increment in a *Y*-cut lithium sulphate plate 0.1 cm thick in a 300 V/cm field.

3.23. An electric field of 10 kV/cm is applied to a *Z*-cut KDP crystal of  $1 \times 1 \times 0.1$  cm<sup>3</sup>, in the phase transition interval. Assuming  $q_3 = -0.6$  CGSE units, find the temperature increment in the plate due to the electrocaloric effect.

## 4. PHYSICAL PROPERTIES OF CRYSTALS DESCRIBED BY TENSORS OF RANK TWO

The properties of crystals described by rank two tensors are the dielectric permittivity and magnetic permeability, susceptibility, electric conductivity and electric resistivity, thermal conductivity, thermal expansion, piezocaloric effect, and some others. Thus, for example, Ohm's law for isotropic media is written in the form

$$\mathbf{j} = \sigma \mathbf{E}$$

where the vectors  $\mathbf{j}$  standing for the current density and  $\mathbf{E}$  standing for the field are parallel, and the electric conductivity  $\sigma$  is a numerical coefficient. In contrast to this, the electric conductivity of crystals is direction-dependent. In the general case, each component of the current density vector is a linear function of all three components of the field vector.

Once an orthogonal coordinate system is chosen, Ohm's law in the differential form for crystals is written in the general case as a system of three equations:

$$\begin{aligned} j_1 &= \sigma_{11}E_1 + \sigma_{12}E_2 + \sigma_{13}E_3 \\ j_2 &= \sigma_{21}E_1 + \sigma_{22}E_2 + \sigma_{23}E_3 \\ j_3 &= \sigma_{31}E_1 + \sigma_{32}E_2 + \sigma_{33}E_3 \end{aligned}$$

By using Einstein's summation rule, we rewrite the above equations in the form

$$j_i = \sigma_{ij}E_j \quad (i, j = 1, 2, 3) \quad (4.1)$$

The summation is carried out over the repeated subscript. The proportionality coefficients  $\sigma_{ij}$  in Eqs. (4.1) define the electric conductivity of the crystal. Thus, in contrast to isotropic media, the number of quantities necessary to define the electric conductivity in a crystal is not one but, in the general case, nine:

$$[\sigma_{ij}] = \begin{bmatrix} \sigma_{11} & \sigma_{12} & \sigma_{13} \\ \sigma_{21} & \sigma_{22} & \sigma_{23} \\ \sigma_{31} & \sigma_{32} & \sigma_{33} \end{bmatrix}$$

The specific values of the coefficients  $\sigma_{11}$ ,  $\sigma_{22}$ ,  $\sigma_{33}$ , and so on depend on the choice of the coordinate system fixed to the crystal. In a transformation from the coordinate system  $X_1$ ,  $X_2$ ,  $X_3$  to a new system  $X'_1$ ,  $X'_2$ ,  $X'_3$ , the coefficients  $\sigma_{ij}$  are transformed in

accord to the law

$$\sigma'_{ij} = C_{ik} C_{jl} \sigma_{kl} \quad (4.2)$$

where  $\sigma'_{ij}$  are the coefficients in the new system  $X'_1, X'_2, X'_3$ ,  $\sigma_{kl}$  are the coefficients in the original system  $X_1, X_2, X_3$ , and  $C_{ik}$ ,  $C_{jl}$  are the direction cosines defining the orientation of the axes  $X'_1, X'_2, X'_3$  with respect to the axes  $X_1, X_2, X_3$ .

Quantities which are defined by nine numbers dependent on the choice of a coordinate system, and in going over to a new coordinate system are transformed according to (4.2), represent a tensor of rank two, or a rank two tensor.

The original coefficients may be expressed in terms of the new ones as follows:

$$\sigma_{ij} = C_{ki} C_{lj} \sigma'_{kl} \quad (4.2a)$$

The following equations describe the passage of electric current through a crystal, thermal expansion and thermal conduction, and the piezocaloric effect which constitutes a change of temperature in a crystal subjected to mechanical stress:

$$\begin{aligned} j_i &= \sigma_{ij} E_j, \quad r_{ij} = \alpha_{ij} \Delta T \\ q_i &= -\lambda_{ij} \frac{dT}{dx_j}, \quad \Delta Q = T \alpha_{ij} t_{ij} \end{aligned}$$

where  $\alpha_{ij}$  are the thermal expansion coefficients,  $q_i$  denotes the components of the heat flux vector,  $\lambda_{ij}$  are the thermal conductivities,  $r_{ij}$  are the components of the mechanical strain tensor, and  $t_{ij}$  are the components of the mechanical stress tensor.

*Magnetic permeability*, as well as *magnetic susceptibility* of paramagnetic and diamagnetic crystals, entering the equations relating the vectors of magnetic field strength  $\mathbf{H}$ , magnetization  $\mathbf{J}$ , and magnetic induction  $\mathbf{B}$  are tensors of rank two. Indeed, at all times  $B_i = \mu_0 H_i + J_i$ , where  $\mu_0$  is a scalar constant called the *magnetic permeability* of vacuum. Furthermore, an additional equation holds for paramagnetic and diamagnetic crystals, for weak and medium-strength fields:

$$J_i = \mu_0 \psi_{ij} H_j$$

where  $\psi_{ij}$  are the components of the *magnetic susceptibility tensor*.

It then follows that  $B_i = \mu_0 H_i + \mu_0 \psi_{ij} H_j = \mu_0 (\delta_{ij} + \psi_{ij}) H_j$ . This equation can be rewritten in the form

$$B_i = \mu_{ij} H_j, \text{ where } \mu_{ij} = \mu_0 (\delta_{ij} + \psi_{ij})$$

The tensor  $[\mu_{ij}]$  is called the *magnetic permeability tensor*. The energy of magnetization of a crystal is  $\psi = (1/2) v \mu_{ij} H_i H_j$ , where  $v$  is the volume of the crystal. A crystal is said to be paramagnetic

or diamagnetic along one of the directions of principal susceptibilities when the magnetic susceptibility along this direction is positive or negative, respectively.

The principal susceptibilities of paramagnetic and diamagnetic crystals are much less than unity ( $\approx 10^{-5}$ ), so that the field produced by a magnetized crystal is small compared with the external field and as a rule can be ignored.

Each element of volume,  $v$ , of a crystal placed in a magnetic field is subjected to a moment of forces

$$G_{ij} = v\mu_0 (-\psi_{ij}H_kH_j + \psi_{ij}H_kH_i)$$

and to forces

$$F_i = \frac{1}{2} v\mu_0 \psi_{jk} \frac{\partial}{\partial x_i} (H_j H_k)$$

The magnetic susceptibility of powder consisting of arbitrarily oriented anisotropic crystalline grains is equal to

$$\frac{1}{3} (\psi_{11} + \psi_{22} + \psi_{33})$$

The electric conductivity, dielectric permittivity and susceptibility, thermal conductivity and thermal expansion, just as magnetic permeability and susceptibility, are described by symmetrical tensors of rank two, and this means that the relations

$$\sigma_{ij} = \sigma_{ji}, \quad \epsilon_{ij} = \epsilon_{ji}, \text{ etc.} \quad (4.3)$$

reducing the number of independent components of the mentioned tensors to six, are valid for them.

**The representation surface of a symmetric rank two tensor.** Tensors of rank two are geometrically interpreted as surfaces of second order; this provides a descriptive representation of the considered properties of crystals, the type of their anisotropy, and the relation to the crystal symmetry. If the components of a symmetrical rank two tensor ( $S_{ij} = S_{ji}$ ) are used as coefficients in the general equation of the second-order surface,

$$S_{11}x_1^2 + S_{22}x_2^2 + S_{33}x_3^2 + S_{12}x_1x_2 + S_{21}x_2x_1 + S_{13}x_1x_3 + S_{31}x_3x_1 + S_{23}x_2x_3 + S_{32}x_3x_2 = 1 \quad (4.4)$$

we obtain a surface referred to as the *representation quadratic of the rank two tensor*.

Thus, in the general case the representation quadratic of electric conductivity of a crystal is described by the equation

$$\sigma_{11}x_1^2 + \sigma_{22}x_2^2 + \sigma_{33}x_3^2 + 2\sigma_{32}x_3x_2 + 2\sigma_{13}x_1x_3 + 2\sigma_{12}x_1x_2 = 1$$

**Geometrical properties of the representation quadratic.** The magnitude of the radius vector  $\mathbf{r}$  of the representation quadratic in a chosen

direction is related to a quantity characterizing the corresponding property in this direction, such as  $\sigma$ , by the formula (Fig. 4.1)

$$r = 1/\sqrt{\sigma} \quad \text{or} \quad \sigma = 1/r^2 \quad (4.4a)$$

If the property to be considered is included in an equation of a vector-vector interaction (vector stimulus and vector response, as in Ohm's law), the representation surface of the property makes it possible to find the direction of the response vector from that of the stimulus vector, and vice versa.

If  $j_i = \sigma_{ij}E_j$ , then the direction of  $j$  for a given  $E$  can be found by drawing the radius vector  $\overline{OP}$  of the characteristic surface parallel to the field  $E$ , and then erecting the perpendicular to the plane tangent to the characteristic surface at the point  $P$  (Fig. 4.2).

**Principal axes of a symmetrical rank two tensor.** Second-order surfaces for which  $S_{ij} = S_{ji}$ , possess the so-called *principal axes*, that is three mutually perpendicular directions such that if they are chosen as the coordinate axes, the general equation of the surface, Eq. (4.4), transforms to the simplest form

$$S_{11}x_1^2 + S_{22}x_2^2 + S_{33}x_3^2 = 1 \quad (4.5)$$

If the quantities  $S_{11}$ ,  $S_{22}$ , and  $S_{33}$  are positive, the surface (4.5) is an ellipsoid; if two coefficients are positive and one negative, the surface (4.5) is a hyperboloid of one sheet. If one coefficient is positive and two are negative, the surface (4.5) is a hyperboloid of two sheets.

At the points of intersection of the principal axes with the representation surface the normal to the surface is parallel to the radius vector; this is considered to be the essential property of the principal axes. If  $P$  denotes a point on the representation surface given by Eq. (4.4), and  $X$  denotes the components of the vector  $\overline{OP}$ , and we

Fig. 4.1. Representation quadratic of electric conductivity.

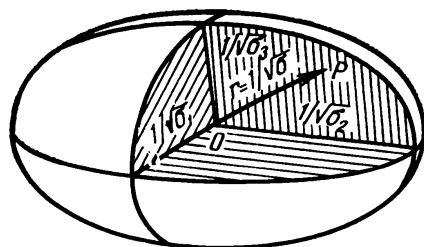
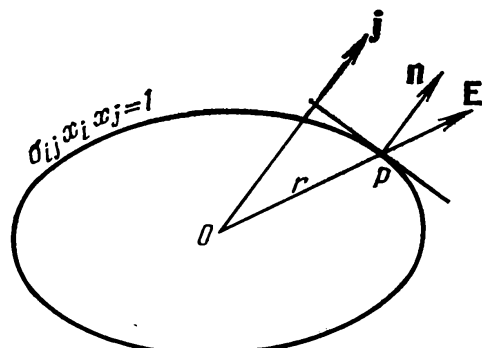


Fig. 4.2. Determination of the direction of response vector on the basis of the direction of stimulus vector, by means of the representation surface.



form a vector  $S_{ij}x_j$ , then this vector is parallel to the surface normal at the point  $P$  in accordance with the properties of radius vector. The radius vector and the normal are parallel if their corresponding components are proportional to each other:

$$S_{ij}x_j = \lambda x_i \quad (4.5a)$$

where  $\lambda$  is a constant. Equation (4.5a) is a system of three linear homogeneous equations in  $x_i$ .

This system has a nonzero solution only if the determinant composed of the coefficients of the equations vanishes:

$$\begin{vmatrix} S_{11} - \lambda & S_{12} & S_{13} \\ S_{12} & S_{22} - \lambda & S_{23} \\ S_{13} & S_{23} & S_{33} - \lambda \end{vmatrix} = 0 \quad (4.5b)$$

The contracted notation is

$$| S_{ij} - \lambda \delta_{ij} | = 0$$

This cubic equation is called the *secular equation*. Its three roots  $\lambda_1$ ,  $\lambda_2$ , and  $\lambda_3$  give three possible values of  $\lambda$  for which the system (4.5a) has a nonzero solution. Each of the roots determines the direction in which the radius vector of a quadratic surface is parallel to the normal to the surface, that is, determines the direction of one of the mutually orthogonal principal axes.

### Lengths of Principal Axes

If a quadratic is referred to its principal axes, the secular equation takes the form

$$\begin{vmatrix} S_1 - \lambda & 0 & 0 \\ 0 & S_2 - \lambda & 0 \\ 0 & 0 & S_3 - \lambda \end{vmatrix} = 0$$

that is,  $(S_1 - \lambda)(S_2 - \lambda)(S_3 - \lambda) = 0$ , and the three roots of Eq. (4.5a),  $\lambda_1$ ,  $\lambda_2$ , and  $\lambda_3$ , are the three *principal coefficients*  $S_1$ ,  $S_2$ , and  $S_3$ , respectively.

The equation of the representation surface of electric conductivity written in terms of the principal axes becomes

$$\sigma_{11}x_1^2 + \sigma_{22}x_2^2 + \sigma_{33}x_3^2 = 1$$

Correspondingly, in the principal coordinate system the rank two tensor is diagonal:

$$\begin{bmatrix} \sigma_{11} & 0 & 0 \\ 0 & \sigma_{22} & 0 \\ 0 & 0 & \sigma_{33} \end{bmatrix} \quad \text{or} \quad \begin{bmatrix} \sigma_1 & 0 & 0 \\ 0 & \sigma_2 & 0 \\ 0 & 0 & \sigma_3 \end{bmatrix}$$

The quantities  $\sigma_1$ ,  $\sigma_2$ , and  $\sigma_3$  are called the *principal components of the electric conductivity tensor*, or the *principal electric conductivities*.

In the principal coordinate system Eqs. (4.1) are also simplified:

$$j_1 = \sigma_1 E_1, \quad j_2 = \sigma_2 E_2, \quad j_3 = \sigma_3 E_3$$

If the electric field is applied along the principal coordinate axis  $X_1$ , then  $E_2 = E_3 = 0$ ; hence,  $j_2 = j_3 = 0$ , and  $\mathbf{j}$  is parallel to  $\mathbf{E}$ .

When studying the effect of crystal symmetry on the form of a rank two tensor, it is especially convenient to write the rank two tensors and the equations of the corresponding representation quadratics in the principal coordinate system.

### *Directions of Principal Axes*

In each particular case the directions of the three principal axes  $X'_1$ ,  $X'_2$ ,  $X'_3$  can be found as follows. First solve equation (4.5b) for  $\lambda$ . Then form three equations (4.5a) with one of the found values of  $\lambda$ , say,  $\lambda_1$ , and solve them for the ratios  $X'_1 : X'_2 : X'_3$ . Repeating these operations with the second root, say,  $\lambda_2$ , we find  $X''_1 : X''_2 : X''_3$ . The third direction  $X'''_1$ ,  $X'''_2$ ,  $X'''_3$  can be found by erecting a perpendicular to the first two.

### *Rotation Around Principal Axes*

A problem typical for numerous physical situations is the transformation of the components of a symmetrical rank two tensor from one coordinate system to another, obtained from the first by a rotation around one of the coordinate axes. Let a tensor  $[S_{ij}]$  be referred to its principal axes:

$$[S_{ij}] = \begin{bmatrix} S_1 & 0 & 0 \\ 0 & S_2 & 0 \\ 0 & 0 & S_3 \end{bmatrix}$$

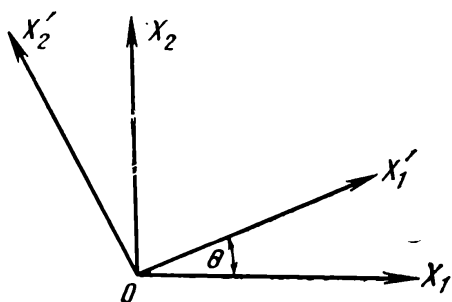


Fig. 4.2a. Rotation of coordinate system around the axis  $X_2$  by an angle  $\theta$ .

Let new axes  $X'_1, X'_2, X'_3$  be obtained from the axes  $X_1, X_2, X_3$  by a rotation around  $X_3$  by an angle  $\theta$  measured by the rotation angle of  $X_1$  toward  $X_2$  (see Fig. 4.2a); the matrix representing this rotation is

$$\begin{pmatrix} \cos \theta & \sin \theta & 0 \\ -\sin \theta & \cos \theta & 0 \\ 0 & 0 & 1 \end{pmatrix}$$

According to (4.2), the transformed tensor is

$$\begin{bmatrix} S'_{11} & S'_{12} & 0 \\ S'_{12} & S'_{22} & 0 \\ 0 & 0 & S_{33} \end{bmatrix}$$

where

$$\begin{aligned} S'_{11} &= S_1 \cos^2 \theta + S_2 \sin^2 \theta = \frac{1}{2} (S_1 + S_2) - \frac{1}{2} (S_2 - S_1) \cos 2\theta \\ S'_{22} &= S_1 \sin \theta \cos \theta + S_2 \cos^2 \theta = \frac{1}{2} (S_1 + S_2) + \frac{1}{2} (S_2 - S_1) \cos 2\theta \\ S'_{12} &= -S_1 \sin \theta \cos \theta + S_2 \sin \theta \cos \theta = \frac{1}{2} (S_2 - S_1) \cos 2\theta \end{aligned}$$

**A quantity characterizing a property in a given direction.** Crystals are generally anisotropic, that is, their properties are direction-dependent. In the general case, when a crystal is exposed to a vector factor, for example, is placed in an electric field, the direction of the generated current does not coincide with that of the field. A quantity characterizing the property of the crystal along a chosen direction is therefore defined as the current density component  $j_{||}$  parallel to  $\mathbf{E}$ , divided by  $\mathbf{E}$ . If a unit field is applied, the electric conductivity along the field is numerically equal to  $j_{||}$ .

If a tensor defining a physical property of a crystal in a fixed coordinate system, for example, the dielectric permittivity tensor  $[\epsilon_{ij}]$ , is known, then the dielectric permittivity along any direction  $\mathbf{n}$  in the crystal is calculated using a relation

$$\epsilon_n = \epsilon_{ij} n_i n_j \quad (4.6)$$

where  $n_i, n_j$  are the components of a unit vector  $\mathbf{n}$  (direction cosines of the fixed direction).

**The effect of crystal symmetry on its properties described by rank two tensors.** The crystal symmetry leads to essential constraints on the number of independent components of rank two tensors. The orientation of the characteristic surface with respect to the crystal symmetry elements is determined in compliance with Neumann's principle, as given in Table 4.1.

Table 4.1

Classification of crystals by optical properties	Crystal system	Characterizing symmetry	Geometry of representation surface and its orientation	The number of independent components of the tensor	Tensor transformed to the chosen coordinate system
Isotropic medium	Cubic	Four axes 3	Sphere	1	$\begin{bmatrix} S & 0 & 0 \\ 0 & S & 0 \\ 0 & 0 & S \end{bmatrix}$
Uniaxial crystals	Tetragonal Hexagonal Trigonal	One axis 4 One axis 6 One axis 3	Surface of revolution around the highest-order symmetry axis $X_3(Z)$	2	$\begin{bmatrix} S_1 & 0 & 0 \\ 0 & S_1 & 0 \\ 0 & 0 & S_3 \end{bmatrix}$
Biaxial crystals	Rhombic	Three mutually perpendicular twofold axes. No axes of higher order	Surface of second order with axes $X_1, X_2, X_3$ parallel to twofold axes: $X, Y, Z$	3	$\begin{bmatrix} S_1 & 0 & 0 \\ 0 & S_2 & 0 \\ 0 & 0 & S_3 \end{bmatrix}$
	Monoclinic	One twofold axis and one plane $m$	Surface of second order with one axis $X_2$ parallel to the twofold axis non-perpendicular to plane $m$	4	$\begin{bmatrix} S_{11} & 0 & S_{13} \\ 0 & S_{22} & 0 \\ S_{13} & 0 & S_{33} \end{bmatrix}$
	Triclinic	Center of symmetry, or no symmetry	Surface of second order. The orientation with respect to crystallographic axes is not defined	6	$\begin{bmatrix} S_{11} & S_{12} & S_{13} \\ S_{12} & S_{22} & S_{23} \\ S_{13} & S_{23} & S_{33} \end{bmatrix}$

The number of independent coefficients in the representation surface equation is exactly equal to the number of components of the corresponding tensor, and the surface symmetry is the same as that of the physical property.

**Measurements on oriented samples.** Relation (4.6) is widely used in practice to calculate the quantities characterizing the physical properties of oriented samples, as well as for the reverse problem,

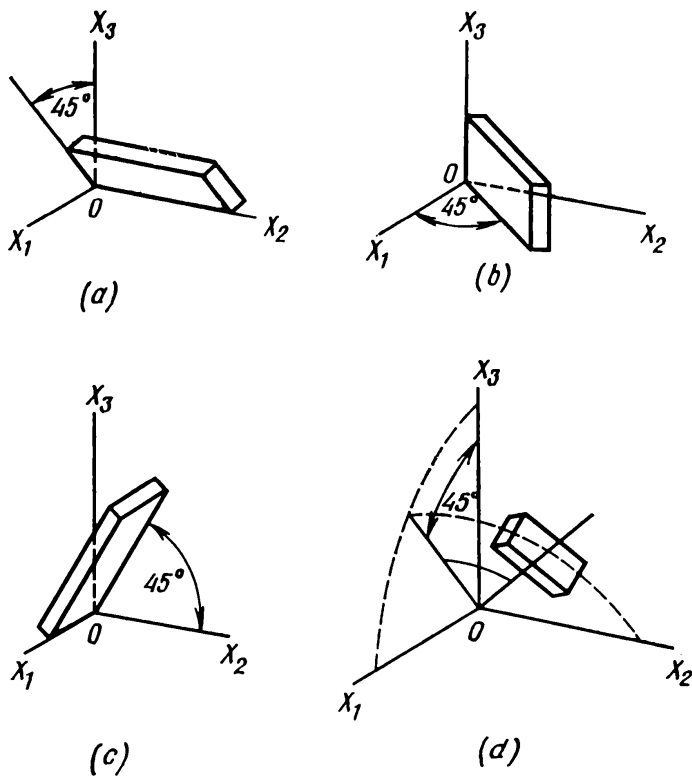
namely, determination of the tensor representing a physical property of a crystal from the data of measurements on oriented samples.

The notation of crystal "cuts" is meant to indicate the directions of the normal to the principal ("working") faces of a plate or bar in the crystallophysical coordinate system. Thus, for example, the  $X$ -,  $Y$ -, and  $Z$ -cuts are plates or slabs in which the normals to the working faces are parallel to the axes  $X$ ,  $Y$ ,  $Z$ , respectively (see Fig. 2.3). The working faces are normally defined as faces to which external factors are applied: electric field, mechanical stress, or others.

The following notations are used to describe the orientation of tilted cuts (these notations were recommended by the International Committee on Piezoelectricity of AIRE in 1946, mostly for piezoelectric crystals).

Some of the cuts are shown in Fig. 4.3. When the properties of tilted cuts related to new axes  $X'_1$ ,  $X'_2$ ,  $X'_3$  (primed axes are directed along the edges of the slab or plate) are studied, relations (4.2) and (4.6) are used. Obviously, each of the coefficients in the frame  $X'_1$ ,  $X'_2$ ,  $X'_3$  will be a linear combination of the principal coefficients.

Fig. 4.3. Examples of various oriented crystal cuts: (a)  $XYl/+45^\circ$ , (b)  $YXb/+45^\circ$ , (c)  $ZYb/+45^\circ$ , (d)  $YXlb/+45^\circ/+45^\circ$ .



Conversely, it is often convenient to find the principal coefficients by measuring the properties on tilted crystal cuts and then going over from the data obtained to the required quantities by the appropriate calculations. The following notations are accepted currently for the description of oriented tilted cuts:

$XYs/\alpha$ ,  $YZsb/\alpha/\gamma$ ,  $XYbl/\alpha/\gamma/\beta$ , etc.

The first two letters denote the crystallophysical axes\* along which are initially aligned the thickness  $s$  and length  $l$  (width  $b$ ) of a crystal cut; the letters placed after them (if they are needed) show which of the edges of the cut is the axis of rotation; Greek letters for angles,  $\alpha$ ,  $\beta$ ,  $\gamma$ , which assume specific values (separated from the letters  $l$ ,  $b$ ,  $s$  by slashes), denote the angles of successive rotations:  $\alpha$  stands for the rotation around the thickness  $s$  of the cut,  $\beta$  for the rotation around the length  $l$ , and  $\gamma$  for the rotation around the width  $b$ . Angles are given in degrees and minutes of arc. Counterclockwise rotation is assumed positive.

Let  $X_1$ ,  $X_2$ ,  $X_3$  be the axes rigidly fixed to a monoclinic crystal in the standard setting, and  $X'_1$ ,  $X'_2$ ,  $X'_3$  be the orthogonal axes fixed to the oriented sample, so that the axis  $X'_3$  lies in the direction along which the dielectric permittivity of the crystal is measured (Fig. 4.4). The corresponding symbol in the frame  $X'_1$ ,  $X'_2$ ,  $X'_3$  is  $\epsilon'_{33}$ . On the other hand, the measured value of  $\epsilon'_{33}$  is expressed, according to Eq. (4.6), in terms of the tensor components  $[\epsilon_{ij}]$  in the standard setting. By measuring the values of  $\epsilon'_{33}$  in samples with four different orientations, we obtain four equations relating the independent components of the tensor  $[\epsilon_{ij}]$  of the monoclinic crystal. By solving them we find the components of the dielectric permittivity tensor in the coordinate system  $X_1$ ,  $X_2$ ,  $X_3$ . Consequently, the measurements on oriented samples enable one to find all the components of the tensor  $[\epsilon_{ij}]$ , and of any rank two tensor describing the physical properties of crystals in the standard setting.

**Magnitude surfaces.** The magnitude surfaces of physical properties of crystals, making it possible to obtain a descriptive image of symmetry and anisotropy, prove very convenient for practical purposes. Thus, for example, the magnitude surface of the dielectric permittivity tensor  $[\epsilon_{ij}]$  is described by the equation

$$\mathbf{r}(n) = \epsilon_{ij} n_i n_j \quad (4.7)$$

which shows that the magnitude surface is formed by the tips of radius vectors  $\mathbf{r}$  whose length is equal, in a chosen scale, to the die-

---

\* By convention, the crystallophysical axes  $X_1$ ,  $X_2$ ,  $X_3$  are denoted by  $X$ ,  $Y$ ,  $Z$ . They must not be confused with the crystallographic coordinate axes (not necessarily orthogonal).

lectric permittivity along any direction  $n$ .

If all the eigenvalues of a rank two tensor describing some physical property of a crystal are positive, then the distance  $r$  to any point on the magnitude surface is also positive. If, however, some of the tensor eigenvalues are negative, then  $r$  will be negative for some directions. In such cases the segments of the surface corresponding to the negative values of  $r$  are drawn exactly as the usual positive segments, but coloured in black to distinguish them from the positive ones, white segments of the surface (see Figs. 3.3 and 4.6).

**Inverse tensors.** Sometimes the calculation of quantities characterizing physical properties of crystals requires a determination of the components of the inverse tensor from the known components of the tensor describing some physical property of crystals. For example, if the tensor of electric conductivity of the crystal whose components enter the equation

$$j_i = \sigma_{ij} E_j$$

are known, one may want to find the resistivity tensor whose components enter the equation

$$E_i = \rho_{ij} j_j$$

In the general case the individual components of the tensor  $[\rho_{ij}]$  are not the reciprocals of the correspondent components of the tensor  $[\sigma_{ij}]$ , but are found from the relation

$$\rho_{ij} = \frac{(-1)^{i+j} \Delta_{ij}^\sigma}{\Delta^\sigma} \quad (4.8)$$

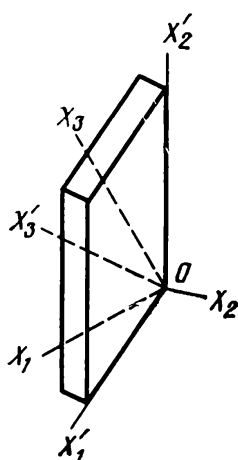


Fig. 4.4. Crystal plate of arbitrary orientation.

where  $\Delta^\sigma$  is a determinant of the type

$$\begin{vmatrix} \sigma_{11} & \sigma_{12} & \sigma_{13} \\ \sigma_{12} & \sigma_{22} & \sigma_{23} \\ \sigma_{13} & \sigma_{23} & \sigma_{33} \end{vmatrix}$$

$\Delta_{ij}^\sigma$  is the minor obtained from the above determinant by crossing out the  $i$ th row and  $j$ th column. It is obvious from Eq. (4.8) that the tensor has an inverse only if all its three principal values are nonzero.

### Examples of Problems with Solutions

**4.1.** Find the magnitude and direction of the current density vector (in the coordinate system  $X_1$ ,  $X_2$ ,  $X_3$ ), for the current generated in a crystal plate with area  $S$  and thickness  $d$  ( $\sqrt{S} \geq d$ ) by an external field  $E$  equal to 150 V/cm and applied in the direction  $(\sqrt{2}/2, \sqrt{2}/2, 0)$ , if the electric conductivity tensor of the crystal in the above coordinate system takes the form

$$[\sigma_{ij}] = \begin{bmatrix} 9 & -2 & 8 \\ -2 & 16 & 0 \\ 8 & 0 & 25 \end{bmatrix} \cdot 10^{-7} \text{ ohm}^{-1} \cdot \text{cm}^{-1}$$

**Solution.** The components of the vector  $\mathbf{E}$  ( $E_1$ ,  $E_2$ ,  $E_3$ ) are:

$$E_1 = 150 \cdot \frac{\sqrt{2}}{2} \text{ V/cm}, \quad E_2 = 150 \cdot \frac{\sqrt{2}}{2} \text{ V/cm}, \quad E_3 = 0$$

$$j_1 = \sigma_{11}E_1 + \sigma_{12}E_2 + \sigma_{13}E_3 = 9 \cdot 10^{-7} \cdot 150 \frac{\sqrt{2}}{2} - 2 \cdot 10^{-7} \cdot 150 \frac{\sqrt{2}}{2} = 7.4 \cdot 10^{-5} \text{ A/cm}^2$$

$$j_2 = \sigma_{21}E_1 + \sigma_{22}E_2 + \sigma_{23}E_3 = -2 \cdot 10^{-7} \cdot 150 \frac{\sqrt{2}}{2} + 16 \cdot 10^{-7} \cdot 150 \frac{\sqrt{2}}{2} = 14.7 \cdot 10^{-5} \text{ A/cm}^2$$

$$j_3 = \sigma_{31}E_1 + \sigma_{32}E_2 + \sigma_{33}E_3 = 8 \cdot 10^{-7} \cdot 150 \frac{\sqrt{2}}{2} = 8.46 \cdot 10^{-5} \text{ A/cm}^2$$

$$|\mathbf{j}| = 18.5 \cdot 10^{-5} \text{ A/cm}^2$$

The direction of the vector  $\mathbf{j}$  is given by the angles  $\alpha$ ,  $\beta$ , and  $\gamma$  between this vector and the coordinate axes. The angles  $\alpha$ ,  $\beta$ , and

$\gamma$  are found from the relations

$$\cos \alpha = \frac{j_1}{|\mathbf{j}|}, \quad \cos \beta = \frac{j_2}{|\mathbf{j}|}, \quad \cos \gamma = \frac{j_3}{|\mathbf{j}|}$$

$$\cos \alpha = 0.398, \quad \alpha = 66^\circ$$

$$\cos \beta = 0.797, \quad \beta = 37^\circ$$

$$\cos \gamma = 0.452, \quad \gamma = 63^\circ$$

4.2. What is the form of the tensor describing the linear expansion of lithium sulphate in the orthogonal coordinate system  $X_1, X_2, X_3$  if (i) the symmetry axis is  $2 \parallel X_3$ ; (ii) the symmetry axis is  $2 \parallel X_2$ ?

**Solution.** In the case of class 2 crystals the operation of rotation by  $180^\circ$  around the axis 2 is an identity transformation. The matrices of direction cosines corresponding to this transformation have the form

$$C_{ij}(X_3, 180^\circ) = \begin{pmatrix} -1 & 0 & 0 \\ 0 & -1 & 0 \\ 0 & 0 & 1 \end{pmatrix}, \quad C_{ij}(X_2, 180^\circ) = \begin{pmatrix} -1 & 0 & 0 \\ 0 & 1 & 0 \\ 0 & 0 & -1 \end{pmatrix}$$

By making use of the transformation law for the rank two tensor components and the given above rotation operators, we obtain for the case  $2 \parallel X_3$

$$\alpha_{11} = \alpha_{11}, \quad \alpha_{21} = \alpha_{21},$$

$$\alpha_{22} = \alpha_{22}, \quad \alpha_{23} = -\alpha_{23},$$

$$\alpha_{33} = \alpha_{33}, \quad \alpha_{31} = -\alpha_{31}.$$

As a result of rotation, the quantities  $\alpha_{23} = \alpha_{32}$  and  $\alpha_{13} = \alpha_{31}$  reversed signs. But since the conditions of symmetric transformation require that these quantities conserve their initial values, this can occur only if they are equal to zero.

Consequently, the thermal expansion of lithium sulphate in the orthogonal coordinate system, whose axis  $X_3$  lies along the symmetry axis 2, is given by the tensor

$$\begin{bmatrix} \alpha_{11} & \alpha_{12} & 0 \\ \alpha_{12} & \alpha_{22} & 0 \\ 0 & 0 & \alpha_{33} \end{bmatrix}$$

Likewise, it can be shown that in the setting ( $2 \parallel X_2$ ) the thermal expansion tensor has the form

$$\begin{bmatrix} \alpha_{11} & 0 & \alpha_{13} \\ 0 & \alpha_{22} & 0 \\ \alpha_{13} & 0 & \alpha_{33} \end{bmatrix}$$

4.3. The electric conductivity tensor of a crystal has the following form:

$$\sigma_{ij} = \begin{bmatrix} 25 & 0 & 0 \\ 0 & 7 & -3\sqrt{3} \\ 0 & -3\sqrt{3} & 13 \end{bmatrix} \cdot 10^{-7} \text{ ohm}^{-1} \cdot \text{m}^{-1}$$

Indicate the directions with respect to the coordinate system in which the tensor  $[\sigma_{ij}]$  has the above-given form, in which the current density vector has the same direction as the applied electric field.

**Solution.** Mathematically, this problem will be solved when we find the eigenvalues and eigenvectors of the given tensor, that is, when we transform it to the principal axes. The principal axes of a tensor have the following property: at the points of intersection of the axes with the representation surface the normal to the surface,  $\mathbf{n}$ , is parallel to the radius vector  $\overline{OP}$  (see Fig. 4.2). We denote by  $P$  a point on the representation surface given by the equation  $\sigma_{ij}x_i x_j = 1$ , and by  $A_i$  the components of the vector  $\overline{OP}$ . In accord with the above property, the radius vector  $\sigma_{ik}A_k$  is parallel to the normal to the surface at the point  $P$ . Since the radius vector and the normal must be parallel, we find that their respective components are proportional, that is,

$$\sigma_{ik}A_k = \lambda A_i$$

where  $\lambda$  is a constant.

This last relation is a system of three homogeneous linear equations in variables  $A_i$  ( $i = 1, 2, 3$ ) which can be written in the form

$$\sigma_{ik}A_k - \lambda A_i = 0$$

or

$$(\sigma_{ik} - \lambda \delta_{ik}) A_k = 0$$

where  $\delta_{ik}$  is the Kronecker delta.

The expanded form of these equations is

$$(\sigma_{11} - \lambda) A_1 + \sigma_{12} A_2 + \sigma_{13} A_3 = 0$$

$$\sigma_{21} A_1 + (\sigma_{22} - \lambda) A_2 + \sigma_{23} A_3 = 0$$

$$\sigma_{31} A_1 + \sigma_{32} A_2 + (\sigma_{33} - \lambda) A_3 = 0$$

This homogeneous system serves to find  $A_1$ ,  $A_2$ , and  $A_3$ ; and we are looking for a nonzero (nontrivial) solution of the system.

A homogeneous system is known to have a nontrivial solution only if its determinant equals zero, that is

$$\begin{vmatrix} \sigma_{11} - \lambda & \sigma_{12} & \sigma_{13} \\ \sigma_{21} & \sigma_{22} - \lambda & \sigma_{23} \\ \sigma_{31} & \sigma_{32} & \sigma_{33} - \lambda \end{vmatrix} = 0$$

which is compactly written in the form

$$|\sigma_{ik} - \lambda\delta_{ik}| = 0$$

The three roots  $\lambda_1$ ,  $\lambda_2$ , and  $\lambda_3$  of the secular equation give three possible values at which the above system of equations has a nonzero solution. Each root determines the direction in which the radius vector of a second-order surface is parallel to one of the principal axes.

In our case the secular equation has the form

$$(25 - \lambda) [(7 - \lambda) (13 - \lambda) - 27] = 0,$$

or

$$\lambda^2 - 20\lambda + 64 = 0$$

This gives

$$\lambda_{2,3} = 10 \pm \sqrt{100 - 64} = 10 \pm 6,$$

$$\lambda_1 = 25, \quad \lambda_2 = 16, \quad \lambda_3 = 4$$

We thus find that the values of the diagonal components of the electric conductivity tensor referred to its principal axes are equal (in  $\text{ohm}^{-1} \cdot \text{m}^{-1}$ ) to

$$\sigma_1 = 25 \cdot 10^{-7}, \quad \sigma_2 = 16 \cdot 10^{-7}, \quad \sigma_3 = 4 \cdot 10^{-7}$$

Now we shall find the directions of the principal axes of the tensor  $\sigma_{ij}$  with respect to the initial coordinate system. Let  $\mathbf{A}^{(1)}$ ,  $\mathbf{A}^{(2)}$ ,  $\mathbf{A}^{(3)}$  be the vectors along the principal axes. The components of the vector  $\mathbf{A}^{(1)}$  will be denoted by  $A_1^{(1)}$ ,  $A_2^{(1)}$ , and  $A_3^{(1)}$ . In order to find these components, we substitute the value  $\lambda = 25$  into the system of linear equations, replacing  $A_1$ ,  $A_2$ , and  $A_3$  by  $A_1^{(1)}$ ,  $A_2^{(1)}$ , and  $A_3^{(1)}$ :

$$25A_1^{(1)} + 0 \cdot A_2^{(1)} + 0 \cdot A_3^{(1)} = 25A_1^{(1)}$$

$$0 \cdot A_1^{(1)} + 7A_2^{(1)} - 3\sqrt{3}A_3^{(1)} = 25A_2^{(1)}$$

$$0 \cdot A_1^{(1)} - 3\sqrt{3}A_2^{(1)} + 13A_3^{(1)} = 25A_3^{(1)}$$

This yields:  $A_1^{(1)}$  is arbitrary, and  $A_2^{(1)}$  and  $A_3^{(1)}$  equal zero. In order to find the direction cosines of the principal axes of the tensor corresponding to the value  $\lambda_1$  with respect to the initial tensor axes, one has to normalize the vector  $\mathbf{A}^{(1)}$ ; in our case this yields

$$A_1^{(1)} = \pm 1, \quad A_2^{(1)} = A_3^{(1)} = 0$$

Following a similar procedure for  $\lambda_2$  and  $\lambda_3$ , we find:

$$A_1^{(2)} = 0, \quad A_2^{(2)} = \frac{1}{2}, \quad A_3^{(2)} = -\frac{\sqrt{3}}{2}$$

$$A_1^{(3)} = 0, \quad A_2^{(3)} = \frac{\sqrt{3}}{2}, \quad A_3^{(3)} = \frac{1}{2}$$

The table of direction cosines fixing the orientation of the principal axes of the tensor  $[\sigma_{ij}]$  with respect to the initial axes then takes the following form:

Table 4.2

Axes	$X_1$	$X_2$	$X_3$
$X'_1$	1	0	0
$X'_2$	0	$+\frac{1}{2}$	$-\frac{\sqrt{3}}{2}$
$X'_3$	0	$\frac{\sqrt{3}}{2}$	$\frac{1}{2}$

4.4. The dielectric permittivities of resorcin were measured on three plates of different cuts shown in Fig. 4.5. The results of measurements are given in the table:

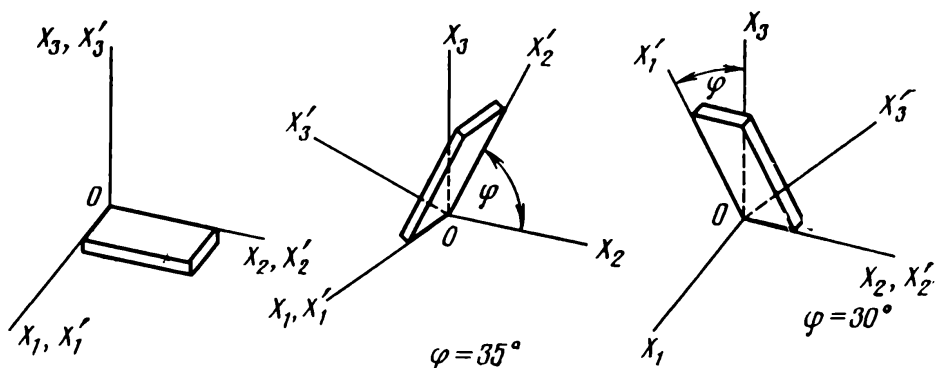
Table 4.3

No. of the cut (Fig. 4.5)	$S, \text{cm}^2$	$t, \text{cm}$	$C \cdot 10^{-12}, \text{F}$
1	3.305	0.179	5.25
2	0.784	0.255	0.92
3	2.672	0.196	3.92

Find the principal dielectric permittivities of resorcin.

**Solution.** The dielectric properties of crystals belonging to class  $mm$  are characterized by three principal values of the dielectric

Fig. 4.5. Orientation of crystal cuts referred to in Problem 4.4.



permittivity:  $\epsilon_1$ ,  $\epsilon_2$ , and  $\epsilon_3$ . Denote the axes of crystallophysical coordinate system fixed to the crystal in the standard setting by  $X_1$ ,  $X_2$ ,  $X_3$ , and the orthogonal axes fixed to the specimen by  $X'_1$ ,  $X'_2$ ,  $X'_3$ . If the metal coating is deposited on the faces parallel to the plane  $X'_1X'_2$ , then the dielectric permittivity  $\epsilon'_{33}$  along  $X'_3$ , that is, along the normal  $\mathbf{n}$  to the plate, can be calculated from the measured capacitance  $C$  and dimensions of the crystal capacitor obtained.

As the components of the tensor  $[\epsilon_{ij}]$  relate to the measured quantities  $\epsilon'_{33}$  via formulas of the type

$$\epsilon'_{33} = n_i n_j \epsilon_{ij},$$

the appropriate measurements on oriented specimens make it possible to determine all components of the tensor in the crystallophysical coordinate system  $X_1$ ,  $X_2$ ,  $X_3$ .

The values of  $\epsilon'_{33}$  are found from the measured capacitance of the plates,  $C = \epsilon'_{33} S / (4\pi t)$ , whence  $\epsilon'_{33} = 4\pi t C / S$  ( $t$  is the thickness, and  $S$  is the area of a plate). Obviously, the measured capacitance of the first plate (Z-cut plate) immediately yields

$$\epsilon_3 = 3.22$$

The orientation of the normal to the second plate with respect to the crystallophysical axes (see Fig. 4.5) is

$$n_1 = 0, \quad n_2 = -\sin \varphi, \quad n_3 = \cos \varphi, \quad \varphi = 35^\circ$$

and its dielectric permittivity is

$$\epsilon''_{33} = \epsilon_2 \sin^2 \varphi + \epsilon_3 \cos^2 \varphi, \quad \epsilon''_{33} = 3.39$$

Correspondingly, for the third plate

$$n_1 = -\cos \varphi, \quad n_2 = 0, \quad n_3 = \sin \varphi, \quad \varphi = 30^\circ$$

$$\epsilon'''_{33} = \epsilon_1 \cos^2 \varphi + \epsilon_3 \sin^2 \varphi$$

Assuming  $\epsilon_3 = 3.22$  in these last equations, and solving them for  $\epsilon_1$  and  $\epsilon_2$  we obtain

$$\epsilon_1 = 3.26, \quad \epsilon_2 = 3.74.$$

**4.5.** It was found that in a monoclinic crystal the thermal expansion coefficient along the twofold symmetry axis [010] is equal to  $41 \cdot 10^{-6}$  K $^{-1}$ . Then the measurements were carried out in the plane (010). It was found that the values of the thermal expansion coefficient along two mutually perpendicular directions in the plane (010) are  $32 \cdot 10^{-6}$  and  $15 \cdot 10^{-6}$  K $^{-1}$ , while in the direction at  $45^\circ$  to these directions the coefficient was  $16 \cdot 10^{-6}$  K $^{-1}$ . Find the coefficients of the tensor  $[\alpha_{ij}]$  in the standard setting, as well as its principal coefficients.

**Solution.** One of the principal axes of the tensor in monoclinic crystals (the axis  $X_2$  in the standard setting) is chosen along [010]

which is either the twofold symmetry axis or the normal to the plane of symmetry. The remaining two principal axes of the tensor may be oriented differently with respect to this direction, so that the tensor  $[\alpha_{ij}]$  of this crystal has four independent components. We direct the axis  $X_2$  along [010], and the two mutually perpendicular directions in the plane (010), along which the thermal expansion coefficients  $32 \cdot 10^{-6}$  and  $15 \cdot 10^{-6} \text{ K}^{-1}$  were measured, along the axes  $X_3$  and  $X_1$ . With this choice of the coordinate system we obtain

$$\alpha_{11} = 15 \cdot 10^{-6} \text{ K}^{-1}, \quad \alpha_{22} = 41 \cdot 10^{-6} \text{ K}^{-1}$$

$$\alpha_{33} = 32 \cdot 10^{-6} \text{ K}^{-1}$$

and the thermal expansion coefficient along the direction at  $45^\circ$  to the axes  $X_3$  and  $X_1$  is then found from relation

$$\alpha_n = \alpha_{ij} n_i n_j = \frac{1}{2} (\alpha_{11} + \alpha_{33} + 2\alpha_{13})$$

whence  $\alpha_{13} = -7.5 \cdot 10^{-6} \text{ K}^{-1}$ .

This means that the thermal expansion tensor of this crystal in the  $X_1$ ,  $X_2$ ,  $X_3$  coordinate system has the form

$$[\alpha_{ij}] = \begin{bmatrix} 15 & 0 & -7.5 \\ 0 & 41 & 0 \\ -7.5 & 0 & 32 \end{bmatrix} \cdot 10^{-6} \text{ K}^{-1}$$

Let us find the principal thermal expansion coefficients by using the method described in Problem 4.3. These are

$$\alpha_1 = 34.8 \cdot 10^{-6} \text{ K}^{-1}, \quad \alpha_2 = 41 \cdot 10^{-6} \text{ K}^{-1},$$

$$\alpha_3 = 12.2 \cdot 10^{-6} \text{ K}^{-1}$$

By converting to the principal axes, we reduce the number of components of the tensor to three, but in this case we shall have to give an additional constant (the angle of rotation around the axis  $X_2$ ) giving the orientation of the frame,  $X'_1$ ,  $X'_2$ ,  $X'_3$  in which the tensor  $[\alpha_{ij}]$  is diagonal, with respect to the axes  $X_1$ ,  $X_2$ ,  $X_3$ .

4.6. The thermal expansion coefficients of a triclinic crystal were measured on a specimen cut in the shape of a cube. The coefficients were measured along the cube edges and its three bulk diagonals. Show how the components of the thermal expansion tensor can be found from these measurement data.

**Solution.** In the general case the thermal expansion of triclinic crystals is characterized by a tensor of the form

$$\begin{bmatrix} \alpha_{11} & \alpha_{12} & \alpha_{13} \\ \alpha_{12} & \alpha_{22} & \alpha_{23} \\ \alpha_{13} & \alpha_{23} & \alpha_{33} \end{bmatrix}$$

The symmetry of triclinic crystals imposes no constraints on the orientation of the representation surface of rank two tensor; furthermore, the orientation of the principal axes of the thermal expansion coefficients in the crystal is not known in advance. Consequently, we orient the axes  $X_1, X_2, X_3$  in an arbitrary manner, for example, directing them along the edges of the cube.

In this case the direction cosines of the directions mentioned in the problem, along which the thermal expansion coefficients were measured, are as follows:

$$(1, 0, 0); \quad (0, 1, 0); \quad (0, 0, 1); \quad (1/\sqrt{3}, 1/\sqrt{3}, 1/\sqrt{3}); \\ (-1/\sqrt{3}, 1/\sqrt{3}, 1/\sqrt{3}); \quad (1/\sqrt{3}, 1/\sqrt{3}, -1/\sqrt{3})$$

Denote the values of the thermal expansion coefficients measured along the mentioned directions by  $\alpha^{(1)}, \alpha^{(2)}, \alpha^{(3)}, \alpha^{(4)}, \alpha^{(5)}$ , and  $\alpha^{(6)}$ , respectively. In the chosen coordinate system fixed to the edges of the cube, we have

$$\alpha^{(1)} = \alpha_{11}, \quad \alpha^{(2)} = \alpha_{22}, \quad \alpha^{(3)} = \alpha_{33}$$

By using equations of the type  $\alpha_n = \alpha_{ij}n_i n_j$ , where  $\alpha_n$  are the thermal expansion coefficients along  $\mathbf{n}$ , we find

$$\alpha^{(4)} = \frac{1}{3} (\alpha_{11} + \alpha_{22} + \alpha_{33} + 2\alpha_{12} + 2\alpha_{23} + 2\alpha_{31})$$

$$\alpha^{(5)} = \frac{1}{3} (\alpha_{11} + \alpha_{22} + \alpha_{33} - 2\alpha_{12} + 2\alpha_{23} - 2\alpha_{31})$$

$$\alpha^{(6)} = \frac{1}{3} (\alpha_{11} + \alpha_{22} + \alpha_{33} + 2\alpha_{12} - 2\alpha_{23} - 2\alpha_{31})$$

We transform these equations to

$$\alpha^{(4)} - \frac{1}{3} (\alpha_{11} + \alpha_{22} + \alpha_{33}) = \frac{2}{3} (\alpha_{12} + \alpha_{23} + \alpha_{31})$$

$$\alpha^{(5)} - \frac{1}{3} (\alpha_{11} + \alpha_{22} + \alpha_{33}) = \frac{2}{3} (-\alpha_{12} + \alpha_{23} - \alpha_{31})$$

$$\alpha^{(6)} - \frac{1}{3} (\alpha_{11} + \alpha_{22} + \alpha_{33}) = \frac{2}{3} (\alpha_{12} - \alpha_{23} - \alpha_{31})$$

whence

$$-\frac{4}{3} \alpha_{31} = (\alpha^{(5)} + \alpha^{(6)}) - \frac{2}{3} (\alpha_{11} + \alpha_{22} + \alpha_{33})$$

$$\alpha_{31} = \frac{1}{2} (\alpha_{11} + \alpha_{22} + \alpha_{33}) - \frac{3}{4} (\alpha^{(5)} + \alpha^{(6)})$$

Likewise,

$$\alpha_{23} = \frac{3}{4} (\alpha^{(4)} + \alpha^{(5)}) - \frac{1}{2} (\alpha_{11} + \alpha_{22} + \alpha_{33})$$

$$\alpha_{12} = \frac{3}{4} (\alpha^{(4)} + \alpha^{(6)}) - \frac{1}{2} (\alpha_{11} + \alpha_{22} + \alpha_{33})$$

This gives us all the independent components of the thermal expansion tensor of the triclinic crystal in the system of coordinates  $X_1$ ,  $X_2$ ,  $X_3$  fixed to the edges of a cube-cut sample.

Evidently, the axes  $X_1$ ,  $X_2$ ,  $X_3$  are not the principal axes of the tensor  $[\alpha_{ij}]$ . In the coordinate system of its principal axes  $X'_1$ ,  $X'_2$ ,  $X'_3$  the tensor  $[\alpha'_{ij}]$  has only three nonzero principal expansion coefficients  $\alpha'_1$ ,  $\alpha'_2$ ,  $\alpha'_3$ . But one needs for the complete description of the thermal expansion of a crystal to know not only the absolute values of the thermal expansion coefficients along the principal axes  $X'_1$ ,  $X'_2$ ,  $X'_3$  but also the orientation of these axes with respect to the fixed axes  $X_1$ ,  $X_2$ ,  $X_3$ . Obviously, one also has to fix three more quantities characterizing the orientation of the axes  $X'_1$ ,  $X'_2$ ,  $X'_3$  with respect to the axes  $X_1$ ,  $X_2$ ,  $X_3$ .

**4.7.** What should be the orientation of a calcite plate in which the thickness of the plate is unaffected by heating?

**Solution.** Calcite belongs to the trigonal crystal class, and its thermal expansion is characterized by three principal coefficients  $\alpha_{11}$ ,  $\alpha_{22}$ , and  $\alpha_{33}$  with  $\alpha_{11} = \alpha_{22} = -5.6 \cdot 10^{-6} \text{ K}^{-1}$ , and  $\alpha_{33} = 25 \cdot 10^{-6} \text{ K}^{-1}$ . Consequently, the thermal expansion of this crystal in certain directions necessarily vanishes. According to Neumann's principle, the symmetry of the magnitude surface of thermal expansion of calcite is  $\infty m$ , so that there is a cone of directions around the threefold axis along which no thermal expansion occurs.

The orientation of the plate is defined by the orientation of the surface normal  $\mathbf{n}$  with respect to the crystallophysical coordinate system. We choose the axis  $X'_3$  along the unit vector  $\mathbf{n}$  normal to the plate. Then the thermal expansion perpendicular to the plate surface is  $\alpha_n = \alpha'_{33}$ . As stated in the problem, the plate must not expand in this direction, and this means that  $\alpha_n = \alpha_{33} = 0$ .

According to (4.6),

$$\alpha'_{33} = n_1^2 \alpha_{11} + n_2^2 \alpha_{22} + n_3^2 \alpha_{33} = \alpha_{11} (n_1^2 + n_2^2) + n_3^2 \alpha_{33}$$

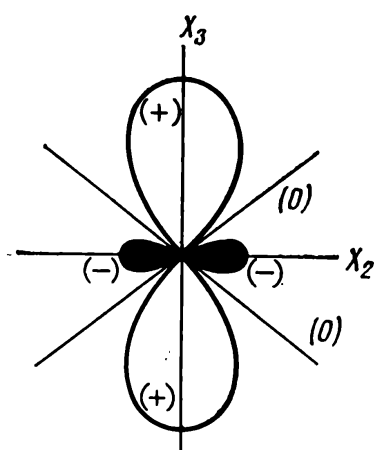


Fig. 4.6. Magnitude surface of thermal expansion coefficient: section by the coordinate plane  $X_1X_3$ .

Taking into account that  $n_1^2 + n_2^2 + n_3^2 = 1$ , we find

$$\alpha'_{33} = \alpha_{11}(1 - n_3^2) + \alpha_{33}n_3^2 = \alpha_{11} + (\alpha_{33} - \alpha_{11})n_3^2$$

Obviously,  $\alpha'_{33} = 0$  for  $n_3^2 = \alpha_{11}/(\alpha_{11} - \alpha_{33})$ . Note that  $n_3$  is the cosine of the angle between the normal  $\mathbf{n}$  to the plate and the threefold symmetry axis of calcite. In the case under discussion, this value of  $n_3$  corresponds to the angle  $64^\circ 43'$ . Hence, a calcite plate with zero thermal expansion must be cut with the normal being at an angle of  $64^\circ 43'$  to the threefold axis.

The magnitude surface of thermal expansion is a surface of revolution of two sheets around the axis  $X_3$ . Its cross section is shown in Fig. 4.6.

#### PROBLEMS

4.8. Show that any property described by a rank two tensor is characteristic of crystals regardless of their symmetry.

4.9. Find the form of the tensor of thermal expansion coefficients in the principal axes for a crystal to have the directions of zero thermal expansion.

4.10. Find the value of the thermal expansion coefficient in the direction perpendicular to the symmetry plane in KDP crystals.

4.11. Find the value of electric resistivity of quartz in the direction of bisector of the angle between the threefold and twofold symmetry axes, and along the bisector of the angle between twofold axes. Explain the obtained result.

4.12. Find the value of the relative dielectric permittivity in rochelle salt along the bisectors of the angles between the axes of each pair of the symmetry axes (throughout the problems to this section, a rochelle salt crystal is assumed to be in the ferroelectric phase whose properties are listed in Table 14).

4.13. Find the value of electric resistivity of the crystal in the direction  $(1/\sqrt{3}, 1/\sqrt{3}, 1/\sqrt{3})$  with respect to the coordinate system in which the electric conductivity tensor of this crystal has the form

$$\begin{bmatrix} -25 & 0 & 0 \\ 0 & 7 & -3\sqrt{3} \\ 0 & -3\sqrt{3} & 13 \end{bmatrix} \cdot 10^{-7} \text{ ohm}^{-1} \text{ cm}^{-1}$$

4.14. Find the angle between the electric field direction and electric current in a quartz crystal when the field is applied to the working faces of a  $45^\circ$   $Y$ -cut plate.

4.15. A gypsum plate  $1 \times 2.5 \text{ cm}^2$  and  $0.4 \text{ cm}$  thick is cut out with the normal to its surface being at the following angles to the

crystallophysical axes:

$$\angle X_1ON = 90^\circ, \quad \angle X_2ON = 30^\circ, \quad \angle X_3ON = 60^\circ$$

The plate is inserted into a plane capacitor. Calculate the capacitance of this system.

**4.16.** Find the total charge generated at the surface of an aragonite crystal plate  $2 \times 4 \times 0.2 \text{ cm}^3$  cut perpendicularly to the direction  $(1/\sqrt{2}, 0, 1/\sqrt{2})$ , when the plate is placed in an electric field  $400 \text{ V/cm}$ . The direction of the field is normal to the plate.

**4.17.** Find the dielectric permittivity tensor of quartz:

(i) in a coordinate system rotated clockwise with respect to the crystallophysical frame by  $30^\circ$  around the axis  $X_1$ ;

(ii) in a coordinate system rotated counterclockwise around the axis  $X_1$  of the crystallophysical frame by  $30^\circ$ ;

(iii) in a coordinate system rotated clockwise and counterclockwise by  $60^\circ$  around the axis  $X_3$  of the crystallophysical frame.

Explain the obtained results.

**4.18.** The relative dielectric permittivity tensor of a crystal with symmetry  $\bar{4}2m$  has the following form in the crystallophysical coordinate system:

$$[\varepsilon_{ij}] = \begin{bmatrix} 89 & 0 & 0 \\ 0 & 89 & 0 \\ 0 & 0 & 173 \end{bmatrix}$$

What will be the form of this tensor in the coordinate system obtained from the initial one by rotating it by  $45^\circ$  around the axis  $X_3$ , that is, in the second crystallophysical setting?

**4.19.** Find the expression for the energy of a polarized rhombic crystal, if the electric field is applied along (i) [100] and (ii) [010].

**4.20.** How should we cut a plate out of a monoclinic crystal to achieve the minimum thermal expansion, if the linear expansion of this crystal is described in the system of orthogonal axes  $X_1$ ,  $X_2$ ,  $X_3$  by a tensor of the type

$$\begin{bmatrix} 10 & -5 & 0 \\ -5 & 20 & 0 \\ 0 & 0 & 80 \end{bmatrix} \cdot 10^{-6} \text{ K}^{-1}$$

**4.21.** How should we cut a calcite plate, for its thermal expansion coefficient normally to the plate to be equal to  $15 \cdot 10^{-6} \text{ K}^{-1}$ ?

**4.22.** Find the crystallographic direction along which graphite crystals are not expanded upon heating.

**4.23.** The dielectric permittivity of a monoclinic crystal in the orthogonal coordinate system  $X_1$ ,  $X_2$ ,  $X_3$  is given by a tensor of

the type

$$\begin{bmatrix} 10 & 5 & 0 \\ 5 & 20 & 0 \\ 0 & 0 & 30 \end{bmatrix}$$

What cut of a crystal plate with fixed dimensions will provide the maximum capacitance?

4.24. Find the orientation of the principal axes of the thermal expansion tensor in a monoclinic crystal with respect to the orthogonal axes  $X_1$ ,  $X_2$ ,  $X_3$ , in which the thermal expansion of the crystal is represented by the tensor

$$\begin{bmatrix} 15 & 0 & -7.5 \\ 0 & 41 & 0 \\ -7.5 & 0 & 32 \end{bmatrix} \cdot 10^{-6} \text{ K}^{-1}$$

4.25. What should be the accuracy of cutting out the rutile crystal plates in  $X$ -,  $Z$ -, and  $45^\circ Y$ -cuts, in order that their dielectric permittivities differ from the calculated ones by not more than 2%?

4.26. Find the temperature increment in a quartz plate oriented as shown in Fig. 4.3b, subjected to a short-duration force ten times its weight. The plate size is  $1 \times 3 \times 10 \text{ mm}^3$ . Analyze three cases of applying force to each pair of mutually parallel faces.

4.27. A crystal  $L$ -cut plate of rochelle salt is placed in an electric field with strength 200 V/cm. Calculate the charge density on its lateral faces, neglecting the electric conductivity of the crystal. Solve the same problem taking this conductivity into account.

4.28. List the symmetry classes in which the direction of the principal axes of tensors describing different properties of crystals ( $\varepsilon_{ij}$ ,  $\alpha_{ij}$ ,  $\sigma_{ij}$ , etc.) coincide. List those where they do not coincide.

4.29. List symmetry classes in which heating changes the directions of the principal axes of the dielectric permittivity tensor.

4.30. Find symmetry classes in which the directions of the principal axes of the electric conductivity and electric resistivity tensors coincide.

4.31. Derive the equation of the index surface for the dielectric permittivity of triclinic crystals.

4.32. A rochelle salt plate is cut with the normal to its surface being at angles of 30, 70, and  $68.6^\circ$ . Calculate the thermal expansion coefficient of the plate.

4.33. Find the thermal conductivity of a quartz plate cut to be parallel to the natural face of rhombohedron,  $(10\bar{1}1)$ , if the angle between the normal to the plate and the axis  $X_3$  is  $52^\circ$ .

4.34. A plate 4 mm thick is cut out of a bismuth single crystal so that the normal to the plate is at an angle of  $30^\circ$  to the threefold

axis. Find the current density through this plate if a voltage of 1 V is applied to its working faces.

4.35. A rod 1 cm in diameter is cut out of a bismuth single crystal, the rod axis being at an angle of  $30^\circ$  to the threefold axis. The potential difference per unit rod length is kept constant and equal to 1 V/cm. Find the maximum potential difference between two diametrically opposite points of a cross section perpendicular to the rod axis.

4.36. Find the components of the magnetic permeability tensor of aragonite and the magnitude of magnetic permeability along the normal to the surface of an *L*-cut plate.

4.37. Write the tensor of magnetic moment,  $G_{ij}$ , in a coordinate system whose axes coincide with the principal axes of the magnetic susceptibility tensor.

4.38. Determine directions along which zirconium crystals evince no magnetic properties.

4.39. A crystal is subjected to magnetic field with strength  $H_1$  along the axis  $X_1$ : then additional field with strength  $H_2$  is applied along  $X_2$ . Show that if the experiment is repeated in the reversed order, the work done by applying the total field  $\mathbf{H}$  ( $H_1, H_2, 0$ ) is the same in both cases only if  $\mu_{12} = \mu_{21}$ .

4.40. An aragonite crystal with volume 1 mm<sup>3</sup> is placed in a non-uniform magnetic field. The field components and some of the gradients along the principal axes (in MKS units) are

$$H_1 = 1.0 \cdot 10^6, \quad H_2 = 0.5 \cdot 10^6, \quad H_3 = 2.0 \cdot 10^6$$

$$\frac{\partial H_1}{\partial x_1} = 1.0 \cdot 10^8, \quad \frac{\partial H_1}{\partial x_2} = 1.2 \cdot 10^8, \quad \frac{\partial H_1}{\partial x_3} = 0.5 \cdot 10^8$$

$$\frac{\partial H_2}{\partial x_2} = 0.8 \cdot 10^8, \quad \frac{\partial H_2}{\partial x_3} = 2.0 \cdot 10^8$$

Find the magnitude and direction of the resultant force and momentum exerted on the crystal.

## 5. STRESS AND STRAIN IN CRYSTALS. ANALYSIS OF STRESSED STATE

A state of uniform stress at a point of a continuous homogeneous medium can be described by nine components of the stress tensor in an arbitrary coordinate system:

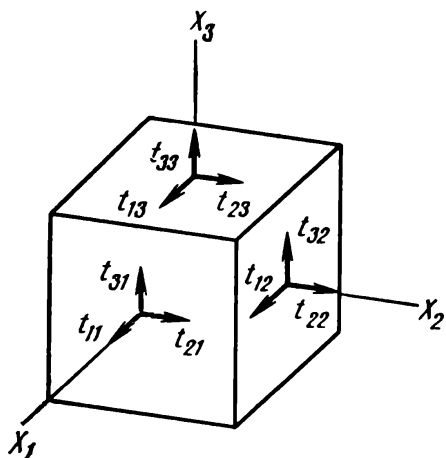
$$t_{ij} = \begin{bmatrix} t_{11} & t_{12} & t_{13} \\ t_{21} & t_{22} & t_{23} \\ t_{31} & t_{32} & t_{33} \end{bmatrix}$$

The following notation has been used for stress: the first subscript of a component of the stress tensor refers to the direction of the force, and the second refers to the elementary face to which the force is applied (Fig. 5.1). For example, the stress  $t_{32}$  denotes the component of the force along the axis  $X_3$  applied to a unit face perpendicular to the axis  $X_2$ . Obviously,  $t_{ii}$ , that is, the diagonal or so-called normal components of the stress tensor are tensile (or compressing) stresses along the coordinate axes;  $t_{ij}$  ( $i \neq j$ ) denote the shear, or tangent, stresses lying in the plane of the faces to which they are applied. As follows from the condition of static equilibrium of the torques with respect to the coordinate axes  $X_1$ ,  $X_2$ ,  $X_3$ , the nondiagonal components of the tensor,  $t_{ij}$ , must be pairwise equal:

$$t_{12} = t_{21}, \quad t_{23} = t_{32}, \quad t_{31} = t_{13} \quad (5.1)$$

Hence, the stressed state is completely described by six independent components of the stress tensor: three normal components  $t_{11}$ ,  $t_{22}$ , and  $t_{33}$ , and three shear components  $t_{12}$ ,  $t_{13}$ , and  $t_{23}$ .

Fig. 5.1. Physical meaning of the components of the stress tensor.



It can be shown that the relation (5.1) remains valid even when the stress is nonuniform, when the body is not in static equilibrium, and when body forces are present, provided body torques are zero.

**Signs of stress.** By convention, the normal and shear stresses are positive if they act in directions shown in Fig. 5.1. This means that the normal stresses corresponding to tension are regarded as positive. It should be mentioned, however, that a reversed sign convention is chosen in treating the piezoelectric and piezooptic effects: here compression stress is regarded as positive.

**Principal axes of the stress tensor and the stress quadratic.** The stress tensor is symmetrical and can be reduced to the principal axes:

$$\begin{bmatrix} t_1 & 0 & 0 \\ 0 & t_2 & 0 \\ 0 & 0 & t_3 \end{bmatrix}$$

where  $t_1$ ,  $t_2$ , and  $t_3$  are the so-called principal stresses.

The principal axes of the stress tensor exhibit the following important property: the components of shear stress are zero on the faces normal to these axes.

The representation second-order surface corresponding to the tensor  $[t_{ij}]$  is called the *stress quadratic*. Its equation is

$$t_{ij}x_i x_j = 1 \quad (5.2)$$

or, in converting to the principal axes,

$$t_1 x_1^2 + t_2 x_2^2 + t_3 x_3^2 = 1$$

As each of the stresses  $t_1$ ,  $t_2$ ,  $t_3$  can be either positive or negative, the stress quadratic may be a real or imaginary ellipsoid or hyperboloid. The direction of the resultant force  $P\delta S$  applied to a surface element  $\delta S$  can be found by making use of the properties of the radius vector and the normal to the stress quadratic (Fig. 5.2). The length of the vector  $\mathbf{r}$  represents the normal stress  $t_n$  applied to the surface element  $\delta S$  shown in Fig. 5.2, namely,

$$t_n = 1/r^2$$

**Total, normal, shear, mean, and effective stress.** The following quantities are often required in solving practical problems:

(i) Total stress  $t_r$  applied to a face with the normal  $\mathbf{n}$  (Fig. 5.3):

$$t_r = \sqrt{t_{ri}^2} \quad (5.3)$$

where

$$t_{ri} = t_{ij} n_j$$

(ii) Normal stress  $t_n$  applied to the face having the same normal:

$$t_n = t_{ij} n_i n_j \quad (5.4)$$

(iii) Shear stress  $t_t$  in the plane of the same elementary face:

$$t_t = \sqrt{t_r^2 - t_n^2} \quad (5.5)$$

(iv) Maximum shear stress  $t_t^{\max}$  applied in the plane  $X_1X_2$ :

$$t_t^{\max} = \left[ \left( \frac{t_{11} - t_{22}}{2} \right)^2 + t_{12}^2 \right]^{1/2} \quad (5.6)$$

Similar relations are valid for the stresses  $t_t^{\max}$  in the planes  $X_1X_3$  and  $X_2X_3$ .

(v) Mean stress  $t_m$ :

$$t_m = \frac{t_{11} + t_{22} + t_{33}}{3} \quad (5.7)$$

(vi) Effective, or generalized, stress:

$$t^2 = \frac{1}{2} [(t_{11} - t_{22})^2 + (t_{22} - t_{33})^2 + (t_{33} - t_{11})^2] + 3(t_{12}^2 + t_{23}^2 + t_{31}^2) \quad (5.8)$$

**Stress tensor as an example of field tensor.** The physical meaning of the stress tensor is close to that of the force applied to a crystal. Consequently, the stress tensor is independent of the crystal symmetry. This tensor has a meaning not only for crystals but also for isotropic bodies in a stressed state. Such tensors are called *field tensors*, to distinguish them from the matter tensors which describe physical properties of crystals and thus are related to their symmetry.

**Strain analysis.** Displacements essential for a strained body are not the absolute displacements of its points but their displacements with respect to one another.

**Fig. 5.2.** Determination of the direction of the resultant force exerted on an element of area  $\delta S$ , by means of the representation stress ellipsoid.

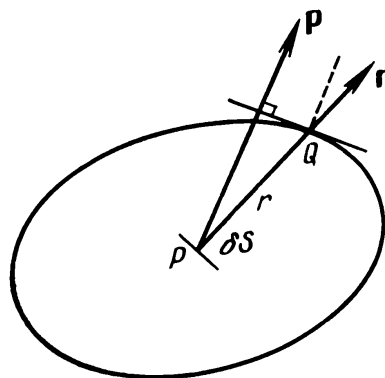
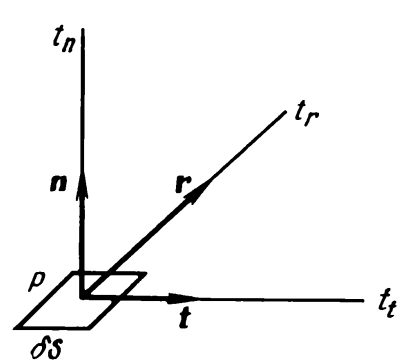


**Fig. 5.3.** Stresses applied to an area element of arbitrary orientation:  $t_r$ —total stress,  $t_t$ —tangential (shear) stress,  $t_n$ —normal stress.



In order to describe a strain in a body, let us fix to this body an orthogonal coordinate system  $X_1, X_2, X_3$ .

Let the strain leave the position of the origin of coordinates non-displaced, while all other points obtain certain displacements. If a point  $A$  (Fig. 5.4) moves to a position  $A'$ , and a point  $B$  at a distance  $\Delta X$  from  $A$  moves to a new position  $B'$ , then the displacements of the points  $A$  and  $B$  are given by the vectors  $\mathbf{u}^A$  and  $\mathbf{u}^B$ , respectively.

The vector  $\mathbf{u}$  is called the *displacement vector*,  $u_i = (x'_i - x_i)$ , where  $i = 1, 2, 3$ ;  $x'_i$  denotes the coordinates of a point before deformation, and  $x_i$  denotes its coordinates after deformation.

Since the factor essential in a deformation is the relative displacement of the points of a body, it is necessary to consider a vector  $\Delta\mathbf{u} = \mathbf{u}^B - \mathbf{u}^A$  which gives the increment in the displacements of the points which originally were spaced by a distance  $\Delta X$ .

If  $u_i = x'_i - x_i$  is constant for all  $i$ 's and for all points of the body, then  $\Delta\mathbf{u} = 0$ , and the body is not deformed, that is, the body is translated parallel to itself. In the case of nonzero deformation, displacements are different for different points.

Strain is defined as *uniform* if the components of the displacement vector are linear functions of coordinates:

$$\left. \begin{aligned} u_1 &= e_{11}x_1 + e_{12}x_2 + e_{13}x_3 \\ u_2 &= e_{21}x_1 + e_{22}x_2 + e_{23}x_3 \\ u_3 &= e_{31}x_1 + e_{32}x_2 + e_{33}x_3 \end{aligned} \right\} \quad (5.9)$$

The values of  $e_{ij}$  are independent of displacements.

In the case of uniform strain the following equations can be written for the increment of displacements:

$$\left. \begin{aligned} \Delta u_1 &= e_{11}\Delta x_1 + e_{12}\Delta x_2 + e_{13}\Delta x_3 \\ \Delta u_2 &= e_{21}\Delta x_1 + e_{22}\Delta x_2 + e_{23}\Delta x_3 \\ \Delta u_3 &= e_{31}\Delta x_1 + e_{32}\Delta x_2 + e_{33}\Delta x_3 \end{aligned} \right\} \quad (5.10)$$

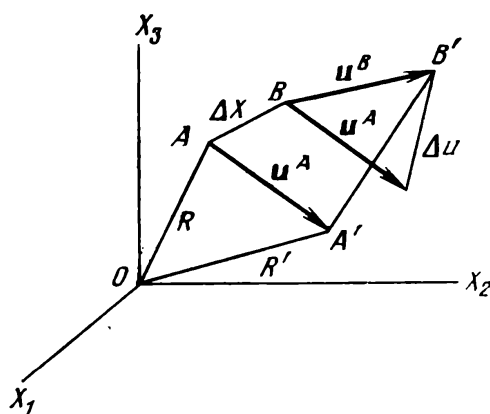


Fig. 5.4. Displacement of points of a body under deformation.

Equations (5.10) describe the vector-vector interaction, and the nine quantities  $e_{ij}$  form a rank two tensor:

$$[e_{ij}] = \left[ \frac{du_i}{dx_j} \right] = \begin{bmatrix} e_{11} & e_{12} & e_{13} \\ e_{21} & e_{22} & e_{23} \\ e_{31} & e_{32} & e_{33} \end{bmatrix} \quad (5.11)$$

The tensor  $[e_{ij}]$  is called the *tensor of small displacements*. In the general case this tensor is nonsymmetrical. It can always be written as a sum of a symmetrical and antisymmetrical tensors:

$$e_{ij} = r_{ij} + \omega_{ij} \quad (5.12)$$

where

$$r_{ij} = \frac{1}{2} (e_{ij} + e_{ji}) = r_{ji} \quad (5.13)$$

Obviously, the tensor  $[r_{ij}]$  is symmetrical. The tensor  $[\omega_{ij}]$  is antisymmetrical:

$$\omega_{ij} = \frac{1}{2} (e_{ij} - e_{ji}) = -\omega_{ji} \quad (5.14)$$

This tensor describes the rotation of a body as a whole around a fixed axis, with no displacements of its points with respect to one another.

The tensor  $[r_{ij}]$  is the strain tensor proper.

The relative increment of the volume of the body is

$$\Delta V/V = r_{ii} = r_{11} + r_{22} + r_{33} \quad (5.15)$$

The diagonal components of the tensor  $[r_{ij}]$ , that is,  $r_{11}$ ,  $r_{22}$ , and  $r_{33}$ , represent the compressional or tensile strains of the unit length elements along the coordinate axes (Fig. 5.5). The non-diagonal components,  $r_{32}$ ,  $r_{23}$ , and  $r_{12}$ , represent the shear strains. For exam-

Fig. 5.5. Deformation of a cube with unit dimensions and edges parallel to the principal axes of strain.

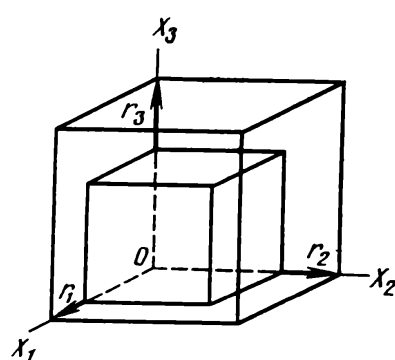
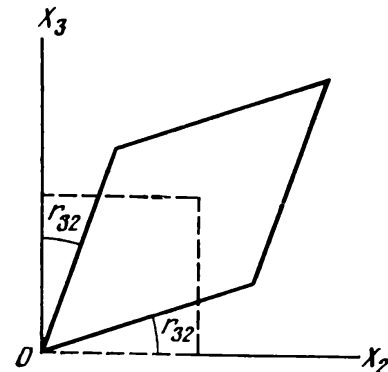


Fig. 5.6. Rotation of segments parallel to coordinate axes under shear strains.



ple, the quantity  $2r_{32}$  is equal to the increment of the angle between two elements which before deformation were parallel to the axes  $X_3$  and  $X_2$  (Fig. 5.6). The components  $r_{13}$  and  $r_{12}$  have a similar meaning.

**Signs of strains.** By convention, tensile strains are considered positive. Shear strains are considered positive if the strain reduces the angle between linear elements singled out in the nonstrained body parallel to the positive directions of the corresponding coordinate axes. For example, the strain  $2r_{32}$  is considered positive if the angle between linear elements parallel to the positive directions of the axes  $X_2$  and  $X_3$  is diminished (see Fig. 5.6).

**Principal axes of the strain tensor and the representation quadratic of the strain tensor.** The strain tensor being symmetrical, it can be reduced to its principal axes:

$$\begin{bmatrix} r_1 & 0 & 0 \\ 0 & r_2 & 0 \\ 0 & 0 & r_3 \end{bmatrix}$$

This means that for an arbitrarily strained body one can always choose a coordinate system in which the deformation of the body can be represented only by compressions and tensions along three mutually perpendicular directions, with no shear.

The strain can be described by the strain representation quadratic whose equation is

$$r_{ij}x_i x_j = 1 \quad (5.16)$$

This surface may be either a real or an imaginary ellipsoid or hyperboloid.

If the strain is uniform, then the displacements caused by it are described by the relation

$$u_i = r_{ij}x_j \quad (5.17)$$

The orientation of the vector  $u$  and the magnitude of  $r$  for any given direction  $\mathbf{l}$  can be found by making use of the property of the radius vector and the normal to the strain quadratic (Fig. 5.7). The

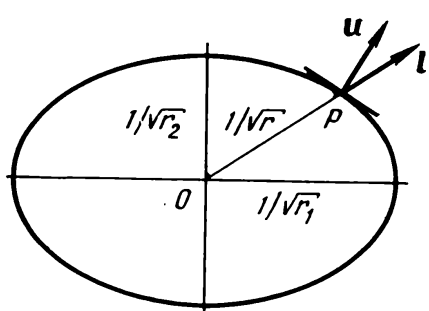


Fig. 5.7. Determination of the direction of displacement of a point by means of the representation strain quadratic.

elongation in an arbitrary direction  $\mathbf{l}$  is given by the relation

$$r = r_{ij}l_il_j \quad (5.18)$$

**Strain ellipsoid.** A descriptive representation of the deformation of a body is obtained by constructing the so-called strain ellipsoid. This is a surface into which transforms a unit radius sphere, singled out in the body before deformation, after this body undergoes straining. The equation of the unit radius sphere is

$$x_1^2 + x_2^2 + x_3^2 = 1$$

Let us fix the radius vector  $\overline{Ox}$  of this sphere. Its coordinates are  $(x_1, x_2, x_3)$ . After straining represented by a tensor

$$\begin{bmatrix} r_1 & 0 & 0 \\ 0 & r_2 & 0 \\ 0 & 0 & r_3 \end{bmatrix}$$

this radius vector transforms to the vector  $\overline{Ox'}$  with coordinates  $(x'_1, x'_2, x'_3)$  (Fig. 5.8). The components of the vector  $\overline{Ox'}$  are related to the components of the vector  $\overline{Ox}$  by the equations

$$x'_1 = x_1(1 + r_1)$$

$$x'_2 = x_2(1 + r_2)$$

$$x'_3 = x_3(1 + r_3)$$

Once the components of the vector  $\overline{Ox}$  are found from these equations and substituted into the equation of the unit radius sphere, we obtain the expression

$$\frac{x'_1^2}{(1+r_1)^2} + \frac{x'_2^2}{(1+r_2)^2} + \frac{x'_3^2}{(1+r_3)^2} = 1 \quad (5.19)$$

This is precisely the equation of the strain ellipsoid. The strain ellipsoid clearly shows the distribution of strain in a body, for

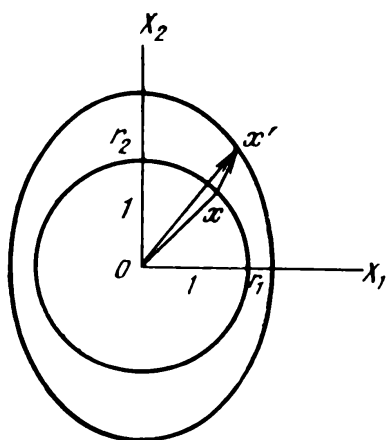


Fig. 5.8. Deformation of a unit-radius sphere.

example, the directions in which the strain is maximum, or minimum, and so on.

**Strain tensor and Neumann's principle.** The strain describing the response of a crystal to an external factor does not represent its physical property. For this reason the strain tensor, like the stress tensor, is not governed by Neumann's principle.

The only exception is the strain induced by variations of temperature of crystals (thermal expansion).

**Thermal expansion.** When the temperature of a crystal is uniformly changed by  $\Delta T$ , the crystal undergoes a uniform strain described by the equation

$$r_{ij} = \alpha_{ij} \Delta T \quad (5.20)$$

where  $\alpha_{ij}$  are the thermal expansion coefficients which are the components of a symmetrical rank two tensor, with three principal thermal expansion coefficients,  $\alpha_1$ ,  $\alpha_2$ , and  $\alpha_3$ , and the corresponding principal directions along which the strain can be found from the relations

$$r_1 = \alpha_1 \Delta T, \quad r_2 = \alpha_2 \Delta T, \quad r_3 = \alpha_3 \Delta T$$

where  $\alpha_1$ ,  $\alpha_2$ , and  $\alpha_3$  are the principal thermal expansion coefficients.

### Examples of Problems with Solutions

**5.1.** A uniaxial mechanical compression stress  $t$  is applied to an  $L$ -cut ADP crystal plate (see Fig. 2.4) normally to its working faces. Write the stress tensor in the crystallophysical coordinate system.

**Solution.** We direct the compression stress  $\mathbf{n}$  ( $n_1$ ,  $n_2$ ,  $n_3$ ) along the axis  $X'_3$  of the new primed coordinate system fixed to the edges of the  $L$ -cut plate. In this case the tensor describing the stressed state of the crystal plate in primed axes is represented by

$$[t'_{kl}] = \begin{bmatrix} 0 & 0 & 0 \\ 0 & 0 & 0 \\ 0 & 0 & t'_{33} \end{bmatrix} = \begin{bmatrix} 0 & 0 & 0 \\ 0 & 0 & 0 \\ 0 & 0 & -t \end{bmatrix}$$

where  $t'_{33} = -t$ .

In order to convert to the crystallophysical coordinate system we have to resort to the transformation law for the components of rank two tensors (4.2a):

$$t_{ij} = C_{2i} C_{3j} t'_{33} = n_i n_j (-t)$$

whence

$$\begin{aligned} t_{11} &= -n_1^2 t, & t_{22} &= -n_2^2 t, & t_{33} &= -n_3^2 t \\ t_{12} = t_{21} &= -n_1 n_2 t, & t_{13} = t_{31} &= -n_1 n_3 t \\ t_{23} = t_{32} &= -n_2 n_3 t \end{aligned}$$

A uniaxial stress in an arbitrary direction  $\mathbf{n}$  ( $n_1, n_2, n_3$ ) with respect to the crystallophysical coordinate system is represented in this system by a general type stress tensor possessing both normal and shear components:

$$\begin{bmatrix} n_1^2 & n_1 n_2 & n_1 n_3 \\ n_1 n_2 & n_2^2 & n_2 n_3 \\ n_1 n_3 & n_2 n_3 & n_3^2 \end{bmatrix} \cdot (-t)$$

**5.2. The stressed state of a quartz crystal in the crystallophysical coordinate system is given as follows:**

$$t_{11} = 10 \text{ N/cm}^2, \quad t_{22} = 20 \text{ N/cm}^2, \quad t_{33} = 30 \text{ N/cm}^2, \quad t_{12} = -5 \text{ N/cm}^2$$

Find: (i) the magnitudes of extremal normal stresses, (ii) the orientation of the plane characterized by the maximal and minimal normal stresses.

**Solution.** (i) Obviously, the prescribed stressed state is represented by the tensor

$$\begin{bmatrix} 10 & -5 & 0 \\ -5 & 20 & 0 \\ 0 & 0 & 30 \end{bmatrix} \text{ N/cm}^2$$

To find the extremal magnitudes of normal stresses one has to find the principal stresses, that is, to reduce the tensor to its principal axes. One of the principal axes is immediately found from the type of the given tensor, namely,  $t_3 = 30 \text{ N/cm}^2$ .

Let us find the principal stresses  $t_1$  and  $t_2$ :

$$\begin{vmatrix} 10-t & -5 & 0 \\ -5 & 20-t & 0 \\ 0 & 0 & 30 \end{vmatrix} = 0$$

$$t^2 - 30t + 175 = 0, \quad t_{1,2} = 15 \pm 7.1, \quad \text{whence } t_1 = 22.1 \text{ N/cm}^2, \quad t_2 = 7.9 \text{ N/cm}^2.$$

Hence, the maximum magnitude of the normal stress applied to the crystal is  $30 \text{ N/cm}^2$ , and the minimal magnitude of this stress is  $7.9 \text{ N/cm}^2$ .

(ii) In order to solve the second part of the problem, one has to find the direction cosines of the principal stresses with respect to the initial crystallophysical axes, by using the method described in

Problem 4.3. This yields

$$\begin{aligned} n_1^{(1)} &= 0.925, & n_2^{(1)} &= -0.384, & n_3^{(1)} &= 0, \\ n_1^{(2)} &= 0.384, & n_2^{(2)} &= 0.925, & n_3^{(2)} &= 0, \\ n_1^{(3)} &= n_2^{(3)} = 0, & n_3^{(3)} &= 1 \end{aligned}$$

We find, therefore, that the maximal normal stress equal to  $30 \text{ N/cm}^2$  exists on a plane whose normal has the direction cosines  $(0, 0, 1)$ . The minimal normal stress equal to  $7.9 \text{ N/cm}^2$  exists on the plane whose normal has the direction cosines  $(0.384, 0.925, 0)$ .

5.3. Electric field applied to the working faces of an  $X$ -cut rochelle salt crystal plate (see Fig. 2.3) induces in this plate a shear strain in the plane  $X_2X_3$ . What should be the direction of the edges of the  $X$ -cut plate in order that the indicated stressed state be the compressional-tensile strain along its edges?

**Solution.** Obviously, the strained state of an  $X$ -cut plate in the system of axes fixed to its edges is described by the tensor

$$\begin{bmatrix} 0 & 0 & 0 \\ 0 & 0 & r_{23} \\ 0 & r_{23} & 0 \end{bmatrix}$$

The tensile and compressional strains are the diagonal components of the tensor  $[r_{ij}]$ , so that the strain tensor must be reduced to its principal axes in order to find these components.

The reduction to the principal axes of the given tensor is realized by a  $45^\circ$  rotation around the axis  $X_1$ ; this transforms the tensor  $[r_{ij}]$  to

$$\begin{bmatrix} 0 & 0 & 0 \\ 0 & r & 0 \\ 0 & 0 & -r \end{bmatrix}$$

where  $|r| = |r_{23}|$ .

Therefore, a rochelle salt plate in which the electric field applied to its working faces causes the compressional-tensile stresses ( $X$ -cut plate), must be cut with the edges at the angles of  $45^\circ$  to the axes  $X_2$  and  $X_3$ . Such plates are called  $45^\circ X$ -cuts.

5.4. The displacements of points in an elastically strained cubic crystal sample  $1 \times 1 \times 1 \text{ cm}^3$  in size are:

$$u_1 = (4x_1 + 3x_2 - 5x_3) \cdot 10^{-4} \text{ cm}$$

$$u_2 = (7x_1 - 13x_2 + 4x_3) \cdot 10^{-4} \text{ cm}$$

$$u_3 = (9x_1 - 2x_2 + 4x_3) \cdot 10^{-4} \text{ cm}$$

Find the changes in the angles between the edges of the cube, and the increment of its volume under strain.

**Solution.** The small displacements tensor, strain tensor, and rotation tensor are, respectively,

$$[e_{ij}] = \begin{bmatrix} 4 & 13 & -5 \\ 7 & -13 & 4 \\ 9 & -2 & 4 \end{bmatrix} \cdot 10^{-4}, \quad [r_{ij}] = \begin{bmatrix} 4 & 5 & 2 \\ 5 & -13 & 1 \\ 2 & 1 & 4 \end{bmatrix} \cdot 10^{-4}$$

$$[\omega_{ij}] = \begin{bmatrix} 0 & -2 & -7 \\ 2 & 0 & 3 \\ 7 & -3 & 0 \end{bmatrix} \cdot 10^{-4}$$

The changes in the angles between the edges of a unit cube are characterized by nondiagonal components of the tensor  $[r_{ij}]$ , that is, by the components  $r_{12}$ ,  $r_{23}$ , and  $r_{13}$ . The angle between the edges parallel to the axes  $X_1$  and  $X_2$  is equal to  $0.5\pi - 2r_{12}$ . The increment of the angle is equal to  $2r_{12}$ .

The changes in the angles between the edges parallel to the axes  $X_1$  and  $X_2$ ,  $X_1$  and  $X_3$ , and  $X_2$  and  $X_3$  prior to deformation, are equal, respectively, to

$$2r_{12} = 3.42', \quad 2r_{13} = 1.2', \quad 2r_{23} = 0.68'$$

The relative change in the volume,  $\Delta V/V$ , is found as the sum of the diagonal components of the tensor  $[r_{ij}]$ , that is, equals  $-5 \cdot 10^{-4}$ .

**5.5. The state of elastic strain of a crystal is given in the form**

$$(i) \begin{bmatrix} 0.001 & 0 & 0 \\ 0 & -0.004 & 0 \\ 0 & 0 & 0.008 \end{bmatrix}, \quad (ii) \begin{bmatrix} 0.0001 & 0 & 0 \\ 0 & +0.001 & 0 \\ 0 & 0 & 0 \end{bmatrix}$$

Find the equation of the strain representation quadratic, as well as the surface to which a unit radius sphere transforms after the deformation represented by the above two tensors.

**Solution.** (i) The strain tensor is already reduced to the principal axes of strain; hence, the equation of the corresponding strain representation quadratic is

$$0.001x_1^2 - 0.004x_2^2 + 0.008x_3^2 = 1$$

This strain quadratic is a hyperboloid of one-sheet. Let us single out in the undeformed crystal a unit-radius sphere. Its equation is

$$x_1^2 + x_2^2 + x_3^2 = 1$$

The coordinates of the points on the new surface obtained by deformation of the sphere are given by the relations

$$x'_1 = x_1 + u_1, \quad x'_2 = x_2 + u_2, \quad x'_3 = x_3 + u_3$$

Since  $u_i = r_{ij}x_j$ , then  $u_1 = r_1x_1$ ,  $u_2 = r_2x_2$ ,  $u_3 = r_3x_3$ ,

$$x'_1 = x_1(1 + r_1), \quad x'_2 = x_2(1 + r_2), \quad x'_3 = x_3(1 + r_3)$$

The equation of the surface obtained by straining the sphere is

$$\frac{x_1'^2}{(1+r_1)^2} + \frac{x_2'^2}{(1+r_2)^2} + \frac{x_3'^2}{(1+r_3)^2} = 1$$

In our case

$$\frac{x_1'^2}{(1+0.001)^2} + \frac{x_2'^2}{(1-0.004)^2} + \frac{x_3'^2}{(1-0.008)^2} = 1$$

Obviously, the sphere singled out in the nonstrained crystal has been converted by strain into a triaxial ellipsoid with semiaxes 1.001, 0.996, and 0.992.

(ii) The equation of the representation strain quadratic takes now the form  $0.0001x_1^2 + 0.001x_2^2 = 1$ , or  $x_1^2 + 10x_2^2 = 10^4$ , that is, the strain quadratic is a cylinder with an elliptic cross section.

Let us single out in the nondeformed crystal a unit-radius sphere

$$x_1^2 + x_2^2 + x_3^2 = 1$$

Deformation turns the unit sphere into a surface

$$\frac{x_1'^2}{(1.0001)^2} + \frac{x_2'^2}{(1.001)^2} + \frac{x_3'^2}{1} = 1$$

which represents a triaxial ellipsoid with semiaxes 1.0001, 1.001 and 1.

5.6. In order to find the thermal expansion coefficients of ethylenediamine tartrate (EDT), the thermal expansion coefficient  $\alpha$  was measured in four different directions (in  $10^{-6}$  K):

Table 5.1

Direction	$\alpha, 10^{-6} \text{ K}^{-1}$
Direction parallel to [010] (twofold symmetry axis)	20.3
Two mutually perpendicular directions in plane (010)	
$\mathbf{n}^{(1)}$	80
$\mathbf{n}^{(2)}$	0
Direction $\mathbf{n}^{(3)}$ , also in plane (010), at $45^\circ$ to $\mathbf{n}^{(1)}$ and $\mathbf{n}^{(2)}$	8

Calculate the coefficients characterizing the linear expansion of EDT crystals upon heating, as well as the maximal and minimal values of the thermal expansion coefficients. What preliminary conclusion on the behaviour of EDT crystals under nonuniform heating can be drawn?

**Solution.** The thermal expansion of class 2 crystals is characterized by four coefficients (see Problem 4.2). We choose the following coordinate axes: axis  $X_2$  along [010], and axes  $X_3$  and  $X_1$  in the plane (010). One of the directions in the plane (010), say, the one along

which the thermal expansion coefficient was found to be  $80 \cdot 10^{-6} \text{ K}^{-1}$ , is denoted by  $X_3$ , and the direction corresponding to zero thermal expansion by  $X_1$ .

Then in the coordinate system we have chosen

$$\alpha_{11} = 0, \quad \alpha_{22} = 20.03 \cdot 10^{-6} \text{ K}^{-1}, \quad \alpha_{33} = 80 \cdot 10^{-6} \text{ K}^{-1}$$

To find the coefficient  $\alpha_{13}$  we shall use the value of the thermal expansion measured along the direction at  $45^\circ$  to the directions of the axes  $X_1$  and  $X_3$ .

Denote this direction by  $l$ ; then its direction cosines with respect to the axes  $X_1$ ,  $X_2$ ,  $X_3$  are  $1/\sqrt{2}$ ,  $0$  and  $1/\sqrt{2}$ , and the thermal expansion along  $l$  obtains from the equation  $\alpha_l = \alpha_{ij}l_il_j$  which in our case takes the form

$$\alpha_l = \frac{1}{2} (\alpha_{11} + \alpha_{33} + 2\alpha_{13})$$

By substituting into this equation the values of  $\alpha_l$ ,  $\alpha_{11}$ , and  $\alpha_{33}$ , we find

$$8 \cdot 10^{-6} = \frac{1}{2} (80 + 2\alpha_{13}) \cdot 10^{-6} \text{ K}^{-1}$$

whence

$$\alpha_{13} = -32 \cdot 10^{-6} \text{ K}^{-1}$$

As a result, the coefficients characterizing the thermal expansion of EDT crystals in the chosen coordinate system  $X_1$ ,  $X_2$ ,  $X_3$ , in the units of  $10^{-6} \text{ K}^{-1}$ , are

$$\alpha_{11} = 0, \quad \alpha_{22} = 20.03$$

$$\alpha_{33} = 80, \quad \alpha_{13} = -32$$

To find the maximal and minimal coefficients, one has to find the principal coefficients  $\alpha_1$ ,  $\alpha_2$ , and  $\alpha_3$ , that is, to reduce the tensor

$$\begin{bmatrix} 0 & 0 & -32 \\ 0 & 20.03 & 0 \\ -32 & 0 & 80 \end{bmatrix} \cdot 10^{-6} \text{ K}^{-1}$$

to its principal axes. Obviously, the axis  $X_2$  is the principal axis of the tensor under discussion, whence  $\alpha_2 = 20.03 \cdot 10^{-6} \text{ K}^{-1}$ .

The values of the coefficients  $\alpha_1$  and  $\alpha_3$  are found as described in Problem 4.3. Therefore, the principal thermal expansion coefficients of EDT crystals, in units of  $10^{-6} \text{ K}^{-1}$ , are

$$\alpha_1 = 91.2 \text{ (maximum)}$$

$$\alpha_2 = 20.03$$

$$\alpha_3 = -11.2 \text{ (minimum)}$$

The values of the thermal expansion coefficients of EDT demonstrate an unusual behaviour of the thermal expansion: very high positive thermal expansion coefficient in one direction ( $91.2 \cdot 10^{-6}$ ), and a small negative coefficient in the direction perpendicular to it ( $-11.2 \cdot 10^{-6}$ ). As a result, the crystal is fragile under rapid nonuniform heating and cooling, with the ensuing difficulties for the applications of the material.

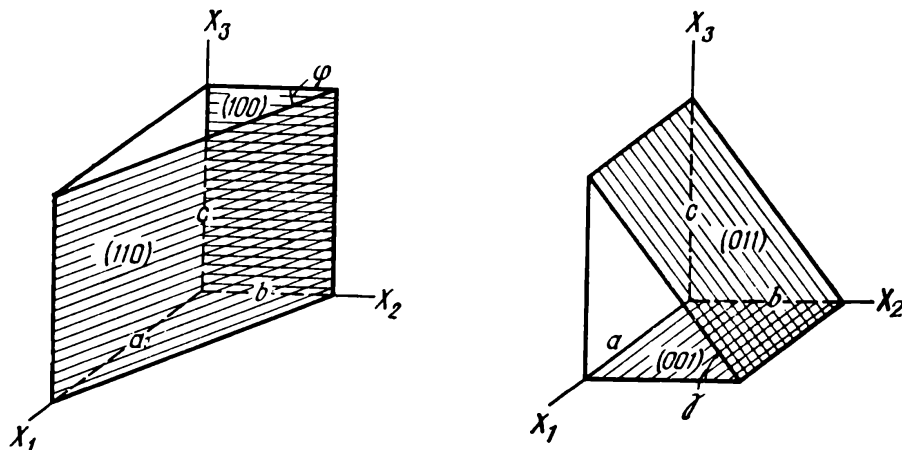
5.7. The ratio of unit cell parameters of aragonite is  $a:b:c = 0.6224:1:0.7206$ . Upon heating from 0 to  $100^\circ\text{C}$ , the angle  $\varphi$  between the faces (100) and (110) diminishes by  $1.14'$ , and the angle  $\gamma$  between the faces (001) and (011) is augmented by  $2.84''$  (Fig. 5.9). The coefficient of volume expansion for this crystal is  $62.0 \cdot 10^{-6} \text{ K}^{-1}$ . Calculate the three principal thermal expansion coefficients.

**Solution.** The thermal expansion of aragonite crystals is described by three principal linear expansion coefficients  $\alpha_1$ ,  $\alpha_2$ , and  $\alpha_3$ , and the coefficient of volume expansion,  $\beta$ , is found as the sum of the linear expansion coefficients, that is,  $\beta = \alpha_1 + \alpha_2 + \alpha_3$ . When heated uniformly by  $\Delta T$ , the crystal undergoes a uniform strain described by the equation  $r_{ij} = \alpha_{ij} \Delta T$ . The changes in the angles between the given crystallographic planes can be expressed as functions of unit cell parameters and linear expansion coefficients of aragonite. We can write

$$\tan \varphi = a/b, \quad \tan \gamma = c/b$$

When crystal's temperature increases by  $\Delta T$ , the unit cell parameters change. The unit cell parameters and angles between the indicated planes in the crystal after the temperature has changed by  $\Delta T$

Fig. 5.9. Angles between faces (100) and (110), (001) and (011) in aragonite crystals.



will be primed, so that

$$a' = a(1 + \alpha_1 \Delta T)$$

$$b' = b(1 + \alpha_2 \Delta T)$$

$$c' = c(1 + \alpha_3 \Delta T)$$

The angles between the planes (100) and (110), (001) and (011) also change, and can be found from the following relations:

$$\begin{aligned} \tan \varphi' &= \frac{a'}{b'} = \frac{(1 + \alpha_1 \Delta T) a}{(1 + \alpha_2 \Delta T) b} = \frac{(1 + \alpha_1 \Delta T)}{(1 + \alpha_2 \Delta T)} \tan \varphi \\ &= [1 + \Delta T (\alpha_1 - \alpha_2)] \tan \varphi \end{aligned}$$

On the other hand,

$$\varphi' = \varphi + \Delta \varphi$$

$$\tan \varphi' = \tan (\varphi + \Delta \varphi) = \tan \varphi + \frac{1}{\cos^2 \varphi} \Delta \varphi$$

By equating the right-hand sides of equations for  $\tan \varphi'$ , we obtain

$$\Delta T (\alpha_1 - \alpha_2) = \frac{1}{\sin \varphi \cos \varphi} \Delta \varphi$$

Since

$$\sin \varphi = a / \sqrt{a^2 + b^2}, \quad \text{then} \quad \alpha_1 - \alpha_2 = \frac{a^2 + b^2}{ab} \frac{\Delta \varphi}{\Delta T}$$

Likewise, if we set  $\tan \gamma = c/b$ , we find

$$\tan \gamma' = \frac{c'}{b'} = \frac{(1 + \alpha_3 \Delta T) c}{(1 + \alpha_2 \Delta T) b} = [1 + \Delta T (\alpha_3 - \alpha_2)] \tan \gamma$$

It then follows that

$$(\alpha_3 - \alpha_2) \Delta T = \frac{1}{\sin \gamma \cos \gamma} \Delta \gamma = \frac{c^2 + b^2}{bc} \Delta \gamma$$

We have arrived at the following relations:

$$\beta = \alpha_1 + \alpha_2 + \alpha_3$$

$$(\alpha_1 - \alpha_2) \Delta T = \frac{a^2 + b^2}{ab} \Delta \varphi, \quad (\alpha_3 - \alpha_2) \Delta T = \frac{c^2 + b^2}{bc} \Delta \gamma$$

Taking into account that  $a:b:c = 0.6224:1:0.7206$ ,  $\Delta \varphi = -1.14'$ ,  $\Delta \gamma = 2.84''$ ,  $\beta = 62 \cdot 10^{-6} \text{ K}^{-1}$ , and resolving the system of the above equations with respect to  $\alpha_1$ ,  $\alpha_2$ , and  $\alpha_3$ , we find

$$\alpha_1 = 9.9 \cdot 10^{-6} \text{ K}^{-1}, \quad \alpha_2 = 17.3 \cdot 10^{-6} \text{ K}^{-1}, \quad \alpha_3 = 34.7 \cdot 10^{-6} \text{ K}^{-1}$$

## PROBLEMS

5.8. The stressed state of an  $L$ -cut rochelle salt crystal plate (see Fig. 2.4) is given in the crystallophysical coordinate system, in  $\text{N/cm}^2$ , by the tensor

$$\begin{bmatrix} -50 & 0 & 0 \\ 0 & 50 & 0 \\ 0 & 0 & 75 \end{bmatrix}$$

Find the total, normal, and shear stresses applied to the plate.

5.9. The stressed state of a crystal specimen is given, in  $10^2 \text{ N/cm}^2$ , by the tensor

$$\begin{bmatrix} 2 & 2 & 0 \\ 2 & 2 & 0 \\ 0 & 0 & 9 \end{bmatrix}$$

Find the coordinate system in which the given stressed state can be considered a system of only compressive and tensile stresses.

5.10. The stressed state of a crystal is given by the tensor

$$\begin{bmatrix} t_{11} & t_{12} & 0 \\ t_{12} & t_{22} & 0 \\ 0 & 0 & t_{33} \end{bmatrix}$$

Find the normal and shear stresses applied to the plane whose normal lies in the plane  $X_1X_2$  and forms an angle  $\alpha$  with the axis  $X_1$ .

5.11. The stressed state at a point of a crystal sample is represented by the following components of the stress tensor (in  $\text{N/m}^2$ ):

$$t_{11} = 50, t_{22} = 0, t_{33} = -30, t_{12} = 50, t_{23} = -75, t_{31} = 80$$

Find the principal, normal, and shear stresses.

5.12. Sawing of sphalerite crystal specimens produced stresses described (in  $\text{N/m}^2$ ) by the tensor

$$\begin{bmatrix} -10 & -60 & 0 \\ -60 & -100 & 0 \\ 0 & 0 & -100 \end{bmatrix}$$

Find the mean pressure, and the maximum shear stress in the crystal sample.

5.13. In the case of infinitesimal strain, each point of a body experiences small displacements:

$$u_1 = (8x_1 + 3x_2 - 5x_3) \cdot 10^{-5} \text{ cm}$$

$$u_2 = (7x_1 + 3x_2 + 4x_3) \cdot 10^{-5} \text{ cm}$$

$$u_3 = (x_1 - 8x_2 + x_3) \cdot 10^{-5} \text{ cm}$$

Find the strain tensor  $[r_{ij}]$  and the rotation tensor  $[\omega_{ij}]$ . Determine the volumetric expansion of the body.

5.14. The displacements of points in a cubic crystal sample  $1 \times 1 \times 1 \text{ cm}^3$  in size, subjected to infinitesimal elastic strain, are

$$u_1 = (4x_1 + 3x_2 - 5x_3) \cdot 10^{-4} \text{ cm}$$

$$u_2 = (7x_1 - 13x_2 + 4x_3) \cdot 10^{-4} \text{ cm}$$

$$u_3 = (9x_1 - 2x_2 + 4x_3) \cdot 10^{-4} \text{ cm}$$

Calculate the changes in the angles between the edges and in the volume of the sample after deformation.

5.15. The elastic strain tensor is given in the form

$$\begin{bmatrix} 8 & -1 & -1 \\ 1 & 6 & 0 \\ -5 & 0 & 2 \end{bmatrix} \cdot 10^{-6}$$

Find the strain tensor  $[r_{ij}]$ , rotation tensor  $[\omega_{ij}]$  and the principal strains.

5.16. After deformation of a crystal its strain is described by the tensor

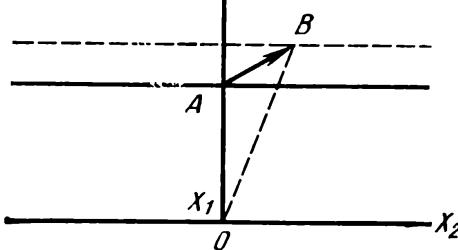
$$\begin{bmatrix} 8 & 0 & -4 \\ 0 & 12 & 0 \\ -4 & 0 & 2 \end{bmatrix} \cdot 10^{-6}$$

Find in the crystal three mutually perpendicular directions which remain perpendicular after deformation.

5.17. As a result of the inverse piezoelectric effect, an  $L$ -cut rochelle salt crystal plate (see Fig. 2.4) undergoes a tensile strain of 0.005 normally to the plate. Refer the strain in the specimen to the crystallophysical coordinate system.

5.18. A cubic rock salt specimen with edges oriented along  $\{100\}$  axes undergoes a plane strain, such that the tensile strain is  $4 \cdot 10^{-5}$  along  $[100]$  and  $12 \cdot 10^{-5}$  along  $[010]$ . Find the tensile strain in the directions  $[111]$ ,  $[121]$ .

Fig. 5.10. Thermal expansion of a plane parallel plate.



5.19. A plane parallel plate cut out of a triclinic crystal is heated by  $\Delta T$  and undergoes a deformation which displaces a point  $A$  to point  $B$  (Fig. 5.10). Find the angle  $AOB$  as a function of the thermal expansion coefficients.

5.20. Find the equation of the surface to which transforms a unit-radius sphere singled out in a rhombic crystal after heating by  $\Delta t^\circ$ .

5.21. Find the thermal expansion coefficients of a hexagonal crystal if the coefficient of volumetric expansion,  $\beta$ , and the change in the unit cell parameters ratio  $c/a$  after heating are known.

5.22. A rectangular crystal bar  $10 \times 4 \times 2 \text{ cm}^3$  is stretched by a force of  $10 \text{ N}$  applied along its length. The bar is elongated thereby by  $22 \mu\text{m}$ , and its width and thickness diminish by  $4 \mu\text{m}$  and  $1 \mu\text{m}$ , respectively.

Find the components of the stress and strain tensors, assuming that the edges of the bar  $10$ ,  $4$  and  $2 \text{ cm}$  long, respectively, are parallel to the axes  $X_1$ ,  $X_2$ ,  $X_3$ .

5.23. A rectangular isotropic bar of  $8 \times 3 \times 2 \text{ cm}^3$  is placed in a fluid at a hydrostatic pressure of  $1000 \text{ N/cm}^2$ . The bar volume is thus reduced by  $1 \text{ mm}^3$ . Find the components of the stress and strain tensors.

5.24. A crystal sample of  $5 \times 5 \times 2 \text{ cm}^3$  is compressed by a force of  $10 \text{ N}$  applied to its  $5 \times 2 \text{ cm}^2$  faces and stretched by the same force applied to the other two  $5 \times 2 \text{ cm}^2$  faces. Find the components of the stress tensor in the coordinate system  $X_1$ ,  $X_2$ ,  $X_3$ , assuming that these axes are parallel to the edges with lengths  $5$ ,  $5$  and  $2 \text{ cm}$ , respectively.

Find the components of the strain tensor if the sample length along  $X_1$  is reduced by  $2 \mu\text{m}$ , and is increased by  $2 \mu\text{m}$  along  $X_2$ .

5.25. A hexagonal crystal cut into a trigonal prism  $5 \text{ cm}$  high, with  $1 \text{ cm}$  wide lateral faces, is subjected to a hydrostatic pressure of  $10,000 \text{ N/cm}^2$ ; the prism height is increased thereby by  $5 \mu\text{m}$ , and the width of the lateral faces is reduced by  $1 \mu\text{m}$ . Find the components of the stress and strain tensors, assuming the lateral edge of the prism to be along the axis  $X_3$ , and one of the edges at the base to be along the axis  $X_1$ .

## 6. PIEZOELECTRIC PROPERTIES OF CRYSTALS. ELECTROSTRICTION

**Direct piezoelectric effect.** The direct piezoelectric effect comprises a group of phenomena in which the mechanical stresses or strains induce in crystals an electric polarization (electric field) proportional to these factors. Besides, the mechanical and electrical quantities are found to be linearly related. Four types of equations describe the direct piezoelectric effect:

$$P_i = d_{ijk} t_{jk} \quad (6.1)$$

$$P_i = e_{ijk} r_{jk} \quad (6.2)$$

$$E_i = -g_{ijk} t_{jk} \quad (6.3)$$

$$E_i = -h_{ijk} r_{jk} \quad (i, j, k = 1, 2, 3) \quad (6.4)$$

where  $P_i$  and  $E_i$  denote the components of the electric polarization vector and electric field strength vector, respectively,  $t_{jk}$  and  $r_{jk}$  are the components of the mechanical stress tensor and strain tensor, respectively, and  $d_{ijk}$ ,  $e_{ijk}$ ,  $g_{ijk}$ , and  $h_{ijk}$  are the piezoelectric coefficients forming a rank three tensor. This means that the piezoelectric coefficients, such as the coefficients  $d_{ijk}$ , are transformed in going from the coordinate system  $X_1$ ,  $X_2$ ,  $X_3$  to the system  $X'_1$ ,  $X'_2$ ,  $X'_3$  according to the law

$$d_{qlm} = C_{qi} C_{lj} C_{mk} d_{ijk} \quad (6.5)$$

The coefficients  $d_{ijk}$  are usually referred to as *piezoelectric moduli*.

**The number of independent piezoelectric moduli. Matrix notation.** The number of components of a rank three tensor is 27, but since the mechanical stress and strain tensors are symmetrical (see Sec. 5),

$$t_{ij} = t_{ji}, \quad r_{ij} = r_{ji} \quad (6.6)$$

that is, the tensors of piezoelectric coefficients are symmetrical with respect to the commutation of the last two subscripts, i.e. satisfy the equalities

$$d_{ijk} = d_{ikj} \quad (6.7)$$

This reduces the number of independent piezoelectric coefficients to 18, making it possible to use a more compact notation of the equations of the piezoelectric effect. This is achieved by introducing a single subscript to replace the two subscripts in the stress

tensor components

$$\begin{bmatrix} t_{11} & t_{12} & t_{13} \\ t_{12} & t_{22} & t_{23} \\ t_{13} & t_{23} & t_{33} \end{bmatrix} \rightarrow \begin{bmatrix} t_1 & t_6 & t_5 \\ t_6 & t_2 & t_4 \\ t_5 & t_4 & t_3 \end{bmatrix}$$

as well as for the strain tensor components:

$$\begin{bmatrix} r_{11} & r_{12} & r_{13} \\ r_{12} & r_{22} & r_{23} \\ r_{13} & r_{23} & r_{33} \end{bmatrix} \rightarrow \begin{bmatrix} r_1 & \frac{1}{2}r_6 & \frac{1}{2}r_5 \\ \frac{1}{2}r_6 & r_2 & \frac{1}{2}r_4 \\ \frac{1}{2}r_5 & \frac{1}{2}r_4 & r_3 \end{bmatrix}$$

In this matrix notation the equations of the direct piezoelectric effect take the form

$$P_i = d_{il}t_l \quad (6.8)$$

$$P_i = e_{il}r_l \quad (6.9)$$

$$E_i = -g_{il}t_l \quad (6.10)$$

$$E_i = -h_{il}r_l \quad (i = 1, 2, 3; l = 1, 2, \dots, 6) \quad (6.11)$$

The coefficients  $d_{il}$ ,  $e_{il}$ ,  $g_{il}$ , and  $h_{il}$  form the matrices consisting of three rows and six columns.

The piezoelectric coefficients in tensor and matrix notations are related by specific formulas, for instance, for coefficients  $d$ :

$$d_{ijk} = d_{in} \quad \text{if } n = 1, 2, 3, \quad i = 1, 2, 3 \quad (6.12)$$

$$2d_{ijk} = d_{in} \quad \text{if } n = 4, 5, 6, \quad i = 1, 2, 3 \quad (6.12a)$$

It must be remembered that if a problem requires a transformation from one coordinate system to another, the tensor and not the matrix notation must be used.

**Constraints due to the crystal symmetry.** The symmetry of crystals imposes constraints on the existence of the piezoelectric effect and on the form of the matrix of piezoelectric moduli. The necessary condition for the piezoelectric effect is the absence of the centre of symmetry in the crystal structure. The  $(d_{ij})$  matrix of crystals without a centre of symmetry, not belonging to the trigonal or hexagonal system, can be obtained by the direct inspection method (Fumi method). This method is based on the fact that the components of rank three tensors are transformed to a new coordinate system similarly to the product of three coordinates of an arbitrary point, namely:

$$x'_i x'_j x'_k = C_{il} C_{jm} C_{kn} x_l x_m x_n \quad (6.13)$$

Thus, for example, if a crystal has a symmetry axis 2 parallel to the axis  $X_3$ , the transformation of the coordinate axes proceeds as follows:

$$X_1 \rightarrow -X'_1, \quad X_2 \rightarrow -X'_2, \quad X_3 \rightarrow X'_3$$

and the coordinates of a point, as follows:

$$x_1 \rightarrow -x'_1, \quad x_2 \rightarrow -x'_2, \quad x_3 \rightarrow x'_3$$

A more compact notation is

$$1 \rightarrow -1, \quad 2 \rightarrow -2, \quad 3 \rightarrow 3$$

In this case  $d_{122}$  is transformed as follows:

$$d_{122} \rightarrow -d'_{122} \quad (6.14)$$

since  $x_1 x'_2 \rightarrow -x'_1 x'_2$ . But as the twofold symmetry axis parallel to  $X_3$  is a symmetry operation, the piezoelectric modulus  $d_{122}$  must be conserved under this coordinate transformation, that is,

$$d_{122} = d'_{122} \quad (6.15)$$

The relations (6.14) and (6.15) can be satisfied simultaneously if and only if  $d_{122} = d'_{122} = 0$ . Hence, the piezoelectric modulus  $d_{122}$  vanishes in crystals with the symmetry axis 2 parallel to the axis  $X_3$ .

After a similar operation with each of the eighteen independent piezoelectric moduli, we arrive at the matrices of piezoelectric moduli for all symmetry classes, with the exception of the trigonal and hexagonal classes in which the piezoelectric moduli in the new coordinate system  $X'_1, X'_2, X'_3$ , related to the original system by a symmetry operation, can only be found by an analytical method, that is, by applying the relation (6.5) and then the relations similar to (6.15).

The forms of matrices  $(d_{ij})$  are listed for different crystallographic classes in Table 6. The matrices of coefficients  $g_{ij}$  coincide with the matrices of  $d_{ij}$  listed in Table 6. The matrices of coefficients  $e_{ij}$  and  $h_{ij}$  differ from the given matrices of  $d_{ij}$  for some of the symmetry classes. In converting from the two-symbol subscripts to three-symbol subscripts in coefficients  $e$  and  $h$  in the formulas similar to (6.12), the factors  $1/2$  should be omitted. The matrices of  $e_{ij}$  and  $h_{ij}$  differing from matrices  $(d_{ij})$  are given in Table 7.

**Converse piezoelectric effect.** The converse piezoelectric effect is the thermodynamic corollary of the direct piezoelectric effect.

The converse effect is described by the equations

$$r_j = d_{ij} E_i \quad (6.16)$$

$$r_j = g_{ij} P_i \quad (6.17)$$

$$t_j = -e_{ij} E_i \quad (6.18)$$

$$t_j = -h_{ij} P_i \quad (6.19)$$

where  $d$ ,  $g$ ,  $h$  and  $e$  with their subscripts are the introduced earlier piezoelectric coefficients [see equations (6.1)-(6.4) or (6.8)-(6.11)].

**Possible applications of piezoelectric crystals and various piezoelectric coefficients.** Piezoelectric crystals are used extensively as electromechanical transducers of energy in a large number of instruments, such as microphones, dynamometers, vibration-sensing devices, seismographs, phonograph pick-ups, ultrasonic emitters, and the like. The modes of operation, and as a consequence the piezoelectric coefficients characterizing the sensitivity of the corresponding instrument, are very different.

Thus, in instruments for measuring small strains by electronic means (piezoelectric seismograph, piezoelectric phonograph pick-up, etc.) the piezoelectric crystal functions in the direct piezoelectric effect mode [Eqs. (6.2) and (6.4)] and must possess as high coefficients  $h$  and  $e$  as possible. In instruments converting electric oscillations into mechanical vibrations, for instance, in ultrasound emitters, the crystal operates in the converse piezoeffect mode [Eq. (6.16)] and must have large piezoelectric moduli  $d$ .

If one of the piezoelectric coefficients of a crystal is much larger than the rest of the coefficients, it is expedient to use this crystal in a suitable mode.

The piezoelectric coefficients  $d$ ,  $g$ ,  $h$  and  $e$  are not independent and can be calculated if one type of the coefficients are known; one has to use then the relations which follow from the equations of the piezoelectric effect, polarization of a dielectric in an external field, and Hook's law:

$$d_{qij} = \frac{\epsilon_{mq}}{4\pi} g_{mij} = s_{ijlm} e_{qln}$$

Applications of piezoelectric crystals essentially depend, in addition to the conversion efficiency, on a number of properties of crystals: mechanical and electrical strength, resistance to humidity effects, stability of dielectric properties, and stability of properties under changing ambient temperature.

**Electromechanical coupling factor.** The most important characteristic of a piezoelectric crystal used as an electromechanical converter of energy is the electromechanical coupling factor:

$$k^2 = \frac{U_{\text{mech}}}{U_{\text{el}}} \quad (6.20)$$

where  $U_{\text{el}}$  is the electric energy delivered to the crystal, and  $U_{\text{mech}}$  is the mechanical energy stored in the crystal.

If the energy conversion is related to the  $i$ th component of the electric field and to the  $j$ th component of strain, the electromechani-

cal coupling coefficient is given by the following formula:

$$k = \frac{d_{ij}}{\sqrt{\frac{1}{4\pi} \epsilon_i^t s_{jj}^E}} \quad (6.21)$$

where  $d_{ij}$  are the piezoelectric moduli which describe piezoelectric excitation,  $\epsilon_i^t$  are the dielectric permittivities of a mechanically free crystal, and  $s_{jj}^E$  are the effective coefficients of elastic compliance measured in constant electric field. (The dielectric permittivities of the mechanically free and mechanically fixed crystal are different in piezoelectric crystals, and especially ferroelectric crystal. The same is true for elastic compliances measured in the conditions of constant field  $E$  or induction  $D$ .)

The electromechanical coupling factors characterize the effect of power conversion in piezoelectric materials, and can be used for a direct comparison between materials with substantially different dielectric permittivities and elastic constants.

**Piezoelectric properties of a crystal plate as a function of its orientation with respect to crystallophysical axes.** Each piezoelectric modulus has a definite physical meaning and a numerical value only in a chosen coordinate system fixed to a crystal. If this frame is crystallophysical, the piezoelectric moduli are called *basic*.

Depending on the symmetry of the crystal, some piezoelectric moduli may vanish in the crystallophysical coordinate system (see Table 6).

On the other hand, it is often possible to find a new coordinate system  $X'_1, X'_2, X'_3$  with respect to which a piezoelectric modulus, nonvanishing in the crystallophysical coordinate system, vanishes in this new system. At the same time, some piezoelectric moduli which equalled zero in the crystallophysical axes may acquire non-zero values.

This means that the properties of a crystal plate depend on its orientation with respect to the crystallophysical axes. New piezoelectric effects absent in standard cuts can be produced by cutting plates oriented in a special way with respect to the crystallophysical axes; conversely, some effects may be suppressed by an appropriate choice of cutting orientation.

**The magnitude surface of the longitudinal piezoelectric effect.** The tensor of piezoelectric moduli  $d_{ijk}$  cannot be represented completely by a single representation quadratic. As a result, only particular cases, important for practical applications of the piezoelectric effect, are considered.

The surfaces of the longitudinal piezoelectric effect are of special interest. The radius vectors of such surfaces are proportional to the charge density induced on the surface perpendicular to the tensile or compressional stress  $t'_{11}$  applied along the radius vector directed along

the axis  $X'_1$  of the auxiliary coordinate system (Fig. 6.1). Since

$$|\sigma| = |P'_1| \quad \text{and} \quad P'_1 = d'_{111} t'_{11}$$

it is obvious that the radius vectors of the longitudinal piezoelectric effect surfaces are proportional to  $d'_{111}$ . As

$$r'_{11} = d'_{111} E'_1$$

this surface also represents the tensile strain produced along the applied field.

**Piezoelectric textures.** The materials widely used in modern piezoelectric equipment are the synthetic piezoelectric systems, the so-called piezoelectric textures (ceramics); the piezoelectric effect in such systems was predicted by A. B. Shubnikov.

A piezoelectric texture (ceramic) is a polycrystalline aggregate consisting of small ferroelectric crystals whose vectors of spontaneous polarization are oriented by the external field and retain their orientation after the field is switched off (polarized ceramics). For piezoelectric ceramics the direction of polarization is the infinite-order symmetry axis. Piezoelectric properties are predicted in ceramics with the symmetries  $\infty$ ,  $\infty m$ ,  $\infty 2$ , and  $\infty/\infty$ , that is, in media without a centre of symmetry.

The matrix of piezoelectric coefficients of a texture with the symmetry  $\infty/\infty$  consists of only zero components.

The textures belonging to the symmetry groups  $\infty$ ,  $\infty m$ , and  $\infty 2$  have nonzero piezoelectric coefficients; the textures have identical matrices of the coefficients  $d$ ,  $g$ ,  $e$ , and  $h$ .

The matrices  $(d_{ij})$  of piezoelectric textures are given in Table 8.

The parameters of piezoelectric textures are calculated via the equations of the direct and converse piezoelectric effect in which  $d$ ,  $g$ ,  $e$ , and  $h$  are the piezoelectric coefficients of the corresponding texture in the crystallophysical coordinate system whose axis  $X_3$  is directed along the infinite-order symmetry axis.

As compared to single crystals, piezoelectric textures have certain advantages. Thus, for example, a ceramic piezoelectric transducer can be made in an arbitrary shape (a plate, a spherical or cylindri-

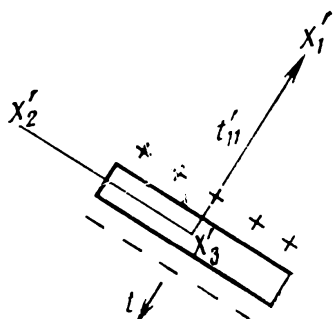


Fig. 6.1. Schematic diagram illustrating longitudinal piezoelectric effect.

cal shell, etc.) by simple technological procedures (grinding, compacting, casting). By producing different directions of the artificial polarization (longitudinal, transverse, radial, etc.), and even producing different polarization directions within different segments of the same piezoelectric transducer, one can infinitely vary the designs of ceramic transducers.

**Vibration modes of piezoelectric oscillators.** If metal electrodes are placed on the opposite faces of a plate cut in a special manner from a piezoelectric crystal, and an ac voltage is applied to these electrodes, the conversed piezoelectric effect leads to mechanical vibrations in such a plate. The amplitude of these vibrations reaches maximum when the frequency of the applied ac voltage is equal to the natural frequency of the mechanical vibrations of the plate.

A vibrating crystal plate with electrodes is called the *piezoelectric oscillator*. A piezoelectric oscillator is equivalent to the oscillatory circuit consisting of a resistor  $R$ , inductance coil  $L$  and capacitor  $C_1$  connected in series in one part of the circuit, and a capacitor  $C_2$  in the parallel branch (Fig. 6.2).

Electromechanical resonators employing a piezoelectric oscillator as a high- $Q$  oscillatory circuit are used in today's electronics to stabilize the frequency of various devices, especially in communication equipment and standard time service.

As an oscillatory circuit, a piezoelectric oscillator has two resonance frequencies:  $f_R$ , the frequency of the series resonance (for  $Z = 0$ , where  $Z$  is the complex resistance of the oscillator) and  $f_A$ , the frequency of the parallel resonance (for  $Z = \infty$ );  $f_R$  is called the resonance frequency, and  $f_A$  the antiresonance frequency. These frequencies are determined by the oscillator size and density, and the elastic, dielectric, and piezoelectric properties of plates. The following formula relates  $f_R$  and  $f_A$  to the electromechanical coupling factor:

$$\frac{f_A - f_R}{f_R} = \frac{4}{\pi} \frac{k^2}{1 - k^2} \quad (6.22)$$

Hence,  $k = \frac{\pi}{2} \sqrt{\frac{\Delta f}{f_R}}$ , where  $\Delta f = f_A - f_R$ . Therefore, it is possible to find the electromechanical coupling factor, related via (6.21) to

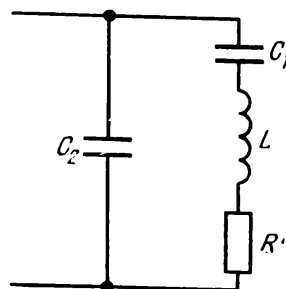


Fig. 6.2. Equivalent circuit of piezoelectric oscillator.

the elastic, piezoelectric, and dielectric constants of the crystal, by measuring  $f_A$  and  $f_R$ .

The vibrations in crystal oscillators are classified by the type of strain and the shape of the piezoelectric transducer determining the resonance frequency. The simplest types of vibrations in piezoelectric oscillators are the lengthwise vibrations of bars (longitudinal vibrations) and thickness shear vibrations of plates. If a bar-shaped oscillator vibrates lengthwise, its natural resonance frequencies are given by the formula

$$f_1 = \frac{n}{2l} \sqrt{\frac{1}{\rho s'_{11}}} \quad (6.23)$$

where  $n$  is the order of the harmonic,  $l$  is the bar length,  $s'_{11}$  is the elastic compliance along the bar length, and  $\rho$  is the density. An oscillator undergoing thickness shear vibrations is usually a circular or square plate whose thickness is small compared with the diameter or edge length. The natural resonance frequency of such a plate is

$$f_d = \frac{n}{2d} \sqrt{\frac{c'_{66}}{\rho}} \quad (6.24)$$

where  $d$  is the plate thickness, and  $c'_{66}$  is the elastic rigidity determining the shear strain along the plate thickness (the coefficients  $s_{ij}$  and  $c_{ij}$  are defined in Sec. 7).

All physical parameters determining the resonance frequency of the oscillator are temperature dependent, so that the resonance frequency itself is also a function of temperature. This temperature dependence is quantitatively characterized by the so-called temperature coefficient of resonance frequency, t.c.f., defined as follows:

$$\text{t.c.f.} = \frac{\Delta f_R}{\Delta T} \frac{1}{f_R}$$

The expression for t.c.f. for each specific mode of vibrations can be obtained by differentiating the appropriate expression for  $f_R$  with respect to temperature. Thus, for a lengthwise vibrating bar of arbitrary orientation the expression for t.c.f. has the following form:

$$\text{t.c.f.} = -\alpha_{ij} l_i l_j + \frac{1}{2} \beta - \frac{1}{2} \frac{\frac{ds_{ijkm}}{dT} l_i l_j l_k l_m}{s_{ijkm} l_i l_j l_k l_m}$$

where  $\alpha_{ij}$  are the thermal expansion coefficients of the crystal,  $\beta$  is the temperature coefficient of density defined via the principal coefficients of thermal expansion:

$$\beta = -(\alpha_{11} + \alpha_{22} + \alpha_{33})$$

$l_i$  are the components of the unit vector along the oscillator length, and  $s_{ijk l}$  are the elastic compliances of the crystal.

The piezoelectric and elastic constants of piezoelectric crystals are found from the measurements of resonance and antiresonance frequencies of oriented bars and plates. It is necessary to excite in the crystal the vibrations of the simplest possible mode and measure the resonance and antiresonance frequencies and capacitance of the crystal at low frequencies. (The dielectric permittivity measured at low frequencies is higher than that at high frequencies. The difference is especially high in ferroelectric crystals.) The results of measuring  $f_R$  and  $f_A$  in crystal plates in which longitudinal vibrations are excited can be used to find all dielectric, piezoelectric, and elastic constants, with the exception of shear elastic constants; these last are usually found by exciting edgewise shear vibrations or thickness shear vibrations in crystal plates.

### *Electrostriction*

In addition to the piezoelectric effect (first-order effect) observable in non-centrosymmetrical crystals, all crystals evince *electrostriction* (second-order effect). Electrostriction induces strain proportional to the square of an electric field applied to a specimen:

$$r_{ij} = R_{ijmn}E_mE_n \quad (6.25)$$

Electrostriction is also described by the following equations:

$$r_{ij} = Q_{ijmn}P_mP_n \quad (6.26)$$

$$t_{ij} = G_{ijmn}P_mP_n \quad (6.27)$$

$$t_{ij} = H_{ijmn}E_mE_n \quad (6.28)$$

where  $R_{ijmn}$ ,  $Q_{ijmn}$ ,  $G_{ijmn}$ , and  $H_{ijmn}$  are the electrostriction constants which are components of rank-four tensors for which  $R_{ijmn} = R_{jimn} = R_{ijnm} = R_{jinm}$ , but  $R_{ijmn} \neq R_{mnij}$ , and so on.

### *Matrix Notation*

By using a single subscript to denote the components of the tensors  $[r_{ij}]$  and  $[t_{ij}]$ , as well as the following notation:  $E_1E_1 = E_1^2$ ,  $E_2E_2 = E_2^2$ ,  $E_3E_3 = E_3^2$ ,  $E_2E_3 = E_3E_2 = E_4^2$ ,  $E_3E_1 = E_1E_3 = E_5^2$ ,  $E_1E_2 = E_2E_1 = E_6^2$ , we obtain the matrix notation for equations (6.25)-(6.28):

$$r_i = R_{ij}E_j^2 \quad (6.29)$$

$$r_i = Q_{ij}P_j^2 \quad (6.30)$$

$$t_i = G_{ij}P_j^2 \quad (6.31)$$

$$t_j = H_{ij}P_j^2 \quad (6.32)$$

The matrices of electrostriction constants in different crystallographic classes have the same form as the matrices of elastooptic coefficients.

The matrix and tensor notations of electrostriction constants are related by the following expressions:

$$\begin{aligned}
 \left. \begin{aligned} G_{mn} &= G_{ijkl} \\ H_{mn} &= H_{ijkl} \end{aligned} \right\} & \text{ for } n = 1, 2, 3 \\
 \left. \begin{aligned} G_{mn} &= 2G_{ijkl} \\ H_{mn} &= 2H_{ijkl} \end{aligned} \right\} & \text{ for } n = 4, 5, 6 \\
 \left. \begin{aligned} R_{mn} &= R_{ijkl} \\ Q_{mn} &= Q_{ijkl} \end{aligned} \right\} & \text{ for } m \text{ and } n = 1, 2, 3 \\
 \left. \begin{aligned} R_{mn} &= 2R_{ijkl} \\ Q_{mn} &= 2Q_{ijkl} \end{aligned} \right\} & \text{ if } m \text{ and } n \text{ equal } 4, 5, 6 \\
 \left. \begin{aligned} R_{mn} &= 4R_{ijkl} \\ Q_{mn} &= 4Q_{ijkl} \end{aligned} \right\} & \text{ if } m \text{ and } n \text{ are equal to } 4, 5, 6
 \end{aligned} \tag{6.33}$$

Electrostriction-induced strain in crystals is normally small and can be observed in pure form only in non-piezoelectric crystals.

In piezoelectric crystals the strain induced by applied electric fields is determined both by the piezoelectric effect and by electrostriction:

$$\begin{aligned} r_{jk} &= d_{ijk}E_i + R_{jkl}E_lE_i = (d_{ijk} + R_{jkl}E_l)E_i \\ r_{jk} &= q_{ijk}P_i + Q_{jkl}P_lP_i = (q_{ijk} + Q_{jkl}P_l)P_i \end{aligned} \tag{6.34}$$

Consequently, the second terms in parentheses must be regarded as electrostriction-induced corrections to piezoelectric constants. In the general case, electric field applied to a crystal may change its symmetry and result in the appearance of new moduli.

Each centrosymmetrical dielectric crystal can be turned into a piezoelectric crystal by an external electric field. The piezoelectric modulus characterizing this artificial piezoelectric material is proportional to electric field and can be found from the relation

$$\frac{\partial r_{ij}}{\partial E_k} = 2R_{ijkl}E_l \tag{6.35}$$

A comparison of equations (6.35) and (6.16) yields

$$d_{kij} = 2R_{ijkl}E_l \tag{6.36}$$

Therefore, Eq. (9.1) can be rewritten in the form

$$r_{ij} = d_{lij}E_l \tag{6.37}$$

Though electrostriction is produced in all crystals, the effect is very small; the only exception is ferroelectric crystals. Crystal plates excited electrostrictively in high-strength fields vibrate at twice the frequency of the applied electric field, and can be employed as modulators.

### Examples of Problems with Solutions

6.1. Find the matrix of piezoelectric moduli for rochelle salt. (In all problems dealing with the piezoelectric effect in rochelle salt we mean crystals in the ferroelectric phase, in the multidomain state.)

**Solution.** The problem can be solved by using the direct inspection method. First consider the symmetry axis 2 along the axis  $X_3$  of the crystallophysical coordinate system. The axis  $2 \parallel X_3$  realizes the following transformation of the coordinate axes:  $X_1 \rightarrow -X_1$ ,  $X_2 \rightarrow -X_2$ ,  $X_3 \rightarrow X_3$ , or in compact notation,  $1 \rightarrow -1$ ,  $2 \rightarrow -2$ ,  $3 \rightarrow 3$ .

Let us successively transform all moduli according to (6.5). If the sign of the modulus is thereby reversed, the corresponding modulus is zero, and if the sign is conserved, the modulus is retained in the matrix of piezoelectric moduli. Obviously, only those moduli  $d_{ij}$  which contain in the subscripts either one or three digits 3 do not vanish. Therefore,

$$\begin{aligned} d_{111} &= 0, \quad d_{112} = 0, \quad d_{113} \neq 0, \quad d_{211} = 0, \quad d_{212} = 0 \\ d_{213} &\neq 0, \quad d_{123} \neq 0, \quad d_{133} = 0, \quad d_{222} = 0, \quad d_{233} = 0 \\ d_{223} &\neq 0, \quad d_{331} = 0, \quad d_{323} = 0, \quad d_{311} \neq 0, \quad d_{312} \neq 0 \\ d_{122} &= 0, \quad d_{322} \neq 0, \quad d_{333} \neq 0 \end{aligned}$$

or, in the matrix notation,

$$\begin{pmatrix} 0 & 0 & 0 & d_{14} & d_{15} & 0 \\ 0 & 0 & 0 & d_{24} & d_{25} & 0 \\ d_{31} & d_{32} & d_{33} & 0 & 0 & d_{36} \end{pmatrix}$$

Now we take the next axis 2 along  $X_2$ . This symmetry axis transforms the coordinate axes as follows:

$$\begin{aligned} X_1 &\rightarrow -X_1, \quad X_2 \rightarrow X_2, \quad X_3 \rightarrow -X_3 \\ 1 &\rightarrow -1, \quad 2 \rightarrow 2, \quad 3 \rightarrow -3 \end{aligned}$$

Among the remaining eight piezoelectric moduli, only those are retained which contain either one or three digits 2, that is, the moduli

$$d_{132} = d_{123} (d_{14}), \quad d_{231} = d_{213} (d_{25}), \quad d_{321} = d_{312} (d_{36})$$

It will be meaningless to analyze the effect of the third twofold axis along  $X_1$ : by virtue of the Euler theorem, it is a generated symmetry element that can be reduced to the already analyzed axes  $2 \parallel X_3$  and  $2 \parallel X_2$ .

Finally, the matrix of piezoelectric moduli of crystals belonging to the symmetry class 222 has the form

$$\begin{pmatrix} 0 & 0 & 0 & d_{14} & 0 & 0 \\ 0 & 0 & 0 & 0 & d_{25} & 0 \\ 0 & 0 & 0 & 0 & 0 & d_{36} \end{pmatrix}$$

**6.2.** Characterize the longitudinal piezoelectric effect in rochelle salt crystals, answering the following questions:

(i) What equation describes the longitudinal piezoelectric effect in an arbitrarily oriented plate?

(ii) Are there directions in which this effect vanishes?

(iii) What is the orientation, with respect to the crystallophysical axes, of plates exhibiting the maximum longitudinal piezoelectric effect?

**Solution.** (i) Consider a plate with the normal  $\mathbf{n}$  ( $n_1, n_2, n_3$ ) oriented arbitrarily with respect to the crystallophysical axes; now stretch (or compress) the plate along the normal. In order to calculate the magnitude of the longitudinal piezoelectric effect, that is, the density of charges generated at the faces perpendicular to the direction of elongation, we use the Eq. (6.1) of the direct piezoelectric effect. Note that the tensor of piezoelectric moduli and the stress tensor must be written in the same coordinate system. The coordinate system can be related to the direction of tension (compression), and in this system the stress tensor will have the simplest form although all eighteen components of the matrix of piezoelectric moduli may then be nonzero. It is unreasonable therefore to relate the coordinate system to this direction. We shall obtain the solution in the crystallophysical coordinate system in which the matrix of piezoelectric moduli is fixed and has the simplest form. The uniaxial tension (compression) in an arbitrary direction  $\mathbf{n}$  ( $n_1, n_2, n_3$ ) is represented in the crystallophysical coordinate system by a tensor whose components are found from the relation  $t_{jk} = tn_j n_k$ , whence

$$[t_{jk}] = \begin{bmatrix} n_1^2 & n_1 n_2 & n_3 n_1 \\ n_1 n_2 & n_2^2 & n_2 n_3 \\ n_3 n_1 & n_2 n_3 & n_3^2 \end{bmatrix} t$$

The longitudinal piezoelectric effect is determined by the component of polarization parallel to the direction of tension (compression), that is,

$$P_{\parallel} = P_i n_i$$

Taking into account that  $P_i = d_{ijk}t_{jk}$ , we obtain  $P_{||} = d_{ijk}tn_in_jn_k$ :

The nonzero piezoelectric moduli in rochelle salt are

$$d_{14} = 2d_{123}, \quad d_{25} = 2d_{231}, \quad d_{36} = 2d_{321}$$

Correspondingly, the longitudinal piezoelectric effect in a rochelle salt plate whose orientation is given by the direction of the normal  $\mathbf{n}$  with respect to the crystallophysical coordinate system is given by the equation

$$P_{||} = n_1n_2n_3 (2d_{123} + 2d_{231} + 2d_{321}) t = n_1n_2n_3 (d_{14} + d_{25} + d_{36}) t$$

(ii) As follows from the expression for  $P_{||}$ , the longitudinal piezoelectric effect vanishes for all directions lying in coordinate planes.

(iii) The longitudinal piezoelectric effect is maximum in crystal plates whose normals are at equal angles to the crystallophysical axes. Such plates (*L*-cuts, see Fig. 2.4) are widely used in applications.

6.3. What should be the directions of edges in a *Z*-cut ADP plate (see Fig. 2.3) in order for it to be polarized by purely normal stresses applied in the directions parallel to its edges?

**Solution.** As follows from the form of the matrix of the piezoelectric moduli belonging to the symmetry class  $\bar{4}2m$ , a *Z*-cut plate will be polarized ( $P_3 \neq 0$ ) only if its stressed state is described by the tensor

$$\begin{bmatrix} 0 & t_6 & 0 \\ t_6 & 0 & 0 \\ 0 & 0 & 0 \end{bmatrix}$$

Let us transform this stress tensor to its principal axes  $X'_1, X'_2, X'_3$  and find the orientation of the principal axes with respect to the initial ones. The sought directions of the edges of a *Z*-cut plate will represent the directions of the principal axes of the stress tensor.

Our tensor is transformed to the principal axes by rotating the initial axes of the tensor around the axis  $X_3$  clockwise by  $45^\circ$ . The stress tensor then takes the form

$$\begin{bmatrix} -t & 0 & 0 \\ 0 & t & 0 \\ 0 & 0 & 0 \end{bmatrix}$$

Therefore, in order to achieve polarization of a *Z*-cut ADP crystal plate by normal stresses, the plate must be cut as shown in Fig. 6.3.

Such plates are called  $45^\circ$  *Z*-cuts.

6.4. To find the piezoelectric moduli of a polarized barium titanate ceramics, a cubic specimen was prepared and subjected to a

compressional stress  $t$  along the polarization axis. Then the same specimen was subjected to hydrostatic compression  $p$ .

Determine the faces of the cube on which these stresses generated electric charges. Which piezoelectric moduli of the barium titanite ceramics can be found from the results of these tests?

**Solution.** As the axis  $X_3$  of the crystallophysical coordinate system of the ceramic is parallel to the direction of polarization, the stressed state is represented by the tensor

$$\begin{bmatrix} 0 & 0 & 0 \\ 0 & 0 & 0 \\ 0 & 0 & -t_{33} \end{bmatrix}$$

The hydrostatic compression is represented by a tensor of the type

$$\begin{bmatrix} -p & 0 & 0 \\ 0 & -p & 0 \\ 0 & 0 & -p \end{bmatrix}$$

so that  $t_1 = t_2 = t_3 = -p$ . Both the uniaxial compression in the indicated direction and the hydrostatic compression induce polarization of the ceramic along its polar axis; in the first case  $P_3 = -d_{33}(-t_3)$ , and in the second case  $P_3 = (2d_{31} + d_{33})(-p)$ . Therefore, two of the three independent piezoelectric moduli of the barium titanite ceramic,  $d_{31}$  and  $d_{33}$ , can be calculated from the experimental results.

6.5. A piezoelectric sound detector consists of a membrane coated on the inside by a stack of thin crystal plates. The plates are spaced with thin metal foil electrodes (Fig. 6.4). Which of the rochelle salt plates have higher sensitivity as transducers:  $45^\circ$   $X$ -cut or  $45^\circ$   $Y$ -cut plates?

Fig. 6.3.  $45^\circ$   $X$ -,  $45^\circ$   $Y$ -, and  $45^\circ$   $Z$ -cuts.

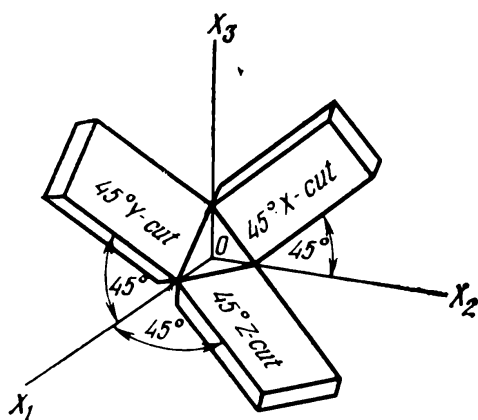
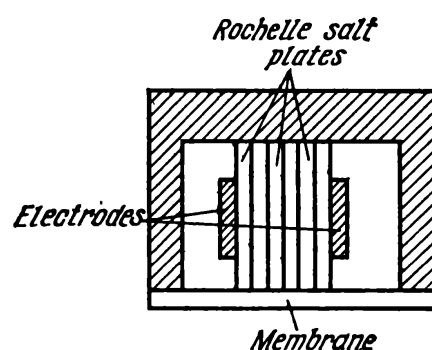


Fig. 6.4. Schematic structure of a piezoelectric sound receiver with rochelle salt plates.



**Solution.** The sensitivity of a transducer can be defined as the ratio of the electric voltage induced by a given mechanical stress (pressure of sound waves) to the magnitude of this mechanical stress, that is, as  $V/t$ .

Acoustic vibrations incident on rochelle salt plates have frequencies much lower than the resonance frequencies, so that we can make use of equation (6.10)

$$E_i = -g_{il}t_l$$

which for  $45^\circ$   $X$ -cut plate takes the form

$$E_l = -g_l t_l$$

where  $t_l$  is the mechanical stress applied lengthwise, that is, at  $45^\circ$  to the crystallophysical axes  $X_2$  and  $X_3$  (see Fig. 6.3), and  $g_l$  is the effective piezoelectric modulus responsible for the excitation of a  $45^\circ$   $X$ -cut plate. This modulus can be calculated from the relation  $g_l = l_i l_j l_k g_{ijk}$ , where  $g_{ijk}$  are the piezoelectric moduli of rochelle salt and  $l_i$  are the direction cosines of the length of the plate with respect to the crystallophysical axes.

The electric field induced by the mechanical stress  $t$  is

$$E_l = \frac{V}{d} = -g_l t_l = 31.5 \cdot 10^{-8} t_l \text{ CGSE units}$$

where  $t_l$  is pressure, dyne/cm<sup>2</sup>,  $d$  is the plate thickness, cm, and  $V$  is the electric voltage induced between the working faces of a rochelle salt  $45^\circ$   $X$ -cut plate, in CGSE units. Hence,

$$V = -dg_l t_l = dg_l t_l$$

In this case the sensitivity of the transducer, defined as  $V/t$ , is equal to  $dg_l$ . Consequently, the sensitivity is proportional to the piezoelectric modulus  $g_l$ . If the membrane is composed of  $n$  transducer plates connected in series, its sensitivity is increased  $n$ -fold.

The piezoelectric moduli  $g_l$  for  $45^\circ$   $X$ - and  $45^\circ$   $Y$ -cuts are, respectively,

$$g_l = \frac{1}{2} g_{14} = 3.15 \cdot 10^{-7} \text{ CGSE units}$$

$$g_l = \frac{1}{2} g_{25} = -9.5 \cdot 10^{-7} \text{ CGSE units}$$

so that  $g_l$  for  $45^\circ$   $X$ -cuts is three times as small as for  $45^\circ$   $Y$ -cuts. As a result, at the same pressure, a  $45^\circ$   $Y$ -cut plate will generate in an open circuit a voltage approximately three times that in a  $45^\circ$   $X$ -cut plate, and have a sensitivity three times higher. The  $45^\circ$   $Y$ -cut plates of rochelle salt are used both in acoustic transducers and as transducers for hydrostatic pressure.

**6.6.** Which of the longitudinally vibrating oscillators, used as ultrasound emitters,  $45^\circ X$ - or  $45^\circ Y$ -cut rochelle salt plates (see Fig. 6.3), has a higher electromechanical coupling factor? Find the vibrational frequencies that can be obtained with 20 mm long emitters. Find the wavelength at which a generator can excite vibrations in thus cut plates.

**Solution.** The coordinate system fixed to the edges of a  $45^\circ X$ -cut oscillator plate is represented by the following table of cosines with respect to the crystallophysical coordinate system:

Table 6.1

Axes	$X_1$	$X_2$	$X_3$
$X'_1$	1	0	0
$X'_2$	0	$\cos 45^\circ$	$\sin 45^\circ$
$X'_3$	0	$-\sin 45^\circ$	$\cos 45^\circ$

The equation of piezoelectric excitation of a  $45^\circ X$ -cut is  $r'_2 = d'_{12}E_1$ , and the electromechanical coupling factor of this cut is

$$k = d'_{12} \sqrt{4\pi/\epsilon_1^T s'_{22}}$$

where  $d'_{12}$  is the piezoelectric modulus, and  $s'_{22}$  is the elastic compliance along the length of the oscillator. According to (6.5),

$$\begin{aligned} d'_{12} = d'_{122} &= C_{1i}C_{2j}C_{2k}d_{ijk} = 2(C_{11}C_{22}C_{23}d_{123} + C_{12}C_{23}C_{21}d_{231} \\ &+ C_{13}C_{21}C_{22}d_{312}) = 2\cos 45^\circ \sin 45^\circ d_{123} = \frac{1}{2}d_{14} \\ &= 5.75 \cdot 10^{-6} \text{ CGSE units} \end{aligned}$$

According to (7.2a),

$$\begin{aligned} s'_{22} = s'_{2222} &= C_{2i}C_{2j}C_{2k}C_{2l}s_{ijkl} = C_{22}^4 s_{22} + C_{23}^4 s_{33} \\ &+ 2C_{22}^2 C_{33}^2 s_{23} + C_{22}^2 C_{23}^2 s_{44} = (\cos 45^\circ)^4 s_{22} + (\sin 45^\circ)^4 s_{33} \\ &+ 2(\cos 45^\circ \sin 45^\circ)^2 s_{23} + (\sin 45^\circ \cos 45^\circ)^2 s_{44} \\ &= \frac{1}{4}(s_{22} + s_{33} + 2s_{23} + s_{44}) = 3.17 \cdot 10^{-12} \text{ CGSE units} \end{aligned}$$

From this,

$$k_{45^\circ X} = 5.75 \cdot 10^{-6} \sqrt{\frac{12.56 \cdot 3.16}{480} \cdot 10^{11}} = 0.524 \approx 52\%$$

The resonance frequency of the  $45^\circ X$ -cut plate is found from the relation

$$f_R = \frac{1}{2l} \sqrt{\frac{1}{\rho s'_{22}}} = \frac{1}{2l} \sqrt{\frac{3.16 \cdot 10^{11}}{1.77}} = 105 \text{ kHz}$$

With the resonance frequency of the crystal plate known, one readily finds the wavelength at which a generator can excite vibrations in a  $45^\circ X$ -cut plate. At resonance the frequency  $f_R$  is equal to the frequency of electric current oscillations, that is,  $f_R = f_{el} = c/\lambda_{el}$ , where  $c = 3 \cdot 10^8 \text{ m/s}$ , and  $\lambda_{el}$  is the wavelength of electric oscillations. This gives the wave factor  $\lambda_{el}/l = 145$  for  $l = 20 \text{ mm}$  and  $\lambda_{el} = 2.9 \cdot 10^3 \text{ mm}$ .

Likewise, for an oscillator made of a  $45^\circ Y$ -cut rochelle salt plate, we obtain a table of cosines.

Table 6.2

Axes	$X_1$	$X_2$	$X_3$
$X'_1$	$\cos 45^\circ$	0	$-\sin 45^\circ$
$X'_2$	0	1	0
$X'_3$	$\sin 45^\circ$	0	$\cos 45^\circ$

The calculations yield

$$r'_3 = d'_{23} E_2, \quad k_{45^\circ Y} = d'_{23} \sqrt{\frac{4\pi}{\epsilon_2^T s'_{33}}}$$

$$d'_{23} = \frac{d_{25}}{2} = -80 \cdot 10^{-8} \text{ CGSE units}$$

$$s'_{33} = \frac{1}{4} (s_{11} + s_{33} + s_{55} + 2s_{13}) = 9.275 \cdot 10^{-12} \text{ cm}^2/\text{dyne}$$

$$k_{45^\circ Y} = 27\%, \quad f_R = \frac{1180 \text{ kHz}}{l}, \quad \frac{\lambda_{el}}{l} = 254$$

(for  $l = 20 \text{ mm}$ ,  $f_R = 59 \text{ kHz}$ ,  $\lambda_{el} = 5.08 \cdot 10^3 \text{ mm}$ )

Oscillators made of  $45^\circ X$ - and  $45^\circ Y$ -cuts of rochelle salt have fairly large electromechanical coupling factors. However, rochelle salt crystals are poor ultrasound emitters because of low mechanical strength of rochelle salt. But the high piezoelectric moduli make rochelle salt plates quite suitable to make ultrasound detectors.

Lengthwise vibrating oscillators are usually employed to generate ultrasound vibrations in the range 20-200 kHz. One of the shortcomings of lengthwise vibrating oscillators is the relatively small emitting area (end faces of the oscillator) which cannot be arbitrarily

increased. At high frequencies, it is preferable to use thicknesswise vibrating oscillators.

6.7. Piezoelectric moduli of quartz crystals were measured at fundamental frequencies by the dynamic method on bars of two different orientations (Fig. 6.5).

The results of measurements are given in Table 6.3.

Table 6.3

Cut orientation	Bar length, mm	$f_R$ , kHz	$f_A$ , kHz	Dielectric permit-tivity of a free crystal, $\epsilon^t$
X-cut	29.99	89.215	89.535	4.49
30° X-cut	32.26	79.96	80.067	4.49

Calculate the values of piezoelectric moduli from the experimental results.

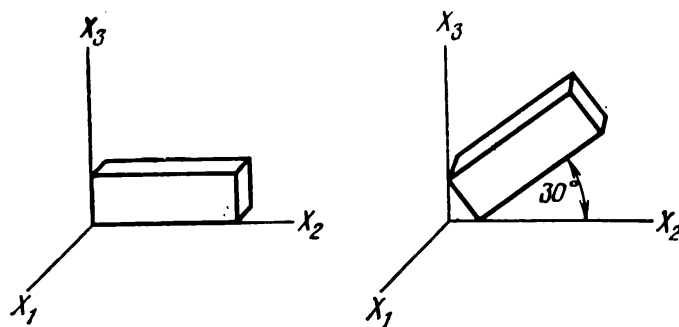
**Solution.** The equation of piezoelectric excitation of a X-cut quartz bar is  $r_2 = d_{12}E_1$ . The piezoelectric modulus  $d_{12}$  responsible for the excitation of X-cuts can be calculated from Eq. (6.21).

$$d_{12} = k \sqrt{\frac{\epsilon_1 s_{22}^E}{4\pi}}$$

provided the electromechanical coupling factor of the bar and the elastic compliance along the length of the bar directed along the axis  $X_2$  are known. According to (6.22), the electromechanical coupling factor is  $\frac{1}{2}\pi\sqrt{\Delta f/f_R}$ , where  $\Delta f = f_A - f_R = 0.32$  kHz; hence  $k = 0.0935$ .

By virtue of (6.23), the fundamental resonance frequency of a longitudinally vibrating X-cut bar stretched lengthwise along  $X_2$  is

Fig. 6.5. Orientation of bars used to determine piezoelectric moduli of quartz by the dynamic technique.



$f_R = 1/2l \sqrt{\rho s_{22}}$ . This yields the compliance  $s_{22}$ :

$$s_{22} = 1/4l^2 \rho f_R^2$$

A substitution into the last formula of the bar length  $l$  (cm), resonance frequency  $f_R$  (Hz) and density of quartz (g/cm<sup>3</sup>) yields

$$s_{22} = 131.6 \cdot 10^{-14} \text{ cm}^2/\text{dyne}$$

In quartz crystals  $s_{11} = s_{22}$  and  $|d_{12}| = |d_{11}|$ . A substitution of the values of  $k$ ,  $s_{22}$ , and dielectric permittivity  $\epsilon_1$  of a free crystal into the expression for  $d_{12}$  yields

$$|d_{12}| = |d_{11}| = 6.45 \cdot 10^{-8} \text{ CGSE units}$$

The lengthwise orientation of a bar used to measure the independent piezoelectric modulus  $d_{14}$  of quartz was chosen at 30° to the axis  $X_2$  (see Fig. 6.5). The following table represents the orientation of the axes  $X'_1$ ,  $X'_2$ ,  $X'_3$  fixed to the edges of the bar with respect to the crystallophysical axes of quartz:

Table 6.4

Axes	$X_1$	$X_2$	$X_3$
$X'_1$	1	0	0
$X'_2$	0	$\sqrt{3}/2$	$1/2$
$X'_3$	0	$-\frac{1}{2}$	$\sqrt{3}/2$

The equation of the piezoelectric excitation of such a bar is

$$r'_2 = d'_{12} E_1$$

where  $d'_{12}$  is the operative piezoelectric modulus responsible for the excitation of vibrations in the bar. We can express  $d'_{12}$  in terms of the principal piezoelectric moduli of quartz:

$$\begin{aligned} d'_{12} &= d'_{122} = C_{1i} C_{2j} C_{2k} d_{ijk} = C_{11} C_{21}^2 d_{111} + C_{11} C_{22}^2 d_{122} \\ &\quad + 2C_{11} C_{22} C_{23} d_{123} + 2C_{12} C_{23} C_{21} d_{213} + 2C_{12} C_{21} C_{22} d_{212} \\ &= \frac{3}{4} d_{12} + \frac{\sqrt{3}}{4} d_{14} = -\frac{3}{4} d_{11} + \frac{\sqrt{3}}{4} d_{14} = -0.75 d_{11} + 0.434 d_{14} \end{aligned}$$

$$d'_{12} = k' \sqrt{\frac{\epsilon_1 s'_{22}}{4\pi}}$$

where  $k'$  is the electromechanical coupling factor of the second bar, equal to  $\frac{1}{2} \pi \sqrt{\Delta f/f_R}$ , and  $s'_{22}$  is the elastic compliance of the bar equal to  $1/4l^2 \rho f_R^2$ .

A substitution of the values of  $f_R$ ,  $\Delta f_R$ , bar length  $l$ , and  $\rho$  yields

$$k' = 0.0577, \quad s'_{22} = 139.6 \cdot 10^{-14} \text{ cm}^2/\text{dyne}$$

This gives

$$d'_{12} = 0.577 \sqrt{\frac{4.49 \cdot 139.6 \cdot 10^{-14}}{12.56}} = 4.06 \cdot 10^{-8} \text{ CGSE units}$$

By substituting the obtained values of  $d_{11}$  and  $d'_{12}$  into the relation  $d'_{12} = -0.75d_{11} + 0.434d_{14}$  and recalling that  $d_{11} = -d_{12}$ , we obtain

$$d_{14} = 1.7 \cdot 10^{-8} \text{ CGSE units}$$

6.8. Which of the electrostriction moduli of monodomain barium titanate crystals can be evaluated from the jump in spontaneous polarization and in unit cell parameters when the crystal temperature is lowered to  $T_C = 120^\circ\text{C}$ ? Calculate these moduli if  $P^s = 18 \times 10^{-2} \text{ C/m}^2$ , and the jumpwise change in the parameters of the initial cubic lattice ( $a \approx 4 \text{ \AA}$ ), by X-ray data, is as follows: two edges of the cell are shortened with the strain  $15.5 \cdot 10^{-4}$ , and the third edge is elongated with the relative strain  $34.2 \cdot 10^{-4}$  (Fig. 6.6).

**Solution.** Above the Curie point ( $120^\circ\text{C}$ ) the symmetry of barium titanate lattice is  $m3m$ , so the piezoelectric properties are absent because of the central symmetry. As temperature is lowered to  $T_C = 120^\circ\text{C}$ , spontaneous polarization arises along one of the four-fold axes. Let us specify that this axis is parallel to  $[001]$ , although the three fourfold axes of the cubic phase are equivalent and the spontaneous polarization could be produced along any of the other two axes. Choosing the direction of  $[001]$  as the axis  $X_3$  of the crystallophysical coordinate system, we obtain that the components of the spontaneous polarization vector are  $P_1^s = P_2^s = 0$ ,  $P_3^s = |\mathbf{P}^s|$ . For the cubic phase the matrix of electrostriction moduli is as follows:

Table 6.5

	$P_1^2$	$P_2^2$	$P_3^2$	$P_4^2$	$P_5^2$	$P_6^2$
$r_1$	$Q_{11}$	$Q_{12}$	$Q_{12}$	0	0	0
$r_2$	$Q_{12}$	$Q_{11}$	$Q_{12}$	0	0	0
$r_3$	$Q_{12}$	$Q_{12}$	$Q_{11}$	0	0	0
$r_4$	0	0	0	$Q_{44}$	0	0
$r_5$	0	0	0	0	$Q_{44}$	0
$r_6$	0	0	0	0	0	$Q_{44}$

We notice that a spontaneous strain along [001] is accompanied by induced spontaneous strains found from the relations  $r_1 = r_2 = = Q_{12}P_3^2$ ,  $r_3 = Q_{11}P_3^2$ . From the experimentally determined values of strain of barium titanate unit cell and from the value of  $P^s$  we find the following values of the moduli  $Q_{11}$  and  $Q_{12}$ :

$$Q_{11} = \frac{r_3}{P_3^2} = 1.17 \cdot 10^{-12} \text{ CGSE units}$$

$$Q_{12} = \frac{r_1}{P_3^2} = -0.53 \cdot 10^{-12} \text{ CGSE units}$$

6.9. Find the change in the shape of the unit cell of triglycin sulphate caused by a ferroelectric phase transition at the Curie point ( $49^\circ\text{C}$ ) which aligns the spontaneous polarization vector  $\mathbf{P}^s$  along [010] of the initial paraelectric phase.

**Solution.** Above the Curie point ( $49^\circ\text{C}$ ) the paraelectric phase of triglycin sulphate belongs to symmetry class  $2/m$  (Fig. 6.7). The ferroelectric phase transition aligns the spontaneous polarization vector [010] which is a twofold symmetry axis and is chosen as the axis  $X_2$  of the crystallophysical coordinate system ( $P_1^s = P_3^s = 0$ ,  $P_2^s = |\mathbf{P}^s|$ ). Since the paraelectric phase is centrosymmetrical, spontaneous polarization in triglycin sulphate crystals is accompanied by spontaneous electrostriction-induced strain. In crystals be-

**Fig. 6.6. Barium titanate unit cells:**  
(a) paraelectric cubic phase, (b) ferroelectric tetragonal phase.

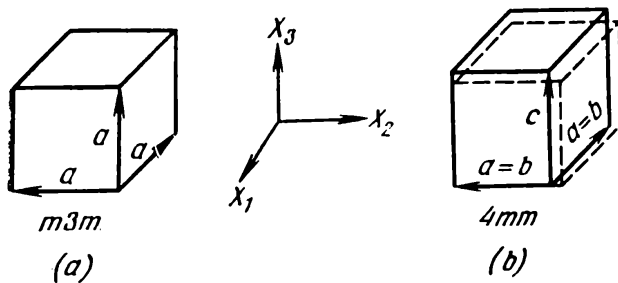
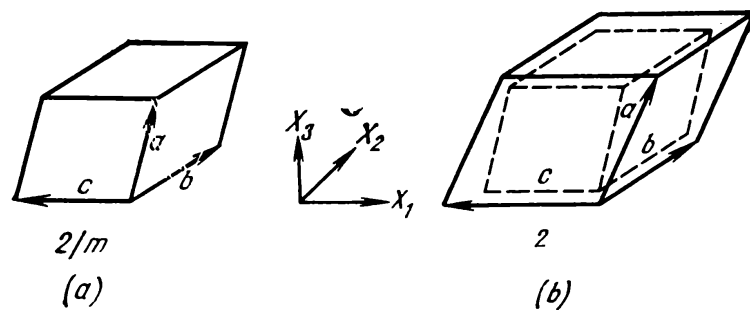


**Fig. 6.7. Triglycin sulphate unit cells:**  
(a) paraelectric monoclinic phase, (b) ferroelectric monoclinic phase.



longing to symmetry class  $2/m$  the tensor of electrostriction moduli takes the following form:

Table 6.6

	$P_1^2$	$P_2^2$	$P_3^2$	$P_4^2$	$P_5^2$	$P_6^2$
$r_1$	$Q_{11}$	$Q_{12}$	$Q_{13}$	0	$Q_{15}$	0
$r_2$	$Q_{21}$	$Q_{22}$	$Q_{23}$	0	$Q_{25}$	0
$r_3$	$Q_{31}$	$Q_{32}$	$Q_{33}$	(1)	$Q_{35}$	(1)
$r_4$	0	(1)	0	$Q_{44}$	0	$Q_{46}$
$r_5$	$Q_{51}$	$Q_{52}$	$Q_{53}$	0	$Q_{55}$	(1)
$r_6$	0	0	0	$Q_{64}$	0	$Q_{66}$

Consequently, spontaneous strains suffered by triglycin sulphate crystals as a result of spontaneous polarization along [010] are

$$r_1 = Q_{12}P_2^2, \quad r_2 = Q_{22}P_2^2, \quad r_3 = Q_{32}P_2^2, \quad r_5 = Q_{52}P_2^2$$

Obviously, a phase transition to ferroelectric phase in triglycin sulphate single crystals results in a compressional (tensile) strains along crystallophysical axes, and in shear strains around the axis  $X_2$ .

These spontaneous strains do not lower the symmetry of the unit cell (it remains monoclinic) but eliminate the mirror symmetry plane and additionally, turn the twofold axis into a polar direction (Fig. 6.7).

6.10. Electrostriction in quartz crystals was analyzed by studying the piezoelectric modulus induced by applying electric field to the working faces of a Z-cut plate as a function of field strength (the piezoelectric modulus was measured in different dc fields by applying to the crystal a weak ac field). The results of measurements are plotted in Fig. 6.8. Find the electrostriction modulus which can be calculated from these data. Calculate the field that must be applied to a Z-cut quartz plate to produce the piezoelectric modulus of the same magnitude as in an X-cut plate.

**Solution.** As follows from the matrix  $(d_{ij})$  for symmetry-32 crystals (the third row contains zero components), the piezoelectric effect vanishes in Z-cut quartz plates. Hence, the electric field applied to

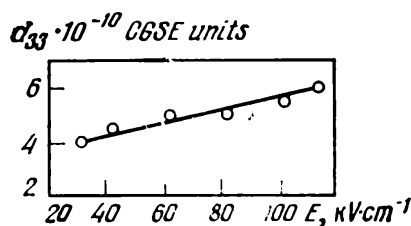


Fig. 6.8. Induced modulus  $d_{33}$  in a quartz plate as a function of strength of dc electric field.

the working faces of a  $Z$ -cut plate ( $E_1 = E_2 = 0$ ,  $E_3 = E$ ) induces only electrostriction strains.

According to (6.36),  $d_{33} = 2R_{33}E_3$ .

Therefore, the data given in the problem yield the modulus  $R_{33}$ .

From the slope of the experimental graph, we find  $R_{33} = 0.3 \times 10^{-12}$  CGSE units.

The graph shows that in the electric field of  $100 \text{ kV} \cdot \text{cm}^{-1}$ , the piezoelectric modulus  $d_{33} = 5 \cdot 10^{-10}$  CGSE units, that is by two orders of magnitude lower than the piezoelectric modulus  $d_{11}$  equal to  $6.76 \cdot 10^{-8}$  CGSE units. This means that for a  $Z$ -cut plate to be equivalent with respect to piezoelectric properties to an  $X$ -cut plate (i.e., to have identical piezoelectric modulus), electric field applied to its working faces must be of the order of  $10^4 \text{ kV} \cdot \text{cm}^{-1}$ .

#### PROBLEMS

6.11. Will a multidomain rochelle salt crystal evince the piezoelectric effect? Will it be found in a multidomain barium titanate crystal?

6.12. Make use of the Fumi method to find the matrix of piezoelectric moduli of crystals belonging to class  $\bar{4}2m$ . Find the matrix  $(d_{ij})$  in the coordinate system  $X'_1$ ,  $X'_2$ ,  $X'_3$  rotated counterclockwise around the axis 4 by  $45^\circ$ .

6.13. Find the number of independent piezoelectric moduli for barium titanate ceramic (symmetry class  $\infty m$ ). Note. To solve this problem, consider not all the eighteen piezoelectric moduli but only those of them which compose the matrix  $(d_{ij})$  for, say, symmetry class  $6mm$  (see Table 6), since those piezoelectric moduli which vanish in class  $6mm$  also vanish in symmetry class  $\infty m$ .

6.14. Find the matrix of piezoelectric moduli for texture of rochelle salt (symmetry class  $\infty 2$ ). Note. To solve the problem, use the matrix of piezoelectric moduli in class  $222$  (see Table 6).

6.15. Show that the crystals belonging to class 4 have the symmetry axis of infinite order with respect to the piezoelectric properties. List the symmetry classes in which the crystals have this property.

6.16. Derive the expression for the longitudinal piezoelectric effect in quartz and sodium chlorate crystals. What are the directions along which the longitudinal piezoelectric effect in these crystals is impossible?

6.17. A quartz parallelepiped with edges  $a$ ,  $b$ ,  $c$ , parallel to the corresponding crystallophysical axes  $X_1$ ,  $X_2$ ,  $X_3$ , is subjected to a force  $F$  which is alternately applied along its edges. Derive the expression for the charge generated at the faces of the parallelepiped.

6.18. A stress of  $10^4 \text{ N/cm}^2$  is applied along [0001] to a Z-cut tourmaline plate. Indicate the faces of the plate between which a potential difference will be generated. Find its magnitude.

6.19. Find the strains of the edges of a  $45^\circ$  X-cut rochelle salt plate (see Fig. 6.3) when a constant electric field with strength  $10^3 \text{ V/cm}$  is applied to its working faces. Is it possible to use this cut to generate longitudinal thickness vibrations?

6.20. Determine the cut of a sphalerite plate required to obtain the maximum charge density on its working faces, when uniaxial tensile stress  $t$  is applied perpendicularly to the plate surface.

6.21. Electric field  $E = 2000 \text{ V/cm}$  is applied along the plane diagonal of a cubic sample of ammonium dihydropophosphate, whose edges are oriented along crystallophysical axes. Find the magnitude and type of strain suffered by the cube.

6.22. Find the absolute displacements of the edge of an X-cut quartz plate of  $0.1 \times 5 \text{ cm}^2$  (see Fig. 2.3), when an electric voltage of 3 kV is applied to the electrodes deposited on its working faces.

6.23. Find the type of strain suffered by X-, Y-, and Z-cut quartz plates (see Fig. 2.3) in the converse piezoelectric effect when the electrodes are deposited on the working faces. Find the vibration modes that can be excited in these plates by applying ac electric field.

6.24. Find the strains of the edges of a  $45^\circ$  Z-cut rochelle salt plate (see Fig. 6.3), produced by applying electric field of  $10^3 \text{ V/cm}$  (the electrodes are on the working faces).

6.25. Derive the equation and calculate the magnitude of the piezoelectric modulus characterizing the piezoelectric excitation of a "rotated" X-cut quartz bar, that is, a bar whose length is at an arbitrary angle  $\varphi$  to the axis  $X_2$  (Fig. 6.9). Analyze the cases when  $\varphi = 0^\circ$  and  $\varphi = 90^\circ$ .

6.26. Derive the equation for the magnitude surface of the longitudinal piezoelectric effect in quartz. Make use of the polar coordinates and construct the section of this surface by the coordinate plane  $X_1X_2$ , and determine the symmetry of this section.

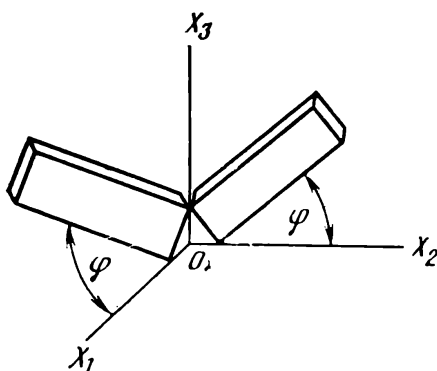


Fig. 6.9. Orientation of "rotated" X- and Y-cut quartz bars.

6.27. A constant uniaxial stress  $t$  is applied to a quartz crystal perpendicularly to its threefold axis. Show that when the direction of  $t$  is rotated around the threefold axis, the piezoelectric polarization vector maintains constant magnitude and rotates around the threefold axis at twice the rotation rate but in the opposite direction.

6.28. What should be the orientation of a sphalerite plate providing the maximum possible strain along the applied electric field?

6.29. What should be the direction of tensile stress with respect to the axis  $\infty$  in piezoelectric texture of symmetry  $\infty 2$ , in order to maximize the charge density at the end faces?

6.30. The charge density produced at the opposite faces of a Z-cut tourmaline plate, used as a hydrostatic pressure transducer, is  $2.5 \cdot 10^{-8} \text{ C/cm}^2$ . Find the magnitude of hydrostatic pressure measured with this plate.

6.31. A rectangular parallelepiped with edges  $a$ ,  $b$ ,  $c$  is textured with the symmetry  $\infty 2$ , and the texture axis is given by an arbitrary direction  $n$  ( $n_1$ ,  $n_2$ ,  $n_3$ ) with respect to the edges. The parallelepiped is stretched along an edge by a stress  $t$ . Find the charges produced on the parallelepiped's faces.

6.32. A Z-cut resorcin plate of  $10 \times 10 \times 1 \text{ mm}^3$  is strained so that one of the faces perpendicular to the short edge is displaced by  $10^{-3} \text{ mm}$ . What is the potential difference between the working faces of the plate? Calculate the magnitude of electric charge on its working faces.

6.33. Find the direction of the maximum longitudinal piezoelectric effect in KDP crystal.

6.34. Find the monoclinic angle in the ferroelectric phase of rochelle salt, produced by spontaneous strain in the phase transition ( $P^s = 0.2 \cdot 10^{-6} \text{ C/cm}^2$ ).

6.35. Find the electromechanical coupling factor of a Z-cut CdS crystal for three possible vibrational modes of this cut.

6.36. Calculate the absolute displacement of a Z-cut CdS crystal plate, caused by electric field of  $3 \cdot 10^3 \text{ V/cm}$  applied between its working faces. The plate thickness is  $10^{-2} \text{ mm}$ .

6.37. Which of the piezoelectric moduli determine the piezoelectric excitation of a  $45^\circ$  Y-cut CdS crystal?

6.38. What should be the orientation of a CdS crystal plate with respect to the crystallophysical axes for the ac electric field, applied to its working faces, to produce thickness shear vibrations?

6.39. Calculate the electromechanical coupling factors of  $45^\circ$  X-cut and L-cut rochelle salt bars (see Figs. 2.3 and 2.4).

6.40. Find the electromechanical coupling factor of a  $45^\circ$  Z-cut and L-cut ADP crystals (see Figs. 2.3 and 2.4).

6.41. A sphalerite plate is cut so that its working faces are perpendicular to [110]. Which of the piezoelectric moduli determine the

thickness shear strain of this plate if the electric field is applied to the working faces?

6.42. A cubic sample of crystalline sodium chlorate has the edges along the directions  $\langle 100 \rangle$ . Derive the formula for the charge density on the faces of the sample when a tensile stress  $t$  is along (i)  $[100]$ , (ii)  $[110]$ , and (iii)  $[111]$ .

6.43. What should be the cut of an EDT (ethylenediamine tartrate) such that the electric field applied to its working faces produced both tensile (or compressional) strains and a shear strain?

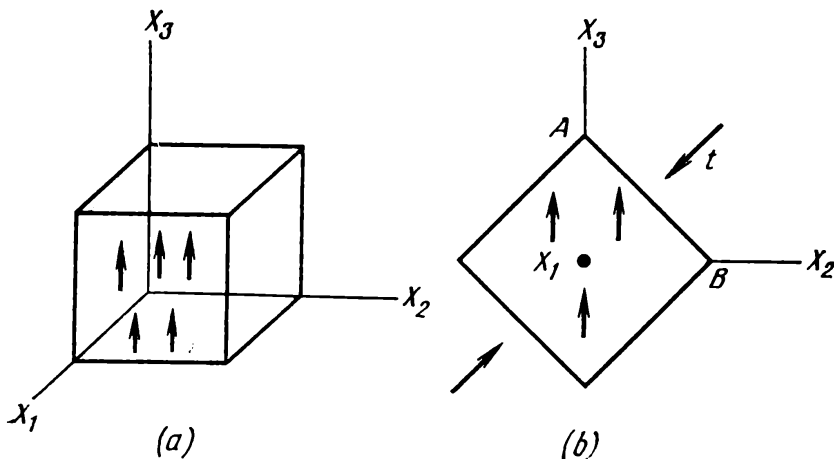
6.44. Find the thickness of an oscillator made of an  $X$ -cut quartz plate (see Fig. 2.3) operating in the thickness vibration mode and tuned to emitting at 30 MHz. Is it possible to make this plate emit 3000 MHz? What should be the thickness of a  $Z$ -cut tourmaline plate (see Fig. 2.3) tuned to emit in the same mode at the same frequency?

6.45. Calculate the electromechanical coupling factors of the plates mentioned in Problem 6.44.

6.46. In order to measure the piezoelectric moduli of polarized barium titanate ceramic, a  $1 \times 1 \times 1 \text{ cm}^3$  cubic specimen (Fig. 6.10a) is compressed by a force of 800 N along the axis  $X_3$  (the direction of polarization), and then by the same force along the axis  $X_1$ . The charge produced on the face perpendicular to  $X_3$  was  $14.8 \cdot 10^{-8} \text{ C}$  in the first case, and  $-6.15 \cdot 10^{-8} \text{ C}$  in the second case. The third independent piezoelectric modulus was found on a sample of the same size oriented as shown in Fig. 6.10b; a force of 800 N applied to the face  $AB$  induced on this face the charge of  $10.3 \cdot 10^{-8} \text{ C}$ .

Calculate the piezoelectric moduli of polarized barium titanate ceramic.

Fig. 6.10. Orientation of specimens used to determine piezoelectric moduli of polarized barium titanate ceramic.



**6.47.** Measurements gave the following values of the resonance and antiresonance frequencies of a sphalerite 45° Z-cut plate (see Fig. 6.3):

$$f_R = 117 \text{ kHz} \text{ and } f_A = 117.146 \text{ kHz}$$

Calculate the piezoelectric modulus of sphalerite.

**6.48.** The spontaneous polarization of proper pyroelectric crystals can be estimated from the magnitude of piezoelectric polarization due to hydrostatic compression (tension), as well as from the change in polarization due to the change in linear dimensions of the crystal. Derive the relations making it possible to estimate the spontaneous polarization in tourmaline and lithium sulphate crystals.

**6.49.** Calculate the strain in quartz bars oriented as shown in Fig. 6.11, in electric field applied to the lateral faces.

**6.50.** Can the piezoelectric effect be observed in KDP crystals in the paraelectric phase? in the ferroelectric phase? Do these phases of KDP crystals have different piezoelectric properties?

**6.51.** Calculate the electromechanical coupling factor of X-cut quartz for the three vibration modes of thus cut bars.

**6.52.** Calculate the electromechanical coupling factor of Y-cut quartz for two possible vibrational modes of thus cut plates.

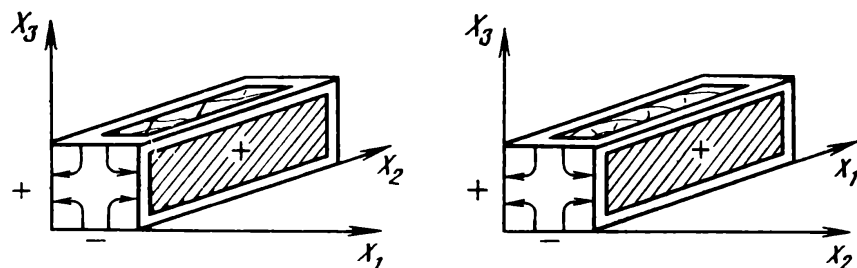
**6.53.** Show that there is no longitudinal piezoelectric effect in any of the directions in the symmetry classes 422 and 622.

**6.54.** Electric field with strength  $E$  is applied to the working faces of X-, Y-, and Z-cut rochelle salt plates (see Fig. 2.3). What strain occurs in such plates?

**6.55.** The crystals of tourmaline, lithium sulphate, and potassium tartrate belong to the polar symmetry classes and can be used as transducers of static or low-frequency hydrostatic pressure. Which of the mentioned crystals has the maximum sensitivity to hydrostatic pressure?

**6.56.** Find all symmetry classes in which electric field applied to the working faces of Z-cut plates generates pure electrostriction-induced strain normally to the plate surface.

**Fig. 6.11.** Orientation of quartz bars used to excite vibrations with non-homogeneous strains.



6.57. Which of the arrangements for measuring piezoelectric moduli do the arrangements for measuring the electrostriction moduli  $Q$ ,  $R$ ,  $G$  and  $H$  correspond?

6.58. At  $T_C = -150^\circ\text{C}$  KDP crystals undergo a transition to a ferroelectric phase with rhombic symmetry (class  $mm$ ), with  $\mathbf{P}^s \parallel [001]$ . Is this phase transition accompanied by spontaneous electrostriction?

6.59. What electric field must be applied to the working faces of  $X$ - and  $Z$ -cut quartz plates to produce in these plates a strain of  $20.4 \cdot 10^{-4}$  normally to the plate surface?

6.60. Which of the electrostriction moduli in monodomain  $\text{BaTiO}_3$  crystals can be found from measurements of spontaneous polarization and deformation accompanying the phase transition to the rhombic modification ( $\mathbf{P}^s$  is parallel to [110] of the initial cubic cell)? Calculate this modulus if  $P^s \approx 30 \cdot 10^{-2} \text{ C} \cdot \text{m}^{-2}$ ,  $r_6 \simeq 0.0029$ .

6.61. A single-crystal cubic specimen of rock salt is placed in electric field of  $30 \text{ kV/cm}$  directed along [110]. Find the type and calculate the strain suffered by the specimen. How can such strains be measured experimentally?

6.62. Evaluate the electrostriction moduli of barium titanate from the following results of piezoelectric measurements on tetragonal-phase single crystals of  $\text{BaTiO}_3$ :

$$g_{15} = 5.07 \cdot 10^{-8} \text{ CGSE units}, \quad g_{31} = -7.67 \cdot 10^{-8} \text{ CGSE units}$$

$$g_{23} = 19.17 \cdot 10^{-8} \text{ CGSE units}, \quad P^s = 26 \cdot 10^{-6} \text{ C/m}^2$$

6.63. Which of the electrostriction moduli of rochelle salt monodomain crystals can be determined from the measurement of spontaneous polarization  $P^s$  ( $\mathbf{P}^s \parallel [100]$ ) and of spontaneous changes in unit cell parameters at the phase-transition point?

6.64. The equilibrium shape and symmetry of domains are known to be determined mostly by the spontaneous deformation of the ferroelectric. If the paraelectric phase of a ferroelectric does not have piezoelectric properties, will the shape of domains in the ferroelectric depend on the sign of spontaneous polarization?

6.65. Find the change in the shape of the unit cell of barium titanate caused by a ferroelectric phase transition in which the spontaneous polarization vector aligns with the direction [110] of the initial paraelectric phase ( $T_C = 5^\circ\text{C}$ ).

6.66. Calculate the electric field strength which produces a piezoelectric modulus of  $4 \cdot 10^{-9} \text{ CGSE units}$  in a rock salt  $Z$ -cut plate.

6.67. Define the "reverse electrostriction" as the effect of electrostriction-induced polarization in a crystal subjected to mechanical stress, such that squared polarization is proportional to strain. Is the "reverse electrostriction" effect possible?

## 7. ELASTIC PROPERTIES OF CRYSTALS. HOOK'S LAW

Crystals subjected to mechanical stress undergo strains. If the stress is below a limiting value called the *proportionality limit*, the strain is reversible.

Strain is proportional to the applied stress for sufficiently low stress. If a crystal is subjected to an arbitrary uniform stress  $[t_{kl}]$ , the uniform strain it causes is such that each of its components  $r_{ij}$  is linearly related to all components of the stress tensor, that is,

$$r_{ij} = s_{ijkl}t_{kl} \quad (i, j, k, l = 1, 2, 3) \quad (7.1)$$

Equation (7.1) is the generalized form of Hook's law. Here  $s_{ijkl}$  are the *elastic compliances* of the crystal. The whole number of compliances  $s_{ijkl}$  is 81. Hook's law can also be written in the form

$$t_{ij} = c_{ijkl}r_{kl} \quad (7.2)$$

where  $c_{ijkl}$  are the *elastic stiffnesses* of the crystal. The coefficients  $s_{ijkl}$  and  $c_{ijkl}$  form tensors of rank four. This means that in a transformation from a coordinate system  $X_1, X_2, X_3$  to  $X'_1, X'_2, X'_3$  the coefficients  $s_{ijkl}$  ( $c_{ijkl}$ ) are transformed to  $s'_{mnop}$  ( $c'_{mnop}$ ) according to the law

$$s'_{mnop} = C_{mi}C_{nj}C_{ok}C_{pl}s_{ijkl} \quad (7.2a)$$

where  $C_{mi}$ ,  $C_{nj}$ ,  $C_{ok}$ , and  $C_{pl}$  are the direction cosines defining the orientation of the axes  $X'_1, X'_2, X'_3$  with respect to the axes  $X_1, X_2, X_3$ . Each coefficient  $s_{ijkl}$  ( $c_{ijkl}$ ) has a definite meaning and a magnitude only with respect to a specific coordinate system fixed to the crystal. If this system coincides with the crystallophysical coordinate system, the coefficients are called *basic*.

As the strain and stress tensors are symmetric, the components of the tensors  $s_{ijkl}$  and  $c_{ijkl}$  are symmetrical pairwise with respect to subscripts  $i$  and  $j$ ,  $k$  and  $l$ , that is

$$s_{ijkl} = s_{jikl}, \quad c_{ijkl} = c_{jikl}, \quad (7.3)$$

$$s_{ijkl} = s_{ijlk}, \quad c_{ijlk} = c_{ijkl} \quad (7.4)$$

Equations (7.3) and (7.4) reduce the number of independent components  $s_{ijkl}$  and  $c_{ijkl}$  down to 36. As  $s_{ijkl}$  and  $c_{ijkl}$  are symmetrical in the first two and the last two subscripts, we can use the matrix notation introduced in Sec. 6. In this notation, equations (7.1) and

(7.2) are written in a more compact form:

$$\left. \begin{array}{l} r_i = s_{ij}t_j \quad (i, j = 1, 2, 3, 4, 5, 6) \\ t_i = c_{ij}r_j \quad (i, j = 1, 2, 3, 4, 5, 6) \end{array} \right\} \quad (7.5)$$

The matrix notation results in a reduced number of terms on the right-hand side of Eq. (7.1), but it becomes necessary to introduce factors 2 and 4 according to the following rule:

$$\left. \begin{array}{l} s_{ijkl} = s_{mn} \text{ when } m \text{ and } n \text{ equal 1, 2, or 3} \\ 2s_{ijkl} = s_{mn} \text{ when } m \text{ or } n \text{ equals 4, 5, or 6} \\ 4s_{ijkl} = s_{mn} \text{ when } m \text{ and } n \text{ equal 4, 5, or 6} \end{array} \right\} \quad (7.6)$$

**Energy of a strained crystal.** Work per unit volume done to produce a small strain in a crystal is given by the formula  $dW = t_i dr_i$ .

If this increment of strain is isothermal and reversible,  $dW$  can be set equal to the increment in free energy  $d\psi$ , that is,

$$d\psi = dW = t_i dr_i \quad (7.7)$$

If Hooke's law holds, Eq. (7.7) takes the form

$$d\psi = c_{ij}r_j dr_i$$

therefore,

$$\frac{d\psi}{dr_i} = c_{ij}r_j$$

Differentiating both sides of the equation with respect to  $r_j$ , we obtain

$$\frac{\partial}{\partial r_j} \left( \frac{d\psi}{dr_i} \right) = c_{ij}$$

However, the order in which the equation is differentiated is unimportant because  $\psi$  is a function of only the state of the body, determined by the components of strain, so that

$$c_{ij} = c_{ji} \quad (7.8)$$

Similarly,

$$s_{ij} = s_{ji} \quad (7.8a)$$

Since the matrices  $(c_{ij})$  and  $(s_{ij})$  are symmetrical, the number of independent stiffnesses and compliances is further reduced, namely, from 36 to 21.

By integrating Eq. (7.7), we find that the work per unit volume of the crystal, required to produce strain  $r_i$  (the so-called *strain energy*) is equal to

$$\frac{1}{2} c_{ij}r_i r_j \quad (7.8b)$$

**Constraints due to symmetry.** Symmetry further reduces the number of independent coefficients  $s_{ij}$  and  $c_{ij}$ .

The matrices of elastic compliances can be obtained by the direct inspection method making it possible to find the number of independent coefficients for all classes with the exception of the classes belonging to the trigonal and hexagonal systems, for which it is necessary to use the analytic method.

The matrices  $(s_{ij})$  and  $(c_{ij})$  for various crystallographic classes, as well as for piezoelectric textures, are listed in Table 9.

**Relations between coefficients  $s_{ij}$  and  $c_{ij}$ .** The following formula relates the elastic compliances  $s_{ij}$  and elastic stiffnesses  $c_{ij}$ :

$$s_{ij} = \frac{(-1)^{i+j} \Delta c_{ij}}{\Delta^c} \quad (7.9)$$

where  $\Delta^c$  is a determinant composed of elastic stiffnesses:

$$\begin{vmatrix} c_{11} & c_{12} & c_{13} & c_{14} & c_{15} & c_{16} \\ c_{12} & c_{22} & c_{23} & c_{24} & c_{25} & c_{26} \\ c_{13} & c_{23} & c_{33} & c_{34} & c_{35} & c_{36} \\ c_{14} & c_{24} & c_{34} & c_{44} & c_{45} & c_{46} \\ c_{15} & c_{25} & c_{35} & c_{45} & c_{55} & c_{56} \\ c_{16} & c_{26} & c_{36} & c_{46} & c_{56} & c_{66} \end{vmatrix}$$

and  $\Delta c_{ij}$  is a minor obtained from this determinant by crossing out the  $i$ th row and  $j$ th column. Likewise,

$$c_{ij} = \frac{(-1)^{i+j} \Delta s_{ij}}{\Delta^s} \quad (7.9a)$$

**Young's modulus, shear modulus, and Poisson ratio.** The following constants are often used for a description of elastic properties of both isotropic and anisotropic media.

*Young's modulus*  $E$ , characterizing elastic properties of a medium in a specific direction, is defined as the ratio of the mechanical stress in this direction to the strain it produces in the same direction.

The *Poisson ratio*  $\nu$  is defined as the ratio of the transverse compressional strain to the longitudinal tensile strain caused by a mechanical stress. The *shear modulus*  $\mu$  is defined as the ratio of shear stress to shear strain it causes.

In isotropic bodies only two of the above-mentioned constants are independent. Elastic properties of isotropic bodies are often described using the constants  $\lambda$  and  $\mu$ , called the *Lame constants*; the constants  $\mu$ ,  $\lambda$ ,  $c_{11}$ , and  $c_{12}$  are related by the following formulas:

$$\mu = \frac{c_{11} - c_{12}}{2} \quad (7.10)$$

$$\lambda = c_{12} \quad (7.11)$$

If the elastic properties of isotropic bodies are characterized by the matrix  $(s_{ij})$  (Table 9), then

$$s_{11} = 1/E, \quad s_{12} = -v/E \quad (7.12)$$

$$2(s_{11} - s_{12}) = 1/\mu \quad (7.13)$$

In isotropic media Young's modulus in an arbitrary direction  $X'_3$  is

$$E = 1/s'_{3333} \quad (7.14)$$

where  $s'_{3333} = C_{3i}C_{3j}C_{3k}C_{3l}s_{ijkl}$  and  $C_{3i}$ ,  $C_{3j}$ ,  $C_{3k}$ , and  $C_{3l}$  are the direction cosines of the axis  $X'_3$  with respect to the crystallophysical coordinate system, and  $s_{ijkl}$  are the basic compliances referred to the crystallophysical coordinate system.

Young's modulus is a function of direction for all crystallographic classes, including cubic classes.

In anisotropic media the Poisson ratio is equal to

$$\nu^{hk} = \frac{s_{hk}}{s_{hh}} \quad (7.15)$$

and represents a measure of lateral compression parallel to  $X_h$  and accompanied by elongation parallel to  $X_k$ .

**Magnitude surfaces of elastic coefficients.** As elastic properties of crystals cannot be represented completely by a single surface, the magnitude surface is usually constructed for one of the elastic coefficients. This surface clearly demonstrates the variation of this coefficient as a function of direction in the crystal.

One practically important surface is the magnitude surface plotting Young's modulus as a function of direction. The radius vector of this surface is proportional to the magnitude of Young's modulus along the radius vector.

**Volumetric and linear compressibility of crystals.** *Volumetric compressibility* is defined as the relative reduction of crystal's volume under unit hydrostatic pressure.

The stress tensor of uniform, or hydrostatic compression is

$$[t_{kl}] = \begin{bmatrix} -p & 0 & 0 \\ 0 & -p & 0 \\ 0 & 0 & -p \end{bmatrix}, \text{ or } t_{kl} = -p\delta_{kl}$$

where  $\delta_{kl}$  is the Kronecker delta.

The strains due to hydrostatic compression are

$$r_{ij} = -ps_{ijkl}\delta_{kl} = -ps_{ijkk} \quad (7.16)$$

and volumetric compression is  $\Delta = \Delta V/V = r_{ii} = -ps_{iikk}$ , where  $V$  is the volume of the crystal. Consequently, the volumetric com-

pressibility is

$$-\frac{\Delta}{p} = s_{iikh} \quad (7.17)$$

The *linear compressibility*  $\beta$  is the relative reduction in the length of a rectilinear segment in crystal subjected to unit hydrostatic pressure.

The relative change in the length of a segment in an arbitrary direction  $\mathbf{n}$  ( $n_1, n_2, n_3$ ) is written as  $r_{ij}n_i n_j$ . This change is caused by the hydrostatic pressure  $p$ , so that  $r_{ij}n_i n_j = -ps_{iikh}n_i n_j$ . Therefore, the linear compressibility is

$$\beta = s_{iikh}n_i n_j \quad (7.18)$$

### Examples of Problems with Solutions

**7.1.** Find the matrix of elastic stiffnesses  $s_{ij}$  of symmetry class 222 comprising the rochelle salt crystals.

**Solution.** Independent elastic compliances  $s_{ij}$  of rochelle salt must be found by the direct inspection method. The compliances  $s_{ij}$  are symmetrical with respect to permutations of subscripts  $i$  and  $j$  ( $s_{ij} = s_{ji}$ ), so that the lower half of the matrix  $(s_{ij})$  can be omitted, and only the coefficients

$$\left( \begin{array}{cccccc} s_{11} & s_{12} & s_{13} & s_{14} & s_{15} & s_{16} \\ s_{21} & s_{22} & s_{23} & s_{24} & s_{25} & s_{26} \\ s_{31} & s_{32} & s_{33} & s_{34} & s_{35} & s_{36} \\ s_{41} & s_{42} & s_{43} & s_{44} & s_{45} & s_{46} \\ s_{51} & s_{52} & s_{53} & s_{54} & s_{55} & s_{56} \\ s_{61} & s_{62} & s_{63} & s_{64} & s_{65} & s_{66} \end{array} \right)$$

can be considered.

Let us write a table of subscripts corresponding to the upper right-hand half of the matrix  $(s_{ij})$ :

11	12	13	14	15	16
22	23	24	25	26	
33	34	35	36		
44	45	46			
55	56				
66					

The symmetry of the point group 222 is completely determined by two twofold axes coinciding with the crystallophysical axes  $X_3$

and  $X_1$  (or by any other pair of twofold symmetry axes), and the third axis is generated by combination of these two.

First consider the action of the axis 2 parallel to  $X_3$ . This transformation can be written as follows:

$$X_1 \rightarrow -X'_1, \quad X_2 \rightarrow -X'_2, \quad X_3 \rightarrow X'_3$$

or, more concisely,

$$1 \rightarrow -1, \quad 2 \rightarrow -2, \quad 3 \rightarrow 3.$$

In the four-subscript notation, the pairs of subscripts are transformed by the rule

$$\begin{aligned} 11 &\rightarrow 11, & 22 &\rightarrow 22, & 33 &\rightarrow 33, \\ 23 &\rightarrow -23, & 31 &\rightarrow -31, & 12 &\rightarrow 12. \end{aligned}$$

In the two-subscript notation, used for the matrix notation, the transformations of subscripts have the form

$$\begin{aligned} 1 &\rightarrow 1, & 2 &\rightarrow 2, & 3 &\rightarrow 3, \\ 4 &\rightarrow -4, & 5 &\rightarrow -5, & 6 &\rightarrow 6. \end{aligned}$$

The table of subscripts is then transformed to

$$\begin{array}{ccccccc} 11 & 12 & 13 & -14 & -15 & 16 \\ 22 & 23 & -24 & -25 & 26 \\ 33 & -34 & -35 & 36 \\ & 44 & 45 & -46 \\ & 55 & -56 \\ & & 66 \end{array}$$

By comparing the components of this table with those of the original table and taking into account that in this transformation compliances  $s_{ij}$  must transform into themselves, we obtain the following matrix:

$$\left( \begin{array}{cccccc} s_{11} & s_{12} & s_{13} & 0 & 0 & s_{16} \\ s_{22} & s_{23} & 0 & 0 & s_{26} \\ s_{33} & 0 & 0 & s_{36} \\ s_{44} & s_{45} & 0 \\ s_{55} & 0 \\ s_{66} \end{array} \right)$$

Consider the effect of an axis 2 parallel to the crystallophysical axis  $X_1$ :

$$1 \rightarrow 1, \quad 2 \rightarrow -2, \quad 3 \rightarrow -3.$$

The pairs of subscripts are transformed according to the rule

$$\begin{aligned} 11 &\rightarrow 11, & 22 &\rightarrow 22, & 33 &\rightarrow 33, \\ 23 &\rightarrow 23, & 31 &\rightarrow -31, & 12 &\rightarrow -12 \end{aligned}$$

or, in the two-subscript notation,

$$\begin{aligned} 1 &\rightarrow 1, & 2 &\rightarrow 2, & 3 &\rightarrow 3, \\ 4 &\rightarrow 4, & 5 &\rightarrow -5, & 6 &\rightarrow -6 \end{aligned}$$

Obviously, those compliances  $s_{ij}$  which have among the subscripts a single digit 5 or 6, that is, all  $s_{i5}$  and all  $s_{i6}$ , will now vanish.

Accordingly, we obtain the following matrix of compliances  $s_{ij}$  for rochelle salt:

$$\begin{pmatrix} s_{11} & s_{12} & s_{13} & 0 & 0 & 0 \\ s_{21} & s_{22} & s_{23} & 0 & 0 & 0 \\ s_{31} & s_{32} & s_{33} & 0 & 0 & 0 \\ & & s_{44} & 0 & 0 & 0 \\ & & s_{55} & 0 & 0 & 0 \\ & & s_{66} & 0 & 0 & 0 \end{pmatrix}$$

The matrix contains nine independent compliances  $s_{ij}$ .

**7.2.** A quartz crystal is subjected to uniaxial compression  $t$  along (i)  $[2\bar{1}10]$ , (ii)  $[0001]$ . Find the type of elastic strain suffered by the crystal.

**Solution.** According to the rules of selecting crystallophysical axes in crystals belonging to the class 32, the axis  $X_1$  is chosen along the axis 2, and the axis  $X_3$  along the axis 3 (see Table 4).

The type of strains suffered by quartz compressed along the mentioned directions will be found by applying Hook's law (7.5).

When quartz is compressed along  $[2\bar{1}10]$ , that is, along the axis 2 coinciding with the axis  $X_1$ , the only component,  $t_1$ , of the tensor of mechanical stress is nonzero, and when it is compressed along  $[0001]$ , this component is  $t_3$ . According to the form of the matrix of elastic compliances (see Table 9), we find that for compressing along  $[2\bar{1}10]$ , that is, along the axis  $X_1$ , the strains are

$$r_1 = s_{11}t_1, \quad r_2 = s_{12}t_1, \quad r_3 = s_{13}t_1$$

that is, the strains are compressional (tensile) along the crystallophysical axes (the sign of strain depends on the sign of elastic compliances), and tangential in the plane  $X_2X_3$ , since  $r_4 = s_{14}t_1$ . In quartz  $s_{11} > 0$ ,  $s_{12} < 0$ ,  $s_{13} < 0$ , so that quartz will experience the tensile strain along the axis  $X_1$ , and compressional strain along the axes  $X_2$  and  $X_3$ .

In the case of compression along [0001] coinciding with the symmetry axis 3, we find

$$r_1 = r_2 = s_{13}t_3, \quad r_3 = s_{33}t_3$$

that is, the strain is compressional along the axes  $X_1$  and  $X_2$  (since  $s_{13} < 0$ ) and tensile along the axis  $X_3$  (since  $s_{33} > 0$ ).

7.3. (i) Find the directions corresponding to the maximum values of Young's modulus for cubic crystals, and the directions corresponding to the minimum values of this modulus, assuming ( $s_{11} - s_{12} - (1/2)s_{44} > 0$ ).

(ii) Describe the magnitude surface of Young's modulus.

(iii) What is the shape of sections of this surface by planes of the type (111)?

**Solution.** (i) According to Eqs. (7.2a) and (7.14), the reciprocal of Young's modulus in an arbitrarily oriented plate is given by

$$s'_{33} = s'_{3333} = C_{3i}C_{3j}C_{3k}C_{3l}s_{ijkl} \text{ or } s'_{3333} = n_i n_j n_k n_l s_{ijkl}$$

where  $C_{3i}$ ,  $C_{3j}$ ,  $C_{3k}$ , and  $C_{3l}$  are the direction cosines of the direction of interest  $\mathbf{n}$  ( $n_1$ ,  $n_2$ ,  $n_3$ ) and  $s_{ijkl}$  are the elastic compliances of cubic crystals.

For all classes of cubic system, the matrix  $(s_{ij})$  in the crystallophysical coordinate system has the form (see Table 9)

$$s_{ij} = \begin{pmatrix} s_{11} & s_{12} & s_{12} & 0 & 0 & 0 \\ s_{12} & s_{11} & s_{12} & 0 & 0 & 0 \\ s_{12} & s_{12} & s_{11} & 0 & 0 & 0 \\ 0 & 0 & 0 & s_{44} & 0 & 0 \\ 0 & 0 & 0 & 0 & s_{44} & 0 \\ 0 & 0 & 0 & 0 & 0 & s_{44} \end{pmatrix}$$

Let us write the nonzero elastic compliances in the tensor notation

$$s_{1111} = s_{2222} = s_{3333}$$

$$s_{1122} = s_{2233} = s_{1133}$$

$$s_{2323} = s_{3131} = s_{2121}$$

Substituting the nonzero elastic compliances into the expression for  $s'_{3333}$  and going over to the matrix notation, we find

$$s'_{33} = s_{11} (C_{31}^4 + C_{32}^4 + C_{33}^4) + (s_{44} + 2s_{12}) (C_{32}^2 C_{33}^2 + C_{33}^2 C_{31}^2 + C_{31}^2 C_{32}^2)$$

After simplifying the formulas, we obtain

$$C_{31}^4 = C_{31}^2 (1 - C_{32}^2 - C_{33}^2) = C_{31}^2 - C_{31}^2 C_{32}^2 - C_{31}^2 C_{33}^2$$

$$C_{32}^4 = C_{32}^2 (1 - C_{31}^2 - C_{33}^2) = C_{32}^2 - C_{32}^2 C_{31}^2 - C_{32}^2 C_{33}^2$$

And finally,

$$C_{33}^4 = C_{33}^2 (1 - C_{31}^2 - C_{32}^2) = C_{33}^2 - C_{31}^2 C_{33}^2 - C_{33}^2 C_{32}^2$$

By substituting the expressions for  $C_{31}^4$ ,  $C_{32}^4$ , and  $C_{33}^4$  into the preceding equation, we find

$$\begin{aligned} s'_{33} &= s_{11} - 2s_{11} (C_{32}^2 C_{33}^2 + C_{33}^2 C_{31}^2 + C_{31}^2 C_{32}^2) \\ &\quad + (s_{44} - 2s_{12}) (C_{32}^2 C_{33}^2 + C_{33}^2 C_{31}^2 + C_{31}^2 C_{32}^2) \\ &= s_{11} - 2 \left( s_{11} - s_{12} - \frac{1}{2} s_{44} \right) (C_{31}^2 C_{32}^2 + C_{32}^2 C_{33}^2 + C_{31}^2 C_{33}^2) \end{aligned}$$

or

$$s'_{33} = s_{11} - 2 \left( s_{11} - s_{12} - \frac{1}{2} s_{44} \right) (n_1^2 n_2^2 + n_2^2 n_3^2 + n_1^2 n_3^2)$$

Hence, Young's modulus for cubic crystals is a function of direction and of the quantity

$$(n_1^2 n_2^2 + n_2^2 n_3^2 + n_1^2 n_3^2)$$

(ii) Let us find the maximum of this quantity by using the method of Lagrange multipliers. Compose a function

$$f = n_1^2 n_2^2 + n_2^2 n_3^2 + n_3^2 n_1^2 - \lambda (n_1^2 + n_2^2 + n_3^2 - 1)$$

Differentiating this function with respect to  $n_1^2$ ,  $n_2^2$  and  $n_3^2$ , and equating the derivatives to zero, we find

$$\frac{\partial f}{\partial n_1^2} = n_2^2 + n_3^2 - \lambda = 0$$

$$\frac{\partial f}{\partial n_2^2} = n_3^2 + n_1^2 - \lambda = 0$$

$$\frac{\partial f}{\partial n_3^2} = n_1^2 + n_2^2 - \lambda = 0$$

Resolving this system of equations, we obtain

$$n_1^2 + n_2^2 = n_3^2 + n_1^2 = n_2^2 + n_3^2 = \lambda$$

Hence,  $n_1^2 = n_2^2 = n_3^2 = 1/3$ ,

$$n_1 = \pm \frac{1}{\sqrt{3}}, \quad n_2 = \pm \frac{1}{\sqrt{3}}, \quad n_3 = \pm \frac{1}{\sqrt{3}}$$

Thus, there are eight directions corresponding to the maximum value of  $n_1^2 n_2^2 + n_2^2 n_3^2 + n_3^2 n_1^2$ :

$$\frac{1}{\sqrt{3}} (1, 1, 1), \quad \frac{1}{\sqrt{3}} (-1, 1, -1), \quad \frac{1}{\sqrt{3}} (-1, 1, 1)$$

$$\frac{1}{\sqrt{3}} (1, 1, -1), \quad \frac{1}{\sqrt{3}} (-1, -1, 1), \quad \frac{1}{\sqrt{3}} (1, -1, -1)$$

$$\frac{1}{\sqrt{3}} (1, -1, 1), \quad \frac{1}{\sqrt{3}} (-1, -1, -1)$$

This means that the maximum magnitude of Young's modulus corresponds to the directions of the type [111], if the quantity  $s_{11} - s_{12} - (1/4)s_{44}$  is positive, and this is true for all cubic crystals (with an exception of molybdenum crystals).

Evidently, the minimum of Young's modulus corresponds to the directions of the type [100], for which the expression  $n_1^2n_2^2 + n_2^2n_3^2 + n_3^2n_1^2$  vanishes. Consequently, we conclude that the magnitude surface of Young's modulus is a cube with rounded corners and depressions at the centres of faces.

(iii) Let us find the sections of this surface by the plane (111). Let a unit vector  $\mathbf{n}$  ( $n_1, n_2, n_3$ ) be perpendicular to [111]. This means that  $n_1 + n_2 + n_3 = 0$ , that is,  $n_3 = -(n_1 + n_2)$ . But  $n_1^2 + n_2^2 + n_3^2 = 1$ ; hence,

$$n_1^2 + n_2^2 + (n_1 + n_2)^2 = 2n_1^2 + 2n_2^2 + 2n_1n_2 = 1$$

or

$$n_1^2 + n_2^2 + n_1n_2 = \frac{1}{2}$$

Taking this relation into account, we can further transform the sum  $n_1^2n_2^2 + n_2^2n_3^2 + n_3^2n_1^2$ :

$$\begin{aligned} n_1^2n_2^2 + n_2^2n_3^2 + n_3^2n_1^2 &= n_1^2n_2^2 + (n_1^2 + n_2^2)(1 - n_1^2 - n_2^2) \\ &= n_1^2n_2^2 + n_1^2 + n_2^2 - (n_1^2 + n_2^2) = n_1^2 + n_2^2 + n_1n_2 - \frac{1}{4} = \frac{1}{4} \end{aligned}$$

As a result, we find that Young's modulus is independent of direction in the plane perpendicular to [111], and the sections of the magnitude surface of Young's modulus, perpendicular to [111], are circular.

**7.4.** (i) Which of the elastic constants of cubic crystals can be determined from the measured longitudinal strain and volumetric compression  $\Delta V/V$  of a crystal specimen subjected to uniaxial compression  $t$  along [100]?

(ii) Does the volumetric compression of cubic crystals depend on the direction of uniaxial mechanical stress?

**Solution.** (i) If a uniaxial mechanical stress acts on a cubic crystal along [100], this signifies that only one component of the stress tensor in the crystallophysical coordinate system,  $t_1$ , is nonzero. Consequently, from the measurement data on the longitudinal strain  $r_1$  we can find, according to (7.5), the compliance  $s_{11} = r_1/t_1$ . The volumetric compression  $\Delta V/V = r_{ii}$  is then equal to  $(2s_{12} + s_{11}) \times (-p)$  so that from the measurement data on  $\Delta V/V$  one can find the compliance  $s_{12}$ .

(ii) Let us fix the uniaxial stress  $t$  along a direction  $\mathbf{n}$  ( $n_1, n_2, n_3$ ), arbitrary with respect to the crystallophysical coordinate system.

We choose the direction of the axis  $X'_3$  of the new primed coordinate

system along  $n$ ; the stressed state in the new coordinate system is represented by the tensor

$$[t'_{kl}] = \begin{bmatrix} 0 & 0 & 0 \\ 0 & 0 & 0 \\ 0 & 0 & t \end{bmatrix}, \text{ where } t = t'_{33}$$

Let us find the stress tensor in the crystallophysical coordinate system making use of the law of transformation of the components of a rank two tensor in a transition from the new to the original coordinate system:  $t_{ij} = C_{ki}C_{lj}t'_{kl}$ . In our case

$$t_{ij} = C_{3i}C_{3j}t'_{33} = n_i n_j t$$

Now we shall find the change in the volume of a cubic crystal subjected to uniaxial tension in an arbitrary direction. Since  $\Delta V/V = r_{ii} = r_{11} + r_{22} + r_{33}$ , and

$$r_{11} = t(s_{1111}n_1^2 + s_{1122}n_2^2 + s_{1133}n_3^2)$$

$$r_{22} = t(s_{2211}n_1^2 + s_{2222}n_2^2 + s_{2233}n_3^2)$$

$$r_{33} = t(s_{3311}n_1^2 + s_{3322}n_2^2 + s_{3333}n_3^2)$$

or, in the matrix notation,

$$r_1 = t(s_{11}n_1^2 + s_{12}n_2^2 + s_{13}n_3^2)$$

$$r_2 = t(s_{21}n_1^2 + s_{22}n_2^2 + s_{23}n_3^2)$$

$$r_3 = t(s_{31}n_1^2 + s_{32}n_2^2 + s_{33}n_3^2)$$

and taking into account that for cubic crystals

$$s_{11} = s_{22} = s_{33}, \quad s_{12} = s_{13} = s_{23}$$

we obtain

$$\frac{\Delta V}{V} = r_1 + r_2 + r_3$$

$$= t(s_{11}n_1^2 + s_{12}n_2^2 + s_{13}n_3^2 + s_{12}n_1^2 + s_{11}n_2^2 + s_{12}n_3^2 + s_{13}n_1^2 + s_{12}n_2^2 + s_{11}n_3^2)$$

Since  $n_1^2 + n_2^2 + n_3^2 = 1$ , we find

$$\frac{\Delta V}{V} = t(s_{11} + 2s_{12})$$

Therefore, the change produced by uniaxial stress in the volume of a cubic crystal is independent of the direction of tensile stress.

7.5. The elastic compliances of quartz crystals were found by measuring the resonance frequency for six differently oriented specimens shown in Fig. 7.1.

The results of measurements are given in the Table 7.1.

Table 7.1

Cut orientation	Vibrational mode	Dimension along the direction of vibrations, mm	Resonance frequency, kHz
X-cut	Longitudinal compression-tension	30.04	89.215
30° X-cut	same	32.18	80.52
—30° X-cut	same	20.00	168.50
60° X-cut	same	20.05	150.00
Y-cut	Face shear	1.60	1453.00
Y-cut	Thickness shear	1.05	1825.00

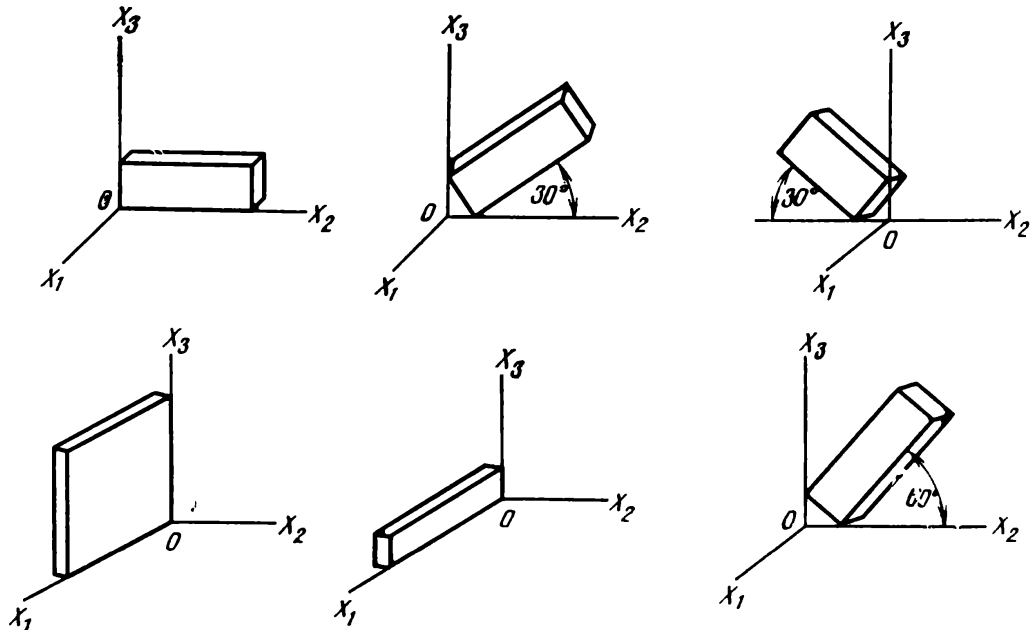
Use the tabulated experimental data to calculate all independent elastic compliances of quartz.

**Solution.** Quartz crystals belong to class 32, so that we have to find six independent elastic compliances (see Table 9):

$$s_{11}, s_{12}, s_{13}, s_{33}, s_{44}, \text{ and } s_{14}$$

The constant  $s_{11}$ , equal to  $s_{22}$  in the case of quartz, is found directly from the data for the X-cut. The equation of piezoelectric excitation of this cut is  $r_2 = s_{22}t_2 + d_{12}E_1$ , so that the resonance frequency of

Fig. 7.1. Orientation of specimens referred to in Problem 7.5.



longitudinal vibrations of the  $X$ -cut elongated in the direction of  $X_2$  is given by the formula  $f_R = 1/(2l \sqrt{\rho s_{22}})$ ; hence,

$$s_{22} = \frac{1}{4f_R^2 l^2 \rho}$$

By substituting the length of the  $X$ -cut (in cm), resonance frequency (in Hz), and the density of quartz (in g/cm<sup>3</sup>) into the above expression, we find

$$s_{22} = 131 \cdot 10^{-14} \text{ cm}^2/\text{dyne} = s_{11}$$

The equation of piezoelectric excitation of long thin specimens of "rotated"  $X$ -cuts whose thickness is along  $X_1$ , and the length is in the direction of  $X'_2$ , is written in the form  $r'_2 = s'_{22} t'_2 + d'_{12} E_1$ , where  $r'_2$ ,  $s'_{22}$ , and  $t'_2$  denote respectively the lengthwise strain, elastic compliance, and mechanical stress in the "rotated"  $X$ -cuts.

The table of direction cosines of the axes related to the edges of these cuts with respect to the crystallophysical axes is as follows:

Table 7.2

Axes	$X_1$	$X_2$	$X_3$
$X'_1$	1	0	0
$X'_2$	0	$\cos \varphi$	$\sin \varphi$
$X'_3$	0	$-\sin \varphi$	$\cos \varphi$

Here  $\varphi = 30^\circ$  for the  $30^\circ$   $X$ -cut,  $\varphi = -30^\circ$  for  $-30^\circ$   $X$ -cut, and  $\varphi = 60^\circ$  for the  $60^\circ$   $X$ -cut. For these cuts

$$\begin{aligned} s'_{22} &= s'_{2222} = C_{2i} C_{2j} C_{2k} C_{2l} s_{ijkl} \\ &= s_{11} \cos^4 \varphi + s_{33} \sin^4 \varphi + 2s_{14} \cos^3 \varphi \sin \varphi + (2s_{13} + s_{44}) \sin^2 \varphi \cos^2 \varphi \end{aligned}$$

(In the case of the  $30^\circ$   $X$ -cut,  $\sin \varphi = 1/2$ ,  $\cos \varphi = \sqrt{3}/2$ .)

As the specimens of the indicated orientations have lengthwise compressional-tensile vibrations along the axis  $X'_2$ , we have  $s'_{22} = 1/4f_R^2 l^2 \rho$ . For the  $30^\circ$   $X$ -cut,  $s'_{22} = 139.6 \cdot 10^{-14} \text{ cm}^2/\text{dyne}$ ; for the  $-30^\circ$   $X$ -cut,  $s'_{22} = 84 \cdot 10^{-14} \text{ cm}^2/\text{dyne}$ ; for the  $60^\circ$   $X$ -cut,  $s'_{22} = 104.5 \cdot 10^{-14} \text{ cm}^2/\text{dyne}$ .

By subtracting the expression for  $s'_{22(+30^\circ)}$  from the expression for  $s'_{22(-30^\circ)}$ , we obtain

$$s'_{22(-30^\circ)} - s'_{22(30^\circ)} = \frac{3}{4} \sqrt{3} s_{14}$$

This yields

$$s_{14} = 42.6 \cdot 10^{-14} \text{ cm}^2/\text{dyne}$$

In order to calculate the other elastic compliances of quartz, shear moduli were found, these were calculated from the known resonance frequencies of thickness shear vibrations and face shear vibrations of  $Y$ -cut specimens. When the field is applied to the working faces of  $Y$ -cut specimens ( $E_1 = E_3 = 0$ ,  $E_2 \neq 0$ ), two types of strain are produced:  $r_5$  ( $r_{13}$ ) and  $r_6$  ( $r_{12}$ ). Both strains are shear strains, the strain  $r_5$  responsible for the deformation of the crystal plate in the plane  $X_1X_3$  is called the *face shear strain*, and the strain  $r_6$  responsible for the deformation of the plate in the  $X_1X_2$  plane is called the *thickness shear strain*, both these modes are excited without difficulties.

By subtracting  $s'_{22(30^\circ)}$  and  $s'_{22(-30^\circ)}$  from  $s'_{22(60^\circ)}$ , we find

$$2s'_{22(60^\circ)} - s'_{22(30^\circ)} - s'_{22(-30^\circ)} = -s_{11} + s_{33} - \frac{\sqrt{3}}{4} s_{14}$$

whence

$$\begin{aligned} s_{33} &= 2s'_{22(60^\circ)} - [s'_{22(-30^\circ)} + s'_{22(30^\circ)}] + s_{11} + \frac{\sqrt{3}}{4} s_{14} \\ &= 98.6 \cdot 10^{-14} \text{ cm}^2/\text{dyne} \end{aligned}$$

Now we can find  $2s_{13} + s_{44}$  by subtracting the terms containing the already determined compliances  $s_{11}$ ,  $s_{33}$ , and  $s_{14}$ , from  $s'_{22(30^\circ)}$ :

$$2s_{13} + s_{44} = \frac{1}{3} (16s'_{22(30^\circ)} - 9s_{11} - s_{33} - 6\sqrt{3}s_{12})$$

The substitution of the numerical values of  $s'_{22(30^\circ)}$ ,  $s_{11}$ ,  $s_{33}$ , and  $s_{13}$  gives

$$2s_{13} + s_{44} = 167.3 \cdot 10^{-14} \text{ cm}^2/\text{dyne}$$

The elastic stiffness  $c_{66}$  can be calculated from the resonance frequency of thickness shear vibrations of an  $Y$ -cut specimen, and the stiffness  $c_{44}$ , from the resonance frequency of face shear vibrations:

$$c_{66} = 4f_R^2 (d^2) \rho = 39 \cdot 10^{10} \text{ dyne/cm}^2$$

$$c_{55} = c_{44} = 4f_R^2 (t^2) \rho = 57.1 \cdot 10^{10} \text{ dyne/cm}^2$$

The transition from stiffnesses  $c_{ij}$  to compliances  $s_{ij}$  is carried out by using relations (7.9a) between these constants.

Let us find the relation between stiffnesses  $c_{44}$  and  $c_{66}$  and compliances  $s_{ij}$ :

$$c_{44} = \frac{s_{11} - s_{12}}{s_{44} (s_{11} - s_{12}) - 2s_{14}^2}, \quad c_{66} = \frac{c_{11} - c_{12}}{2} = \frac{s_{44}}{2s_{44} (s_{11} - s_{12}) 2s_{14}^2}$$

whence

$$s_{44} = \frac{1}{c_{44}} + \frac{2s_{14}^2}{\frac{1}{4c_{66}} + \sqrt{\frac{1}{(4c_{66})^2} + \frac{s_{14}^2 c_{44}}{c_{66}}}}$$

$$(s_{11} - s_{12}) = \frac{1}{4c_{66}} + \sqrt{\frac{1}{(4c_{66})^2} + \frac{s_{14}^2 c_{44}}{c_{66}}}$$

The substitution of the measured quantities into the above expressions gives  $s_{44} = 199.3 \cdot 10^{-14}$ ,  $s_{11} - s_{12} = 145.6 \cdot 10^{-14}$ ,  $s_{12} = -14.10^{-14}$  cm<sup>2</sup>/dyne.

Knowing  $s_{44}$ , we find  $s_{13}$  from the relation

$$2s_{13} + s_{44} = 167.3 \cdot 10^{-14}$$
 cm<sup>2</sup>/dyne

This gives  $s_{13} = -16 \cdot 10^{-14}$  cm<sup>2</sup>/dyne.

The six independent coefficients  $s_{ij}$  for quartz are thus found from six measurements of resonance frequencies of crystal specimens with different orientations:

$$s_{11} = 131 \cdot 10^{-14}, s_{12} = -14 \cdot 10^{-14}, s_{13} = -16 \cdot 10^{-14}$$

$$s_{33} = 98.6 \cdot 10^{-14}, s_{14} = -42.6 \cdot 10^{-14}, s_{44} = 199.3 \cdot 10^{-14}$$

As the measurements were carried out by the dynamic technique the calculated elastic constants refer to adiabatic conditions at constant electric field,  $s_{ijkl}^{E,s}$  (see Sec. 13).

7.6. Elastic compliances of sphalerite were measured at room temperature by the dynamic technique on three differently oriented Z-cut bars shown in Fig. 7.2. The electrodes were applied to the working faces. The averaged results of measurements are listed in Table 7.3.

Table 7.3

Cut orientation (see Fig. 7.2)	Dimensions, mm			Vibration mode	Resonance ( $f_R$ ) and antireson- ance ( $f_A$ ) frequency, kHz	Relative dielectric permitt- ivity of free crystal
	$l$	$t$	$d$			
22.5° Z-cut	20	2.7	1.0	Longitudinal vibrations at fundamental frequency	$f_R = 101.7$	
45° Z-cut	20	2.7	1.0	Same	$f_R = 117$ $f_A = 117.146$	8.37
0° Z-cut	30	6.0	1.0	Face shear vibrations at fundamental frequency	$f_R = 279$	

Making use of the listed data, calculate the elastic compliances of sphalerite.

**Solution.** Sphalerite crystals (point symmetry group  $43m$ ) are characterized by three elastic compliances:  $s_{11}$ ,  $s_{12}$ , and  $s_{44}$ . All these constants can be measured on three differently oriented bars.

As shown in the figure, all three bars are cut perpendicularly to the axis  $X_3$ , that is, to one of the three equivalent crystallophysical axes each of which is a fourfold inversion axis. The lengths of the first two bars, the so-called "rotated" Z-cuts, are chosen to be larger than their width and thickness. Sphalerite crystals are piezoelectric, so that ac electric field applied to the working faces generates in them lengthwise compressional-tensile vibrations; the longer axis of the bar is taken for the axis  $X'_1$ . In this case, the elastic compliance of the plates is  $s'_{11}$ . According to (6.23), the resonance frequency of longitudinal vibrations at the fundamental frequency is

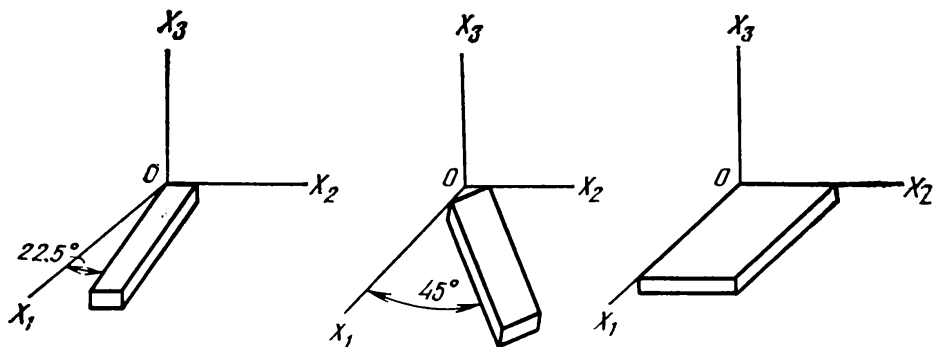
$$f_R = \frac{1}{2l \sqrt{\rho s'_{11}}}$$

Consequently, the measured resonance frequencies of such bars directly yield the compliances  $s'_{11}$ . The orientation of the axes  $X'_1$ ,  $X'_2$ ,  $X'_3$ , fixed to the edges of the "rotated" Z-cut bars, is given by the following table of direction cosines, with respect to the crystallophysical axes of sphalerite:

Table 7.4

Axes	$X_1$	$X_2$	$X_3$
$X'_1$	$\cos \varphi$	$\sin \varphi$	0
$X'_2$	$-\sin \varphi$	$\cos \varphi$	0
$X'_3$	0	0	1

Fig. 7.2. Orientation of specimens referred to in Problem 7.6.



The elastic compliance  $s'_{11}$  along the length of the "rotated" Z-cut bars can be found from Eq. (7.2a) which, in our case, takes the form

$$s'_{11} = s_{11} (\cos^4 \varphi + \sin^4 \varphi) + (2s_{12} + s_{44}) \sin^2 \varphi \cos^2 \varphi$$

The compliance  $s_{44}$  is found from the data on the  $0^\circ$  Z-cut plate whose length is much larger than its width. The vibrations excited in such a plate are the face shear vibrations. The resonance frequency of face shear vibrations is given by the formula

$$f_R = \frac{1}{2t} \sqrt{\frac{c_{66}}{\rho}}$$

where  $t$  is the plate width.

In cubic crystals  $c_{66} = c_{44} = 1/s_{44}$ ; hence,

$$s_{44} = \frac{1}{(2tf_R)^2 \rho}$$

By using these relations, as well as the experimental and reference data, one can calculate all elastic compliances of sphalerite.

The values of  $s'_{11}$  will be found from the formula for resonance frequencies of longitudinally vibrating "rotated" Z-cut bars:

$$s'_{11} = \frac{1}{(2lf_R)^2 \rho}$$

whence

$$s'_{11(22.5^\circ)} = 14.73 \cdot 10^{-13} \text{ cm}^2/\text{dyne}$$

$$s'_{11(45^\circ)} = 11.08 \cdot 10^{-13} \text{ cm}^2/\text{dyne}$$

On the other hand,

$$s'_{11} = s_{11} (\cos^4 \varphi + \sin^4 \varphi) + (2s_{12} + s_{44}) \sin^2 \varphi \cos^2 \varphi$$

for the  $22.5^\circ$  Z-cut,  $\sin \varphi = 0.3827$ ,  $\cos \varphi = 0.9239$ , and  $s'_{11} = 0.75s_{11} + 0.125(2s_{12} + s_{44})$ ; for the  $45^\circ$  Z-cut,  $\sin \varphi = \cos \varphi = 0.7071$ , and  $s'_{11} = 0.5s_{11} + 0.25(2s_{12} + s_{44})$ .

By solving these equations for  $s_{11}$  and  $2s_{12} + s_{44}$ , we find

$$s_{11} = 2s'_{11(22.5^\circ)} - s'_{11(45^\circ)} = 18.42 \cdot 10^{-13} \text{ cm}^2/\text{dyne}$$

$$2s_{12} + s_{44} = 6s'_{11(45^\circ)} - 4s'_{11(22.5^\circ)}$$

To find  $s_{44}$ , we use the data for the  $0^\circ$  Z-cut:

$$s_{44} = \frac{1}{(2 \cdot 0.6 \cdot 279 \cdot 10^3)^2 \cdot 4.102} = 21.7 \cdot 10^{-13} \text{ cm}^2/\text{dyne}$$

Next we find

$$s_{12} = \frac{(7.56 - 21.7) \cdot 10^{-13}}{2} = -7.07 \cdot 10^{-13} \text{ cm}^2/\text{dyne}$$

The elastic compliances of sphalerite are, therefore,  
 $s_{11} = 18.42 \cdot 10^{-13}$ ,  $s_{12} = -7.07 \cdot 10^{-13}$ ,  $s_{44} = 21.7 \cdot 10^{-13}$  CGSE units

#### PROBLEMS

7.7. Into what groups of components, similar in their physical meaning, can the matrix of elastic compliances ( $s_{ij}$ ) for triclinic crystals be divided?

7.8. Using Table 9, answer the following questions:

(i) What should be the symmetry of crystals undergoing shear strain under the action of uniform compression?

(ii) Is it possible for uniform compression to change only the shape of a crystal specimen without affecting its volume?

7.9. Using the direct inspection method, show that the matrix ( $s_{ij}$ ) for the crystals of KDP group has six independent components.

7.10. A compressional stress of  $1500 \text{ N/cm}^2$  is applied along one of the twofold axes of a sodium chlorate crystal.

Calculate the strain suffered by the crystal along the directions of the type [111].

7.11. A sodium chlorate crystal is subjected to a uniaxial tensile stress of  $10^4 \text{ N/cm}^2$  in an arbitrary direction.

What should be the increment in temperature in order for the relative change in the volume of this crystal to be the same as in the case of the strain caused by the indicated uniaxial tension?

7.12. As a result of the converse piezoelectric effect, an  $L$ -cut ADP plate (see Fig. 2.4) undergoes a compressional thickness strain equal to  $6 \cdot 10^{-3}$ . Describe the stressed state of the plate in the crystallophysical coordinate system.

7.13. Calculate the bulk compressibility of tourmaline and rochelle salt crystals; compare these compressibilities.

7.14. Find Young's modulus along the crystallophysical axes  $X_1$  and  $X_3$ , as well as along the length of an ADP  $45^\circ$  Z-cut bar (see Fig. 6.3).

7.15. Derive the equation of the magnitude quadratic of the compliance  $s'_{33}$  (the quantity reciprocal of Young's modulus) for quartz crystals. What is the shape of the section of this surface by the plane  $X_1X_2$ ?

7.16. Derive the equation of the magnitude quadratic of the compliance  $s'_{33}$  (the quantity reciprocal to Young's modulus) for wurtzite crystals. What can be said about the symmetry of this surface?

7.17. An  $X$ -cut quartz plate of  $1 \times 1 \times 0.3 \text{ cm}^3$  (see Fig. 2.3) is compressed by a force of 800 N, applied to the working faces of the plate. Find the work of deformation.

7.18. A  $1 \times 1 \times 1 \text{ cm}^3$  cube is cut from a quartz crystal. The cube is subjected to uniform compressional stress of  $500 \text{ N/cm}^2$ . Calculate the change in the internal energy of the deformed cube.

7.19. Find the energy of deformation of a single crystal silicon cube subjected to uniaxial compression along the direction with direction cosines  $(0.705, 0.705, 0)$  with respect to crystallophysical coordinate system. The compressional stress is  $400 \text{ N/cm}^2$ .

7.20. Show that the reciprocal of compressibility in cubic crystals is related to elastic stiffnesses by the formula

$$\frac{1}{\beta} = \frac{c_{11} + 2c_{12}}{3}$$

7.21. Show that the following relation holds for crystals belonging to symmetry class  $4/mmm$ :  $c_{11} - c_{12} = 1/(s_{11} - s_{12})$ .

7.22. Show that in cubic crystals the elastic stiffness  $c_{11}$  is related to the elastic compliances  $s_{11}$  and  $s_{12}$  by the formula

$$c_{11} = \frac{s_{11} + s_{12}}{(s_{11} - s_{12})(s_{11} + 2s_{12})}$$

7.23. Which of the elastic compliances can be found from measurements of the bulk compression  $\Delta V/V$  and of the longitudinal strain of a wurtzite specimen compressed along  $[0001]$ ?

7.24. A single-crystal silicon specimen is subjected to compressional stress  $1.5 \cdot 10^3 \text{ N/cm}^2$  along  $[100]$ ; the longitudinal strain produced in the specimen was  $1.13 \cdot 10^{-4}$ . The specimen was then subjected to hydrostatic pressure of  $10^4 \text{ N/cm}^2$ ; this generated a relative reduction of volume of  $1.1 \cdot 10^{-3}$ . Which of the constants  $s_{ij}$  can be found from these experimental results?

7.25. Two specimens shaped into elongated parallelepipeds with square cross section were made from polarized barium titanate ceramic in order to measure its elastic constants (Fig. 7.3). In both cases the axis of polarization of the ceramic was the axis  $X_3$ , and the uniaxial compressional stress acted along the normal to the square cross section of the specimens. Which of the constants characterizing the elastic properties of the ceramic can be calculated from the measured longitudinal strain and volumetric compression of the specimens?

7.26. Which of the elastic constants of quartz can be calculated from the measurements of strain suffered by the edges of a bar, loaded lengthwise, whose geometry is shown in Fig. 7.3 on the left?

7.27. The constants necessary to characterize the elastic properties of a cubic crystal were found by measuring the resonance frequencies of three specimens with different orientations, as shown in Fig. 7.2.

The averaged measurement data are listed in Table 7.5.

Find which of the coefficients can be determined from the measurement data, and calculate their values.

Table 7.5

Cut orientation	Dimensions, mm			Vibrational mode	Resonance frequency, kHz
	<i>l</i>	<i>t</i>	<i>d</i>		
22.5° Z-cut	20.1	2.69	1.0	Longitudinal vibrations at fundamental frequency	95.976
45° Z-cut	20.38	2.7	1.01	Same	89.205
0° Z-cut	29.9	6.02	1.01	Face shear vibrations at fundamental frequency	180.398

7.28. Show that the relative change in volume,  $\Delta V/V$ , of a cubic crystal is independent of the direction of uniaxial tension.

7.29. Show that the plane (0001) in crystals belonging to symmetry class 6mm is the plane of elastic isotropy with respect to the elastic properties.

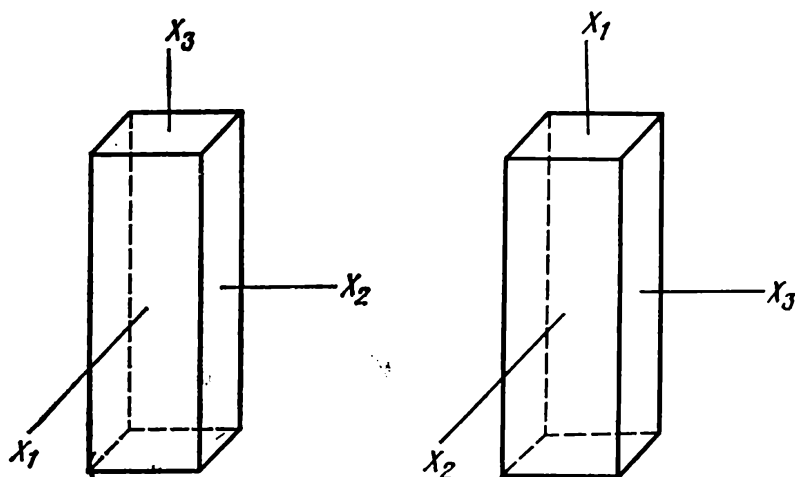
7.30. Show that with respect to elastic properties, crystals belonging to the hexagonal system have a symmetry axis of infinite order.

7.31. Show that with respect to elastic properties, the symmetry axis 2 is equivalent to a symmetry plane perpendicular to this axis.

7.32. Find the maximum values of admissible elastic compressional strains for KCl if the corresponding elastic limit (proportionality limit) for uniaxial compression along [100] is 800 N/cm<sup>2</sup>.

7.33. Find the maximum admissible values of electric fields used to excite a piezoelectric transducer made of KDP crystal if the mechanical strength of this crystal is 120 N/cm<sup>2</sup>. Analyze the *L*-cut.

Fig. 7.3. Orientation of specimens referred to in Problem 7.25.



7.34. Calculate the stresses acting in a  $45^\circ$  Z-cut rochelle salt plate (Fig. 6.3) in the electric field of  $10^3$  V/cm applied to its working faces.

7.35. Which of the elastic compliances of ADP crystals can be found by measuring the resonance frequency of longitudinally vibrating  $22.5^\circ X$ -,  $45^\circ X$ -, and  $67.5^\circ X$ -cut bars?

7.36. A single-crystal silicon specimen is compressed by a stress  $1.5 \cdot 10^7$  N/m<sup>2</sup> along [100]; the longitudinal strain thus produced was  $1.13 \cdot 10^{-4}$ . The specimen was then subjected to hydrostatic pressure of  $10^7$  N/m<sup>2</sup>, and the relative change in volume was  $1.1 \cdot 10^{-3}$ . Which of the compliances  $s_{ij}$  can be found from these measurements?

7.37. Find the strains of specimens made of polarized barium titanate ceramic, whose orientation is shown in Fig. 6.7, under the action of stresses given in Problem 6.46.

7.38. Derive the expression for the temperature coefficient of frequency of cubic crystals. Analyze the derived expression and determine the cases in which zero temperature coefficient of frequency  $f_T$  is possible in cubic piezoelectric materials (for solving Problems 7.38-7.43, see Sec. 6).

7.39. Calculate the temperature coefficient of frequency for a longitudinally vibrating  $X$ -cut quartz bar.

7.40. Find the relative change in the resonance frequency of an  $X$ -cut quartz bar caused by heating it to  $60^\circ\text{C}$ . The bar length is 15 mm.

7.41. Find the admissible temperature variations for a longitudinally vibrating  $X$ -cut quartz oscillator if the relative variation of its frequency,  $\Delta f/f$ , must not exceed  $10^{-4}$ .

7.42. A normal to the working face of an  $X$ -cut quartz bar lies in the coordinate plane  $X_1X_3$  and is at the angle of  $5^\circ$  to the axis  $X_1$ . Find the temperature coefficient of frequency for this oscillator.

7.43. Calculate the relative variation of resonance frequency of the oscillator described in Problem 7.42 in the  $-60^\circ\text{--}+60^\circ\text{C}$  temperature range.

## 8. PIEZORESISTIVITY IN SEMICONDUCTOR CRYSTALS

Piezoresistivity constitutes a variation in the electric resistivity of crystals, produced by applied mechanical stresses. This effect is to a smaller or larger extent inherent to most crystals, and is maximal in semiconductors.

In the absence of mechanical stresses, Ohm's law for crystals is

$$E_i = \rho_{ii} j_i \quad (8.1)$$

where  $E_i$  and  $j_i$  are the components of the electric field vector and the current density, respectively, and  $\rho_{ii}$  are the components of the resistivity tensor in the absence of mechanical stresses.

When mechanical stresses act on a crystal, its resistivity is changed, and Ohm's law takes the form

$$E_i = (\rho_{ii} + \Delta\rho_{ii}) j_i \quad (8.2)$$

If mechanical stresses are small, the increment  $[\Delta\rho_{ii}]$  to the resistivity tensor is a linear function of stress, that is

$$\Delta\rho_{ii} = P_{ilmn} t_{mn} \quad (8.3)$$

where  $P_{ilmn}$  are the coefficients forming a rank four tensor.

Equation (8.2) now takes the form

$$E_i = (\rho_{ii} + P_{ilmn} t_{mn}) j_i$$

Usually the piezoresistive properties of crystals are described by the tensor of piezoresistivities  $\Pi_{klmn}$  which is related to the tensor  $P_{ilmn}$ :

$$P_{ilmn} = \rho_{ik}^0 \Pi_{klmn} \quad (8.4)$$

so that the equation of piezoresistivity takes the form

$$E_i = \rho_{ik}^0 (\delta_{kl} + \Pi_{klmn} t_{mn}) j_i \quad (8.5)$$

In the crystals of cubic system comprising most of the semiconductor crystals employed as piezoresistors,  $\rho_{ik}^0 = \rho^0 \delta_{ik}$  and

$$E_k = \rho^0 (\delta_{kl} + \Pi_{klmn} t_{mn}) j_l \quad (8.6)$$

Another aspect of piezoresistivity, namely, the dependence of resistivity on strain,  $r_{pg}$  is described by the equation

$$E_i = \rho_{ik}^0 (\delta_{kl} + m_{klpg} r_{pg}) j_l \quad (8.7)$$

The components of the tensor of elastoresistivity,  $m_{klpg}$ , are related to the components of the tensor of piezoresistivity:

$$m_{klpg} = \Pi_{klmn} c_{mnpq}, \quad \Pi_{klmn} = m_{klpg} s_{pgmn} \quad (8.8)$$

in which  $c_{mnpq}$  are the elastic stiffnesses, and  $s_{pgmn}$  are the elastic compliances.

*Matrix notation.* As the tensors  $[\rho_{kl}]$ ,  $[t_{mn}]$ , and  $[r_{pg}]$  are symmetrical in subscripts, the components of the tensors of piezoresistivities and elastoresistivities are symmetrical in the first and second pairs of subscripts:

$$\Pi_{klmn} = \Pi_{lkmn} = \Pi_{klnm} = \Pi_{lknm} \quad (8.9)$$

These tensors can be written in the two-subscript notation: usually  $\Pi_{\lambda\mu}$  are related to  $\Pi_{klmn}$  as follows:

$$\Pi_{\lambda\mu} = \begin{cases} \Pi_{klmn} (\lambda = 1, \dots, 6, \mu = 1, 2, 3) \\ 2\Pi_{klmn} (\lambda = 1, \dots, 6, \mu = 4, 5, 6) \end{cases} \quad (8.10)$$

and  $m_{\lambda\nu}$  to  $m_{klpg}$  by

$$m_{\lambda\nu} = m_{klpg} (\lambda = 1, \dots, 6; \nu = 1, \dots, 6) \quad (8.11)$$

*Crystal symmetry and the number of independent piezoresistivities.* By virtue of the symmetry of the coefficients  $\Pi_{\mu\nu}$  and  $m_{\mu\nu}$  with respect to  $\mu$  and  $\nu$ , the number of independent coefficients in the general case is 36. The symmetry of a crystal reduces this number. The matrices of piezoresistivities in crystals belonging to different crystallographic classes and the values of piezoresistivities in a number of semiconductors crystals are listed in Tables 10 and 14.

*Longitudinal, transverse, and shear piezoresistivity.* Let a uniaxial mechanical stress act on a crystal evincing piezoresistivity.

If the directions of the current and electric field coincide with that of the mechanical stress (Fig. 8.1a), the change induced in the resistivity of the crystal is called the *longitudinal piezoresistive effect*.

If the directions of the current and the field are perpendicular to the direction of the mechanical stress (Fig. 8.1b), this effect is called *transverse*. Thus, for example, in the case of uniaxial stress along the axis  $X_1$  the coefficient  $\Pi_{11}$  represents the longitudinal effect, and the coefficients  $\Pi_{12}$  and  $\Pi_{13}$  represent the transverse effects.

A change in the resistivity of a crystal produced by shear stresses is called the *shear piezoresistive effect*. The shear coefficients  $\Pi_{14}$ ,  $\Pi_{24}$ ,  $\Pi_{34}$  describe the variation of resistivity produced by a shear stress  $t_4$  in the case when the directions of the electric field and current coincide; the coefficient  $\Pi_{44}$  characterizes the change in resistivity induced by the same stress  $t_4$  in the case when the field is parallel to the axis  $X_2$ , and the current density, to the axis  $X_3$ .

*Piezoresistive effect as a function of direction in the crystal.* In most cases the maximum value of the longitudinal, transverse, or shear piezoresistive effect is not related to the direction of crystallophysical axes. In order to find the directions corresponding to the extremal values of piezoresistivities, we can use the appropriate transformation law:

$$\Pi'_{ijkl} = C_{im} C_{jn} C_{kp} C_{lg} \Pi_{mnpq} \quad (8.12)$$

and analyze this expression for extrema. Here  $C_{im}$ ,  $C_{jn}$ ,  $C_{kp}$ , and  $C_{lg}$  are the direction cosines defining the orientation of the axes  $X'_1$ ,  $X'_2$ ,  $X'_3$  with respect to the crystallophysical axes with which the constants  $\Pi_{mnpq}$  are related.

*Transducers operating in the longitudinal, transverse, and shear piezoresistivity modes.* Single-crystal transducers of this type are thin oriented rods or bars whose length lies along the direction of the maximum longitudinal piezoresistivity for a given crystal (Fig. 8.2). Assume that a specimen whose length direction  $\mathbf{n}$  coincides with the direction  $X'_1$  is subjected to a mechanical stress. If  $j_2 = j_3 = 0$ ,

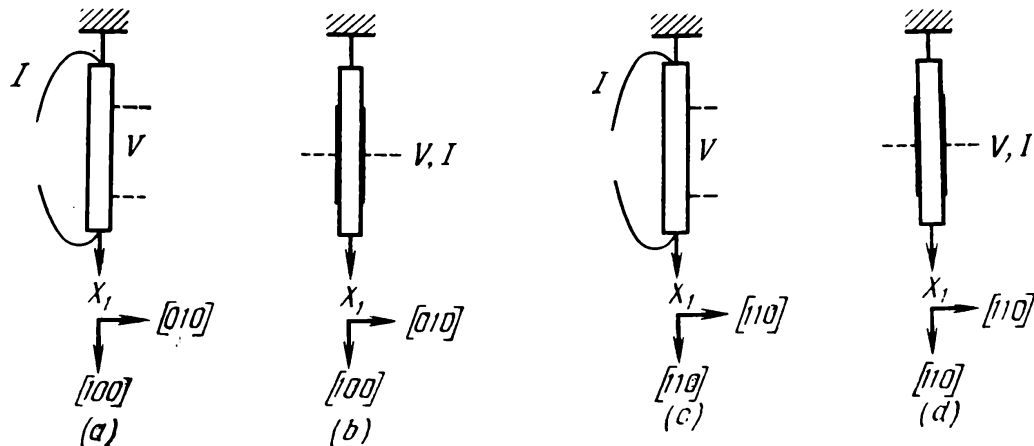
$$E'_1 = j'_1 (1 + \Pi'_{11} t'_1) \rho \quad (8.13)$$

Since  $E'_1 = j'_1 (\rho + \Delta\rho)$ ,

$$\Delta\rho/\rho = \Pi'_{11} t'_1 \text{ or } \Delta\rho/\rho = \Pi_n t_n \quad (8.14)$$

where  $\Pi_n$  is the magnitude of the longitudinal piezoresistivity along  $\mathbf{n}$ . As follows from (8.14), the constant  $\Pi_n$  can be termed the voltage sensitivity factor ( $\Pi_n = \Delta\rho/\rho t$ ).

Fig. 8.1. Schematic representation of the longitudinal and transverse piezoresistivity effect.



One of the most important characteristics of the discussed transducers is the *stress sensitivity factor*  $K$  defined by

$$K = \frac{\Delta R}{Rr} \quad (8.15)$$

where  $\frac{\Delta R}{R}$  and  $r$  are the increment in resistivity and strain, respectively, measured lengthwise.

As follows from (8.15), the factor  $K$  characterizes the sensitivity of a transducer to strain.

Taking Hook's law into account, we find that

$$K = \frac{\Delta R}{R t_n s_n} = \Pi_n E_n$$

where  $t_n$  is the stress acting along the length of the transducer, that is, along  $n$ , and  $s_n$  and  $E_n$  are the elastic compliance and Young's modulus, respectively, along the length of the transducer.

For crystals belonging to the cubic system,

$$s_n = s_{11} - 2 \left( s_{11} - s_{12} + \frac{1}{2} s_{44} \right) (n_1^2 n_2^2 + n_2^2 n_3^2 + n_3^2 n_1^2) \quad (8.16)$$

Since for semiconductor crystals  $\Pi_{44} \neq 0$ , the crystals can be used to measure shear stresses and torques.

Transducers for measuring strains in a free surface are based on the transverse and shear effects. A schematic representation of such a transducer is shown in Fig. 8.3. Three measurements are required for a complete determination of strains: measurement of resistivity in two perpendicular directions (for example, along  $X'_1$  and  $X'_2$ ), provided the currents in transverse directions are zero, and measure-

Fig. 8.2. Semiconductor stress transducer operating in the longitudinal piezoelectricity mode.

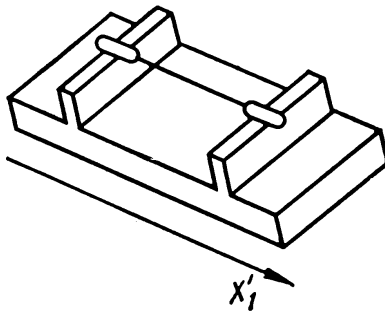
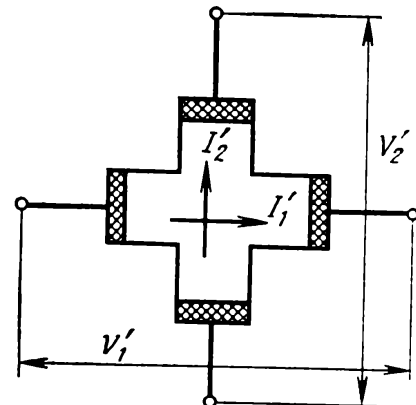


Fig. 8.3. Stress transducer measuring the sum of stresses in a plane.



ment, say, of  $V'_2/I'_1$  for  $I'_2 = 0$ . Evidently, the results of these three measurements can yield strains in two perpendicular directions and a shear strain in the plane tangent to the surface.

### Examples of Problems with Solutions

**8.1.** Relative strains in various structural elements are usually measured with germanium or silicon transducers made of thin oriented rods operating in the longitudinal piezoresistivity mode. Derive the expression for the longitudinal piezoresistivity of such transducers with an arbitrary orientation. What should be the orientation of *p*- and *n*-type germanium transducers and *n*-type silicon transducers giving the maximum longitudinal effect?

**Solution.** Let  $\mathbf{n}$  ( $n_1, n_2, n_3$ ) lie lengthwise of the transducer. Directing the axis  $X'_1$  along  $\mathbf{n}$ , we find from (8.12) that the longitudinal piezoresistivity is given by the constant

$$\Pi_{\mathbf{n}} = \Pi'_{11} = \Pi'_{1111} = C_{1i} C_{1j} C_{1k} C_{1l} \Pi_{ijkl} = n_i n_j n_k n_l \Pi_{ijkl}$$

By substituting the nonzero constants  $\Pi_{ijkl}$  for symmetry class  $m3m$  (comprising germanium and silicon crystals) into the above expression, we obtain

$$\Pi'_{11} = (n_1^4 + n_2^4 + n_3^4) \Pi_{11} + 2(\Pi_{12} + \Pi_{44}) (n_1^2 n_2^2 + n_3^2 n_1^2 + n_2^2 n_3^2)$$

$$\text{where } \Pi_{44} = 2\Pi_{2323} = 2\Pi_{3131} = 2\Pi_{1212}.$$

Raising the expression  $n_1^2 + n_2^2 + n_3^2 = 1$  to the second power, we find

$$n_1^4 + n_2^4 + n_3^4 = 1 - 2(n_1^2 n_2^2 + n_3^2 n_1^2 + n_2^2 n_3^2)$$

Taking this into account, we can write for  $\Pi'_{11}$

$$\begin{aligned} \Pi'_{11} &= \Pi_{11} - 2(\Pi_{11} - \Pi_{12} - \Pi_{44})(n_1^2 n_2^2 + n_3^2 n_1^2 + n_2^2 n_3^2) \\ &= \Pi_{11} - 2\Pi_A (n_1^2 n_2^2 + n_3^2 n_1^2 + n_2^2 n_3^2) \end{aligned}$$

$$\text{where } \Pi_A = \Pi_{11} - \Pi_{12} - \Pi_{44}.$$

In order to find the range of variation of  $\Pi'_{11}$ , it is necessary to find the range of variation of  $(n_1^2 n_2^2 + n_3^2 n_1^2 + n_2^2 n_3^2)$ . This expression varies from 0 to  $1/3$ , so that  $\Pi'_{11}$  varies from  $\Pi_{11}$  to  $\Pi_{11} - \frac{2}{3}\Pi_A$ .

The extremum  $\Pi'_{11} = \Pi_{11}$  corresponds to three directions  $\{100\}$ , and the extremum  $\Pi'_{11} = \Pi_{11} - \frac{2}{3}\Pi_A$  corresponds to eight directions.

The maximum and minimum values of  $\Pi'_{11}$  depend on the signs of  $\Pi_{11}$  and  $\Pi_A$ . For *p*- and *n*-type germanium transducers the maximum values of  $\Pi'_{11}$  correspond to directions  $\langle 111 \rangle$ , and for *n*-type silicon transducers, to the directions  $\langle 100 \rangle$  (see Table 14).

Therefore, *n*- and *p*-type germanium transducers must be oriented along  $\langle 111 \rangle$  and *n*-type silicon transducers, along  $\langle 100 \rangle$ .

8.2. Calculate the change in the resistivity of a filament-shaped *n*-type silicon piezoresistive transducer of  $6 \times 1 \times 1 \text{ mm}^3$ , oriented along [100] and operating in the longitudinal piezoresistivity mode, for a 0.05% strain (i) as a result of the change in resistivity, and (ii) as a result of changing geometrical dimensions.

Calculate the stress sensitivity factor and the output signal for a 0.05% strain, if the dc current through the transducer is 5 A.

**Solution.** (i) All stresses, with the exception of the longitudinal stress  $t_1$ , vanish in a semiconductor stress transducer shaped into a thin rod oriented along [100]. Strains corresponding to this stress are

$$r_1 = s_{11}t_1, \quad r_2 = s_{21}t_1, \quad r_3 = s_{31}t_1$$

The transducer operates in the longitudinal effect mode, so that  $j_2 = j_3 = 0$ ,  $E_2 = E_3 = 0$ , and according to (8.6)

$$E_1/\rho = j_1 (1 + \Pi_{11}t_1) = j_1 \left( 1 + \frac{\Pi_{11}r_1}{s_{11}} \right)$$

The relative change in the resistivity of the transducer is

$$\Delta\rho/\rho = \Pi_{11}t_1 = \Pi_{11}r_1/s_{11}$$

For *n*-type silicon,  $\rho = 11.7 \text{ ohm}\cdot\text{cm}$ ,  $\Pi_{11} = 102.2 \cdot 10^{-12} \text{ cm}^2/\text{dyne}$ ,  $s_{11} = 0.768 \cdot 10^{-12} \text{ cm}^2/\text{dyne}$ , and for the strain  $r_1 = 5 \cdot 10^{-4}$ ,  $\Delta R/R = \Delta\rho/\rho = 0.665$ .

(ii) The relative change in the resistance of a piezoresistivity transducer due to a change in its dimensions is

$$\frac{\Delta R}{R} = \left( 1 - \frac{s_{21} + s_{31}}{s_{11}} \right) r_1 = \left( 1 - \frac{2s_{12}}{s_{11}} \right) r_1$$

The first term in the parentheses appears as a result of elongation of the specimen, and the term  $(-s_{21} + s_{31})/s_{11}$  appears as a result of a change in the cross-sectional area; numerically

$$\frac{\Delta R}{R} = \left( 1 + \frac{0.428}{0.768} \right) \cdot 5 \cdot 10^{-4} = 0.008$$

The total change in the resistance of a filament-shaped piezoresistivity transducer oriented along [100] is

$$\frac{\Delta R}{R} = (1 - 2s_{12}/s_{11} + \Pi_{11}) r_1 = r_1$$

As follows from the calculations for thin silicon transducers, the main contribution to the resistance increment (99% in the present case) results from a change in its resistivity. The same is true for other semiconductor piezoresistance transducers of this type.

The stress sensitivity factor of the transducer is

$$K = \frac{\Delta R}{Rr} = 1 - \frac{2s_{12}}{s_{11}} + \Pi_{11} + \frac{1}{s_{11}} \approx \Pi_{11} \cdot \frac{1}{s_{11}} \approx -133$$

The output signal for  $5 \cdot 10^{-4}$  strain is

$$|V| = I\Delta R = IR \frac{\Delta \rho}{\rho} = I\rho \frac{l}{s} \frac{\Pi_{11}}{s_{11}} r_1 \approx 2.3 \text{ V}$$

8.3. Derive the expression for calculating the transverse piezoresistivity effect in semiconductor crystals belonging to symmetry classes  $m3m$  and  $43m$ , in an arbitrary direction. Find extremal values of transverse piezoresistivities, and the extremal directions corresponding to them.

**Solution.** The transverse piezoresistivity is described by coefficients  $\Pi_{ij}$ , where  $i \neq j$ ,  $i, j = 1, 2, 3$ .

If the mechanical stress acts along the axis  $X_2$ , and the current density and field vectors are parallel to the axis  $X_1$ , the effect is represented by the coefficient  $\Pi_{12}$ . Consider the case when a uniaxial mechanical stress acts in the direction  $\mathbf{n}$  ( $n_1, n_2, n_3 \parallel X'_2$ ), and the current and field are in the direction  $\mathbf{l}$  ( $l_1, l_2, l_3 \parallel X'_1$ ). In this case

$$\begin{aligned} \Pi'_{12} = \Pi'_{1122} &= l_i l_j n_h n_l \Pi_{ijkl} = \Pi_{11} (n_1^2 l_1^2 + n_2^2 l_2^2 + n_3^2 l_3^2) \\ &+ \Pi_{12} (n_1^2 l_1^2 + n_2^2 l_1^2 + n_1^2 l_3^2 + n_3^2 l_1^2 + n_2^2 l_3^2 + n_3^2 l_2^2) \\ &+ 2\Pi_{44} (n_2 n_3 l_2 l_3 + n_1 n_3 l_1 l_3 + n_1 n_2 l_1 l_2) \end{aligned}$$

In order to simplify the expression for  $\Pi'_{12}$ , make use of the squared condition of orthogonality of the vectors  $\mathbf{n}$  and  $\mathbf{l}$ :

$$\begin{aligned} (n_1 l_1 + n_2 l_2 + n_3 l_3)^2 &= 0 \text{ or } n_1^2 l_1^2 + n_2^2 l_2^2 + n_3^2 l_3^2 \\ &+ 2(n_1 n_2 l_1 l_2 + n_1 n_3 l_1 l_3 + n_2 n_3 l_2 l_3) = 0 \end{aligned}$$

and of the fact that  $\mathbf{n}$  and  $\mathbf{l}$  are unit vectors:

$$(n_1^2 + n_2^2 + n_3^2)(l_1^2 + l_2^2 + l_3^2) = 1$$

With these relations taken into account, we find the following expression for  $\Pi'_{12}$ :

$$\Pi'_{12} = \Pi_{12} + \Pi_A (n_1^2 l_1^2 + n_2^2 l_2^2 + n_3^2 l_3^2), \text{ where } \Pi_A = \Pi_{11} - \Pi_{12} - \Pi_{44}$$

The extremum values of  $\Pi'_{12}$  are determined by the sum  $n_1^2 l_1^2 + n_2^2 l_2^2 + n_3^2 l_3^2$ , whose minimum is apparently zero. This corresponds to the following directions of  $\mathbf{n}$  and  $\mathbf{l}$ :

$\mathbf{n}$	$\mathbf{l}$	$\mathbf{n}$	$\mathbf{l}$
$(1, 0, 0)$	$(0, l_2, l_3)$	$(0, n_2, n_3)$	$(1, 0, 0)$
$(0, 1, 0)$	$(l_1, 0, l_3)$ or $(n_1, 0, n_3)$	$(0, 1, 0)$	
$(0, 0, 1)$	$(l_1, l_2, 0)$	$(n_1, n_2, 0)$	$(0, 0, 1)$

To find the maximum value of the sum  $n_1^2 l_1^2 + n_2^2 l_2^2 + n_3^2 l_3^2$ , we use the method of the Lagrange multipliers, constructing a function

$$f = (n_1^2 l_1^2 + n_2^2 l_2^2 + n_3^2 l_3^2) - \lambda_1 (n_1^2 + n_2^2 + n_3^2 - 1) - \lambda_2 (l_1^2 + l_2^2 + l_3^2 - 1) - \lambda (n_1 l_1 + n_2 l_2 + n_3 l_3)$$

By differentiating  $f$  with respect to  $n_i$  and  $l_i$  and equating the derivatives to zero, we obtain

$$\frac{\partial f}{\partial n_i} = 2n_i l_i^2 - 2\lambda_1 n_i - \lambda l_i = 0$$

$$\frac{\partial f}{\partial l_i} = 2l_i n_i^2 - 2\lambda_2 l_i - \lambda n_i = 0$$

Multiplying  $\partial f / \partial n_i$  by  $n_i$ ,  $\partial f / \partial l_i$  by  $l_i$ , and comparing the obtained expressions, we find  $n_i^2 = l_i^2$ , or  $n_i = \pm l_i$ . The expression  $n_1 l_1 + n_2 l_2 + n_3 l_3 = 0$  now takes the form

$$\pm n_1^2 \pm n_2^2 \pm n_3^2 = 0$$

The choice of only positive or only negative signs with all  $n_1$ ,  $n_2$ ,  $n_3$  does not satisfy the normalization of the vector  $\mathbf{n}$ . Consider one of the six remaining combinations of signs, for instance,  $n_1^2 - n_2^2 + n_3^2 = 0$ . By subtracting this equality from the normalization condition for  $\mathbf{n}$ , we find

$$n_2^2 = \frac{1}{2}, \quad n_2 = \pm \frac{1}{\sqrt{2}}$$

In addition,

$$\mathbf{n} = \left( n_1; \pm \frac{1}{\sqrt{2}}; n_3 \right), \quad \mathbf{l} = \left( n_1; \pm \frac{1}{\sqrt{2}}; n_3 \right)$$

and  $n_2^2 l_1^2 + n_2^2 l_2^2 + n_2^2 l_3^2 = n_1^4 + 1/4 + n_3^4$ . Taking into account that  $n_1^2 + n_3^2 = 1/2$ , we find that the maximum of  $\Pi'_{12}$  corresponds to the directions of the type  $\mathbf{n} \left( \frac{1}{\sqrt{2}}, \frac{1}{\sqrt{2}}, 0 \right)$ ,  $\mathbf{l} \left( \frac{1}{\sqrt{2}}, -\frac{1}{\sqrt{2}}, 0 \right)$  (there are six such directions altogether) and is equal to  $-1/2$ . The transverse effect coefficient varies, therefore, from  $\Pi_{12}$  to  $\Pi_{12} + (1/2) (\Pi_{11} - \Pi_{12} - \Pi_{44})$ , and its maximum and minimum values depend on the sign of  $(\Pi_{11} - \Pi_{12} - \Pi_{44})$ .

8.4. Single-crystal  $p$ -PbTe specimens with carrier concentration  $1-3 \cdot 10^{18} \text{ cm}^{-3}$  and cross section  $10^{-2} \text{ cm}^2$  were prepared to determine piezoresistivities (symmetry class  $m3m$ ). The orientation of the cuts and the schematic of the experiment are shown in Fig. 8.1. When the specimens were compressed by 9.8 N, the dc resistivity of the first, second, and third specimens (Figs. 8.1a, b and c, respectively) decreased by 0.24%, 0.15%, and 1.27%, respectively. Calculate the piezoresistivities of  $p$ -PbTe crystals.

**Solution.** As shown by Fig. 8.1, the effects used are the longitudinal effect in the first and third specimens (the directions of field and current coincide with that of the mechanical stress), and the transverse effect in the case of the second specimen (field and current are perpendicular to the stress).

The piezoresistive properties of lead telluride are described by three independent coefficients  $\Pi_{11}$ ,  $\Pi_{12}$ , and  $\Pi_{44}$ , while resistivity is a scalar. In the first specimen (Fig. 8.1a)  $t_1 = -t$ ,  $t_2 = t_3 = 0$ ,  $j_1 = j$ ,  $j_2 = j_3 = 0$ ,  $E_1 = E$ ,  $E_2 = E_3 = 0$ , so that the equation of piezoresistance takes the form

$$E_1/j_1 = \rho (1 + \Pi_{11}t_1) = \rho + \Delta\rho, \quad \frac{\Delta\rho}{\rho} = \Pi_{11}t_1$$

whence

$$\Pi_{11} = \frac{(-\Delta\rho/\rho)}{-t} = \frac{(-\Delta\rho/\rho)}{(-F/S)} = \frac{24 \cdot 10^{-4}}{10^6 \cdot 10^2} = 24 \cdot 10^{-12} \text{ cm}^2/\text{dyne}$$

In the second specimen (Fig. 8.1b)  $t_1 = -t$ ,  $t_2 = t_3 = 0$ ,  $j_2 = j$ ,  $j_1 = j_3 = 0$ ,  $E_2 = E$ ,  $E_1 = E_3 = 0$ , and the equation of piezoresistance takes the form

$$\frac{E_2}{j_2} = \rho (1 + \Pi_{12}t_1), \quad \frac{\Delta\rho}{\rho} = \Pi_{12}t_1, \quad \Pi_{12} = \frac{-\Delta\rho/\rho}{-t} = 15 \cdot 10^{-12} \text{ cm}^2/\text{dyne}$$

For the third specimen (Fig. 8.1c) the equation of piezoresistance takes the form

$$\frac{E_l}{j_l} = \rho (1 + \Pi_l t_l)$$

where  $l$  is the direction of the length of the sample defined by direction cosines  $(1/\sqrt{2}, 1/\sqrt{2}, 0)$ . Therefore, according to (8.12),  $\Pi_l = \frac{1}{2}(\Pi_{11} + \Pi_{12} + \Pi_{44})$ , and

$$\frac{\Delta\rho}{\rho} = \frac{1}{2} \frac{\Pi_{11} + \Pi_{12} + \Pi_{44}}{t},$$

$$\Pi_{11} + \Pi_{12} + \Pi_{44} = 2 \frac{(-\Delta\rho/\rho)}{-t} = 254 \cdot 10^{-12} \text{ cm}^2/\text{dyne}$$

This yields  $\Pi_{44} = 215 \cdot 10^{-12} \text{ cm}^2/\text{dyne}$ .

**8.5.** Shear stresses and torques can be measured by semiconductor transducers operating in the shear piezoresistance mode. Derive the equation of this effect in an arbitrary direction in semiconductor crystals belonging to symmetry classes  $m3m$ ,  $\bar{4}3m$ . Find the extremal values of the effect, and the directions corresponding to these extrema.

**Solution.** The shear piezoresistance is described by the constants  $\Pi_{ij}$  ( $i = 1, 2, 3$ ;  $j = 4, 5, 6$ , and  $i, j = 4, 5, 6$ ).

If the electric field and electric current are parallel, the shear stress, for instance  $t_4$ , affects the resistance of a semiconductor via

the coefficients  $\Pi_{14}$ ,  $\Pi_{24}$ , and  $\Pi_{34}$ . On the other hand, the same shear stress  $t_4$  affects the ratio of the field along the axis  $X_2$  to the current density along the axis  $X_2$  via the constant  $\Pi_{44}$ . In semiconductor crystals belonging to symmetry classes  $m3m$  and  $\bar{4}3m$ , all constants of the first type ( $\Pi_{14}$ ,  $\Pi_{24}$ , and  $\Pi_{34}$ ), are zero so that in these crystals the piezoresistance effect is determined by nonzero and equal coefficients

$$\Pi_{44} = \Pi_{55} = \Pi_{66}$$

Consequently, the magnitude of the piezoresistance effect in the crystals belonging to the indicated symmetry classes in arbitrary direction is determined by the constant  $\Pi'_{44}$  along this direction.

Consider the cases in which the mechanical shear stress  $t'_4$  ( $t'_{23}$  and  $t'_{32}$ ) is along the directions  $X'_2 \parallel \mathbf{n}$  ( $n_1, n_2, n_3$ ) and  $X'_3 \parallel \mathbf{l}$  ( $l_1, l_2, l_3$ ), the field strength is along the axis  $X_2$  and the current density along the axis  $X_3$ . Then

$$\begin{aligned} \frac{\Pi'_{44}}{2} &= \Pi'_{2323} = n_i l_i n_k l_k \Pi_{ijkl} = \Pi_{2323} (n_2^2 l_3^2 \\ &\quad + n_3^2 l_2^2 + n_3^2 l_1^2 + n_1^2 l_2^2 + n_2^2 l_1^2) \\ &\quad + 2\Pi_{2323} (n_2 n_3 l_2 l_3 + n_3 n_1 l_3 l_1 + n_1 n_2 l_1 l_2) \\ &\quad + \Pi_{1111} (n_1^2 l_1^2 + n_2^2 l_2^2 + n_3^2 l_3^2) - 2\Pi_{1122} (n_1^2 n_2^2 + l_1^2 l_2^2 + n_3^2 l_3^2) \\ &\quad - \Pi_{2323} (n_1^2 l_1^2 + n_2^2 l_2^2 + n_3^2 l_3^2) = \Pi_{2323} + (\Pi_{1111} - 2\Pi_{2323} - \Pi_{1122}) \\ &\quad \times (n_1^2 l_1^2 + n_2^2 l_2^2 + n_3^2 l_3^2) = \frac{\Pi_{44}}{2} + \Pi_A (n_1^2 l_1^2 + n_2^2 l_2^2 + n_3^2 l_3^2), \end{aligned}$$

$$\Pi'_{44} = \Pi_{44} + 2\Pi_A (n_1^2 l_1^2 + n_2^2 l_2^2 + n_3^2 l_3^2)$$

Looking for extrema of  $\Pi'_{44}$  (see Problem 8.3), we find that the first extremum, equal to  $\Pi_{44}$ , corresponds to  $\mathbf{n}$  of the type  $(1, 0, 0)$  and to  $\mathbf{l}$  of the type  $(0, l_2, l_3)$ , as well as to  $\mathbf{l}$  of the type  $(1, 0, 0)$  and  $\mathbf{n}$  of the type  $(0, n_2, n_3)$ .

The second extremum of  $\Pi'_{44}$  is equal to  $\Pi_{44} + \Pi_A = \Pi_{11} - \Pi_{12}$ , and corresponds to the directions of  $\mathbf{n}$  of the type  $(1/\sqrt{2}, 1/\sqrt{2}, 0)$  and directions of  $\mathbf{l}$  of the type  $(1/\sqrt{2}, -1/\sqrt{2}, 0)$ .

As a result, the coefficients  $\Pi'_{44}$  vary as functions of the direction of shear stress in the range from  $\Pi_{44}$  to  $\Pi_{11} - \Pi_{12}$ , and the minimum and maximum values of  $\Pi'_{44}$  depend on the magnitudes and signs of piezoresistances in different crystals.

8.6. A technology of manufacturing semiconductor piezoresistive transducers that gained wide acceptance in recent years is the growth of germanium dendrite ribbon in the direction [211] on special seeds. The main advantage of this technology is the simple manufacturing process requiring only cutting the ribbon into transducers and providing the necessary leads. Calculate the stress sensitivity factor

of transducers made of *n*-germanium dendrite ribbon operating in the longitudinal piezoresistance mode and used for (i) measuring strains, and (ii) for measuring stress, compare this sensitivity to that of transducers cut along [111].

**Solution.** (i) The stress sensitivity factors of a transducer prepared for measuring strain in the longitudinal piezoresistive mode is defined as follows:

$$K = \frac{\Delta R}{R_r} = \Pi_1 E_1$$

where  $\Pi_1$  and  $E_1$  stand for the piezoresistance and Young's modulus along transducer's length.

In a dendrite ribbon transducer  $\mathbf{l} \parallel [211]$ , ( $l_1 = 2/\sqrt{6}$ ,  $l_2 = l_3 = 1/\sqrt{6}$ ), and the values of  $\Pi_1$  and  $E_1$  are found from equations (8.12) and (8.17), respectively:

$$\Pi_1 = \Pi_{[211]} = \Pi_{11} + \frac{1}{2} (\Pi_{44} + \Pi_{12} - \Pi_{11}) = -73.8 \cdot 10^{-12} \text{ cm}^2/\text{dyne}$$

$$E_1 = E_{[211]} = \frac{1}{s_{11} - 0.5(s_{11} - s_{12} - 0.5s_{44})} = 1.37 \cdot 10^{12} \text{ dyne/cm}^2$$

$$K = \Pi_{[211]} E_{[211]} = -101$$

(ii) The stress sensitivity factor of a transducer for measuring stress is equal to the magnitude of piezoresistance along the transducer's axis, that is

$$\Pi_{[211]} = -73.8 \cdot 10^{-12} \text{ cm}^2/\text{dyne}$$

In an *n*-germanium transducer cut along [111],  $\Pi_{[111]} = (1/3) \Pi_{11} + (2/3) (\Pi_{12} - \Pi_{44}) = -96.84 \cdot 10^{-12} \text{ cm}^2/\text{dyne}$ .

A comparison of these constants shows that the sensitivity factors of stress and strain transducers made of *n*-germanium dendrite ribbon are lower by a factor of 1, 3, and 1.75, respectively, than those of transducers cut along [111].

**8.7.** Longitudinal strains in design members of aircraft structures were measured with a *p*-silicon transducer  $6 \times 0.5 \times 1 \text{ mm}^3$ , oriented along [111]. The transducer was connected in an electric circuit supplying it with a direct current of 0.02 A, and with counter voltage across reference transducer (Fig. 8.4). What was the strain in the tested member of the structure if the output signal was 0.63 V?

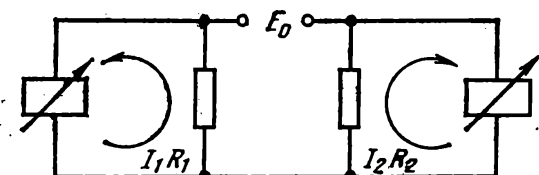


Fig. 8.4. Schematic of a silicon stress transducer for measuring longitudinal strain.

**Solution.** If the circuit, used for measurements is that given in Fig. 8.4, then at zero strain of the active transducer we have

$$I_1 R_1 = I_2 R_2, \quad \text{that is,} \quad V_{\text{out}} = 0$$

When the active transducer is strained, its resistance changes by  $\Delta R_1$ , so that

$$V_{\text{out}} = I_1 (R_1 + \Delta R_1) - I_2 R_2 = I_1 (R_1 + \Delta R_1) - I_1 R_1 = I_1 \Delta R_1$$

Therefore, the output signal is proportional to the increment in resistance. According to (8.15),

$$\Delta R_1 = R r K_{[111]} = \rho \frac{l}{S} r \Pi_{[111]} E_{[111]}$$

whence

$$r = \frac{V_{\text{out}}}{I \rho S^{-1} \Pi_{[111]} E_{[111]}}$$

The piezoresistance and Young's modulus along [111] are found from relations (8.12) and (8.17), respectively, and for *p*-silicon are  $\Pi_{[111]} = 93.53 \cdot 10^{-12} \text{ cm}^2/\text{dyne}$ ,  $E_{[111]} = 1.88 \cdot 10^{-12} \text{ dyne/cm}^2$ ,  $r = 2.06 \cdot 10^{-4}$ .

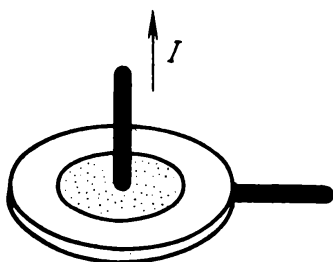
**8.8.** An *n*-germanium piezoresistive transducer, measuring the sum of principal stresses in a plane, is shown in Fig. 8.5.

The transducer plane is oriented along (111), and the electric current is passed normally to this plane. What was the measured strain if the relative change in the transducer's resistance was 0.12%?

**Solution.** If the current and electric field strength in the transducer lie along  $\mathbf{n}$ , the increment in the resistance of the transducer due to the stresses  $[t_{kl}]$  is given by the formula  $\Delta R/R = n_i n_j \Pi_{ijkl} t_{kl}$ . In our case  $\mathbf{n} = (1/\sqrt{3}, 1/\sqrt{3}, 1/\sqrt{3})$ ,

$$\begin{aligned} \frac{\Delta R}{R} = \frac{1}{3} t_{kl} & \left( \Pi_{11kl} + \Pi_{22kl} + \Pi_{33kl} + 2\Pi_{12kl} + 2\Pi_{23kl} \right. \\ & \left. + 2\Pi_{31kl} \right) = \frac{1}{3} \Pi_{11} (t_1 + t_2 + t_3) + \frac{2}{3} \Pi_{12} (t_1 + t_2 + t_3) \\ & + \frac{2}{3} \Pi_{44} (t_4 + t_5 + t_6) \end{aligned}$$

**Fig. 8.5.** Schematic of a germanium stress transducer for measuring the sum of principal stresses in a plane.



The strains are in the plane of the plate, so that  $t_{ik}n_k = 0$ . Hence,  $t_{i1} + t_{i2} + t_{i3} = 0$ , that is,

$$\begin{aligned} t_{12} + t_{13} &= -t_{11} & t_6 + t_5 &= -t_1 \\ t_{21} + t_{23} &= -t_{22} \quad \text{or} \quad t_6 + t_4 &= -t_2 \\ t_{31} + t_{32} &= -t_{33} & t_5 + t_4 &= -t_3 \end{aligned}$$

whence

$$2(t_6 + t_5 + t_4) = -(t_1 + t_2 + t_3)$$

Substituting  $t_4 + t_5 + t_6$  into the expression for  $\Delta R/R$ , we find

$$\frac{\Delta R}{R} = \frac{1}{3}(\Pi_{11} + 2\Pi_{12} - \Pi_{44})(t_1 + t_2 + t_3)$$

Denote the principal stresses in the plane of the plate by  $t_a$  and  $t_b$ . Since  $t_1 + t_2 + t_3$  is the trace of the tensor of stress suffered by the plate, it is equal to the sum of eigenvalues of the tensor, that is,  $t_a + t_b$ .

In *n*-type germanium  $\Pi_{11} + 2\Pi_{12} - \Pi_{44} = 123.2 \cdot 10^{-12} \text{ cm}^2/\text{dyne}$ , so that

$$t_a + t_b = \frac{3\Delta R}{R(\Pi_{11} + 2\Pi_{12} - \Pi_{44})} \simeq 3 \cdot 10^6 \text{ Pa}$$

**8.9.** One of the practical applications of semiconductor piezoresistive transducers is to measure pressure. Which of semiconductor crystal materials, *p*-Ge, *p*-PbTe, or *p*-InSb, has the maximum sensitivity in sensors of hydrostatic pressure?

**Solution.** The sensitivity of a semiconductor transducer of hydrostatic pressure, based on the piezoresistance effect, is defined as the ratio of the relative change of resistance of a specimen,  $\Delta R/R$ , due to hydrostatic pressure, to this pressure, that is

$$\Pi_p = \frac{\Delta R}{R(-p)} = -(\Pi_{11} + 2\Pi_{12})$$

Consequently, the sensitivity of *p*-Ge is 2.7, for *p*-PbTe, 115, and for *p*-InSb, 300, in units of  $10^{-12} \text{ cm}^2/\text{dyne}$ . The sensitivity of a *p*-InSb pressure transducer is thus three times that of a *p*-PbTe transducer, and 100 times that of a *p*-Ge transducer.

#### PROBLEMS

**8.10.** Calculate the change in the resistance of an indium antimonide crystal specimen subjected to hydrostatic pressure of  $10^7 \text{ Pa}$ .

**8.11.** An *n*-silicon piezoresistive transducer, shown in Fig. 8.5, was used to measure the principal stresses in a plane. The current is passed normally to the transducer plane parallel to (100).

What is the sum of the measured stresses if the resistance of the transducer was 0.11 %?

8.12. Calculate the stress sensitivity factor of a *p*-silicon stress transducer cut along [111], operating in the mode of (i) longitudinal piezoresistance and (ii) transverse piezoresistance measured along [110].

8.13. Calculate the minimum strain measurable by a semiconductor transducer with the stress sensitivity factor 50 and the resistance 100 ohm, if the thermal noise voltage of this transducer  $V_T \simeq \simeq 1.3 \cdot 10^{-9}$  V, and the output signal must exceed the noise voltage by a factor of 10.

Assume that the current through the transducer is equal to 0.01 A.

8.14. Piezoresistances of *n*-Ge single crystals with resistivity  $9.9 \cdot 10^{-2}$  ohm were measured on three specimens of  $6 \times 1 \times 1$  mm<sup>3</sup>. The cuts and the schematic of the experiment are shown in Fig. 8.1. A uniaxial compressive stress of  $10^2$  Pa increased the resistances of the first, second, and third specimens (Figs. 8.1a, b, and c, respectively) by 0.279, 0.279, and 4.37 ohm, respectively.

Calculate piezoresistivities of these single crystals.

8.15. Compare the output signals generated by a metal and a semiconductor transducers operating at a 0.05 % strain in a circuit shown in Fig. 8.4, if the transducer current is 20 mA. For the metal transducer the stress sensitivity factor is  $K = 2$ , and  $R = 120$  ohm. For the semiconductor transducer made of *n*-Ge and oriented along [111]  $R = 350$  ohm.

8.16. The resistance of a semiconductor transducer of hydrostatic pressure, made of *p*-InSb, changed by 3.24 ohm. The transducer size is  $1.6 \times 1 \times 0.8$  mm<sup>3</sup>. Calculate the corresponding pressure.

8.17. Compare the stress sensitivity factor of a long thin stress transducer made of *p*-Si oriented along [111], with those of transducers made of the same material and oriented along [100] and [110].

8.18. Find the range of possible variation of the coefficient determining the shear piezoresistance in germanium and silicon crystals with *p*-type conductivity.

8.19. Before piezoresistance of semiconductor crystals was discovered, metal stress transducers with stress sensitivity factor from 2 to 4 were widely used in measurement instruments for stress analysis. Calculate the range of stress sensitivity factors for *p*-type silicon and germanium stress transducers operating in the longitudinal piezoresistance mode, and compare it with the stress sensitivity factor of metal transducers.

8.20. Calculate elastoresistances of silicon crystals.

8.21. Calculate the mechanical stress measurable by a thin *p*-Si stress transducer oriented along [111], if the output signal level exceeding by a factor of 10 the voltage of thermal noise in such

a transducer is  $1.3 \cdot 10^{-3}$  V. The transducer resistance is 100 ohm, and the current through the transducer is 10 mA.

8.22. A thin *p*-Ge transducer oriented along [111] and a metal transducer operate under  $8 \cdot 10^{-4}$  strain in a circuit shown in Fig. 8.4. Calculate the output signal for both transducers, for transducer resistance 25 ohm, transducer current 20 mA, and metal transducer's sensitivity factor 2.

8.23. A *p*-Si filament stress transducer oriented along [111], with dimensions  $15 \times 1 \times 0.5$  mm<sup>3</sup>, was glued to an aircraft element to test its strain in the course of strength tests. What was the strain in the element if the maximum increment of the transducer's resistance was 2.44 ohm?

8.24. Pressure in a high-temperature medium was measured with an *n*-Si transducer. Calculate the pressure in the medium if the transducer's resistance increment was 0.09%.

8.25. Calculate the range of values of the stress sensitivity factor for *n*-Si wire transducers, on the basis of the extreme values of piezo-resistance.

8.26. Which of the piezoresistances of rutile (symmetry class 4/mmm) can be found in an experiment schematically shown in Fig. 8.1?

## 9. OPTICAL PROPERTIES OF CRYSTALS

The main feature of the propagation of light through crystals, as compared to its propagation through isotropic media, is the existence of birefringence, also called double refraction: in the general case, not one but two light waves polarized in mutually perpendicular planes propagate along any direction in a crystal; these waves have different velocities and, consequently, different indices of refraction. This phenomenon is caused by the dielectric anisotropy of crystals. For light, the refractive index  $n = \sqrt{\epsilon\mu} = c/v$ , where  $\epsilon$  is the relative dielectric permittivity,  $\mu$  is the magnetic permeability, and  $c$  and  $v$  are the light velocities in the vacuum and in the medium. For a transparent nonconducting medium we can safely assume that in the range of optical frequencies  $\mu \simeq 1$  so that  $n \simeq \sqrt{\epsilon}$ .

In isotropic media the dielectric permittivity, and with it, refractive index are independent of the direction:  $\mathbf{D} = \epsilon \mathbf{E}$ , and the vectors  $\mathbf{D}$  and  $\mathbf{E}$  are collinear. In anisotropic media,  $D_i = \epsilon_{ij}E_j$ , where  $\epsilon_{ij}$  is a rank two tensor. In the general case, the vectors  $\mathbf{D}$  and  $\mathbf{E}$  have different directions.

All the peculiarities in light propagation through crystals follow from the solution of the Maxwell equations, taking into account the above matter equation,  $D_i = \epsilon_{ij}E_j$ , or the equation

$$E_k = \eta_{km}D_m \quad (9.1)$$

The vectors  $\mathbf{D}$ ,  $\mathbf{H}$ , and  $\mathbf{m}$  are mutually orthogonal. In other words, the vectors  $\mathbf{D}$  and  $\mathbf{H}$  are in the wave front plane perpendicular to  $\mathbf{m}$ , which means that light waves are transverse. The vectors  $\mathbf{H}$  and  $\mathbf{E}$  are also orthogonal, but  $\mathbf{E}$  is not parallel to  $\mathbf{D}$  and lies in a plane perpendicular to the wavefront, at a certain angle to it (Fig. 9.1).

By using the Maxwell equations and the matter equation in the form  $E_i = \eta_{ij}D_j$ , we can derive a system of equations which enable us to find the refractive indices and directions of the vectors  $\mathbf{D}$  for different directions  $\mathbf{m}$  of light propagation through a crystal, provided the dielectric impermeability of the crystal  $\eta_{ij}$  is known.

The Maxwell equations yield the following relation between the vectors  $\mathbf{m}$ ,  $\mathbf{E}$ , and  $\mathbf{D}$  for a plane light wave propagating along  $\mathbf{m}$ :

$$n^2\mathbf{m} \times (\mathbf{m} \times \mathbf{E}) = -\mathbf{D}$$

Removing the brackets in the triple vector product and taking into account the mutual orientation of the vectors  $\mathbf{E}$ ,  $\mathbf{D}$ , and  $\mathbf{m}$ , we find

$$\mathbf{E} - \mathbf{m} (\mathbf{m} \cdot \mathbf{E}) = \frac{1}{n^2} \mathbf{D} \quad (9.2)$$

The left-hand side of (9.2) involves the component of  $\mathbf{E}$  lying in the wavefront plane, that is, the component of  $\mathbf{E}$  parallel to  $\mathbf{D}$  (Fig. 9.1). In the coordinate form, we can rewrite (9.2), taking into account (9.1), as

$$(\eta_{ij} - m_i m_j \eta_{jk}) D_j = \frac{1}{n^2} D_k \quad (9.3)$$

Equation (9.3) is a system of three equations in unknown components of  $\mathbf{D}$ , that is,  $D_1$ ,  $D_2$ ,  $D_3$ , which has a nontrivial solution for a certain value of  $n$  determined from the condition of compatibility of the system (9.3), namely, the condition of zero determinant of the system.

Equations (9.3) thus yield the refractive indices of light waves,  $n$ , and the orientation of the vectors  $\mathbf{D}$  with respect to coordinate system in which the tensor  $[\eta_{ij}]$  is given.

Consider the system (9.3) in the coordinate system  $X_1$ ,  $X_2$ ,  $X_3$  chosen so that the axis  $X_3$  is parallel to  $\mathbf{m}$ , and the axes  $X_1$  and  $X_2$  lie in the wavefront plane. In this frame we have  $\mathbf{D}$  ( $D_1$ ,  $D_2$ , 0),  $\mathbf{m}$  (0, 0,  $m_3$ ), and equations (9.3) take the form

$$(\eta_{11} - n^{-2}) D_1 + \eta_{12} D_2 = 0$$

$$\eta_{12} D_1 + (\eta_{22} - n^{-2}) D_2 = 0$$

where  $n^{-2}$  are the eigenvalues of a two-dimensional tensor

$$\begin{vmatrix} \eta_{11} & \eta_{12} \\ \eta_{12} & \eta_{22} \end{vmatrix} \quad (9.4)$$

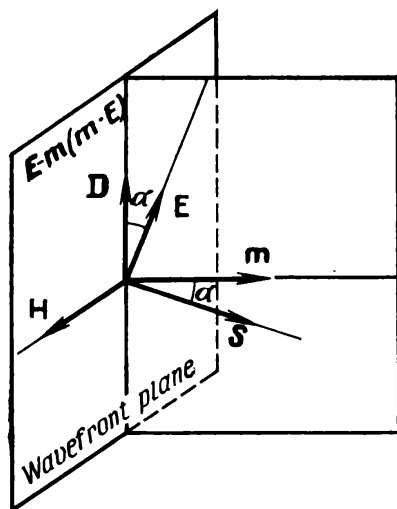


Fig. 9.1. Mutual arrangement of vectors  $\mathbf{D}$ ,  $\mathbf{E}$ ,  $\mathbf{H}$ ,  $\mathbf{m}$ , and  $\mathbf{S}$  in the case of light propagation in an anisotropic medium.

and can be found from the condition

$$\begin{vmatrix} \eta_{11} - n^{-2} & \eta_{12} \\ \eta_{12} & \eta_{22} - n^{-2} \end{vmatrix} = 0$$

This gives (see the solution to Problem 4.3)

$$n_{(1,2)}^{-2} = \frac{1}{2} [(\eta_{11} + \eta_{22}) \pm \sqrt{(\eta_{11} - \eta_{22})^2 + (2\eta_{12})^2}]$$

We thus find that two waves propagate in the direction  $\mathbf{m}$ , with refractive indices  $n_{(1)}$  and  $n_{(2)}$  expressible in terms of the components of the tensor  $\eta_{ij}$  in the chosen coordinate system  $X_1, X_2, X_3$ . The velocities of these waves are

$$v_{(1)} = c/n_{(1)}, \quad v_{(2)} = c/n_{(2)}$$

Clearly, as the direction  $\mathbf{m}$  changes, so change  $n_{(1)}$  and  $n_{(2)}$ ,  $v_{(1)}$ , and  $v_{(2)}$  since for any new direction  $\mathbf{m}$ , that is, in a new coordinate system, the components of the tensor  $\eta_{ij}$  of the crystal will change accordingly.

Each eigenvalue  $n^{-2}$  corresponds to an eigenvector  $\mathbf{D}$ . Let us find the eigenvector  $\mathbf{D}^{(1)}$  for a wave propagating at a velocity  $v_{(1)}$ :

$$(\eta_{11} - n_{(1)}^{-2}) D_1^{(1)} + \eta_{12} D_2^{(1)} = 0, \quad \eta_{12} D_1^{(1)} + (\eta_{22} - n_{(2)}^{-2}) D_2^{(1)} = 0 \quad (9.5)$$

If the coordinate axes  $X_1$  and  $X_2$  are chosen so that  $\eta_{12} = 0$  and  $\eta_{11} > \eta_{22}$ , equations (9.5) yield that  $\mathbf{D}^{(1)}$  is parallel to  $X_1$  since only the component  $D_1^{(1)}$  of  $\mathbf{D}^{(1)}$  does not vanish. For a wave with induction  $\mathbf{D}^{(1)}$  the refractive index  $n_{(1)} = 1/\sqrt{\eta_{11}}$ . The same arguments show that  $\mathbf{D}^{(2)}$  is parallel to  $X_2$ , and  $n_{(2)} = 1/\sqrt{\eta_{22}}$ .

The problem of finding the refractive indices and the directions of induction vectors  $\mathbf{D}^{(1)}$  and  $\mathbf{D}^{(2)}$  for two waves propagating along  $\mathbf{m}$  is thus rephrased to reducing to principal axis the two-dimensional tensor in the coordinate plane  $X_1, X_2$  coinciding with the wavefront plane (see Problem 4.3).

The above arguments become geometrically clear if we use the representation surface of the tensor of dielectric impermeability  $\eta_{ij}$ , also called the index ellipsoid, or optical indicatrix (Fig. 9.2). The

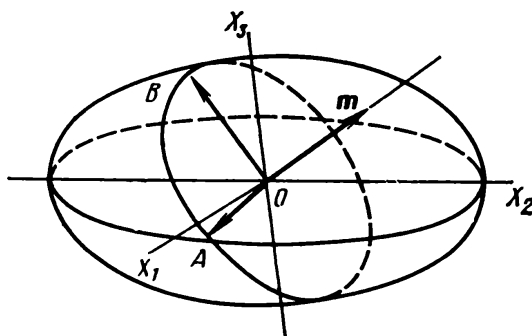


Fig. 9.2. Construction of index ellipsoid of a crystal.

equation of the index ellipsoid is

$$\eta_{ij}x_i x_j = 1 \quad (9.6)$$

This surface is an ellipsoid with the following important property: the central section perpendicular to  $\mathbf{m}$  is an ellipse. The refractive indices of two waves propagating along  $\mathbf{m}$ ,  $n_{(1)}$  and  $n_{(2)}$ , are given by the lengths of the semiaxes of this ellipse, and the directions of these semiaxes give the directions of oscillation of the vectors  $\mathbf{D}^{(1)}$  and  $\mathbf{D}^{(2)}$  for each of the two waves.

In the lowest-symmetry crystals the rank two tensor characterizing a property of a crystal (in the present case it is the tensor of dielectric impermeability  $[\eta_{ij}]$ ) has three independent components; in the medium-symmetry crystals it has two, and in the highest-symmetry crystals only one independent component. The quantities  $\eta_{11}$ ,  $\eta_{22}$ , and  $\eta_{33}$  are essentially positive, so that the index ellipsoid for the lowest-symmetry crystals is a triaxial ellipsoid

$$\eta_{11}x_1^2 + \eta_{22}x_2^2 + \eta_{33}x_3^2 = 1$$

or

$$\frac{x_1^2}{n_1^2} + \frac{x_2^2}{n_2^2} + \frac{x_3^2}{n_3^2} = 1$$

where  $n_1 = 1/\sqrt{\eta_{11}}$ ,  $n_2 = 1/\sqrt{\eta_{22}}$ , and  $n_3 = 1/\sqrt{\eta_{33}}$  are the so-called principal refractive indices of the crystal.

In medium-symmetry crystals  $\eta_{11} = \eta_{22}$ , so that the index ellipsoid is an ellipsoid of revolution:

$$\eta_{11}(x_1^2 + x_2^2) + \eta_{33}x_3^2 = 1$$

or

$$\frac{x_1^2 + x_2^2}{n_1^2} + \frac{x_3^2}{n_3^2} = 1$$

In the highest-symmetry group of crystals the index ellipsoid degenerates into a sphere:

$$\eta_{11}(x_1^2 + x_2^2 + x_3^2) = 1 \text{ or } \frac{x_1^2 + x_2^2 + x_3^2}{n^2} = 1$$

If one of the sections of the index ellipsoid is a circle, this means that in the direction perpendicular to this section the propagating waves have identical phase velocities and identical refractive indices, and the direction of oscillations of the vector  $\mathbf{D}$  is not defined. Only one wave with a velocity determined by the radius of the circular section of the index ellipsoid propagates in this direction, that is, birefringence is absent. This direction is called the optical axis of the crystal.

A triaxial ellipsoid has two circular sections whose radius is equal to the medium-magnitude semiaxis of the ellipsoid (Fig. 9.3). Con-

sequently, the lowest-symmetry crystals have two optical axes, and are called optically biaxial. The following notation for refractive indices is usual:  $N_g$  is the maximum,  $N_p$  is the minimum, and  $N_m$  is the medium refractive index. Light propagating along an optical axis has the refractive index  $N_m$ . The optical axes lie in the plane of the ellipsoid determined by its semiaxes  $N_g$  and  $N_p$ ; this plane is referred to as the plane of optical axes. The acute angle between the optical axes is called the optical axes angle and is denoted by  $2V$  (Fig. 9.4).

An ellipsoid of revolution has a single central circular section perpendicular to its symmetry axes of indefinite order. The direction of this axis coincides with the optical axis of the crystal. The medium-symmetry crystals thus have a single optical axis, and are said to be optically uniaxial. The direction of the optical axis is that of the symmetry axis of maximum order. All other central sections of the ellipsoid of revolution necessarily have one semiaxis equal to the radius of the circular section (Fig. 9.5). The length of the other semiaxes varies from the radius of the circular section to the length of the semiaxis in the direction of the infinite-fold symmetry axis of the ellipsoid of revolution. This means that one wave in the uniaxial crystal has the same refractive index independent of the direction of propagation; this wave is said to be ordinary, and its refractive index is denoted by  $N_o$ . The refractive index of the other wave depends on the direction of propagation, and varies from  $N_o$  to  $N_e$ . This wave is called extraordinary.

By convention, uniaxial crystals are subsummed into optically positive ( $N_e > N_o$ ) and optically negative ( $N_o > N_e$ ). The difference  $\Delta n = N_e - N_o$  is a measure of birefringence of a crystal, and gives one of its most important optical characteristics.

The optical indicatrix of cubic crystals is a sphere. Any of its central sections is a circle. Consequently, only one wave propagates

Fig. 9.3. Index ellipsoid of a biaxial crystal.

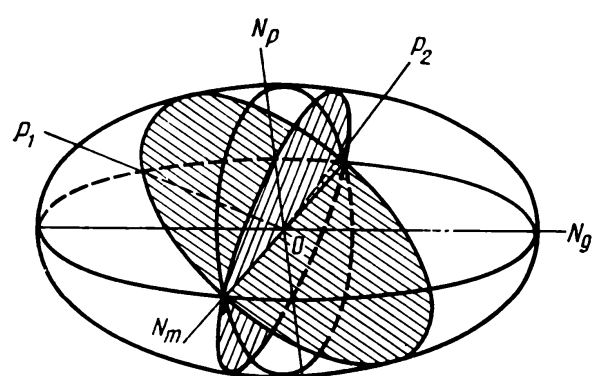
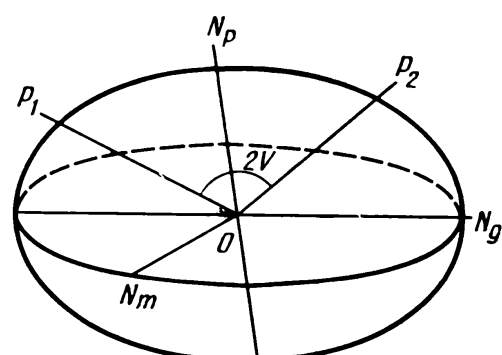


Fig. 9.4. Index ellipsoid of a biaxial crystal, with a given angle between optic axes.



through cubic crystals in any direction, and its refractive index is independent of direction and equal to the radius of the sphere. Cubic crystals behave as isotropic media with respect to light propagation.

In biaxial crystals, the refractive index of each of the two waves depends on direction, therefore, both waves are extraordinary. A biaxial crystal is said to be positive when  $N_g - N_m > N_g - N_p$ , that is,  $N_g$  is the bisector of the acute angle  $2V$ . Biaxial crystals in which the bisector of the acute angle is  $N_p$  are said to be optically negative.

In addition to birefringence, dielectric anisotropy of crystals results in another important feature of optical phenomena in crystals: in the general case, the direction of the normal to the wavefront, that is, the direction of propagation of the wavefront or of the phase of oscillations does not coincide with the direction of the light beam, that is, with the direction of energy propagation of the light wave. Consequently, the phase and wave velocity and the corresponding refractive indices for the wave and the beam become different.

Indeed, the propagation of energy in an electromagnetic wave is described by the Pointing vector:

$$\mathbf{S} = \frac{1}{4\pi} \mathbf{E} \times \mathbf{H}$$

The vector  $\mathbf{H}$  lies in the wavefront plane, and  $\mathbf{E}$  does not, so that the vector product of these vectors,  $\mathbf{S}$ , is not parallel to  $\mathbf{m}$  but lies in the plane of the vectors  $\mathbf{D}$  and  $\mathbf{E}$ . Two waves, one with  $\mathbf{D}^{(1)}$  and another with  $\mathbf{D}^{(2)}$ , propagate along  $\mathbf{m}$ , so that two beams  $\mathbf{S}^{(1)}$  and  $\mathbf{S}^{(2)}$  propagate at angles  $\alpha$  and  $\beta$  to  $\mathbf{m}$  (Fig. 9.6).

These angles are equal to the angles between the vectors  $\mathbf{D}$  and  $\mathbf{E}$  and can be calculated by the formulas

$$\cos \alpha = \frac{\mathbf{D}^{(1)} \cdot \mathbf{E}^{(1)}}{|\mathbf{D}^{(1)}| |\mathbf{E}^{(1)}|}, \quad \cos \beta = \frac{\mathbf{D}^{(2)} \cdot \mathbf{E}^{(2)}}{|\mathbf{D}^{(2)}| |\mathbf{E}^{(2)}|}$$

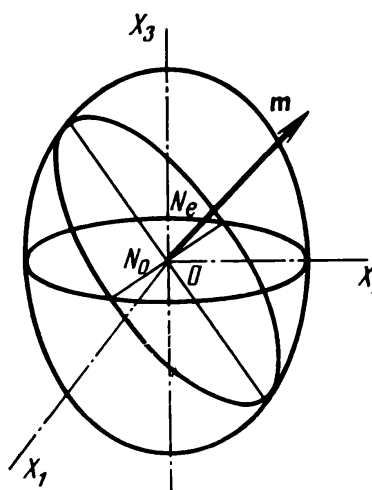


Fig. 9.5. Index ellipsoid of a uniaxial crystal.

Correspondingly, the velocity of light wave propagation along one of the beams is  $u = v/\cos \alpha$ . We may introduce a quantity  $q = u/c$ , reciprocal of the refractive index for the beam and related to the refractive index of the wave,  $n$ , by the formula

$$q = 1/(n \cos \alpha)$$

The quantity  $q$  for the second beam with the wave normal  $\mathbf{m}$  is defined in a similar manner.

### Examples of Problems with Solutions

**9.1.** Find the angle between the normal to the wavefront and the beam for a light wave propagating in the direction  $\mathbf{m}$  ( $m_1, m_2, m_3$ ) if the dielectric impermeability of the crystal is

$$[\eta_{ij}] = \begin{bmatrix} \eta_1 & 0 & 0 \\ 0 & \eta_2 & 0 \\ 0 & 0 & \eta_3 \end{bmatrix}$$

*Plan of Solution.* The graphic solution of this problem, using the index ellipsoid, goes through the following stages:

- Construction of the section of the index ellipsoid, perpendicular to  $\mathbf{m}$ .
- Calculation of the lengths and directions of semiaxes of the obtained elliptical section.

The lengths of semiaxes will give the values of refractive indices,  $n_{(1)}$  and  $n_{(2)}$ , of the two waves, and the directions of semiaxes will give the directions of the vectors  $\mathbf{D}^{(1)}$  and  $\mathbf{D}^{(2)}$  of these waves (Fig. 9.7).

The index ellipsoid will not be required at the further stages in the solution.

Equation  $E_i = \eta_{ij}D_j$  will give the direction of the vectors  $\mathbf{E}^{(1)}$  and  $\mathbf{E}^{(2)}$  for each of the vectors  $\mathbf{D}^{(i)}$ . For each wave propagating along  $\mathbf{m}$  at its specific velocity, we find a specific angle between

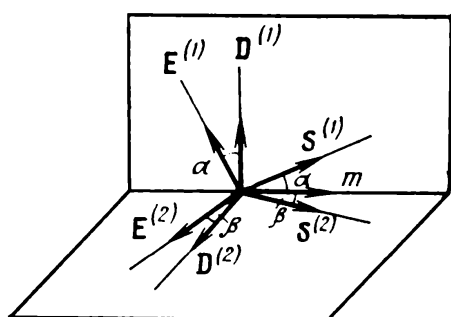


Fig. 9.6. Mutual arrangement of the wavefront normal  $\mathbf{m}$  of light wave and two vectors  $\mathbf{s}^{(1)}$  and  $\mathbf{s}^{(2)}$  of the rays corresponding to the light wave.

the vectors  $\mathbf{D}$  and  $\mathbf{E}$ , and correspondingly, two directions of light beam propagation,  $\mathbf{s}^{(1)}$  and  $\mathbf{s}^{(2)}$ .

The analytical solution of this problem follows a similar programme.

(i) To construct the section of the index ellipsoid, perpendicular to  $\mathbf{m}$ , a coordinate system  $X'_1, X'_2, X'_3$ , such that  $X'_1$  is parallel to  $\mathbf{m}$ , and  $X'_2$  and  $X'_3$  satisfy the conditions of orthogonality and right-handedness of the coordinate system, is chosen.

(ii) The matrix of transition from  $X_1, X_2, X_3$  to  $X'_1, X'_2, X'_3$  is found.

(iii)  $\eta'_{ij}$  and the section of the ellipsoid, perpendicular to  $X'_1$ , whose equation is written in terms of the components of a two-dimensional tensor

$$\begin{bmatrix} \eta'_{22} & \eta'_{23} \\ \eta'_{23} & \eta'_{33} \end{bmatrix}$$

is found in the new coordinate system; this tensor is reduced to the principal axes, that is, its principal values are found, making it possible to find the refractive indices of the two waves and the directions of semiaxes, that is, the directions of the vectors  $\mathbf{D}^{(1)}$  and  $\mathbf{D}^{(2)}$  with respect to the coordinate system  $X'_1, X'_2, X'_3$ .

(iv) The vectors  $\mathbf{E}^{(1)}$  and  $\mathbf{E}^{(2)}$  are then found:

$$E_i^{(1)} = \eta'_{ij} D_j^{(1)}$$

$$E_i^{(2)} = \eta'_{ij} D_j^{(2)}$$

(v) The angle between the beam and the normal to the wavefront,  $\varphi$ , is equal to the angle between the vectors  $\mathbf{E}$  and  $\mathbf{D}$  so that

$$\cos \varphi = \frac{\mathbf{E}^{(1)} \cdot \mathbf{D}^{(1)}}{|\mathbf{E}^{(1)}| |\mathbf{D}^{(1)}|}$$

Likewise, the value of  $\varphi_2$  is found.

**Solution.** (i) Let us find the unit vectors  $\mathbf{y}^{(1)}, \mathbf{y}^{(2)}, \mathbf{y}^{(3)}$  of the coordinate system  $X'_1, X'_2, X'_3$ . By virtue of the conditions imposed

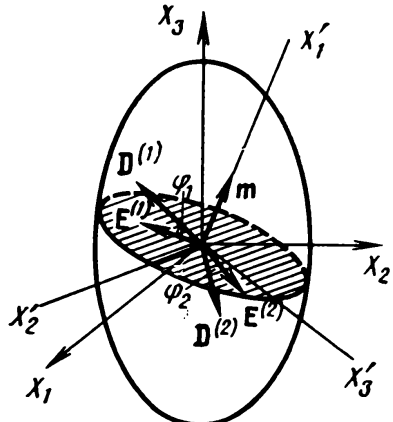


Fig. 9.7. Construction of the section of index ellipsoid perpendicular to wavefront normal  $\mathbf{m}$ .

on the choice of the frame  $X'_1, X'_2, X'_3$ ,  $\mathbf{y}^{(1)} = (m_1, m_2, m_3)$ ;  $\mathbf{y}^{(2)}$  is chosen to be orthogonal to  $\mathbf{y}^{(1)}$ , and  $\mathbf{y}^{(3)}$  to be orthogonal to  $\mathbf{y}^{(1)}$  and  $\mathbf{y}^{(2)}$ . As a result,

$$\mathbf{y}^{(1)} = (m_1, m_2, m_3)$$

$$\mathbf{y}^{(2)} = (1, 0, 0) + \mu \mathbf{y}^{(1)}$$

$$\mathbf{y}^{(3)} = (0, 1, 0) + \mu_1 \mathbf{y}^{(1)} + \mu_2 \mathbf{y}^{(2)}$$

where  $\mu, \mu_1$ , and  $\mu_2$  are numerical factors found from the constraints

$$\mathbf{y}^{(1)} \cdot \mathbf{y}^{(2)} = 0, \quad \mathbf{y}^{(1)} \cdot \mathbf{y}^{(3)} = 0, \quad \mathbf{y}^{(2)} \cdot \mathbf{y}^{(3)} = 0$$

For  $\mathbf{y}^{(2)}$  we find the value of  $\mu$ :

$$\mathbf{y}^{(2)} \cdot \mathbf{y}^{(1)} = m_1 + \mu \mathbf{y}^{(1)} \cdot \mathbf{y}^{(1)} = 0$$

$$\mu = -\frac{m_1}{\mathbf{y}^{(1)} \cdot \mathbf{y}^{(1)}} = -m_1$$

For  $\mathbf{y}^{(3)}$  we find  $\mu_1$  and  $\mu_2$ :

$$\mathbf{y}^{(3)} \cdot \mathbf{y}^{(1)} = m_2 + \mu_1 \mathbf{y}^{(1)} \cdot \mathbf{y}^{(1)} + \mu_2 \mathbf{y}^{(2)} \cdot \mathbf{y}^{(1)} = 0$$

$$\mu_1 = -\frac{m_2}{\mathbf{y}^{(1)} \cdot \mathbf{y}^{(1)}} = -m_2$$

$$\mathbf{y}^{(3)} \cdot \mathbf{y}^{(2)} = -m_1 m_2 + \mu_1 \mathbf{y}^{(1)} \cdot \mathbf{y}^{(2)} + \mu_2 \mathbf{y}^{(2)} \cdot \mathbf{y}^{(2)}, \quad \mu_2 = \frac{m_1 m_2}{\mathbf{y}^{(2)} \cdot \mathbf{y}^{(2)}} = \frac{m_1 m_2}{1 - m_2^2}$$

As a result,

$$\mathbf{y}^{(1)} = (m_1, m_2, m_3)$$

$$\mathbf{y}^{(2)} = (1 - m_1^2, -m_1 m_2, -m_1 m_2)$$

$$\mathbf{y}^{(3)} = \left( -m_1 m_2 + m_1 m_2, 1 - m_2^2 - \frac{m_1^2 m_2^2}{1 - m_1^2}, -m_2 m_3 - \frac{m_1^2 m_2^2 m_3^2}{1 - m_1^2} \right)$$

After normalizing each of the vectors  $\mathbf{y}^{(i)}$  to unity, we find:

$$\mathbf{y}^{(1)} = (m_1, m_2, m_3)$$

$$\mathbf{y}^{(2)} = \left( \sqrt{1 - m_1^2}, -\frac{m_1 m_2}{\sqrt{1 - m_1^2}}, -\frac{m_1 m_3}{\sqrt{1 - m_1^2}} \right)$$

$$\mathbf{y}^{(3)} = \left( 0, \frac{m_3}{\sqrt{1 - m_1^2}}, -\frac{m_2}{\sqrt{1 - m_1^2}} \right)$$

Correspondingly, the matrix of transition from  $X_1, X_2, X_3$  to  $X'_1, X'_2, X'_3$  is

$$C_{ij} = \begin{pmatrix} m_1 & m_2 & m_3 \\ \sqrt{1 - m_1^2} & -\frac{m_1 m_2}{\sqrt{1 - m_1^2}} & -\frac{m_1 m_3}{\sqrt{1 - m_1^2}} \\ 0 & \frac{m_3}{\sqrt{1 - m_1^2}} & -\frac{m_2}{\sqrt{1 - m_1^2}} \end{pmatrix}$$

The determinant of this matrix equals  $-1$ . Hence, the transformation by means of the matrix  $C_{ij}$  transforms the right-handed system into a left-handed one. To keep the system  $X'_1, X'_2, X'_3$  right-handed, we commute the subscripts in the coordinate axes  $X'_2$  and  $X'_3$ , thus commuting the second and third rows of the matrix  $C_{ij}$ . Denoting  $f = \sqrt{1 - m_1^2}$ , we finally obtain

$$C_{ij} = \begin{pmatrix} m_1 & m_2 & m_3 \\ 0 & \frac{m_3}{f} & -\frac{m_2}{f} \\ f & -\frac{m_1 m_2}{f} & -\frac{m_1 m_3}{f} \end{pmatrix}$$

(ii). Let us transform the tensor  $[\eta'_{ij}]$  to the new coordinate system via the formula

$$[\eta'_{ij}] = C_{ik} C_{jl} \eta_{kl}$$

This gives

$$[\eta'_{ij}] = \begin{bmatrix} m_1^2 \eta_1 + m_2^2 \eta_2 + m_3^2 \eta_3 & \frac{m_2 m_3}{f} \eta_2 - \frac{m_2 m_3}{f} \eta_3 & f m_1 \eta_1 - \frac{m_1 m_2^2}{f} \eta_2 - \frac{m_2 m_3^2}{f} \eta_3 \\ \frac{m_3^2}{f^2} \eta_2 + \frac{m_2^2}{f^2} \eta_3 & -\frac{m_1 m_2 m_3}{f^2} \eta_2 + \frac{m_1 m_2 m_3}{f^2} \eta_3 & f^2 \eta_1 + \frac{m_1^2 m_2^2}{f^2} \eta_2 + \frac{m_1^2 m_3^2}{f^2} \eta_3 \end{bmatrix}$$

To simplify the formulas, introduce the notations

$$\begin{bmatrix} a & b \\ b & c \end{bmatrix}$$

for the two-dimensional tensor

$$\begin{bmatrix} \frac{m_3^2 \eta_2}{f^2} + \frac{m_2^2 \eta_3}{f^2} & \frac{m_1 m_2 m_3}{f^2} (\eta_3 - \eta_2) \\ \frac{m_1 m_2 m_3}{f^2} (\eta_3 - \eta_2) & f^2 \eta_1 + \frac{m_1^2 m_2^2}{f^2} \eta_2 + \frac{m_1^2 m_3^2}{f^2} \eta_3 \end{bmatrix}$$

and transform this tensor to the principal axes by the method described in Problem 4.3:

$$\begin{vmatrix} a - \lambda & b \\ b & c - \lambda \end{vmatrix} = 0; \quad \lambda^2 - \lambda (a + c) + ac - b^2 = 0$$

$$\lambda_{1,2} = \frac{(a + c) \pm \sqrt{(c - a)^2 + 4b^2}}{2}$$

Note that  $\lambda_1 = n_{(1)}^{-2}$ , where  $n_{(1)}$  is the refractive index of one of the waves propagating along  $\mathbf{m}$ ,  $\lambda_2 = n_{(2)}^{-2}$ , where  $n_{(2)}$  is the refractive index of the other wave.

The refractive indices  $n_{(1)}$  and  $n_{(2)}$  can be expressed in terms of the basic values of dielectric impermeability,  $\eta_1$ ,  $\eta_2$ , and  $\eta_3$ , and the direction cosines of the wave propagation direction, that is, the components of the vector  $\mathbf{m}$ .

The directions of eigenvectors  $\mathbf{d}^{(1)}$  and  $\mathbf{d}^{(2)}$  of the two-dimensional tensor will be found from the conditions

$$\begin{aligned}\eta'_{ij}d_j^{(1)} &= \lambda_1 d_i^{(1)}, \quad \eta'_{ij}d_j^{(2)} = \lambda_2 d_i^{(2)} \\ ad_2^{(1)} + bd_3^{(1)} &= \lambda_1 d_2^{(1)}, \quad bd_2^{(1)} + cd_3^{(1)} = \lambda_1 d_3^{(1)} \\ (a - \lambda_1) d_2^{(1)} + bd_3^{(1)} &= 0, \quad bd_2^{(1)} + (c - \lambda_1) d_3^{(1)} = 0\end{aligned}$$

which gives

$$\frac{d_2^{(1)}}{d_3^{(1)}} = -\frac{b}{a - \lambda_1} \quad \text{or} \quad \frac{d_2^{(1)}}{d_3^{(1)}} = -\frac{c - \lambda_1}{b}$$

Let

$$\frac{d_2^{(1)}}{d_3^{(1)}} = -\frac{b}{a - \lambda_1} \quad \text{and} \quad d_3^{(1)} = 1, \quad \text{then} \quad d_2 = -b/(a - \lambda_1)$$

Finally, this gives the vector  $\mathbf{d}^{(1)}$ :

$$\mathbf{d}^{(1)} = \left( 0, -\frac{2b}{(a - c) + \sqrt{(a - c)^2 + 4b^2}}, 1 \right)$$

The components of  $\mathbf{d}^{(2)}$  can be found from the condition of orthogonality of the vectors  $\mathbf{d}^{(1)}$ ,  $\mathbf{d}^{(2)}$ , and  $\mathbf{m}$ :

$$\mathbf{d}^{(2)} = \left( 0, 1, \frac{2b}{(a - c) + \sqrt{(a - c)^2 + 4b^2}} \right)$$

Now that the directions of the vectors  $\mathbf{D}^{(1)}$  and  $\mathbf{D}^{(2)}$  of the light waves are known, we find in the coordinate system  $X'_1$ ,  $X'_2$ ,  $X'_3$ :

$$E_i^{(1)} = \eta_{ij} D_j^{(1)}, \quad E_i^{(2)} = \eta_{ij} D_j^{(2)}$$

and finally

$$\cos \varphi_1 = \frac{\mathbf{E}^{(1)} \cdot \mathbf{D}^{(1)}}{|\mathbf{E}^{(1)}| |\mathbf{D}^{(1)}|}, \quad \cos \varphi_2 = \frac{\mathbf{E}^{(2)} \cdot \mathbf{D}^{(2)}}{|\mathbf{E}^{(2)}| |\mathbf{D}^{(2)}|}$$

**9.2.** Find the angle between the normal to the wavefront  $\mathbf{m}$  and the beam direction  $\mathbf{s}$  for light waves propagating in a  $\text{LiNbO}_3$  crystal in a direction at  $30^\circ$  to the optic axis of the crystal.

**Solution.** A section of the index ellipsoid of the crystal by the coordinate plane  $X_1 X_2$  is given in Fig. 9.8. We are solving for the direction  $\mathbf{m}$  lying in this plane. As the symmetry axis 3 is a symmetry axis of infinite order with respect to the optical properties, the result obtained will be valid for all directions generated from  $\mathbf{m}$  by rotating around  $X_3$ , and forming a continuous cone of directions.

To solve the problem, we shall use the results of Problem 9.1. It is clear from Fig. 9.8 that  $\mathbf{m} = \mathbf{m}(\sin \theta, 0, \cos \theta)$ . The matrix

of transition from  $X_1, X_2, X_3$  to  $X'_1, X'_2, X'_3$  is

$$C_{ij} = \begin{pmatrix} \sin \theta & 0 & \cos \theta \\ 0 & 1 & 0 \\ \cos \theta & 0 & -\sin \theta \end{pmatrix}$$

In the  $X'_1, X'_2, X'_3$  coordinate system the tensor  $[\eta'_{ij}]$  is:

$$[\eta'_{ij}] = \begin{bmatrix} \sin^2 \theta \eta_1 + \cos^2 \theta \eta_3 & 0 & \sin \theta \cos \theta \eta_1 - \cos \theta \sin \theta \eta_3 \\ 0 & \eta_1 & 0 \\ \sin \theta \cos \theta \eta_1 - \cos \theta \sin \theta \eta_3 & 0 & \cos^2 \theta \eta_1 + \sin^2 \theta \eta_3 \end{bmatrix}$$

As follows from the solution to Problem 9.1,  $\mathbf{d}^{(1)} = (0, 0, 1)$ . Let  $|\mathbf{D}^{(1)}| = 1$ . Then we obtain for  $\mathbf{E}^{(1)}$ :

$$E_1^{(1)} = (\sin \theta \cos \theta \eta_1 - \cos \theta \sin \theta \eta_3)$$

$$E_2^{(1)} = 0$$

$$E_3^{(1)} = (\cos^2 \theta \eta_1 + \sin^2 \theta \eta_3)$$

For  $\varphi$  we now find

$$\begin{aligned} \cos \varphi_1 &= \frac{\mathbf{E}^{(1)} \cdot \mathbf{D}^{(1)}}{|\mathbf{E}^{(1)}| |\mathbf{D}^{(1)}|} \\ &= \frac{\cos^2 \theta \eta_1 + \sin^2 \theta \eta_3}{(\sin^2 \theta \cos^2 \theta \eta_1^2 + \cos^2 \theta \sin^2 \theta \eta_3^2 + \cos^4 \theta \eta_1^2 + \sin^4 \theta \eta_3^2)^{1/2}} \\ &= \frac{\cos^2 \theta \eta_1 + \sin^2 \theta \eta_3}{[\eta_1^2 (\cos^4 \theta + \sin^2 \theta \cos^2 \theta) + \eta_3^2 (\sin^4 \theta + \sin^2 \theta \cos^2 \theta)]^{1/2}} \end{aligned}$$

For  $\text{LiNbO}_3$  we find  $\eta_1 = 0.023$ ,  $\eta_3 = 0.030$ ,  $\theta = 30^\circ$ ,  $\cos \varphi_1 = 0.992$ ,  $\varphi_1 = 6^\circ$ ,  $\mathbf{d}^{(2)} = (0, 1, 0)$ , and  $\mathbf{E}^{(2)} = (0, \eta_2 D_2, 0)$ . The vectors  $\mathbf{E}^{(2)}$  and  $\mathbf{D}^{(2)}$  are collinear:  $\cos \varphi_2 = 1$ ,  $\varphi_2 = 0$ .

We thus see that for a wave with the plane of oscillations coinciding with the plane of the drawing, that is, for the extraordinary wave, the directions  $\mathbf{m}$  and  $\mathbf{s}$  do not coincide and are at an angle  $\varphi$ .

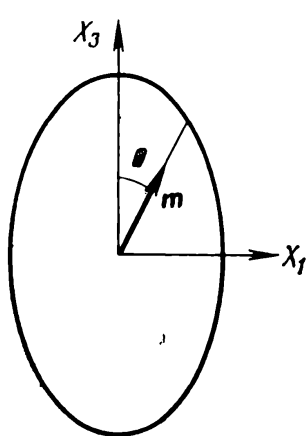


Fig. 9.8. Section of index ellipsoid of a crystal by the coordinate plane  $X_1 X_3$ .

For a wave with the plane of oscillations perpendicular to that of the drawing, that is, for the ordinary wave,  $\varphi = 0$  and  $\mathbf{m} \parallel \mathbf{s}$ . In optically biaxial crystals both waves would be extraordinary, and the angles  $\varphi_1$  and  $\varphi_2$  would be nonzero and not equal to each other.

**9.3.** Calculate the birefringence of an *L*-cut rochelle salt plate. Calculate the thickness of a plate creating the optical path difference equal to a half-wavelength for  $\lambda = 0.63 \mu\text{m}$ .

**Solution.** Quantitatively, birefringence of a crystal plate is defined as the difference between refractive indices  $n_1$  and  $n_2$  of two waves propagating normally to the plate:

$$\Delta n = n_1 - n_2$$

The principal dielectric impermeabilities of rochelle salt are

$$\eta_1 = \frac{1}{\varepsilon_1} = 0.4462, \quad \eta_2 = \frac{1}{\varepsilon_2} = 0.4704, \quad \eta_3 = \frac{1}{\varepsilon_3} = 0.4505$$

As the birefringence must be found for the *L*-cut (see Fig. 2.4), we have  $\mathbf{m} (1/\sqrt{3}, 1/\sqrt{3}, 1/\sqrt{3})$ .

To move further, we shall use the results of Problem 9.1:

$$n_1^{-2} = \frac{(a+c) + \sqrt{(a-c)^2 + 4b^2}}{2}, \quad n_2^{-2} = \frac{(a+c) - \sqrt{(a-c)^2 + 4b^2}}{2}$$

where  $a$ ,  $b$ , and  $c$  are the components of the two-dimensional tensor which in our case takes the form

$$\begin{bmatrix} 0.460 & -0.005 \\ -0.005 & 0.365 \end{bmatrix}$$

Substituting the values of  $a$ ,  $b$ , and  $c$  into the formulas for  $n_1$  and  $n_2$ , we find these indices and birefringence  $\Delta n = 0.181$ .

For a given birefringence of a plate,  $\Delta n$ , the path difference between light waves transmitted through a plate of thickness  $d$  is

$$\Gamma = \Delta n \cdot d$$

In our case  $\Gamma = \lambda/2 = 0.5 \cdot 63 \cdot 10^{-6} \text{ cm}$ . Consequently, the required plate thickness is  $d = 16.5 \cdot 10^{-6} \text{ cm}$ .

**9.4.** Find the angle of refraction  $r$  of the extraordinary wave in a calcite crystal plate for light incident at the plate at an angle of  $30^\circ$ . The cut of the plate is such that the optical axis is at an angle of  $15^\circ$  to the normal to the plate, and lies in the plane of incidence.

**Solution.** This problem can be solved by using the Huygens construction. Let us make use of the momentum conservation of a light wave in the course of refraction. The vector  $\mathbf{k}$  of a light wave is the momentum of the corresponding photon, and must be conserved under refraction. Consequently, the component of  $\mathbf{k}$  parallel to the interface is continuous on this interface.

In order to determine the angle  $r$ , draw a circle centred at the incidence point  $P$ , with the radius  $\mathbf{k}_1$ , where  $\mathbf{k}_1$  is the wave vector of the incident wave, and an ellipse centred at the same point representing the locus of the tips of wave vectors for different directions of light propagation in the crystal (see Fig. 9.9). In order to find the directions of refracted waves, extend the incident wave to its intersection with the circle, and then draw through this intersection point a perpendicular to the interface.

The line connecting the point  $P$  with the point of intersection of the perpendicular and the ellipse gives the direction of the refracted wave. Indeed, both of the thus constructed vectors  $\mathbf{k}_1$  and  $\mathbf{k}_2$  have identical components parallel to the crystal surface.

Note that since  $\mathbf{k} = (\omega/c) \mathbf{n}\mathbf{m}$ , the above-constructed ellipse can be considered as the section of the index ellipsoid by the light incidence plane, rotated by  $90^\circ$  with respect to the perpendicular to the incidence plane. Let us write the equation of the section using the principal axes of the surface as coordinate axes:

$$\eta_2 x_2^2 + \eta_3 x_3^2 = 1$$

Let us transform the coordinate system so that the axis  $X'_3$  be parallel to the crystal surface. This transformation corresponds to rotating the coordinate axes by an angle  $\alpha$  between the optic axis of the crystal and the normal to the plate surface.

The corresponding matrix of transformation is

$$C_{ij} = \begin{pmatrix} 1 & 0 & 0 \\ 0 & \cos \alpha & -\sin \alpha \\ 0 & \sin \alpha & \cos \alpha \end{pmatrix}$$

In the new coordinate system the sought section of the index ellipsoid will have the equation

$$(\cos^2 \alpha \eta_2^2 + \sin^2 \alpha \eta_3^2) x_2'^2 + (\sin^2 \alpha \eta_2^2 + \cos^2 \alpha \eta_3^2) x_3'^2 + (\eta_2^2 - \eta_3^2) \sin 2\alpha x_2' x_3' = 1 \quad (9.7)$$

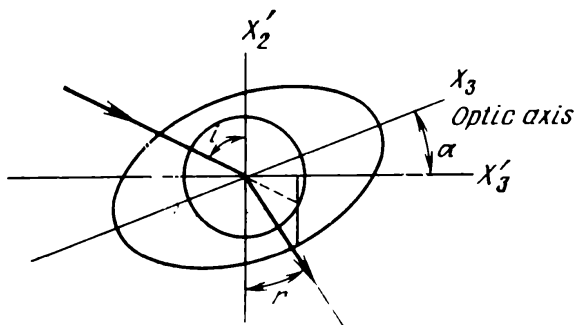


Fig. 9.9. Section of index ellipsoid of a crystal by the incidence plane.

As follows from Fig. 9.9,  $\cot r = x'_2/x'_3$ , and  $\sin i = x'_3$ . By substituting this into (9.7), we find

$$\begin{aligned} & (\sin^2 \alpha \eta_2^2 + \cos^2 \alpha \eta_3^2) \cot^2 r + (\eta_2^2 - \eta_3^2) \sin 2\alpha \cot r \\ & + (\cos^2 \alpha \eta_2^2 + \sin^2 \alpha \eta_3^2) - 1/\sin^2 i = 0 \\ \cot r = & \frac{(\eta_3^2 - \eta_2^2) \sin 2\alpha \pm \sqrt{\eta_2^2 \sin^2 \alpha / \sin^2 i + \eta_3^2 \cos^2 \alpha / \sin^2 i - \eta_2^2 \eta_3^2}}{2(\sin^2 \alpha \eta_2^2 + \cos^2 \alpha \eta_3^2)} \end{aligned}$$

At the conditions given in the problem, we obtain for the refraction of light by calcite plate

$$\cot r = 2.764, \quad r = 19^\circ 7'.$$

**9.5.** An optical system is formed by a polarizer, a crystal, and an analyzer (Fig. 9.10). Find the intensity of the light transmitted through this system if the planes of oscillation in the analyzer and the polarizer are at an angle  $\gamma$ , and the plane of oscillations in the crystal is at angles  $\alpha$  and  $\beta$  to the corresponding planes in the polarizer and analyzer.

Find the mutual arrangement of the polarizer, analyzer, and crystal providing the maximum intensity of the transmitted light, and that for the minimum intensity of the transmitted light.

**Solution.** Figure 9.10 shows the section of the index ellipsoid by the surface of the crystal plate which is perpendicular to the incident wave coming from the polarizer;  $I$  and  $II$  denote the directions of semiaxes of this section, and hence, the directions of oscillations in the crystal.

Let  $n_1$  and  $n_2$  be the refractive indices for waves with oscillation directions  $I$  and  $II$ , respectively. After the passage through a  $d$ -thick plate the two waves gain a phase difference

$$\varphi = \frac{2\pi}{\lambda} d (n_1 - n_2)$$

The intensity of light leaving the analyzer is

$$I = (OA_1)^2 + (OA_2)^2 - 2(OA_1)(OA_2) \cos \varphi$$

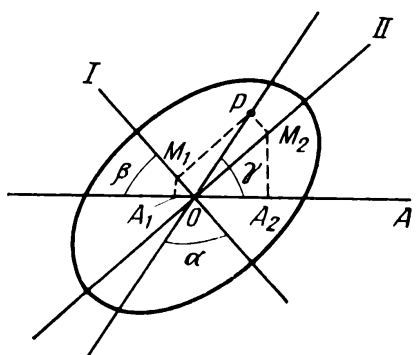


**Fig. 9.10.** Schematic diagram clarifying the calculation of intensity of light transmitted by the analyzer-polarizer system.

where  $OA_1$  and  $OA_2$  are the amplitudes of the transmitted waves, and can be expressed in terms of the amplitudes of light transmitted through the polarizer and the amplitudes of light in the crystal,  $OM_1$  and  $OM_2$ .

Denote the intensity of the light transmitted through the polarizer by  $OP$ . Then  $OP = \sqrt{I_0}$ ,  $OM_1 = \sqrt{I_0} \cos \alpha$ ,  $OM_2 = \sqrt{I_0} \sin \alpha$ ,  $OA_1 = \sqrt{I_0} \cos \alpha \cos \beta$ ,  $OA_2 = \sqrt{I_0} \sin \alpha \sin \beta$ .

After substituting these expressions into the formula for the output intensity, we find

$$I = I_0 \cos^2 \gamma + I_0 \sin 2\alpha \sin 2\beta \sin^2 \frac{\varphi}{2}$$

In crossed Nicol prisms,  $I = I_0 \sin^2 2\alpha \sin^2 \frac{\varphi}{2}$ . In this case the maximum light intensity is observed for the crystal thickness corresponding to the phase difference  $\varphi = \pi$ . When the crystal is rotated  $360^\circ$  around the normal to the plate, the total extinction will be observed four times, and total transparency four times. If, however,  $\varphi = 2\pi$  for any setting of the plate, that is, for any  $\alpha$ , the screen will never be illuminated.

If the analyzer and polarizer are parallel,

$$I = I_0 - I_0 \sin^2 2\alpha \sin^2 \frac{\varphi}{2}$$

The maximum transparency of the plate in crossed Nicol prisms will correspond to extinction in parallel Nicols.

### PROBLEMS

9.6. Calculate birefringence in a quartz plate cut parallel to the optic axis of the crystal. Find the phase difference between the ordinary and extraordinary wavelengths for  $\lambda = 5.9 \cdot 10^{-5}$  cm, for the plate thickness 0.1 mm.

9.7. What is the birefringence of quartz along the normal to the face of a rhombohedron? The rhombohedron face  $(10\bar{1}1)$  is at an angle of  $142^\circ$  to the prism face  $(10\bar{1}0)$ .

9.8. Find the optical sign of a rhombic crystal if the  $X$ -cut plate has the birefringence 0.019, and the  $Y$ -cut plate, 0.036.

9.9. Calculate the thickness of a calcite plate cleaved along the cleavage plane  $(10\bar{1}1)$  providing the path difference  $\Gamma = 1000$  nm.

9.10. What should be the orientation of a gypsum plate to provide maximum path difference at the minimum thickness? Calculate the plate thickness making it a quarter-wave plate for the light with  $\lambda = 5.46 \cdot 10^{-5}$  cm.

9.11. Calculate the thickness of an  $X$ -cut calcite plate capable of compensating for the natural birefringence of lithium iodate plate

1 mm thick, cut at an angle of  $28.9^\circ$  to the axis  $X_3$ . The light wavelength is  $\lambda = 0.43 \mu\text{m}$ .

9.12. What pattern will be observed on the screen if a narrow non-polarized beam passes through two identical calcite plates cleaved along cleavage planes, when the plates have (i) parallel optic axes? (ii) the second plate is rotated around the normal to the plate by  $45^\circ$  with respect to the initial position? (iii) by  $90^\circ$ ? (iv) by  $180^\circ$ ?

9.13. Find the angle between the wavefront normal and the extraordinary beam when the light wave propagates at an angle of  $60^\circ$  to the optic axis of a tourmaline crystal.

9.14. Find the "beam displacement" \* in the case of light propagation along the synchronism direction in a KDP crystal, for the plate thickness 8 mm, and the synchronism direction at  $49^\circ$  to the axis  $\bar{4}$ .

9.15. Find the angle of maximum separation of the ordinary and extraordinary waves in calcite. What is the crystallographic direction for which this angle is realized?

9.16. Compare the values of maximum birefringence and maximum angular separation of the ordinary and extraordinary waves in quartz, calcite, saltpeter, and rutile crystals.

9.17. Find the orientation of a plate with respect to the optic axis in an optically uniaxial crystal, for which the refracted extraordinary beam is in the same plane with the incident beam and the normal to the surface, that is, in the incidence plane. What is the plate orientation when the beam is out of the incidence plane?

9.18. What pattern will be observed on a screen when a narrow non-polarized light beam is transmitted through a cleaved calcite plate? What will happen when the plate is rotated around the normal to its surface? Obtain the answers by using the Huygens construction.

9.19. Find the distance on the screen between two beams formed after the light beam passes through a 2 mm thick cleaved calcite plate.

9.20. Find the intensity of light transmitted through a polarizer-crystal-analyzer system if the polarizer and analyzer are crossed, and the plate cut from a KDP crystal parallel to its optic axis is oriented with the optic axis at  $45^\circ$  to the plane of oscillations in the polarizer. The plate thickness is 5 mm,  $\lambda = 0.54 \mu\text{m}$  (in Problems 9.20 through 9.25 neglect the absorption of light in crystals).

9.21. Find the orientation of the plate in Problem 9.20, giving the maximum intensity of the transmitted light.

9.22. Calculate the thickness of a plate cut from a tourmaline crystal parallel to its optic axis, for which the intensity of light transmitted through the polarizer-crystal-analyzer system is independent

---

\* On beam displacement, see Sec. 12, p. 214.

of the angle of rotation of the plate around the direction perpendicular to its surface. Assume  $\lambda = 0.43 \mu\text{m}$ .

9.23. The intensity of light is diminished when the beam is transmitted through a polarizer and analyzer rotated to form an angle  $\varphi$  between the respective polarization planes. Find the relative error in determining light intensity produced by an error  $\Delta\varphi$  in measuring the angle between the polarizer and analyzer oscillation planes.

9.24. Calculate the ratio of intensities of the ordinary and extraordinary beams traversing successively two cleaved calcite plates of identical thickness, rotated with respect to each other by  $90^\circ$ .

9.25. Calculate intensity of light transmitted through a polarizer-crystal-analyzer system if the polarizer and analyzer are crossed, and the crystal is a rochelle salt cube cut with the edges parallel to the symmetry axes 2, with the edge length of 1 cm. Consider the cases of light incident on the specimen's face coinciding with the plane of optic axes, and on the face perpendicular to the bisector of the angle between the optic axes. Denote the incident light intensity by  $I_0$ , and assume  $\lambda = 1.06 \mu\text{m}$ .

9.26. A narrow light beam is incident at a glancing angle on an ammonium sulphate crystal plate cut parallel to the optic axis. The ordinary and extraordinary beams emerging from the plate are displaced by 1.75 mm. Find the plate thickness.  $N_o = 1.525$ ,  $N_e = 1.479$ .

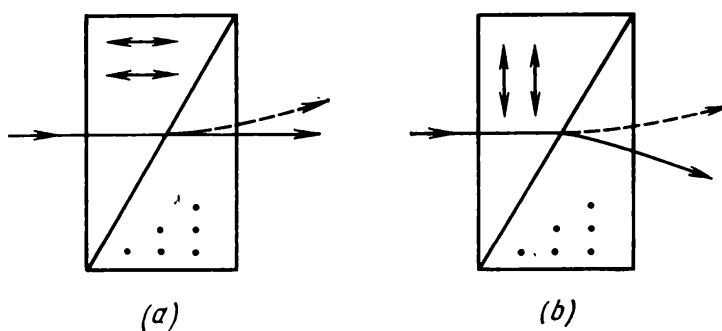
9.27. Show that in a plate cut from a uniaxial crystal with the optic axis perpendicular to the refracting surface, the refracted beams and the optic axis lie in the same plane.

9.28. What is the difference between the principles of beam separation in the Wollaston and Rochon prisms (Fig. 9.11)?

9.29. A Wollaston prism is cut from calcite. The refraction angle of the prism is  $15^\circ$ . Find the beam separation angle produced by this prism.

9.30. Calculate the refraction angle of a Rochon prism giving the beam separation angle  $5^\circ$ .

Fig. 9.11. (a) Rochon prism, and  
(b) Wollaston prism.



9.31. What is the beam separation angle in a Wollaston prism with the refraction angle  $30^\circ$ ?

9.32. Find the maximum angle between the beam and the wave-front normal in crystalline lithium niobate.

9.33. A thin calcite plate cut parallel to the optic axis is placed between the crossed polarizer and analyzer. The plate can be rotated around the normal to its surface. Find the rotation angle corresponding to the maximum intensity of light transmitted by the system.

9.34. Calculate the plate thickness which transforms the white light transmitted through the system described in Problem 9.33 into the red light. What effect will be observed if the polarizer and analyzer are rotated synchronously?

9.35. Calculate the thickness of calcite and quartz plates which can be used as quarter-wave plates for red, green, and violet light (neglect the dispersion of light).

9.36. Calculate exactly the necessary thickness of a quarter-wave calcite plate for  $\lambda = 889$  nm, under the constraint that  $d \geq 1$  mm.

9.37. Indicate the difference produced by rotating, between an analyzer and a polarizer (see Problem 9.5), (i) a single-crystal mica plate, and (ii) a stack of randomly oriented mica plates with the aggregate thickness equal to that of the single-crystal plate.

9.38. What is the reason for coloring of a thin birefringent plate placed between crossed Nicols and illuminated by white light?

9.39. Calculate the optic sign of a biaxial crystal if  $N_g - N_m = 0.036$ ,  $N_g - N_p = 0.019$ .

## 10. PIEZOOPTICAL PROPERTIES OF CRYSTALS

The piezooptical effect (photoelasticity) consists in changes in the optical properties of crystals produced by static or alternating external mechanical stresses, and is described in terms of changes in the index ellipsoid.

When a crystal is placed in a mechanical stress field, the shape and orientation of the index ellipsoid are changed, and in the general case the new principal axes deviate from those of the original ellipsoid. The general equation of the index ellipsoid in an arbitrary coordinate system  $X_1, X_2, X_3$ , whose origin coincides with that of the main (crystallophysical) coordinate system, can be written in the following form:

$$\eta_{11}x_1^2 + \eta_{22}x_2^2 + \eta_{33}x_3^2 + 2\eta_{23}x_2x_3 + 2\eta_{13}x_1x_3 + 2\eta_{12}x_1x_2 = 1 \quad (10.1)$$

An applied mechanical stress produces changes  $\Delta\eta_{ij}$  in dielectric impermeability (polarization constants, as the coefficients of the tensor of dielectric impermeability are usually termed in the literature dealing with the piezooptic, elastooptic, and electrooptic effects):

$$\Delta\eta_{ij} = \eta_{ij}^0 - \eta_{ij} \quad (10.2)$$

To the accuracy of first-order terms, the increments in the dielectric impermeability tensor components are proportional to mechanical stresses:

$$\Delta\eta_{ij} = \pi_{ijkl}t_{kl} \quad (10.3)$$

These increments can also be expressed in terms of strains:

$$\Delta\eta_{ij} = p_{ijkl}r_{kl} \quad (10.4)$$

Such a change in the optical indicatrix of the crystal due to straining is called the *elastooptical effect*. The coefficients  $\pi_{ijkl}$  and  $p_{ijkl}$  form a rank four tensor, and are called the *piezooptical* and *elastooptical constants*, respectively. As

$$\Delta\eta_{ij} = \Delta\eta_{ji}, \quad t_{kl} = t_{lk}$$

we find for zero bulk moments

$$\pi_{ijkl} = \pi_{jikl} = \pi_{ijlk} = \pi_{jilk}$$

*Matrix Notation*

In the matrix notation Eqs. (10.3) and (10.4) can be rewritten in the form

$$\Delta\eta_m = \pi_{mn} t_n \quad (10.5)$$

$$\Delta\eta_m = P_{mn} r_n \quad (10.6)$$

where

$$\pi_{mn} = \pi_{ijkl} \text{ if } n = 1, 2, \text{ or } 3$$

$$\pi_{mn} = 2\pi_{ijkl} \text{ if } n = 4, 5, \text{ or } 6$$

and  $P_{mn}$  are dimensionless elastooptical coefficients, and  $P_{mn} = P_{ijkl}$  for all  $m$  and  $n$ . In the general case

$$\pi_{mn} \neq \pi_{nm}, \quad P_{mn} \neq P_{nm}$$

The piezooptical and elastooptical coefficients are related by the following formulas:

$$P_{mn} = \pi_{mr} c_{rn}, \quad \pi_{mn} = P_{mr} s_{rn} \quad (10.7)$$

where  $c_{rn}$  are elastic stiffnesses and  $s_{rn}$  are elastic compliances.

Matrices  $(\pi_{ij})$  and  $(P_{ij})$  for crystals belonging to various crystallographic classes are listed in Table 11.

The piezooptical and elastooptical effects are observed in crystals of all symmetries because the elastooptical and piezooptical coefficients are components of the even-rank tensor.

To solve specific problems, it is convenient to represent equations (10.5) and (10.6) by the following table.

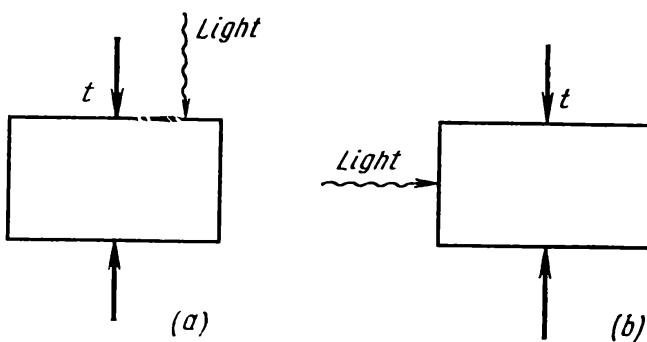
Table 10.1

	$t_1$	$t_2$	$t_3$	$t_4$	$t_5$	$t_6$
$\Delta\eta_1$	$\pi_{11}$	$\pi_{12}$	$\pi_{13}$	$\pi_{14}$	$\pi_{15}$	$\pi_{16}$
$\Delta\eta_2$	$\pi_{21}$	$\pi_{22}$	$\pi_{23}$	$\pi_{24}$	$\pi_{25}$	$\pi_{26}$
$\Delta\eta_3$	$\pi_{31}$	$\pi_{32}$	$\pi_{33}$	$\pi_{34}$	$\pi_{35}$	$\pi_{36}$
$\Delta\eta_4$	$\pi_{41}$	$\pi_{42}$	$\pi_{43}$	$\pi_{44}$	$\pi_{45}$	$\pi_{46}$
$\Delta\eta_5$	$\pi_{51}$	$\pi_{52}$	$\pi_{53}$	$\pi_{54}$	$\pi_{55}$	$\pi_{56}$
$\Delta\eta_6$	$\pi_{61}$	$\pi_{62}$	$\pi_{63}$	$\pi_{64}$	$\pi_{65}$	$\pi_{66}$

*Longitudinal  
and Transverse  
Piezooptical Effect*

The longitudinal and transverse effects are very important for practical applications. The longitudinal piezooptical effect is the effect of induced birefringence, observed in the direction of applica-

**Fig. 10.1.** Schematic representation of the (a) longitudinal and (b) transverse piezooptical effect.



tion of a uniaxial mechanical stress (the mechanical stress and light propagation directions are parallel) (Fig. 10.1a).

The transverse piezooptical effect is the effect observed in the direction perpendicular to a uniaxial mechanical stress (Fig. 10.1b).

### Examples of Problems with Solutions

**10.1.** A mechanical stress is applied along a fourfold axis to a  $1 \times 1 \times 1 \text{ cm}^3$  cubic specimen of rock salt cleaved along the planes (100). Calculate this stress if the path difference for the ordinary and extraordinary beams with wavelength  $5890 \text{ \AA}$ , measured along [100], was found to be  $10.2 \cdot 10^{-5} \text{ cm}$ .

**Solution.** The symmetry of rock salt is  $m3m$  (see Table 14); hence, at zero stress the index ellipsoid of this cube degenerates to a sphere

$$\eta_0 (x_1^2 + x_2^2 + x_3^2) = 1$$

where  $\eta_0 = 1/n_0^2$ . In the case of uniaxial tension of a cube along [100], the mechanical stress tensor has a single component  $t_1 = t$ . The corresponding increments of the components of the dielectric impermeability tensor are

$$\Delta\eta_1 = \pi_{11}t$$

$$\Delta\eta_2 = \Delta\eta_3 = \pi_{12}t$$

$$\Delta\eta_4 = \Delta\eta_5 = \Delta\eta_6 = 0$$

The equation of the modified index ellipsoid takes the form

$$(\eta_0 + \Delta\eta_1)x_1^2 + (\eta_0 + \Delta\eta_2)x_2^2 + (\eta_0 + \Delta\eta_3)x_3^2 = 1$$

or

$$\eta_1 x_1^2 + \eta_2 (x_2^2 + x_3^2) = 1$$

Since  $\eta_4 = \eta_5 = \eta_6 = 0$ , the axes of this index ellipsoid coincide with the crystallophysical axes  $X_1, X_2, X_3$ ; this means that a tension along [100] only deforms but does not rotate the axes of the index ellipsoid in rock salt.

Let us find the three principal refractive indices:

$$\begin{aligned} n_1 &= \frac{1}{\sqrt{\eta_1}} = \frac{1}{\sqrt{\eta_0 + \Delta\eta_1}} = \frac{1}{\sqrt{\eta_0}} \frac{1}{\sqrt{1 + \Delta\eta_1/\eta_0}} \\ &= \frac{1}{\sqrt{\eta_0}} \left( 1 - \frac{1}{2} \frac{\Delta\eta_1}{\eta_0} \right) = \frac{1}{\sqrt{\eta_0}} - \frac{1}{2} \frac{\Delta\eta_1}{\eta_0 \sqrt{\eta_0}} \\ &= N_0 - \frac{1}{2} N_0^3 \Delta\eta_1 = N_0 - \frac{1}{2} N_0^3 \pi_{11} t \end{aligned}$$

Similarly,

$$n_2 = n_3 = N_0 - \frac{1}{2} N_0^3 \pi_{12} t$$

Hence, the optical indicatrix of rock salt extended along [100] becomes an ellipsoid of revolution, and a rock salt cube behaves as a uniaxial crystal.

The same result can be derived from the Curie principle (see Problem 2.3).

The birefringence for light beams propagating along [010] is given by the relation

$$\Delta n = n_1 - n_3 = -\frac{1}{2} N_0^3 (\pi_{11} - \pi_{12}) t$$

whence

$$t = \frac{\Delta n d}{\frac{1}{2} N_0^3 (\pi_{12} - \pi_{11}) d} = \frac{10.2 \cdot 10^{-5} \cdot 1}{\frac{1}{2} (1.51)^3 \cdot 1.21 \cdot 10^{-11} \cdot 1} = 5 \cdot 10^5 \text{ Pa}$$

**10.2.** A photoelastic germanium birefringence modulator used to modulate radiation in the infrared range is oriented with the axis [111] in the direction of uniaxial mechanical stress. Calculate the maximum birefringence induced by mechanical stress along [111]. What mode, longitudinal or transverse, must be chosen for this modulator?

**Solution.** The equation of index ellipsoid of unstressed  $m3m$  crystal is

$$\eta(x_1^2 + x_2^2 + x_3^2) = 1$$

In the crystallophysical coordinate system a uniaxial mechanical stress along [111] is represented by a tensor

$$\frac{1}{3} \begin{bmatrix} t & t & t \\ t & t & t \\ t & t & t \end{bmatrix}$$

According to (10.5), the increments of polarization constants are

$$\Delta\eta_1 = \Delta\eta_2 = \Delta\eta_3 = \frac{1}{3}(\pi_{11} + 2\pi_{12})$$

$$\Delta\eta_4 = \Delta\eta_5 = \Delta\eta_6 = \frac{1}{3}\pi_{44}$$

In the initial coordinate system the equation of index ellipsoid becomes

$$\left[ \eta + \frac{1}{3}(\pi_{11} + 2\pi_{12}) t \right] (x_1^2 + x_2^2 + x_3^2) + \frac{1}{3}\pi_{44} (x_1 x_2 + x_1 x_3 + x_2 x_3) = 1$$

and the tensor of polarization constants then takes the form

$$\begin{bmatrix} c & b & b \\ b & c & b \\ b & b & c \end{bmatrix}$$

where

$$c = \eta + \frac{1}{3}t(\pi_{11} + 2\pi_{12}), \quad b = \frac{1}{3}\pi_{44}$$

By determining the principal values of the tensor  $[\eta_{ij}]$ , we find

$$\lambda_1 = \lambda_2 = c - b, \quad \lambda_3 = c + 2b,$$

and the directions  $X'_1, X'_2, X'_3$ , corresponding to the principal values of the tensor  $[\eta_{ij}]$ , are defined by the vectors

$$\frac{1}{\sqrt{6}}(2, -1, -1), \quad \frac{1}{\sqrt{2}}(0, 1, 1), \quad \frac{1}{\sqrt{3}}(1, 1, 1)$$

Hence, the direction of the axis  $X'_3$  coincides with the direction of the mechanical stress.

In order to find the refractive indices of the stressed crystal, the index ellipsoid must be referred to its principal axes  $X'_1, X'_2, X'_3$ :

$$\begin{aligned} \left[ \eta + \frac{1}{3}(\pi_{11} + 2\pi_{12} - \pi_{44}) t \right] (x'_1)^2 + (x'_2)^2 \\ + \left[ \eta + \frac{1}{3}(\pi_{11} + 2\pi_{12} + 2\pi_{44}) t \right] (x'_3)^2 = 1 \end{aligned}$$

The refractive indices along the principal axes  $X'_1, X'_2, X'_3$  are

$$n'_1 = n'_2 = N_0 - \frac{1}{6}N_0^3 t (\pi_{11} + 2\pi_{12} + 2\pi_{44})$$

$$n'_3 = N_0 - \frac{1}{6}N_0^3 t (\pi_{11} + 2\pi_{12} - \pi_{44})$$

The maximum birefringence induced by applying a uniaxial mechanical stress along [111] is

$$n'_1 - n'_3 = - \frac{N_0^3 \pi_{44} t}{2}$$

This modulator will be inoperative in the longitudinal effect mode when the mechanical stress and light propagation are both parallel to [111] since  $n'_1 = n'_2$  and the induced birefringence is of course zero. The modulator will be operative only in the transverse-effect mode.

**10.3.** The total internal reflection angle in crystals is a function of applied mechanical stresses (or electric field) applied perpendicularly to the incidence plane. This effect can be used to design deflectors, that is, devices controlling the light propagation direction.

Figure 10.2 gives the orientation of the beam-deflecting prism with controlled total internal reflection angle.

In this case a linearly polarized light beam whose polarization plane is in the light incidence plane, is deflected owing to the piezo-optical or electrooptical effect from the direction of nonperturbed beam by an angle  $\psi$  equal to

$$\frac{1}{2} N_0^3 (\Delta \eta'_{11} - \Delta \eta'_{22})$$

where  $\Delta\eta'_{11}$  and  $\Delta\eta'_{22}$  are the increments in polarization constants due to mechanical stress (electric field). Calculate the value of  $\psi$  obtainable by a deflecting NaCl prism for light with wavelength  $\lambda = 0.589 \text{ } \mu\text{m}$  under a mechanical stress equal to  $10^7 \text{ N/m}^2$ .

**Solution.** As follows from Fig. 10.2, the incident light comes along the axis  $X'_1$ , the reflected light along  $X'_2$ , and the uniaxial mechanical stress is parallel to  $X'_3$ .

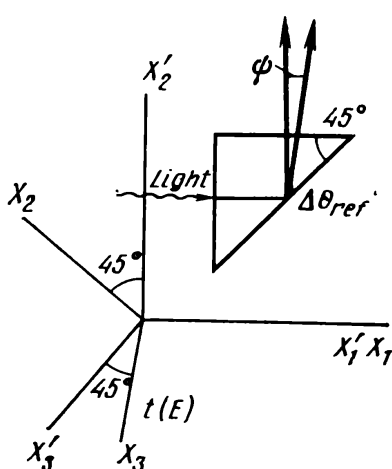


**Fig. 10.2.** Orientation of a rotation prism with controlled angle of total internal reflection.

The orientation of the coordinate system  $X'_1, X'_2, X'_3$  with respect to crystallophysical axes  $X_1, X_2, X_3$  is given by the following matrix of direction cosines:

Table 10.2

	$X_1$	$X_2$	$X_3$
$X'_1$	1	0	0
$X'_2$	0	$1/\sqrt{2}$	$1/\sqrt{2}$
$X'_3$	0	$-1/\sqrt{2}$	$1/\sqrt{2}$

According to (10.5),  $\Delta\eta'_{ij} = \pi'_{ijkl}t'_{kl}$ . As the uniaxial mechanical stress is applied along  $X'_3$ , the only non-zero component of the tensor  $[t_{ij}]$  is  $t'_{33}$ . Consequently,

$$\Delta\eta'_{11} = \pi'_{1133}t'_{33}, \quad \Delta\eta'_{22} = \pi'_{2233}t'_{33}$$

where

$$\pi'_{1133} = C_{1i}C_{1j}C_{3k}C_{3l}\pi_{ijkl}$$

$$\pi'_{2233} = C_{2i}C_{2j}C_{3k}C_{3l}\pi_{ijkl}$$

Here  $\pi_{ijkl}$  are the piezooptical coefficients in the crystallophysical coordinate system, and  $C_{ij}$  are the elements of the above-given matrix of cosines. Taking into account the non-zero coefficients for symmetry class  $m3m$  comprising NaCl crystals, we find

$$\pi'_{1133} = \frac{1}{2}(\pi_{1122} + \pi_{1133}) = \pi_{12}$$

$$\pi'_{2233} = \frac{1}{4}(\pi_{2222} + \pi_{2233} + \pi_{3333} - 4\pi_{2323}) = \frac{1}{4}(2\pi_{11} + 2\pi_{12} - 2\pi_{44})$$

Assuming  $t'_{33} = t$ , we obtain

$$\Delta\eta'_{11} = \pi_{12}t, \quad \Delta\eta'_{22} = \frac{1}{2}(\pi_{11} + \pi_{12} - \pi_{44})t$$

whence

$$\psi = \frac{1}{2}N_0^3(\Delta\eta'_{11} - \Delta\eta'_{22}) = -\frac{1}{4}N_0^3(\pi_{11} - \pi_{12} - \pi_{44})t; \quad \psi = 2.1'$$

**10.4.** The specimen used to study piezooptical properties of RDP crystals (symmetry class  $\bar{4}2m$ ) was a  $45^\circ$  Z-cut crystal plate (see Fig. 11.5) elongated in the direction [110].

The plate was extended by a tensile stress along [110] and simultaneously compressed by a compressional stress along [1\bar{1}0]. The half-wavelength path difference for light with wavelength  $0.535 \mu\text{m}$

propagating, along [001], was achieved for the stress  $0.776 \text{ kgf/cm}^2$ . Which of the piezooptical coefficients can be calculated from the results of the experiment? Calculate this coefficient for the plate thickness 10 mm, wavelength  $\lambda = 0.535 \mu\text{m}$ , and  $N_o = 1.509$ .

**Solution.** In the system of axes fixed to the edges of a  $45^\circ$  Z-cut plate, the stressed state of the crystal plate is written in the form

$$\begin{bmatrix} t & 0 & 0 \\ 0 & -t & 0 \\ 0 & 0 & 0 \end{bmatrix}$$

In the crystallophysical coordinate system this stressed state is obviously described by the tensor

$$\begin{bmatrix} 0 & t & 0 \\ t & 0 & 0 \\ 0 & 0 & 0 \end{bmatrix}$$

involving only shear components denoted by  $t_6$  in the matrix notation.

The equation of the index ellipsoid of a non-stressed crystal is

$$\eta_1(x_1^2 + x_2^2) + \eta_3 x_3^2 = 1$$

where

$$\eta_1 = \frac{1}{N_o^2}, \quad \eta_3 = \frac{1}{N_e^2}$$

According to (10.5), the increment in polarization constants due to mechanical stress  $t_6$  is  $\Delta\eta_6 = \pi_{66}t$ , so that the index ellipsoid equation becomes

$$\eta_1(x_1^2 + x_2^2) + \eta_3 x_3^2 + 2\pi_{66}t x_1 x_2 = 1$$

The change in refraction properties is determined by the section of the index ellipsoid, perpendicular to the light propagation direction. Since light propagates along [001], the equation of this section is

$$\eta_1(x_1^2 + x_2^2) + 2\pi_{66}t x_1 x_2 = 1$$

In the principal axes this equation becomes

$$(\eta_1 + \pi_{66}t) x_1'^2 + (\eta_1 - \pi_{66}t) x_2'^2 = 1$$

This readily yields the values of new refractive indices of RDP:

$$n'_1 = N_o + \frac{1}{2} N_o^3 \pi_{66} t$$

$$n'_2 = N_o - \frac{1}{2} N_o^3 \pi_{66} t$$

The induced birefringence is found as the difference between the new refractive indices:

$$\Delta n = n'_2 - n'_1 = N_0^3 \pi_{66} t$$

The half-wavelength path difference was reached for  $t \approx 10^4$  Pa, that is

$$\lambda/2 = N_0^3 \pi_{66} t_{\lambda/2} d$$

As a result, the available experimental data yield the piezooptical coefficient  $\pi_{66}$  equal to

$$\pi_{66} = \frac{\lambda}{2n_0^3 t_{\lambda/2} d} = 10.5 \cdot 10^{-11} \text{ Pa}^{-1}$$

**10.5.** Uniaxial mechanical stress is applied along [100] to an ADP crystal. Derive the expressions required to evaluate the refractive indices of the stressed crystal.

**Solution.** The index ellipsoid of the unstressed crystal is an ellipsoid of revolution with the equation

$$\eta_1 (x_1^2 + x_2^2) + \eta_3 x_3^2 = 1$$

The crystal is subjected to a uniaxial mechanical stress along [100], that is along the axis  $X_1$  of the crystallophysical coordinate system; hence, the mechanical stress tensor has a single non-zero component,  $t_1$ . According to (10.5) and to the form of the matrix  $(\pi_{ij})$  for crystals belonging to symmetry class  $\bar{4}2m$ , the increments of polarization constants are

$$\Delta \eta_1 = \pi_{11} t_1, \quad \Delta \eta_2 = \pi_{12} t_1, \quad \Delta \eta_3 = \pi_{13} t_1$$

and the equation of the index ellipsoid is

$$(\eta_1 + \pi_{11} t_1) x_1^2 + (\eta_2 + \pi_{12} t_1) x_2^2 + (\eta_3 + \pi_{13} t_1) x_3^2 = 1$$

This equation shows that uniaxial mechanical stress along [100] induces only a deformation of the index ellipsoid along its principal axes.

With rotation absent, the values of new principal refractive indices can be calculated directly from the last equation:

$$n'_1 = N_0 - (1/2) \pi_{11} t_1 N_0^3$$

$$n'_2 = N_0 - (1/2) \pi_{12} t_1 N_0^3$$

$$n'_3 = N_0 - (1/2) \pi_{13} t_1 N_0^3$$

#### PROBLEMS

**10.6.** Using only symmetry-based arguments, show that in crystals belonging to symmetry classes 23 and 3, the piezooptical coefficient  $\pi_{12}$  is not equal to  $\pi_{13}$ .

10.7. A sphalerite crystal is compressed along [110]. What change is thereby induced in the index ellipsoid? Is the direction of tension related to the direction of the axes of the index ellipsoid in the crystal?

10.8. Will the longitudinal piezooptical effect be observed in a rock salt cube cleaved along {100} when subjected to a mechanical stress applied along <100>? Will the transverse effect be observed?

10.9. List the symmetry classes of crystals whose index ellipsoids are not only deformed but also rotated when the crystals are subjected to hydrostatic pressure.

10.10. Transverse piezooptical effect is observed in a fluorite plate 1 cm thick, cut perpendicularly to [111]. For monochromatic light with wavelength 0.590  $\mu\text{m}$  the half-wavelength path difference was obtained at compression equal to 3.2 kgf/cm<sup>2</sup>. Find the value of the piezooptical coefficient that can be calculated from the given experimental data.

10.11. What mechanical tensile stress must be applied along [110] to a 45° Z-cut ADP plate 5 mm thick, with a compressional stress applied simultaneously along [110], in order to obtain the quarter-wavelength path difference for monochromatic light with wavelength 0.535  $\mu\text{m}$  propagating along [001]? Assume  $N_0 = 1.525$  for  $\lambda = 0.535 \mu\text{m}$ .

10.12. Calculate birefringence along the directions [010] and [001] in aluminium potassium sulphate crystals, induced by uniaxial mechanical stress along [100].

10.13. An ADP crystal is subjected to uniaxial mechanical stress  $t$  along [100]. Derive expressions making it possible to evaluate refractive indices of the stressed crystal.

10.14. Will the longitudinal piezooptical effect be observed in a Z-cut KDP plate (Fig. 2.3)? Will the transverse piezooptical effect be observed?

10.15. A photoelastic modulator, used in narrow-band systems (such as lidars), operating in the transverse effect mode, is an ittrium-iron garnet plate 3 mm thick, with the normal to the plate along [111]. Calculate the controlling mechanical stress required to produce half-wavelength path difference for light with  $\lambda = 1.15 \mu\text{m}$ .

10.16. A quartz crystal cube with edges parallel to its crystallophysical axes was compressed along the axis  $X_1$ . Which of the piezo-optical coefficients of quartz can be calculated from the results of the experiment in which increments of refractive indices along the edges of the cube were measured?

10.17. A photoelastic modulator made of a single crystal corundum Z-cut plate (symmetry class  $\bar{3}m$ ) of  $1 \times 1 \times 0.3 \text{ cm}^3$  (Fig. 2.3) operates in the transverse effect mode. What thickness strain must be generated in this plate to obtain the half-wavelength path difference for light with  $\lambda = 0.63 \mu\text{m}$  propagating along  $X_1$ ? Assume  $P_{13} = 0.08$ ,  $N_0 = 1.765$ ,  $N_e = 1.759$ .

**10.18.** What thickness strain must be produced in a square Z-cut lithium niobate plate of  $1 \times 1 \times 0.3 \text{ cm}^3$  in order to obtain the half-wavelength path difference for light with wavelength  $0.63 \mu\text{m}$ , propagating along [0001]?

**10.19.** Calculate the shear stress  $t_{12}$  giving the half-wavelength path difference in ADP and DKDP unit-dimension specimens for light with  $\lambda = 0.535 \mu\text{m}$ , propagating along [001].

## 11. ELECTROOPTICAL PROPERTIES OF CRYSTALS

**Linear electrooptical effect.** By definition, the *linear electrooptical effect* is the change in refractive indices of the medium, proportional to the applied dc or ac electric field. One of the important characteristics of the linear electrooptical effect is its small inertia making it possible to realize light modulation at frequencies up to tens of Gigahertz. Furthermore, nonlinearity introduced by modulation is relatively small because the refractive index is a linear function of electric field. An analytical description of the electrooptical effect is based on the relation between the increments of polarization constants and electric field:

$$\Delta\eta_{ij} = r_{ijk}E_k \quad (11.1)$$

where  $r_{ijk}$  are the coefficients forming a polar rank-three tensor, the so-called *tensor of linear electrooptical effect*. In describing the spontaneous electrooptical effect in ferroelectrics, Eq. (11.1) is written in the form

$$\Delta\eta_{ij} = m_{ijk}P_k \quad (11.2)$$

where  $m_{ijk}$  are coefficients similar to coefficients  $r_{ijk}$ .

Electrooptic properties of ferroelectrics essentially depend on whether the crystal is short-circuited ( $E = \text{const}$ ) or open-circuited ( $D = \text{const}$ ) in the process of measurement. As follows from Eqs. (11.1) and (11.2), the coefficients  $r_{ijk}$  are found for constant strength of electric field, and the coefficient  $m_{ijk}$ , for constant electric induction.

### Matrix Notation

By virtue of the symmetric nature of the tensor of polarization constants, Eqs. (11.1) and (11.2) can be rewritten in matrix notation:

$$\Delta\eta_n = r_{nl}E_l \quad (11.3)$$

$$\Delta\eta_n = m_{nl}P_l \quad (11.4)$$

No factors 2 and 1/2 appear when  $r_{ijk}$  ( $m_{ijk}$ ) are replaced by  $r_{nl}$  ( $m_{nl}$ ).

For the sake of convenience in solving problems, equations (11.3) are written in a tabulated form:

Table 11.1

	$E_1$	$E_2$	$E_3$
$\Delta\eta_1$	$r_{11}$	$r_{12}$	$r_{13}$
$\Delta\eta_2$	$r_{21}$	$r_{22}$	$r_{23}$
$\Delta\eta_3$	$r_{31}$	$r_{32}$	$r_{33}$
$\Delta\eta_4$	$r_{41}$	$r_{42}$	$r_{43}$
$\Delta\eta_5$	$r_{51}$	$r_{52}$	$r_{53}$
$\Delta\eta_6$	$r_{61}$	$r_{62}$	$r_{63}$

### Constraints Due to Symmetry

In the general case we have 18 independent coefficients  $r_{ij}$ . Crystal symmetry reduces this number, just as we saw in the case of piezoelectric moduli. The forms of matrices coincide, to within constant factors, with those of transposed piezoelectric matrices and are listed in Table 12. As any other effect described by a polar rank-three tensor, the linear electrooptical effect is not possible in crystals with a centre of symmetry.

### Primary and Secondary Electrooptical Effect

The linear electrooptical effect is possible only in crystals without a centre of symmetry, that is, in the crystals in which the piezoelectric effect is observable. Hence, if a crystal is mechanically free (stresses are absent), the electric field will produce strains owing to the converse piezoelectric effect, and these strains must produce, according to Eq. (10.12), changes in refractive indices owing to the elasto-optical effect. Consequently, if a crystal can be deformed without mechanical constraints, that is, in static or low-frequency electric fields, the net effect is observed. The change in polarization constants due to applied electric field, not related to the converse piezoelectric effect (via the elasto-optical effect), is called the *primary ("true") electro-optical effect*. In other words, the "true" linear electrooptical effect is only the direct result of application of electric field to dielectrics. Obviously, the primary ("true") electrooptical effect is observed in crystals with "forbidden" deformation, that is, in mechanically "clamped" crystals. The conditions of mechanical clamping of a crystal are realized when the electrooptical effect is observed in a high-frequency electric field whose frequency is much higher than the

frequency of natural vibrations of the crystal. The *secondary*, or “*false*” *linear electrooptical effect* is the change in polarization constants due to the converse piezoelectric effect (via the elastooptical effect). The following equation relates the two effects:

$$\Delta\eta_{ij} = r_{ijk}E_k = r_{ijk}^*E_k + P_{ijlm}r_{lm} = (r_{ijk}^* + P_{ijlm}d_{klm})E_k \quad (11.5)$$

whence

$$r_{ijk} = r_{ijk}^* + P_{ijlm}d_{klm} \quad (11.6)$$

where  $r_{ijk}^*$  are the coefficients of the primary (“true”) electrooptic effect,  $P_{ijlm}$  are the elastooptical coefficients, and  $d_{klm}$  are the piezoelectric moduli.

Likewise,

$$\Delta\eta_{ij} = (m_{ijk}^* + P_{ijlm}g_{klm})P_k \quad (11.7)$$

where  $m_{ijk}^*$  are the coefficients of the primary (“true”) electrooptical effect, and  $g_{klm}$  are the piezoelectric constants.

**Quadratic Electrooptical Effect (Kerr Effect).** Electric field  $E$  applied to a crystal may produce both linear (proportional to  $E$ ) and quadratic (proportional to  $E^2$ ) effects.

Changes in polarization constants due to electric field applied to an electrooptic medium can be found, to within the terms of second order of smallness, from the relation

$$\Delta\eta_{ij} = r_{ijk}E_k + R_{ijk}E_kE_l$$

Here the terms  $r_{ijk}E_k$  characterize the linear electrooptical effect, and the terms  $R_{ijk}E_kE_l$ , the quadratic effects. Thus, the change in polarization constants due to the quadratic electrooptical effect can be found from the equations

$$\Delta\eta_{ij} = R_{ijk}E_kE_l \quad (11.8)$$

The change in polarization constants due to appearance, or change in, spontaneous polarization  $P^s$  in ferroelectrics because of the quadratic electrooptical effect is found from the equations

$$\Delta\eta_{ij} = M_{ijk}P_k^sP_l^s \quad (11.9)$$

The coefficients of the quadratic electrooptical effect,  $R_{ijk}^l$ , are the components of a rank-four tensor which, similarly to electrostriction coefficients, are symmetric both in the pair of subscripts  $i$  and  $j$ , and in the pair  $l$  and  $k$ , that is,

$$R_{ijk}^l = R_{jik}^l \quad (11.10)$$

but do not commute in the pairs of subscripts:

$$R_{ijk}^l \neq R_{kli}^j \quad (11.11)$$

By introducing the notations

$$\begin{aligned} E_1 \cdot E_1 &= E_1^2; \quad E_2 \cdot E_2 = E_2^2; \quad E_3 \cdot E_3 = E_3^2; \quad E_2 \cdot E_3, \quad E_3 \cdot E_2 = E_4^2; \\ E_3 \cdot E_1, \quad E_1 \cdot E_3 &= E_5^2; \quad E_1 \cdot E_2, \quad E_2 \cdot E_1 = E_6^2 \end{aligned} \quad (11.12)$$

we can rewrite Eqs. (11.8) and (11.9) in the matrix form:

$$\Delta\eta_i = R_{ij} E_j^2 \quad (11.13)$$

$$\Delta\eta_i = M_{ij} P_j^2 \quad (11.14)$$

For the convenience of specific calculations, Eqs. (11.13) are written in a more detailed form:

Table 11.2

	$E_1^2$	$E_2^2$	$E_3^2$	$E_4^2$	$E_5^2$	$E_6^2$
$\Delta\eta_1$	$R_{11}$	$R_{12}$	$R_{13}$	$R_{14}$	$R_{15}$	$R_{16}$
$\Delta\eta_2$	$R_{21}$	$R_{22}$	$R_{23}$	$R_{24}$	$R_{25}$	$R_{26}$
$\Delta\eta_3$	$R_{31}$	$R_{32}$	$R_{33}$	$R_{34}$	$R_{35}$	$R_{36}$
$\Delta\eta_4$	$R_{41}$	$R_{42}$	$R_{43}$	$R_{44}$	$R_{45}$	$R_{46}$
$\Delta\eta_5$	$R_{51}$	$R_{52}$	$R_{53}$	$R_{54}$	$R_{55}$	$R_{56}$
$\Delta\eta_6$	$R_{61}$	$R_{62}$	$R_{63}$	$R_{64}$	$R_{65}$	$R_{66}$

Equation (11.14) is written in a similar manner. The matrices of coefficients  $(R_{ij})$  and  $(M_{ij})$  are identical to those of electrostriction coefficients  $(G_{ij})$  and  $(H_{ij})$ .

The quadratic electrooptical effect is observed in crystals of any symmetry, as well as in isotropic media.

### Primary and Secondary Quadratic Electrooptical Effect

The *primary* ("true") *quadratic electrooptical effect* consists in a change in polarization constants proportional to squared applied electric field (polarization) only due to the applied field (polarization).

"*False*" *quadratic electrooptical effect* is a change in polarization constants proportional to squared electric field (polarization) due to strains in the crystal because of electrostriction.

The changes in polarization constants due both to the "true" and to the "false" effects are found from the relations

$$\Delta\eta_{ij} = R_{ijkl}^* E_k E_l + P_{ijmn} r_{mn} \quad (11.15)$$

$$\Delta\eta_{ij} = M_{ijkl}^* P_k P_l + P_{ijmn} r_{mn} \quad (11.16)$$

which can be rewritten in the form

$$\Delta\eta_{ij} = (R_{ijkl}^* + P_{ijmn}L_{mnkl}) E_k E_l \quad (11.17)$$

$$\Delta\eta_{ij} = (M_{ijkl}^* + P_{ijmn}Q_{mnkl}) P_k P_l \quad (11.18)$$

where  $R_{ijkl}^*$ ,  $M_{ijkl}^*$  are the coefficients of the "true" quadratic electro-optical effect,  $P_{ijmn}$  are the elasto-optical coefficients, and  $L_{mnkl}$ ,  $Q_{mnkl}$  are the electrostriction coefficients. A comparison of Eqs. (11.8) and (11.9) with Eqs. (11.17) and (11.18) yields

$$R_{ijkl} = R_{ijkl}^* + P_{ijmn}L_{mnkl} \quad (11.19)$$

$$M_{ijkl} = M_{ijkl}^* + P_{ijmn}Q_{mnkl} \quad (11.20)$$

The following relation holds in practically achievable electric fields:

$$1 \gg r_{ijk} E \gg R_{ijkl} E_k E_l$$

that is, the quadratic effect contributes terms small compared with the linear increments of polarization constants. However, for crystals with a centre of symmetry and for isotropic bodies, for example, liquids in which  $r_{ijk} = 0$ , the quadratic effect is predominant.

### Examples of Problems

#### with Solutions

11.1. A high-speed electrooptic light gate used to generate a sequence of pulses and to increase the peak power of laser output is a Z-cut KDP plate placed between crossed polarizers (Fig. 11.1). Conducting electrodes are deposited on the working faces of the plate. What voltage must be applied to the gate to make it completely open for light with  $\lambda = 0.546 \mu\text{m}$ ? Calculate the voltage for a similar gate made of a Z-cut DKDP plate.

**Solution.** The "open" mode of a gate is achieved when the crystal plate is subjected to a voltage producing the half-wavelength path difference, the so-called half-wavelength voltage  $V_{\lambda/2}$ ; this voltage can be found from the condition  $\Delta n \cdot d = \lambda/2$ , where  $d$  is the light path length in the crystal plate ( $d$  is the plate thickness in this case),

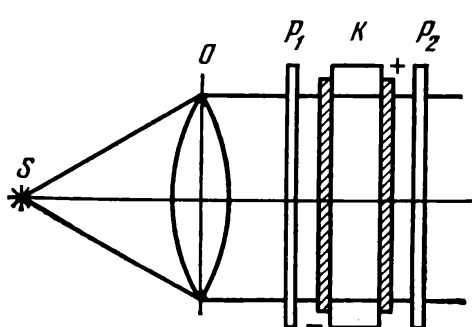


Fig. 11.1. Schematic of an electrooptic light gate.

and  $\Delta n$  is the birefringence induced by the applied voltage. In symmetry class  $\bar{4}2m$  the matrix of coefficients of the linear electrooptical effect has three nonzero components:  $r_{41}$ ,  $r_{52} = r_{41}$ , and  $r_{63}$  (see Table 14). In zero electric field the equation of the index ellipsoid is written in the following form:

$$\eta_1(x_1^2 + x_2^2) + \eta_3 x_3^2 = 1$$

where

$$\eta_1 = 1/N_o^2; \quad \eta_3 = 1/N_e^2,$$

and  $N_o$ ,  $N_e$  are the ordinary and extraordinary refractive indices, respectively. The field  $\mathbf{E}$  is applied to the faces of the Z-cut plate, so that  $E_1 = E_2 = 0$ ,  $E_3 = |\mathbf{E}|$ . According to (11.3), this yields  $\Delta\eta_6 = \eta_6 = r_{63}E_3$ , so that the equation of the optic indicatrix in the system of initial axes  $X_1$ ,  $X_2$ ,  $X_3$  takes the form

$$\eta_1(x_1^2 + x_2^2) + \eta_3 x_3^2 + 2r_{63}E_3 x_1 x_3 = 1$$

As the light propagates along the axis  $X_3$ , the values of refractive indices are equal to the lengths of semiaxes of the section of the index ellipsoid, perpendicular to  $X_3$ . The section of the index ellipsoid by the coordinate plane  $X_1 X_2$  is an ellipse. The semiaxes of this ellipse do not coincide with the crystallophysical axes  $X_1$  and  $X_2$ . The equation of the ellipse,

$$(x_1^2 + x_2^2)/N_o^2 + 2r_{63}x_1 x_2 E_3 = 1$$

is symmetrical with respect to the commutation of the coordinate axes  $X_1$  and  $X_2$ ; we conclude, therefore, that the semiaxes of the ellipse are at angles of  $45^\circ$  to the initial crystallophysical coordinate axes  $X_1$  and  $X_2$  (Fig. 11.2). This result also obtains from the Curie principle. In zero electric field, the principal axes of a crystal in symmetry class  $\bar{4}2m$  coincide with the axes 2. When field  $\mathbf{E}$  is applied along [001], the crystal symmetry becomes  $mm2$ , one of the axes,  $X'_3$ , coincides with  $X_3$ , and the axes  $X'_1$  and  $X'_2$  are normal to the planes  $m$  arranged at  $45^\circ$  with respect to the principal axes  $X_1$  and  $X_2$  in the absence of the field. Let us calculate new principal

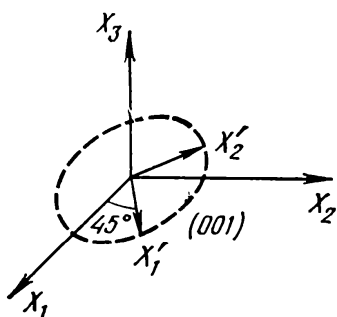


Fig. 11.2. Rotation of the axis of index ellipsoid of crystals belonging to symmetry class  $\bar{4}2m$  upon application of electric field.

refractive indices of the crystal,  $n_{x_1}'$  and  $n_{x_2}'$ . To do this, we refer the equation of the ellipse to the principal axes:

$$\left( \frac{1}{N_0^2} + r_{63}E_3 \right) x_1'^2 + \left( \frac{1}{N_0^2} - r_{63}E_3 \right) x_2'^2 = 1$$

Obviously, the new refractive indices will have the values

$$\frac{1}{n_1'^2} = \frac{1}{N_0^2} + r_{63}E_3$$

whence

$$\frac{1}{n_2'^2} = \frac{1}{N_0^2} - r_{63}E_3$$

$$n_1'^2 = \frac{N_0^2}{1 + r_{63}E_3N_0^2}, \quad n_1' = N_0 \sqrt{\frac{1}{1 + r_{63}E_3N_0^2}}$$

$$n_2'^2 = \frac{N_0^2}{1 - r_{63}E_3N_0^2}, \quad n_2' = N_0 \sqrt{\frac{1}{1 - r_{63}E_3N_0^2}}$$

The quantity  $r_{63}E_3N_0^2$  is small, so that we can use a familiar expression valid for small  $\alpha$ :

$$\sqrt{\frac{1}{1 + \alpha}} \approx 1 - \alpha/2$$

This yields

$$n_1' = N_0 - \frac{1}{2} r_{63}E_3N_0^2, \quad n_2' = N_0 + \frac{1}{2} r_{63}E_3N_0^2$$

In our case, therefore, we have a biaxial crystal with principal refractive indices

$$n_1' = N_0 - \frac{1}{2} r_{63}E_3N_0^2, \quad n_2' = N_0 + \frac{1}{2} r_{63}E_3N_0^2, \quad n_3' = N_0$$

For light propagating in a Z-cut plate perpendicularly to its faces the birefringence is

$$\Delta n = n_2' - n_1' = r_{63}E_3N_0^2$$

The path length of light in the crystal is  $d$ , so that

$$r_{63}E_3N_0^2 d = \lambda/2$$

For  $\lambda = 0.540 \text{ } \mu\text{m}$ , we find  $r_{63} = 30 \cdot 10^{-8}$  CGSE units,  $N_0 = 1.51152$ , and  $V_{\lambda/2} = 7.9 \text{ kV}$ .

Likewise, for a light gate made of a Z-cut DKDP crystal plate we find  $V_{\lambda/2} = 3.4 \text{ kV}$ .

**11.2. Devices producing both the low- and high-frequency light modulation (in the range  $10-10^9 \text{ Hz}$ ) employ ADP crystal plates as modulators. Calculate the control voltage  $V_{\lambda/2}$  ( $\lambda = 0.516 \text{ } \mu\text{m}$ ) for a modulator made of a Z-cut ADP plate operating in the longitudinal**

electrooptical mode in the cases of (i) low-frequency modulation, and (ii) microwave-frequency modulation.

**Solution.** Electric field applied to the working faces of a Z-cut ADP plate induces birefringence equal to  $r_{63}E_3N_0^3$  (see Problem 11.1), and the path difference corresponding to  $\lambda/2$  is equal to  $r_{63}V_{\lambda/2}N_0^3$ , whence

$$V_{\lambda/2} = \frac{\lambda}{2r_{63}N_0^3}$$

In the case of low-frequency electric fields (field frequency much smaller than the resonance frequency of the plate), the coefficient  $r_{63}$  defines the electrooptic properties of the plate and is the sum of the coefficients of the primary and secondary effects, and thus equals  $25 \cdot 10^{-8}$  CGSE units. The half-wavelength voltage  $V_{\lambda/2}$  in the Z-cut ADP plate used as the low-frequency modulator equals 9.2 kV. At frequencies above the resonance frequency, electrooptic elements operate in the piezoelectric clamping mode; the modulation is then caused only by the primary ("true") electrooptical effect, and the electric properties of the Z-cut plate are determined by the coefficient  $r_{63}^*$ .

According to (11.6),

$$r_{63} = r_{63}^* + P_{66}d_{36} = r_{63}^* + \pi_{66}c_{66}d_{36}$$

whence  $r_{63}^* = r_{63} - \pi_{66}c_{66}d_{36}$ .

This gives  $V_{\lambda/2}^* = 13.1$  kV for Z-cut ADP plates used for light modulation at microwave frequencies.

**11.3.** High-frequency modulation of light can be realized by using the quadratic electrooptical effect in cubic (class  $m3m$ ) crystals of potassium niobate-tantalate (KTN) crystals, because the quadratic effect in perovskite crystals has negligible inertia at frequencies up to 200 GHz.

Which of the modes of the quadratic electrooptical effect, longitudinal or transverse, must be chosen for a high-frequency modulator made of a Z-cut KTN plate (Fig. 2.3)?

**Solution.** We shall use the matrix of coefficients of the electrooptical effect given in Table 13.

In zero electric field the equation of the index ellipsoid is  $\eta(x_1^2 + x_2^2 + x_3^2) = 1$ . When the electric field is applied along [100] ( $E_1 = E$ ,  $E_2 = E_3 = 0$ ), Eq. (11.13) gives

$$\Delta\eta_1 = R_{11}E_1^2, \quad \Delta\eta_2 = \Delta\eta_3 = R_{12}E_1^2$$

and the equation of the index ellipsoid becomes

$$(\eta + R_{11}E_1^2)x_1^2 + (\eta + R_{12}E_1^2)(x_2^2 + x_3^2) = 1$$

Here  $\eta$  is the polarization constant for zero field. The last equation shows that electric field turns the KTN crystal into an optically

uniaxial crystal with the optic axis aligned with the field direction. The principal axes of the indicatrixes of the crystal before and after the field is applied coincide. Let us calculate the new refractive indices:

$$\frac{1}{n_1'^2} = \frac{1}{n_{x_1'}^2} = \frac{1}{N_0^2} + R_{11}E_1^2 = \frac{1 + R_{11}E_1^2}{N_0^2} N_0^2$$

$$n_1' = N_0 \left( 1 - \frac{R_{11}E_1^2 N_0^2}{2} \right)$$

Likewise,

$$n_2' = n_3' = N_0 \left( 1 - \frac{R_{12}E_1^2 N_0^2}{2} \right)$$

As  $n_2' = n_3'$ , the birefringence of an  $X$ -cut plate will be zero for the longitudinal electrooptical effect. Both the  $X$ -, and the  $Y$ - and  $Z$ -cuts can work only in the transverse quadratic electrooptical effect mode in which the field and the light propagation directions are mutually perpendicular.

**11.4.** The principle of operation of a crystal deflector with controlled angle of reflection is described in Problem 10.3. Figure 11.3 gives a schematic of the copper chloride deflector prism (symmetry class  $\bar{4}3m$ ), indicating the directions of the incident and reflected light, and the direction of the applied electric field. Calculate the control electric field required to deflect the light emerging from a CuCl prism ( $\lambda = 0.535 \mu\text{m}$ ) by  $20^\circ$  from the beam direction in zero field. Find the control field for the same deflection of the beam if a multiple internal reflection deflector (Fig. 11.4) is used: the number of reflections is  $10^3$ , and the beam deflection is  $\theta = \psi m$ , where  $m$  is the number of internal reflections, and  $\psi$  is the deflection angle per reflection.

Fig. 11.3. Orientation of rotating prism made of copper chloride.

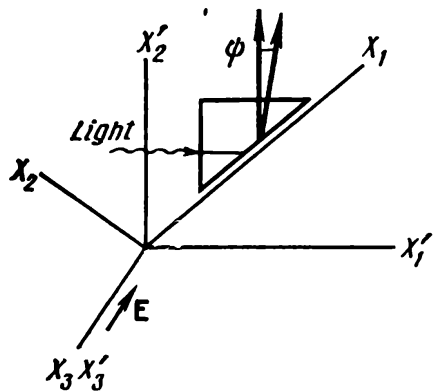
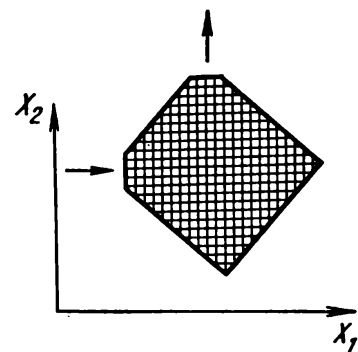


Fig. 11.4. Schematic of total internal reflection deflector.



**Solution.** As follows from Fig. 11.3, the incident light propagates along the axis  $X'_1$ , and the electric field is aligned with  $X'_3$ . The orientation of the coordinate system  $X'_1, X'_2, X'_3$  with respect to the crystallophysical axes  $X_1, X_2, X_3$  is given by the following matrix of direction cosines:

Table 11.3

	$X_1$	$X_2$	$X_3$
$X'_1$	$1/\sqrt{2}$	$1/\sqrt{2}$	0
$X'_2$	$-1/\sqrt{2}$	$1/\sqrt{2}$	0
$X'_3$	0	0	1

According to (11.2),  $\Delta\eta'_{ij} = r'_{ijk}E'_k$ . As the electric field acts along the axis  $X'_3$ , the only nonzero component of the field is  $E_3 = |\mathbf{E}|$ . Therefore,

$$\Delta\eta'_{11} = r'_{113}E'_3, \quad \Delta\eta'_{22} = r'_{223}E'_3$$

The coefficients  $r'_{ijk}$  are the components of a rank-three polar tensor, consequently

$$r'_{113} = C_{1i}C_{1j}C_{3k}r_{ijk}, \quad r'_{223} = C_{2i}C_{2j}C_{3k}r_{ijk}$$

where  $r_{ijk}$  are nonzero electrooptical coefficients referred to the crystallophysical coordinate system, and  $C$  are the elements of the above matrix of direction cosines.

The nonzero coefficients  $r$  in the crystallophysical coordinate system for symmetry class  $\bar{4}3m$  are  $r_{14}, r_{25}, r_{36}$ , where

$$r_{14} = r_{25} = r_{36}, \quad r'_{113} = C_{11}C_{12}C_{33}r_{123} + C_{12}C_{11}C_{33}r_{213} = r_{123} = r_{63}$$

Likewise,

$$r'_{223} = C_{21}C_{22}C_{33}r_{123} + C_{22}C_{21}C_{33}r_{123} = -r_{123} = -r_{63}$$

Since  $\psi = N_0^3 r_{63} E$ , we obtain  $E = 1.2 \cdot 10^6$  V/cm.

In a deflector with the number of reflections  $10^3$ ,  $E = 1.2 \cdot 10^3$  V/cm. As a result, by using a multiple internal reflection deflector (Fig. 11.4) it is possible to reduce the electric field to conventional level ( $10^3$ - $10^4$  V/cm).

**11.5.** A modulator is made of a  $45^\circ$  Z-cut ADP crystal of  $3 \times 3 \times 100$  mm $^3$  ( $l = 100$  mm,  $d = 3$  mm). What gain in modulation is achieved by using the transverse electrooptical effect (Fig. 11.5) in this modulator instead of the longitudinal effect?

**Solution.** Figure 11.5 shows that  $E_1 = E_2 = 0$ ,  $E_3 = |\mathbf{E}|$ . The equation of the indicatrix of ADP then takes the form

$$\eta_1(x_1^2 + x_2^2) + \eta_3 x_3^2 + 2r_{63}E_3 x_2 x_1 = 1$$

It has been shown in Problem 11.1 that the principal axes of the indicatrix,  $X'_1$ ,  $X'_2$ ,  $X'_3$ , are referred to the initial axes  $X_1$ ,  $X_2$ ,  $X_3$  by a  $45^\circ$  rotation around  $X_3$  (Fig. 11.2). Hence, the light propagation direction [110] coincides with one of the principal axes of the indicatrix, namely,  $X'_1$ . The section of the index ellipsoid by the plane  $X'_1 = 0$  is an ellipse

$$(\eta_1 + r_{63}E) x''_2^2 + \eta_3 x''_3^2 = 1$$

whence

$$n'_2 = N_0 \left( 1 - \frac{1}{2} N_0^3 r_{63} E \right), \quad n'_3 = N_e$$

and the light beam components polarized along the axes  $X'_2$  and  $X'_3$  ( $X_3$ ) propagate at velocities

$$v'_2 = \frac{c}{N_0} \left( 1 - \frac{1}{2} N_0^3 r_{63} E \right)^{-1}, \quad v'_3 = \frac{c}{N_e}$$

The total phase difference between the light beam components polarized along the axes  $X'_2$  and  $X'_3$  is equal to

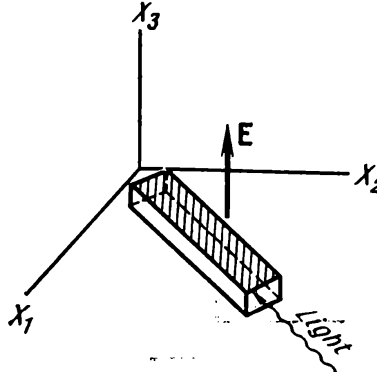
$$F = \frac{2\pi l}{\lambda} (N_e - N_0) + \frac{\pi N_0^3 r_{63} E l}{\lambda}$$

The term  $2\pi (N_e - N_0)/\lambda$  represents the inherent anisotropy of the crystal, and the term  $\pi N_0^3 r_{63} E l/\lambda$  is caused by the applied electric field. The half-wavelength voltage corresponding to the phase difference of  $\pi$  is now equal to

$$V_{\lambda/2} = \frac{\lambda d}{l N_0^3 r_{63}}$$

By comparing this quantity with the half-wavelength voltage of a modulator operating in the longitudinal effect mode (see Problem 11.1), we find that  $V_{\lambda/2}$  of the transverse-effect modulator is smaller by a factor of  $l/2d$  (a factor of 17 for ADP crystals) than  $V_{\lambda/2}$  of a longitudinal-effect modulator. Another advantage offered

Fig. 11.5.  $45^\circ$  Z-cut modulating element.



by the transverse electrooptical effect is a simplification of the electrode system, since the need to transmit the light through the electrodes is eliminated.

**11.6.** The angle of rotation of the index ellipsoid in a rochelle salt crystal (single domain) due to the spontaneous electrooptical effect and the spontaneous polarization  $\mathbf{P}^s \parallel [100]$  were found to be  $0.8^\circ$  and  $7.5 \cdot 10^2$  CGSE units (the index ellipsoid rotation angle is measured as the angle between extinction positions of contiguous domains in an  $X$ -cut plate). Which of the electrooptical coefficients of rochelle salt can be calculated from these experimental results? Calculate its value, assuming that the increments in refractive indices  $n_2$  and  $n_3$  are negligible. Evaluate the ratio of the "true" and "false" effect.

**Solution.** The equation of the index ellipsoid of the paraelectric phase of rochelle salt is

$$\eta_1 x_1^2 + \eta_2 x_2^2 + \eta_3 x_3^2 = 1$$

where

$$\eta_1 = \frac{1}{n_1^2}, \quad \eta_2 = \frac{1}{n_2^2}, \quad \eta_3 = \frac{1}{n_3^2}$$

According to Eq. (11.4), the increments of polarization constants due to the spontaneous polarization  $\mathbf{P}^s \parallel [100]$  ( $P_1 = |\mathbf{P}^s|$ ,  $P_2 = P_3 = 0$ ) in crystals with symmetry 2, prescribed by the form of the matrix  $(m_{ij})$ , is

$$\Delta \eta_4 = m_{41} P_1 = m_{41} P^s$$

In this case the indicatrix equation becomes

$$\eta_1 x_1^2 + \eta_2 x_2^2 + \eta_3 x_3^2 + 2m_{41} P^s x_2 x_3 = 1$$

This equation shows that in the ferroelectric phase the indicatrix is rotated by an angle  $\alpha$  around the axis  $X_1$ . In order to find  $\alpha$ , it is necessary to find the eigenvectors of the following matrix:

$$\begin{vmatrix} \frac{1}{n_2^2} & m_{41} P^s \\ m_{41} P^s & \frac{1}{n_3^2} \end{vmatrix}$$

The eigenvalues of this matrix are

$$\lambda_{1,2} = \frac{1}{2} \left( \frac{1}{n_2^2} + \frac{1}{n_3^2} \right) \pm \sqrt{\frac{1}{4} \left( \frac{1}{n_2^2} - \frac{1}{n_3^2} \right) + m_{41}^2 P^{s^2}}$$

Since the quantity  $m_{41} P^s$  is small, we find

$$\lambda_{1,2} = \frac{1}{2} \left( \frac{1}{n_2^2} + \frac{1}{n_3^2} \right) \pm \frac{1}{2} \left( \frac{1}{n_2^2} - \frac{1}{n_3^2} \right) \left[ 1 + \frac{1}{2} \frac{4m_{41}^2 P^{s^2}}{\frac{1}{n_2^2} - \frac{1}{n_3^2}} \right]$$

Finally,

$$\lambda_1 = \frac{1}{n_{X'_2}^2} = \frac{1}{n_2^2} + m_{41} P^s$$

$$\lambda_2 = \frac{1}{n_{X'_3}^2} = \frac{1}{n_3^2} - m_{41} P^s$$

By substituting the values of  $\lambda_1$  and  $\lambda_2$  into the matrix, we obtain the corresponding principal directions.

The value of  $\tan \alpha$  is given by

$$\frac{\frac{m_{41}^2 P^{s^2}}{1}}{\frac{1}{n_2^2} - \frac{1}{n_3^2}} / m_{41} P^s$$

Since the angle  $\alpha$  is small, we find

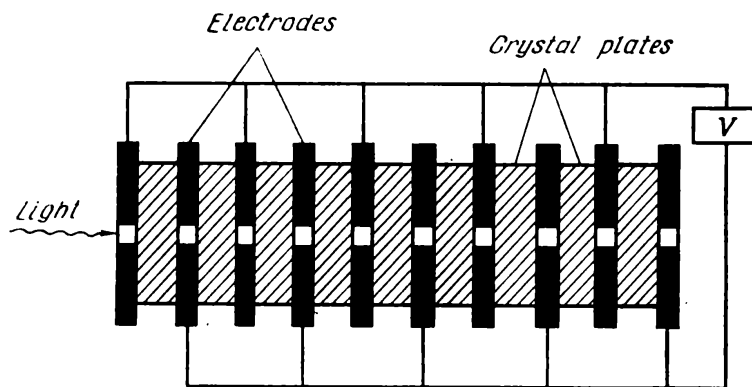
$$\tan \alpha \approx \alpha \approx \frac{m_{41} P^s}{1/n_2^2 - 1/n_3^2}$$

and thus the coefficient  $m_{41}$  can be found from the experimental data. By substituting the values of  $\alpha$ ,  $P^s$  at  $0^\circ\text{C}$ , and the values of  $n_2$  and  $n_3$  (see Appendix) into the expression for  $m_{41}$ , we obtain  $m_{41} = 0.88 \cdot 10^{-7}$ . The ratio of the "true" and "false" effects can be evaluated from (2.8), which in our case can be rewritten in the form  $m_{41} = m_{41}^* + P_{44} g_{14}$ .

In rochelle salt crystals  $g_{14} = 6.7 \cdot 10^{-7}$  CGSE units,  $P_{44} = 8.95 \times 10^{-3}$  CGSE units, and  $P_{44} g_{14} = 0.6 \cdot 10^{-8}$  CGSE units, so that the "false effect" in rochelle salt comes to 27% of the "true effect".

11.7. Figure 11.6 gives a schematic of a modulator cell consisting of  $N$  crystal plates of Z-cut KDP, separated by electrodes with sign-alternating electric fields. What should be the orientation of these plates in order for the phase difference add up? Calculate the

Fig. 11.6. Schematic diagram of a multicell modulator.



half-wavelength voltage of such a cell with ten plates ( $N = 10$ ) if the cell is designed for low-frequency modulation of light with  $\lambda = 0.546 \mu\text{m}$ . Calculate the half-wavelength voltage in the case of a modulator consisting of a single Z-cut KDP plate.

**Solution.** As follows from Fig. 11.6, the modulating Z-cut KDP crystal plates operate in the longitudinal electrooptical effect mode. Consequently, the birefringence induced by the electric field applied along [001] for a light beam propagating in the same direction is  $r_{63}N_o^3E$  (see Problem 11.1), and the corresponding phase difference (phase retardation) of the light signal over a path length  $d$  (plate thickness) is

$$\frac{2\pi}{\lambda} N_o^3 E d = \frac{2\pi}{\lambda} N_o^3 V$$

Therefore, the phase difference (and, correspondingly, the modulation factor) is a function of voltage applied to a plate, and is independent of the plate thickness. A modulating element should thus be cut as a thin plate. If we take a stack of such plates and apply to each one of them the same voltage  $V$ , the total phase difference  $\Gamma$  between the orthogonally polarized components of the beam will be  $N\Gamma$ , where  $N$  is the number of plates. If an electric field is applied to a KDP crystal along [001],

$$n'_1 = N_o \left( 1 + \frac{1}{2} N_o^2 r_{63} E \right), \quad n'_2 = N_o \left( 1 - \frac{1}{2} N_o^2 r_{63} E \right)$$

(see Problem 11.1). This means that the velocity of the component polarized along  $X'_1$ , equal to  $c/N_o(1 + N_o^2 r_{63} E/2)$ , is smaller than the velocity of the component polarized along  $X'_2$ , equal to  $c/N_o(1 - N_o^2 r_{63} E/2)$ ; the phase retardation is positive,  $\Gamma > 0$ . When the electric field is reversed,

$$n'_1 = N_o \left( 1 - \frac{1}{2} N_o^2 r_{63} E \right), \quad n'_2 = N_o \left( 1 + \frac{1}{2} N_o^2 r_{63} E \right)$$

In this case the component polarized along  $X'_1$  has a higher velocity than the component polarized along  $X'_2$ , and  $\Gamma < 0$ . Obviously, the phase retardation produced by two adjacent KDP plates will be equal to the sum of phase retardations of the light beam in each of the plates if each plate is rotated by  $90^\circ$  around  $X'_3$  with respect to the preceding plate. The control voltage  $V_{\lambda/2}$  in one low-frequency modulator plate is

$$V_{\lambda/2} = \lambda/(2r_{63}N_o^3) \approx 7.9 \text{ kV}$$

which gives  $V_{\lambda/2} \approx 7.9 \text{ kV}$  for  $\lambda = 0.546 \mu\text{m}$ . Thus, the control voltage in a modulator cell consisting of ten plates is approximately 0.79 kV.

**11.8.** Ferroelectric perovskite crystals require the lowest control voltages and are thus most promising as crystals for electrooptical modulation of light. Calculate the control voltage  $V_{\lambda/2}$  of a modulator made of potassium tantalate-niobate specimen of  $1 \times 1 \times 1 \text{ cm}^3$  operating at the room temperature in the transverse electrooptical effect mode (Fig. 11.7) for  $\lambda = 0.633 \text{ } \mu\text{m}$ .

**Solution.** The crystals of symmetry class  $4mm$  have five coefficients  $r_{mn}$  (see Table 12), and  $r_{13} = r_{23}$ ,  $r_{42} = r_{51}$ . As shown in Fig. 11.7, the electric field is aligned with the crystallophysical axis  $X_3$ , that is  $E_1 = E_2 = 0$ ,  $E_3 = |\mathbf{E}|$ , and the equation of the index ellipsoid takes the form

$$(\eta_1 + r_{13}E_3)x_1^2 + (\eta_1 + r_{13}E_3)x_2^2 + (\eta_3 + r_{33}E_3)x_3^2 = 1$$

where

$$\eta_1 = 1/N_0^2, \quad \eta_3 = 1/N_e^2$$

This equation yields expressions for the new principal refractive indices (see Problem 11.1):

$$n'_1 = n'_2 = N_0 + \frac{1}{2} N_0^3 r_{13} E_3$$

$$n'_3 = N_e^2 + \frac{1}{2} N_e^3 r_{33} E_3$$

When light propagates along  $[010]$ , that is, along the axis  $X_2$ , the phase difference between the light components polarized parallel and perpendicular to the axis  $X_3$ , is

$$\Gamma = \frac{2\pi}{\lambda} (N_0 - N_e) l + \frac{\pi}{\lambda} (N_e^3 r_{33} - N_0^3 r_{13}) V \frac{l}{d}$$

The first term in the expression for  $\Gamma$  is caused by the inherent anisotropy of the crystal, the second by the applied electric field  $E = V/d$ , where  $d$  is the crystal thickness along the field and  $V$  is the voltage applied to the crystal. The modulating voltage corresponding to a change of  $\Gamma$  by  $\pi$  in a unit-size specimen ( $l = d$ ) for  $\lambda = 0.633 \text{ } \mu\text{m}$  is

$$V_{\lambda/2} = \frac{\lambda}{N_e^3 r_{33} - N_0^3 r_{13}} = 107 \text{ V}$$

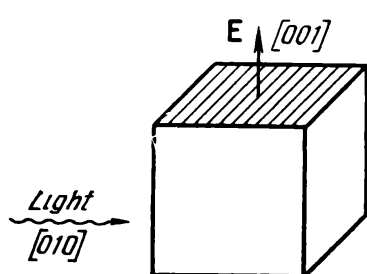


Fig. 11.7. Cell operating in the transverse electrooptic effect mode.

11.9. Calculate the control voltage  $V_{\lambda/2}$  for a light gate made of an  $Y$ -cut calcium pyroniobate plate of  $5 \times 5 \times 20 \text{ mm}^3$ , operating in the transverse electrooptical effect mode, when the light beam with  $\lambda = 0.546 \mu\text{m}$  propagates along [100].

**Solution.** Calcium pyroniobate crystals belong to class 2, and are optically biaxial (see Table 14).

In the crystallophysical coordinate system the equation of index ellipsoid in zero field is

$$\eta_1 x_1^2 + \eta_2 x_2^2 + \eta_3 x_3^2 = 1$$

When electric field is applied along the axis  $X_2$  ( $E_1 = E_3 = 0$ ,  $E_2 = |\mathbf{E}|$ ), the equation of index ellipsoid becomes

$$(\eta_1 + r_{12}E) x_1^2 + (\eta_2 + r_{22}E) x_2^2 + (\eta_3 + r_{32}E) x_3^2 + 2r_{52}Ex_1x_3 = 1$$

Taking into account only the terms linear in electric field, we arrive at the following expressions for the new refractive indices:

$$n'_1 = n_1 - \frac{1}{2} n_1^3 r_{12} E$$

$$n'_2 = n_2 - \frac{1}{2} n_2^3 r_{22} E$$

$$n'_3 = n_3 - \frac{1}{2} n_3^3 r_{32} E$$

When light propagates along  $X_1$ , the essential difference in refraction is that between the refractive indices  $n'_2$  and  $n'_3$ . The path length is  $l$ , so that a field applied along the axis  $X_2$  produces the phase difference

$$\Gamma = \Gamma^* + \frac{\pi}{\lambda} (n_2^3 r_{22} - n_3^3 r_{32}) El$$

where

$$\Gamma^* = \frac{2\pi}{\lambda} (n_2 - n_3) l$$

The control voltage  $V$  corresponding to the additional half-wavelength phase difference is given by the formula

$$V_{\lambda/2} = \frac{\lambda d}{(n_2^3 r_{22} - n_3^3 r_{32}) l} \approx 1 \text{ kV}$$

11.10. The quadratic electrooptical effect in KDP crystals was studied on specimens of  $1 \times 1 \times 1 \text{ cm}^3$ . The half-wavelength voltages for light with  $\lambda = 0.540 \mu\text{m}$  are listed in Table 11.4 for the specific orientations of electric field and light propagation directions.

Which of the coefficients  $R_{ij}$  or their combinations (Table 13) can be calculated from these data? What are their values?

Table 11.4

Direction of electric field	Direction of light propagation	Control voltage $V_{\lambda/2}$ , kV/cm
(i) [001]	[010]	13.2
(ii) [110]	[001]	42.4

**Solution.** (i) Electric field aligned with the axis  $X_3$  of the crystallophysical coordinate system ( $X_3 \parallel [001]$ ) transforms the initial equation of the index ellipsoid

$$\eta_1(x_1^2 + x_2^2) + \eta_3 x_3^2 = 1$$

to the following form:

$$(\eta_1 + R_{13}E_3^2)(x_1^2 + x_2^2) + (\eta_3 + R_{33}E_3^2)x_3^2 = 1$$

This yields the values of the new refractive indices:

$$n'_1 = n'_2 = N_o - \frac{1}{2} N_o^3 R_{13} E_3^2, \quad n'_3 = N_e - \frac{1}{2} N_e^3 R_{33} E_3^2$$

The birefringence  $n'_1 - n'_3$  for light propagation along [010] is, therefore,

$$\begin{aligned} n'_1 - n'_3 &= (N_o - N_e) + \frac{1}{2} (N_e^3 R_{33} - N_o^3 R_{13}) E_3^2 \\ &= (N_o - N_e) \pm \frac{1}{2} R_a E_3^2 \end{aligned}$$

and the birefringence induced by the applied field is

$$\frac{1}{2} (N_e^3 R_{33} - N_o^3 R_{13}) E_3^2 = \frac{1}{2} R_a E_3^2$$

Consequently, by measuring the control voltage  $V_{\lambda/2}$ , we can find the coefficient  $R_a$ , namely  $R_a = 3.4 \cdot 10^{-18}$  CGSE units.

(ii) If the electric field aligns with [110], then  $E_1 = E_2 \neq 0$ ,  $E_3 = 0$ , whence  $E_1 E_2 = E_2 E_2 = E_1 E_2 \neq 0$ ; in the matrix notation  $E_1^2 = E_2^2 = E_6^2 \neq 0$ , and the equation of the index ellipsoid of KDP becomes

$$\begin{aligned} &(\eta_1 + R_{11}E_1^2 + R_{12}E_2^2)x_1^2 + (\eta_2 + R_{12}E_1^2 + R_{11}E_2^2)x_2^2 \\ &+ [\eta_3 + R_{31}(E_1^2 + E_2^2)]x_3^2 + 2R_{66}E_6^2 x_1 x_2 = 1 \end{aligned}$$

When light propagates along [001], the measure of birefringence is the difference  $n'_1 - n'_2$ . In our case the refractive indices  $n'_1$  and  $n'_2$  are

$$n'_1 = N_0 - \frac{1}{2} N_0^3 (R_{11} + R_{12}) E^2 - \frac{1}{2} N_0^3 R_{66} E^2$$

$$n'_2 = N_0 - \frac{1}{2} N_0^3 (R_{11} + R_{12}) E^2 + \frac{1}{2} N_0^3 R_{66} E^2$$

$$n'_2 - n'_1 = N_0^3 R_{66} E^2$$

Consequently, the following quantities can be found from the data listed in Table 11.4:

$$R_a = N_e^3 R_{33} - N_0^3 R_{13} \text{ and } R_{66}$$

11.11. The refractive index of barium tantanate crystals along the ferroelectric axis [001] was observed to drop sharply in the vicinity of the Curie point (120 °C) from 2.42 in the cubic phase to 2.38 in the tetragonal phase, with the refractive indices along [100] and [010] remaining practically unaltered. Evaluate the coefficient characterizing the observed spontaneous electrooptical effect, and the fractions of the “true” and “false” effects.

**Solution.** The paraelectric phase of barium titanate crystals belongs to class  $m3m$  (see Table 14), and thus cannot manifest the linear electrooptic effect. Consequently, the spontaneous electrooptical effect in  $\text{BaTiO}_3$  at the Curie point is quadratic.

The equation of the index ellipsoid of paraelectric barium titanate phase is

$$\eta (x_1^2 + x_2^2 + x_3^2) = 1$$

According to Eq. (12.14) and to the form of the matrix  $(M_{ij})$  for crystals belonging to class  $m3m$ , the spontaneous polarization  $\mathbf{P}^s$  along [001] ( $P_3^s = |\mathbf{P}^s|$ ,  $P_1^s = P_2^s = 0$ ) results in the following changes in the dielectric impermeabilities ( $\Delta\eta_1$ ,  $\Delta\eta_2$ ,  $\Delta\eta_3$ ) defining the changes in refractive indices in the directions [100], [010], and [001], respectively:

$$\Delta\eta_1 = \Delta\eta_2 = M_{12} (P^s)^2, \quad \Delta\eta_3 = M_{33} (P^s)^2 = M_{11} (P^s)^2$$

As the refractive indices along [100] and [010] remain practically constant, the index ellipsoid equation takes the form

$$\eta (x_1^2 + x_2^2) + [\eta + M_{33} (P^s)^2] x_3^2 = 1$$

whence

$$\begin{aligned} n_1 = n_2 &= \frac{1}{\sqrt{\eta}}; \quad n'_3 = \frac{1}{\sqrt{\eta + M_{33} (P^s)^2}} \\ &= \frac{1}{\sqrt{\eta}} \left( 1 - \frac{M_{33} (P^s)^2}{2\eta} \right); \quad n'_3 = n_3 - \frac{1}{2} n_3^3 M_{33} (P^s)^2 \end{aligned}$$

Assuming that at the Curie point  $n'_3 = 2.38$ ,  $n_3 = 2.42$ , and  $P_3^s = |\mathbf{P}^s| = 54 \cdot 10^3$  CGSE units

we find that  $M_{33} = 1.88 \cdot 10^{-12}$  CGSE units. According to Eq. (11.20),

$$M_{33} = M_{33}^* + P_{3m}Q_{m3}$$

where  $M_{33}^*$  is the coefficient of the "true" quadratic electrooptical effect, and  $P_{3m}Q_{m3}$  is the electrostriction correction term characterizing the contribution of the "false" effect. Furthermore, since  $Q_{12} = Q_{13} = -0.53 \cdot 10^{-12}$  CGSE units (see Table 14), and the coefficients  $P_{3m}$  are of the order of 0.1 CGSE units, so that  $P_{3m}Q_{m3} \simeq \simeq 10^{-14}$  CGSE units, we find  $M_{33}^* \simeq 1.87 \cdot 10^{-12}$  CGSE units. This shows that the effect observed in barium titanate crystals at the Curie point is the 99% "true" quadratic electrooptical effect.

**11.12.** A prismatic crystal deflector based on varying the total internal reflection angle by applied electric fields, is schematically shown in Fig. 11.3.

What control field must be applied to a cubic barium titanate specimen in order to deflect the beam emerging from the prism by 30' from the non-perturbed direction of the beam?

**Solution.** The effect responsible for the possibility to control the direction of a light beam by a cubic barium titanate deflecting prism placed in an electric field is the quadratic electrooptical effect.

If the axis  $X'_1$  is chosen along the direction of the incident light beam, the axis  $X'_2$  along the direction of reflected light, and the axis  $X'_3$  along the applied electric field, the orientation of these axes with respect to crystallophysical axes  $X_1$ ,  $X_2$ ,  $X_3$  is given by the following matrix of cosines:

Table 11.5

	$X_1$	$X_2$	$X_3$
$X'_1$	$1/\sqrt{2}$	$1/\sqrt{2}$	0
$X'_2$	$-1/\sqrt{2}$	$1/\sqrt{2}$	0
$X'_3$	0	0	1

Since  $E_1 = E_2 = 0$ ,  $E_3 = |\mathbf{E}|$ , the increment of polarization constants in the expression for  $\Delta\theta_{\text{ref}}$  can be found, according to (11.8), from the following relations:

$$\Delta\eta'_{11} = R'_{1133}E_3^2 = R'_{1133}E^2, \quad \Delta\eta'_{22} = R'_{2233}E^2$$

where  $R'_{1133}$  and  $R'_{2233}$  are the coefficients of the quadratic electrooptical effect in the coordinate system  $X'_1$ ,  $X'_2$ ,  $X'_3$ . The coefficients

$R_{ijkl}$  are the components of a rank-four tensor, so that

$$R'_{1133} = C_{1i} C_{1j} C_{3k} C_{3l} R_{ijkl}, \quad R'_{2233} = C_{2i} C_{2j} C_{3k} C_{3l} R_{ijkl}$$

where  $C_{ij}$  are the elements of the cosine matrix, and  $R_{ijkl}$  are the coefficients of the quadratic electrooptical effect in the crystallophysical coordinate system. Taking into account the form of the matrix ( $R_{ij}$ ) for crystals with symmetry  $m3m$ , we find that

$$R'_{1133} = \frac{1}{2} (R_{1122} + R_{1133}) = \frac{1}{2} (R_{12} + R_{13})$$

For crystals of the cubic system,  $R_{12} = R_{13}$  (see Table 14), whence  $R'_{1133} = R_{1122}$ , and

$$R'_{2233} = \frac{1}{2} (R_{11} + R_{12} - R_{44})$$

Therefore,

$$\Delta\theta = \frac{1}{2} n^3 (\Delta\eta'_{11} - \Delta\eta'_{22}) = -\frac{1}{4} n^3 (R_{11} - R_{12} - R_{44}) E^2, \quad E = 0.3 \text{ kV}$$

#### PROBLEMS

11.13. How can the electrooptical effect be used with a  $Z$ -cut KDP plate to rotate the light polarization plane by  $90^\circ$ ?

11.14. Find the orientation of a lithium niobate crystal plate to be used as required in Problem 11.13?

11.15. Calculate the voltage rotating the polarization plate of light incident on a  $Z$ -cut ADP crystal plate by  $90^\circ$  (use the results obtained in solving Problem 11.13).

11.16. Use the matrices of electrooptical coefficients given in Table 13 and answer the following questions:

(i) To what symmetry classes the crystals do belong, in which electric field applied along the axis  $X_3$  only changes the magnitudes of the principal refractive indices without modifying the number of optical axis of the crystal? Can the number of optical axes be changed in these crystals by aligning the field with other directions?

(ii) To what symmetry classes do the crystals belong in which electric field applied along  $X_3$  changes the number of optical axes but conserves the directions of the principal axes of the index ellipsoid?

(iii) To which symmetry classes do the crystals belong, in which both the principal refractive indices and the directions of the principal axes of the index ellipsoid are changed by electric field?

11.17. Electric field is applied along [111] to a single-crystal gallium phosphide specimen. Will the longitudinal electrooptical effect be produced in this case? And the transverse effect?

11.18. Indicate the tetragonal symmetry classes in which the index ellipsoid of a crystal changes its symmetry under the action of electric field applied in any direction (including the configuration  $E \parallel [001]$ ).

11.19. High optical quality of quartz makes it possible to use it in modulators despite its low electrooptical constants. Is it possible to use Z-cut quartz plates to achieve light modulation on the basis of the linear electrooptical effect?

11.20. Which of the uniaxial crystals do not change their optical properties in the linear approximation, when placed in an electric field aligned with the highest-symmetry axis?

11.21. Figure 11.8 plots the effective electrooptical constant  $r_3 = r_{63}n_0^3$  of KDP and DKDP crystals as a function of temperature, recorded in the static mode for light wavelength  $0.535 \mu\text{m}$ . Suppose that modulators are made of  $45^\circ$  Z-cut KDP and DKDP plates and operate in the longitudinal electrooptical effect mode at temperatures in the vicinity of the Curie point; by what factor is the half-wavelength control voltage  $V_{\lambda/2}$  reduced at these temperatures in comparison with that required for modulation at the room temperature?

What difficulties are encountered in the modulation at temperatures close to  $T_C$ ?

11.22. Derive expressions making it possible to calculate the spontaneous birefringence of a KDP crystal (single domain) at the Curie point ( $T_C$ ), if birefringence is caused by the spontaneous polarization vector  $\mathbf{P}^s$  aligned with [001], for light propagating along [100], [010], or [001].

11.23. Which of the electrooptical coefficients of lithium tantalate can be found from the measurements of the half-wavelength voltage applied to a Z-cut plate if the longitudinal electrooptical effect is observed in the plate?

11.24. Gallium arsenide single crystals doped with chromium and iron are used in modulators for the IR range. Calculate the phase difference which can be obtained by a single-crystal gallium arse-

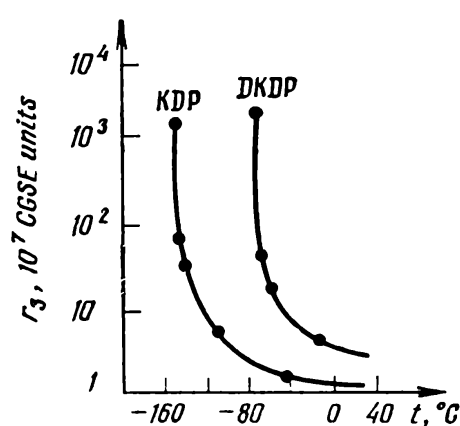


Fig. 11.8. Temperature dependence of effective electrooptic coefficient of KDP and DKDP crystals.

nide plate in the longitudinal electrooptical effect mode, if the electric field strength along [110] is  $10^4$  V/cm, and the path length for light with  $\lambda = 1.25$   $\mu\text{m}$  propagating along [110] is 20 mm.

11.25. CdS greenockite crystals, transparent in the IR range, can be used as modulators for this range. Calculate the control voltage required for a greenockite Z-cut plate modulator operating in the longitudinal electrooptical effect mode, for light with  $\lambda = 0.515$   $\mu\text{m}$ .

11.26. Calculate the thickness of a gallium arsenide plate whose working faces are perpendicular to [110], if the transverse electrooptical effect observed in the direction [110] produces a quarter-wavelength path difference ( $\lambda = 0.546$   $\mu\text{m}$ ) for the electric field strength  $E = 5.25$  kV/cm.

11.27. A Z-cut ADP plate was used as the transducer of a unit designed to record static stresses. What is the magnitude of the measured stress if complete extinction of light with  $\lambda = 0.546$   $\mu\text{m}$  at the centre of the interference pattern was obtained for the analyzer rotation angle  $30^\circ$ ?

11.28. The electrooptical effect is observed in an X-cut quartz plate 0.5 cm thick, with a voltage of 30 kV applied to its working faces. Characterize the changes in the properties of this plate and evaluate the angle by which the axes of the index ellipsoid are rotated by the applied electric field.

11.29. It was found in studying the tetragonal phase barium titanate crystals that an increment of polarization by  $24 \cdot 10^3$  CGSE units corresponds to an increment in refractive indices of  $-0.03$ . Evaluate the electrooptical coefficient that can be calculated from the results of this experiment.

11.30. An X-cut rochelle salt crystal plate is placed in electric field with strength  $\mathbf{E}$ . Calculate the new refractive indices, and the angle of rotation of the index ellipsoid in this field.

11.31. Calculate the thickness of a Z-cut KDP plate used as a light gate for a high-speed movie camera if the application of electric field  $E = 10$  kV/cm to the opposite faces of the plate gives a quarter-wavelength path difference for light with  $\lambda = 0.546$   $\mu\text{m}$  propagating along [001].

11.32. The measurement of the longitudinal electrooptical effect in a mechanically free Z-cut KDP plate gave  $r_{63} = -30 \cdot 10^{-3}$  CGSE units. Evaluate this coefficient if the plate is used in a high-frequency ac field (assume that the frequency and plate thickness are such that no resonance is produced).

11.33. Which of the electrooptical coefficients of quartz can be found by using an oriented X-cut specimen and measuring the half-wavelength control voltage  $V_{\lambda/2}$  for a light beam with a known wavelength, propagating along the optic axis?

11.34. An electric field  $\mathbf{E}$  is applied to the working faces of a sphalerite plate oriented perpendicular to [111]. Find the refractive in-

dices characterizing the optical properties of this plate. Find the expression for the phase retardation of light polarized along [111] and propagating in a direction perpendicular to [111].

11.35. An analysis of electrooptical properties of KTN crystals at a temperature  $T = T_C$  for light with  $\lambda = 0.633 \mu\text{m}$  revealed that an electric field acting along [100] changed the refractive index along [010] by  $\Delta n$ ; at field strength  $10^4 \text{ V/cm}$  the increment of the refractive index,  $\Delta n$ , was equal to  $6 \cdot 10^{-4}$ . Which of the electrooptical coefficients can be determined from these data? Calculate its magnitude.

11.36. Two unit-size KDP and DKDP crystal specimens are placed in an electric field so that  $\mathbf{E} \parallel [001]$ , and light propagates along [110]. Calculate the potential difference necessary to produce a half-wavelength path difference for  $\lambda = 0.535 \mu\text{m}$  in both plates.

11.37. Calculate the phase retardation of light with  $\lambda = 0.633 \mu\text{m}$  obtainable by the Z-cut lithium tantalate plate operating in the longitudinal electrooptical effect mode, if the voltage applied to the electrodes deposited on the working faces is 30 kV.

11.38. Calculate the thickness of a gallium arsenide plate with the normal to the surface [111], such that an electric field  $10^3 \text{ V/cm}$  applied between the working faces produces a quarter-wavelength path difference for light with  $\lambda = 1.25 \mu\text{m}$ .

11.39. Evaluate the angle by which the index ellipsoid of KDP crystals is rotated when an electric field of  $10^4 \text{ V/cm}$  is applied along [100].

11.40. The transverse electrooptical effect is observed on a single-crystal gallium arsenide specimen oriented as shown in Fig. 11.9. Field  $\mathbf{E}$  is parallel to [110], and light propagates along [110].

Calculate the principal refractive indices of gallium arsenide in the field. Determine the phase retardation induced by the electric field for light polarized along [001].

11.41. Is it possible to realize light modulation by employing the quadratic electrooptical effect in cubic perovskite crystals in the directions

(i) [100], [010], and (ii) [110]?

Note: In solving problems 11.42-11.46 use the Curie principle and take into account that the symmetry of the product  $E_k E_l$  [eq. (11.8)] is  $\infty/\text{mm}$ .

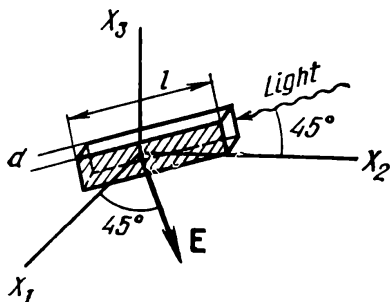


Fig. 11.9. Schematic arrangement for observation of transverse electrooptic effect on a gallium arsenide specimen.

11.42. Determine the change induced by the quadratic electrooptical effect in the index ellipsoid of crystals belonging to symmetry classes 23 and  $m3$  when electric field is aligned with directions  $\langle 100 \rangle$ .

11.43. Find the crystallographic directions in medium-symmetry classes of crystals such that the electrooptical effect induced by electric field aligned with these directions does not lower the symmetry of the corresponding index ellipsoids.

11.44. Determine the changes in the optical properties of  $X$ - and  $Z$ -cut quartz plates due to the quadratic electrooptical effect, if the vector of electric field strength is perpendicular to the plate surface.

11.45. Is it possible to observe the linear and quadratic longitudinal electrooptical effect in tourmaline crystals in the direction  $[0001]$ ?

11.46. Determine the changes in the optical properties of rock salt and sphalerite crystals due to the (i) linear electrooptical effect, and (ii) quadratic electrooptical effect, when electric field is aligned with directions  $\langle 100 \rangle$ .

11.47. It is important in any experimental study of the quadratic electrooptical effect in noncentrosymmetrical crystals to separate it from the linear effect. Which of the crystallographic directions,  $[100]$ ,  $[010]$ , or  $[001]$ , make it possible to observe the pure longitudinal quadratic electrooptical effect in class 2 crystals?

11.48. The quadratic electrooptical effect was studied on KDP crystal specimens of  $1 \times 1 \times 1 \text{ cm}^3$ . The values of control voltages required to produce a half-wavelength path difference for light with  $\lambda = 0.540 \mu\text{m}$  are listed in Table 11.6 for particular directions of electric field and light propagation.

Table 11.6

Direction of electric field	Direction of light propagation	Control voltage, $V_{\lambda/2}$ (kV)
$[100]$	$[010]$	20.0
$[010]$	$[001]$	24.6

Which of the coefficients  $R_{ij}$  (or combinations of coefficients) can be calculated from these data?

11.49. Calculate the control voltage  $V_{\lambda/2}$  of an ADP modulator of  $1 \times 1 \times 1 \text{ cm}^3$ , operating in the transverse quadratic electrooptical effect mode (electric field along  $[110]$ , light propagation along  $[001]$ , wavelength  $\lambda = 0.540 \mu\text{m}$ ). Find the ratio of the half-wavelength control voltage of the described modulator employing the quadratic electrooptical effect to the corresponding voltage of an

ADP modulator employing the longitudinal linear electrooptical effect in the direction [001].

11.50. One of the most important technical characteristics of optical deflectors used in optical communication systems is the resolving power  $N$  defined as the number of resolvable light-emitting elements. Evaluate the maximum resolving power of a deflector made of a KTN (potassium niobate-tantalate) prism with the base length 1 cm, placed in an electric field of  $10^4$  V/cm (Fig. 11.10), operating in the temperature range 20-30°C (wavelength  $\lambda = 0.633 \mu\text{m}$ ).

**Note:** The maximum resolving power  $N_{\max}$  is defined as  $N_{\max} = l\Delta n/\lambda$ , where  $l$  is the length of the prism base,  $\lambda$  is the light wavelength, and  $\Delta n$  is the increment in the refractive index.

11.51. Which of the constants of the quadratic electrooptical effect in ADP crystals can be determined from the results of an experiment represented schematically in Fig. 11.11, if the half-wavelength voltage  $V_{\lambda/2}$  is 52 kV in a  $1 \times 1 \times 1 \text{ cm}^3$  specimen?

11.52. Calculate the control voltage  $V_{\lambda/2}$  for a high-frequency modulator made of a Z-cut potassium niobatetantalate (KTN) plate 1 mm thick and 10 mm long, operating at the room temperature in the transverse quadratic electrooptical effect mode.

11.53. Calculate the birefringence induced in triglycin sulphate (TGS) crystals by electric field aligned with [010] for the light propagation direction [100] (i) in the paraelectric phase, and (ii) in the ferroelectric phase.

11.54. Cubic single crystals of strontium titanate,  $\text{SrTiO}_3$ , may prove practically important for designing wide-aperture modulator devices for the low-temperature conditions. Calculate the half-wavelength control voltage  $V_{\lambda/2}$  of a  $\text{SrTiO}_3$  modulator, realized on a Z-cut plate with the length  $l = 2.5 \text{ cm}$  along [010] and width  $d = 0.3 \text{ cm}$ .

**Fig. 11.10. Prism of a deflector.**

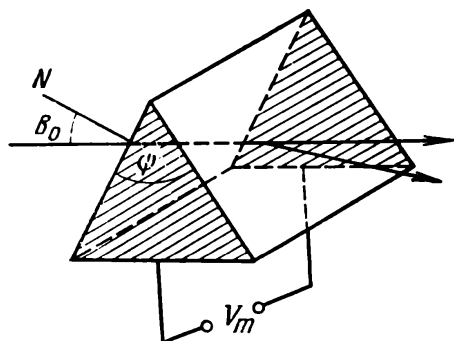
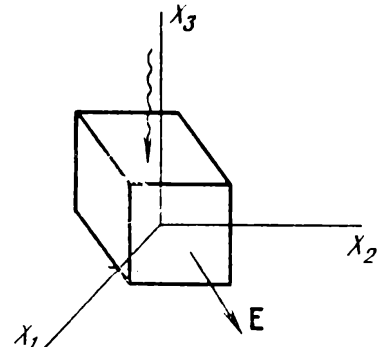


**Fig. 11.11. Experimental arrangement for observing the quadratic electrooptic effect in ADP crystals.**



A plate is used in the transverse quadratic electrooptical effect mode (electric field is applied along [001] and light propagates along [100]) and  $V_{\lambda/2} = 6.5$  kV/cm in a unit-size specimen at  $-100^{\circ}\text{C}$ .

11.55. The longitudinal electrooptical effect is observed in the direction [010] in triglycin sulphate crystals. Calculate birefringence induced by an electric field.

11.56. Is it possible to observe the longitudinal quadratic electrooptical effect in crystals with symmetry 422 in the directions [100], [010], and [001]?

11.57. The simplest beam scanners employ a prism made of an electrooptical crystal placed in an electric field (Fig. 11.10). When the refractive index of the prism is changed, the refracted beam is deflected. Calculate the increment in the refractive index of a barium titanate prism placed in the electric field of  $10^4$  V/cm, used for static deflection in the temperature range  $130\text{--}140^{\circ}\text{C}$ , for wavelength  $\lambda = 0.633$   $\mu\text{m}$ .

11.58. Figure 11.12 plots the spontaneous birefringence of barium titanate crystals as a function of squared spontaneous polarization; the birefringence is caused by the spontaneous polarization  $\mathbf{P}^s \parallel [001]$  at the Curie point. Which of the quadratic electrooptical coefficients (or combinations of coefficients) can be calculated from these data? Find its magnitude.

11.59. The results of the experimental study of the quadratic electrooptical effect on oriented unit-size specimens of RDP crystals are listed in Table 11.7 (wavelength  $\lambda = 0.540$   $\mu\text{m}$ ).

Calculate the coefficients  $R_{ij}$  (or combinations of coefficients) which can be found from the data given.

11.60. Figure 11.3 gives the spontaneous birefringence of rochelle salt crystals as a function of the squared spontaneous polarization

Fig. 11.12. Spontaneous birefringence of  $\text{BaTiO}_3$  crystals as a function of squared spontaneous polarization.

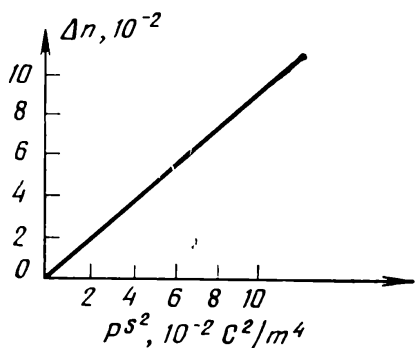


Fig. 11.13. Spontaneous birefringence of rochelle salt crystals as a function of squared spontaneous polarization.

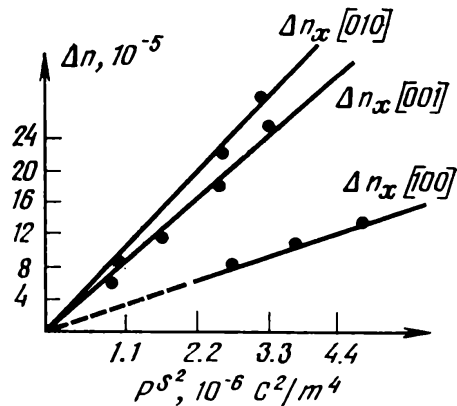


Table 11.7

Direction of electric field	Direction of light propagation	Control voltage, $V_{\lambda/2}$ (kV)
[110]	[001]	32
[010]	[001]	24.9

$(\mathbf{P}^s \parallel [100])$  in the directions [100], [010], and [001]. Which of the coefficients of the quadratic electrooptical effect (or combinations of coefficients) can be found from these data? Calculate their magnitudes.

## 12. GENERATION OF OPTICAL HARMONICS

The main laws of crystal optics for light with relatively low intensity follow from the solutions to the Maxwell equations on an assumption that the crystalline medium is linear in the dielectric properties of the medium. The matter equation  $D_i = \epsilon_{ij}E_j$ , used in Sec. 9 is linear in  $\mathbf{E}$  and yields a linear dependence of polarization  $\mathbf{P}$  on  $\mathbf{E}$ :  $P_i = \kappa_{ij}E_j$ , where  $\kappa_{ij}$  is the tensor of polarizability of the medium, related to  $\epsilon_{ij}$  by the expression

$$\kappa_{ij} = \frac{1 - \epsilon_{ij}}{4\pi}$$

The quantities  $\epsilon_{ij}$  and  $\kappa_{ij}$  were assumed independent of the field.

In stronger interactions, when the strength of the external field is high, the linear approximation proves insufficient, and a correct description of the interaction between the strong field and a dielectric must take into account the terms of the matter equation quadratic in field. We are dealing here with optical phenomena following from the dielectric nonlinearity of crystals; taking into account that the electric field of the light wave may act as the “external” field, we shall introduce the frequencies of the electric field and polarization.

Consider the polarization produced by fields  $\mathbf{E}(\omega_1)$  and  $\mathbf{E}(\omega_2)$ . By expanding  $\mathbf{P}$  in powers of  $\mathbf{E}(\omega_1)$  and  $\mathbf{E}(\omega_2)$  and assuming  $\mathbf{P} = \mathbf{P}_0$  at the initial time moment when  $\mathbf{E}(\omega_1) = \mathbf{E}(\omega_2) = 0$ , we find

$$\begin{aligned} P_i(\omega) = P_{0i} + \frac{\partial P_i}{\partial E_j(\omega_1)} E_j(\omega_1) + \frac{\partial P_i}{\partial E_j(\omega_2)} E_j(\omega_2) \\ + \frac{\partial^2 P_i}{\partial E_j(\omega_1) \partial E_k(\omega_1)} E_j(\omega_1) E_k(\omega_1) \quad (12.1) \\ + \frac{\partial^2 P_i}{\partial E_j(\omega_2) \partial E_k(\omega_2)} E_j(\omega_2) E_k(\omega_2) \\ + \frac{\partial^2 P_i}{\partial E_j(\omega_1) \partial E_k(\omega_2)} E_j(\omega_1) E_k(\omega_2) \end{aligned}$$

The first derivatives in Eq. (12.1) are polarizabilities  $\kappa_{ij}$  describing the propagation of light in the linear approximation when the frequency of the induced polarizations equals the electric field frequency.

The second derivatives are the nonlinear polarizabilities or the quadratic susceptibility  $\chi_{ijk}(\omega, \omega_1, \omega_2)$ ; these are the rank-three

tensor whose components are functions of frequencies  $\omega_1$ ,  $\omega_2$  and the generated frequency  $\omega$ . The physical meaning of the components of tensor  $\chi_{ijk}$  follows from the equation for the nonlinear component of polarization, quadratic in field:

$$P_i(\omega) = \chi_{ijk}(\omega, \omega_1, \omega_2) E_j(\omega_1) E_k(\omega_2) \quad (12.2)$$

Let us introduce relationships between frequencies  $\omega$ ,  $\omega_1$ , and  $\omega_2$  for nonlinear terms in (12.1). Let the fields  $\mathbf{E}(\omega_1)$  and  $\mathbf{E}(\omega_2)$  at any fixed point of the crystal be harmonic in time:

$$E_j(\omega_1) = E_{0j} \cos(\omega_1 t)$$

$$E_k(\omega_2) = E_{0k} \cos(\omega_2 t + \varphi)$$

where  $\varphi$  is the phase shift between the fields at the chosen point. Since

$$E_j(\omega_1) E_k(\omega_2) = \frac{1}{2} E_{0j} E_{0k} \{ \cos[(\omega_1 - \omega_2)t - \varphi] + \cos[(\omega_1 + \omega_2)t + \varphi] \}$$

the polarization quadratic in field either has a difference ( $\omega_1 - \omega_2$ ) or sum ( $\omega_1 + \omega_2$ ) frequency, and the tensor  $\chi_{ijk}(\omega, \omega_1, \omega_2)$  is non-zero in only two cases:

$$\chi_{ijk} = \chi_{ijk}(\omega_1 - \omega_2, \omega_1, \omega_2)$$

or

$$\chi_{ijk} = \chi_{ijk}(\omega_1 + \omega_2, \omega_1, \omega_2)$$

If a crystal is illuminated with a high-intensity light at frequency  $\omega$ , and the nonlinear polarizability of the medium due to the electric field of the light wave is taken into account, then

$$\chi_{ijk} = \chi_{ijk}(0, \omega, \omega)$$

$$\chi_{ijk} = \chi_{ijk}(2\omega, \omega, \omega)$$

Consequently, taking the dielectric nonlinearity into account results in a constant component of polarization and generation of the second harmonic of the fundamental frequency (SHG). In what follows, SHG is the only light frequency conversion in the nonlinear medium that will be of interest to us.

Generation of a double frequency of light can be illustrated by the following diagram (Fig. 12.1). The incident wave  $\mathbf{E}(\omega)$  propagates at a velocity  $v_1 = c/n_1$  and generates a polarization wave  $\mathbf{P}(2\omega)$  propagating at the same velocity  $v_1$ . The polarization  $\mathbf{P}(2\omega)$  generates a light wave with twice the initial frequency,  $\mathbf{E}(2\omega)$ , propagating at a different velocity  $v_2 = c/n_2$ . Because of dispersion of the medium,  $n_1(\omega) \neq n_2(2\omega)$ .

The emerging light wave  $\mathbf{E}(2\omega)$  is sufficiently intensive outside the crystal if the quadratic polarization amplifies the wave with the fundamental frequency passing through this point of emergence, that is, if the waves  $\mathbf{E}(\omega)$  and  $\mathbf{E}(2\omega)$  interfere constructively.

The interference of waves with frequencies  $\omega$  and  $2\omega$  is possible if  $v_1 = v_2$ . This requirement is equivalent to requiring that the refractive indices for frequencies  $\omega$  and  $2\omega$  be equal:  $n_1(\omega) = n_2(2\omega)$ , or, dropping the subscripts,

$$n(\omega) = n(2\omega) \quad (12.3)$$

The condition of equal refractive indices for the fundamental frequency wave and its second harmonic (SH) is called the wave synchronism, or index matching. This condition is fulfilled only in particular crystals, in specific directions called synchronism directions. Indeed, the constraint  $n(\omega) = n(2\omega)$  cannot hold in an isotropic body because  $n$  is an increasing function of frequency in the normal dispersion region. In the region of anomalous dispersion synchronism is only possible for frequencies close to the resonance absorption frequency. In this frequency range absorption is high, and thus it is impossible to generate a sufficiently intensive SH in isotropic media.

In birefringent crystals refractive indices are functions of direction. Consequently, synchronism can be satisfied even in the range of normal dispersion for two waves propagating in the same direction. Figure 12.2a shows index quadratics for waves with frequencies  $\omega$  and  $2\omega$  in a positive uniaxial crystal. Clearly, the surfaces corresponding to  $n_e(2\omega)$  and  $n_o(\omega)$  intersect in directions at an angle  $\theta$  to the optic axis of the crystal. This means that in the directions shown by the arrow the synchronism holds for the ordinary fundamental frequency beam and the extraordinary SH beam. Figure 12.3 demonstrates a case when no synchronism is attainable in a crystal with high dispersion and relatively low anisotropy.

When crystals are used for SHG, it is essential to achieve the maximum intensity of SH, realizable in the synchronism direction, and to know what deviations from synchronism affect this intensity.

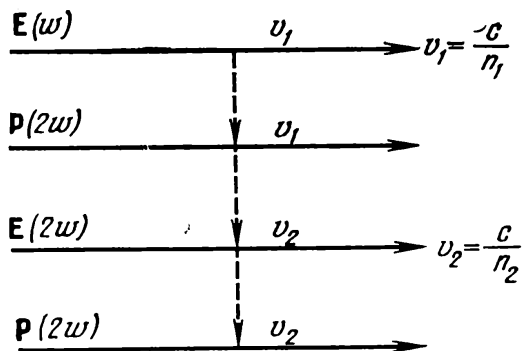


Fig. 12.1. Schematic diagram illustrating the generation of second harmonic.

To find the intensity of SH, consider the Maxwell equations with nonlinear polarization included:

$$\operatorname{curl} \mathbf{H} = -\frac{1}{c} \frac{\partial \mathbf{D}}{\partial t} \quad (12.4a)$$

$$\operatorname{curl} \mathbf{E} = \frac{1}{c} \frac{\partial \mathbf{H}}{\partial t} \quad (12.4b)$$

$$D_i = \epsilon_{ij} E_j + 4\pi P_i \quad (12.4c)$$

The additional term  $4\pi P_i$  in the matter equation (12.4c) represents the nonlinear part of polarization, and  $\epsilon_{ij} E_j$  is the linear part of induction  $D_i$ .

The intensity of light is expressed in terms of amplitude  $E_0$  of light wave, so that we need to express the amplitude of SH wave in terms of the amplitude of the fundamental frequency wave. To achieve this, we solve the system (12.4a, b, c) for the field of double frequency  $2\omega$ , taking the nonlinear term  $P$  into account.

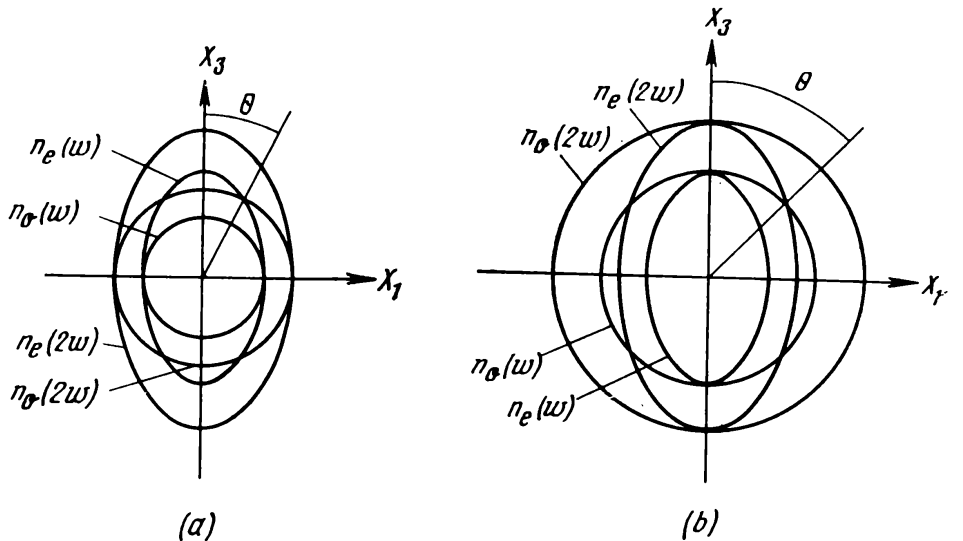
Let us rewrite the Maxwell equations (12.4a, b, c) by differentiating (12.4a) with respect to time, and taking the curl of the right- and left-hand sides of equation (12.4b):

$$\frac{\partial}{\partial t} \operatorname{curl} \mathbf{H} = -\frac{1}{c} \frac{\partial^2 \mathbf{D}}{\partial t^2}$$

$$\operatorname{curl} \operatorname{curl} \mathbf{E} = \frac{1}{c} \operatorname{curl} \frac{\partial}{\partial t} \mathbf{H}$$

Fig. 12.2. Sections of refractive index ellipsoids of uniaxial crystals in optically positive and

optically negative crystals. The direction of synchronism is at an angle  $\theta$  to the optic axis.



By writing explicitly  $\operatorname{curl} \operatorname{curl} \mathbf{E}$  and substituting the expression for  $\frac{\partial}{\partial t} \operatorname{curl} \mathbf{H}$  from the second into the first equation, we find

$$\nabla^2 \mathbf{E} = \frac{1}{c} \frac{\partial^2 \mathbf{D}}{\partial t^2} \quad (12.5)$$

In the one-dimensional case, when light propagates along the axis  $X_3$ , Eq. (12.5) takes the form

$$\frac{\partial^2 \mathbf{E}}{\partial x_3^2} = \frac{1}{c^2} \frac{\partial^2 \mathbf{D}}{\partial t^2}$$

or, using (12.4c),

$$\frac{\partial^2 \mathbf{E}}{\partial x_3^2} = \frac{\epsilon}{c^2} \frac{\partial^2 \mathbf{E}}{\partial t^2} + \frac{4\pi}{c^2} \frac{\partial^2 \mathbf{P}}{\partial t^2} \quad (12.6)$$

Let  $E_1 = E_{01}(x_3) \exp[-i(\omega t - k_1 x_3)]$  denote the fundamental frequency wave,  $E_2 = E_{02}(x_3) \exp[-i(2\omega t - k_1 x_3)]$  the SH wave, and  $P_2 = \chi E_{01}(x_3) \exp[-i(2\omega t - k_1 x_3)]$  the polarization wave with frequency  $2\omega$ .

If synchronism does not hold,  $2k_1 \neq k_2$ . We denote  $2k_1 - k_2 = \Delta k$ , and regard  $\Delta k$  as a measure of departure from synchronism.

Let us find derivatives of all quantities in (12.6), and substitute them into this equation:

$$\begin{aligned} 2 \frac{\partial E_{02}}{\partial x_3} i k_2 \exp[-i(2\omega t - k_2 x_3)] \\ = \frac{4\pi}{c^2} \chi 4\omega^2 E_{01}^2(x_3) \exp[-i(2\omega t - 2k_2 x_3)] \end{aligned}$$

Multiply both sides of the equation by  $i$  and divide them by  $\exp[-i(2\omega t - k_2 x_3)]$ :

$$\frac{\partial E_{02}(x_3)}{\partial x_3} = \frac{8\pi i}{c^2 k_2} \chi \omega^2 E_{01}^2(x_3) \exp[i\Delta k x_3] dx_3 \quad (12.7)$$

Equation (12.7) is the equation for the SH amplitude  $E_{02}(x_3)$ . Integration of (12.7) with respect to  $x_3$  on an assumption that the fundamental frequency amplitude  $E_{01}(x_3)$  is weakly dependent on  $x_3$

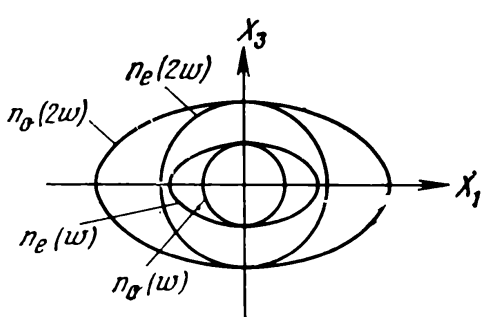


Fig. 12.3. Section of refractive index surfaces of an optically positive crystal without synchronism directions.

gives the amplitude of SH wave at a point with coordinate  $L$ :

$$E_{02}(L) = \frac{8\pi i}{c^2 k_2} \chi \omega_1^2 E_{01}^2 \int_0^L \exp[i\Delta k x_3] dx_3$$

The intensity of double frequency light can now be found by using the formula

$$I = \frac{cn}{2\pi} EE^*$$

where  $E$  and  $E^*$  are complex conjugate amplitudes of the light wave.

For SH,

$$E_{02}E_{02}^* = \left( \frac{8\pi\omega^2}{c^2 k_2} \chi \right)^2 E_{01}E_{01}^* \int_0^L e^{i\Delta k x_3} dx_3 \int_0^L e^{-i\Delta k x_3} dx_3$$

By using the Euler formula,  $e^{ix} = \cos x + i \sin x$ , expressing  $E_{01}E_{01}^*$  via the intensity  $I_1$  of the fundamental frequency light, and taking into account that  $k_2 = 2\pi n_2/\lambda_2$ ,  $k_1 = 2\pi n_1/\lambda_1$ , and  $\lambda_2 = \lambda_1/2$ , we find the following expression for the intensity  $I_2$  of the SH wave:

$$I_2 = \frac{64\pi^5}{cn_1^2 n} \frac{L^2}{\lambda_1^2} \chi^2 I_1^2 \left( \frac{\sin \frac{\Delta k L}{2}}{\frac{\Delta k L}{2}} \right) \quad (12.8)$$

where  $n_1$  is the refractive index at the fundamental frequency, that is,  $n(\omega)$ ;  $n_2 = n(2\omega)$ ;  $\lambda_1$  is the wavelength at the fundamental frequency, and  $\chi$  is the nonlinear susceptibility of the medium.

As follows from formula (12.8), the SH intensity is proportional to squared intensity at the fundamental frequency. The intensity  $I$  is a periodical function of  $\Delta k L/2$ , and its dependence on the length of a crystal is given by

$$\left( \frac{\sin \left( \frac{\Delta k L}{2} \right)}{\frac{\Delta k L}{2}} \right)^2$$

If  $\Delta k \neq 0$ ,  $I$  reaches the first maximum for  $L = \pi/\Delta k$ . This length is called the coherence length  $L_{coh}$  of the crystal.

Let us express  $L_{coh}$  in terms of the refractive indices  $n(\omega)$  and  $n(2\omega)$ . If the primary wave and its SH have the common wavefront normal  $m$ , then

$$\Delta k = \frac{2\omega}{c} [n(2\omega) - n(\omega)] = \frac{2\omega}{c} \Delta n \quad (12.9)$$

This yields

$$L_{coh} = \frac{2\pi c}{2\omega\Delta n}$$

The coherence length is a very small quantity. Thus, for example, in quartz illuminated with Nd laser radiation ( $\lambda = 1.06 \mu\text{m}$ ) we find  $\Delta n = 10^{-2}$  and  $L_{coh} = 13 \mu\text{m}$ . Clearly, the maximum intensity obtainable in a crystal with  $\Delta k \neq 0$  is equal to the intensity generated over one coherence length of the crystal, regardless of its total length.

If the synchronism condition is not satisfied, the SH intensity is very small even for the coherence length of the crystal.

When the synchronism condition is satisfied, Eq. (12.8) shows that the SH intensity is proportional to the crystal length, and the SH intensity is considerable. But in this case very long crystals cannot be used because of the so-called "beam displacement". The "beam displacement" for light propagating in the synchronism direction, not coinciding with one of the semiaxes of the index ellipsoid in an optically uniaxial crystal, is the deviation of the extraordinary beam from the direction of wavefront normal and from that of the ordinary beam. The extraordinary beam energy is thus moved away from the ordinary beam, and the effective length of beam interaction becomes smaller than the crystal length, and the more so the larger is the angle between the wavefront normal and the beam for the extraordinary wave. Consequently, the transformation efficiency is maximum for the so-called 90 degrees synchronism, that is,  $\theta = 90^\circ$ . To achieve the  $90^\circ$  synchronism, it is possible to use the temperature dependence of refractive indices at the fundamental and double frequencies, as well as the dependence of these quantities on crystal composition.

Dielectric nonlinearity of crystals in the optical frequency range is described by the quadratic susceptibility constants  $\chi_{ijk}$  and nonlinearity coefficients  $d_{ijk}$ . Current literature operates with the quadratic susceptibility constants relating the complex polarizability to the complex electric field:

$$P_i(2\omega) = \chi_{ijk} E_j(\omega) E_k(\omega) \quad (12.10)$$

Experimenters operate with nonlinearity coefficients which relate the real values of polarization and electric field:

$$\{P_i(2\omega)\} = d_{ijk} \{E_j(\omega)\} \{E_k(\omega)\} \quad (12.11)$$

Taking into account that for a wave propagating along the axis  $X_3$ , we have

$$P(2\omega) = \frac{\{P\}}{2} e^{-2ikx_3} \quad \text{and} \quad E(\omega) = \frac{\{E\}}{2} e^{-ikx_3}$$

it can be shown that

$$d_{ijk} = \frac{\chi_{ijk}}{2}$$

Usually the handbooks on the properties of nonlinear optic materials give the tables listing the components of the tensor  $d_{ijk}$ . Note that nonlinear optic effects, and SHG among them, are observed only in noncentrosymmetrical crystals, and the matrices of  $d_{ijk}$  for these crystals are identical in form with the matrices of piezoelectric moduli.

In the case of SHG, relation (12.11) can be written in the following detailed matrix form:

$$\begin{vmatrix} P_1 \\ P_2 \\ P_3 \end{vmatrix} = \begin{vmatrix} d_{11} & d_{12} & d_{13} & d_{14} & d_{15} & d_{16} \\ d_{21} & d_{22} & d_{23} & d_{24} & d_{25} & d_{26} \\ d_{31} & d_{32} & d_{33} & d_{34} & d_{35} & d_{36} \end{vmatrix} \begin{vmatrix} E_1^2 \\ E_2^2 \\ E_3^2 \\ E_2 E_3 \\ E_1 E_3 \\ E_1 E_2 \end{vmatrix}$$

where  $P_1$ ,  $P_2$ , and  $P_3$  are the components of nonlinear polarization  $\mathbf{P}$  ( $2\omega$ ), and  $E_1$ ,  $E_2$ , and  $E_3$  the components of the electric field of light wave at the fundamental frequency,  $\mathbf{E}$  ( $\omega$ ).

For a particular light wave propagating in a direction  $\mathbf{m}$  coinciding, for example, with the synchronism direction of a crystal, the directions of the components of  $P_i$  and  $E_i$  with respect to the crystallophysical axes are determined, and the summation prescribed by (12.11) for the matrix  $d_{ijk}$ , corresponding to the symmetry of the crystal, can be carried out. The summation yields a coefficient  $d_{\text{eff}}$  which expresses the actual polarization as a function of actual electric field:

$$\{P(2\omega)\} = d_{\text{eff}} \{E(\omega)\}^2 \quad (12.12)$$

The coefficient  $d_{\text{eff}}$  for an interaction under consideration can then be used to calculate the SH intensity via (12.8), taking into account (12.12).

### Examples of Problems with Solutions

**12.1.** Determine the effective nonlinearity coefficient  $d_{\text{eff}}$  for different types of interactions in directions at an angle  $\theta$  to the optic axis for crystals belonging to symmetry class  $\bar{4}2m$ .

Calculate  $d_{\text{eff}}$  for the  $oo \rightarrow e$  coupling in KDP, that is, for SHG.

**Solution.** As follows from Fig. 12.2a, the synchronism (index matching) in optically positive uniaxial crystals is realized in SHG for the extraordinary incident wave and ordinary SH wave. The compact notation for this coupling is  $ee \rightarrow o$ . In optically negative crystals the situation is reversed, that is, the  $oo \rightarrow e$ , coupling is realized. Synchronism may also be attained if the incident radiation is a superposition of an ordinary and extraordinary waves. The coupling of two incident waves, ordinary and extraordinary, to the ordinary SH wave in a positive crystal,  $oe \rightarrow o$ , and to the extraordinary wave in a negative crystal,  $oe \rightarrow e$ , proves index-matched.

Consider the general case of finding  $d_{\text{eff}}$  in a  $\bar{4}2m$  crystal, with no restriction on the optic sing of crystals.

Equation (12.11) relating the nonlinear component of polarization to the electric field strength of fundamental-frequency waves is

$$P_i(2\omega) = d_{ijk} E_j(\omega) E_k(\omega)$$

where  $d_{ijk}$  for class  $\bar{4}2m$  is

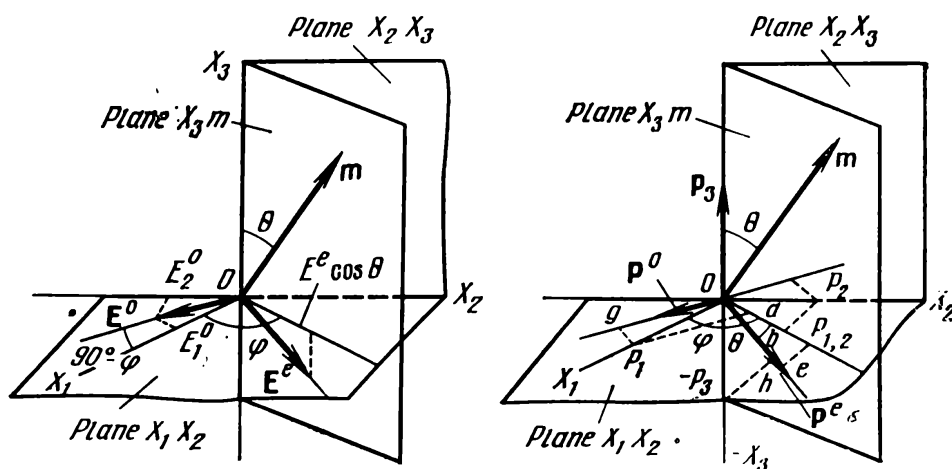
$$\begin{pmatrix} 0 & 0 & 0 & d_{14} & 0 & 0 \\ 0 & 0 & 0 & 0 & d_{14} & 0 \\ 0 & 0 & 0 & 0 & 0 & d_{36} \end{pmatrix}$$

By definition,

$$d_{\text{eff}} = \frac{\{P(2\omega)\}}{\{E(\omega)\}^2}$$

and can be calculated for a crystal of a given symmetry class as a function of the direction of propagation of the fundamental- and double frequency light waves.

Fig. 12.4. Diagram clarifying the derivation of the expression for  $d_{\text{eff}}$  for KDP crystals.



In order to calculate  $d_{\text{eff}}$ , we make use of Eq. (12.11) and Fig. 12.4 which shows the arrangement of the vectors  $\mathbf{m}$ ,  $\mathbf{E}^{\text{o}}(\omega)$ , and  $\mathbf{E}^{\text{e}}(\omega)$  for the incident waves, and  $\mathbf{P}^{\text{o}}(2\omega)$  and  $\mathbf{P}^{\text{e}}(2\omega)$  for the SH wave in the crystallophysical coordinate system. The optic axis of the crystal and vector  $\mathbf{m}$  lie in the principal plane defined by these two directions in the crystal, at an angle  $\varphi$  to the axis  $X_1$ ;  $\mathbf{E}^{\text{e}}(\omega)$  is in the same plane, and  $\mathbf{E}^{\text{o}}(\omega)$  is perpendicular to  $\mathbf{m}$ , lies in the plane  $X_1X_2$ , at an angle  $(90^\circ - \varphi)$  to  $X_1$ .

In the tensor and not matrix notation of the coefficients  $d_{ijk}$  the components of nonlinear polarization  $P_i(2\omega)$  are

$$P_1 = d_{123}E_2^{\text{o}}E_3^{\text{e}} + d_{132}E_3^{\text{o}}E_2^{\text{e}}$$

$$P_2 = d_{213}E_1^{\text{o}}E_3^{\text{e}} + d_{231}E_3^{\text{o}}E_1^{\text{e}}$$

$$P_3 = d_{312}E_1^{\text{o}}E_2^{\text{e}} + d_{321}E_2^{\text{o}}E_1^{\text{e}}$$

In the matrix notation, taking into account that  $d_{14} = d_{25}$ , we find

$$P_1 = d_{14}(E_2^{\text{o}}E_3^{\text{e}} + E_3^{\text{o}}E_2^{\text{e}})$$

$$P_2 = d_{14}(E_1^{\text{o}}E_3^{\text{e}} + E_3^{\text{o}}E_1^{\text{e}})$$

$$P_3 = d_{36}(E_1^{\text{o}}E_2^{\text{e}} + E_2^{\text{o}}E_1^{\text{e}})$$

The components  $E^{\text{o}}$  and  $E^{\text{e}}$  along the coordinate axes are

$$E_1^{\text{o}} = E^{\text{o}} \sin \varphi, \quad E_1^{\text{e}} = E^{\text{e}} \cos \theta \cos \varphi$$

$$E_2^{\text{o}} = -E^{\text{o}} \cos \varphi, \quad E_2^{\text{e}} = E^{\text{e}} \cos \theta \sin \varphi$$

$$E_3^{\text{o}} = 0, \quad E_3^{\text{e}} = -E^{\text{e}} \sin \theta$$

Correspondingly, the components of nonlinear polarization are

$$P_1 = d_{14}(E^{\text{o}} \cos \varphi E^{\text{e}} \sin \theta) = d_{14}E^{\text{o}}E^{\text{e}} \sin \theta \cos \varphi$$

$$P_2 = -d_{14}E^{\text{o}}E^{\text{e}} \sin \varphi \sin \theta$$

$$P_3 = -d_{36}E^{\text{o}}E^{\text{e}}(\sin^2 \varphi \cos \theta - \cos^2 \varphi \cos \theta) = -d_{36}E^{\text{o}}E^{\text{e}} \cos \theta \cos^2 \varphi$$

Now, to find  $d_{\text{eff}}$  we have to determine the projections of the components of the vector  $\mathbf{P}(2\omega)$  onto the directions of the vectors  $\mathbf{E}^{\text{o}}(\omega)$  and  $\mathbf{E}^{\text{e}}(\omega)$ , that is, the values of  $P^{\text{e}}(2\omega)$  and  $P^{\text{o}}(2\omega)$ .

As follows from Fig. 12.4,  $P^e$  ( $2\omega$ ) lies in the principal plane of the crystal, and can be given by the following formulas:

$$\begin{aligned}
 P^e &= oe + oh; \quad oa = P_1 \cos \varphi; \quad ob = P_2 \sin \varphi \\
 P_{1,2} &= P_1 \cos \varphi + P_2 \sin \varphi; \quad oe = P_{1,2} \cos \theta \\
 &\quad = (P_1 \cos \varphi + P_2 \sin \varphi) \cos \theta \\
 oh &= -P_3 \sin \theta; \quad P^e = oe + oh = -oh - oe \\
 P^e &= d_{36} E^0 E^e \cos \theta \sin \theta \cos 2\varphi \\
 &\quad + E^e E^0 d_{14} (\sin 2\varphi \cos \theta \sin \theta - \cos^2 \varphi \sin \theta \cos \theta) \\
 &\quad = -(d_{14} + d_{36}) \cos 2\varphi \cos \theta \sin \theta E^0 E^e \quad (12.13)
 \end{aligned}$$

$$\begin{aligned}
 P^0 &= og + of = P_1 \sin \varphi + P_2 \cos \varphi \\
 &= d_{14} (\cos \varphi \sin \varphi \sin \theta + \sin \varphi \cos \varphi \sin \theta) \\
 &\quad = d_{14} \sin \theta \sin 2\varphi E^0 E^e \quad (12.14)
 \end{aligned}$$

Equations (12.13) and (12.14) yield

$$d_{\text{eff}} = -(d_{14} + d_{36}) \cos 2\varphi \cos \theta \sin \theta$$

for the  $oo \rightarrow e$  coupling, and

$$d_{\text{eff}} = d_{14} \sin \theta \sin 2\varphi$$

for the  $oe \rightarrow o$  coupling.

We shall now calculate  $d_{\text{eff}}$  for the  $oo \rightarrow e$  coupling in KDP crystals. In this case  $P_1 = 0$ ,  $P_2 = 0$ , and

$$\begin{aligned}
 P_3 &= -d_{36} \sin \varphi \cos \theta (E^0)^2; \quad oe = P_{1,2} \cos \theta = 0; \\
 P^e &= oe + oh = 0 - P_3 \sin \theta = -d_{36} \sin \varphi \cos \varphi \sin \theta (E^0)^2
 \end{aligned}$$

This means that

$$d_{\text{eff}} = -d_{36} \sin \theta \sin 2\varphi$$

reaches maximum for  $\varphi = \pi/4$  and  $\theta = 41^\circ$ , that is, in the direction of index matching.

For  $\lambda = 1.06 \mu\text{m}$ ,  $d_{36} = 1.04 \cdot 10^{-9} \text{ cm/dyne}^{1/2}$ . Finally,  $d_{\text{eff}} = -1.04 \cdot 10^{-9} \cdot 0.65 = 0.67 \cdot 10^{-9} \text{ cm/dyne}^{1/2}$ .

**12.2.** Determine the orientation of the synchronism axis in KDP for  $\lambda = 0.694 \mu\text{m}$ , if  $N_o = 1.51$ ,  $N_e = 1.47$  for  $\lambda = 0.694 \mu\text{m}$ , and  $N_o = 1.54$ ,  $N_e = 1.49$  for  $\lambda = 0.347 \mu\text{m}$ .

**Solution.** The symmetry of KDP crystals is  $\bar{4}2m$ ; as  $N_o > N_e$ , the crystal is uniaxial and negative. Hence, it allows for  $oo \rightarrow e$  synchronous coupling. Index matching is realized in uniaxial negative crystals if the principal refractive indices at the appropriate fre-

quencies satisfy the relation (see Fig. 12.2b)

$$N_o(\omega) \geq N_e(2\omega)$$

In the case under discussion  $1.51 > 1.49$ , so that the crystal indeed has a direction satisfying the index matching condition. Let us find this direction using the following arguments.

For the index-matching coupling  $oo \rightarrow e$  along the synchronism direction the refractive index of the fundamental-frequency ordinary wave must be equal to that of the double-frequency extraordinary wave  $n_e^0(2\omega)$ :

$$N_o(\omega) = n_e^0(2\omega) \quad (12.15)$$

Since the refractive index of the extraordinary wave is a function of direction of its wavefront normal, we shall express  $n_e^0$  as a function of angle  $\theta$  between the wavefront normal  $\mathbf{m}$  and the optic axis of the crystal, that is, the crystallophysical axis  $X_3$  (Fig. 12.5). The value of  $n_e^0$  can be found as the radius vector  $\mathbf{r}$  of the indicatrix lying in the same plane with the wavefront normal and perpendicular to it. The angle between  $\mathbf{r}$  and the optic axis is  $(90^\circ - \theta)$ . In uniaxial crystals the indicatrix has a symmetry axis of infinite order, coinciding with the coordinate axis  $X_3$ , and the vector  $\mathbf{r}$  and the normal  $\mathbf{m}$  to the plate can be aligned in the coordinate plane  $X_2X_3$ ; the coordinates of  $\mathbf{r}$  are  $(0, r_2, r_3)$ .

The equation of the section of the index ellipsoid by the coordinate plane  $X_2X_3$  is

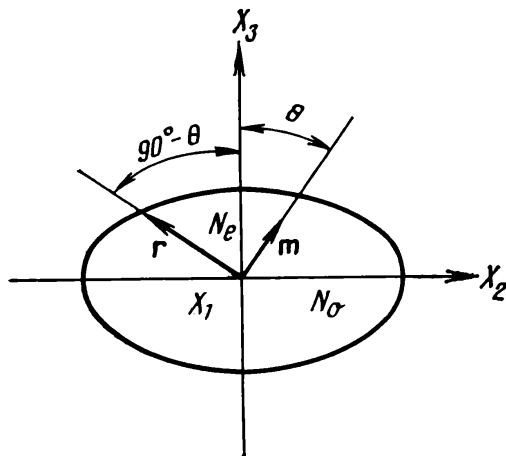
$$\frac{x_2^2}{N_o^2} + \frac{x_3^2}{N_e^2} = 1 \quad (12.16)$$

Since  $(90^\circ - \theta)$  is the angle between  $\mathbf{r}$  and  $X_3$ , we have

$$x_2 = r \sin(90^\circ - \theta) = r \cos \theta$$

$$x_3 = r \cos(90^\circ - \theta) = r \sin \theta$$

Fig. 12.5. Section of the index ellipsoid of an optically uniaxial crystal by the coordinate plane  $X_2X_3$ .



Substitution of  $x_2$  and  $x_3$  into (12.16) yields

$$\frac{r^2 \cos^2 \theta}{N_o^2} + \frac{r^2 \sin^2 \theta}{N_e^2} = 1$$

whence

$$r^2 = \frac{1}{\frac{\cos^2 \theta}{N_o^2} + \frac{\sin^2 \theta}{N_e^2}} = \frac{N_o^2 N_e^2}{N_e^2 \cos^2 \theta + N_o^2 \sin^2 \theta} \quad (12.17)$$

From this

$$n_e^\theta = \frac{N_o N_e}{(N_e^2 \cos^2 \theta + N_o^2 \sin^2 \theta)^{1/2}}$$

or

$$(n_e^\theta)^{-2} = N_o^{-2} \cos^2 \theta + N_e^{-2} \sin^2 \theta$$

Substituting the expression for  $n_e^\theta$  into (12.15) and taking into account that  $n_e^\theta$  corresponds to frequency  $2\omega$ , we find

$$N_o^{-2}(\omega) = N_o^{-2}(2\omega) \cos^2 \theta + N_e^{-2}(2\omega) \sin^2 \theta$$

By solving this equation for  $\sin \theta$ , we obtain

$$\sin \theta = \sqrt{\frac{N_o^{-2}(\omega) - N_o^{-2}(2\omega)}{N_e^{-2}(2\omega) - N_o^{-2}(2\omega)}} \quad (12.18)$$

Using the numerical values of refractive indices of KDP crystals in (12.18), we find

$$\sin \theta = 0.76$$

whence  $\theta = 50^\circ$ .

**12.3.** Find the radiant flux density of SH radiation generated in a KDP crystal for the fundamental-frequency wavelength  $\lambda = 1.06 \mu\text{m}$ , incident flux density  $10^9 \text{ W/cm}^2$ , and crystal length 2.5 cm.

**Solution.** For this calculation, we use the results of the preceding problem and the formula for the SH radiant flux density (in  $\text{W/cm}^2$ ):

$$P(2\omega) = \frac{52.2 d_{\text{eff}}^2 L^2 P^2(\omega)}{N_o^2(\omega) N_e(2\omega) \lambda^2(\omega)} \left( \frac{\sin \frac{\Delta k L}{2}}{\frac{\Delta k L}{2}} \right)^2 \quad (12.19)$$

Note that formula (12.19) can be derived from (12.8) by choosing an appropriate system of units.

Since we consider a cut of a KDP crystal, corresponding to the synchronism direction, the factor in parenthesis in (12.19) is assumed equal to unity. This gives

$$P(2\omega) = \frac{52.2 (0.67 \cdot 10^9) \cdot 0.5^2 \cdot 10^{18}}{1.51^2 \cdot 1.49 \cdot 0.694^2 \cdot 10^{-8}} = 0.3 \cdot 10^9 \text{ W/cm}^2$$

**12.4.** Find the change in the SH radiant flux density when the incident wave deviates from the synchronism direction,  $\theta_s$ , by an angle  $\Delta\theta$ , in the  $oo \rightarrow e$  coupling (the case realized, for instance, in KDP crystals).

**Solution.** The basis for the solution is formula (12.17) in which the  $\theta$ -dependent quantities are the factors

$$d_{\text{eff}} \text{ and } \left( \frac{\sin \frac{\Delta k L}{2}}{\frac{\Delta k L}{2}} \right)^2$$

For the sake of brevity, the factor in front of them will be denoted by  $A$ :

$$P(2\omega) = Ad_{\text{eff}}^2 \left( \frac{\sin \frac{\Delta k L}{2}}{\frac{\Delta k L}{2}} \right)^2$$

In order to solve the problem, we shall analyze how the factor

$$\left( \frac{\sin \frac{\Delta k L}{2}}{\frac{\Delta k L}{2}} \right)^2$$

equal to unity for  $\theta = \theta_s$ , varies with  $\theta$ . For the  $oo \rightarrow e$  coupling in KDP we have

$$\begin{aligned} \Delta k &= \frac{2\omega}{c} [n_e^\theta(2\omega) - N_o(\omega)] \\ &= \frac{2\omega}{c} \left[ \frac{N_o(2\omega) N_e(2\omega)}{(N_e^2(2\omega) \cos^2 \theta + N_o^2(2\omega) \sin^2 \theta)^{1/2}} - N_o(\omega) \right] \quad (12.20) \end{aligned}$$

If  $\theta = \theta_s$ , then  $\Delta k = 0$ .

Differentiation of (12.18) yields  $\Delta k$  corresponding to the angle differing from  $\theta_s$  by  $\Delta\theta$ :

$$\Delta k = \frac{\omega}{c} N_o^3(\omega) \left[ \frac{1}{N_e^2(2\omega)} - \frac{1}{N_o^2(2\omega)} \right] \sin(2\theta_s) \Delta\theta$$

Now we find an increment in  $P(2\omega)$  as a function of  $\Delta\theta$ , that is,  $\Delta P_{2\omega}(\Delta\theta)$ . This will be done by expanding  $\sin^2 \frac{\Delta k L}{2}$  into a series in the neighbourhood of  $\Delta k = 0$ . Since  $\sin x = x - \frac{1}{3!} x^3$ , we find that

$$\sin^2 x = \left( x - \frac{1}{3!} x^3 \right) \left( x - \frac{1}{3!} x^3 \right) \simeq x^2 - \frac{2}{3!} x^4$$

and

$$P_{2\omega}(\theta + \Delta\theta) = Ad_{\text{eff}}^2(\theta + \Delta\theta) \left(1 - \frac{2}{3!} x^2\right)$$

$$P_{2\omega}(\theta + \Delta\theta) = Ad_{\text{eff}}^2(\theta + \Delta\theta) \left\{1 - \frac{2}{3!} \frac{L^2}{4} \frac{\omega^2}{c^2} N_0^6(\omega) \right.$$

$$\left. \times \left[ \frac{1}{N_e^2(2\omega)} - \frac{1}{N_0^2(2\omega)} \right]^2 \sin^2(2\theta_s) \Delta\theta^2\right\}$$

$$\Delta P_{2\omega} = P_{2\omega}(\theta_s) - P_{2\omega}(\theta_s + \Delta\theta)$$

$$\Delta P_{2\omega} = -\frac{A[d_{\text{eff}}^2(\theta_s + \Delta\theta) - d_{\text{eff}}^2(\theta_s)]}{3} \frac{L^2}{4}$$

$$\times \frac{\omega^2 N_0^6(\omega)}{c^2} \left( \frac{1}{N_e^2(2\omega)} - \frac{1}{N_0^2(2\omega)} \right)^2 \sin^2(2\theta_s) \Delta\theta^2$$

#### PROBLEMS

**12.5.** What should be the relationship between  $N_e(\omega)$ ,  $N_o(\omega)$ , and  $N_e(2\omega)$ ,  $N_o(2\omega)$  for a synchronous coupling of waves in optically positive uniaxial crystals? In optically negative uniaxial crystals?

**12.6.** Is synchronous coupling possible in cadmium selenide crystals (symmetry  $6mm$ ) in the YAG : Nd<sup>3+</sup> ( $\lambda = 1.06 \mu\text{m}$ ) and CO<sub>2</sub> laser radiation ( $\lambda = 10.6 \mu\text{m}$ )? The optical dispersion in CdSe crystals is given by the formulas

$$N_o^2 = 4.2243 + \frac{1.766\lambda^2}{\lambda^2 - 0.227} + \frac{3.12\lambda^2}{\lambda^2 - 3380}$$

$$N_e^2 = 4.2009 + \frac{1.8875\lambda^2}{\lambda^2 - 0.2171} + \frac{3.6461\lambda^2}{\lambda^2 - 3629}$$

**12.7.** Is synchronous coupling possible in proustite crystals, Ag<sub>3</sub>AsS<sub>3</sub> (symmetry  $3m$ ), for the CO<sub>2</sub> laser radiation, if the dispersion in these crystals is given by

$$N_o^2 = 9.220 + \frac{0.4454}{\lambda^2 - 0.1264} + \frac{1733}{1000 - \lambda^2}$$

$$N_e^2 = 7.007 + \frac{0.3230}{\lambda^2 - 0.1192} + \frac{660}{1000 - \lambda^2}$$

**12.8.** Is synchronous coupling possible in quartz crystals at wavelength  $\lambda = 0.347 \mu\text{m}$ ?

**12.9.** Find the temperature of the 90°-synchronism in lithium niobate crystals of a given stoichiometric composition for  $\lambda = 1.064 \mu\text{m}$ , for the following dispersion and temperature dependencies of refractive indices in crystals with this composition:

$$N_o^2 = 4.9130 + \frac{0.1173 + 1.65 \cdot 10^{-8} T^2}{\lambda^2 - (0.212 + 2.7 \cdot 10^{-8} T^2)^2} - 2.78 \cdot 10^{-2} \lambda^2$$

$$N_e^2 = 4.5567 + 2.605 \cdot 10^{-7} T^2 + \frac{0.097 + 2.7 \cdot 10^{-8} T^2}{\lambda^2 - (0.201 + 5.4 \cdot 10^{-8} T^2)^2} - 2.24 \cdot 10^{-2} \lambda^2$$

12.10. Show that  $d_{\text{eff}}$  for the  $ee \rightarrow o$  coupling in symmetry class 422 is independent of the angle  $\varphi$  between the principal plane and coordinate plane  $X_1X_3$  in the crystal.

12.11. Show that  $d_{\text{eff}}$  for the  $oo \rightarrow e$  coupling in symmetry class 3 is equal to the sum of  $d_{\text{eff}}$  in symmetry classes  $\bar{6}$  and 6.

12.12. Show that  $d_{\text{eff}}$  for the  $oo \rightarrow e$  coupling in symmetry class  $3m$  is equal to the sum of  $d_{\text{eff}}$  for classes  $\bar{6}m2$  and  $6mm$ .

12.13. Find the crystallographic directions in lithium niobate in which  $d_{\text{eff}}$  for the  $oo \rightarrow e$  coupling is a function of  $d_{31}$  only. Will the transformation of the fundamental-frequency light into SH be more or less effective than in other synchronism directions possible in the crystal?

12.14. Show that  $d_{\text{eff}} = 0$  for the  $oo \rightarrow e$  coupling in crystals with symmetry 622 and 422.

12.15. Find the orientation of the synchronism axis in cinnabar (HgS) crystals for  $\lambda = 10.6 \mu\text{m}$  if the refractive indices are

$$N_o = 2.83, N_e = 3.15 \text{ for } \lambda = 5.3 \mu\text{m}$$

$$N_o = 2.60, N_e = 2.85 \text{ for } \lambda = 10.6 \mu\text{m}$$

12.16. Find the flux density of SH of a  $\text{CO}_2$  laser radiation, generated in a cinnabar crystal 0.8 cm long, for the incident flux density  $10^7 \text{ W/cm}^2$ .

12.17. Find the coherence length of a quartz crystal generating SH in the directions at angles  $30^\circ$  and  $90^\circ$  to the optic axis of the crystal, for  $\lambda = 1.06 \mu\text{m}$ .

12.18. Find the flux density of SH generated in a quartz crystal in the directions given in the preceding problem.

The incident flux density is  $10^9 \text{ W/cm}^2$ , and the crystal length equals the coherence length in the corresponding direction.

12.19. Find the coherence length of a KDP crystal in directions deviating from the synchronism direction by  $5^\circ$ , that is,  $(\theta_s + 5^\circ)$  and  $(\theta_s - 5^\circ)$ .

12.20. Calculate the change in the output flux density of SH generated in a lithium niobate crystal for a deflection from the synchronism angle by  $5^\circ$ ,  $10^\circ$ , and  $15^\circ$ , for  $\lambda = 1.06 \mu\text{m}$  and crystal composition allowing for the  $90^\circ$ -synchronism. Make use of the data given in Problem 12.9.

12.21. Find the orientation of the synchronism direction in gallium selenide crystals for  $\lambda = 10.6 \mu\text{m}$ , for the following refractive indices:

$$N_o = 2.81, N_e = 2.44 \text{ for } \lambda = 10.6 \mu\text{m}$$

$$N_o = 2.83, N_e = 2.46 \text{ for } \lambda = 0.53 \mu\text{m}$$

**12.22.** Find the orientations of the synchronism direction at which the beam displacement imposes no restriction on the actual length of synchronous coupling for  $\Delta k = 0$ .

**12.23.** Find the SH flux density in a lithium niobate crystal in the case of  $90^\circ$ -synchronism for crystal length  $L = 1$  cm,  $\lambda = 1.06 \mu\text{m}$ , incident radiant flux  $5 \cdot 10^5 \text{ W}$ , and beam cross-sectional area  $S = 1 \text{ cm}^2$ . What will be the change in the SH flux when the beam cross-sectional area is reduced to  $0.01 \text{ cm}^2$ , with the flux conserved?

**12.24.** Calculate the incident radiant flux at which the output SH flux will be 50% and 90% of the incident flux in lithium niobate crystal for  $90^\circ$ -synchronism. Assume  $L = 1 \text{ cm}$ ,  $\lambda = 1.06 \mu\text{m}$ , and  $S = 0.01 \text{ cm}^2$ .

**12.25.** Calculate the actual coupling length in a KDP crystal, taking into account the beam displacement, when the fundamental-frequency wave propagates in the synchronism direction ( $\theta = 49^\circ$ ), for the incident beam diameter  $d = 1 \text{ mm}$ .

**12.26.** Recalculate the preceding problem for  $d = 1 \text{ cm}$ .

**12.27.** Find the angle between the wavefront normal and the beam propagating in the synchronism direction, in a cinnabar crystal for  $\lambda = 10.6 \mu\text{m}$ . What is the coupling length for  $d = 1 \text{ cm}$ ?

**12.28.** Find the change in the SH output flux when the beam diameter is reduced from 1 to  $0.1 \text{ cm}$  in a KDP crystal, taking into account the effect of beam diameter on the synchronous coupling length. The light beam propagates in the synchronism direction ( $\theta = 49^\circ$ ), the incident radiant flux is  $10^8 \text{ W}$ .

## 13. ROTATION OF POLARIZATION PLANE (OPTICAL ACTIVITY)

When a plane-polarized monochromatic light passes through some isotropic media, the polarization plane is rotated, and the rotation angle is proportional to the optical path length. This phenomenon is called the rotation of light polarization plane, or optical activity. This phenomenon is also observed in some cubic crystals, as well as in many uniaxial and biaxial crystals when light propagates along the optical axis, that is, along a direction in which the usual birefringence is absent.

*Rotation of Polarization Plane  
in Isotropic Media, Cubic Crystals,  
and in Other Crystals when Light Propagates Along an Optic Axis*

In this cases there are two circularly polarized waves of opposite hand, propagating through the medium without a change in the polarization state. These waves propagate at different velocities, corresponding to the refractive indices  $n_r$  and  $n_l$  (the indices r and l refer to the right-handed and left-handed components). The incident plane-polarized wave splits into two circularly polarized components and emerges from the medium as a plane-polarized wave whose polarization plane is rotated by an angle  $\varphi$  (Fig. 13.1). The angle of rotation is given by the formula

$$\varphi = \frac{\pi d}{\lambda_0} (n_l - n_r) \quad (13.1)$$

where  $d$  is the path length in the medium, and  $\lambda_0$  is the wavelength in vacuum.

The path difference of the two circularly polarized components is  $2\varphi$ .

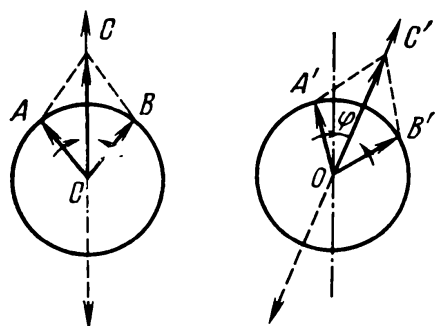


Fig. 13.1. Rotation of polarization plane when light passes through a crystal in a direction in which ordinary birefringence is absent:  
(a) arrangement of vectors at the point of entrance into the medium,  
(b) arrangement of vectors at the point of emergence from the crystal.

The angle of rotation of polarization plane per unit path length in a given medium,  $\rho = \phi/d$ , is called the *specific rotation*:

$$\rho = \frac{\pi}{\lambda_0} (n_1 - n_r) \quad (13.2)$$

Clockwise rotation for an observer facing the beam propagation is by convention the right-hand rotation. The sign of  $\rho$  is positive if both the rotation and the coordinate system are right- or left-handed; the sign is negative if the rotation is right-handed (left-handed) and the coordinate system is left-handed (right-handed).

This means that the sign of specific rotation must change in converting from a right-handed to a left-handed (and vice versa) coordinate system:

$$\rho' = \pm \rho \quad (13.3)$$

where the plus sign refers to transformations which conserve the hand of the coordinate system, and the minus sign refers to transformations which convert a right-handed system into a left-handed system (and vice versa). (A physical quantity behaving in this manner is called *pseudoscalar*.)

*Rotation of Polarization Plane in Uniaxial and Biaxial Crystals along Directions Tilted with Respect to an Optic Axis*

In this case an arbitrary wave normal corresponds to two waves which pass through an optically active crystal without changing the state of polarization. In the general case these waves are elliptically polarized, with the shape of the ellipses defining the polarization state being identical for both, but with the opposite directions of rotation. The major axes of the ellipses are mutually perpendicular and coincide with the principal directions of oscillations that would be realized or a given normal if the crystal were optically inactive. The refractive indices of these waves are positive roots of the equation

$$(n^2 - n'^2) (n^2 - n''^2) = G^2 \quad (13.4)$$

where  $n'$  and  $n''$  are refractive indices for zero optical activity, and  $G$  is the gyration, the quantity determining the optical activity in a given direction. The gyration  $G$  is a function of direction, written in the form

$$G = g_{ij} l_i l_j \quad (g_{ij} = g_{ji}) \quad (13.5)$$

where  $g_{ij}$  are the components of the gyration tensor.

The forms of tensors  $[g_{ij}]$  for crystals belonging to various crystallographic classes are given in Appendix (Table 13a). Specific rota-

tion  $\rho$  is related to  $G$  as follows:

$$\rho = \frac{\pi G}{\lambda_0 \bar{n}} \quad (13.6)$$

where  $\bar{n} = \sqrt[n]{n' n''}$ .

Like  $\rho$ ,  $G$  is a pseudoscalar, that is,

$$G' = \pm G \quad (13.7)$$

and its sign depends on whether the hand of the coordinate system is changed upon transformation.

Tensor  $[g_{ij}]$  is an axially symmetric tensor of rank two transformed as follows:

$$g_{ij} = \pm c_{ik} c_{jl} g_{kl} \quad (13.8)$$

where the plus sign indicates transformations conserving the hand of the coordinate system, and the minus sign refers to transformations changing the hand of the coordinate system.

As any symmetric tensor, the gyration tensor can be converted to the diagonal form:

$$[g_{ij}] = \begin{bmatrix} g_{11} & 0 & 0 \\ 0 & g_{22} & 0 \\ 0 & 0 & g_{33} \end{bmatrix}$$

where  $g_{11}$ ,  $g_{22}$ ,  $g_{33}$  are the gyration tensor components along the principal axes.

Referred to the principal axes, Eq. (13.5) is greatly simplified:

$$g_{11}n_1^2 + g_{22}n_2^2 + g_{33}n_3^2 = G$$

The surface described by this equation, that is, the surface with radius vectors proportional to  $G$ , is called the gyration surface.

### Examples of Problems with Solutions

**13.1.** Show that crystals belonging to class  $m$ , though not enantiomorphous, are optically active.

**Solution.** According to the rules of choosing crystallophysical axes in class  $m$  crystals (see Table 3), the axis  $X_2$  is chosen perpendicular to  $m$ .

In this case the plane  $m$  transforms the initial coordinate system in such a manner that  $X_1 \rightarrow X_1$ ,  $X_2 \rightarrow -X_2$ ,  $X_3 \rightarrow +X_3$  or, in a compact form,  $1 \rightarrow 1$ ,  $2 \rightarrow -2$ ,  $3 \rightarrow +3$ . The operation of reflection in a symmetry plane is the second-kind operation, that is, it converts a right-handed coordinate system into a left-handed system (and vice versa); consequently, according to (13.8), the components of the

gyration tensor in the new coordinate system should have minus sign. By using the direct inspection method and taking into account (13.8), we find that the components of  $[g_{ij}]$  are transformed as follows:

$$g_{11} \rightarrow -g_{11}, \text{ i.e. } g_{11} = 0, \quad g_{12} \rightarrow g_{12}, \quad g_{31} \rightarrow -g_{31}, \text{ i.e. } g_{31} = 0$$

$$g_{22} \rightarrow -g_{22}, \text{ i.e. } g_{22} = 0, \quad g_{23} \rightarrow g_{23}, \quad g_{33} \rightarrow -g_{33}, \text{ i.e. } g_{33} = 0$$

so that the tensor  $[g_{ij}]$  takes the form

$$\begin{bmatrix} 0 & g_{12} & 0 \\ g_{12} & 0 & g_{23} \\ 0 & g_{23} & 0 \end{bmatrix}$$

Since the coefficients  $g_{ij}$  of the gyration tensor for class  $m$  crystals are nonzero, the crystals of this class, though not enantiomorphous, are optically active.

**13.2.** What should be the orientation of a precisely machined quartz plate possessing no optical activity?

**Solution.** Quartz crystals are optically active; the optical activity of quartz is determined by two independent coefficients  $g_{ij}$ :  $g_{11} = g_{22}$ ,  $g_{33}$ , with the coefficients  $g_{11}$  and  $g_{22}$  being of opposite signs (see Table 13a).

Therefore, quartz can rotate the polarization plane not only along the optic axis, but also in perpendicular directions, and the signs of these rotations are opposite. Correspondingly, the gyration surface is described by the equation

$$G = g_{11} (n_1^2 + n_2^2) - g_{33} n_3^2$$

Denote the angle between a radius vector of the gyration surface and the optic axis by  $\varphi$ . Then we find for the section coinciding with the coordinate plane  $X_2X_3$ :  $n_3 = \cos \varphi$ ,  $n_2 = \sin \varphi$ ,  $n_1 = 0$ .

A substitution of these expressions for  $n_1$ ,  $n_2$ , and  $n_3$  into the equation of the quartz gyration surface yields

$$\pm G = g_{11} \sin^2 \varphi - g_{33} \cos^2 \varphi$$

The sought value of the angle  $\varphi$  must ensure zero optical activity. Consequently,  $0 = g_{11} \sin^2 \varphi - g_{33} \cos^2 \varphi$ , whence

$$\tan^2 \varphi = \frac{g_{33}}{g_{11}} = 2.23, \quad \tan \varphi = 1.493, \quad \varphi = 56^\circ 10'$$

Therefore, for zero optical activity of a quartz plate it must be cut in such a manner that the normal to the plate be at an angle  $56^\circ 10'$  to the three-fold axis. Obviously, this result can be used in optic industry to manufacture quartz plates and quartz wedges not rotating the light polarization plane.

## PROBLEMS

13.3. Show that centrosymmetrical crystals cannot be optically active.

13.4 Indicate non-enantiomorphous symmetry classes in which optical activity can be observed.

13.5. Find the number of independent components of the duration tensor for rochelle salt.

13.6. Optical axes of rochelle salt lie in the plane (010). Use symmetry arguments only and find the magnitude and sign of specific rotation along optical axes.

13.7. Find the number of independent components of the gyration tensor for crystals belonging to symmetry classes  $\bar{4}$  and  $\bar{4}2m$ . What are the crystallographic directions of such crystals in which optical activity is zero?

13.8. Show that all components of the gyration tensor  $[g_{ij}]$  are zero for crystals with symmetry  $4mm$ .

13.9. What are the restrictions imposed by symmetry on the rotation of polarization plane along the optic axis in the case of symmetry class  $mm$ ?

13.10. Can the rotation of polarization plane be observed along optic axes in crystals with symmetry  $m$  if (i) the symmetry plane contains both optic axes, (ii) the symmetry plane is the bisector of the angle between the optic axes? Find the sign and magnitude of specific rotation along optic axes in these cases.

13.11. Find the change in the point symmetry of crystals belonging to classes  $\bar{3}m$ ,  $3m$ ,  $32$ ,  $4/mmm$ ,  $4/m$ , and  $\bar{4}2m$ , caused by a phase transition accompanied by the optical activity described by a gyration surface with symmetry  $\infty\infty$ .

13.12. Find the change in the point symmetry of crystals belonging to classes  $m3m$  and  $432$ , caused by a phase transition accompanied by the appearance of optical activity with gyration surfaces having the following symmetry: (i)  $\infty\infty$ , (ii)  $\infty 2$ , (iii)  $\bar{4}2m$ , (iv)  $2$ , provided the principal axes of these gyration surfaces are along the crystallographic directions (a)  $\langle 100 \rangle$  or (b)  $\langle 111 \rangle$ .

13.13. What should be the orientation of a crystal plate of tartaric acid (TA) so that the effect of rotation of polarization plane can be observed in its pure form?

13.14. The plane (010) of sugar crystals, in which the optic axes of the crystal lie, is perpendicular to the two-fold symmetry axis. By using only symmetry arguments, find the magnitude and sign of the specific rotation along the optic axes.

13.15. Calculate the difference between refractive indices of two circularly polarized components of light with wavelength  $0.556 \mu\text{m}$  propagating in a sodium chlorate crystal plate.

13.16. Find the orientation of the principal axes of the gyration tensor in class  $m$  crystals with respect to the symmetry plane. Find the tensor  $[g_{ij}]$  referred to the principal axes.

13.17. The optic axes of tartaric crystal lie in the same plane with the two-fold symmetry axis. By using only symmetry arguments, find the sign and magnitude of specific rotation along the optic axes of the crystal.

13.18. A quartz plate cut perpendicular to the optic axis is placed between parallel nicols. The difference  $n_l - n_r$  for wavelength  $0.589 \mu\text{m}$  is equal to  $7.1 \cdot 10^{-5}$  along the optic axis. Find the plate thickness which gives complete extinction of light at this wavelength.

13.19. Find the minimal difference  $\Delta n$  in refractive indices of circularly polarized beams, with right- and left-handed polarization and wavelength  $0.76 \mu\text{m}$ , detectable in a cinnabar plate  $2 \text{ mm}$  thick, for specific rotation of these beams equal to  $325^\circ/\text{mm}$ .

13.20. A quartz plate  $1 \text{ mm}$  thick is cut perpendicular to the optic axis and placed between crossed nicols. Explain why the plate is never opaque, whatever the light wavelength.

13.21. Estimate birefringence of an oriented quartz plate for light wavelength  $\lambda = 0.510 \mu\text{m}$  if the angle between the normal to the plate and its optic axis is  $60^\circ$ ; calculate the additional birefringence due to optical activity of quartz.

## 14. ELASTIC WAVES IN CRYSTALS

### *Bulk Elastic Waves in Non-Piezoelectric Crystals*

The wave equation describing the propagation of elastic (acoustic) waves in crystals can be derived from Newton's second law

$$\rho \frac{\partial^2 u_i}{\partial t^2} = \frac{\partial t_{ij}}{\partial x_j}$$

and Hooke's law (7.2)

$$\rho \ddot{u}_j = c_{jklm} \frac{\partial^2 u_m}{\partial x_k \partial x_l} \quad (14.1)$$

where  $u_j$  are the components of *displacement vector of the medium*,  $\rho$  is the density, and  $c_{jklm}$  are the elastic stiffnesses.

The solution of Eq. (14.1) is the plane monochromatic wave of elastic displacements:

$$u_j = u_j^0 e^{i k [(n_1 x_1 + n_2 x_2 + n_3 x_3) - vt]} \quad (14.2)$$

where  $u_j^0$  is the displacement amplitude along the  $j$ th axis,  $k$  is the wave number equal to  $2\pi/\lambda$ ,  $n_1$ ,  $n_2$ ,  $n_3$  are the components of unit vector of wavefront normal,  $\lambda$  is the wavelength, and  $v$  is the *phase velocity*.

The substitution of the expression for  $u_j$  into the equation of motion yields

$$(c_{jklm} n_k n_l - \rho v^2 \delta_{jm}) u_j^0 = 0 \quad (14.3)$$

Let us introduce a rank two tensor

$$\begin{aligned} \Lambda_{jm} &= \lambda_{jklm} n_k n_l = \frac{1}{\rho} c_{jklm} n_k n_l \\ \lambda_{jklm} &= \frac{1}{\rho} c_{jklm} \end{aligned} \quad (14.4)$$

called the *Green-Christoffel tensor* for a given propagation direction of the acoustic wave; this tensor is a positively definite symmetric tensor of rank two. With this tensor, Eq. (14.3) can be written in the form

$$(\Lambda_{im} - v^2 \delta_{im}) u_m^0 = 0 \quad (14.5)$$

where  $\delta_{im}$  is the Kronecker delta.

Equation (14.5) is called the *Green-Christoffel equation* for a given direction of propagation of an acoustic wave. In the most general

case of a triclinic crystal, each component of the tensor  $[\Lambda_{im}]$  is found from relations of the form

$$\Lambda_{im} = \lambda_{iklm} n_k n_l = \frac{1}{\rho} \{ c_{i11m} n_1^2 + c_{i22m} n_2^2 + c_{i33m} n_3^2 + (c_{i23m} + c_{i32m}) n_2 n_3 + (c_{i31m} + c_{i13m}) n_3 n_1 + (c_{i12m} + c_{i21m}) n_1 n_2 \}$$

for  $i, m = (11), (22), (33), (23), (31), (12)$ .

The contraction  $\Lambda_{jm} = c_{ijlm} n_i n_l$ , corresponding to the tensor  $[\Lambda_{jm}]$ , is given in full form in Table 14.1. By using this table and

Table 14.1

**Matrix Components of the Green-Christoffel Tensor \***  $\Lambda_{ik} = \frac{1}{\rho} c_{ijkl}^E n_j n_l$   
**Used to Determine Phase Velocities of Acoustic Waves Propagating**  
**in Triclinic Crystals**

$\Lambda_{ik}$	$n_j n_l$	$n_1^2$	$n_2^2$	$n_3^2$	$n_2 n_3$	$n_1 n_3$	$n_1 n_2$
$\Lambda_{11}$	11	66	55		$2 \times 56$	$2 \times 15$	$2 \times 16$
$\Lambda_{22}$	66	22	44		$2 \times 24$	$2 \times 46$	$2 \times 26$
$\Lambda_{33}$	55	44	33		$2 \times 34$	$2 \times 35$	$2 \times 45$
$\Lambda_{23}$	56	24	34		$23+44$	$36+45$	$25+46$
$\Lambda_{13}$	15	46	35		$36+45$	$13+55$	$14+56$
$\Lambda_{12}$	16	26	45		$25+46$	$14+56$	$12+66$

\* The squares of this and other similar tables list the indices of the corresponding tensors in the matrix notation. In the specific case of Table 14.1, this means that 11 stands for  $c_{11}^E$ ,  $2 \times 56$  is equivalent to  $2c_{56}^E$ , and  $25+46$  to  $c_{25}^E + c_{46}^E$ .

knowing the matrix of elastic stiffnesses ( $c_{ij}$ ) of a specific crystal, it is easy to find the components of tensor for any chosen direction of the wavefront normal.

For the solution of Eq. (14.2) to be nonzero, the determinant of the coefficients of the system (14.5) must vanish:

$$|\Lambda_{im} - v^2 \delta_{im}| = 0 \quad (14.6)$$

or, in a more detailed form,

$$|\Lambda_{11} - v^2| |\Lambda_{22} - v^2| |\Lambda_{33} - v^2| - \Lambda_{23}^2 |\Lambda_{11} - v^2| - \Lambda_{13}^2 |\Lambda_{22} - v^2| + 2\Lambda_{12}\Lambda_{13}\Lambda_{33} = 0$$

Since equation (14.6) is cubic in  $v^2$ , three waves propagate in the general case along a given direction of wavefront normal  $\mathbf{n}$ , at different velocities  $v_1$ ,  $v_2$ , and  $v_3$ ; each wave has its own vector  $\mathbf{u}^{(1)}$ ,  $\mathbf{u}^{(2)}$ , and  $\mathbf{u}^{(3)}$  determining the direction of displacement in the wave (Fig. 14.1). Waves with a common wavefront normal  $\mathbf{n}$  are called *isonormal*.

**Isotropic medium.** In isotropic media the tensor  $[\Lambda_{im}]$  is uniaxial for any direction of wavefront normal. It can be shown that in isotropic media the tensor of elastic stiffnesses is given by the following expression:

$$c_{iklm} = a_1 \delta_{ik} \delta_{lm} + a_2 (\delta_{il} \delta_{km} + \delta_{im} \delta_{kl})$$

where  $a_1$ ,  $a_2$  are scalar coefficients, and  $\delta_{ik}$  is the Kronecker delta; hence

$$\Lambda_{im} = \frac{1}{\rho} c_{iklm} n_k n_l = a_2 \delta_{im} + (a_1 + a_2) n_i n_m$$

This means that the axis of the tensor  $[\Lambda_{im}]$  is the wavefront normal  $\mathbf{n}$ , and one of the eigenvectors of the uniaxial tensor is aligned along  $\mathbf{n}$ . Consequently, the vector of displacement  $\mathbf{u}_1$  in the corresponding wave oscillates along the wavefront normal. Such waves are called *purely longitudinal*. Two other linearly independent displacement vectors can be chosen in an arbitrary manner in the plane perpendicular to  $\mathbf{n}$ . These waves are called *purely shear waves*, or *transverse waves*, and their phase velocities are identical.

The direction of propagation of two waves with identical velocities is called the *acoustic axis*. The following condition must be satisfied for the propagation of purely longitudinal and purely transverse waves:

$\mathbf{u} \times \mathbf{n} = 0$ : the condition of the purely longitudinal wave (14.7)

$\mathbf{u} \cdot \mathbf{n} = 0$ : the condition of a purely transverse wave (14.8)

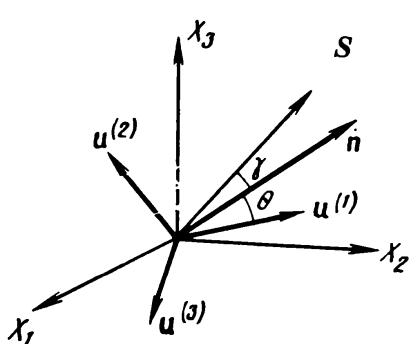


Fig. 14.1. Isonormal waves in anisotropic media.  $\theta$ —angle between the wavefront normal  $\mathbf{n}$  and displacement vector  $\mathbf{u}^{(1)}$  of a wave propagating at a velocity  $v_1$ ;  $\gamma$ —angle between  $\mathbf{n}$  and the group velocity vector  $\mathbf{S}$ .

Consequently, elastic waves in isotropic media have the following properties.

- (i) One of the three isonormal waves is always purely longitudinal (the directions along which the purely longitudinal wave can propagate are said to be longitudinal normals). Any wavefront normal in an isotropic medium is a longitudinal normal.
- (ii) Purely transverse waves propagate along each wavefront normal.
- (iii) Two waves with identical velocities propagate along each wavefront normal.

**Anisotropic medium.** In contrast to isotropic media, in crystals none of the three isonormal waves is, in the general case, either purely longitudinal or purely transverse, that is, in most directions  $\mathbf{u} \times \mathbf{n} \neq 0$  and  $\mathbf{u} \cdot \mathbf{n} \neq 0$  (Fig. 14.1). However, in any case one of the waves has a displacement vector at a minimum angle to the wavefront normal, as compared with the displacement vectors of the other two waves. Such a wave is called *quasilongitudinal*, and the other two *quasitransverse* (*quasishear*) waves. Experiments show that in practically all crystals the quasilongitudinal wave has a velocity greater than that of the two isonormal waves (the only known exception is paratellurite,  $\text{TeO}_2$ , in whose crystals longitudinal waves propagate at a velocity smaller than that of shear waves). The fact that as a rule elastic waves in crystals are neither purely longitudinal nor purely transverse is one of the main manifestations of anisotropy of elastic properties in crystals.

The tensor  $[\Lambda_{im}]$  has in crystals three distinct eigenvalues, and therefore three eigenvectors with clearly defined directions. For almost all directions of the wavefront normal each of the displacement vectors of three isonormal waves remains parallel to some fixed straight line, while its magnitude varies periodically. This means that, as a rule, plane elastic waves in crystals are linearly polarized, except for those directions  $\mathbf{n}$  for which the tensor  $[\Lambda_{im}]$  becomes uniaxial. Waves of a different polarization can propagate along these directions together with linearly polarized waves.

**Singular directions in crystals.** In any crystal, except for those belonging to the triclinic system, there are directions of the normal  $\mathbf{n}$  such that elastic waves propagating along these directions possess one or several of the properties characteristic for isotropic media. These directions are said to be *singular*.

Equation (14.6) is considerably simplified in the cases of singular directions. An analysis shows that

- (i) a longitudinal and purely shear waves propagate along the symmetry axes;
- (ii) shear waves propagate along the axes 3, 4, and 6 at identical velocities;
- (iii) in symmetry plane or in planes perpendicular to the axes 2, 4,

and 6 one of the waves is purely transverse, with the condition (14.8) satisfied. The set of singular directions satisfying conditions (14.7) and (14.8) are of special interest for manufacturing piezoelectric devices.

Owing to the absence of elastic coupling between different types of vibrations (piezoelectric coupling may exist), plates cut perpendicular to these directions vibrate at a single frequency of thickness vibrations.

An analysis also shows that the singular directions in crystals form a cone of order eight, degenerated to a number of discrete directions, and that there are at least two such directions in any crystal.

**Wave surfaces.** In studying the propagation of elastic waves in crystals, it is very useful to introduce certain surfaces which make it possible to describe a number of properties of these waves in an illustrative manner.

Mostly three types of surfaces are used, each giving a locus of the ends of one of the vectors characterizing the propagations of waves.

**Surface of phase velocities.** If the vectors of phase velocities are drawn from an origin 0 in all possible directions of the wavefront normal  $\mathbf{n}$ , the locus of the ends of these vectors is called the *phase-velocity surface*.

Obviously, the radius vector of this surface is the vector of phase velocity

$$\mathbf{r} = \mathbf{v} = v\mathbf{n} \quad (14.9)$$

In the general case the equation of the phase-velocity surface is an equation of order 12. Three different values of phase velocity correspond to each direction of the wavefront normal, and this means that any straight line drawn from the origin intersects the surface in three points, and the surface consists of three sheets. One of these sheets,  $L$ , corresponds to the velocities of quasilongitudinal waves  $v_1$ . Two other sheets,  $T_1$  and  $T_2$ , correspond to quasitransverse waves  $v_2$  and  $v_3$ . Obviously, the surfaces of phase velocities of quasitransverse waves are tangent or intersect along the acoustic axes (Fig. 14.2b).

#### *Surface of Inverse Velocities (Refractive Surface)*

Let us introduce a vector  $\mathbf{M} = \mathbf{n}/v$  aligned along the wavefront normal, with the magnitude equal to the reciprocal of phase velocity. This vector is said to be the *vector of refraction*, and the locus of the ends of refraction vectors drawn from the origin is said to be the surface of inverse velocities (*refraction surface*).

The equation of refraction surface is an equation of order six in the components of refraction vector. The refraction surface, as the phase-velocity surface, consists of three sheets corresponding to the quasilongitudinal ( $L$ ) and quasitransverse ( $T_1$  and  $T_2$ ) waves.

The phase-velocity surface and refraction surface are related because the product of their radius vectors drawn in the same direction is unity:

$$| \mathbf{v} | | \mathbf{M} | = 1$$

Therefore, each one of these surfaces can be obtained from the other by inversion.

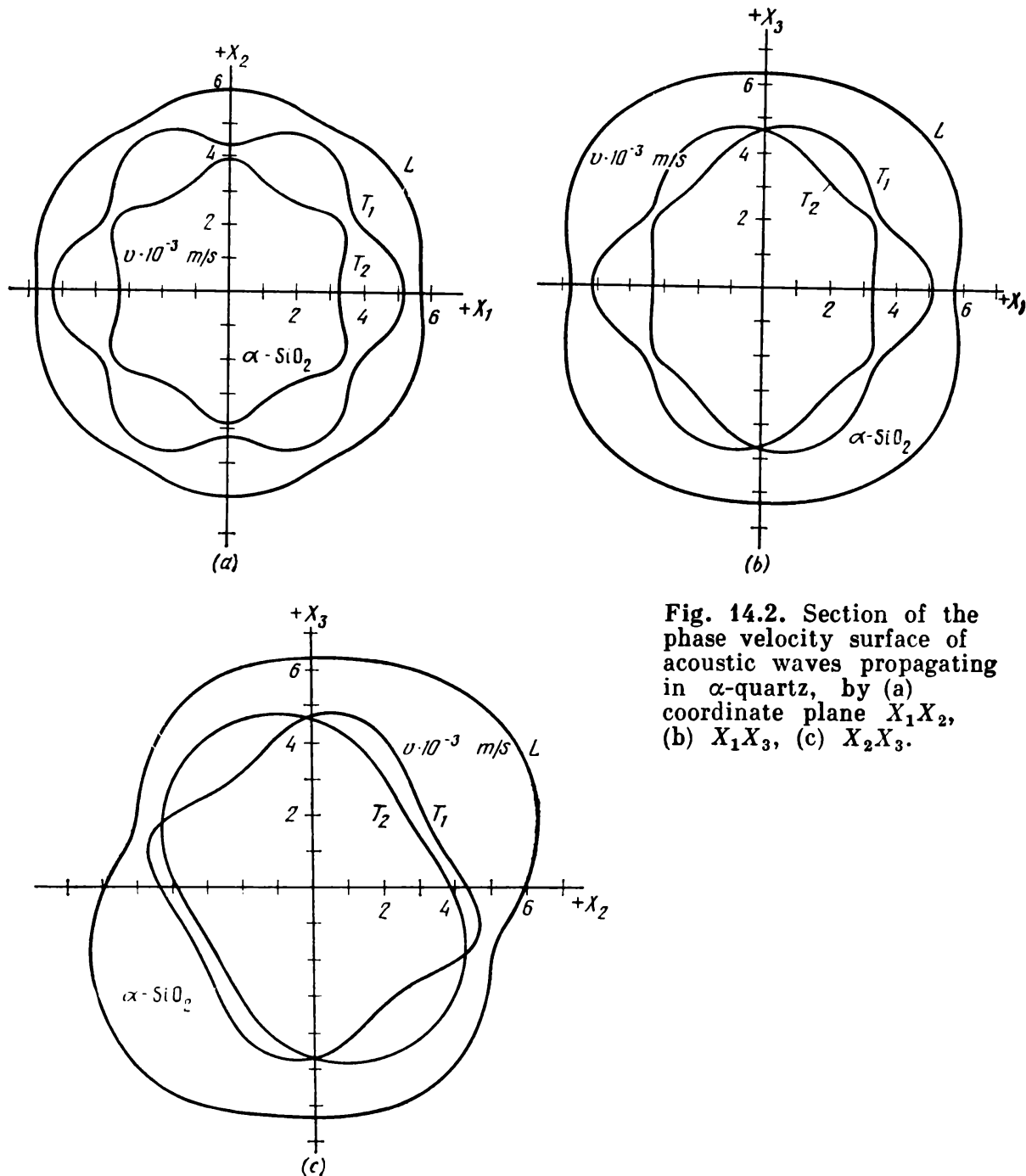


Fig. 14.2. Section of the phase velocity surface of acoustic waves propagating in  $\alpha$ -quartz, by (a) coordinate plane  $X_1X_2$ , (b)  $X_1X_3$ , (c)  $X_2X_3$ .

*Sections  
of Wave Surfaces*

As wave surface equations may be of quite high orders, sections of these surfaces by various planes, such as coordinate and symmetry planes, are widely used to analyze these surfaces and the related physical properties of acoustic waves. In a symmetry plane, Eq. (14.6) always separates into a linear and a quadratic equations. The sections of phase-velocity surfaces by various coordinate planes are shown in Fig. 14.2a-c for acoustic waves propagating in  $\alpha$ -quartz crystals.

*Calculation  
of Characteristics  
of Phase Velocities  
for Bulk Acoustic Waves*

The procedure used to calculate the characteristics of phase velocities for bulk acoustic waves and to determine the corresponding polarizations is as follows.

For each given direction of wavefront normal  $\mathbf{n}$ , the components of the Green-Christoffel tensor  $[\Lambda_{ik}]$  are found from the known matrix of elastic stiffnesses of a crystal by using Table 14.1.

Then the cubic equation (14.6) is solved for  $v^2$ , and the phase velocities of the three bulk acoustic waves are calculated. The wave polarization is found by solving the system of homogeneous equations for a given phase velocity of the wave  $v^p$  ( $p = 1, 2, 3$  are the indices of one of eigenvalues):

$$(\Lambda_{ik} - v^p{}^2 \delta_{ik}) u_k^p = 0$$

Here we take into account that  $(u_k^p)^2 = 1$ . The next step is to find the angle  $\theta$  between the displacement vector and the direction of the wavefront normal  $\mathbf{n}$ , determining the type of the wave (Fig. 14.1), from the known components of the unit displacement vector:

$$\theta = \arccos(n_i u_i).$$

*Energy Flux  
and Group Velocities  
of Bulk Acoustic Waves*

As a result of anisotropy of elastic properties in crystals, in the general case the direction of the energy flux vector of an acoustic wave does not coincide, in contrast to the case of isotropic media, with the direction of wavefront normal  $\mathbf{n}$ , that is, there is a certain

nonzero angle  $\gamma$  between these two vectors (Fig. 14.3). Consequently, group velocity does not coincide with phase velocity even in the case of zero dispersion. The *group velocity* of an elastic wave,  $S$ , is the velocity of energy flux. The relation between the group and phase velocities is

$$\mathbf{S}^p \cdot \mathbf{n} = v_p \quad (14.10)$$

that is, phase velocity is equal to the projection of group velocity onto the direction of sound propagation. When a wave propagates along an acoustic axis, the energy flux of shear waves may deviate from the direction of wave propagation, and the direction of deviation depends on the polarization of the wave. By analogy to optical phenomena, this effect is called the *internal conical refraction*: as the polarization plane of a shear wave is rotated, the acoustic beam also rotates, moving along a cone which is a locus of possible directions of energy flux. The semivertical angle of the cone  $\psi$  (Fig. 14.4) is called the *angle of conical refraction*.

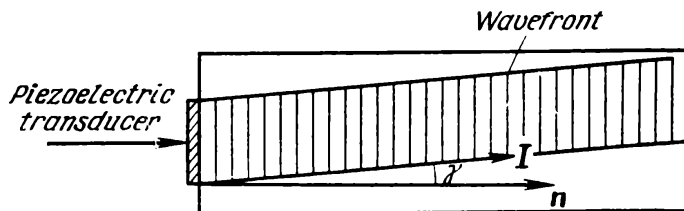


Fig. 14.3. Energy flux and wavefront normal in an anisotropic medium.

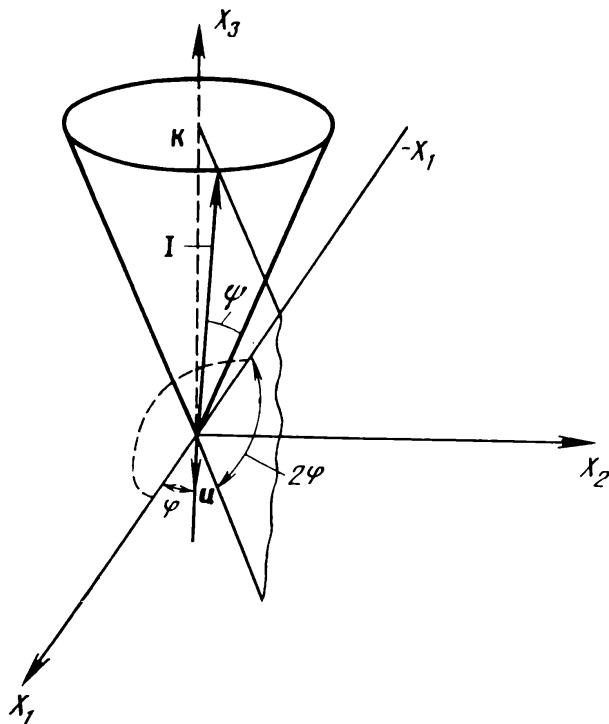


Fig. 14.4. The cone of internal conical refraction.

Group velocity is given by the relation

$$S_i^p = \frac{1}{\rho v^p} c_{ijkl} n_j u_k u_l \quad (14.11)$$

that is, the group velocity of bulk elastic waves can be calculated if the phase velocity of a wave in a given direction and the components of its displacement vector are known. To facilitate calculations, a vector  $\mathcal{E}$  with components

$$\mathcal{E}_v^c = c_{ijsv} n_i u_j u_s \quad (14.12)$$

is introduced. To simplify the operations with equation (14.11), the contracted terms in this equation are usually written in detail. Table 14.2 lists detailed notation of the contracted so-called "elastic" vector  $\mathcal{E}_v^c$ .

Let us introduce a unit vector of energy flux along the flux propagation direction:

$$I_i = \frac{c_{ijlm} u_j u_m n_l}{\rho v^p |S^p|} \quad (14.13)$$

The angle between the wave propagation direction and energy flux, the so-called "displacement" angle, is given by the relation

$$\gamma = \arccos (I_i n_i) \quad (14.14)$$

and sometimes reaches tens of degrees.

### Piezoelectric Effect in the Theory of Elastic Waves

Mechanical stress and strain generated by elastic waves propagating in piezoelectric

Table 14.2  
Components of Contracted "Elastic" Vector  $\mathcal{E}_v^c = c_{vilm}^E u_j u_m n_l$  Required for Calculation of Group Velocities  
of Bulk Acoustic Waves

$n_l u_j u_m$	$n_1$			$n_2$			$n_3$				
	$u_1^2$	$u_2^2$	$u_3^2$	$u_1 u_3$	$u_2 u_3$	$u_1 u_2$	$u_1^2$	$u_2^2$	$u_3^2$	$u_1 u_3$	$u_1 u_2$
$\mathcal{E}_1^c$	11	66	55	2 $\times$ 56	2 $\times$ 15	2 $\times$ 16	16	26	45	25 $\times$ 46	14 $\times$ 56
$\mathcal{E}_2^c$	16	26	45	25 $\times$ 46	14 $\times$ 56	12 $\times$ 66	66	22	44	2 $\times$ 24	2 $\times$ 46
$\mathcal{E}_3^c$	15	46	35	36 $\times$ 45	13 $\times$ 55	14 $\times$ 56	56	24	34	23 $\times$ 44	36 $\times$ 45
							34	23 $\times$ 44	36 $\times$ 45	55	44
							33	2 $\times$ 34	2 $\times$ 35		
											25 $\times$ 46
											14 $\times$ 56

crystals and textures produce dielectric polarization (direct piezoelectric effect). The electric field produced thereby affects, in its turn, the original strain and stress (reverse piezoelectric effect). As a result, the velocities of elastic waves propagating in piezoelectric crystals are different from those obtained by solving the ordinary Christoffel equation (14.5).

An analysis of wave propagation in piezoelectric media involves a joint solution of equations of motion (14.1) and Maxwell equations. High-frequency elastic waves in piezoelectric crystals are accompanied by electromagnetic waves they generate, and vice versa.

In the general case, three elastic and two electromagnetic waves propagate in piezoelectric media because of the above-described coupling. These waves are of two types: some have phase velocities nearly equal to that of electromagnetic waves, while the velocity of others is nearly equal to that of elastic waves. Among them there are "fast" elastic waves interpreted as mechanical strain accompanying an ordinary electromagnetic wave, and "slow" electromagnetic waves caused by time-dependent electric field generated in a normal elastic wave.

The equations of state of a piezoelectric medium take the form

$$t_{ij} = c_{ijkl} r_{kl} - e_{mij} E_m \quad (14.15)$$

$$D_m = e_{mkl} r_{kl} + \epsilon_{mj} E_j \quad (14.16)$$

By substituting Eq. (14.15) into that of Newton's second law, we obtain

$$\rho \ddot{u}_i = c_{ijkl} \frac{\partial r_{kl}}{\partial x_j} - e_{mij} \frac{\partial E_m}{\partial x_j} \quad (14.17)$$

The electrodynamics equation  $\operatorname{div} \mathbf{D} = \operatorname{curl} \mathbf{E} = 0$  yields

$$e_{jlk} \frac{\partial r_{kl}}{\partial x_j} + \epsilon_{mj} \frac{\partial E_m}{\partial x_j} = 0 \quad (14.18)$$

Taking into account that  $r_{kl} = \frac{1}{2} \left( \frac{\partial u_k}{\partial x_l} + \frac{\partial u_l}{\partial x_k} \right)$  and

$$E_i = - \frac{\partial \varphi}{\partial x_i}$$

we find

$$\rho \ddot{u}_i = c_{ijkl} \frac{\partial^2 u_k}{\partial x_j \partial x_l} + e_{mij} \frac{\partial^2 \varphi}{\partial x_j \partial x_m} \quad (14.19)$$

and

$$0 = e_{jkl} \frac{\partial^2 u_k}{\partial x_j \partial x_l} - \epsilon_{mj} \frac{\partial^2 \varphi}{\partial x_j \partial x_m} \quad (14.20)$$

In a plane wave

$$u_k = u_{k0} \exp [i(\mathbf{k} \cdot \mathbf{r} - \omega t)] \text{ and } \varphi = \varphi_0 \exp [i(\mathbf{k} \cdot \mathbf{r} - \omega t)]$$

Substituting these expressions into (14.18) and (14.19), we find

$$\rho\omega^2 u_i = c_{ijkl} k_j k_l u_k + e_{mij} k_j k_m \varphi \quad (14.21)$$

$$0 = e_{jkl} k_j k_l u_k - e_{mij} k_j k_m \varphi \quad (14.22)$$

Taking into account that  $\mathbf{k} = \frac{\omega}{v} \mathbf{n}$  and eliminating  $\varphi$ , we obtain

$$\left[ \frac{1}{\rho} c_{ijkl} n_j n_l + \frac{1}{\rho} \frac{(n_m e_{mij} n_j) (n_j e_{jkl} n_l)}{n_m e_{mij} n_j} - v^2 \delta_{ik} \right] u_k = 0 \quad (14.23)$$

Introducing the symbols

$$\mathcal{E}_i^n = n_m e_{mij} n_j, \quad \varepsilon^n = \rho n_m e_{mij} n_j \quad (14.24)$$

we rewrite equation (14.23) in the form

$$(\Lambda_{ik} + \mathcal{E}_i^n \mathcal{E}_k^n / \varepsilon^n - v^2 \delta_{ik}) u_k = 0 \quad (14.25)$$

or

$$(\Lambda_{ik} + \Delta \Lambda_{ik}) u_k = v^2 u_i \quad (14.25a)$$

where  $\Lambda_{ik}$  are the components of the Green-Christoffel tensor calculated according to (14.4);  $\Delta \Lambda_{ik} = \mathcal{E}_i^n \mathcal{E}_k^n / \varepsilon^n$  is a "piezoelectric increment" to the components  $\Lambda_{ik}$ ,  $\mathcal{E}_i^n$  are the components of the so-called contracted piezoelectric vector, and  $\mathcal{E}^n$  is the "effective" dielectric permittivity along  $\mathbf{n}$  times  $\rho$ . To simplify the calculation of the characteristics of acoustic waves in piezoelectric crystals, a detailed form of the contracted "piezoelectric" vector  $\mathcal{E}_i^n$  and effective dielectric permittivity is used (see Table 14.3).

Table 14.3

Components of Contracted Vector  $\mathcal{E}_v^n = e_{ivj} n_i n_j$  Required for Calculation of Phase Velocities of Acoustic Waves in Piezoelectric Crystals

$\mathcal{E}_v^n$	$n_i n_j$	$n_1^2$	$n_2^2$	$n_3^2$	$n_2 n_3$	$n_1 n_3$	$n_1 n_2$
$\mathcal{E}_1^n$	11	26	35	25+36	15+31	16+21	
$\mathcal{E}_2^n$	16	22	34	24+32	14+36	12+26	
$\mathcal{E}_3^n$	15	24	33	23+34	13+35	14+25	
$\mathcal{E}^n$	11	22	33	2×23	2×13	2×12	

As a rule,  $\Delta\Lambda_{ik}^n$  is a very small addition to the tensor  $\Lambda_{ik}^n$  so that

$$v^2 = v_0^2 + \Delta v^2$$

$$\mathbf{u} = \mathbf{u}_0 + \Delta \mathbf{u}$$

where  $v_0$ ,  $\mathbf{u}_0$  are the velocity and polarization, respectively, of elastic wave when the piezoelectric effect is neglected;  $\Delta v$  and  $\Delta \mathbf{u}$  are the corresponding small corrections, and one can assume that

$$u_i \Delta u_i = 0$$

By multiplying (14.25a) by  $u_i$  and summing up over  $i$ , we find the expression yielding the piezoelectric correction to the velocity of elastic waves:

$$\Delta v^2 = \frac{1}{\epsilon^n} (\mathcal{E}_i^n u_i^0)^2 \quad (14.26)$$

Piezoelectric properties considerably affect the propagation of acoustic waves if the propagation direction and the motion of particles in a wave are such that the longitudinal component of piezoelectric polarization is generated. Such acoustic waves accompanied by intensive longitudinal piezoelectric fields are called "*piezoelectrically active*" waves.

The polarization of elastic waves in piezoelectric crystals is defined precisely as the polarization in nonpiezoelectric crystals but takes into account the piezoelectric increment  $\Delta\Lambda_{ik}$ . The components of the group velocity vector in piezoelectric crystals are given by the expression

$$S_v = \frac{1}{\rho v} \left\{ \mathcal{E}_v^c + \frac{1}{\epsilon} \mathcal{E}^e \left[ (\mathcal{E}_v^c + ' \mathcal{E}_v^e) - \frac{1}{\epsilon} \mathcal{E}^e \mathcal{E}_v^e \right] \right\} \quad (14.27)$$

where

$$\mathcal{E}_v^c = c_{ijsv}^E n_i u_j u_s; \quad \mathcal{E}^e = e_{mij} n_m n_i u_j$$

$$\epsilon = n_a \epsilon_{ab} n_b; \quad \mathcal{E}_v^e = e_{mvj} n_m u_j$$

$$' \mathcal{E}_v^e = e_{vij} n_i u_j; \quad \mathcal{E}_v^e = \epsilon_{va} n_a$$

In order to simplify Eq. (14.27), it is necessary to convert to the detailed notation of contracted components in this equation, given in Tables 14.5-14.6. Table 14.3 gives the detailed notation of the first term in Eq. (14.27), that is, the components of the contracted "elastic" vector:

$$\mathcal{E}_v^c = c_{ijsv}^E n_i u_j u_s$$

*Calculation  
of Characteristics  
of Group Velocities  
of Bulk Acoustic Waves  
in Piezoelectric Crystals*

The calculation of characteristics of the group velocity of an elastic wave propagating in a piezoelectric medium is carried out in the following order:

(i) the phase velocity  $v$  of an elastic wave and the corresponding vector of polarization  $\mathbf{u}$  are calculated for a given direction of the wavefront normal  $\mathbf{n}$ ;

(ii) the group velocity components  $S_1$ ,  $S_2$  and  $S_3$  are calculated from Eq. (4.27);

(iii) the magnitude of group velocity  $S$  is found by the formula  

$$S = (S_1^2 + S_2^2 + S_3^2)^{1/2} \quad (14.28)$$

(iv) the formula

$$\mathbf{I} = \frac{1}{S} (s_1 \mathbf{e}_1 + s_2 \mathbf{e}_2 + s_3 \mathbf{e}_3) \quad (14.29)$$

yields the unit vector indicating the direction of energy flux in the given elastic wave;  $\mathbf{e}_1$ ,  $\mathbf{e}_2$  and  $\mathbf{e}_3$  are the unit vectors of the crystallophysical coordinate system;

(v) the angle of deviation of energy flux in the considered elastic wave from the wavefront normal  $\mathbf{n}$  is found from the equation

$$\gamma = \arccos (\mathbf{I} \cdot \mathbf{n}) \quad (14.30)$$

Table 14.4 gives the components of the contracted "piezoelectric" vector

$$\mathcal{E}_v^e + ' \mathcal{E}_v^e = e_{mvj} n_m u_j + e_{vij} n_i u_j$$

Table 14.4

Components of Contracted Vector  $\mathcal{E}_v^e + ' \mathcal{E}_v^e = e_{vij} n_i u_j + e_{vij} n_i u_j$   
 Required to Calculate Group Velocities of Acoustic Waves  
 in Piezoelectric Crystals

$n_i u_j$	$n_1$			$n_2$			$n_3$		
$\mathcal{E}_v^e, ' \mathcal{E}_v^e$	$u_1$	$u_2$	$u_3$	$u_1$	$u_2$	$u_3$	$u_1$	$u_2$	$u_3$
$\mathcal{E}_1^e + ' \mathcal{E}_1^e$	2×11	2×16	2×15	16+21	12+26	14+25	15+31	14+36	13+35
$\mathcal{E}_2^e + ' \mathcal{E}_2^e$	16+21	12+26	14+25	2×22	2×24	2×36	25+36	24+32	23+34
$\mathcal{E}_3^e + ' \mathcal{E}_3^e$	15+31	14+36	13+35	25+36	24+32	23+34	2×35	2×34	2×33

which are the sums of the second and third components in Eq. (14.27). The contracted form  $\mathcal{E}^e = e_{mij}n_m n_i u_j$  is a scalar product of the polarization vector  $\mathbf{u}$  and “piezoelectric” contracted vector whose components are  $\mathcal{E}_j^e = e_{mij}n_m n_i$ , given in detailed form in Table 14.3. This table also gives the detailed notation of the effective dielectric permittivity  $\epsilon$  of the piezoelectric material.

The components of the contracted “electric” vector  $\mathcal{E}_v^e = \epsilon_{va} n_a$  are listed in Table 14.5.

Table 14.5

Components of Contracted Vector $\mathcal{E}_v^e = \epsilon_{vp}^u n_p$ Required to Calculate Group Velocities of Acoustic Waves in Piezoelectric Crystals			
$\mathcal{E}_v^e$	$n_1$	$n_2$	$n_3$
$\mathcal{E}_1^e$	11	12	13
$\mathcal{E}_2^e$	12	22	23
$\mathcal{E}_3^e$	13	23	33

### Electromechanical Coupling Factor

The electromechanical coupling factor  $K^2$  found from the relation

$$K^2 = \frac{v^2 - v_0^2}{v_0^2} \quad (14.31)$$

where  $v$  and  $v_0$  are phase velocities along a given direction, when the piezoelectric effect taken into account and not taken into account, respectively, is a generalized characteristic of elastic and piezoelectric properties of crystals.

### Examples of Problems with Solutions

**14.1.** Using only symmetry arguments, show that one purely longitudinal and two purely transverse waves propagate in any crystal along the two-fold axis and along the normal to the symmetry plane.

**Solution.** Assume that an elastic wave with the wavefront normal parallel to the two-fold axis corresponds to the displacement vector

$\mathbf{u}$  at an angle not equal to 0 or  $\pi/2$  with respect to the two-fold axis (Fig. 14.5). Since  $\mathbf{n} \parallel 2$ , the introduction of a favoured direction of the wavefront normal does not change the symmetry of the crystal-elastic wave system as compared to the symmetry of the crystal itself. Consequently, as a result, a rotation of the system by the angle  $\pi$  around the axis 2 leaves the system unchanged. Obviously, this is only possible if the displacement vector is either parallel or perpendicular to  $\mathbf{n}$ ; otherwise it would switch from the position  $\mathbf{u}$  to the position  $\mathbf{u}'$ , and the crystal-wave system would not coincide with itself upon rotation.

This shows that only a pure longitudinal and two pure transverse waves can propagate along a two-fold symmetry axis. A symmetry plane is equivalent, with respect to elastic properties, to a two-fold axis, and therefore, the above arguments are valid for the wavefront normal perpendicular to the symmetry plane.

**14.2.** Electronic devices storing the colour signal for each frame in a colour TV receiver and then transmitting the signal to the electronic gun of the colour picture tube at the end of each frame employ ultrasonic delay line (UDL) with  $60 \mu\text{s}$  delay time. Such delay lines, used in electronics to condition and process radio signals, usually consist of a solid acoustic waveguide coupled to transducers, one to generate elastic vibrations in the acoustic waveguide by applied electric voltage, and another to receive and transform them into electric signals (Fig. 14.6).

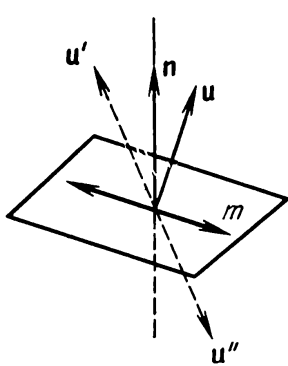
Determine the dimensions of a UDL made of fused quartz operating on (i) longitudinal vibrations, (ii) shear vibrations. By what percentage can the length of the line be reduced if shear waves are employed instead of longitudinal ones?

**Solution.** Fused quartz is an isotropic medium, and its elastic properties are determined by two independent elastic stiffnesses  $c_{11}$  and  $c_{12}$ .

In accordance with the matrix of stiffnesses  $c_{ij}$  of isotropic media, the tensor  $[\Lambda_{ij}]$  takes the form

$$\Lambda_{ij} = \lambda_{44} \delta_{ij} + (\lambda_{11} - \lambda_{44}) n_i n_j$$

Fig. 14.5. Figure to Problem 14.1.



Denote the velocity of a longitudinal wave by  $v_l$ , and that of a transverse wave by  $v_t$ .

The polarization vector of a longitudinal wave propagating along  $\mathbf{n}$  is  $u_i = un_i$ . By substituting this relation into Eq. (14.5), we find

$$\Lambda_{ij}n_j = v_l^2 n_i$$

or

$$[\lambda_{44}\delta_{ij} + (\lambda_{11} - \lambda_{44})n_i n_j]n_j = v_l^2 n_i$$

$$[\lambda_{44} + (\lambda_{11} - \lambda_{44})]n_i = v_l^2 n_i$$

whence

$$v_l^2 = \lambda_{11}; \quad v_l = \sqrt{\frac{c_{11}}{\rho}} = \sqrt{\frac{E}{\rho}}$$

For a transverse wave propagating along  $\mathbf{n}$ ,  $\mathbf{u} \cdot \mathbf{n} = 0$ . Consequently,

$$[\lambda_{44}\delta_{ij} + (\lambda_{11} - \lambda_{44})n_i n_j]u_j = v_t^2 u_i$$

$$\lambda_{44}u_i = v_t^2 u_i$$

whence

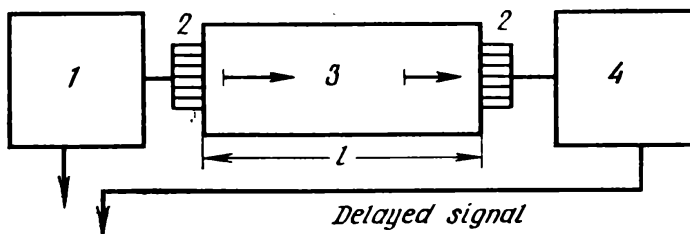
$$v_t^2 = \lambda_{44}$$

$$v_t = \sqrt{\frac{c_{44}}{\rho}} = \sqrt{\frac{\frac{1}{2}(c_{11} - c_{12})}{\rho}}$$

According to (4.19), in isotropic media

$$s_{11} = \frac{1}{E}; \quad s_{12} = -\frac{\sigma}{E}$$

Fig. 14.6. Schematic diagram of ultrasonic delay line with straight acoustic waveguide: 1—pulse generator, 2—transducer, 3—acoustic waveguide, 4—amplifier.



According to (7.9a),  $c_{ij}$  are related to  $s_{ij}$  as follows:

$$c_{11} = \frac{s_{11} + s_{12}}{(s_{11} - s_{12})(s_{11} + 2s_{12})} = E \frac{1 - \sigma}{(1 + \sigma)(1 - 2\sigma)}$$

$$c_{12} = \frac{-s_{12}}{(s_{11} - s_{12})(s_{11} + 2s_{12})} = E \frac{\sigma}{(1 + \sigma)(1 - 2\sigma)}$$

Having found the values of  $c_{11}$  and  $c_{12}$ , we substitute them into the expressions for  $v_1$  and  $v_t$  and find:  $v_1 = 5.75 \cdot 10^5$  cm/s,  $v_t = 3.76 \times 10^5$  cm/s. The signal delay time in a straight acoustic waveguide is  $l/v$ , so that the length of a fused quartz UDL with delay time 60  $\mu$ s is 34.5 cm in the longitudinal vibrations mode, and 22.56 cm in the shear vibrations mode; the UDL length can thus be reduced by 37%.

**14.3.** Find phase velocities of elastic waves propagating in polarized ceramic PZT-4 along the axis  $X_3$ . Which of the waves, longitudinal or transverse, will be piezoelectrically active? What is the piezoelectric correction to the phase velocity of a piezoelectrically active wave?

**Solution.** The elastic properties of piezoelectric ceramic PZT-4 with symmetry  $\infty m$  are characterized by the same set of coefficients  $c_{ij}$  as hexagonal crystals (see Table 9). Correspondingly, the tensor  $[\Lambda_{ij}]$  has the following form (see Table 14.1):

$$\Lambda_{11} = \lambda_{11} n_1^2 + \lambda_{66} n_2^2 + \lambda_{44} n_3^2, \quad \Lambda_{23} = (\lambda_{13} + \lambda_{44}) n_2 n_3$$

$$\Lambda_{22} = \lambda_{66} n_1^2 + \lambda_{11} n_2^2 + \lambda_{44} n_3^2, \quad \Lambda_{31} = (\lambda_{13} + \lambda_{44}) n_1 n_3$$

$$\Lambda_{33} = \lambda_{44} (n_1^2 + n_2^2) + \lambda_{33} n_3^2, \quad \Lambda_{12} = (\lambda_{11} - \lambda_{66}) n_1 n_2$$

(i) For the direction parallel to the axis  $X_3$  we get

$$n_1 = n_2 = 0, \quad n_3 = 1.$$

In this case the tensor  $[\Lambda_{im}]$  is diagonal:

$$\begin{bmatrix} \lambda_{44} & 0 & 0 \\ 0 & \lambda_{44} & 0 \\ 0 & 0 & \lambda_{33} \end{bmatrix}$$

The velocity of an elastic wave,  $-v_1$ , with the displacement vector aligned with the wavefront normal is equal to  $\sqrt{\lambda_{33}}$ , that is,  $v_1 = \sqrt{\frac{c_{33}}{\rho}}$  and the velocities of shear waves with displacement vector perpendicular to  $X_3$  are identical and equal to  $\sqrt{\lambda_{44}}$ , that is,  $v_t = \sqrt{c_{44}/\rho}$ . Now let us find the tensor  $[\Delta\Lambda_{ij}] = \mathcal{E}_i^n \mathcal{E}_j^n / \epsilon$ , where  $\mathcal{E}_i^n = e_{hij} n_h n_j$ .

Since  $\mathbf{n} = (0, 0, 1)$ ,  $\mathcal{E}_i = e_{3i3}$ . In polarized ceramics PZT-4 the nonzero coefficients are  $e_{15}$ ,  $e_{24} = e_{15}$ ,  $e_{31}$ ,  $e_{32} = e_{31}$ ,  $e_{33}$  (see Table 6);

consequently, as follows from Table 14.3, the vector  $\mathcal{E}$  has the form  $\mathcal{E} = (0, 0, 1) e_{33}$ , and

$$[\Delta \Lambda_{ij}] = \begin{bmatrix} 0 & 0 & 0 \\ 0 & 0 & 0 \\ 0 & 0 & \frac{e_{33}^2}{\epsilon^n} \end{bmatrix}$$

where  $\epsilon^n = \frac{\rho}{4\pi e_3}$ .

This shows that among the elastic waves propagating in PZT-4 ceramic along the axis  $X_3$ , only the longitudinal wave with velocity  $\sqrt{c_{33}/\rho} = 4.6 \cdot 10^5$  cm/s is piezoelectrically active. The piezoelectric increment  $\Delta v$  to this velocity is

$$\sqrt{\frac{4\pi e_{33}^2}{\rho e_3}} = 8.2 \cdot 10^3 \text{ cm/s}$$

The velocity of the shear wave propagating along  $X_3$  is

$$\sqrt{\frac{c_{44}}{\rho}} = 8.5 \cdot 10^5 \text{ cm/s}$$

**14.4.** Delay lines used in indicators of moving targets in radar stations have delay time of the order of 1 ms ( $10^{-3}$  s). The dimensions and the level of noise are known to be minimal in polyhedral ultrasonic delay lines (Fig. 14.7). Calculate the linear dimensions of a fused quartz delay line operating in the shear vibrations mode and giving the delay time 1.5 ms. The geometry of the waveguide is (i) straight acoustic waveguide (Fig. 14.6), (ii) 14-hedral waveguide.

**Note.** To calculate the diameter of 14-hedral waveguide use the relation  $R = v\tau/\eta$ , where  $v$  is the elastic wave velocity,  $\tau$  the delay time, and  $\eta$  the coefficient determining the path of the signal in the waveguide,  $\eta = 54.5$ .

**Solution.** The shear wave velocity in fused quartz is given by the relation  $v_t = \sqrt{\frac{c_{44}}{\rho}}$  (see Problem 14.2),  $v_t = 3.76 \cdot 10^5$  cm/s. The linear size of a straight fused quartz waveguide with delay time 1.5 ms is  $l_1 = v_t \tau = 5.64$  m. The diameter of a 14-hedral waveguide with the same delay time is

$$D = 2R = v_t \tau / \eta \approx 10.3 \text{ cm}$$

**14.5.** Find phase velocities and polarization of elastic waves propagating in germanium crystals along (i) [100], (ii) [110], (iii) [111].

**Solution.** The problem of determining phase velocities and polarization of elastic waves in a crystal along a direction  $\mathbf{n}$  ( $n_1, n_2, n_3$ )

is reduced to finding eigenvalues and eigenvectors of the tensor  $[\Lambda_{im}]$ . By using Table 14.1, we find the components of the tensor  $[\Lambda_{im}]$  for cubic crystals:

$$\Lambda_{11} = (\lambda_{11} - \lambda_{44}) n_1^2 + \lambda_{44}, \quad \Lambda_{23} = (\lambda_{12} + \lambda_{44}) n_2 n_3$$

$$\Lambda_{22} = (\lambda_{11} - \lambda_{44}) n_2^2 + \lambda_{44}, \quad \Lambda_{31} = (\lambda_{12} + \lambda_{44}) n_3 n_1$$

$$\Lambda_{33} = (\lambda_{11} - \lambda_{44}) n_3^2 + \lambda_{44}, \quad \Lambda_{12} = (\lambda_{12} + \lambda_{44}) n_1 n_2$$

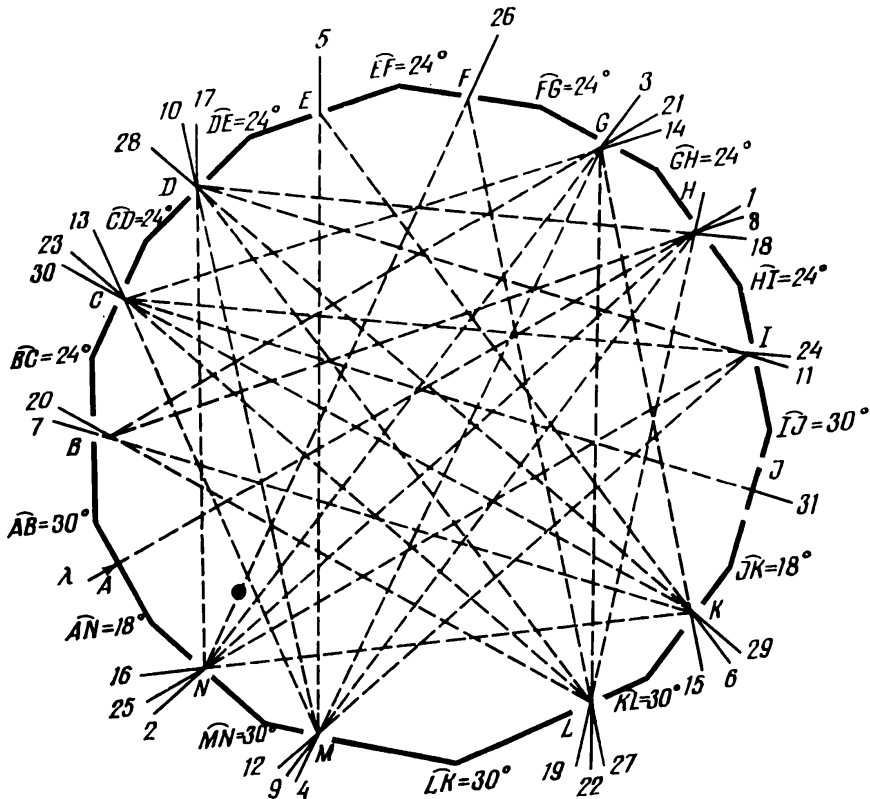
(i) When the elastic wave propagates along [100], we have  $n_1 = 1$ ,  $n_2 = n_3 = 0$ ,

$$\Lambda_{11} = \lambda_{11} \quad \Lambda_{22} = \Lambda_{33} = \lambda_{44}$$

$$\Lambda_{23} = \Lambda_{31} = \Lambda_{12} = 0$$

$$[\Lambda_{im}] = \begin{bmatrix} \lambda_{11} & 0 & 0 \\ 0 & \lambda_{44} & 0 \\ 0 & 0 & \lambda_{44} \end{bmatrix}$$

**Fig. 14.7.** Polyhedral delay line with multiple reflections.



Obviously, the eigenvalues and eigenvectors of this tensor are equal to

$$v_1^2 = \lambda_{11}, \quad \mathbf{u}_1 \sim (1, 0, 0)$$

$$v_2^2 = \lambda_{44}, \quad \mathbf{u}_2 \sim (0, 1, 0)$$

$$v_3^2 = \lambda_{44}, \quad \mathbf{u}_3 \sim (0, 0, 1)$$

Since  $\mathbf{u}_1 \parallel \mathbf{n}$ , the value  $\sqrt{c_{11}/\rho}$  corresponds to the velocity  $v_1$  of the longitudinal wave, and the value  $\sqrt{c_{44}/\rho}$  corresponds to the velocities  $v_2$  and  $v_3$  of two shear (transverse) waves whose displacement vectors are perpendicular to the wavefront propagation direction. In germanium crystals  $\rho = 5.32 \text{ g/cm}^3$ ,  $c_{11} = 12.86 \cdot 10^{11} \text{ dyne/cm}^2$ ,  $c_{12} = 4.83 \cdot 10^{11} \text{ dyne/cm}^2$ , and  $c_{44} = 6.71 \cdot 10^{11} \text{ dyne/cm}^2$  (see Table 14); this gives  $v_1 = 4.99 \cdot 10^5 \text{ cm/s}$ ,  $v_{t_1} = 3.55 \cdot 10^5 \text{ cm/s}$ .

(ii)  $\mathbf{n} \parallel [110]$ ,  $n_1 = n_2 = 1/\sqrt{2}$ ,  $n_3 = 0$ . In this case the components of the tensor  $[\Lambda_{im}]$  are

$$\Lambda_{11} = \Lambda_{22} = \frac{1}{2}(\lambda_{11} + \lambda_{44}); \quad \Lambda_{33} = \lambda_{44}$$

$$\Lambda_{12} = \frac{1}{2}(\lambda_{12} + \lambda_{44})$$

$$[\Lambda_{im}] = \begin{bmatrix} \frac{1}{2}(\lambda_{11} + \lambda_{44}) & \frac{1}{2}(\lambda_{12} + \lambda_{44}) & 0 \\ \frac{1}{2}(\lambda_{12} + \lambda_{44}) & \frac{1}{2}(\lambda_{11} + \lambda_{44}) & 0 \\ 0 & 0 & \lambda_{44} \end{bmatrix}$$

This means that  $v_3^2 = \lambda_{44}$ ,  $\mathbf{u}_3 \sim (0, 0, 1)$ .

Since  $\mathbf{u} \perp \mathbf{n}$ , the value  $v_3 = \sqrt{c_{44}/\rho}$  corresponds to a shear wave. Now we shall find  $v_1$  and  $v_2$ :

$$\begin{bmatrix} \frac{1}{2}(\lambda_{11} + \lambda_{44}) - v^2 & \frac{1}{2}(\lambda_{12} + \lambda_{44}) \\ \frac{1}{2}(\lambda_{12} + \lambda_{44}) & \frac{1}{2}(\lambda_{11} + \lambda_{44}) - v^2 \end{bmatrix} = 0$$

$$v^4 - (\lambda_{11} + \lambda_{44})v^2 + \frac{1}{4}(\lambda_{11} + \lambda_{44})^2 - \frac{1}{4}(\lambda_{12} + \lambda_{44})^2 = 0$$

$$v_1^2 = \frac{\lambda_{11} + \lambda_{12} + 2\lambda_{44}}{2}; \quad v_1 = \sqrt{\frac{c_{11} + c_{12} + 2c_{44}}{2\rho}}$$

$$v_2^2 = \frac{\lambda_{11} - \lambda_{12}}{2}; \quad v_2 = \sqrt{\frac{c_{11} - c_{12}}{2\rho}}$$

The displacement vector corresponding to the velocity  $v_1$  is

$$\begin{bmatrix} -\frac{1}{2}(\lambda_{12} + \lambda_{44}) & \frac{1}{2}(\lambda_{12} + \lambda_{44}) \\ \frac{1}{2}(\lambda_{12} + \lambda_{44}) & -\frac{1}{2}(\lambda_{12} + \lambda_{44}) \end{bmatrix} \begin{pmatrix} u_1^{(1)} \\ u_2^{(1)} \end{pmatrix} = 0$$

$$\frac{1}{2}(\lambda_{12} + \lambda_{44}) \begin{bmatrix} -1 & 1 \\ 1 & -1 \end{bmatrix} \begin{pmatrix} u_1^{(1)} \\ u_2^{(1)} \end{pmatrix} = 0$$

This gives

$$\begin{aligned} -u_1^{(1)} + u_2^{(1)} &= 0 \\ u_1^{(1)} - u_2^{(1)} &= 0 \end{aligned}$$

whence  $u_1^{(1)} = u_2^{(1)}$  and  $\mathbf{u}^{(1)} = (1/\sqrt{2}, 1/\sqrt{2}, 0) u$ .

In the case under discussion  $\mathbf{u}^{(1)} \parallel \mathbf{n}$ , therefore, the wave corresponding to  $v_1$  is longitudinal.

The displacement vector of the wave corresponding to  $v_2$  is found in a similar manner:

$$\frac{1}{2}(\lambda_{12} + \lambda_{44}) \begin{bmatrix} 1 & 1 \\ 1 & 1 \end{bmatrix} \begin{pmatrix} u_1^{(2)} \\ u_2^{(2)} \end{pmatrix} = 0$$

$$u_1^{(2)} + u_2^{(2)} = 0$$

$$u_1^{(2)} = -u_2^{(2)}$$

and, consequently,  $\mathbf{u}^{(2)} = \frac{1}{\sqrt{2}} (1, -1, 0) u$ .

Since  $\mathbf{u}_2 \cdot \mathbf{n} = 0$ , the wave corresponding to  $v_2 = \sqrt{(c_{11} - c_{12})/2\rho}$  is a shear wave.

Therefore, the waves propagating in germanium crystals along [110] are one longitudinal wave with velocity  $v_1 = v_1 = 5.41 \times 10^5$  cm/s, and two shear waves with velocities  $v_1^{[1\bar{1}0]} = 2.75 \times 10^5$  cm/s and  $v_2^{[001]} = 6.71 \cdot 10^5$  cm/s.

The superscripts indicate the directions of polarization of shear waves.

(iii) When elastic waves propagate in a cubic crystal along [111], we have

$$n_1^2 = n_2^2 = n_3^2 = n_1 n_2 = n_2 n_3 = n_3 n_1 = 1/3$$

so that in correspondence with Table 14.1, the tensor  $[\Lambda_{im}]$  is

$$\frac{1}{3} \begin{bmatrix} \lambda_{11} + 2\lambda_{44} & \lambda_{12} + \lambda_{44} & \lambda_{12} + \lambda_{44} \\ \lambda_{12} + \lambda_{44} & \lambda_{11} + 2\lambda_{44} & \lambda_{12} + \lambda_{44} \\ \lambda_{12} + \lambda_{44} & \lambda_{12} + \lambda_{44} & \lambda_{11} + 2\lambda_{44} \end{bmatrix}$$

Introduce the following notations:

$$\frac{1}{3}(\lambda_{11} + 2\lambda_{44}) = a, \quad \frac{1}{3}(\lambda_{12} + \lambda_{44}) = b$$

This gives

$$[\Lambda_{im}] = \begin{bmatrix} a & b & b \\ b & a & b \\ b & b & a \end{bmatrix}$$

Equation (14.5) then becomes in the present case

$$\begin{vmatrix} a - v^2 & b & b \\ b & a - v^2 & b \\ b & b & a - v^2 \end{vmatrix} = 0$$

$$(a - v^2)^3 + 2b^3 - 3b^2(a - v^2) = 0$$

Denote  $v^2 - a$  by  $x$ ; then

$$x^3 - 2b^3 - 3b^2x = 0 \quad (14.32)$$

Let us check whether this equation has a solution for  $x = 2b$ :

$$8b^3 - 6b^3 - 2b^3 = 0$$

The cubic trinomial can therefore be represented in the form

$$(x - 2b)(x^2 + \alpha x + \beta) \quad (14.33)$$

Equation (14.33) has two solutions:

$$x - 2b = 0, \quad (x^2 + \alpha x + \beta) = 0 \quad (14.34)$$

Obviously, the first root  $x_1$  of Eq. (14.33) equals  $2b$ . As  $v^2 - a = x$ , we have  $v_1^2 = 2b + a$ , and

$$v_1^2 = \frac{1}{3}(\lambda_{11} + 2\lambda_{12} + 4\lambda_{44})$$

$$v_1 = \sqrt{\frac{1}{3}(\lambda_{11} + 2\lambda_{12} + 4\lambda_{44})}$$

To find the roots  $x_2$  and  $x_3$  of Eq. (14.34), corresponding to the velocities  $v_2$  and  $v_3$ , it is necessary to find the coefficients  $\alpha$  and  $\beta$  in this equation.

Aligning equation (14.33) with (14.32),

$$x^3 - 2b^3 - 3b^2x = 0$$

$$x^3 - 2bx^2 + \alpha x^2 - 2b\alpha x + \beta x - 2\beta b = 0$$

and comparing coefficients of  $x^2$ , we find

$$\alpha - 2b = 0, \quad \alpha = 2b$$

A comparison of the coefficients of  $x$  yields

$$-2b\alpha + \beta = -3b^2$$

Likewise, the comparison of coefficients of free terms yields

$$-2b\beta = -2b^3, \quad \beta = b^2$$

From this we have  $\alpha = 2b$  and  $\beta = b^2$ . After substituting the values  $\alpha$  and  $\beta$  into Eq. (14.34), we find

$$x^2 + 2bx + b^2 = 0; \quad x_{2,3} = -b \pm \sqrt{b^2 - b^2} = -b$$

Consequently, three waves propagate in cubic crystals along [111]. The velocity of one of them is

$$v_1 = \sqrt{\frac{1}{3} \frac{c_{11} + 2c_{12} + 4c_{44}}{\rho}} = 5.56 \cdot 10^5 \text{ cm/s}$$

the other two waves have identical velocities

$$v_2 = v_3 = \sqrt{\frac{c_{11} - c_{12} + c_{44}}{3\rho}} = 3.04 \cdot 10^5 \text{ cm/s}$$

Let us find the polarization of the wave propagating at the velocity  $v_1$ :

$$\begin{bmatrix} -2b & b & b \\ b & -2b & b \\ b & b & -2b \end{bmatrix} \cdot \begin{pmatrix} u_1 \\ u_2 \\ u_3 \end{pmatrix} = 0$$

$$b \begin{bmatrix} -2 & 1 & 1 \\ 1 & -2 & 1 \\ 1 & 1 & -2 \end{bmatrix} \cdot \begin{pmatrix} u_1 \\ u_2 \\ u_3 \end{pmatrix} = 0$$

or

$$-2u_1 + u_2 + u_3 = 0 \quad (14.35)$$

$$u_1 - 2u_2 + u_3 = 0 \quad (14.36)$$

$$u_1 + u_2 - 2u_3 = 0 \quad (14.37)$$

The determinant of this system of linear equations vanishes, consequently, only two of these equations are independent. Subtract Eq. (14.36) from (14.35):

$$-3u_1 + 3u_2 = 0, \text{ and thus } u_1 = u_2$$

Substituting  $u_1 = u_2$  into (14.37), we find

$$-2u_1 + u_1 + u_3 = 0, \quad u_1 = u_3$$

Hence,  $u_1 = u_2 = u_3$ , and the polarization vector of the wave propagating at the velocity  $v_1$  is  $\mathbf{u} = \frac{1}{\sqrt{3}}(1, 1, 1)$ . Since  $\mathbf{u} \parallel \mathbf{n}$ ,  $v_1$  corresponds to the longitudinal wave.

Likewise, it can be shown that the waves propagating at the velocities  $v_2 = v_3$  are shear waves, and their polarization vector may be any vector lying in the plane (111).

**14.6.** Find the maximum magnitude of piezoelectric correction to the phase velocity of shear elastic waves propagating in sphalerite crystals in the plane (001) and polarized along [001]. Find the directions lying in the plane (001) in which the velocity of shear waves is not affected by the piezoelectric effect.

**Solution.** The following piezoelectric coefficients  $e_{ij}$  do not vanish in sphalerite crystals belonging to symmetry class  $\bar{4}3m$ :  $e_{14}$ ,  $e_{25}$ ,  $e_{36}$  ( $e_{14} = e_{25} = e_{36}$ ) (see Table 6).

According to Table 14.3, the expressions for  $\mathcal{E}^n$  then have the form

$$\mathcal{E}^n = 2e_{14}(n_2n_3, n_3n_1, n_1n_2)$$

and

$$\varepsilon^n = \frac{1}{4\pi} \mathcal{E}$$

In our case  $\mathbf{n}$  ( $n_1, n_2, 0$ ),  $n_1 = \cos \varphi$ ,  $n_2 = \sin \varphi$  ( $\varphi$  is the angle between  $\mathbf{n}$  and the axis  $X_1$ ), and  $u_0 = (1, 0, 0)$ ,  $v_0^2 = \lambda_{44}$ . According to (14.26),

$$\Delta v^2 = \frac{4\pi e_{14}^2 \sin^2 2\varphi}{\rho \varepsilon}$$

As follows from the expression for  $\Delta v^2$ , the piezoelectric correction to velocity is a function of direction  $\mathbf{n}$  (the function of angle  $\varphi$ ). The maximum value of  $\Delta v^2$ , equal to  $\frac{4\pi e_{14}^2}{\rho \varepsilon}$ , corresponds to  $\varphi = \pm 45^\circ$ , that is, to directions  $\langle 110 \rangle$ ; for  $\varphi = 0$  and  $\varphi = 90^\circ$ , that is along the directions  $\langle 100 \rangle$ ,  $\Delta v^2 = 0$  and the piezoelectric effect does not affect the velocity of shear waves.

**14.7.** Calculate the phase velocity and polarizations of bulk acoustic waves propagating in lithium niobate crystals along its crystallophysical axes. Which of these waves are piezoelectrically active?

**Solution.** In accordance with the form of the matrix  $(c_{\alpha\beta})$  for symmetry class  $3m$  (see Table 9), the components of the tensor  $[\Lambda_{kl}]$  are written, by using Table 14.1, in the form

$$\begin{aligned} \Lambda_{11} &= \lambda_{11}n_1^2 + \lambda_{66}n_2^2 + \lambda_{44}n_3^2 + 2\lambda_{14}n_2n_3 \\ \Lambda_{22} &= \lambda_{66}n_1^2 + \lambda_{11}n_2^2 + \lambda_{44}n_3^2 - 2\lambda_{14}n_2n_3 \\ \Lambda_{33} &= \lambda_{44}(n_1^2 + n_2^2) + \lambda_{33}n_3^2 \\ \Lambda_{23} &= (\lambda_{13} + \lambda_{44})n_2n_3 + \lambda_{14}(n_1^2 - n_2^2) \\ \Lambda_{13} &= (\lambda_{13} + \lambda_{44})n_1n_3 + 2\lambda_{14}n_1n_2 \\ \Lambda_{12} &= (\lambda_{11} - \lambda_{66})n_1n_2 + 2\lambda_{14}n_1n_3. \end{aligned} \tag{14.38}$$

By solving Eq. (14.5) and taking into account (14.38) for a given wavefront normal  $\mathbf{n}$ , we find the velocities and polarizations of elastic waves in the considered crystalline medium.

(i) The components of the wavefront normal in the case of the elastic wave propagating along the axis  $X_1$  are:  $n_1 = 1$ ,  $n_2 = n_3 = 0$ , and, in accordance with (14.38),

$$\Lambda_{11} = \frac{1}{\rho} c_{11}; \quad \Lambda_{22} = \frac{1}{\rho} c_{66}; \quad \Lambda_{33} = \frac{1}{\rho} c_{44};$$

$$\Lambda_{23} = \frac{1}{\rho} c_{14}; \quad \Lambda_{13} = \Lambda_{12} = 0,$$

where  $c_{11}$ ,  $c_{14}$ ,  $c_{44}$ , and  $c_{66}$  are the effective elastic moduli, and  $c_{\alpha\beta} = c_{\alpha\beta}^E + \Delta c_{\alpha\beta}$ , where  $c_{\alpha\beta}^E$  are the elastic moduli of the crystal, and  $\Delta c_{\alpha\beta}$  are the piezoelectric corrections which can be found from Table 14.3. From the matrix of piezoelectric constants ( $e_{i\alpha}$ ) (see Table 7) and the tensor of dielectric permittivities [ $\epsilon_{mn}$ ] for symmetry class  $3m$ , we find:

$$\Delta c_{11} = 0, \quad \Delta c_{14} = -e_{15}e_{22}/\epsilon_{11}, \quad \Delta c_{44} = e_{15}^2/\epsilon_{11}, \quad \Delta c_{66} = e_{22}^2/\epsilon_{11}$$

Corrections to the remaining elastic coefficients vanish in the present case.

The characteristic equation is

$$\begin{vmatrix} c_{11} - \rho v^2 & 0 & 0 \\ 0 & c_{66} - \rho v^2 & c_{14} \\ 0 & c_{14} & c_{44} - \rho v^2 \end{vmatrix} = 0 \quad (14.39)$$

where

$$c_{14} = c_{14}^E - \frac{e_{15}e_{22}}{\epsilon_{11}}; \quad c_{44} = c_{44}^E + \frac{e_{15}^2}{\epsilon_{11}}; \quad c_{66} = c_{66}^E + \frac{e_{22}^2}{\epsilon_{11}}$$

As follows from (14.39),  $v_1 = \sqrt{c_{11}/\rho}$ , and  $\mathbf{u} (1, 0, 0)$ . The velocity  $v_1$  corresponds to the longitudinal piezoelectrically nonactive wave because  $\mathbf{u}_1 \parallel \mathbf{n}_1$ . Furthermore,

$$v_2 = \sqrt{\frac{1}{\rho} \left[ \frac{c_{44} + c_{66}}{2} + \sqrt{\frac{(c_{44} - c_{66})^2}{4} + c_{24}^2} \right]}$$

$$\mathbf{u}_2 \left( 0; \frac{1}{\sqrt{2\sqrt{k^2+1}(\sqrt{k^2+1}+k)}}, \frac{\sqrt{k^2+1}+k}{\sqrt{2\sqrt{k^2+1}(\sqrt{k^2+1}+k)}} \right)$$

$$v_3 = \sqrt{\frac{1}{\rho} \left[ \frac{c_{44} + c_{66}}{2} - \sqrt{\frac{(c_{44} - c_{66})^2}{4} + c_{14}^2} \right]}$$

$$\mathbf{u}_3 \left( 0; \frac{1}{\sqrt{2\sqrt{k^2+1}(\sqrt{k^2+1}-k)}}, \frac{\sqrt{k^2+1}-k}{\sqrt{2\sqrt{k^2+1}(\sqrt{k^2+1}-k)}} \right)$$

where  $k = (c_{44} - c_{66})/(2c_{14})$ .

The velocities  $v_2$  and  $v_3$  correspond to two quasitransverse waves, with  $v_2$  corresponding to the fast, and  $v_3$  to the slow quasitransverse wave.

(ii) The elastic wave propagates along the axis  $X_2$ , that is,  $n_1 = 0$ ,  $n_2 = 1$ ,  $n_3 = 0$ .

In this case the characteristic equation is

$$\begin{vmatrix} c_{66} - \rho v^2 & 0 & 0 \\ 0 & c_{11} - \rho v^2 & -c_{14} \\ 0 & -c_{14} & c_{44} - \rho v^2 \end{vmatrix} = 0 \quad (14.40)$$

where

$$c_{11} = c_{11}^E + \frac{e_{22}^2}{\varepsilon_{11}}; \quad c_{14} = c_{14}^E + \frac{e_{15}e_{22}}{\varepsilon_{11}}; \quad c_{44} = c_{44}^E + \frac{e_{15}^2}{\varepsilon_{11}}$$

As follows from (14.40),  $v_3 = \sqrt{c_{66}/\rho}$ ,  $\mathbf{u} (1, 0, 0)$ , that is, the velocity  $v_3$  corresponds to the shear piezoelectrically nonactive wave. Furthermore

$$v_1 = \sqrt{\frac{1}{\rho} \left[ \frac{c_{11} + c_{44}}{2} + \sqrt{\frac{(c_{11} - c_{44})^2}{4} + c_{14}^2} \right]}$$

$$\mathbf{u}_1 \left( \frac{1}{\sqrt{2} \sqrt{k^2 + 1} (\sqrt{k^2 + 1} - k)}; \quad 0; \quad -\frac{\sqrt{k^2 + 1} - k}{\sqrt{2} \sqrt{k^2 + 1} (\sqrt{k^2 + 1} - k)} \right)$$

$$v_2 = \sqrt{\frac{1}{\rho} \left[ \frac{c_{11} + c_{44}}{2} - \sqrt{\frac{(c_{11} - c_{44})^2}{4} + c_{14}^2} \right]}$$

$$\mathbf{u}_2 \left( \frac{1}{\sqrt{2} \sqrt{k^2 + 1} (\sqrt{k^2 + 1} + k)}; \quad 0; \quad \frac{\sqrt{k^2 + 1} + k}{\sqrt{2} \sqrt{k^2 + 1} (\sqrt{k^2 + 1} + k)} \right)$$

where  $k = (c_{11} - c_{44})/(2c_{14})$ .

The velocity  $v_1$  corresponds to the quasilongitudinal wave, and  $v_2$ , to the quasitransverse wave.

(iii) The elastic wave propagates along the axis  $X_3$ , that is,  $n_1 = n_2 = 0$ ,  $n_3 = 1$ .

In this case the characteristic equation is

$$\begin{vmatrix} c_{44} - \rho v^2 & 0 & 0 \\ 0 & c_{44} - \rho v^2 & 0 \\ 0 & 0 & c_{33} - \rho v^2 \end{vmatrix} = 0 \quad (14.41)$$

As follows from (14.41),  $v_1 = \sqrt{c_{33}/\rho}$ ,  $\mathbf{u}_1 (0, 0, 1)$ , and  $v_1$  corresponds to the longitudinal piezoelectrically active wave. Furthermore,  $v_2 \Rightarrow v_3 = \sqrt{c_{44}/\rho}$ .

These velocities correspond to two pure transverse piezoelectrically nonactive waves with polarization vectors in the plane  $X_1OX_2$ . Obviously, the direction of the axis  $X_3$  is the acoustic axis.

14.8. Determine group velocities and the direction of energy flux of bulk acoustic waves propagating in lithium niobate crystals along the crystallophysical axes  $X_1, X_2, X_3$ .

**Solution.** According to (14.27), the first step in calculating the components of group velocities is the calculation of contracted components

$$\mathcal{E}_v^c, \mathcal{E}_v^e, \mathcal{E}_v^e + ' \mathcal{E}_v^e, \mathcal{E}_v^e$$

This is conveniently done by using Tables 14.2-14.5. In accordance with the form of elastic stiffness matrices ( $c_{ij}$ ) for crystals belonging to symmetry class  $3m$  (see Table 9), matrices of piezoelectric moduli ( $e_{ij}$ ) (see Table 7), and matrices of dielectric permittivity coefficients ( $\epsilon_{ij}$ ) (see Table 14.5), Tables 14.2-14.5 are transformed into Tables 14.6-14.9.

(i) The acoustic wave propagates along the axis  $X_1$ , that is,  $\mathbf{n} (1, 0, 0)$ . We begin with Table 14.7, because the components of contracted vectors,

$$\mathcal{E}_v^e = e_{mvj} n_m u_j \text{ and}$$

$$\epsilon = n_a \epsilon_{ab} n_b$$

are identical for all three types of waves propagating along a given direction  $\mathbf{n}$ . We thus obtain from Table 14.7 that  $\mathcal{E}_1^e = 0$ ,  $\mathcal{E}_2^e = -e_{22}$ ,  $\mathcal{E}_3^e = e_{15}$ , and  $\epsilon = \epsilon_{11}$ . For the longitudinal wave we obtain in the present case  $v_1 = \sqrt{c_{11}^E/\rho}$  and  $\mathbf{u} (1, 0, 0)$ , and therefore  $\mathcal{E}^e = \mathcal{E}_j u_j = 0$ . It is obvious from Table 14.6 that  $\mathcal{E}_1^c = c_{11}^E$ ,

Table 14.6

Components of Contracted "Elastic" Vector  $\mathcal{E}_v^c = c_{ijsv}^E n_i u_j n_s$  in Symmetry Classes  $32, 3m$ , and  $\bar{3}m$

	$n_1$			$n_2$			$n_3$										
	$u_1^2$	$u_2^2$	$u_3^2$	$u_1 u_3$	$u_2 u_3$	$u_1 u_2$	$u_2^2$	$u_3^2$	$u_1^2$	$u_2^2$	$u_3^2$	$u_1 u_3$	$u_1 u_2$	$u_2 u_3$	$u_1 u_2$	$u_1 u_3$	$u_1 u_2$
$\mathcal{E}_1^c$	11	66	44	2 $\times$ 14	—	—	—	—	—	2 $\times$ 14	12 + 66	—	—	—	—	13 + 44	2 $\times$ 14
$\mathcal{E}_2^c$	—	—	—	—	2 $\times$ 14	12 + 66	66	11	44	—	—	14	—	13 + 44	—	—	—
$\mathcal{E}_3^c$	—	—	—	—	—	13 + 44	2 $\times$ 14	14	—	13 + 44	—	—	44	44	33	—	—

Table 14.7

**Components of Contracted “Piezoelectric” Vector  $\mathcal{E}_v^e = e_{mvj} n_m u_j$  and of Effective Dielectric Permittivity  $\epsilon = n_a \epsilon_{ab}^v n_b$  for Symmetry Class  $3m$**

	$n_1^2$	$n_2^2$	$n_3^2$	$n_2 n_3$	$n_1 n_3$	$n_1 n_2$
$\mathcal{E}_1^e$	—	—	—	—	15+31	$-2 \times 22$
$\mathcal{E}_2^e$	$-22$	22	—	15+31	—	—
$\mathcal{E}_3^e$	15	15	33	—	—	—
$\epsilon$	11	11	33	—	—	—

Table 14.8

**Components of Contracted “Piezoelectric” Vector  $\mathcal{E}_v^e + ' \mathcal{E}_v^e = e_{mvj} n_m u_j + e_{vij} n_i u_j$  for Symmetry Class  $3m$**

	$n_1$			$n_2$			$n_3$		
	$u_1$	$u_2$	$u_3$	$u_1$	$u_2$	$u_3$	$u_1$	$u_2$	$u_3$
$\mathcal{E}_1^e + ' \mathcal{E}_1^e$	—	$-2 \times 22$	$2 \times 15$	$-2 \times 22$	—	—	15+31	—	—
$\mathcal{E}_2^e + ' \mathcal{E}_2^e$	$-2 \times 22$	—	—	—	$2 \times 22$	$2 \times 15$	—	15+31	—
$\mathcal{E}_3^e + ' \mathcal{E}_3^e$	15+31	—	—	—	15+31	—	—	—	$2 \times 33$

Table 14.9

**Components of Contracted “Electric” Vector  $\mathcal{E}_v^e = \epsilon_{v\alpha}^r n_\alpha$  for Medium-Symmetry Crystals**

	$n_1$	$n_2$	$n_3$
$\mathcal{E}_1^e$	11	—	—
$\mathcal{E}_2^e$	—	11	—
$\mathcal{E}_3^e$	—	—	33

$\mathcal{E}_2^c = \mathcal{E}_3^c = 0$ ; hence, these relations substituted into Eq. (14.27) yield:  $S_1 = c_{11}^E/\rho v_1 = v_1$ ,  $S_2 = S_3 = 0$ . Finally we obtain for the longitudinal elastic wave propagating along the axis  $X_1$ :  $S^1 = v_1$ ,  $\mathbf{l}(1, 0, 0)$  and  $\gamma_1 = 0^\circ$ . For shear waves we find for  $\mathbf{n}(1, 0, 0)$ :  $v_{2,3}$  and  $\mathbf{u}_{2,3}(0, u_2, u_3)$  (see Problem 14.7) and, as follows from Table 14.6 in this case,

$$\mathcal{E}_1^c = c_{66}^E u_2^2 + 2c_{14}^E u_2 u_3 + c_{44}^E u_3^2, \quad \mathcal{E}_2^c = \mathcal{E}_3^c = 0.$$

We also find

$$\mathcal{E}^e = \mathcal{E}_j u_j = -e_{22} u_2 + e_{15} u_3 \text{ and } \varepsilon = \varepsilon_{11}$$

As follows from Table 14.8,

$$\mathcal{E}_1^e + ' \mathcal{E}_1^e = -2e_{22} u_2 + 2e_{15} u_3, \quad \mathcal{E}_2^e + ' \mathcal{E}_2^e = \mathcal{E}_3^e + ' \mathcal{E}_3^e = 0$$

and from Table 14.9,

$$\mathcal{E}_1^e = \varepsilon_{11}, \quad \mathcal{E}_2^e = \mathcal{E}_3^e = 0$$

After the obtained relations are substituted into Eq. (14.27), we obtain

$$\begin{aligned} S_1 &= \frac{1}{\rho v} \left[ c_{66}^E u_2^2 + 2c_{14}^E u_2 u_3 + c_{44}^E u_3^2 + \frac{1}{\varepsilon_{11}^r} (e_{15} u_3 - e_{22} u_2) \right. \\ &\quad \times \left. \left( 2e_{15} u_3 - 2e_{22} u_2 - \frac{1}{\varepsilon_{11}^r} (e_{15} u_3 - e_{22} u_2) \varepsilon_{11}^\gamma \right) \right] \\ &= \frac{1}{\rho v} \left[ c_{66}^E u_2^2 + 2c_{14}^E u_2 u_3 + c_{44}^E u_3^2 + \frac{1}{\varepsilon_{11}^r} (e_{15} u_3 - e_{22} u_2)^2 \right] \\ &= \frac{1}{\rho v} \left[ \left( c_{66}^E + \frac{e_{22}^2}{\varepsilon_{11}^r} \right) u_2^2 + 2 \left( c_{14}^E - \frac{e_{15} e_{22}}{\varepsilon_{11}^r} \right) u_2 u_3 + \left( c_{44}^E + \frac{e_{15}^2}{\varepsilon_{11}^r} \right) u_3^2 \right. \\ &\quad \left. = \frac{1}{\rho v} (c_{66}^E u_2^2 + 2c_{14}^E u_2 u_3 + c_{44}^E u_3^2), \quad S_2 = S_3 = 0 \right] \end{aligned}$$

Taking into account the specific relations for  $v_2$ ,  $u_2$  and  $v_3$ ,  $u_3$  (see Problem 14.7), we finally obtain for transverse waves propagating along the axis  $X_1$

$$S_{2,3} = v_{2,3}, \quad \mathbf{l}_{2,3}(1, 0, 0) \text{ and } \gamma_{2,3} = 0^\circ$$

(ii) The elastic wave propagates along the axis  $X_2$ , that is,  $\mathbf{n}(0, 1, 0)$ . In this case Table 14.7 gives  $\mathcal{E}_1^e = 0$ ,  $\mathcal{E}_2^e = e_{22}$ ,  $\mathcal{E}_3^e = e_{15}$ , and  $\varepsilon = \varepsilon_{11}$ . For the quasilongitudinal and quasitransverse waves  $\mathbf{u}_{1,2}(0, u_2, u_3)$  (see Problem 14.7), consequently,

$$\mathcal{E}^e = \mathcal{E}_j u_j = e_{22} u_2 + e_{15} u_3$$

Table 14.6 yields

$$\mathcal{E}_1^c = 0, \quad \mathcal{E}_2^c = c_{11}^E u_2^2 - 2c_{14}^E u_2 u_3 + c_{44}^E u_3^2$$

$$\mathcal{E}_3^c = -c_{14}^E u_2^2 + (c_{13}^E + c_{14}^E) u_2 u_3$$

We then find from Table 14.8 that

$$\mathcal{E}_1^e + ' \mathcal{E}_1^e = 0, \quad \mathcal{E}_2^e + ' \mathcal{E}_2^e = 2e_{22}u_2 + 2e_{15}u_3, \quad \mathcal{E}_3^e + ' \mathcal{E}_3^e = (e_{15} + e_{31})u_2$$

and from Table 14.9,

$$\mathcal{E}_1^e = \mathcal{E}_3^e = 0 \text{ and } \mathcal{E}_2^e = \varepsilon_{11}^r$$

By substituting the derived relations into Eq. (14.27), we find

$$\begin{aligned} S_2 &= \frac{1}{\rho v} \left[ c_{11}^E u_2^2 - 2c_{14}^E u_2 u_3 + c_{44}^E u_3^2 + \frac{e_{22}u_2 + e_{15}u_3}{\varepsilon_{11}^r} \right. \\ &\quad \times \left. \left( 2e_{22}u_2 + 2e_{15}u_3 - \frac{e_{22}u_2 + e_{15}u_3}{\varepsilon_{11}^r} \varepsilon_{11}^r \right) \right] \\ &= \frac{1}{\rho v} \left[ \left( c_{14}^E + \frac{e_{22}^2}{\varepsilon_{11}^r} \right) u_2^2 - 2 \left( c_{14}^E - \frac{e_{15}e_{22}}{\varepsilon_{11}^r} \right) u_2 u_3 + \left( c_{44}^E + \frac{e_{15}^2}{\varepsilon_{11}^r} \right) u_3^2 \right] \\ &\quad = \frac{1}{\rho v} (c_{11}u_1^2 - 2c_{14}u_2u_3 + c_{44}u_3^2) \\ S_3 &= \frac{1}{\rho v} \left\{ (c_{13}^E + c_{44}^E) u_2 u_3 - c_{14}^E u_2^2 + \frac{e_{22}u_2 + e_{15}u_3}{\varepsilon_{11}^r} \right. \\ &\quad \times \left. \left[ (e_{15} + e_{31})u_2 - \frac{e_{22}u_2 + e_{15}u_3}{\varepsilon_{11}^r} \varepsilon_{11}^r \right] \right\} \\ &= \frac{1}{\rho v} \left\{ \left[ -c_{14}^E + \frac{1}{\varepsilon_{11}^r} e_{22} (e_{15} - e_{22} + e_{31}) \right] u_2^2 \right. \\ &\quad \left. + \left[ c_{13}^E + c_{44}^E + \frac{1}{\varepsilon_{11}^r} e_{15} (e_{15} - 2e_{22} + e_{31}) \right] u_2 u_3 - \frac{e_{15}^2}{\varepsilon_{11}^r} u_3^2 \right\} \end{aligned}$$

The relations thus obtained are used to calculate, via Eqs. (14.29) and (14.30), the magnitude and direction of group velocity, as well as the angle deviation of energy flux from the wavefront normal of the quasilongitudinal and quasitransverse waves, respectively.

In the case of a transverse wave,  $v_3 = \sqrt{c_{66}^E/\rho}$  and  $\mathbf{u} (1, 0, 0)$  (see Problem 14.7). This gives  $\mathcal{E}^e = \mathcal{E}_i^e u_i = 0$ , so that the piezoelectric effect does not change the group velocity of the transverse wave. Furthermore, Table 14.6 yields

$$\mathcal{E}_1^c = 0, \quad \mathcal{E}_2^c = c_{66}^E, \quad \text{and} \quad \mathcal{E}_3^c = c_{14}^E$$

We thus find that

$$S_1 = 0, \quad S_2 = c_{66}^E / \rho v_3, \quad S_3 = c_{14}^E / \rho v_3$$

whence

$$S_3 = \frac{1}{\rho v_3} \sqrt{(c_{66}^E)^2 + (c_{14}^E)^2} = \sqrt{\frac{1}{\rho} \left( c_{66}^E + \frac{c_{14}^E}{c_{66}^E} c_{14}^E \right)}$$

Now it is not difficult to calculate  $\mathbf{I}_3$  and  $\gamma_3$  from Eqs. (14.29) and (14.30).

(iii) The elastic wave propagates along the axis  $X_3$ , that is,  $\mathbf{n} (0, 0, 1)$ . Table 14.7 yields

$$\mathcal{E}_1^e = \mathcal{E}_2^e = 0, \quad \mathcal{E}_3^e = e_{33} \text{ and } \varepsilon = \varepsilon_{33}$$

In the case of a longitudinal wave  $v_1 = \sqrt{c_{33}/\rho}$  and  $\mathbf{u}_1 (0, 0, 1)$ . Therefore,  $\mathcal{E}^e = \mathcal{E}_i^e u_i = e_{33}$ . Furthermore, Table 14.6 yields  $\mathcal{E}_1^c = \mathcal{E}_2^c = 0$ ,  $\mathcal{E}_3^c = c_{33}^E$ . From Table 14.8 we have

$$\mathcal{E}_1^e + ' \mathcal{E}_1^e = \mathcal{E}_2^e + ' \mathcal{E}_2^e = 0 \text{ and } \mathcal{E}_3^e + ' \mathcal{E}_3^e = 2e_{33},$$

and from Table 14.6

$$\mathcal{E}_1^e = \mathcal{E}_2^e = 0 \text{ and } \mathcal{E}_3^e = \varepsilon_{33}^r$$

As a result, we obtain for the longitudinal wave  $S_1 = S_2 = 0$ ,

$$\begin{aligned} S_3 &= \frac{1}{\rho v_1} \left[ c_{33}^E + \frac{e_{33}}{\varepsilon_{33}^r} \left( 2e_{33} - \frac{e_{32}}{\varepsilon_{33}^r} \varepsilon_{33}^r \right) \right] \\ &= \frac{1}{\rho v_1} \left( c_{33}^E + \frac{e_{33}^2}{\varepsilon_{33}^r} \right) = \frac{c_{33}}{\rho v_1} = \frac{v_1^2}{v_1} = v_1 \end{aligned}$$

that is,  $S^1 = v_1$ ,  $\mathbf{I} (0, 0, 1)$ , and  $\gamma_1 = 0^\circ$ .

In the case of transverse waves (see Problem 14.7),

$$v_{2,3} = \sqrt{c_{44}^E/\rho} \text{ and } \mathbf{u}_{2,3} \perp \mathbf{n}$$

Hence,  $\mathcal{E}^e = \mathcal{E}_i^e u_i = 0$ , that is, the piezoelectric effect does not change the values of the group velocities of transverse waves. From Table 14.6, we find that

$$\mathcal{E}_1^c = 2c_{14}^E u_1 u_2, \quad \mathcal{E}_2^c = c_{14}^E u_1^2 - c_{14}^E u_2^2, \quad \mathcal{E}_3^c = c_{44}^E u_1^2 + c_{44}^E u_2^2$$

Taking into account that  $u_1^2 + u_2^2 = 1$ , we can now write

$$\begin{aligned} S_1 &= \frac{1}{\rho v_{2,3}} 2c_{14}^E u_1 u_2, \quad S_2 = \frac{1}{\rho v_{2,3}} c_{14}^E (u_1^2 - u_2^2), \quad S_3 = \frac{1}{\rho v_{2,3}} c_{44}^E \\ S_{2,3} &= \frac{1}{\rho v_{2,3}} \sqrt{(c_{14}^E)^2 + (c_{44}^E)^2} = \sqrt{\frac{1}{\rho} \left( c_{44}^E + \frac{c_{14}^E}{c_{44}^E} c_{14}^E \right)} \end{aligned}$$

It is not difficult now to calculate  $\mathbf{I}_{2,3}$  ( $I_1, I_2, I_3$ ) and  $\gamma_{2,3}$  from Eqs. (14.29) and (14.30). Note that from

$$\gamma_{2,3} = \arccos(\mathbf{l}_{2,3} \cdot \mathbf{n}) = \arccos(c_{44}^E / \rho v_{2,3} s^{2,3})$$

follows that  $\gamma_2 = \gamma_3$  for any orientation of polarization vectors  $\mathbf{u}_2$  and  $\mathbf{u}_3$  in the plane  $X_1OX_2$ ; this is caused by internal conical refraction of elastic waves in crystals.

14.9. In designing single crystal UDL acoustic waveguides the case of special interest is that of shear wave propagation in the symmetry plane, because a reflection of shear waves without generation of new types of waves is possible only in such planes.

Find the maximum and minimum velocity of a pure shear wave propagating in artificial sapphire crystals in the symmetry plane, as well as the direction of their propagation.

**Solution.** Sapphire crystals belong to class  $\bar{3}m$ . According to the rules of selecting crystallophysical axes in crystals of this class, the plane  $X_2OX_3$  is the symmetry plane (see Table 4). We are thus interested in the transverse wave propagating in the plane  $X_2OX_3$ , that is, the wave with the wavefront normal  $\mathbf{n} (0, n_2, n_3)$  and displacement vector along the axis  $X_1$  ( $\mathbf{u} = u (1, 0, 0)$ ) (Fig. 14.8).

As follows from the matrix of coefficients  $c_{ij}$  for crystals belonging to symmetry class  $\bar{3}m$  (see Table 9), the tensor  $[\Lambda_{ij}]$  for the directions of propagation of elastic waves, which are of interest here, is

$$[\Lambda_{jm}] = \begin{bmatrix} -\Lambda_{12} & 0 & 0 \\ 0 & \Lambda_{22} & \Lambda_{23} \\ 0 & \Lambda_{23} & \Lambda_{33} \end{bmatrix}$$

According to Table 14.1, we have

$$\Lambda_{11} = \lambda_{66}n_2^2 + \lambda_{44}n_3^2 + 2\lambda_{14}n_2n_3$$

$$\Lambda_{22} = \lambda_{11}n_2^2 + \lambda_{44}n_3^2 - 2\lambda_{14}n_2n_3$$

$$\Lambda_{23} = (\Lambda_{13} + \Lambda_{44})n_2n_3 - \lambda_{14}n_2^2$$

$$\Lambda_{33} = \lambda_{44}n_2^2 + \lambda_{33}n_3^2$$

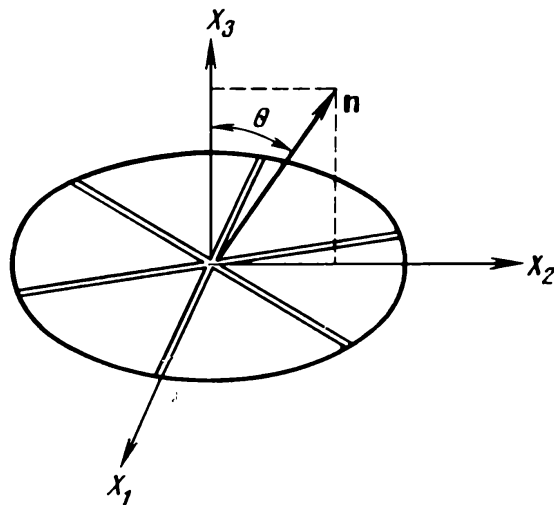
By writing the appropriate Christoffel equation, we find that the velocity of the shear wave polarized along  $\mathbf{u} (1, 0, 0)$  can be found from the relation

$$v_2 = \lambda_{66}n_2^2 + \lambda_{44}n_3^2 + 2\lambda_{14}n_2n_3$$

or

$$v_2 = \frac{c_{66}n_2^2 + c_{44}n_3^2 + 2c_{14}n_2n_3}{\rho}$$

Fig. 14.8. Figure to Problem 14.9.



By denoting the angle between the wave propagation direction and the axis  $X_3$  by  $\theta$ , we find

$$v_2 = \frac{1}{\rho} (c_{66} \cos^2 \theta + c_{44} \sin^2 \theta + 2c_{14} \cos \theta \sin \theta)$$

The extremal values of velocities can be obtained by differentiating the expression for velocity with respect to the angle  $\theta$ :

$$2v_2 \frac{\partial v_2}{\partial \theta} = \frac{1}{\rho} (-c_{66} \sin 2\theta + c_{44} \sin 2\theta + 2c_{14} \cos 2\theta)$$

As  $2v_2 \neq 0$ , the vanishing of the derivative is equivalent to setting the right-hand side of the above expression equal to zero:

$$-c_{66} \sin 2\theta_0 + c_{44} \sin 2\theta_0 + 2c_{14} \cos 2\theta_0 = 0$$

whence

$$\tan 2\theta_0 = \frac{2c_{14}}{c_{66} - c_{44}}$$

In this case the expression for  $v_2$  takes the form

$$v_2 = \frac{1}{2} (\lambda_{66} + \lambda_{44}) + \sqrt{\frac{1}{4} (\lambda_{66} - \lambda_{44})^2 + \lambda_{14}^2} \cos^2(\theta - \theta_0)$$

Substituting the angles corresponding to the extremal values of velocities into the expression for  $v_2$ , we derive the following expressions:

$$v_{2 \max} = \frac{1}{\rho} (c_{66} \cos^2 \theta_0 + c_{44} \sin^2 \theta_0 + c_{14} \sin 2\theta_0)$$

$$v_{2 \min} = \frac{1}{\rho} (c_{66} \sin^2 \theta_0 + c_{44} \cos^2 \theta_0 - c_{14} \sin 2\theta_0)$$

In the case of sapphire  $\theta_0 = 33^\circ 51'$ ,  $v_{2 \max} = 6.8 \cdot 10^5$  m/s,  $v_{2 \min} = 5.668 \cdot 10^5$  m/s.

**14.10.** Elastic stiffnesses of non-piezoelectric crystals belonging to the rhombic system can be found from the measured velocities of three isonormal waves propagating along [100], [010], [001], and from the measured velocities of quasitransverse or quasilongitudinal waves propagating in the coordinate planes.

Derive expressions which make it possible to calculate all independent elastic stiffnesses of rhombic crystals from the known values of the above-mentioned velocities.

**Solution.** The elastic properties of rhombic crystals are determined by nine independent stiffnesses  $c_{ij}$ ; according to Table 14.1 the components of the tensor  $[\Lambda_{ij}]$  in these crystals are

$$\Lambda_{11} = \lambda_{11} n_1^2 + \lambda_{66} n_2^2 + \lambda_{55} n_3^2, \quad \Lambda_{23} = (\lambda_{23} + \lambda_{44}) n_2 n_3$$

$$\Lambda_{22} = \lambda_{66} n_1^2 = \lambda_{22} n_2^2 + \lambda_{44} n_3^2, \quad \Lambda_{31} = (\lambda_{13} + \lambda_{55}) n_3 n_1$$

$$\Lambda_{33} = \lambda_{55} n_1^2 + \lambda_{44} n_2^2 + \lambda_{33} n_3^2, \quad \Lambda_{12} = (\lambda_{12} + \lambda_{66}) n_1 n_2$$

When an elastic wave propagates along [100], the tensor  $[\Lambda_{ij}]$  takes the form

$$[\Lambda_{ij}] = \begin{bmatrix} -\lambda_{11} & 0 & 0 \\ 0 & \lambda_{66} & 0 \\ 0 & 0 & \lambda_{55} \end{bmatrix}$$

whence

$$v_1^2 = \lambda_{11}$$

$$c_{11} = \rho v_1^2$$

where  $v_1$  is the velocity of the longitudinal wave.

By convention the velocity of a shear wave with displacement vector  $\mathbf{u}$  ( $u_1, u_2, u_3$ ) will be denoted by  $v_t^{(u_1, u_2, u_3)}$ . With this notation,

$$(v_t^{(010)})^2 = \lambda_{66}, \quad c_{66} = \rho (v_t^{(010)})^2$$

$$(v_t^{(001)})^2 = \lambda_{55}, \quad c_{55} = \rho (v_t^{(001)})^2$$

By measuring the velocities of the longitudinal and shear waves propagating in rhombic crystals along [100], we can find the stiffnesses  $c_{11}$ ,  $c_{66}$ , and  $c_{55}$ .

Likewise, if an elastic wave propagates along [010], then

$$[\Lambda_{ij}] = \begin{bmatrix} -\lambda_{66} & 0 & 0 \\ 0 & \lambda_{22} & 0 \\ 0 & 0 & \lambda_{44} \end{bmatrix}$$

and

$$c_{22} = \rho v_1^2$$

$$c_{66} = \rho (v_t^{(100)})^2$$

$$c_{44} = \rho (v_t^{(001)})^2$$

Obviously, when the wave propagates along [001], then

$$[\Lambda_{ij}] = \begin{bmatrix} -\lambda_{55} & 0 & 0 \\ 0 & \lambda_{44} & 0 \\ 0 & 0 & \lambda_{33} \end{bmatrix}$$

and

$$c_{33} = \rho v_1^2$$

$$c_{55} = \rho (v_t^{(100)})^2$$

$$c_{44} = \rho (v_t^{(010)})^2$$

Therefore, by measuring the velocity of longitudinal vibrations, and the velocities of transverse vibrations with different polariza-

tions, propagating along coordinate axes, we can determine six coefficients  $c_{ij}$ :  $c_{11}$ ,  $c_{22}$ ,  $c_{33}$ ,  $c_{44}$ ,  $c_{55}$ , and  $c_{66}$ . The expressions making it possible to find the stiffnesses  $c_{12}$ ,  $c_{13}$ , and  $c_{23}$  will be found by analyzing the propagation of elastic waves in directions lying in the coordinate planes. If the direction of the wavefront normal is  $\mathbf{n}$  ( $n_1, n_2 \neq 0$ ), then the corresponding tensor  $[\Lambda_{ij}]$  is

$$\begin{bmatrix} -\lambda_{11}n_1^2 + \lambda_{66}n_2^2 & (\lambda_{12} + \lambda_{66})n_1n_2 & 0 \\ (\lambda_{12} + \lambda_{66})n_1n_2 & \lambda_{66}n_1^2 + \lambda_{22}n_2^2 & 0 \\ 0 & 0 & \lambda_{55}n_1^2 + \lambda_{44}n_2^2 \end{bmatrix}$$

It then follows that

$$\rho(v_t^{(001)})^2 = c_{55}n_1^2 + c_{44}n_2^2$$

but this result is of no interest because it does not involve  $c_{12}$ . Now we shall derive the expressions for the velocities of the quasitransverse,  $v_t = v_2$ , and quasilongitudinal,  $v_l = v_1$ , elastic waves which represent the eigenvalues of the above tensor. By using the already known relations, we find

$$v_1^2 = \frac{1}{2}[(n_1^2(\lambda_{11} + \lambda_{66}) + n_2^2(\lambda_{22} + \lambda_{66})) + r]$$

$$v_2^2 = \frac{1}{2}[n_1^2(\lambda_{11} + \lambda_{66}) + n_2^2(\lambda_{22} + \lambda_{66})] - r$$

where

$$r = \sqrt{\frac{1}{4}[(\lambda_{66} - \lambda_{11})n_1^2 + (\lambda_{22} - \lambda_{66})n_2^2]^2 - [(\lambda_{12} + \lambda_{66})n_1n_2]^2}$$

As  $v_2 < v_1$ , it is obvious that  $v_2$  corresponds to the quasitransverse wave, and  $v_1$  to the quasilongitudinal wave, since shear waves in most media propagate at smaller velocities than longitudinal waves.

Assume that the experimentally determined velocity is  $v_2$ . The expression for  $v_2^2$  yields  $r$ :

$$r = \frac{1}{2}[n_1^2(\lambda_{11} + \lambda_{66}) + n_2^2(\lambda_{66} + \lambda_{22})] - v_2^2$$

Raising both sides of this equality to second power gives

$$r^2 = \left[ \frac{1}{2}(\lambda_{11}n_1^2 + \lambda_{22}n_2^2 + \lambda_{66}) - v_2^2 \right]^2$$

By substituting  $r$  and retaining on the right-hand side only the terms involving  $\lambda_{12}$ , we find

$$\begin{aligned} n_1^2n_2^2(\lambda_{12} + \lambda_{66})^2 &= \left[ \frac{1}{2}(n_1^2\lambda_{11} + n_2^2\lambda_{22} + \lambda_{66}) - v_2^2 \right]^2 \\ &\quad - \frac{1}{4}[\lambda_{56}n_1^2 - \lambda_{66}n_2^2 + \lambda_{22}n_2^2 - \lambda_{11}n_1^2]^2 \end{aligned}$$

or

$$n_1^2 n_2^2 (\lambda_{12} + \lambda_{66})^2 = [\lambda_{66} n_1^2 + \lambda_{22} n_2^2 - v_2^2] [\lambda_{66} n_2^2 + \lambda_{11} n_1^2 - v_2^2]$$

whence

$$\lambda_{12} = \sqrt{\frac{(\lambda_{66} n_1^2 + \lambda_{22} n_2^2 - v_2^2)(\lambda_{66} n_2^2 + \lambda_{11} n_1^2 - v_2^2)}{n_1^2 n_2^2}} - \lambda_{66}$$

Taking into account that  $\lambda_{ij} = \frac{1}{\rho} c_{ij}$  and denoting by  $\varphi$  the angle between the wavefront normal and the axis  $X_1$  ( $n_1 = \cos \varphi$ ,  $n_2 = \sin \varphi$ , and  $n_3 = 0$ ), we obtain

$$c_{12} = \frac{[(c_{66} \cos^2 \varphi + c_{22} \sin^2 \varphi - \rho v_2^2)(c_{11} \cos^2 \varphi + c_{66} \sin^2 \varphi - \rho v_2^2)]^{1/2}}{\cos \varphi \sin \varphi} - c_{66}$$

The stiffness  $c_{12}$  could be found in the same manner by using the value of  $v_1$ , the velocity of the quasilongitudinal wave.

Likewise, if the velocity of a quasitransverse wave propagating in the direction  $\mathbf{n}$  ( $0, n_2, n_3$ ) is known ( $n_2 = \cos \psi$ ,  $n_3 = \sin \psi$ , where  $\psi$  is the angle between  $\mathbf{n}$  and the axis  $X_2$ ), we obtain

$$c_{23} = \left[ \frac{(c_{22} \cos^2 \psi + c_{44} \sin^2 \psi - \rho v_1^2)(c_{44} \cos^2 \psi + c_{33} \sin^2 \psi - \rho v_1^2)}{\cos^2 \psi \sin^2 \psi} \right]^{1/2} - c_{44}$$

If the direction of wave propagation is  $\mathbf{n}$  ( $n_1, 0, n_3$ ), where  $n_1 = \cos \theta$ ,  $n_3 = \sin \theta$ , and  $\theta$  is the angle between  $\mathbf{n}$  and the axis  $X_3$ , we find

$$c_{13} = \left[ \frac{(c_{11} \sin^2 \theta + c_{55} \cos^2 \theta - \rho v_1^2)(c_{55} \sin^2 \theta + c_{33} \cos^2 \theta - \rho v_1^2)}{\cos^2 \theta \sin^2 \theta} \right]^{1/2} - c_{55}$$

**14.11.** Because of the importance of delay time stability for many applications of UDL, there is constant research for the methods of reducing the temperature coefficient of delay time (TCDT) characterizing the thermal stability of a material used for acoustic waveguides.

In the first approximation, the temperature coefficient of delay time,  $T_\tau$ , is defined as follows:

$$T_\tau = \frac{1}{\tau} \frac{\partial \tau}{\partial T} = \frac{\partial \ln \tau}{\partial T}$$

$$\ln \tau = \ln l - \ln v$$

$$T_\tau = \frac{1}{\tau} \frac{\partial \tau}{\partial T} = \alpha_l - T_v$$

where  $\alpha_l$  is the thermal expansion coefficient in the direction  $\mathbf{l}$ , and  $T_v$  is the temperature coefficient of propagation velocity.

The delay time may be thermally stabilized by choosing such orientation of acoustic waveguide with respect to crystallophysical axes of a single crystal that TCDT of individual rays cancel one

another out; this can be clearly illustrated by polar diagrams of TCDT.

Derive a relation making it possible to construct a polar TCDT diagram of shear waves propagating in sapphire crystals along the symmetry plane.

*Solution.* Let  $\mathbf{n} = (0, n_2, n_3)$  be the direction of the wavefront normal of a shear wave propagating in sapphire crystals (symmetry class  $\bar{3}m$ ) in the plane  $X_2OX_3$ . In this case

$$\alpha_1 = \alpha_{\mathbf{n}} = \alpha_{ij}n_i n_j = \alpha_{11}n_2^2 + \alpha_{33}n_3^2$$

The equation of phase velocity of a pure transverse wave propagating in the plane  $X_2OX_3$  is

$$v^2 = \frac{1}{\rho} (c_{66}n_2^2 + c_{44}n_3^2 + 2c_{14}n_2n_3)$$

which gives  $v$  as a function of  $\rho$  and  $c_{ij}$ .

This gives the expression for the temperature coefficient of propagation velocity:

$$T_v = \frac{1}{2v^2} \frac{\partial v^2}{\partial T} = \frac{1}{2} \beta + \frac{1}{2} \frac{T_{c_{66}}c_{66}n_2^2 + T_{c_{44}}c_{44}n_3^2 + 2T_{c_{14}}c_{14}n_2n_3}{c_{66}n_2^2 + c_{44}n_3^2 + 2c_{14}n_2n_3}$$

where  $\beta = \sum_i \alpha_{ij}$  is the thermal expansion coefficient, and  $T_{c_{66}}$ ,  $T_{c_{44}}$ ,  $T_{c_{14}}$  are the temperature coefficients of elastic stiffnesses  $c_{66}$ ,  $c_{44}$ ,  $c_{14}$ . The final expression for  $T_v$  in the case of shear waves propagating in the plane  $X_2OX_3$  in sapphire crystals is

$$T_v = \alpha_1 - \frac{1}{2} \beta - \frac{1}{2} \frac{T_{c_{66}}c_{66}n_2^2 + T_{c_{44}}c_{44}n_3^2 + 2T_{c_{14}}c_{14}n_2n_3}{c_{66}n_2^2 + c_{44}n_3^2 + 2c_{14}n_2n_3}$$

By using this expression, one can construct the polar diagrams of the coefficient  $T_v$  of sapphire crystals. Obviously, this relation can be used to construct similar diagrams of other crystals belonging to the trigonal system.

#### PROBLEMS



**14.12.** Prove that if a crystal has a symmetry axis of order above two, it is always the acoustic axis, that is, such direction of wavefront normal for which phase velocities of two isonormal waves coincide.

**14.13.** Find crystallographic directions, parallel to wavefront normals, along which pure longitudinal and pure transverse waves propagate in: (i) quartz crystals, (ii) lithium niobate crystals, (iii) alkali halide crystals.

**14.14.** Imagine two cubic specimens of identical dimensions and weight. One of them is known to be made of an isotropic material,

and the second to be a cubic-symmetry single crystal, with one of the cube edges coinciding with the direction [111]. Indicate acoustic experiments capable of distinguishing which of the cubes is monocrystalline.

14.15. Find crystallographic directions which are singular for the propagation of bulk acoustic waves in crystals of (i) potassium dihydrophosphate and (ii) bismuth germanate.

14.16. Using only symmetry arguments, show that if the wave-front normal is in the symmetry plane or in a plane perpendicular to a four-fold symmetry axis, then one of the waves is pure transverse and its displacement vector is perpendicular to this plane. Is a pure longitudinal wave unavoidable in this case?

14.17. Are common points possible for the sheets  $L$ ,  $T_1$ , and  $T_2$  of which the phase-velocity surface is composed? (Sheet  $L$  represents the velocity of longitudinal and quasilongitudinal waves, and the sheets  $T_1$  and  $T_2$  the velocities of transverse or quasitransverse waves.) Indicate directions on which the common points of sheets  $T_1$  and  $T_2$  lie in crystals of (i) cubic-symmetry and (ii) medium-symmetry classes. Will there be common points of surfaces  $T_1$  and  $T_2$  in crystals of lower symmetry classes?

14.18. Is it possible to find all independent elastic stiffnesses of a cubic crystal by measuring the velocities of longitudinal and shear elastic waves propagating along  $\langle 110 \rangle$ ?

14.19. Elastic stiffnesses of wurtzite crystals were determined by measuring the velocities of ultrasonic wave propagation along the following directions:  $(1, 0, 0)$ ,  $(0, 0, 1)$ , and  $\left(\frac{1}{\sqrt{2}}, 0, \frac{1}{\sqrt{2}}\right)$ .

The results of measurements are listed in Table 14.10.

Calculate elastic stiffnesses  $c_{ij}$  in wurtzite.

Table 14.10

No.	Wave propagation direction	Polarization (orientation of displacement vector)	Velocity, $10^5$ cm/s
1	$(0, 0, 1)$	$(0, 0, 1)$	$v_1 = 5.852$
2	$(0, 0, 1)$	$(1, 0, 0)$	$v_2 = 2.647$
3	$(1, 0, 0)$	$(1, 0, 0)$	$v_3 = 5.512$
4	$(1, 0, 0)$	$(0, 1, 0)$	$v_4 = 2.799$
5	$\frac{1}{\sqrt{2}} (1, 0, 1)$	quasilongitudinal	$v_5 = 5.362$

14.20. Show that the plane  $(001)$  in crystals with tetragonal symmetry is the plane of elastic isotropy for a pure transverse wave propagating along this plane with polarization vector perpendicular to the propagation plane. Will the basal plane of a crystal belong-

ing to a medium-symmetry system possess similar property? Find such symmetry classes.

**14.21.** Using Table 14.2, find which of the directions [100], [110], [111] in bismuth germanate crystals possess longitudinal piezoelectric activity and for what type of waves.

**14.22.** Determine the electromechanical coupling factor of a pure transverse wave for piezoelectric crystals (i) in  $\alpha\text{-SiO}_2$ , when the wavefront normal  $\mathbf{n} \parallel X_1$ , and (ii) in CdS, when  $\mathbf{n} \perp X_3$ .

**14.23.** Determine the phase velocity as a function of propagation direction in the plane (100) of NaCl crystals for longitudinal and transverse waves.

**14.24.** Calculate the group velocity of a longitudinal wave propagating in gallium arsenide crystals along [110]. Does the beam velocity coincide with the phase velocity?

**14.25.** To determine elastic stiffnesses of aragonite crystals (aragonite belongs to rhombic system), the velocities of longitudinal and transverse isonormal high-frequency elastic waves, propagating along [100], [010], and [001], were measured. The results of measurements are listed in Table 14.11. Which of the coefficients can be calculated from the experimental results? Find these stiffnesses if the crystal density is  $\rho = 2.7 \text{ g/cm}^3$ .

Table 14.11

Wave type	Polarization (orientation of displacement vector)	Velocity, $10^5 \text{ cm/s}$
Propagation along $X_1$		
longitudinal	$X_1$	7.68
transverse	$X_2$	3.96
transverse	$X_3$	3.08
Propagation along $X_2$		
longitudinal	$X_2$	5.68
transverse	$X_1$	3.96
transverse	$X_3$	3.90
Propagation along $X_3$		
longitudinal	$X_3$	5.59
transverse	$X_1$	3.07
transverse	$X_2$	3.90

**14.26.** Single crystal delay lines widely used in electronics to condition and process radio signals are normally manufactured in the USSR from alkali halide crystals (AHC). The optimal conditions for propagation of elastic vibrations without losses caused by

the transformation in other types of vibration are: acoustic wave-guide oriented along the planes [100] and propagation of a shear wave in these planes with displacement vector perpendicular to the plane of propagation. Which of the three AHC crystals, NaCl, KBr, or RbI, is characterized by the maximum ratio of signal delay time to the weight of the delay line?

**14.27.** Calculate the velocity at which elastic longitudinal vibrations propagate in gallium arsenide single crystals along [100], [110], and [111]. Find the propagation velocity in the same directions for shear vibrations.

**14.28.** To determine elastic stiffnesses in rutile, propagation velocities of high-frequency elastic waves were measured in various crystallographic directions. The results are listed in Table 14.12.

Table 14.12

Wave propagation direction	Polarization (orientation of displacement vector)	Velocity, $10^5$ cm/s
[100]	[100]	$v_1 = 9.13$
[100]	[010]	$v_2 = 5.86$
[100]	[001]	$v_3 = 5.10$
[001]	[001]	$v_4 = 11.20$
[110]	[110]	$v_5 = 1.14$

Which of the stiffnesses  $c_{ij}$  can be determined from the data listed in the table? Calculate their values. Which of the independent stiffnesses  $c_{ij}$  remains to be determined? Propose an experimental arrangement to find this stiffness.

**14.29.** Calculate the linear dimensions of a delay line made of KBr operating in the shear vibrations mode, with the wave propagating along [100] and giving delay time 0.5 ms.

**14.30.** What are the stiffnesses  $c_{ij}$  of potassium iodide crystals if the velocities of high-frequency longitudinal and transverse isonormal waves propagating along [100] proved to be  $2.92 \cdot 10^5$  cm/s and  $1.16 \cdot 10^5$  cm/s, and the velocity of longitudinal waves propagating along [110],  $2.51 \cdot 10^5$  cm/s? The density of potassium iodide is  $3.13$  g/cm<sup>3</sup>.

**14.31.** Calculate the maximum and minimum velocity of shear ultrasonic waves propagating in rutile crystals in the plane  $X_2OX_3$ .

Find a symmetry plane of rutile in which a shear wave propagates at a velocity independent of the direction of its wavefront normal.

**14.32.** Determine elastic stiffnesses of polarized barium titanate ceramic by using the measured velocities of ultrasonic waves in this ceramic; the velocities are given in Table 14.13.

Table 14.13

Wave propagation direction	Polarization (orientation of displacement vector)	Type of wave	Velocity $10^5$ cm/s
(0, 0, 1)	(0, 0, 1)	longitudinal	5.85
(0, 0, 1)	( $n_1$ , $n_2$ , 0)	transverse	3.15
(1, 0, 0)	(1, 0, 0)	longitudinal	5.52
(1, 0, 0)	(0, 1, 0)	transverse	2.86
$\frac{1}{\sqrt{2}} (0, 1, 1)$	—	quasilongitudinal	5.87

**14.33.** Is it possible to determine all independent elastic stiffnesses of cubic symmetry crystals by measuring the velocities of pure longitudinal and pure shear waves on an oriented specimen given in Fig. 14.9? Directions of elastic wave propagation are shown by arrows.

**14.34.** Find the angle between the wavefront normal corresponding to the minimum velocity of shear waves propagating in one of symmetry planes of lithium niobate, and the highest-order symmetry axis.

**14.35.** Which of the elastic stiffnesses of rubi can be calculated from measured values of the velocities of longitudinal and shear waves propagating along [0001] and [1120]?

**14.36.** Are two oriented specimens shown in Fig. 14.10 sufficient to find all stiffnesses  $c_{ij}$  of the ADP-group crystals? The directions of elastic wave propagation are shown by arrows.

**14.37.** Calculate the velocity of propagation of longitudinal and shear ultrasonic vibrations in indium antimonide crystals along (i) [110], and (ii) [111].

**14.38.** Are two oriented rubi specimens shown in Fig. 14.10 sufficient to find all its independent elastic stiffnesses? The directions of elastic wave propagation are shown by arrows.

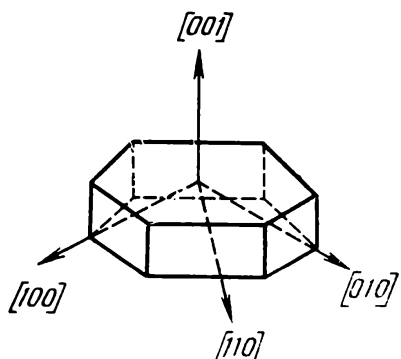


**Fig. 14.9.** Orientation of a specimen for the measurement of elastic stiffnesses of cubic symmetry crystals.

**14.39.** Which of the independent elastic stiffnesses of wurtzite can be found by measuring the velocities of ultrasonic waves on two oriented specimens shown in Fig. 14.10? The directions of elastic wave propagation are shown by arrows.

**14.40.** Find the direction of the wavefront normal corresponding to the maximum value of velocity of ultrasonic shear vibrations propagating in ADP crystals in the symmetry plane. Calculate the minimum and maximum velocities of such vibrations in the indicated plane.

**14.41.** Find the maximum contribution, in per cent, of the piezoelectric correction to the phase velocity of a shear wave propagating in KDP crystals in the plane (100) with polarization along [100]. Find the directions in the plane (100) along which propagate piezoelectrically active shear waves with this polarization.

**14.42.** Which of the elastic waves propagating in wurtzite crystals along [0001], namely, longitudinal or transverse, are piezoelectrically active? The following coefficients  $e_{ij}$  are nonzero in wurtzite:  $e_{24} = e_{15}$ ,  $e_{31}$ ,  $e_{32} = e_{31}$ ,  $e_{33}$ .

**14.43.** To determine the elastic stiffnesses of cadmium selenide single crystals, CdSe, the velocities of elastic wave propagation were measured in the directions  $(1, 0, 0)$ ,  $(0, 0, 1)$  and  $(\frac{1}{\sqrt{2}}, 0, \frac{1}{\sqrt{2}})$ .

The results of measurements are listed in Table 14.14.

Find the stiffnesses  $c_{ij}$  of cadmium selenide crystals.

**14.44.** Derive the expression for the temperature coefficient of delay time in cubic crystals (see Problem 14.11). Calculate  $T_\tau$  for potassium chloride and barium fluoride.

**14.45.** The velocity of high-frequency elastic vibrations propagating in a beryl crystal along  $n(0, 0, 1)$  and  $n(1, 0, 0)$  are (in  $10^5$  cm/s):

**Fig. 14.10.** Orientation of a specimen for measuring elastic stiffnesses of medium-symmetry crystals.

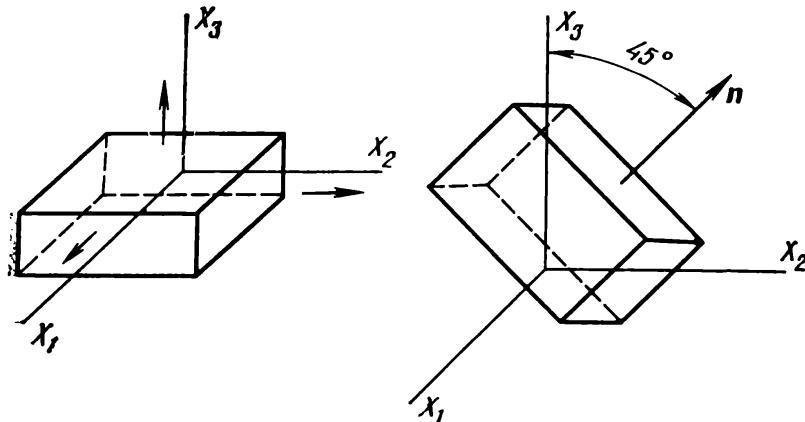


Table 14.14

No.	Wave propagation direction	Polarization (orientation of displacement vector)	Velocity, $10^5$ cm/s	Density, g/cm <sup>3</sup>
1	(0, 0, 1)	(0, 0, 1)	$v_1 = 3.630$	5.684
2	(0, 0, 1)	(1, 0, 0)	$v_2 = 1.521$	
3	(1, 0, 0)	(1, 0, 0)	$v_3 = 3.630$	
4	(1, 0, 0)	(0, 1, 0)	$v_4 = 1.592$	
5	$\left( \frac{1}{\sqrt{2}}, 0, \frac{1}{\sqrt{2}} \right)$	quasilongitudinal	$v_5 = 3.572$	

(i)  $\mathbf{n} (0, 0, 1)$ ;  $v_l = 12.7$ ,  $v_t = 9.11$

(ii)  $\mathbf{n} (1, 0, 0)$ ;  $v_l = 12.25$ ,  $v_t^{(0,0,1)} = 9.1$ ,  $v_t^{(0,1,0)} = 9.04$ ;  $v_t^{(0,0,1)}$  is the shear wave with displacement vector along (0, 0, 1);  $v_t^{(0,1,0)}$  is the shear wave with displacement vector along (0, 1, 0). Calculate stiffnesses  $c_{ij}$  of beryl; beryl density is 1.87 g/cm<sup>3</sup>.

14.46. Derive a relation making it possible to construct the TCDT polar diagram for shear waves propagating in the symmetry plane in KDP-group crystals (see Problem 14.1).

14.47. Calculate linear dimensions of a KCl delay line operating on shear vibrations propagating along [100], giving the signal delay time 1.5 ms. What could you suggest to reduce the size of the line?

14.48. What is the maximum contribution, in per cent, of the piezoelectric correction to the phase velocity of a shear wave propagating in KDP crystals in the plane (001), polarized along [001]? Find the directions in the plane (001) along which propagate (i) piezoelectrically nonactive shear waves with this polarization, and (ii) waves of the given type with the maximum piezoelectric activity.

14.49. Construct the TCDT polar diagram of shear waves propagating in sapphire crystals in the symmetry plane  $X_2OX_3$ .

14.50. The results of measuring the velocity of high-frequency elastic waves in cadmium single crystals (symmetry class 6/mmm) along the axis  $X_3$  are:

$$v_1 = 2.44 \cdot 10^5 \text{ cm/s}, \quad v_t = 2.11 \cdot 10^5 \text{ cm/s}$$

The corresponding velocities in the direction of the axis  $X_1$  are:  $v_1 = 3.74 \cdot 10^5 \text{ cm/s}$ ,  $v_t = 2.05 \cdot 10^5 \text{ cm/s}$  (the displacement vector is parallel to the axis  $X_2$ ).

Calculate the elastic stiffnesses which can be determined from the given values of velocities.

14.51. A shear wave propagating in a lithium niobate crystal along the axis  $X_3$  is polarized at 40° to the axis  $X_1$ . Determine the direction of energy flux of this wave.

## 15. THERMODYNAMICS OF CRYSTALS

*Linear effects.* A state of a dielectric crystal regarded as a thermodynamic system is defined by the following characteristics: mechanical stresses  $t_{ij}$  and strains  $r_{ij}$ , strength  $E_i$  and induction  $D_i$  (or polarization  $P_i$ ) of electric field, temperature  $T$  and entropy  $S$ .

Entropy, electric induction, and strain are usually regarded as generalized thermodynamical coordinates, and temperature, electric field strength, and mechanical stresses as generalized forces. However, in conventional experiments it is easier to measure temperature, electric field strength, and mechanical strains, and determine quantitatively the changes in these quantities, regarding them as independent variables. It is difficult to control changes in entropy, electric induction, and strain directly. In general, any three characteristics of the mechanical, electric, and thermal state of the crystal can be chosen as independent variables. The remaining characteristics then become functions of the chosen independent variables.

Ten independent variables must be fixed to characterize the state of a crystal unambiguously: six components of the mechanical stress tensor (or strain tensor), three components of the electric field vector (or electric induction vector), and temperature (or entropy).

As follows from the first law of thermodynamics, there is only one function of ten selected independent variables, whose increment is a total differential. Each particular choice of independent variables corresponds to a specific thermodynamic function.

Consider two of all possible variants of independent variables and their functions:

$$\begin{array}{ll} 1. r_{ij} = r_{ij} (t_{ij}, E_i, T) & 2. t_{ij} = t_{ij} (r_{ij}, D_i, S) \\ D_i = D_i (t_{ij}, E_i, T) & E_i = E_i (r_{ij}, D_i, S) \\ S = S (t_{ij}, E_i, T) & T = T (r_{ij}, D_i, S). \end{array}$$

The first of these sets is the most natural for actually conducted experiments.

The second set is basic for ferroelectric crystals in which it is convenient to select the electric polarization (induction) generated spontaneously in phase transition, and the strain as independent variables.

In the first case the thermodynamic potential with respect to independent variables  $t_{ij}$ ,  $E_i$ ,  $T$  is the Gibbs function:

$$dG = -r_{ij}t_{ij} - D_m dE_m - S \, dT$$

Let us expand  $r_{kl}$ ,  $D_m$ , and  $S$  into the Taylor series in a neighbourhood of an arbitrary point  $(t_{kl}^0, E_m^0, T_0)$ , that is, in a neighbourhood of the initial state of the crystal, truncating the series to first-order terms:

(differentiation is carried out with respect to one variable for fixed values of all other variables).

This gives us a system of ten equations: six equations to determine strains  $r_{ij}$ , three for induction  $D_m$ , and one for entropy.

As the initial state we choose a mechanically nonstressed state  $t_{kl}^0 = 0$  in zero electric field,  $E_i^0 = 0$ . Therefore, only the initial temperature of the crystal is nonzero,  $T = T_0$ . We assume that in the initial state the crystal is nonstrained and nonpolarized:

$$\left( \frac{\partial G}{\partial t_{kl}} \right)_0 = 0, \quad \left( \frac{\partial G}{\partial E_m} \right)_0 = 0 \quad \text{and} \quad \left( \frac{\partial G}{\partial T} \right) = S_0$$

that is, we assume that  $T_0$  is the reference point for temperature-induced strains and pyroelectric polarization. Denote  $T - T_0 = \Delta T$  and  $S - S_0 = \Delta S$ .

The system of equations (15.1) can be rewritten in the following form:

$$\begin{aligned} r_{ij} &= - \left( \frac{\partial^2 G}{\partial t_{ij} \partial t_{kl}} \right)_0 t_{kl} - \left( \frac{\partial^2 G}{\partial t_{ij} \partial E_m} \right)_0 E_m - \left( \frac{\partial^2 G}{\partial t_{ij} \partial T} \right)_0 \Delta T \\ D_m &= - \left( \frac{\partial^2 G}{\partial E_m \partial t_{kl}} \right)_0 t_{kl} - \left( \frac{\partial^2 G}{\partial E_m \partial E_l} \right)_0 E_l - \left( \frac{\partial^2 G}{\partial E_m \partial T} \right)_0 \Delta T \\ \Delta S &= - \left( \frac{\partial^2 G}{\partial T \partial t_{kl}} \right)_0 t_{kl} - \left( \frac{\partial^2 G}{\partial T \partial E_l} \right)_0 E_l - \left( \frac{\partial^2 G}{\partial T^2} \right)_0 \Delta T \end{aligned}$$

Consider all the coefficients in these equations:

$$\left( \frac{\partial^2 G}{\partial t_{ij} \partial t_{kl}} \right) = \left( \frac{\partial r_{ij}}{\partial t_{kl}} \right) = s_{ij;kl}^T$$

is the elastic compliance measured at constant electric field and temperature,

$$\left( \frac{\partial^2 G}{\partial t_{ij} \partial E_m} \right) = \left( \frac{\partial r_{ij}}{\partial E_m} \right) = d_{mi;j}^T$$

is the piezoelectric coefficient at  $T = \text{const}$ ,

$$\left( \frac{\partial^2 G}{\partial t_{ij} \partial T} \right) = \left( \frac{\partial r_{ij}}{\partial T} \right) = \alpha_{ij;E}^T$$

is the thermal expansion coefficient measured at constant stress and constant electric field,

$$\left( \frac{\partial^2 G}{\partial E_m \partial t_{ij}} \right) = \left( \frac{\partial D_m}{\partial t_{ij}} \right) = d'_{mi;j}$$

is the piezoelectric coefficient,

$$\left( \frac{\partial^2 G}{\partial E_m \partial E_l} \right) = \left( \frac{\partial D_m}{\partial E_l} \right) = \epsilon_{ml}^{T,t}$$

is the dielectric permittivity,

$$\left( \frac{\partial^2 G}{\partial E_m \partial T} \right) = \left( \frac{\partial D_m}{\partial T} \right) = \gamma_m^t$$

is the pyroelectric coefficient,

$$\left( \frac{\partial^2 G}{\partial T \partial t_{ij}} \right) T = \left( \frac{\partial S}{\partial t_{ij}} \right) T = \frac{\partial Q}{\partial t_{ij}} = \alpha'_{ij}$$

is the coefficient of thermoelastic stress,

$$\left( \frac{\partial^2 G}{\partial T \partial E_m} \right) T = \left( \frac{\partial S}{\partial E_m} \right) T = \frac{\partial Q}{\partial E_m} = \gamma'_m$$

is the coefficient of the electrocaloric effect, and  $c^{t,E}$  is the heat capacity at constant electric field and mechanical stress. Here and throughout this Chapter the conditions of measurement are given by superscripts.

Since  $dG$  is a total differential, the value of the second derivative of function  $G$  is independent of the order in which differentiation is carried out, and the following relation exists among the above-listed coefficients:

$$\frac{\partial r_{ij}}{\partial E_m} = \frac{\partial D_m}{\partial t_{ij}}, \text{ hence, } d_{mij} = d'_{mij}$$

$$\frac{\partial D_m}{\partial T} = \frac{\partial S}{\partial E_m} \text{ and } \gamma_m = \frac{\gamma'_m}{T}, \quad \frac{\partial r_{ij}}{\partial T} = \frac{\partial S}{\partial t_{ij}},$$

$$\text{and } \alpha_{ij} = \frac{\alpha'_{ij}}{T}$$

Multiply the last equation of (15.1) by  $T$ :

$$\Delta S \cdot T = \Delta Q = - \left( \frac{\partial^2 G}{\partial T \partial t_{kl}} \right)_0 T t_{kl} - \left( \frac{\partial^2 G}{\partial T \partial E_m} \right)_0 T E_m - \left( \frac{\partial^2 G}{\partial T^2} \right) T \Delta T$$

Finally, equations (15.1) become:

$$\left. \begin{aligned} r_{ij} &= s_{ijkl}^{E,T} t_{kl} + d_{mij}^T E_m + \alpha_{ij}^{t,E} \Delta T \\ D_m &= d_{mkl}^T t_{kl} + \epsilon_{ml}^{t,T} E_l + \gamma_m^t \Delta T \\ \Delta Q &= T \cdot \alpha_{kl}^{E,T} t_{kl} + T \cdot \gamma_m^t E_m + \rho c^t \Delta T \end{aligned} \right\} \quad (15.2)$$

This system of equations describes the set of electric, mechanical, and thermal phenomena observed when mechanical stresses, electric field, and temperature of a dielectric crystal are changed: strain induced by mechanical stresses and temperature variations, direct and converse piezoelectric effect, polarization of a dielectric in an external field, pyroelectric effect, and so on.

For the second choice of independent variables and their functions, we again expand  $t_{ij}$ ,  $E_i$ ,  $T$  into the Taylor series, making use of the internal energy  $U$ .

Introducing the notation for expansion coefficients, we obtain the second system of equations in the following form:

$$\begin{aligned} t_{ij} &= c_{ijkl}^{D,S} r_{kl} - h_{mij}^S D_m - p_{ij}^{r,D} \Delta Q \\ E_i &= -h_{imk}^S r_{mk} + \eta_{im}^{r,S} D_m - g_i^{r,D} \Delta Q \\ \Delta T &= -T p_{ij}^{D,S} r_{ij} - T g_m^{r,S} D_m + \frac{\Delta Q}{\rho c^{r,D}} \end{aligned} \quad (15.3)$$

Note that by convention the coefficients  $h_{mij}$ ,  $p_{ij}$ , and  $g_i$  are given in the minus sign.

In contrast to the system (15.2), system (15.3) describes the electric, mechanical, and thermal phenomena in crystals due to variations in strain, electric induction, and entropy.

*Second-order effects.* Equations discussed above operated with mechanical stress and electrical field in crystals as linear functions

of strain and induction. The same was true for strain and induction as functions of mechanical stresses and electric field.

If the analysis is not limited to the first-order terms in the expansions of  $r_{ij}$ ,  $D_i$ ,  $S$ , and  $t_{ij}$ ,  $E_i$ ,  $T$ , and higher-order terms are taken into account, it is possible to describe a number of physical phenomena, the so-called second-order effects observed in crystals. These effects are particularly well pronounced and are of practical importance in ferroelectric crystals.

The role played by thermal phenomena in second-order effects is negligible, therefore in this subsection we regard only mechanical stresses and induction as independent variables, and strains and electric field as their functions, assuming the conditions to be isothermal. An analysis for adiabatic conditions is similar.

For the same initial conditions as in equations (15.3) and with the terms of the second order of smallness in a Taylor series taken into account, mechanical stresses and electric field can be written in the following form:

$$\begin{aligned} t_{ij} &= \left( \frac{\partial t_{ij}}{\partial r_{kl}} \right)^D r_{kl} + \left( \frac{\partial t_{ij}}{\partial D_m} \right)_0^r D_m + \frac{1}{2!} \left[ \left( \frac{\partial^2 t_{ij}}{\partial r_{kl} \partial r_{pq}} \right)_0 r_{kl} r_{pq} \right. \\ &\quad \left. + 2 \left( \frac{\partial t_{ij}}{\partial r_{kl} \partial D_m} \right)_0 r_{kl} D_m + \left( \frac{\partial^2 t_{ij}}{\partial D_m \partial D_n} \right)_0 D_m D_n \right] \\ E_m &= \left( \frac{\partial E_m}{\partial r_{kl}} \right)^D r_{kl} + \left( \frac{\partial E_m}{\partial D_n} \right)_0^r D_n + \frac{1}{2!} \left[ \left( \frac{\partial^2 E_m}{\partial r_{kl} \partial r_{pq}} \right)_0 r_{kl} r_{pq} \right. \\ &\quad \left. + 2 \left( \frac{\partial^2 E_m}{\partial r_{kl} \partial D_n} \right)_0 r_{kl} D_n + \left( \frac{\partial^2 E_m}{\partial D_q \partial D_p} \right)_0 D_q D_p \right] \end{aligned}$$

In these equations

$$\left( \frac{\partial t_{ij}}{\partial r_{kl}} \right)^D, \quad \left( \frac{\partial t_{ij}}{\partial D_m} \right)^r = \left( \frac{\partial E_m}{\partial r_{ij}} \right)^D, \quad \text{and} \quad \left( \frac{\partial E_m}{\partial D_n} \right)$$

are the familiar elastic stiffnesses  $c_{ijkl}^D$ , piezoelectric constants  $h_{mij}$ , and dielectric impermeabilities  $\eta_{mn}$ .

We denote now

$$\begin{aligned} \left( \frac{\partial^2 t_{kl}}{\partial r_{ij} \partial D_n} \right) &= \left( \frac{\partial^3 U}{\partial r_{kl} \partial r_{ij} \partial D_n} \right) = \left( \frac{\partial^2 E_n}{\partial r_{kl} \partial r_{ij}} \right) = -\frac{\partial h_{nkl}}{\partial r_{ij}} = 2M_{nkl}^D \\ \left( \frac{\partial^2 t_{ij}}{\partial r_{kl} \partial r_{pq}} \right) &= \frac{\partial c_{ijkl}}{\partial r_{pq}} = N_{ijklpq}^D \\ \left( \frac{\partial^2 t_{kl}}{\partial D_n \partial D_q} \right) &= \left( \frac{\partial^3 U}{\partial r_{kl} \partial D_n \partial D_q} \right) = \left( \frac{\partial^2 E_n}{\partial r_{kl} \partial D_q} \right) \\ &= -\frac{\partial h_{nkl}}{\partial D_q} = \frac{\partial \eta_{nq}}{\partial r_{kl}} = 2p_{kl} \eta_q \\ \left( \frac{\partial^2 E_m}{\partial D_q \partial D_p} \right) &= \frac{\partial \eta_{mq}}{\partial D_p} = 2f_{mq} \end{aligned}$$

The physical meaning of the above-introduced coefficients  $M_{nkl}^{ijkl}$ ,  $N_{ijklpq}$ ,  $p_{kl}^{lnq}$ ,  $f_{mnp}$  is quite clear. Thus, the coefficients  $M_{nkl}^{ijkl}$ , forming a rank five tensor, describe piezoelectric constants as functions of strains  $r_{ij}$ ; the coefficients  $p_{kl}^{lnq}$  describe the same piezoelectric constants as functions of induction  $D_q$  or dielectric impermeability  $\eta_{nq}$  as a function of strains  $r_{kl}$ , and so forth.

Equations (15.4) can now be rewritten in the form

$$t_{kl} = c_{kl}^D r_{ij} - h_{nkl} D_n + N_{ijklpq}^D r_{ij} r_{pq} + M_{nkl}^{ijkl} r_{ij} D_n + p_{kl}^{lnq} D_m D_e \quad (15.4)$$

$$E_m = -h_{mkl} r_{kl} + \eta_{mn} D_n + M_{mpqkl} r_{kl} + p_{klmn} r_{kl} D_n + f_{mnp} D_q D_{np}$$

or

$$t_{kl} = (c_{kl}^D + N_{ijklpq}^D r_{pq} + M_{nkl}^{ijkl} D_n) r_{ij} + (-h_{nkl} + p_{klmn} D_m) D_n \quad (15.5)$$

$$E_m = (-h_{mkl} + M_{mpqkl}^D r_{pq}) r_{kl} + (\eta_{mn}^t + p_{klmn}^t r_{kl} + f_{mnp}^t D_q) D_n$$

The expression in parentheses in front of  $r_{ij}$  is the elastic stiffness corrected for nonzero strain  $N_{ijklpq}^D r_{pq}$  and induction  $M_{nkl}^{ijkl} D_n$  (after contracting over indices  $pq$  and  $n$ , this gives a rank four tensor). The expression in parentheses in front of  $D_n$  represents piezoelectric constants corrected for nonzero electric induction,  $p_{klmn} D_m$ .

The expression in parentheses in front of  $r_{kl}$  represents piezoelectric constants corrected for strains  $M_{mpqkl}^D r_{pq}$ . The second expression in parentheses in front of  $D_n$  represents the dielectric impermeability corrected for strain  $p_{klmn} r_{kl}$  and induction  $f_{mnp}^t D_q$ .

And finally, equations (15.5) can be rewritten in the following form:

$$t_{kl} = (c_{kl}^D + \Delta c_{kl}^D) r_{ij} - (h_{nkl} + \Delta h_{nkl}) D_n, \quad (15.6)$$

$$E_m = -(h_{mkl} + \Delta h_{mkl}) r_{kl} + (\eta_{mn}^t + \Delta_1 \eta_{mn}^t + \Delta_2 \eta_{mn}^t) D_n \quad (15.7)$$

Let us discuss in more detail the corrections to dielectric impermeability of the crystal,  $\Delta_1 \eta_{mn}$  and  $\Delta_2 \eta_{mn}$ :

$$\Delta_1 \eta_{mn}^t = f_{mnp}^t D_q \quad (15.8)$$

$$\Delta_2 \eta_{mn}^t = p_{klmn}^D r_{kl} \quad (15.9)$$

Equation (15.8) is the equation of the electrooptic effect considered to be linear in the sense that the change in the dielectric impermeability of a crystal in (15.8) is a linear function of induction. However, this linear dependence is a result of a nonlinear relationship between the generalized coordinates, that is, nonlinear dependence of  $E$  on  $D$ ; this is represented by a dependence of dielec-

tric properties,  $\eta_{ij}$  in the present case, on the magnitude of electric factor  $\mathbf{D}$ .

In general, the thermodynamic theory for the electrooptic effect offers four different systems of equations and four types of electrooptic constants, depending on whether the external factor is the induction  $\mathbf{D}$  or electric field  $\mathbf{E}$ , and whether the dielectric properties are characterized by the tensors  $\eta_{ij}$ ,  $\epsilon_{ij}$ ,  $\alpha_{ij}$  ( $E_i = \alpha_{ij}P_j$ ) or  $\kappa_{ij}$  ( $P_i = \kappa_{ij}E_j$ ):

$$\left. \begin{array}{l} \Delta\eta_{mn} = f_{mnq}D_q \\ \Delta\epsilon_{ij} = \rho_{ijk}E_k \\ \Delta\alpha_{ml} = \delta_{mlq}P_q \\ \Delta\kappa_{mn} = \chi_{mn}E_l \end{array} \right\} \quad (15.10)$$

All these equations and electrooptic constants are equally valid, and can be used to describe the electrooptic effect in appropriate physical conditions. However, the coefficients used most frequently are those not listed above, and appearing in the equation (see Sec. 11, (11.1)):

$$\Delta\eta_{mn} = r_{mnk}E_k \quad (15.11)$$

This equation is the easiest to interpret by invoking the geometric arguments of deformation introduced into the index ellipsoid by the applied external electric field.

Equation (15.9) describes the so-called elastooptic effect (photoelasticity), that is, changes introduced into the optical properties of crystals by mechanical stress.

Finally, by retaining the third-order terms in equations (15.1) and (15.3) we can derive the expression for the so-called quadratic electrooptic effect:

$$\begin{aligned} E_m &= (-h_{mkl}r_{kl} + B_{mpql}r_{pq})r_{kl} \\ &\quad + (\beta_{mn} + p_{klmn}r_{kl} + f_{mnq}D_q + F_{mnqp}D_qD_p)D_n \\ D_m &= 4\pi d_{mkl}t_{kl} + (\epsilon_{mn} + \mu_{mnh}t_{hl} + \rho_{mnq}E_q + K_{mnpq}E_qE_p)E_n \end{aligned}$$

The last terms in parentheses in these equations,  $F_{mnqp}D_qD_p$  and  $K_{mnpq}E_qE_p$ , take into account the quadratic dependence of dielectric properties ( $\eta_{ij}$  and  $\epsilon_{ij}$ ) on induction  $\mathbf{D}$  and electric field  $\mathbf{E}$ , respectively:

$$\left. \begin{array}{l} \Delta\eta_{ij} = F_{ijk}D_kD_l \\ \Delta\epsilon_{ij} = K_{jkl}E_hE_l \end{array} \right\} \quad (15.12)$$

Equations (15.12) give two of the four possible forms of representing the quadratic electrooptic effect;  $F_{ijk}$  and  $K_{jkl}$  are the coefficients of the quadratic electrooptic effect. They form a rank

four tensor, so that this effect is observable in crystals of arbitrary symmetry.

However, this effect is easier to observe in centrosymmetrical crystals, because of the absence of the linear effect which usually greatly exceeds the quadratic effect.

The form of matrices of the coefficients of the quadratic electrooptic effect in different symmetry classes is identical to that of elastic compliance and stiffness,  $s_{ijkl}$  and  $c_{ijkl}$ .

Electrostriction is another second-order effect of practical significance. Electrostriction realizes as the strain of a crystal quadratic in electric field:

$$r_{ij} = R_{ijmn}E_mE_n$$

The equation of electrostriction indicates that the reversal of electric field does not change the sign of strain.

Three additional equations express electrostriction as a function of observation conditions:

$$r_{ij} = Q_{ijmn}P_mP_n, \quad t_{ij} = G_{ijmn}P_mP_n, \quad t_{ij} = E_{ijmn}E_mE_n$$

The electrostriction constants  $R_{ijmn}$ ,  $Q_{ijmn}$ ,  $G_{ijmn}$ ,  $H_{ijmn}$  are not independent (see Sec. 6, p. 96).

**Relation between the coefficients measured in different conditions.** As follows from the above arguments, the values of the coefficients describing mechanical, electrical, thermal, as well as piezo- and pyroelectric properties of crystals depend on the conditions of measurement. Thus, mechanical properties depend on thermal and electrical conditions, electrical properties, on mechanical and thermal conditions, heat capacity on mechanical conditions, and so on.

Let us single out the *most important* measurement conditions.

Thermal conditions:

1.  $T = \text{const}$  (isothermal measurements). This situation is realized in low-rate processes, when the crystal is at all times in equilibrium with the ambient. The corresponding tests of crystals are called static.

2.  $S = \text{const}$  (adiabatic measurements). This situation is realized in high-rate processes when no heat exchange is possible between parts of the crystal and between the crystal and the ambient. The corresponding tests are called dynamic and are realized in the case of elastic vibrations of crystals at frequencies much higher than the natural vibration frequency.

Electric conditions:

1.  $E = \text{const}$  (electrically free crystal). In this case the surface of the crystal as a whole must have the same potential. This requires that the electrodes deposited on a crystal plate be electrically connected, that is, the external circuit of the crystal be closed.

2.  $D = \text{const}$  (electrically “clamped” crystal). Experimentally this condition is hardly feasible. The closest realizable measurement conditions are those of the open external circuit of the crystal.

Mechanical conditions:

1.  $t_{ij} = \text{const}$  (mechanically free crystal). This situation is realized when the crystal can be deformed by external forces without constraints; this is possible in static tests.

2.  $r_{ij} = \text{const}$  (mechanically “clamped” crystal). A realization of this situation requires that the crystal be surrounded by a medium with infinitely large stiffness. In practice, the condition  $r_{ij} = \text{const}$  is realizable in dynamic high-frequency tests when crystal deformations are too slow to follow the external forces.

### Examples of Problems with Solutions

**15.1.** Calculate the contributions of the primary and secondary pyroelectric effects in barium nitrite crystals.

**Solution.** Owing to the polar symmetry and the absence of an inversion centre, pyroelectric crystals are at the same time piezoelectric. Consequently, a thermal deformation of the crystal produced in experimental observations of pyroelectric polarization in uniformly heated crystals inevitably produces the piezoelectric effect. If the crystal is mechanically clamped, that is, cannot deform, the piezoelectric effect is caused by thermally generated mechanical stresses in the clamped crystal.

Therefore, the pyroelectric effect observed experimentally includes, in addition to the “true” pyroelectric effect, that is, in addition to the direct effect of temperature changes on polarization, also a “false” pyroelectric effect, namely, the piezoelectric effect caused by thermal deformation of the crystal. If the constant of the “true” pyroelectric effect is denoted by  $\gamma'$ , and that of the “false” pyroelectric effect by  $\gamma''$ , then  $\gamma = \gamma' + \gamma''$  (see Sec. 3).

The following thermodynamical treatment of this phenomenon makes it possible to calculate the primary and secondary contributions to the net pyroelectric effect. Let us choose as independent variables characterizing the state of the crystal the following quantities:  $\mathbf{E}$ —the strength of an external electric field,  $r_{kl}$ —the strains suffered by the crystal, and  $T$ —the temperature of the crystal.

The quantities: electric induction  $\mathbf{D}$ , mechanical stresses  $t_{ij}$ , and entropy  $S$  are the functions of  $\mathbf{E}$ ,  $r_{kl}$  and  $T$ :

$$D_i = D_i(E_m, r_{kl}, T), \quad t_{ij} = t_{ij}(E_m, r_{kl}, T), \quad S = S(E_m, r_{kl}, T)$$

Consider the vector of induction  $\mathbf{D}$  as a function of temperature in zero external electric field ( $\mathbf{E} = 0$ ).

Since  $D_i = \epsilon_0 E_i + P_i$ , then for  $E = 0$

$$\left( \frac{\partial D_i}{\partial T} \right)_{t, E} = \left( \frac{\partial P_i}{\partial T} \right)_{t, E} = \gamma_i$$

As  $D_i = D_i(T, r_{kl})$  and  $r_{kl} = r_{kl}(t_{ij}, T)$ , we can write

$$\left. \begin{aligned} dD_i &= \left( \frac{\partial D_i}{\partial T} \right)_{r_{kl}} dT + \left( \frac{\partial D_i}{\partial r_{kl}} \right)_T dr_{kl} \\ dr_{kl} &= \left( \frac{\partial r_{kl}}{\partial t_{ij}} \right)_T dt_{ij} + \left( \frac{\partial r_{kl}}{\partial T} \right)_{t_{ij}} dT \end{aligned} \right\} \quad (15.13)$$

If measurements are taken at a constant external pressure, then  $dt_{ij} = 0$ , and

$$dr_{kl} = \left( \frac{\partial r_{kl}}{\partial T} \right) dT \quad (15.14)$$

A substitution of  $dr_{kl}$  from (15.14) into (15.13) yields

$$dD_i = \left[ \left( \frac{\partial D_i}{\partial T} \right)_{r_{kl}} + \frac{\partial D_i}{\partial r_{kl}} \frac{\partial r_{kl}}{\partial T} \right] dT \quad (15.15)$$

The expression in brackets is the coefficient of the net pyroelectric effect. The term  $\gamma'_i = \left( \frac{\partial D_i}{\partial T} \right)_{r_{kl}}$  represents the primary ("true") pyroelectric effect; the term  $\gamma''_i = \frac{\partial D_i}{\partial r_{kl}} \frac{\partial r_{kl}}{\partial T}$  represents the secondary ("false") effect due to the piezoelectric effect thermal expansion of the crystal.

Obviously,  $\frac{\partial r_{kl}}{\partial T} = \alpha_{kl}$ ,  $\frac{\partial D_i}{\partial r_{kl}} = \frac{\partial D_i}{\partial t_{mn}} \frac{\partial t_{mn}}{\partial r_{kl}} = d_{imn} c_{mnkl}^E$ , where  $\alpha_{kl}$  are the thermal expansion coefficients,  $d_{imn}$  are the piezoelectric moduli,  $c_{mnkl}$  are the elastic stiffnesses of the crystal measured at constant electric field, so that the coefficient of the secondary pyroelectric effect can be written in the form

$$\gamma''_i = d_{imn} c_{mnkl}^E \alpha_{kl} \quad (15.16)$$

The right-hand side of (15.16) includes quantities measurable in experiments. The coefficient  $\gamma''_i$  can therefore be calculated; as a result, if the coefficient  $\gamma_i$  is known, we can evaluate the primary and secondary contributions into the pyroelectric effect.

Barium nitrite crystals have a single pyroelectric constant  $\gamma_3 = \gamma'_3 + \gamma''_3$ , and equation (15.13) transforms into

$$\gamma''_3 = d_{3j} c_{jk} \alpha_k$$

where  $\alpha_k$  are the thermal expansion coefficients,  $d_{3j}$  are the piezoelectric moduli in the third row of the matrix  $(d_{ij})$ , and  $c_{jk}$  are the elastic stiffnesses of the crystal.

The nonzero coefficients  $d_{3j}$  for barium nitrite are (see Table 9):  $d_{31}$ ,  $d_{32} = d_{31}$ ,  $d_{33}$ .

Taking into account this property, and the form of the matrices  $(\alpha_k)$  and  $(c_{jk})$  (see Tables 4, 5, 9) for barium nitrite, we arrive at the following expression for  $\gamma''_3$ :

$$\begin{aligned}\gamma''_3 = d_{3j}c_{jk}\alpha_k &= d_{31}(c_{11}\alpha_1 + c_{12}\alpha_2 + c_{13}\alpha_3) \\ &+ d_{32}(c_{21}\alpha_1 + c_{22}\alpha_2 + c_{23}\alpha_3) + d_{33}(c_{31}\alpha_1 + c_{32}\alpha_2 + c_{33}\alpha_3)\end{aligned}$$

Or, taking into account that  $c_{11} = c_{22}$ ,  $c_{13} = c_{23}$ ,  $\alpha_1 = \alpha_2$ , we find

$$\gamma''_3 = 2d_{31}[(c_{11} + c_{12})\alpha_1 + c_{13}\alpha_3] + 2d_{33}c_{31}\alpha_1 + d_{33}c_{33}\alpha_3$$

With coefficients  $d_{3j}$ ,  $c_{jk}$ , and  $\alpha_k$  substituted from Table 14, we obtain  $\gamma''_3 = 0.72$  CGSE units. As the net constant of pyroelectric effect is equal to  $-8$  CGSE units, the contribution of the secondary pyroelectric effect into the total effect is approximately 9% at room temperature. Predominantly (about 90%) the pyroelectric effect in barium nitrite crystals is due to the primary ("true") pyroelectric effect.

**15.2.** Find the relationship between elastic compliances measured in isothermal and adiabatic conditions.

**Solution.** To solve the problem, we shall use the equations relating the mechanical and thermal characteristics of the state of a crystal, neglecting electrical phenomena:

$$\begin{aligned}r_{ij} &= r_{ij}(t_{ij}, T); \quad S = S(t_{ij}, T) \\ dr_{ij} &= \left(\frac{\partial r_{ij}}{\partial t_{kl}}\right)^T dt_{kl} + \left(\frac{\partial r_{ij}}{\partial T}\right)^t dT\end{aligned}\quad (15.17)$$

$$dS = \left(\frac{\partial S}{\partial t_{kl}}\right)^T dt_{kl} + \left(\frac{\partial S}{\partial T}\right)^t dT \quad (15.18)$$

Assume the measurement conditions to be adiabatic, that is,  $S = \text{const}$  and  $dS = 0$  in (15.18). Now find  $dT$  from (15.18) and substitute it into (15.17). This gives

$$dr_{ij} = \left(\frac{\partial r_{ij}}{\partial t_{kl}}\right)^T dt_{kl} - \frac{(\partial r_{ij}/\partial T)^t (\partial S/\partial t_{kl})^T dt_{kl}}{(\partial S/\partial T)^t} \quad (15.19)$$

Taking into account that for each choice of independent variables and their functions the increment of the appropriate thermodynamical function,  $dG$ , is the total differential, we find

$$-\left(\frac{\partial^2 G}{\partial t_{ij} \partial T}\right) = -\left(\frac{\partial r_{ij}}{\partial T}\right)^t = -\left(\frac{\partial S}{\partial t_{ij}}\right)^T$$

The relations thus obtained are substituted into (15.19):

$$\left(\frac{\partial r_{ij}}{\partial t_{kl}}\right)^S - \left(\frac{\partial r_{ij}}{\partial t_{kl}}\right)^T = -\left(\frac{\partial r_{ij}}{\partial T}\right)^t \left(\frac{\partial r_{kl}}{\partial T}\right)^t \left(\frac{\partial T}{\partial S}\right)^t$$

With the notations introduced above, we obtain:

$$s_{ijkl}^S - s_{ijkl}^T = -\alpha_{ij}\alpha_{kl} \frac{T}{ct}$$

**15.3.** Find the matrix of elastoelectric coefficients for symmetry class 32.

**Solution.** From the first of equations (15.5) we can write for the increments of elastic stiffnesses as functions of electric induction in the crystal:

$$\Delta c_{ijkl} = M_{nijkl} D_n \quad (15.20)$$

Equation (15.20) can be regarded as the equation of elastoelectric effect. If the external factor is an electric field, then

$$\Delta c_{ijkl} = g_{mijkl} E_m$$

The components of the tensor  $g_{mijkl}$  are related with  $M_{nijkl}$  via the dielectric permittivities.

Operations chosen as group generators for crystals of symmetry class 32 can be rotations around axis 2 parallel to  $X_1$  and rotations by  $120^\circ$  around the axis 3 parallel to  $X_3$ . The order in which these generators are applied is immaterial, so that it is expedient to consider first the result of transformation by the axis 2, since it allows for the Fumi method (see Sections 6, 7):

$$C_{2 \parallel X_1} = \begin{pmatrix} 1 & 0 & 0 \\ 0 & -1 & 0 \\ 0 & 0 & -1 \end{pmatrix}$$

We can now consider the result of rotations around the axis 3:

$$C_{3 \parallel X_3} = \begin{pmatrix} -1/2 & -\sqrt{3}/2 & 0 \\ \sqrt{3}/2 & -1/2 & 0 \\ 0 & 0 & 1 \end{pmatrix}$$

which requires the use of the direct inspection method, that is, the following system of equations must be resolved:

$$g'_{pqrs} = C_{pm} C_{qi} C_{rj} C_{sk} C_{tl} g_{mijkl}$$

Ultimately this gives us three matrices for class 32:

$$\begin{bmatrix} g_{111} - (g_{111} + g_{122}) & g_{113} & g_{114} & 0 & 0 \\ g_{122} & -g_{113} & g_{124} & 0 & 0 \\ 0 & g_{134} & 0 & 0 & 0 \\ g_{144} & 0 & 0 & 0 & 0 \\ & g_{144} (g_{124} - g_{144}) - 2(g_{111} + g_{122}) & & & \end{bmatrix}$$

$$\begin{bmatrix} 0 & 0 & 0 & 0 & -g_{124} & g_{111} + 3g_{122} \\ 0 & 0 & 0 & -g_{114} & -(3g_{111} + g_{122}) \\ 0 & 0 & -g_{134} & -2g_{113} \\ 0 & g_{144} & -g_{114} - g_{124} \\ 0 & 0 & 0 \\ 0 & & & \end{bmatrix}$$

$$\begin{bmatrix} 0 & 0 & 0 & 0 & g_{315} & 0 \\ 0 & 0 & 0 & -g_{315} & 0 \\ 0 & 0 & 0 & 0 \\ 0 & 0 & -g_{315} \\ 0 & 0 & 0 \\ 0 & & & \end{bmatrix}$$

which offer an easy way to present a rank five tensor in matrix notation:  $g_{1mk}$ ,  $g_{2lq}$ ,  $g_{3ij}$ . The subscripts  $m, k, l, q, i, j$  are obtained by contraction over two pairs of subscripts referring to elastic constants, and running from 1 to 6.

For the purpose of illustration, it is convenient to represent the effect of an electric field on elasticity of the crystal by a table which in the case of class 32 is

$c_{11} + g_{111}E_1$	$-\frac{c_{12}}{(g_{111} + g_{112})E_1}$	$c_{13} + g_{113}E_1$	$c_{14} + g_{144}E_1$	$-\frac{g_{124}E_2 +}{+g_{315}E_3}$	$(g_{111} + 3g_{122})E_2$
$c_{12} - \frac{(g_{111} + g_{122})E_1}{+g_{112}E_1}$	$c_{11} + g_{122}E_1$	$c_{13} - g_{113}E_1$	$-\frac{c_{14} +}{+g_{124}E_1}$	$-\frac{g_{114}E_2 +}{+g_{315}E_3}$	$-(3g_{111} + g_{122})E_2$
$c_{13} + g_{113}E_1$	$c_{13} - g_{113}E_1$	$c_{33}$	$g_{134}E_1$	$-g_{134}E_2$	$-2g_{113}E_2$
$c_{14} + g_{114}E_1$	$-\frac{c_{14} +}{+g_{124}E_1}$	$g_{134}E_1$	$c_{44} + g_{114}E_1$	$2g_{114}E_2$	$-\frac{(g_{114} - g_{124})E_2 -}{-2g_{315}E_3}$
$-\frac{g_{124}E_2 +}{+g_{315}E_3}$	$-\frac{g_{114}E_2 -}{-g_{315}E_3}$	$-g_{134}E_2$	$2g_{144}E_2$	$c_{44} - g_{144}E_1$	$-\frac{(g_{121} - g_{144})E_1}{-g_{144}E_1}$
$(g_{111} + 3g_{122})E_2$	$-(3g_{111} + g_{122})E_2$	$-2g_{113}E_2$	$-\frac{(g_{114} - g_{124})E_2 -}{-2g_{315}E_3}$	$-\frac{(g_{124} - g_{114})E_1}{-g_{114}E_1}$	$-\frac{c_{66} -}{2(g_{111} + g_{112})E_1}$

15.4. The constants of linear electrooptic effect  $r_{22}$  and  $r_{33}$  of lithium niobate crystals were measured in an electric field at a frequency exceeding the natural frequency of the specimen vibration; the corresponding figures are

$$r_{22}^* = 0.1 \cdot 10^{-6} \text{ CGSE units}, \quad r_{33}^* = 0.9 \text{ CGSE units}$$

Calculate the corresponding constants characterizing electrooptic properties of lithium niobate in static and low-frequency fields. Which of the given constants depends on frequency most strongly?

*Solution.* The electrooptic constants given above characterize the "true" electrooptic effect since they were measured at frequencies above the natural vibration frequencies of the specimens. In this case a crystal is mechanically "clamped" since its deformation is too slow to follow those of the external electric field. The values of electrooptic constants  $r_{22}$  and  $r_{33}$ , characterizing the properties of lithium niobate in low-frequency and static fields, are greater by the value of the contribution of the elastooptic effect, since in this case the crystal, being mechanically "free", is deformed, and this deformation in its turn causes an additional change in polarization constants. Equation (11.6) makes possible the calculation of the constants of interest.

The matrices  $(d_{ij})$  and  $(P_{ij})$ , required to calculate  $r_{22}$  and  $r_{33}$  in crystals with symmetry  $3m$ , comprising lithium niobate crystals, are shown in Tables 6 and 11.

According to (12.6), and in correspondence with the form of matrices  $(d_{ij})$  and  $(P_{ij})$ , we find:  $r_{222} = r_{222}^* + P_{2211}d_{211} + P_{2222}d_{222} + 2P_{2223}d_{223}$ , or, in matrix notation,

$$\begin{aligned} r_{22} &= r_{22}^* + P_{21}d_{21} - P_{22}d_{21} + 2P_{24}d_{24} \\ &= r_{22}^* + (P_{12} - P_{11})d_{21} - P_{14}d_{15} = 0.194 \times 10^{-6} \text{ CGSE units} \end{aligned}$$

The constant  $r_{22}$  characterizing the electrooptic properties of lithium niobate in a low-frequency or static electric field is thus twice as large as  $r_{22}^*$  which characterizes these properties in a high-frequency field. Now let us find  $r_{33}$ :

$$r_{33} = r_{33}^* + 2P_{31}d_{31} + P_{33}d_{33} = 0.0004 \cdot 10^{-6} \text{ CGSE units}$$

This means that  $r_{33}$  differs from  $r_{33}^*$  by 0.4%.

Obviously, the strongest dependence on frequency will be evinced by  $r_{22}$ .

#### PROBLEMS

15.5. Describe the phenomena observed in (i) homogeneous and (ii) inhomogeneous heating of crystals belonging to symmetry classes 3, 32, and  $m3$ .

15.6. What physical phenomena are possible only in crystals of ten polar symmetry classes?

15.7. What physical phenomena are possible, when second-order effects are taken into account, when crystals with symmetry  $2$ ,  $mm$ , and  $23$  are placed in a uniform electric field?

15.8. Table 14 gives elastic compliances of quartz measured in isothermal conditions,  $s_{ij}^T$ . Use the data of this table and calculate adiabatic elastic compliances of quartz,  $s_{ij}^S$ .

15.9. Find the relation between the components of the dielectric permittivity tensor, measured on a mechanically free ( $\epsilon_{ij}^t$ ) and mechanically clamped ( $\epsilon_{ij}^r$ ) crystals. In what symmetry classes of crystals are these components different and in what are they identical?

15.10. Find the relation between the components of the dielectric permittivity tensor measured in isothermal ( $\epsilon_{ij}^T$ ) and adiabatic ( $\epsilon_{ij}^S$ ) conditions. In what symmetry classes of crystals are these components different and in what identical?

15.11. Find the relative increment of capacitance of a capacitor made of an  $X$ -cut rochelle salt plate, when the capacitor operates at frequencies (i) below and (ii) above the natural resonance frequency of vibrations in the plate (the capacitance of a mechanically free and mechanically clamped crystal).

15.12. Will the capacitance of a mica capacitor be different in low- and high-frequency ranges?

15.13. Could the resonance frequencies of piezoelectric oscillators be calculated on the basis of elastic compliances from the data on sound velocities in crystals?

15.14. Show that the adiabatic coefficient  $S_{44}^S$  in cubic symmetry crystals is equal to the isothermal coefficient  $S_{44}^T$ .

15.15. Find the relations between the adiabatic and isothermal piezoelectric moduli. Are these moduli different for (i) lithium niobate, (ii) quartz, and (iii) KDP crystals?

15.16. Find the change in the temperature of a quartz plate oriented as shown in Fig. 4.3b, under a short-time action of a force ten times the weight of the plate. The plate dimensions are  $1 \times 3 \times 10$  mm $^3$ . Analyze three cases in which the force is applied to each pair of mutually parallel faces.

15.17. Determine the matrix of elastoelectric constants for symmetry class  $\bar{4}2m$ .

15.18. Find the matrix of elastoelectric constants for symmetry class  $3m$ .

15.19. What will be the change in the resonance frequency of a piezoelectric oscillator made of an  $X$ -cut quartz bar 10 mm long, performing compressional-tensile lengthwise vibrations, if it is placed in a constant electric field of  $10^6$  V/cm along the axis  $2$ ?

15.20. Calculate the relative change in the resonance frequency of a piezoelectric oscillator, made of a  $Y$ -cut quartz plate, operating in the thickness shear vibration mode, when constant electric field  $5 \cdot 10^5$  V/cm is aligned with the axis  $X_1$ .

15.21. Find the change in Young's modulus of lithium niobate along the axis 3 if the crystal is placed in an electric field of  $10^6$  V/m aligned at equal angles to the crystallophysical axes?

15.22. Derive the expression and plot the section of the representation quadratic of the stiffness  $c'_{33}$  of lithium niobate by the coordinate plane  $X_1X_2$ , if the crystal is placed in electric field aligned along the bisector of the angle between the axes  $X_1$  and  $X_2$ .

15.23. What field must be applied to a  $Z$ -cut of quartz to obtain the electrostriction strain  $r_{33}$  equal to the piezoelectric strain  $r_{11}$  of an  $X$ -cut in the field  $E = 10^5$  V/cm? For quartz  $R_{33} = 0.3 \cdot 10^{-12}$  CGSE units.

## ANSWERS TO PROBLEMS

### § 3

3.8. (i)  $\sigma = 36$  CGSE units; (ii)  $\sigma = 18$  CGSE units; (iii)  $\sigma = 0$ .  
 3.9.  $\Delta T = 5.7 \cdot 10^{-7}$  K. The plate must be cut perpendicularly to the axis [2.  
 3.10.  $\sim 750$  V/cm. 3.11.  $3.2 \cdot 10^3$  V.  
 3.12. The lower Curie point will be shifted by  $1.4^\circ$  to higher temperatures if the field  $E$  is parallel to  $P^s$ . If  $E$  is antiparallel to  $P^s$ , the lower Curie point will be shifted by the same amount to lower temperatures.  
 3.13.  $\gamma \approx 6 \cdot 10^4$  CGSE units. 3.14. 156 V. 3.15. In classes 1 and  $m$ .  
 3.16.  $\Delta T = 3 \cdot 10^{-4}$  K. 3.17.  $Q = 4.8 \cdot 10^{-7}$  C. 3.21.  $Q = 5 \cdot 10^{-9}$  C,  
 $V = 1200$  V. 3.22.  $\Delta T = 5 \cdot 10^{-5}$  K. 3.23.  $\Delta T = 5 \cdot 10^{-5}$  K. 3.24.  $\Delta T = -0.2$  K.

### § 4

4.10.  $3.6 \cdot 10^{-6}$  K $^{-1}$ . 4.11.  $200 \cdot 10^{14}$  ohm $\cdot$ cm;  $100 \cdot 10^{14}$  ohm $\cdot$ cm.  
 4.12. 246; 245; 11. 4.13.  $1.7 \cdot 10^6$  ohm $\cdot$ cm. 4.14.  $0^\circ$ .  
 4.15.  $1.4 \cdot 10^{-12}$  F. 4.16.  $1.4 \cdot 10^{-5}$  C. 4.17. (i) and (ii)

$$\varepsilon'_{ij} = \begin{bmatrix} 4.5 & 0 & 0 \\ 0 & 4.52 & -0.04 \\ 0 & -0.04 & 4.57 \end{bmatrix}; \text{ (iii) remains unchanged.}$$

4.20. The plate must be cut perpendicularly to  $n$  (0.92; 0.33; 0). 4.21.  $34^\circ 52'$ .  
 4.22. In directions at  $86^\circ 50'$  to the highest-order symmetry axis. 4.23. The plate must be cut perpendicularly to [001]. 4.24. The principal axes of the tensor  $[\alpha_{ij}]$  are related to the original axes by a counterclockwise rotation by  $20.7^\circ$  around  $X_2$ . 4.25.  $2^\circ$  for the  $X$ -cut,  $57'$  for the  $Y$ -cut.  
 4.26.  $\Delta T_1 = 2.3 \cdot 10^{-3}$  K;  $\Delta T_2 = 4 \cdot 10^{-3}$  K. 4.27.  $3.3 \cdot 10^{-8}$  C/cm $^2$ .  
 4.32.  $0.628 \cdot 10^{-6}$  K $^{-1}$ . 4.33.  $20.8 \cdot 10^{-3}$  cal $\cdot$ K $^{-1}$ cm $^{-1}$ s $^{-1}$ .  
 4.34.  $1.92 \cdot 10^{-8}$   $\mu$ m. 4.35. 0.096 V.

### § 5

5.9. The sought coordinate system is related to the original axes of the tensor by a counterclockwise rotation by  $45^\circ$  around the axis  $X_3$ .  
 5.10.  $t_n = t_{11} \cos^2 \alpha + t_{22} \sin^2 \alpha + t_{12} \sin 2\alpha$ ;  
 $t_t = \frac{1}{2} (t_{22} - t_{11}) \cdot \sin 2\alpha + t_{12} \cos 2\alpha$ .  
 5.11.  $t_1 \approx 99.3$  N/cm $^2$ ;  $t_2 \approx 58.8$  N/cm $^2$ ;  $t_3 = -1380$  N/cm $^2$ .  
 5.12.  $P_{av} = -700$  N/cm $^2$ ;  $t_{t\max} = 75$  N/cm $^2$ .  
 5.13.

$$r_{ij} = \begin{bmatrix} 8 & 5 & -2 \\ 5 & 3 & -2 \\ -2 & -2 & 1 \end{bmatrix} \cdot 10^{-5}; \quad \omega_{ij} = \begin{bmatrix} 0 & -2 & -3 \\ 2 & 0 & 6 \\ 3 & -6 & 0 \end{bmatrix} \cdot 10^{-5}$$

$\Delta V/V = 12 \cdot 10^{-5}$ .  
 5.16.  $n_1$  (0.8945; 0; -0.4470);  $n_2$  (0, 1, 0);  $n_3$  (0.4470; 0; 0.8945).  
 5.18.  $5.33 \cdot 10^{-5}$ ;  $8.67 \cdot 10^{-5}$ .

5.19.  $\varphi = 2 \cdot \Delta T \sqrt{\alpha_{13}^2 + \alpha_{23}^2}$ . 5.22.  $t_{11} = 1250 \text{ N/cm}^2$ ;  
 $r_{11} = 2.2 \cdot 10^{-4}$ ;  $r_{22} = -10^{-4}$ ;  $r_{33} = -0.5 \cdot 10^{-4}$ .  
 5.23.  $t_{11} = t_{22} = t_{33} = 9.81 \cdot 10^3 \text{ N/cm}^2$ ;  $t_{12} = t_{23} = t_{31} = 0$ ;  
 $r_{11} = r_{22} = r_{33}$ ;  $r_{12} = r_{23} = r_{31} = 0$ .  
 5.24.  $t_{11} = 1 \text{ N/cm}^2$ ;  $t_{22} = -1 \text{ N/cm}^2$ ,  $t_{33} = 0$ ,  $t_{12} = t_{23} = t_{31} = 0$ ;  
 $r_{11} = -0.4 \cdot 10^{-4}$ ;  $r_{22} = 0.4 \cdot 10^{-4}$ ;  $r_{33} = r_{12} = r_{23} = r_{31} = 0$ .  
 5.25.  $t_{11} = t_{22} = t_{33} = 10^4 \text{ N/cm}^2$ ;  $t_{12} = t_{23} = t_{31} = 0$ ;  $r_{33} = 10^{-4}$ ;  $r_{11} = -10^{-4}$ .

## § 6

6.16. (i) In quartz  $P_{11} = n_1(n_1^2 - 3n_2^2)d_{11}t$ ; the longitudinal effect is impossible along [0001]. (ii) In sodium chlorate  $P_{11} = 3n_1n_2n_3d_{14}t$ ; the longitudinal effect is impossible in the directions lying in the coordinate planes, i.e. in the directions [hk0].

6.17.  $Q = F \cdot d_{11}$ ;  $Q = -F \cdot d_{11} \text{ V/A}$ ;  $Q = 0$ . 6.18. 5.5 CGSE units.  
 6.19.  $r'_2 = -1.9 \cdot 10^{-5}$ ;  $r'_3 = -r_2$ . 6.20.  $n(\sqrt{3}/3; \sqrt{3}/3; \sqrt{3}/3)$ .  
 6.21.  $r_4 = r_5 = -7.5 \cdot 10^{-6}$ . 6.22.  $\Delta x_1 = -6.7 \cdot 10^{-7} \text{ cm}$ ;  $\Delta x_2 = 3.38 \cdot 10^{-5} \text{ cm}$ .  
 6.24. The relative strain of edges in the plane of the working faces is  $5.83 \cdot 10^{-7}$ . 6.25.  $d'_{12} = -d_{11} \cdot \cos^2 \varphi + d_{14} \cdot \sin \varphi \cos \varphi$ ; for  $\varphi = 0^\circ$ ,  
 $d'_{12} = -d_{11}$ ; for  $\varphi = 90^\circ$   $d'_{12} = 0$ . 6.26.  $r = n_1 \cdot (n_1^2 - 3n_2^2) d_{11}$ . 6.28. The unit normal to the plate in the crystallophysical coordinate system must have the components  $n_1 = n_2 = n_3 = 0.5774$ . 6.29.  $45^\circ$ . 6.30.  $1.01 \cdot 10^6 \text{ N/cm}^2$ .  
 6.31.  $Q_1 = d_{14}n_2n_3t \cdot b \cdot c$ ;  $Q_2 = d_{14}n_1n_3t \cdot a \cdot c$ ;  $Q_3 = 0$ . 6.32.  $Q = 1.4 \cdot 10^{-5} \text{ C}$ ,  
 $V = 45 \text{ V}$ . 6.33.  $n(\sqrt{3}/3, \sqrt{3}/3, \sqrt{3}/3)$ . 6.34. Monoclinic angle  $90^\circ 2''$ .  
 6.35.  $K = 3\%$ . 6.36. The displacement of the plate edge is approximately  $10^{-6} \mu\text{m}$ . 6.40.  $K = 22\%$  for  $45^\circ$  Z-cut and  $K = 32\%$  for L-cut. 6.41.  $d_{14}$ .  
 6.42. (i)  $\sigma = 0$  on all faces; (ii)  $\sigma = d_{14}t/2$  on the face perpendicular to [001], and  $\sigma = 0$  on all other faces; (iii)  $\sigma = d_{14}t/3$  on all faces. 6.43. Y-cut.  
 6.44. 0.27 cm. 6.45.  $K = 10\%$ ;  $K = 9\%$ .  
 6.46.  $d_{33} = 5.63 \cdot 10^{-6}$ ,  $d_{31} = -2.35 \cdot 10^{-6}$ ,  $d_{15} = 7.8 \cdot 10^{-6}$  (in CGSE units).  
 6.47.  $d_{14} = 9.52 \cdot 10^{-8}$  CGSE units. 6.48.  $P^s = \frac{2(d_{31} + d_{33})}{s_{33} - 2s_{11} - 2s_{12}}$  for tourmaline;

$$P^s = \frac{d_{21} + d_{22} + d_{23}}{s_{22} - s_{11} - s_{33} - 2s_{13}} \text{ for lithium sulphate.} \quad 6.51. \quad 1\%; \quad 1\%; \quad 0.3\%.$$

6.52. 0.3%; 1.3%.

6.56. 32, 422, 622,  $\bar{6}$ ,  $\bar{6}m2$ . 6.57. The conditions of determination of the coefficients  $Q$ ,  $R$ ,  $G$ , and  $H$  correspond to those of determination of the coefficients  $g$ ,  $d$ ,  $h$ , and  $e$ , respectively. 6.58. It is not; the spontaneous deformation accompanying the appearance of  $P^s$  along [001] is of a piezoelectric nature. 6.59.  $E = 100 \text{ V/cm}$  in an X-cut plate. 6.60.  $Q_{44}$ .  
 6.62.  $Q_{11} = 1.23 \cdot 10^{-12}$  CGSE units;  $Q_{12} = -0.49 \cdot 10^{-12}$  CGSE units;  
 $Q_{44} = 0.65 \cdot 10^{-12}$  CGSE units. 6.64. Since spontaneous deformation in ferroelectrics of this type is induced by electrostriction, the shape of their domains is independent of the sign of spontaneous polarization.  
 6.66.  $\approx 200 \text{ kV/cm}$ . 6.67. Impossible. Consider a centrosymmetrical crystal, with no piezoelectric effect but with electrostriction. A centrosymmetrical influence (mechanical stress or deformation) conserves the central symmetry of the crystal and therefore, suppresses the appearance of polarization.

## § 7

7.10.  $1.82 \cdot 10^{-4}$ . 7.11. By  $4^\circ$ . 7.12.  $t_1 = t_2 = 180 \text{ N/cm}^2$ ;  $t_3 = 146 \text{ N/cm}^2$ ;  
 $t_4 = t_5 = 17.3 \text{ N/cm}^2$ ;  $t_6 = 12 \text{ N/cm}^2$ . 7.13.  $1.026 \cdot 10^{-8} \text{ cm}^2/\text{dyne}$ ;  
 $2.67 \cdot 10^{-12} \text{ cm}^2/\text{dyne}$ . 7.14.  $5.52 \cdot 10^{11} \text{ dyne/cm}^2$ ;  $2.08 \cdot 10^{11} \text{ dyne/cm}^2$ ;

1.95.  $10^{11}$  dyne/cm<sup>2</sup>. 7.15.  $s'_{33} = \frac{1}{E} = s_{11} \cdot (1 - \cos^2 \theta_3)^2 +$   
 $+ (s_{44} + 2 \cdot s_{13}) \cdot \cos \theta_3 \cdot (1 - \cos^2 \theta_3) + s_{33} \cos^4 \theta_3 +$   
 $+ 2s_{14} \cdot \cos \theta_2 \cdot \cos \theta_3 \cdot (3 \cos^2 \theta_1 - \cos^2 \theta_2)$ , where  $\theta_1$ ,  $\theta_2$ , and  $\theta_3$  are the angles between an arbitrary  $X_3$  axis and the crystallophysical axes.  
 7.16.  $s'_{33} = s_{11} \sin^4 \theta + s_{33} \cos^4 \theta + (s_{44} + 2s_{13}) \sin^2 \theta \cdot \cos^2 \theta$ , where  $\theta$  is the angle between an arbitrary direction  $X_3$  and the highest-order symmetry axis.  
 7.17. 1200 erg. 7.18. 3320 erg. 7.23.  $s_{33}$  and  $s_{13}$ . 7.25.  $s_{13}$ ,  $s_{33}$ . 7.26.  $s_{13}$ ,  $s_{33}$ .  
 7.27.  $s_{11} = 2.34 \cdot 10^{-12}$ ,  $s_{12} = -0.515 \cdot 10^{-12}$ ,  $s_{44} = 8.54 \cdot 10^{-12}$  (in cm<sup>2</sup>/dyne).  
 7.33. 1.5 kV/cm. 7.34.  $1.2 \cdot 10^3$  N/m<sup>2</sup>. 7.35.  $s_{12}$ ,  $s_{13}$ . 7.39.  $-3.7 \cdot 10^{-6}$  K<sup>-1</sup>.  
 7.41.  $\Delta T = 0.27$  K. 7.42.  $f_T = 1.9 \cdot 10^{-5}$  K<sup>-1</sup>.

### § 8

8.10. By 3%. 8.11.  $19.6 \cdot 10^4$  Pa. 8.12. (i)  $-80 \cdot 10^{-12}$  cm<sup>2</sup>/dyne,  
 (ii)  $42.4 \cdot 10^{-12}$  cm<sup>2</sup>/dyne. 8.13.  $2.6 \cdot 10^{-10}$ . 8.14.  $\Pi_{11} = -4.7 \cdot 10^{-12}$  cm<sup>2</sup>/dyne,  
 $\Pi_{12} = -5 \cdot 10^{-12}$  cm<sup>2</sup>/dyne,  $\Pi_{44} = -137.9 \cdot 10^{-12}$  cm<sup>2</sup>/dyne. 8.15. (i) 0.002 V,  
 (ii) 0.525 V. 8.16.  $P \approx 9.8 \cdot 10^6$  Pa. 8.17. (i) By a factor of 14, (ii) by a factor of 1.3. 8.18. For  $p$ -Ge:  $96.7 \cdot 10^{-12}$  cm<sup>2</sup>/dyne  $\geq \Pi_{44} \geq -0.5 \cdot 10^{-12}$  cm<sup>2</sup>/dyne.  
 8.19. For  $p$ -Ge:  $144 \geq K \geq 8.58$ ; for  $p$ -Si:  $66.02 \geq K \geq -3.78$ .  
 8.21.  $t \approx 14$  Pa. 8.22. (i) 0.3 V, (ii)  $6.4 \cdot 10^{-4}$  V. 8.25.  $133 \geq K \geq 13$ .

### § 9

9.6.  $\Delta n = 0.009$ ,  $\Delta\phi = 0.24$  rad. 9.7.  $\Delta n = 0.006$ . 9.8. The crystal is optically negative. 9.9. 0.011 mm; 9.10. 0.014 mm; 9.11. 1.53 mm; 9.13.  $1.03^\circ$ ;  
 9.14. 0.48 mm; 9.15.  $3.06^\circ$ ; 9.16.  $0.17^\circ$ ,  $3.06^\circ$ ,  $2.07^\circ$ ; 9.19. 0.203 mm;  
 9.20.  $I/I_0 = 0.616$ ; 9.22.  $4.5 \cdot 10^{-3}$  mm; 9.24. The ratio of intensities is 1.  
 9.25.  $I/I_0 = 0.029 \sin^2 \alpha$ ,  $I/I_0 = 0.094 \sin^2 \alpha$ ; 9.29.  $5.3^\circ$ ; 9.30.  $13.5^\circ$ .  
 9.31.  $11.4^\circ$ . 9.32.  $3.4^\circ$ . 9.36. 1.003 mm.

### § 10

10.7. The index ellipsoid of the sphalerite crystal is deformed by stress so that the sphere is transformed into a triaxial ellipsoid, with one of the axes of the ellipsoid parallel to the direction of stress. 10.8. The longitudinal effect is zero, and the transverse effect is  $\frac{1}{2} N_0^3 (\pi_{11} - \pi_{12})$ . 10.9. The classes belonging to triclinic and monoclinic systems. 10.10.  $\pi_{44} = 0.706 \cdot 10^{-11}$  cm<sup>2</sup>/dyne.  
 10.11.  $\sim 8.8$  kgf/cm<sup>2</sup>. 10.12.  $B_{[010]} = -1/2 N_0^3 \cdot (\pi_{11} - \pi_{12}) t$ ;  $B_{[001]} = -1/2 N_0^3 \cdot (\pi_{11} - \pi_{12}) t$ .

$$10.13. n_{x'_1} = N_0 - \frac{\pi_{11} t}{2} N_0^3; \quad n_{x'_2} = N_0 - \frac{\pi_{12} t}{2} N_0^3; \quad n_{x'_3} = N_0 - \frac{\pi_{31} t}{2} N_0^3.$$

10.16.  $\pi_{11}$ ,  $\pi_{12}$ ,  $\pi_{31}$ . 10.18.  $1.65 \cdot 10^{-4}$ . 10.19. 8.8 kgf/cm<sup>2</sup> for ADP,  
 22.8 kgf/cm<sup>2</sup> for DKDP.

### § 11

11.11.  $\bar{4}$ ,  $\bar{4}2m$ . 11.19. Impossible. 11.20. Crystals with symmetry 422, 32, 622,  $\bar{3}m$ , and  $\bar{6}m2$ . 11.21. By a factor of  $\sim 660$  for KDP and  $u \approx 500$  for DKDP.  
 11.22.  $B_{[100]} = \frac{1}{2} P^s (n_3^3 m_{33} - n_2^3 m_{23})$ ,  $B_{[010]} = (1/2) P^s (n_3^3 m_{33} - n_1^3 m_{13})$ ,  
 $B_{[001]} = \frac{1}{2} P^s (n_2^3 m_{23} - n_1^3 m_{13})$ . 11.23.  $r_{13}$ . 11.26. 0.2 cm. 11.27. 12.3 kV.  
 11.28.  $\sim 16'$ . 11.29.  $m_{33} = 1.87 \cdot 10^{-7}$  CGSE units. 11.30.  $n_{x'} = n_1$ ;

$$\frac{1}{n_{x'_2}} = \frac{1}{n_2^2} + \frac{r_{41}^2 E_1^2}{\frac{1}{n_2^2} - \frac{1}{n_3^2}}; \quad \frac{1}{n_{x'_3}} = \frac{1}{n_3^2} - \frac{r_{41}^2 E_1'}{\frac{1}{n_2^2} - \frac{1}{n_3^2}}.$$

11.31.  $\sim 0.4$  cm. 11.32.  $\sim 27.8 \cdot 10^{-8}$  CGSE units.

$$11.34. n_{x'_1} = n_{x'_2} = N_0 + \frac{1}{2\sqrt{3}} N_0^3 r_{41} E; \quad n_{x'_3} = N_0 - \frac{1}{2\sqrt{3}} N_0^3 r_{41} E;$$

$$\Gamma = \frac{2\pi}{\sqrt{3}} \lambda N_0^3 r_{41} E l.$$

11.35.  $r_{42} = 24 \cdot 10^{-6}$  CGSE units. 11.36.  $V_{\lambda/2} = 15.6$  kV for KDP,  $V_{\lambda/2} = 6.7$  kV for DKDP. 11.37.  $0.34\pi$ . 11.39.  $\sim 13'$ . 11.47. Along [010].

11.48.  $N_e^3 R_{31} - N_0^3 R_{11} = 1.35 \cdot 10^{-13}$   $\text{cm}^2 \cdot \text{V}^{-2}$ ,  $N_0^3 (R_{12} - R_{11}) = -0.89 \cdot 10^{-13}$   $\text{cm} \cdot \text{V}^{-2}$ . 11.49.  $V_{\lambda/2}$  of a modulator based on the quadratic electrooptic effect is six times that of a modulator based on the linear effect.

11.50.  $N_{\max} = 100$ . 11.51.  $R_{66} = 0.20 \cdot 10^{-13}$   $\text{cm}^2 \cdot \text{V}^{-2}$ .

11.53. (i)  $(1/2) (R_{33} n_3^3 - R_{22} n_2^3) E_2^2$ ; (ii)  $(1/2) (r_{32} n_3^3 - r_{22} n_2^3) E_2 + (1/2) (r_{32} n_3^3 - R_{22} n_2^3) \cdot E_2^2$ . 11.54. 3.9 kV.

11.55.  $(1/2) (n_3^3 \cdot R_{32} - n_1^3 \cdot R_{12}) E_2^2 + \Delta n_\phi$ , where  $\Delta n_\phi$  is the birefringence due to the rotation of the index ellipsoid. 11.56. The longitudinal quadratic electrooptic effect can be observed along [100] and [010]. 11.57.  $\sim 6 \cdot 10^{-3}$ .

11.58.  $M_{11} - M_{12} = 1.67 \cdot 10^{-12}$  CGSE units. 11.59.  $n_0^3 R_{66} = 0.5 \cdot 10^{-13}$   $\text{cm}^2 \cdot \text{V}^{-2}$ .

$N_0^3 (R_{12} - R_{11}) = 0.87 \cdot 10^{-13}$   $\text{cm}^2 \cdot \text{V}^{-2}$ . 11.60.  $(1/2) (n_3 \cdot M_{31} - n_2^3 \cdot M_{21}) = 5 \cdot 10^{-11}$  CGSE units;  $(1/2) (n_3^3 \cdot M_{11} - n_3 \cdot M_{33}) = 12 \cdot 10^{-11}$  CGSE units;  $(1/2) (n_2^3 M_{21} - n_1^3 M_{11}) = 11 \cdot 10^{-11}$  CGSE units.

## § 12

12.9. 44 °C. 12.15.  $\theta = 21^\circ$ . 12.16.  $1.8 \cdot 10^6$  W/cm<sup>2</sup>. 12.17.  $L_{\text{coh}} = 52.5$  μm for  $\theta = 30^\circ$ . 12.18.  $P_{2\omega} = 1.46 \cdot 10^4$  W/cm<sup>2</sup> for  $\theta = 30^\circ$ ,  $P_{2\omega} = 0$  for  $\theta = 90^\circ$ .

12.19.  $L_{\text{coh}} = 35.5$  μm for  $\theta + 5^\circ$  and  $L_{\text{coh}} = 49.3$  μm for  $\theta - 5^\circ$ .

12.20. SH output power reduction factor is  $2.6 \cdot 10^{-4}$ ,  $8.4 \cdot 10^{-6}$ , and  $8.7 \cdot 10^{-7}$ , respectively. 12.21.  $\theta = 11.5^\circ$ . 12.25. 37.5 mm. 12.26. 53 mm. 12.28. SH output power is reduced by a factor of 100.

## § 13:

13.4.  $m$ ,  $mm$ ,  $\bar{4}$ ,  $\bar{4}2m$ . 13.6. In accord with the symmetry of rochelle salt (symmetry class 222), the two optic axes are equivalent; hence, the magnitude and sign of the specific rotation along the optic axes must be the same. 13.7. Along [001]. 13.9. Rotation angle is zero if the optic axes lie in the plane perpendicular to  $X_1$  or  $X_2$ . Rotation angles are equal but of opposite hands if the optic axes lie in the plane perpendicular to  $X_3$ . 13.10. (i) forbidden by virtue of the symmetry conditions; (ii) allowed; specific rotations along the optic axes must be of equal magnitudes and opposite hands. 13.13. Perpendicular to one of the optic axes. 13.14. Differ both in sign and in magnitude.

13.15.  $n_1 - n_r = 0.44 \cdot 10^{-5}$ . 13.16. One of the principal axes of the tensor  $[g_{ij}]$ , say,  $X_3$ , lies in the symmetry plane, and two others,  $X_1$  and  $X_2$ , are at  $45^\circ$  to the symmetry plane. In this case the tensor referred to the principal axes is

$$\begin{bmatrix} \sqrt{g_{12}^2 + g_{23}^2} & 0 & 0 \\ 0 & -\sqrt{g_{12}^2 + g_{23}^2} & 0 \\ 0 & 0 & 0 \end{bmatrix}$$

13.17. Identical for both axes. 13.18.  $d \simeq 4.16$  mm. 13.20. Because of rotation of the polarization plane in quartz, the angle of rotation in the plate of the indicated thickness is below  $180^\circ$  for visible light of any colour.

§ 14

14.25.  $c_{ij}$  in  $10^{11}$  dyne/cm $^2$ :  $c_{11} = 16$ ,  $c_{22} = 8.72$ ,  $c_{44} = 4.12$ ,  $c_{55} = 4.27$ ,  $c_{66} = 4.27$ . 14.26. RbI. 14.27. The velocities of longitudinal and shear waves propagating along [100], [110], and [111] in units of  $10^5$  cm/s are, respectively:

$v_l$	1.9	1.84	1.82
$v_t$	1.01	1.11	1.08

14.28.  $c_{ij}$  in  $10^{11}$  dyne/cm $^2$ :  $c_{11} = 35.8$ ,  $c_{33} = 47.9$ ,  $c_{44} = 12.5$ ,  $c_{66} = 14.7$ ,  $c_{12} = 26.9$ . 14.29. 6.8 cm. 14.30.  $c_{ij}$  in  $10^{11}$  dyne/cm $^2$ :  $c_{11} = 2.65$ ,  $c_{12} = 0.43$ ,  $c_{44} = 0.42$ . 14.32.  $c_{ij}$  in  $10^{11}$  dyne/cm:  $c_{11} = 16.8$ ,  $c_{12} = 7.82$ ,  $c_{13} = 7.10$ ,  $c_{33} = 18.9$ ,  $c_{44} = 5.46$ . 14.34.  $\approx 25^\circ$ . 14.35.  $c_{33}$ ,  $c_{44}$ ,  $c_{12}$ ,  $c_{11}$ ,  $c_{14}$ .

14.37.  $v$  in  $10^5$  cm/s: (i)  $v_l = 3.77$ ,  $v_t = 1.63$ , (ii)  $v_l = 3.89$ ,  $v_t = 1.87$ .

14.40.  $v_{\max} = 2.168 \cdot 10^5$  cm/s,  $v_{\min} = 1.811 \cdot 10^5$  cm/s. 14.43.  $c_{ij}$  in  $10^{11}$  dyne/cm $^2$ :  $c_{11} = 7.49$ ,  $c_{33} = 8.45$ ,  $c_{66} = 1.44$ ,  $c_{44} = 1.32$ . 14.46. For shear waves propagating in the plane  $X_2X_3$  ( $\mathbf{n}(0, n_2, n_3)$ ,  $\mathbf{u}(1, 0, 0)$ )

$$T_\tau = \alpha_{11}n_2^2 + \alpha_{33}n_3^2 - \frac{1}{2}\beta - \frac{1}{2} \frac{T_c 66 c_{66} n_2^2 + T_c 44 c_{44} n_3^2}{c_{66} n_2^2 + c_{44} n_3^2}$$

14.47. 2.68 cm. 14.48. If  $\theta$  is the angle between the wavefront normal and the axis  $X_1$ , then the piezoelectrically nonactive waves correspond to the following values of  $\theta$ :  $0^\circ$ ,  $90^\circ$ ,  $180^\circ$ ,  $270^\circ$ . The waves with maximum piezoelectric activity correspond to the following values of  $\theta$ :  $45^\circ$ ,  $135^\circ$ ,  $225^\circ$ ,  $315^\circ$ . 14.50.  $c_{ij}$  in  $10^{11}$  dyne/cm $^2$ :  $c_{11} = 12.10$ ,  $c_{12} = 4.82$ ,  $c_{33} = 5.13$ ,  $c_{44} = 1.85$ ,  $c_{66} = 3.65$ .

§ 15

15.8.  $s_{mn}^S$  in  $10^{-13}$  CGSE units:  $s_{11}^S = 12.77$ ,  $s_{33}^S = 9.73$ ,  $s_{12}^S = -1.81$ ,  $s_{13}^S = -1.23$ ,  $s_{44}^S = 19.98$ ,  $s_{66}^S = 29.16$ ,  $s_{14}^S = 4.52$ . 15.11. The capacitor's capacitance at high frequencies is twice as small as that at low frequencies.

15.16.  $\Delta T_1 = 2.33 \cdot 10^{-3}$  K,  $\Delta T_2 = 4 \cdot 10^{-3}$  K. 15.19.  $\Delta f/f = 1.3 \cdot 10^{-5}$ .

15.20.  $\Delta f/f = 2 \cdot 10^{-6}$ .

## REFERENCES

1. Nye, J.F. *Physical Properties of Crystals*, Oxford, Clarendon Press, 1964.
2. Sirotin, Yu.I., Shaskol'skaya, M.P. *Fundamentals of Crystal Physics*, Mir Publishers, Moscow, 1982.
3. Shaskol'skaya, M.P. *Crystallography*, Vissaya Shkola, Moscow, 1976 (in Russian).
4. Wooster, W.A. *Tensors and Group Theory for the Physical Properties of Crystals*, Clarendon Press, Oxford, 1973.
5. Zernike, F., Midwinter, J.E. *Applied Nonlinear Optics*, John Wiley and Sons, New York, Sydney, Toronto, London, 1973.
6. Voronkova, E.M., Grechushnikov, B.N., Distler, G.I., Petrov., I.P. *Optical Materials for Infrared Technology*, Nauka, Moscow, 1965 (in Russian).
7. Zheludev, I.S. *Physics of Crystal Dielectrics*, Nauka, Moscow, 1968 (in Russian).
8. Mustel', E.R., Parygin, V.N. *Methods of Modulation and Scanning of Light*, Nauka, Moscow, 1970 (in Russian).
9. Shubnikov, A.V. *Selected Works on Crystallography*, Nauka, Moscow, 1970 (in Russian).
10. Sonin, A.S., Vasilevskaya, A.S. *Electrooptic Crystals*, Atomizdat, Moscow, 1973 (in Russian).
11. Landolt-Bornstein, Lahlenwerte und Functionen aus Naturwissenschaften und Technik Neue Serie, Yrapp III. Band 1, Springer Verlag, 1966.
12. Shubnikov, A.V. *Optical Crystallography*, Publishing House of the USSR Academy of Sciences, 1950 (in Russian).
13. Mason, W.P. *Piezoelectric Crystals and Their Application to Ultrasonics*, New York, 1950.
14. *Modern Crystallography*, Vol. 4, Nauka, Moscow, 1981 (in Russian).
15. Fedorov, F.I. *Theory of Elastic Waves in Crystals*, Plenum Press, New York, 1968.
16. Physical Acoustics, ed. W.P. Mason, Vol. 1, p.A., p.B., Academic Press, New York-London, 1964.
17. *Ultrasound—Little Encyclopaedia*, ed. I.P. Golyamina, Soviet Encyclopaedia, Moscow, 1979.
18. Bondarenko, V.S., Blistanov, A.A., Perelomova, N.V. *Acoustic Crystals*, ed. M.P. Shaskolskaya, Nauka, Moscow, 1982 (in Russian).

# APPENDIX

*Table 1*  
**Notation of 32 Symmetry Classes**

System of symmetry	Notation		
	international	after Schoenflies	symmetry formula
Triclinic	1	$C_1$	$L_1$
	$\bar{1}$	$C_i$	$C$
Monoclinic	2	$C_2$	$L_2$
	$m$	$C_s$	$P$
	$2/m$	$C_{2h}$	$L_2PC$
Rhombic	222	$D_2$	$3L_2$
	$mm2$	$C_{2v}$	$L_22P$
	$mmm$	$D_{2h}$	$3L_23PC$
Tetragonal	4	$C_4$	$L_4$
	$4/m$	$C_{4h}$	$L_4PC$
	422	$D_4$	$L_44L_2$
	$4mm$	$C_{4v}$	$L_44P$
	$4/mmm$	$D_{4h}$	$L_44L_25PC$
	$\bar{4}$	$S_4$	$L_{\bar{4}}$
	$\bar{4}2m$	$D_{2d}$	$L_{\bar{4}}2L_22P$
Trigonal	3	$C_3$	$L_3$
	$\bar{3}$	$C_{3i}$	$L_3C$
	32	$D_3$	$L_33L_2$
	$3m$	$C_{3v}$	$L_33P$
	$\bar{3}m$	$D_{3d}$	$L_33L_23PC$
Hexagonal	6	$C_6$	$L_6$
	$6/m$	$C_{6h}$	$L_6PC$
	622	$D_6$	$L_66L_2$
	$6mm$	$C_{6v}$	$L_66P$
	$6/mmm$	$D_{6h}$	$L_66L_27PC$
	$\bar{6}$	$C_{3h}$	$L_3P$
	$\bar{6}m2$	$D_{3h}$	$L_33L_24P$

Table 1 (cont'd)

System of symmetry	Notation		
	international	after Schoenflies	symmetry formula
Cubic	23	$T$	$4L_33L_2$
	$m3$	$T_h$	$4L_33L_23PC$
	432	0	$4L_33L_46L_2$
	$\bar{4}3m$	$T_d$	$4L_33L_46P$
	$m3m$	$0_h$	$4L_33L_46L_29PC$

Table 2  
Symbols of Symmetry Elements on Stereographic Projections

Symmetry element	Symbol	International symbol
Centre of symmetry	No symbol	$\bar{1}$
Plane of mirror reflection	Solid line or arc of circle	$m$
Rotational axes		
Twofold (diad) axis		2
Threefold axis		3
Fourfold axis		4
Sixfold axis		6
Inversion axes		
Onefold axis $\equiv$ center of symmetry	No symbol	$\bar{1}$
Twofold axis $\equiv$ mirror reflection plane perpendicular to the axis	Same as for mirror reflection plane	$\bar{2} (\equiv m)$
Threefold axis		$\bar{3}$
Fourfold axis		$\bar{4}$
Sixfold axis		$\bar{6} (\equiv 3/m)$

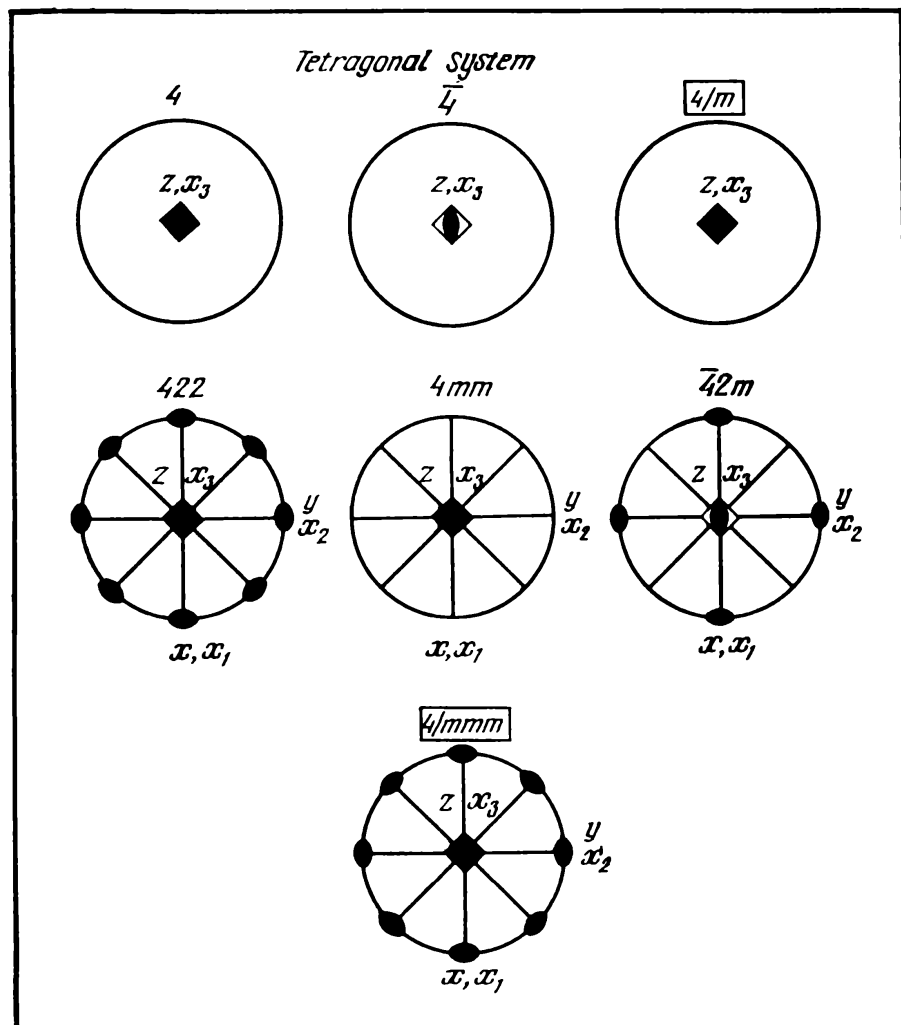
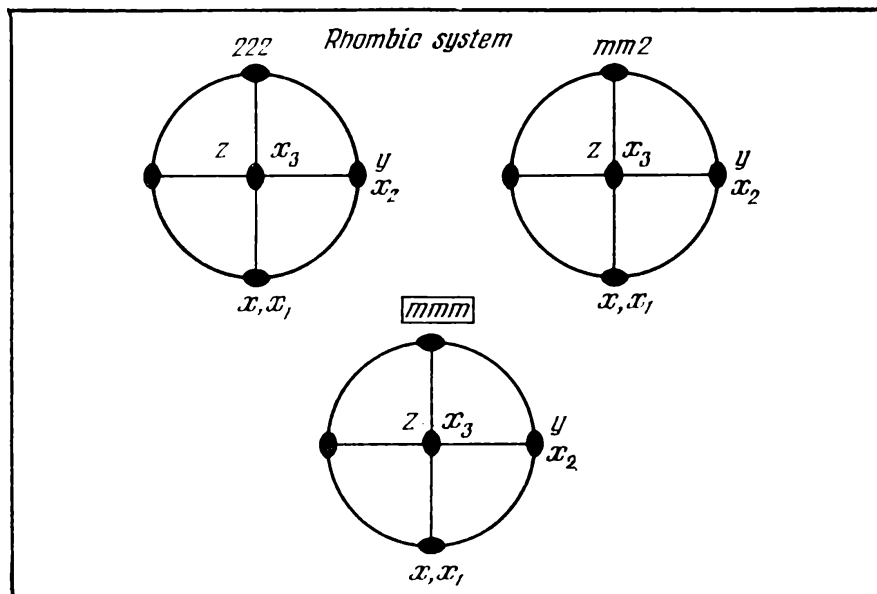
**Table 3**  
**Rules for Setting of Crystals According to Symmetry System**

<p><b>Notation:</b>  <math>z</math> 2,3,4,6-symmetry axes  <math>m</math>-normal to the symmetry plane  <math>c_0</math></p>	<p><b>Triclinic</b></p> $a_0 \neq b_0 \neq c_0$ $\alpha \neq \beta \neq \gamma \neq 90^\circ$	<p><b>Monoclinic</b></p> $a_0 \neq b_0 \neq c_0$ $\alpha = \gamma = 90^\circ \neq \beta$	<p><b>Rhombic</b></p> $2, m$ $a_0 \neq b_0 \neq c_0$ $\alpha = \beta = \gamma = 90^\circ$
<p><b>Trigonal and hexagonal</b></p> $6, \bar{6}, 3, \bar{3}$ $a_0 = b_0 \neq c_0$ $\alpha = \beta = 90^\circ$ $\gamma = 120^\circ$	<p><b>Tetragonal</b></p> $4, \bar{4}$ $a_0 = b_0 \neq c_0$ $\alpha = \beta = \gamma = 90^\circ$	<p><b>Cubic</b></p> $4, \bar{4}, 2$ $a_0 = b_0 = c_0$ $\alpha = \beta = \gamma = 90^\circ$	

**Table 4**  
**Symmetry Elements and Rules for Choosing Axes for 32 Crystallographic Classes (symbols referring to centrosymmetrical classes are given in boxes)**

<p><b>Triclinic system</b></p>	
<p><b>Monoclinic system</b></p>	

Table 4 (cont'd)



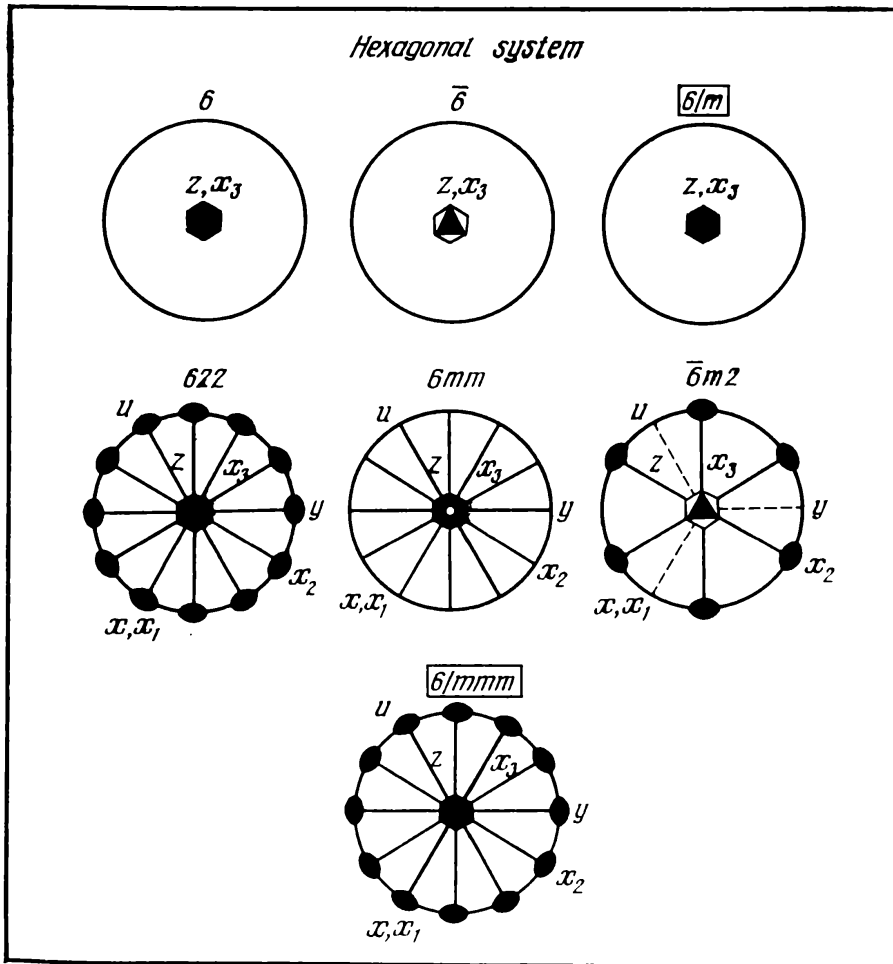
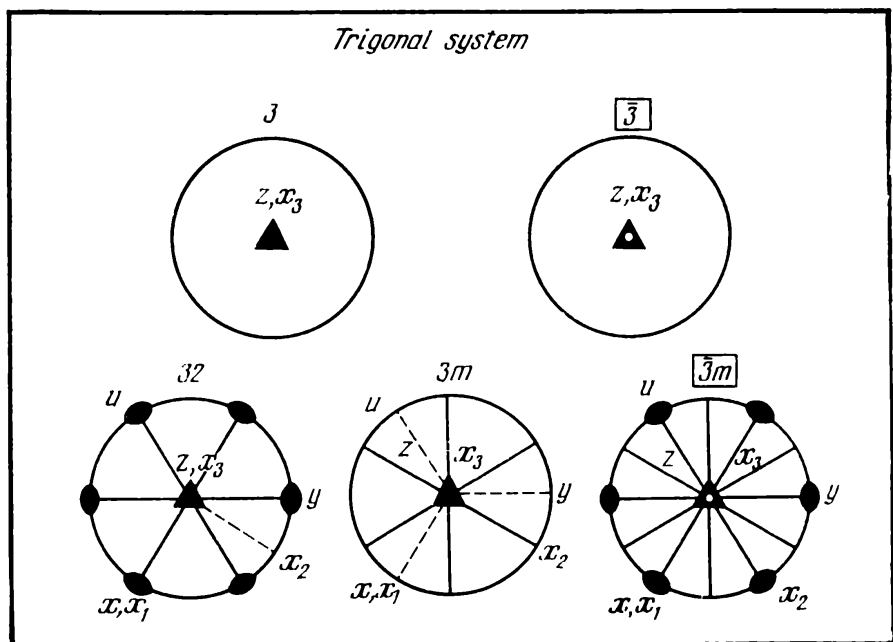


Table 4 (cont'd)

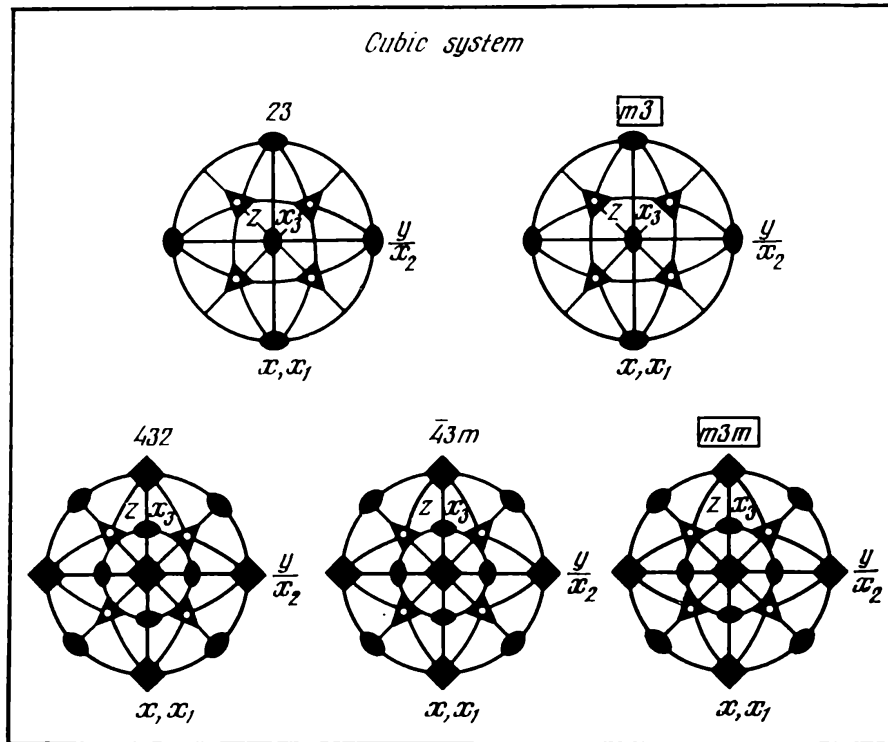


Table 5  
Rules for Choosing Crystallophysical Axes

Symmetry system	$x_3$	$x_2$	$x_1$
Triclinic	[001]	In the plane perpendicular to [001]	
Monoclinic	[001]	[010]	In the plane (100)
Rhombic	[001]	[010]	[100]
Tetragonal	[001]	[010]	[100]
Trigonal and hexagonal	[0001]	[0110]	[2110]
Cubic	[001]	[010]	[100]

Table 6

Matrices of Piezoelectric Moduli ( $d_{ij}$ ) and Piezoelectric Constants ( $g_{ij}$ )

*Centrosymmetrical classes: all moduli equal zero.*  
*Noncentrosymmetrical classes:*

*Triclinic system*  
 Class 1

$$\begin{pmatrix} d_{11} & d_{12} & d_{13} & d_{14} & d_{15} & d_{16} \\ d_{21} & d_{22} & d_{23} & d_{24} & d_{25} & d_{26} \\ d_{31} & d_{32} & d_{33} & d_{34} & d_{35} & d_{36} \end{pmatrix}_{(18)}$$

*Monoclinic system*

Class 2,  $2||X_2$   
 (standard orientation)

$$\begin{pmatrix} 0 & 0 & 0 & d_{14} & 0 & d_{16} \\ d_{21} & d_{22} & d_{23} & 0 & d_{25} & 0 \\ 0 & 0 & 0 & d_{34} & 0 & d_{36} \end{pmatrix}_{(8)}$$

Class 2,  $2||X_3$

$$\begin{pmatrix} 0 & 0 & 0 & d_{14} & d_{15} & 0 \\ 0 & 0 & 0 & d_{24} & d_{25} & 0 \\ d_{31} & d_{32} & d_{33} & 0 & 0 & d_{36} \end{pmatrix}_{(8)}$$

Class  $m$ ,  $m \perp X_2$  (standard orientation)

$$\begin{pmatrix} d_{11} & d_{12} & d_{13} & 0 & d_{15} & 0 \\ 0 & 0 & 0 & d_{24} & 0 & d_{26} \\ d_{31} & d_{32} & d_{33} & 0 & d_{35} & 0 \end{pmatrix}_{(10)}$$

Class  $m$ ,  $m \perp X_3$

$$\begin{pmatrix} d_{11} & d_{12} & d_{13} & 0 & 0 & d_{16} \\ d_{21} & d_{22} & d_{23} & 0 & 0 & d_{26} \\ 0 & 0 & 0 & d_{34} & d_{35} & 0 \end{pmatrix}_{(10)}$$

*Rhombic system*

Class 222

$$\begin{pmatrix} 0 & 0 & 0 & d_{14} & 0 & 0 \\ 0 & 0 & 0 & 0 & d_{25} & 0 \\ 0 & 0 & 0 & 0 & 0 & d_{36} \end{pmatrix}_{(3)}$$

Class  $mm2$

$$\begin{pmatrix} 0 & 0 & 0 & 0 & d_{15} & 0 \\ 0 & 0 & 0 & d_{24} & 0 & 0 \\ d_{31} & d_{32} & d_{33} & 0 & 0 & 0 \end{pmatrix}_{(5)}$$

*Tetragonal system*

Class 4

$$\begin{pmatrix} 0 & 0 & 0 & d_{14} & -d_{15} & 0 \\ 0 & 0 & 0 & d_{15} & d_{14} & 0 \\ d_{31} & d_{31} & d_{33} & 0 & 0 & 0 \end{pmatrix}_{(4)}$$

Class  $\bar{4}$

$$\begin{pmatrix} 0 & 0 & 0 & d_{14} & d_{15} & 0 \\ 0 & 0 & 0 & -d_{15} & d_{14} & 0 \\ d_{31} & -d_{31} & 0 & 0 & 0 & d_{36} \end{pmatrix}_{(4)}$$

Class 422

$$\begin{pmatrix} 0 & 0 & 0 & d_{14} & 0 & 0 \\ 0 & 0 & 0 & 0 & -d_{14} & 0 \\ 0 & 0 & 0 & 0 & 0 & 0 \end{pmatrix}_{(1)}$$

Class 4mm

$$\begin{pmatrix} 0 & 0 & 0 & 0 & d_{15} & 0 \\ 0 & 0 & 0 & d_{15} & 0 & 0 \\ d_{31} & d_{31} & d_{33} & 0 & 0 & 0 \end{pmatrix}_{(3)}$$

Table 6 (cont'd)

Class  $\bar{4}2m, 2||X_1$   
(standard orientation)

$$\begin{pmatrix} 0 & 0 & 0 & d_{14} & 0 & 0 \\ 0 & 0 & 0 & 0 & d_{14} & 0 \\ 0 & 0 & 0 & 0 & 0 & d_{36} \end{pmatrix}_{(2)}$$

Trigonal system

Class 3

$$\begin{pmatrix} d_{11} & -d_{11} & 0 & d_{14} & -d_{15} & -2d_{22} \\ -d_{22} & d_{22} & 0 & d_{15} & -d_{14} & -2d_{11} \\ d_{31} & d_{31} & d_{33} & 0 & 0 & 0 \end{pmatrix}_{(6)} \quad \begin{pmatrix} d_{11} & -d_{11} & 0 & d_{14} & 0 & 0 \\ 0 & 0 & 0 & 0 & -d_{14} & -2d_{11} \\ 0 & 0 & 0 & 0 & 0 & 0 \end{pmatrix}_{(2)}$$

Class  $3m, m \perp X_1$  (standard orientation)

$$\begin{pmatrix} 0 & 0 & 0 & 0 & d_{15} & -2d_{22} \\ -d_{22} & d_{22} & 0 & d_{15} & 0 & 0 \\ d_{31} & d_{31} & d_{33} & 0 & 0 & 0 \end{pmatrix}_{(4)} \quad \begin{pmatrix} d_{11} & -d_{11} & 0 & 0 & d_{15} & 0 \\ 0 & 0 & 0 & d_{15} & 0 & -2d_{11} \\ d_{31} & d_{31} & d_{33} & 0 & 0 & 0 \end{pmatrix}_{(4)}$$

Hexagonal system

Class 6

$$\begin{pmatrix} 0 & 0 & 0 & d_{14} & -d_{15} & 0 \\ 0 & 0 & 0 & d_{15} & -d_{14} & 0 \\ d_{31} & d_{31} & d_{33} & 0 & 0 & 0 \end{pmatrix}_{(4)} \quad \begin{pmatrix} 0 & 0 & 0 & 0 & d_{15} & 0 \\ 0 & 0 & 0 & d_{15} & 0 & 0 \\ d_{31} & d_{31} & d_{33} & 0 & 0 & 0 \end{pmatrix}_{(3)}$$

Same as class 4:

Class 622

Same as class 4mm;

Class  $\bar{6}$

$$\begin{pmatrix} 0 & 0 & 0 & d_{14} & 0 & 0 \\ 0 & 0 & 0 & 0 & -d_{14} & 0 \\ 0 & 0 & 0 & 0 & 0 & 0 \end{pmatrix}_{(1)} \quad \begin{pmatrix} -d_{11} & -d_{11} & 0 & 0 & 0 & -2d_{22} \\ -d_{22} & d_{22} & 0 & 0 & 0 & -2d_{11} \\ 0 & 0 & 0 & 0 & 0 & 0 \end{pmatrix}_{(2)}$$

Same as class 422;  
class  $\bar{6}m2, m \perp X_1$   
(standard orientation)

Class  $\bar{6}m2, m \perp X_2$

$$\begin{pmatrix} 0 & 0 & 0 & 0 & 0 & -2d_{22} \\ -d_{22} & d_{22} & 0 & 0 & 0 & 0 \\ 0 & 0 & 0 & 0 & 0 & 0 \end{pmatrix}_{(1)} \quad \begin{pmatrix} d_{11} & -d_{11} & 0 & 0 & 0 & 0 \\ 0 & 0 & 0 & 0 & 0 & -2d_{11} \\ 0 & 0 & 0 & 0 & 0 & 0 \end{pmatrix}_{(1)}$$

Cubic system

Class 432

$$\begin{pmatrix} 0 & 0 & 0 & 0 & 0 & 0 \\ 0 & 0 & 0 & 0 & 0 & 0 \\ 0 & 0 & 0 & 0 & 0 & 0 \end{pmatrix}_{(0)} \quad \begin{pmatrix} 0 & 0 & 0 & d_{14} & 0 & 0 \\ 0 & 0 & 0 & 0 & d_{14} & 0 \\ 0 & 0 & 0 & 0 & 0 & d_{14} \end{pmatrix}_{(1)}$$

Table 7

**Matrices of Piezoelectric Constants ( $h_{ij}$ ) and ( $e_{ij}$ )  
for Crystals in Which These Matrices Differ from  
( $d_{ij}$ ) and ( $g_{ij}$ )**

Class 3	Class 32
$\begin{pmatrix} h_{11} & -h_{11} & 0 & h_{14} & h_{15} & -h_{22} \\ -h_{22} & h_{22} & 0 & h_{15} & -h_{14} & -h_{11} \\ h_{31} & h_{31} & h_{33} & 0 & 0 & 0 \end{pmatrix}_{(6)}$	$\begin{pmatrix} h_{11} & -h_{11} & 0 & h_{14} & 0 & 0 \\ 0 & 0 & 0 & 0 & -h_{14} & -h_{11} \\ 0 & 0 & 0 & 0 & 0 & 0 \end{pmatrix}_{(2)}$
Class $\bar{6}$	Class $3m, m \perp X_1$
$\begin{pmatrix} h_{11} & -h_{11} & 0 & 0 & 0 & -h_{22} \\ -h_{22} & h_{22} & 0 & 0 & 0 & -h_{11} \\ 0 & 0 & 0 & 0 & 0 & 0 \end{pmatrix}_{(3)}$	$\begin{pmatrix} 0 & 0 & 0 & 0 & h_{15} & -h_{22} \\ -h_{22} & h_{22} & 0 & h_{15} & 0 & 0 \\ h_{31} & h_{31} & h_{33} & 0 & 0 & 0 \end{pmatrix}_{(4)}$
Class $\bar{6m}2$	
$\begin{pmatrix} h_{11} & -h_{11} & 0 & 0 & 0 & 0 \\ 0 & 0 & 0 & 0 & 0 & -h_{11} \\ 0 & 0 & 0 & 0 & 0 & 0 \end{pmatrix}_{(1)}$	

Table 8

**Matrices of Piezoelectric Moduli ( $d_{ij}$ )  
for Piezoelectric Textures**

Group $\infty$	Group $\infty m$
$\begin{pmatrix} 0 & 0 & 0 & d_{14} & d_{15} & 0 \\ 0 & 0 & 0 & d_{15} & -d_{14} & 0 \\ d_{31} & d_{31} & d_{33} & 0 & 0 & 0 \end{pmatrix}_{(4)}$	$\begin{pmatrix} 0 & 0 & 0 & 0 & d_{15} & 0 \\ 0 & 0 & 0 & d_{15} & 0 & 0 \\ d_{31} & d_{31} & d_{33} & 0 & 0 & 0 \end{pmatrix}_{(3)}$
Group $\infty 2$	
$\begin{pmatrix} 0 & 0 & 0 & d_{14} & 0 & 0 \\ 0 & 0 & 0 & 0 & -d_{14} & 0 \\ 0 & 0 & 0 & 0 & 0 & 0 \end{pmatrix}_{(4)}$	

Table 9

**Matrices of Elastic Compliances ( $s_{ij}$ )  
and Elastic Stiffnesses ( $c_{ij}$ )**

*Triclinic system*  
Both classes

$\begin{pmatrix} s_{11} & s_{12} & s_{13} & s_{14} & s_{15} & s_{16} \\ s_{12} & s_{22} & s_{23} & s_{24} & s_{25} & s_{26} \\ s_{13} & s_{23} & s_{33} & s_{34} & s_{35} & s_{36} \\ s_{14} & s_{24} & s_{34} & s_{44} & s_{45} & s_{46} \\ s_{15} & s_{25} & s_{35} & s_{45} & s_{55} & s_{56} \\ s_{16} & s_{26} & s_{36} & s_{46} & s_{56} & s_{66} \end{pmatrix}_{(21)}$	$\begin{pmatrix} c_{11} & c_{12} & c_{13} & c_{14} & c_{15} & c_{16} \\ c_{12} & c_{22} & c_{23} & c_{24} & c_{25} & c_{26} \\ c_{13} & c_{23} & c_{33} & c_{34} & c_{35} & c_{36} \\ c_{14} & c_{24} & c_{34} & c_{44} & c_{45} & c_{46} \\ c_{15} & c_{25} & c_{35} & c_{45} & c_{55} & c_{56} \\ c_{16} & c_{26} & c_{36} & c_{46} & c_{56} & c_{66} \end{pmatrix}_{(21)}$
---	---

Table 9 (cont'd)

*Monoclinic system*All classes,  $2 \parallel X_2$  (standard orientation)

$$\begin{pmatrix} s_{11} & s_{12} & s_{13} & 0 & s_{15} & 0 \\ s_{12} & s_{22} & s_{23} & 0 & s_{25} & 0 \\ s_{13} & s_{23} & s_{33} & 0 & s_{35} & 0 \\ 0 & 0 & 0 & s_{44} & 0 & s_{46} \\ s_{15} & s_{25} & s_{35} & 0 & s_{55} & 0 \\ 0 & 0 & 0 & s_{46} & 0 & s_{66} \end{pmatrix} \quad (13)$$

$$\begin{pmatrix} c_{11} & c_{12} & c_{13} & 0 & c_{15} & 0 \\ c_{12} & c_{22} & c_{23} & 0 & c_{25} & 0 \\ c_{13} & c_{23} & c_{33} & 0 & c_{35} & 0 \\ 0 & 0 & 0 & c_{44} & 0 & c_{46} \\ c_{15} & c_{25} & c_{35} & 0 & c_{55} & 0 \\ 0 & 0 & 0 & c_{46} & 0 & c_{66} \end{pmatrix} \quad (13)$$

*Rhombic system*

All classes

$$\begin{pmatrix} s_{11} & s_{12} & s_{13} & 0 & 0 & 0 \\ s_{12} & s_{22} & s_{23} & 0 & 0 & 0 \\ s_{13} & s_{23} & s_{33} & 0 & 0 & 0 \\ 0 & 0 & 0 & s_{44} & 0 & 0 \\ 0 & 0 & 0 & 0 & s_{55} & 0 \\ 0 & 0 & 0 & 0 & 0 & s_{66} \end{pmatrix} \quad (9)$$

$$\begin{pmatrix} c_{11} & c_{12} & c_{13} & 0 & 0 & 0 \\ c_{12} & c_{22} & c_{23} & 0 & 0 & 0 \\ c_{13} & c_{23} & c_{33} & 0 & 0 & 0 \\ 0 & 0 & 0 & c_{44} & 0 & 0 \\ 0 & 0 & 0 & 0 & c_{55} & 0 \\ 0 & 0 & 0 & 0 & 0 & c_{66} \end{pmatrix} \quad (9)$$

*Tetragonal system*Classes  $4, \bar{4}, 4/m$ 

$$\begin{pmatrix} s_{11} & s_{12} & s_{13} & 0 & 0 & s_{16} \\ s_{12} & s_{11} & s_{13} & 0 & 0 & -s_{16} \\ s_{13} & s_{13} & s_{33} & 0 & 0 & 0 \\ 0 & 0 & 0 & s_{44} & 0 & 0 \\ 0 & 0 & 0 & 0 & s_{44} & 0 \\ s_{16} & -s_{16} & 0 & 0 & 0 & s_{66} \end{pmatrix} \quad (7)$$

$$\begin{pmatrix} c_{11} & c_{12} & c_{13} & 0 & 0 & c_{16} \\ c_{12} & c_{11} & c_{13} & 0 & 0 & -c_{16} \\ c_{13} & c_{13} & c_{33} & 0 & 0 & 0 \\ 0 & 0 & 0 & c_{44} & 0 & 0 \\ 0 & 0 & 0 & 0 & c_{44} & 0 \\ c_{16} & -c_{16} & 0 & 0 & 0 & c_{66} \end{pmatrix} \quad (7)$$

Classes  $4mm, \bar{4}2m, 422, 4/mmm$ 

$$\begin{pmatrix} s_{11} & s_{12} & s_{13} & 0 & 0 & 0 \\ s_{12} & s_{11} & s_{13} & 0 & 0 & 0 \\ s_{13} & s_{13} & s_{33} & 0 & 0 & 0 \\ 0 & 0 & 0 & s_{44} & 0 & 0 \\ 0 & 0 & 0 & 0 & s_{44} & 0 \\ 0 & 0 & 0 & 0 & 0 & s_{66} \end{pmatrix} \quad (6)$$

$$\begin{pmatrix} c_{11} & c_{12} & c_{13} & 0 & 0 & 0 \\ c_{12} & c_{11} & c_{13} & 0 & 0 & 0 \\ c_{13} & c_{13} & c_{33} & 0 & 0 & 0 \\ 0 & 0 & 0 & c_{44} & 0 & 0 \\ 0 & 0 & 0 & 0 & c_{44} & 0 \\ 0 & 0 & 0 & 0 & 0 & c_{66} \end{pmatrix} \quad (6)$$

*Trigonal system*Classes  $3, \bar{3}$ 

$$\begin{pmatrix} s_{11} & s_{12} & s_{13} & s_{14} & -s_{25} & 0 \\ s_{12} & s_{11} & s_{13} & -s_{14} & s_{25} & 0 \\ s_{13} & s_{13} & s_{33} & 0 & 0 & 0 \\ s_{14} & -s_{14} & 0 & s_{44} & 0 & 2s_{25} \\ -s_{25} & s_{25} & 0 & 0 & s_{44} & 2s_{14} \\ 0 & 0 & 0 & 2s_{25} & 2s_{14} & 2(s_{11} - s_{12}) \end{pmatrix} \quad (7)$$

Table 9 (cont'd)

$$\left( \begin{array}{cccccc} c_{11} & c_{12} & c_{13} & c_{14} & -c_{25} & 0 \\ c_{12} & c_{11} & c_{13} & -c_{14} & c_{25} & 0 \\ c_{13} & c_{13} & c_{33} & 0 & 0 & 0 \\ c_{14} & -c_{14} & 0 & c_{44} & 0 & c_{25} \\ -c_{25} & c_{25} & 0 & 0 & c_{44} & c_{14} \\ 0 & 0 & 0 & c_{25} & c_{14} & \frac{1}{2}(c_{11}-c_{12}) \end{array} \right) (7)$$

Classes 32,  $\bar{3}m$ , 3m

$$\left( \begin{array}{cccccc} s_{11} & s_{12} & s_{13} & s_{14} & 0 & 0 \\ s_{12} & s_{11} & s_{13} & -s_{14} & 0 & 0 \\ s_{13} & s_{13} & s_{33} & 0 & 0 & 0 \\ s_{14} & -s_{14} & 0 & s_{44} & 0 & 0 \\ 0 & 0 & 0 & 0 & s_{24} & 2s_{14} \\ 0 & 0 & 0 & 0 & 2s_{14} & 2(s_{11}-s_{12}) \end{array} \right) (6)$$

$$\left( \begin{array}{cccccc} c_{11} & c_{12} & c_{13} & c_{14} & 0 & 0 \\ c_{12} & c_{11} & c_{13} & -c_{14} & 0 & 0 \\ c_{13} & c_{13} & c_{33} & 0 & 0 & 0 \\ c_{14} & -c_{14} & 0 & c_{44} & 0 & 0 \\ 0 & 0 & 0 & 0 & c_{44} & c_{14} \\ 0 & 0 & 0 & 0 & c_{14} & \frac{1}{2}(c_{11}-c_{12}) \end{array} \right) (6)$$

Hexagonal system  
All classes

$$\left( \begin{array}{cccccc} s_{11} & s_{12} & s_{13} & 0 & 0 & 0 \\ s_{12} & s_{11} & s_{13} & 0 & 0 & 0 \\ s_{13} & s_{13} & s_{33} & 0 & 0 & 0 \\ 0 & 0 & 0 & s_{44} & 0 & 0 \\ 0 & 0 & 0 & 0 & s_{44} & 0 \\ 0 & 0 & 0 & 0 & 0 & 2(s_{11}-s_{12}) \end{array} \right) (5)$$

$$\left( \begin{array}{cccccc} c_{11} & c_{12} & c_{13} & 0 & 0 & 0 \\ c_{12} & c_{11} & c_{13} & 0 & 0 & 0 \\ c_{13} & c_{13} & c_{33} & 0 & 0 & 0 \\ 0 & 0 & 0 & c_{44} & 0 & 0 \\ 0 & 0 & 0 & 0 & c_{44} & 0 \\ 0 & 0 & 0 & 0 & 0 & \frac{1}{2}(c_{11}-c_{12}) \end{array} \right) (5)$$

Table 9 (cont'd)

*Cubic system*  
All classes

$$\begin{pmatrix} s_{11} & s_{12} & s_{12} & 0 & 0 & 0 \\ s_{12} & s_{11} & s_{12} & 0 & 0 & 0 \\ s_{12} & s_{12} & s_{11} & 0 & 0 & 0 \\ 0 & 0 & 0 & s_{44} & 0 & 0 \\ 0 & 0 & 0 & 0 & s_{44} & 0 \\ 0 & 0 & 0 & 0 & 0 & s_{44} \end{pmatrix} (3) \quad \begin{pmatrix} c_{11} & c_{12} & c_{12} & 0 & 0 & 0 \\ c_{12} & c_{11} & c_{12} & 0 & 0 & 0 \\ c_{12} & c_{12} & c_{11} & 0 & 0 & 0 \\ 0 & 0 & 0 & c_{44} & 0 & 0 \\ 0 & 0 & 0 & 0 & c_{44} & 0 \\ 0 & 0 & 0 & 0 & 0 & c_{44} \end{pmatrix} (3)$$

Homogeneous continuous structures (textures) represented by groups  $\infty m$ ,  $\infty$ ,  $\infty/m$ ,  $\infty/mmm$ ,  $\infty 2$

$$\begin{pmatrix} s_{11} & s_{12} & s_{13} & 0 & 0 & 0 \\ s_{12} & s_{11} & s_{13} & 0 & 0 & 0 \\ s_{13} & s_{13} & s_{33} & 0 & 0 & 0 \\ 0 & 0 & 0 & s_{44} & 0 & 0 \\ 0 & 0 & 0 & 0 & s_{44} & 0 \\ 0 & 0 & 0 & 0 & 0 & 2(s_{11} - s_{12}) \end{pmatrix}$$

$$\begin{pmatrix} c_{11} & c_{12} & c_{13} & 0 & 0 & 0 \\ c_{12} & c_{11} & c_{13} & 0 & 0 & 0 \\ c_{13} & c_{13} & c_{33} & 0 & 0 & 0 \\ 0 & 0 & 0 & c_{44} & 0 & 0 \\ 0 & 0 & 0 & 0 & c_{44} & 0 \\ 0 & 0 & 0 & 0 & 0 & \frac{1}{2} (c_{11} - c_{12}) \end{pmatrix}$$

*Isotropic medium*

$$\begin{pmatrix} s_{11} & s_{12} & s_{12} & 0 & 0 & 0 \\ s_{12} & s_{11} & s_{12} & 0 & 0 & 0 \\ s_{12} & s_{12} & s_{11} & 0 & 0 & 0 \\ 0 & 0 & 0 & 2(s_{11} - s_{12}) & 0 & 0 \\ 0 & 0 & 0 & 0 & 2(s_{11} - s_{12}) & 0 \\ 0 & 0 & 0 & 0 & 0 & 2(s_{11} - s_{12}) \end{pmatrix} (2)$$

$$\begin{pmatrix} c_{11} & c_{12} & c_{12} & 0 & 0 & 0 \\ c_{12} & c_{11} & c_{12} & 0 & 0 & 0 \\ c_{12} & c_{12} & c_{11} & 0 & 0 & 0 \\ 0 & 0 & 0 & \frac{1}{2} (c_{11} - c_{12}) & 0 & 0 \\ 0 & 0 & 0 & 0 & \frac{1}{2} (c_{11} - c_{12}) & 0 \\ 0 & 0 & 0 & 0 & 0 & \frac{1}{2} (c_{11} - c_{12}) \end{pmatrix} (2)$$

Table 10

Matrices of Piezoresistivity Constants ( $\Pi_{ij}$ )

## Triclinic system

## Both classes

$$\begin{pmatrix} \Pi_{11} & \Pi_{12} & \Pi_{13} & \Pi_{14} & \Pi_{15} & \Pi_{16} \\ \Pi_{21} & \Pi_{22} & \Pi_{23} & \Pi_{24} & \Pi_{25} & \Pi_{26} \\ \Pi_{31} & \Pi_{32} & \Pi_{33} & \Pi_{34} & \Pi_{35} & \Pi_{36} \\ \Pi_{41} & \Pi_{42} & \Pi_{43} & \Pi_{44} & \Pi_{45} & \Pi_{46} \\ \Pi_{51} & \Pi_{52} & \Pi_{53} & \Pi_{54} & \Pi_{55} & \Pi_{56} \\ \Pi_{61} & \Pi_{62} & \Pi_{63} & \Pi_{64} & \Pi_{65} & \Pi_{66} \end{pmatrix} \quad (36)$$

## Monoclinic system

## All classes

Axis 2  $\parallel X_2$ 

$$\begin{pmatrix} \Pi_{11} & \Pi_{12} & \Pi_{13} & 0 & \Pi_{15} & 0 \\ \Pi_{21} & \Pi_{22} & \Pi_{23} & 0 & \Pi_{25} & 0 \\ \Pi_{31} & \Pi_{32} & \Pi_{33} & 0 & \Pi_{35} & 0 \\ 0 & 0 & 0 & \Pi_{44} & 0 & \Pi_{46} \\ \Pi_{51} & \Pi_{52} & \Pi_{53} & 0 & \Pi_{55} & 0 \\ 0 & 0 & 0 & \Pi_{64} & 0 & \Pi_{66} \end{pmatrix} \quad (20)$$

Axis 2  $\parallel X_3$ 

$$\begin{pmatrix} \Pi_{11} & \Pi_{12} & \Pi_{13} & 0 & 0 & \Pi_{16} \\ \Pi_{21} & \Pi_{22} & \Pi_{23} & 0 & 0 & \Pi_{26} \\ \Pi_{31} & \Pi_{32} & \Pi_{33} & 0 & 0 & \Pi_{36} \\ 0 & 0 & 0 & \Pi_{44} & \Pi_{45} & 0 \\ 0 & 0 & 0 & \Pi_{54} & \Pi_{55} & 0 \\ \Pi_{61} & \Pi_{62} & \Pi_{63} & 0 & 0 & \Pi_{66} \end{pmatrix} \quad (20)$$

## Rhombic system

## All classes

$$\begin{pmatrix} \Pi_{11} & \Pi_{12} & \Pi_{13} & 0 & 0 & 0 \\ \Pi_{21} & \Pi_{22} & \Pi_{23} & 0 & 0 & 0 \\ \Pi_{31} & \Pi_{32} & \Pi_{33} & 0 & 0 & 0 \\ 0 & 0 & 0 & \Pi_{44} & 0 & 0 \\ 0 & 0 & 0 & 0 & \Pi_{55} & 0 \\ 0 & 0 & 0 & 0 & 0 & \Pi_{66} \end{pmatrix} \quad (12)$$

## Tetragonal system

Classes 4,  $\bar{4}$ ,  $4/m$ 

$$\begin{pmatrix} \Pi_{11} & \Pi_{12} & \Pi_{13} & 0 & 0 & \Pi_{16} \\ \Pi_{12} & \Pi_{11} & \Pi_{13} & 0 & 0 & -\Pi_{16} \\ \Pi_{31} & \Pi_{31} & \Pi_{33} & 0 & 0 & 0 \\ 0 & 0 & 0 & \Pi_{44} & \Pi_{45} & 0 \\ 0 & 0 & 0 & -\Pi_{45} & \Pi_{44} & 0 \\ \Pi_{61} & -\Pi_{61} & 0 & 0 & 0 & \Pi_{66} \end{pmatrix} \quad (10)$$

Table 10 (cont'd)

Classes  $4mm$ ,  $42m$ ,  $422$ ,  $4/mmm$ 

$$\begin{pmatrix} \Pi_{11} & \Pi_{12} & \Pi_{13} & 0 & 0 & 0 \\ \Pi_{12} & \Pi_{11} & \Pi_{13} & 0 & 0 & 0 \\ \Pi_{31} & \Pi_{31} & \Pi_{33} & 0 & 0 & 0 \\ 0 & 0 & 0 & \Pi_{44} & 0 & 0 \\ 0 & 0 & 0 & 0 & \Pi_{44} & 0 \\ 0 & 0 & 0 & 0 & 0 & \Pi_{66} \end{pmatrix} \quad (7)$$

Trigonal system

Classes  $3$ ,  $\bar{3}$ 

$$\begin{pmatrix} \Pi_{11} & \Pi_{12} & \Pi_{13} & \Pi_{14} & -\Pi_{25} & 2\Pi_{62} \\ \Pi_{12} & \Pi_{11} & \Pi_{13} & -\Pi_{14} & \Pi_{25} & -2\Pi_{62} \\ \Pi_{31} & \Pi_{31} & \Pi_{33} & 0 & 0 & 0 \\ \Pi_{41} & -\Pi_{41} & 0 & \Pi_{44} & \Pi_{45} & 2\Pi_{52} \\ -\Pi_{52} & \Pi_{52} & 0 & -\Pi_{45} & \Pi_{44} & -2\Pi_{41} \\ -\Pi_{62} & \Pi_{62} & 0 & \Pi_{25} & \Pi_{14} & (\Pi_{11} - \Pi_{12}) \end{pmatrix} \quad (12)$$

Classes  $3m$ ,  $32$ ,  $\bar{3}m$ 

$$\begin{pmatrix} \Pi_{11} & \Pi_{12} & \Pi_{13} & \Pi_{14} & 0 & 0 \\ \Pi_{12} & \Pi_{11} & \Pi_{13} & -\Pi_{14} & 0 & 0 \\ \Pi_{31} & \Pi_{31} & \Pi_{33} & 0 & 0 & 0 \\ \Pi_{41} & -\Pi_{41} & 0 & \Pi_{44} & 0 & 0 \\ 0 & 0 & 0 & 0 & \Pi_{44} & 2\Pi_{41} \\ 0 & 0 & 0 & 0 & \Pi_{14} & (\Pi_{11} - \Pi_{12}) \end{pmatrix} \quad (8)$$

Hexagonal system

Classes  $6$ ,  $\bar{6}$ ,  $6/m$ 

$$\begin{pmatrix} \Pi_{11} & \Pi_{12} & \Pi_{13} & 0 & 0 & -2\Pi_{61} \\ \Pi_{12} & \Pi_{11} & \Pi_{13} & 0 & 0 & 2\Pi_{61} \\ \Pi_{31} & \Pi_{31} & \Pi_{33} & 0 & 0 & 0 \\ 0 & 0 & 0 & \Pi_{44} & \Pi_{45} & 0 \\ 0 & 0 & 0 & -\Pi_{45} & \Pi_{44} & 0 \\ \Pi_{61} & -\Pi_{61} & 0 & 0 & 0 & (\Pi_{11} - \Pi_{12}) \end{pmatrix} \quad (8)$$

Classes  $\bar{6}m2$ ,  $6mm$ ,  $622$ ,  $6/mmm$ 

$$\begin{pmatrix} \Pi_{11} & \Pi_{12} & \Pi_{13} & 0 & 0 & 0 \\ \Pi_{12} & \Pi_{11} & \Pi_{13} & 0 & 0 & 0 \\ \Pi_{31} & \Pi_{31} & \Pi_{33} & 0 & 0 & 0 \\ 0 & 0 & 0 & \Pi_{44} & 0 & 0 \\ 0 & 0 & 0 & 0 & \Pi_{44} & 0 \\ 0 & 0 & 0 & 0 & 0 & (\Pi_{11} - \Pi_{12}) \end{pmatrix} \quad (6)$$

Table 10 (cont'd)

## Cubic system

Classes 23,  $m3$ 

$$\begin{pmatrix} \Pi_{11} & \Pi_{12} & \Pi_{13} & 0 & 0 & 0 \\ \Pi_{13} & \Pi_{11} & \Pi_{12} & 0 & 0 & 0 \\ \Pi_{12} & \Pi_{13} & \Pi_{11} & 0 & 0 & 0 \\ 0 & 0 & 0 & \Pi_{44} & 0 & 0 \\ 0 & 0 & 0 & 0 & \Pi_{44} & 0 \\ 0 & 0 & 0 & 0 & 0 & \Pi_{44} \end{pmatrix} (4)$$

Classes  $\bar{4}3m$ ,  $432$ ,  $m3m$ 

$$\begin{pmatrix} \Pi_{11} & \Pi_{12} & \Pi_{12} & 0 & 0 & 0 \\ \Pi_{12} & \Pi_{11} & \Pi_{12} & 0 & 0 & 0 \\ \Pi_{12} & \Pi_{12} & \Pi_{11} & 0 & 0 & 0 \\ 0 & 0 & 0 & \Pi_{44} & 0 & 0 \\ 0 & 0 & 0 & 0 & \Pi_{44} & 0 \\ 0 & 0 & 0 & 0 & 0 & \Pi_{44} \end{pmatrix} (3)$$

## Isotropic medium

$$\begin{pmatrix} \Pi_{11} & \Pi_{12} & \Pi_{12} & 0 & 0 & 0 \\ \Pi_{12} & \Pi_{11} & \Pi_{12} & 0 & 0 & 0 \\ \Pi_{12} & \Pi_{12} & \Pi_{11} & 0 & 0 & 0 \\ 0 & 0 & 0 & \Pi_{11} - \Pi_{12} & 0 & 0 \\ 0 & 0 & 0 & 0 & \Pi_{11} - \Pi_{12} & 0 \\ 0 & 0 & 0 & 0 & 0 & \Pi_{11} - \Pi_{12} \end{pmatrix} (2)$$

Table 11

Matrices of Piezooptical Constants ( $\pi_{kl}$ ) and Elastooptical Constants ( $p_{kl}$ )

## Triclinic system

## Both classes

$$\begin{pmatrix} \pi_{11} & \pi_{12} & \pi_{13} & \pi_{14} & \pi_{15} & \pi_{16} \\ \pi_{21} & \pi_{22} & \pi_{23} & \pi_{24} & \pi_{25} & \pi_{26} \\ \pi_{31} & \pi_{32} & \pi_{33} & \pi_{34} & \pi_{35} & \pi_{36} \\ \pi_{41} & \pi_{42} & \pi_{43} & \pi_{44} & \pi_{45} & \pi_{46} \\ \pi_{51} & \pi_{52} & \pi_{53} & \pi_{54} & \pi_{55} & \pi_{56} \\ \pi_{61} & \pi_{62} & \pi_{63} & \pi_{64} & \pi_{65} & \pi_{66} \end{pmatrix} (36) \quad \begin{pmatrix} p_{11} & p_{12} & p_{13} & p_{14} & p_{15} & p_{16} \\ p_{21} & p_{22} & p_{23} & p_{24} & p_{25} & p_{26} \\ p_{31} & p_{32} & p_{33} & p_{34} & p_{35} & p_{36} \\ p_{41} & p_{42} & p_{43} & p_{44} & p_{45} & p_{46} \\ p_{51} & p_{52} & p_{53} & p_{54} & p_{55} & p_{56} \\ p_{61} & p_{62} & p_{63} & p_{64} & p_{65} & p_{66} \end{pmatrix} (36)$$

Table 11 (cont'd)

## Monoclinic system

## All classes

Axis 2||X<sub>2</sub> (standard orientation)

$$\begin{pmatrix} \pi_{11} & \pi_{12} & \pi_{13} & 0 & \pi_{15} & 0 \\ \pi_{21} & \pi_{22} & \pi_{23} & 0 & \pi_{25} & 0 \\ \pi_{31} & \pi_{32} & \pi_{33} & 0 & \pi_{35} & 0 \\ 0 & 0 & 0 & \pi_{44} & 0 & \pi_{46} \\ \pi_{51} & \pi_{52} & \pi_{53} & 0 & \pi_{55} & 0 \\ 0 & 0 & 0 & \pi_{64} & 0 & \pi_{66} \end{pmatrix} (20) \quad \begin{pmatrix} p_{11} & p_{12} & p_{13} & 0 & p_{15} & 0 \\ p_{21} & p_{22} & p_{23} & 0 & p_{25} & 0 \\ p_{31} & p_{32} & p_{33} & 0 & p_{35} & 0 \\ 0 & 0 & 0 & p_{44} & 0 & p_{46} \\ p_{51} & p_{52} & p_{53} & 0 & p_{55} & 0 \\ 0 & 0 & 0 & p_{64} & 0 & p_{66} \end{pmatrix} (20)$$

Axis 2||X<sub>3</sub>

$$\begin{pmatrix} \pi_{11} & \pi_{12} & \pi_{13} & 0 & 0 & \pi_{16} \\ \pi_{21} & \pi_{22} & \pi_{23} & 0 & 0 & \pi_{26} \\ \pi_{31} & \pi_{32} & \pi_{33} & 0 & 0 & \pi_{36} \\ 0 & 0 & 0 & \pi_{44} & \pi_{45} & 0 \\ 0 & 0 & 0 & \pi_{54} & \pi_{55} & 0 \\ \pi_{61} & \pi_{62} & \pi_{63} & 0 & 0 & \pi_{66} \end{pmatrix} (20) \quad \begin{pmatrix} p_{11} & p_{12} & p_{13} & 0 & 0 & p_{16} \\ p_{21} & p_{22} & p_{23} & 0 & 0 & p_{26} \\ p_{31} & p_{32} & p_{33} & 0 & 0 & p_{36} \\ 0 & 0 & 0 & p_{44} & p_{45} & 0 \\ 0 & 0 & 0 & p_{54} & p_{55} & 0 \\ p_{61} & p_{62} & p_{63} & 0 & 0 & p_{66} \end{pmatrix} (20)$$

## Rhombic system

## All classes

$$\begin{pmatrix} \pi_{11} & \pi_{12} & \pi_{13} & 0 & 0 & 0 \\ \pi_{21} & \pi_{22} & \pi_{23} & 0 & 0 & 0 \\ \pi_{31} & \pi_{32} & \pi_{33} & 0 & 0 & 0 \\ 0 & 0 & 0 & \pi_{44} & 0 & 0 \\ 0 & 0 & 0 & 0 & \pi_{55} & 0 \\ 0 & 0 & 0 & 0 & 0 & \pi_{66} \end{pmatrix} (12) \quad \begin{pmatrix} p_{11} & p_{12} & p_{13} & 0 & 0 & 0 \\ p_{21} & p_{22} & p_{23} & 0 & 0 & 0 \\ p_{31} & p_{32} & p_{33} & 0 & 0 & 0 \\ 0 & 0 & 0 & p_{44} & 0 & 0 \\ 0 & 0 & 0 & 0 & p_{55} & 0 \\ 0 & 0 & 0 & 0 & 0 & p_{66} \end{pmatrix} (12)$$

## Tetragonal system

Classes 4,  $\bar{4}$ , 4/m

$$\begin{pmatrix} \pi_{11} & \pi_{12} & \pi_{13} & 0 & 0 & \pi_{16} \\ \pi_{12} & \pi_{11} & \pi_{13} & 0 & 0 & -\pi_{16} \\ \pi_{31} & \pi_{31} & \pi_{33} & 0 & 0 & 0 \\ 0 & 0 & 0 & \pi_{44} & \pi_{45} & 0 \\ 0 & 0 & 0 & -\pi_{45} & \pi_{44} & 0 \\ \pi_{61} & -\pi_{61} & 0 & 0 & 0 & \pi_{66} \end{pmatrix} (10) \quad \begin{pmatrix} p_{11} & p_{12} & p_{13} & 0 & 0 & p_{16} \\ p_{12} & p_{11} & p_{13} & 0 & 0 & -p_{16} \\ p_{31} & p_{31} & p_{33} & 0 & 0 & 0 \\ 0 & 0 & 0 & p_{44} & p_{45} & 0 \\ 0 & 0 & 0 & -p_{45} & p_{44} & 0 \\ p_{61} & -p_{61} & 0 & 0 & 0 & p_{66} \end{pmatrix} (10)$$

Table 11 (cont'd)

Classes  $4mm$ ,  $\bar{4}2m$ ,  $422$ ,  $4/mmm$ 

$$\left( \begin{array}{cccccc} \pi_{11} & \pi_{12} & \pi_{13} & 0 & 0 & 0 \\ \pi_{12} & \pi_{11} & \pi_{13} & 0 & 0 & 0 \\ \pi_{31} & \pi_{31} & \pi_{33} & 0 & 0 & 0 \\ 0 & 0 & 0 & \pi_{44} & 0 & 0 \\ 0 & 0 & 0 & 0 & \pi_{44} & 0 \\ 0 & 0 & 0 & 0 & 0 & \pi_{66} \end{array} \right) (7) \quad \left( \begin{array}{cccccc} p_{11} & p_{12} & p_{13} & 0 & 0 & 0 \\ p_{12} & p_{11} & p_{13} & 0 & 0 & 0 \\ p_{31} & p_{31} & p_{33} & 0 & 0 & 0 \\ 0 & 0 & 0 & p_{44} & 0 & 0 \\ 0 & 0 & 0 & 0 & p_{44} & 0 \\ 0 & 0 & 0 & 0 & 0 & p_{46} \end{array} \right) (7)$$

Trigonal system

Classes  $3$  and  $\bar{3}$ 

$$\left( \begin{array}{cccccc} \pi_{11} & \pi_{12} & \pi_{13} & \pi_{14} & -\pi_{25} & 2\pi_{62} \\ \pi_{12} & \pi_{11} & \pi_{13} & -\pi_{14} & \pi_{25} & -2\pi_{62} \\ \pi_{31} & \pi_{31} & \pi_{33} & 0 & 0 & 0 \\ \pi_{41} & -\pi_{41} & 0 & \pi_{44} & \pi_{45} & 2\pi_{52} \\ -\pi_{52} & \pi_{52} & 0 & -\pi_{45} & \pi_{44} & 2\pi_{41} \\ -\pi_{62} & \pi_{62} & 0 & \pi_{25} & \pi_{14} & \pi_{11} - \pi_{12} \end{array} \right) (12)$$

$$\left( \begin{array}{cccccc} p_{11} & p_{12} & p_{13} & p_{14} & -p_{25} & p_{62} \\ p_{12} & p_{11} & p_{13} & -p_{14} & p_{25} & -p_{62} \\ p_{31} & p_{31} & p_{33} & 0 & 0 & 0 \\ p_{41} & -p_{41} & 0 & p_{44} & p_{45} & p_{52} \\ -p_{52} & p_{52} & 0 & -p_{45} & p_{44} & p_{41} \\ -p_{62} & p_{62} & 0 & p_{25} & p_{14} & \frac{1}{2}(p_{11} - p_{12}) \end{array} \right) (12)$$

Classes  $3m$ ,  $32$ ,  $\bar{3}m$ 

$$\left( \begin{array}{cccccc} \pi_{11} & \pi_{12} & \pi_{13} & \pi_{14} & 0 & 0 \\ \pi_{12} & \pi_{11} & \pi_{13} & -\pi_{14} & 0 & 0 \\ \pi_{31} & \pi_{31} & \pi_{33} & 0 & 0 & 0 \\ \pi_{41} & -\pi_{41} & 0 & \pi_{44} & 0 & 0 \\ 0 & 0 & 0 & 0 & \pi_{44} & 2\pi_{41} \\ 0 & 0 & 0 & 0 & \pi_{14} & \pi_{11} - \pi_{12} \end{array} \right) (8)$$

$$\left( \begin{array}{cccccc} p_{11} & p_{12} & p_{13} & p_{14} & 0 & 0 \\ p_{12} & p_{11} & p_{13} & -p_{14} & 0 & 0 \\ p_{31} & p_{31} & p_{33} & 0 & 0 & 0 \\ p_{41} & -p_{41} & 0 & p_{44} & 0 & 0 \\ 0 & 0 & 0 & 0 & p_{44} & p_{41} \\ 0 & 0 & 0 & 0 & p_{14} & \frac{1}{2}(p_{11} - p_{12}) \end{array} \right) (8)$$

Table 11 (cont'd)

## Hexagonal system

Classes  $\bar{6}$ ,  $6$ ,  $6/m$ 

$$\left\{ \begin{array}{cccccc} \pi_{11} & \pi_{12} & \pi_{13} & 0 & 0 & 2\pi_{62} \\ \pi_{12} & \pi_{11} & \pi_{13} & 0 & 0 & -2\pi_{62} \\ \pi_{31} & \pi_{31} & \pi_{33} & 0 & 0 & 0 \\ 0 & 0 & 0 & \pi_{44} & \pi_{45} & 0 \\ 0 & 0 & 0 & -\pi_{45} & \pi_{44} & 0 \\ -\pi_{62} & \pi_{62} & 0 & 0 & 0 & \pi_{11} - \pi_{12} \end{array} \right\} (8)$$

$$\left\{ \begin{array}{cccccc} p_{11} & p_{12} & p_{13} & 0 & 0 & p_{62} \\ p_{12} & p_{11} & p_{13} & 0 & 0 & -p_{62} \\ p_{31} & p_{31} & p_{33} & 0 & 0 & 0 \\ 0 & 0 & 0 & p_{44} & p_{45} & 0 \\ 0 & 0 & 0 & -p_{45} & p_{44} & 0 \\ -p_{62} & p_{62} & 0 & 0 & 0 & \frac{1}{2} (p_{11} - p_{12}) \end{array} \right\} (8)$$

Classes  $\bar{6}m2$ ,  $6mm$ ,  $622$ ,  $6/mmm$ 

$$\left\{ \begin{array}{cccccc} \pi_{11} & \pi_{12} & \pi_{13} & 0 & 0 & 0 \\ \pi_{12} & \pi_{11} & \pi_{13} & 0 & 0 & 0 \\ \pi_{31} & \pi_{31} & \pi_{33} & 0 & 0 & 0 \\ 0 & 0 & 0 & \pi_{44} & 0 & 0 \\ 0 & 0 & 0 & 0 & \pi_{44} & 0 \\ 0 & 0 & 0 & 0 & 0 & \pi_{11} - \pi_{12} \end{array} \right\} (6)$$

$$\left\{ \begin{array}{cccccc} p_{11} & p_{12} & p_{13} & 0 & 0 & 0 \\ p_{12} & p_{11} & p_{13} & 0 & 0 & 0 \\ p_{31} & p_{31} & p_{33} & 0 & 0 & 0 \\ 0 & 0 & 0 & p_{44} & 0 & 0 \\ 0 & 0 & 0 & 0 & p_{44} & 0 \\ 0 & 0 & 0 & 0 & 0 & \frac{1}{2} (p_{11} - p_{12}) \end{array} \right\} (6)$$

## Cubic system

Classes  $23$  and  $m3$ 

$$\left\{ \begin{array}{cccccc} \pi_{11} & \pi_{12} & \pi_{13} & 0 & 0 & 0 \\ \pi_{13} & \pi_{11} & \pi_{12} & 0 & 0 & 0 \\ \pi_{12} & \pi_{13} & \pi_{11} & 0 & 0 & 0 \\ 0 & 0 & 0 & \pi_{44} & 0 & 0 \\ 0 & 0 & 0 & 0 & \pi_{44} & 0 \\ 0 & 0 & 0 & 0 & 0 & \pi_{44} \end{array} \right\} (4)$$

$$\left\{ \begin{array}{cccccc} p_{11} & p_{12} & p_{13} & 0 & 0 & 0 \\ p_{13} & p_{11} & p_{12} & 0 & 0 & 0 \\ p_{12} & p_{13} & p_{11} & 0 & 0 & 0 \\ 0 & 0 & 0 & p_{44} & 0 & 0 \\ 0 & 0 & 0 & 0 & p_{44} & 0 \\ 0 & 0 & 0 & 0 & 0 & p_{44} \end{array} \right\} (4)$$

Table 11 (cont'd)

Classes  $\bar{4}3m, 432, m3m$ 

$$\left( \begin{array}{cccccc} \pi_{11} & \pi_{12} & \pi_{12} & 0 & 0 & 0 \\ \pi_{12} & \pi_{11} & \pi_{12} & 0 & 0 & 0 \\ \pi_{12} & \pi_{12} & \pi_{11} & 0 & 0 & 0 \\ 0 & 0 & 0 & \pi_{44} & 0 & 0 \\ 0 & 0 & 0 & 0 & \pi_{44} & 0 \\ 0 & 0 & 0 & 0 & 0 & \pi_{44} \end{array} \right)_{(3)} \quad \left( \begin{array}{cccccc} p_{11} & p_{12} & p_{12} & 0 & 0 & 0 \\ p_{12} & p_{11} & p_{12} & 0 & 0 & 0 \\ p_{12} & p_{12} & p_{11} & 0 & 0 & 0 \\ 0 & 0 & 0 & p_{44} & 0 & 0 \\ 0 & 0 & 0 & 0 & p_{44} & 0 \\ 0 & 0 & 0 & 0 & 0 & p_{44} \end{array} \right)_{(3)}$$

Isotropic medium

$$\left( \begin{array}{cccccc} \pi_{11} & \pi_{12} & \pi_{12} & 0 & 0 & 0 \\ \pi_{12} & \pi_{11} & \pi_{12} & 0 & 0 & 0 \\ \pi_{12} & \pi_{12} & \pi_{11} & 0 & 0 & 0 \\ 0 & 0 & 0 & \pi_{11} - \pi_{12} & 0 & 0 \\ 0 & 0 & 0 & 0 & \pi_{11} - \pi_{12} & 0 \\ 0 & 0 & 0 & 0 & 0 & \pi_{11} - \pi_{12} \end{array} \right)_{(2)}$$

$$\left( \begin{array}{cccccc} p_{11} & p_{12} & p_{12} & 0 & 0 & 0 \\ p_{12} & p_{11} & p_{12} & 0 & 0 & 0 \\ p_{12} & p_{12} & p_{11} & 0 & 0 & 0 \\ 0 & 0 & 0 & \frac{1}{2} (p_{11} - p_{12}) & 0 & 0 \\ 0 & 0 & 0 & 0 & \frac{1}{2} (p_{11} - p_{12}) & 0 \\ 0 & 0 & 0 & 0 & 0 & \frac{1}{2} (p_{11} - p_{12}) \end{array} \right)_{(2)}$$

Table 12

Matrices of Linear Electrooptical Effect Constants ( $r_{ij}$ )

Triclinic system

$$\left( \begin{array}{ccc} r_{11} & r_{12} & r_{13} \\ r_{21} & r_{22} & r_{23} \\ r_{31} & r_{32} & r_{33} \\ r_{41} & r_{42} & r_{43} \\ r_{51} & r_{52} & r_{53} \\ r_{61} & r_{62} & r_{63} \end{array} \right)_{(18)}$$

Table 12 (cont'd)

*Monoclinic system*

## Class 2

2  $\parallel X_2$       2  $\parallel X_3$ 

$$\begin{pmatrix} 0 & r_{12} & 0 \\ 0 & r_{22} & 0 \\ 0 & r_{32} & 0 \\ r_{41} & 0 & r_{43} \\ 0 & r_{52} & 0 \\ r_{61} & 0 & r_{63} \end{pmatrix} (8) \quad \begin{pmatrix} 0 & 0 & r_{13} \\ 0 & 0 & r_{23} \\ 0 & 0 & r_{33} \\ r_{41} & r_{42} & 0 \\ r_{51} & r_{52} & 0 \\ 0 & 0 & r_{63} \end{pmatrix} (8)$$

Class  $m$  $m \perp X_2$        $m \perp X_3$ 

$$\begin{pmatrix} r_{11} & 0 & r_{13} \\ r_{21} & 0 & r_{23} \\ r_{31} & 0 & r_{33} \\ 0 & r_{42} & 0 \\ r_{51} & 0 & r_{53} \\ 0 & r_{62} & 0 \end{pmatrix} (10) \quad \begin{pmatrix} r_{11} & r_{12} & 0 \\ r_{21} & r_{22} & 0 \\ r_{31} & r_{32} & 0 \\ 0 & 0 & r_{43} \\ 0 & 0 & r_{53} \\ r_{61} & 0 & 0 \end{pmatrix} (10)$$

*Rhombic system*

## Class 222

$$\begin{pmatrix} 0 & 0 & 0 \\ 0 & 0 & 0 \\ 0 & 0 & 0 \\ r_{41} & 0 & 0 \\ 0 & r_{52} & 0 \\ 0 & 0 & r_{63} \end{pmatrix} (3)$$

Class  $mm2$ 

$$\begin{pmatrix} 0 & 0 & r_{13} \\ 0 & 0 & r_{23} \\ 0 & 0 & r_{33} \\ 0 & r_{42} & 0 \\ r_{51} & 0 & 0 \\ 0 & 0 & 0 \end{pmatrix} (5)$$

*Tetragonal system*

## Class 4

$$\begin{pmatrix} 0 & 0 & r_{13} \\ 0 & 0 & r_{13} \\ 0 & 0 & r_{33} \\ r_{41} & r_{51} & 0 \\ r_{51} & -r_{41} & 0 \\ 0 & 0 & 0 \end{pmatrix} (4)$$

Class  $\bar{4}$ 

$$\begin{pmatrix} 0 & 0 & r_{13} \\ 0 & 0 & -r_{13} \\ 0 & 0 & 0 \\ r_{41} & r_{51} & 0 \\ -r_{51} & r_{41} & 0 \\ 0 & 0 & r_{63} \end{pmatrix} (4)$$

Table 12 (cont'd)

Class 422	Class 4mm
$\begin{pmatrix} 0 & 0 & 0 \\ 0 & 0 & 0 \\ 0 & 0 & 0 \\ r_{41} & 0 & 0 \\ 0 & -r_{41} & 0 \\ 0 & 0 & 0 \end{pmatrix} (1)$	$\begin{pmatrix} 0 & 0 & r_{13} \\ 0 & 0 & r_{13} \\ 0 & 0 & r_{33} \\ 0 & r_{51} & 0 \\ r_{51} & 0 & 0 \\ 0 & 0 & 0 \end{pmatrix} (3)$
<b>Class <math>\bar{4}2m</math>, <math>2 \parallel X_1</math></b>	
$\begin{pmatrix} 0 & 0 & 0 \\ 0 & 0 & 0 \\ 0 & 0 & 0 \\ r_{41} & 0 & 0 \\ 0 & r_{41} & 0 \\ 0 & 0 & r_{63} \end{pmatrix} (2)$	
<i>Trigonal system</i>	
Class 3	Class 32
$\begin{pmatrix} r_{11} & -r_{22} & r_{13} \\ -r_{11} & r_{22} & r_{13} \\ 0 & 0 & r_{33} \\ r_{41} & r_{51} & 0 \\ r_{51} & -r_{41} & 0 \\ -r_{22} & r_{11} & 0 \end{pmatrix} (6)$	$\begin{pmatrix} r_{11} & 0 & 0 \\ -r_{11} & 0 & 0 \\ 0 & 0 & 0 \\ r_{41} & 0 & 0 \\ 0 & -r_{41} & 0 \\ 0 & 2r_{11} & 0 \end{pmatrix} (2)$
Class $3m$ , $m \perp X_1$	Class $3m$ , $m \perp X_2$
$\begin{pmatrix} 0 & -r_{22} & r_{13} \\ 0 & r_{22} & r_{13} \\ 0 & 0 & r_{33} \\ 0 & r_{51} & 0 \\ r_{51} & 0 & 0 \\ -2r_{22} & 0 & 0 \end{pmatrix} (4)$	$\begin{pmatrix} r_{11} & 0 & r_{13} \\ -r_{11} & 0 & r_{13} \\ 0 & 0 & r_{33} \\ 0 & r_{51} & 0 \\ r_{51} & 0 & 0 \\ 0 & -r_{11} & 0 \end{pmatrix} (4)$
<i>Hexagonal system</i>	
Class 6	Class 6mm
$\begin{pmatrix} 0 & 0 & r_{13} \\ 0 & 0 & r_{13} \\ 0 & 0 & r_{33} \\ r_{41} & r_{51} & 0 \\ r_{51} & -r_{41} & 0 \\ 0 & 0 & 0 \end{pmatrix} (4)$	$\begin{pmatrix} 0 & 0 & r_{13} \\ 0 & 0 & r_{13} \\ 0 & 0 & r_{33} \\ 0 & r_{51} & 0 \\ r_{51} & 0 & 0 \\ 0 & 0 & 0 \end{pmatrix} (3)$

Table 12 (cont'd)

Class 622

$$\begin{pmatrix} 0 & 0 & 0 \\ 0 & 0 & 0 \\ 0 & 0 & 0 \\ r_{41} & 0 & 0 \\ 0 & -r_{41} & 0 \\ 0 & 0 & 0 \end{pmatrix} (1)$$

Class  $\bar{6}$ 

$$\begin{pmatrix} r_{11} & -r_{22} & 0 \\ -r_{11} & r_{22} & 0 \\ 0 & 0 & 0 \\ 0 & 0 & 0 \\ 0 & 0 & 0 \\ -2r_{22} & -2r_{11} & 0 \end{pmatrix} (2)$$

Class  $\bar{6}m2, m \perp X_1$ 

$$\begin{pmatrix} 0 & r_{12} & 0 \\ 0 & -r_{12} & 0 \\ 0 & 0 & 0 \\ 0 & 0 & 0 \\ 0 & 0 & 0 \\ -2r_{12} & 0 & 0 \end{pmatrix} (1)$$

Class  $\bar{6}m2, m \perp X_2$ 

$$\begin{pmatrix} r_{11} & 0 & 0 \\ -r_{11} & 0 & 0 \\ 0 & 0 & 0 \\ 0 & 0 & 0 \\ 0 & 0 & 0 \\ 0 & -r_{11} & 0 \end{pmatrix} (1)$$

*Cubic system*

Class 432

$$\begin{pmatrix} 0 & 0 & 0 \\ 0 & 0 & 0 \\ 0 & 0 & 0 \\ 0 & 0 & 0 \\ 0 & 0 & 0 \\ 0 & 0 & 0 \end{pmatrix} (0)$$

Classes  $\bar{4}3m, 23$ 

$$\begin{pmatrix} 0 & 0 & 0 \\ 0 & 0 & 0 \\ 0 & 0 & 0 \\ r_{41} & 0 & 0 \\ 0 & r_{41} & 0 \\ 0 & 0 & r_{41} \end{pmatrix} (1)$$

Table 13

Matrices of Quadratic Electrooptical Effect Constants ( $R_{ij}$ )*Triclinic system*

## Both classes

$$\begin{pmatrix} R_{11} & R_{12} & R_{13} & R_{14} & R_{15} & R_{16} \\ R_{21} & R_{22} & R_{23} & R_{24} & R_{25} & R_{26} \\ R_{31} & R_{32} & R_{33} & R_{34} & R_{35} & R_{36} \\ R_{41} & R_{42} & R_{43} & R_{44} & R_{45} & R_{46} \\ R_{51} & R_{52} & R_{53} & R_{54} & R_{55} & R_{56} \\ R_{61} & R_{62} & R_{63} & R_{64} & R_{65} & R_{66} \end{pmatrix} (36)$$

Table 13 (cont'd)

*Monoclinic system*

## All classes

Classes  $2 \parallel X_2, X_2 \perp m$ 

$$\begin{pmatrix} R_{11} & R_{12} & R_{13} & 0 & R_{15} & 0 \\ R_{21} & R_{22} & R_{23} & 0 & R_{25} & 0 \\ R_{31} & R_{32} & R_{33} & 0 & R_{35} & 0 \\ 0 & 0 & 0 & R_{44} & 0 & R_{46} \\ R_{51} & R_{52} & R_{53} & 0 & R_{55} & 0 \\ 0 & 0 & 0 & R_{64} & 0 & R_{66} \end{pmatrix} (20)$$

Classes  $2 \parallel X_3, X_3 \perp m$ 

$$\begin{pmatrix} R_{11} & R_{12} & R_{13} & 0 & 0 & R_{16} \\ R_{21} & R_{22} & R_{23} & 0 & 0 & R_{26} \\ R_{31} & R_{32} & R_{33} & 0 & 0 & R_{36} \\ 0 & 0 & 0 & R_{44} & R_{45} & 0 \\ 0 & 0 & 0 & R_{54} & R_{55} & 0 \\ R_{61} & R_{62} & R_{63} & 0 & 0 & R_{66} \end{pmatrix} (20)$$

*Rhombic system*

## All classes

$$\begin{pmatrix} R_{11} & R_{12} & R_{13} & 0 & 0 & 0 \\ R_{21} & R_{22} & R_{23} & 0 & 0 & 0 \\ R_{31} & R_{32} & R_{33} & 0 & 0 & 0 \\ 0 & 0 & 0 & R_{44} & 0 & 0 \\ 0 & 0 & 0 & 0 & R_{55} & 0 \\ 0 & 0 & 0 & 0 & 0 & R_{66} \end{pmatrix} (12)$$

*Tetragonal system*Classes  $4, \bar{4}, 4/m$ 

$$\begin{pmatrix} R_{11} & R_{12} & R_{13} & 0 & 0 & R_{16} \\ R_{12} & R_{11} & R_{13} & 0 & 0 & -R_{16} \\ R_{31} & R_{31} & R_{33} & 0 & 0 & 0 \\ 0 & 0 & 0 & R_{44} & R_{45} & 0 \\ 0 & 0 & 0 & R_{45} & R_{44} & 0 \\ R_{61} & -R_{61} & 0 & 0 & 0 & R_{66} \end{pmatrix} (10)$$

Classes  $4mm, \bar{4}2m, 422, 4/mmm$ 

$$\begin{pmatrix} R_{11} & R_{12} & R_{13} & 0 & 0 & 0 \\ R_{12} & R_{11} & R_{13} & 0 & 0 & 0 \\ R_{31} & R_{31} & R_{33} & 0 & 0 & 0 \\ 0 & 0 & 0 & R_{44} & 0 & 0 \\ 0 & 0 & 0 & 0 & R_{44} & 0 \\ 0 & 0 & 0 & 0 & 0 & R_{66} \end{pmatrix} (7)$$

*Trigonal system*Classes  $3, \bar{3}$ 

$$\begin{pmatrix} R_{11} & R_{12} & R_{13} & R_{14} & -R_{25} & 2R_{26} \\ R_{12} & R_{11} & R_{13} & -R_{14} & R_{25} & -2R_{26} \\ R_{31} & R_{31} & R_{33} & 0 & 0 & 0 \\ R_{41} & -R_{41} & 0 & R_{44} & R_{45} & 2R_{52} \\ -R_{52} & R_{52} & 0 & -R_{45} & R_{44} & 2R_{41} \\ -R_{62} & R_{62} & 0 & R_{25} & R_{14} & (R_{11} - R_{12}) \end{pmatrix} (12)$$

Table 13 (cont'd)

Classes  $3m$ ,  $\overline{3}m$ , 32

$$\left( \begin{array}{cccccc} R_{11} & R_{12} & R_{13} & R_{14} & 0 & 0 \\ R_{12} & R_{11} & R_{13} & -R_{14} & 0 & 0 \\ R_{31} & R_{31} & R_{33} & 0 & 0 & 0 \\ R_{41} & -R_{41} & 0 & R_{44} & 0 & 0 \\ 0 & 0 & 0 & 0 & R_{44} & 2R_{44} \\ 0 & 0 & 0 & 0 & R_{14} & (R_{11}-R_{12}) \end{array} \right) (8)$$

Textures  $\infty$ ,  $\infty/m$ 

$$\left( \begin{array}{cccccc} R_{11} & R_{12} & R_{13} & 0 & 0 & 2R_{62} \\ R_{12} & R_{11} & R_{13} & 0 & 0 & -2R_{62} \\ R_{31} & R_{31} & R_{33} & 0 & 0 & 0 \\ 0 & 0 & 0 & R_{44} & R_{45} & 0 \\ 0 & 0 & 0 & -R_{45} & R_{44} & 0 \\ -R_{62} & R_{62} & 0 & 0 & 0 & (R_{11}-R_{12}) \end{array} \right) (8)$$

Textures  $\infty m$ ,  $\infty/2$ 

$$\left( \begin{array}{cccccc} R_{11} & R_{12} & R_{13} & 0 & 0 & 0 \\ R_{12} & R_{11} & R_{13} & 0 & 0 & 0 \\ R_{31} & R_{31} & R_{33} & 0 & 0 & 0 \\ 0 & 0 & 0 & R_{44} & 0 & 0 \\ 0 & 0 & 0 & 0 & R_{44} & 0 \\ 0 & 0 & 0 & 0 & 0 & (R_{11}-R_{12}) \end{array} \right) (6)$$

Isotropic medium

$$\left( \begin{array}{cccccc} R_{11} & R_{12} & R_{12} & 0 & 0 & 0 \\ R_{12} & R_{11} & R_{12} & 0 & 0 & 0 \\ R_{12} & R_{12} & R_{11} & 0 & 0 & 0 \\ 0 & 0 & 0 & (R_{11}-R_{12}) & 0 & 0 \\ 0 & 0 & 0 & 0 & (R_{11}-R_{12}) & 0 \\ 0 & 0 & 0 & 0 & 0 & (R_{11}-R_{12}) \end{array} \right) (2)$$

Table 13a

Gyration Tensor  $[g_{ij}]$ 

Triclinic system

Class 1

$$\begin{bmatrix} g_{11} & g_{12} & g_{13} \\ g_{12} & g_{22} & g_{23} \\ g_{13} & g_{23} & g_{33} \end{bmatrix} (6)$$

Table 13a (cont'd)

*Monoclinic system*

Class 2 $2 \parallel X_2$ (standard orientation)	Class 2 $2 \parallel X_2$
$\begin{bmatrix} g_{11} & 0 & g_{13} \\ 0 & g_{22} & 0 \\ g_{13} & 0 & g_{33} \end{bmatrix}_{(4)}$	$\begin{bmatrix} g_{11} & g_{12} & 0 \\ g_{12} & g_{22} & 0 \\ 0 & 0 & g_{33} \end{bmatrix}_{(4)}$
Class $m$ $m \perp X_2$ (standard orientation)	Class $m$ $m \perp X_2$
$\begin{bmatrix} 0 & g_{12} & 0 \\ g_{12} & 0 & g_{23} \\ 0 & g_{23} & 0 \end{bmatrix}_{(2)}$	$\begin{bmatrix} 0 & 0 & g_{13} \\ 0 & 0 & g_{23} \\ g_{13} & g_{23} & 0 \end{bmatrix}_{(2)}$

*Rhombic system*

Class 222	Class $mm2$
$\begin{bmatrix} g_{11} & 0 & 0 \\ 0 & g_{22} & 0 \\ 0 & 0 & g_{33} \end{bmatrix}_{(3)}$	$\begin{bmatrix} 0 & g_{12} & 0 \\ g_{12} & 0 & 0 \\ 0 & 0 & 0 \end{bmatrix}_{(1)}$

*Tetragonal system*

Classes 4, 422	Class $\bar{4}$	Class $\bar{4}2m$
$\begin{bmatrix} g_{11} & 0 & 0 \\ 0 & g_{11} & 0 \\ 0 & 0 & g_{33} \end{bmatrix}_{(2)}$	$\begin{bmatrix} g_{11} & g_{12} & 0 \\ g_{12} & -g_{11} & 0 \\ 0 & 0 & 0 \end{bmatrix}_{(2)} 2 \parallel X$	$\begin{bmatrix} 0 & g_{12} & 0 \\ g_{12} & 0 & 0 \\ 0 & 0 & 0 \end{bmatrix}_{(2)}$

*Tetragonal and hexagonal systems**Classes 3, 32, 6, 622*

$\begin{bmatrix} g_{11} & 0 & 0 \\ 0 & g_{11} & 0 \\ 0 & 0 & g_{33} \end{bmatrix}_{(2)}$
--

*Cubic system**Classes 432, 23*

$\begin{bmatrix} g_{11} & 0 & 0 \\ 0 & g_{11} & 0 \\ 0 & 0 & g_{11} \end{bmatrix}_{(1)}$
--

*Isotropic medium*

$\begin{bmatrix} g_{11} & 0 & 0 \\ 0 & g_{11} & 0 \\ 0 & 0 & g_{11} \end{bmatrix}_{(1)}$
--

Table 14

## Reference Data Required for Solving the Problems

Substances are arranged in alphabetic order.

Unless stated otherwise, the listed values of physical constants refer to room temperature.

Where the experimental conditions are not given, assume that the constants were measured on mechanically free crystals, at constant temperature.

**Ammonium dihydrophosphate (ADP) ( $\text{NH}_4\text{H}_2\text{PO}_4$ );  $\bar{4}2m$**

$$\rho = 1.803 \text{ g/cm}^3 \text{ For } \lambda = 0.546 \mu\text{m}, \quad N_o = 1.52662, \quad N_e = 1.48072$$

$d, 10^{-8}$ CGSE units	$s, 10^{-12}$ CGSE units	$c, 10^{11}$ CGSE units	$\epsilon$	$\alpha, 10^{-6} \text{ K}^{-1}$
$d_{14} = 5.27$	$s_{11} = 1.82$	$c_{11} = 6.17$	$\epsilon_1 = \epsilon_2 = 56.4$	$\alpha_1 = \alpha_2 = 30.1$
$d_{36} = -145$	$s_{33} = 4.35$	$c_{33} = 3.28$	$\epsilon_3 = 16.4$	$\alpha_3 = 4.1$
	$s_{44} = 11.53$	$c_{44} = 0.85$		
	$s_{66} = 16.46$	$c_{66} = 0.59$		
	$s_{12} = 0.19$	$c_{12} = 0.72$		
	$s_{13} = -1.18$	$c_{13} = 1.19$		

**Aragonite ( $\text{CaCO}_3$ );  $mmm$**

$$\rho = 2.6 \text{ g/cm}^3, \quad T_{\text{melt}} = 129 \text{ }^\circ\text{C}.$$

$$\alpha_1 = 35 \cdot 10^{-6} \text{ K}^{-1}, \quad \alpha_2 = 17 \cdot 10^{-6} \text{ K}^{-1}, \quad \alpha_3 = 11 \cdot 10^{-6} \text{ K}^{-1}.$$

$$\epsilon_1 = 9.8, \quad \epsilon_2 = 7.7, \quad \epsilon_3 = 6.6.$$

**Barium fluoride ( $\text{BaF}_2$ );  $m3m$**

$$\rho = 4.83 \text{ g/cm}^3, \quad T_{\text{melt}} = 1280 \text{ }^\circ\text{C}.$$

$$c_{11} = 9.01 \cdot 10^{11} \text{ CGSE units}, \quad c_{12} = 4.04 \cdot 10^{11} \text{ CGSE units},$$

$$c_{44} = 2.49 \cdot 10^{11} \text{ CGSE units}.$$

**Barium nitrite ( $\text{Ba}(\text{NO}_2)_2 \cdot \text{H}_2\text{O}$ );  $6$**

$$\alpha_1 = \alpha_2 = 16 \cdot 10^{-6} \text{ K}^{-1}, \quad \alpha_3 = 76 \cdot 10^{-6} \text{ K}^{-1}, \quad \gamma_3 = -8 \text{ CGSE units},$$

$$d_{31} = 5.3 \cdot 10^{-8} \text{ CGSE units}, \quad d_{33} = 5.1 \cdot 10^{-8} \text{ CGSE units}$$

$$c_{11} = 0.525 \cdot 10^{12} \text{ CGSE units}, \quad c_{33} = 0.3 \cdot 10^{12} \text{ CGSE units}$$

$$c_{12} = 2.5 \cdot 10^{12} \text{ CGSE units}, \quad c_{13} = 0.15 \cdot 10^{12} \text{ CGSE units}.$$

**Barium titanate ( $\text{BaTiO}_3$ )**

$$\rho = 5.9 \text{ g/cm}^3, \quad T_{\text{melt}} = 1625 \text{ }^\circ\text{C}.$$

Symmetry is  $m3m$  above  $120 \text{ }^\circ\text{C}$ . The phase stable between  $120 \text{ }^\circ\text{C}$  and  $5 \text{ }^\circ\text{C}$  is tetragonal,  $4mm$ . The direction of spontaneous polarization is parallel to  $\langle 100 \rangle$  of the initial cubic unit cell,  $P^s = 54 \cdot 10^3 \text{ CGSE units}$ . Below  $5 \text{ }^\circ\text{C}$  a new ferroelectric phase appears, with spontaneous polarization parallel to  $\langle 110 \rangle$  of the initial unit cell. The symmetry of this phase is  $mm$ , and it is stable between  $5 \text{ }^\circ\text{C}$  and  $-90 \text{ }^\circ\text{C}$ .

At  $-90 \text{ }^\circ\text{C}$  the third phase transition takes place, with spontaneous polarization of the new phase parallel to  $\langle 111 \rangle$  of the initial cubic unit cell; the symmetry of the new phase is  $3m$ .

Cubic phase:  $n = 2.4$ ,  $R_{11} = R_{12} = 1.4 \cdot 10^{-12} \text{ CGSE units}$ ,  $R_{44} = 1.88 \cdot 10^{-12} \text{ CGSE units}$ .

**Bismuth germanate** ( $\text{Bi}_{12}\text{GeO}_{20}$ ); 23  
 $\rho = 9.2 \text{ g/cm}^3$ ,  $T_{\text{melt}} = 930^\circ\text{C}$ ,  
 $c_{11} = 1.2 \cdot 10^{10}$  CGSE units,  $c_{12} = 0.39 \cdot 10^{10}$  CGSE units,  $c_{44} = 0.25 \cdot 10^{10}$  CGSE units  
 $\epsilon = 3.8$ ,  $e_{14} = 0.987 \text{ cm/m}^2$ .

**Cadmium selenide** ( $\text{CdSe}$ ); 6mm  
 $\rho = 5.81 \text{ g/cm}^3$ ,  $T_{\text{melt}} > 1350^\circ\text{C}$ .

**Cadmium sulphide** ( $\text{CdS}$ ); 6mm  
 $\rho = 4.82 \text{ g/cm}^3$ ,  $T_{\text{melt}} = 1500^\circ\text{C}$  at a pressure of 100 atm.  
For  $\lambda = 0.515 \mu\text{m}$ :  $N_o = 2.743$ ,  $N_e = 2.726$   
 $r_{13} = 3.3 \cdot 10^{-8}$  CGSE units,  $r_{33} = 7.2 \cdot 10^{-8}$  CGSE units  
 $r_{51} = 11.1 \cdot 10^{-8}$  CGSE units

$d, 10^{-8}$ CGSE units	$s, 10^{-12}$ CGSE units	$c, 10^{11}$ CGSE units	$\epsilon$	$\alpha, 10^{-4} \text{ K}^{-1}$
$d_{31} = -1.7$	$s_{11} = 2.22$	$c_{11} = 8.1$	$\epsilon_1 = \epsilon_2 = 9.3$	$\alpha_1 = \alpha_2 = 5.0$
$d_{33} = -3.4$	$s_{12} = -0.87$	$c_{12} = 4.9$	$\epsilon_3 = 10.3$	$\alpha_3 = 3.5$
$d_{15} = 4.7$	$s_{13} = -0.80$	$c_{13} = 4.8$		
	$s_{33} = 2.19$	$c_{33} = 8.0$		
	$s_{44} = 7.0$	$c_{44} = 1.43$		

**Calcite (Iceland spar)** ( $\text{CaCO}_3$ );  $\bar{3}m$   
 $\rho = 2.6\text{--}2.8 \text{ g/cm}^3$ ,  $T_{\text{melt}} = 1339^\circ\text{C}$  at a pressure of about 102.5 atm. Cleaves along planes parallel to rhombohedron faces ( $(10\bar{1}1)$ ). The normal to a rhombohedron's face is at  $44^\circ$  to the axis  $\bar{3}$ .

For  $\lambda = 0.589 \mu\text{m}$ :  $N_o = 1.658$ ,  $N_e = 1.486$ ,  
 $\alpha_1 = \alpha_2 = -5.6 \cdot 10^{-6} \text{ K}^{-1}$ ,  $\alpha_3 = 25 \cdot 10^{-6} \text{ K}^{-1}$ .

**Ceramic**,  $\text{BaTiO}_3$ , polarized;  $\infty m$   
**Artificial ferroelectric**,  $\rho = 5.5 \text{ g/cm}^3$ ,  $T_C = 115^\circ\text{C}$ .

$d, g, 10^{-8}$ CGSE units	$c, 10^{11}$ CGSE units	$\epsilon$
$d_{33} = 5.73$	$c_{11} = 16.8$	$\epsilon_1 = 1596$
$d_{31} = -2.35$	$c_{33} = 18.9$	$\epsilon_2 = 1872$
$d_{15} = 7.8$	$c_{44} = 5.46$	
$g_{33} = 3.84$	$c_{12} = 7.82$	
$g_{31} = -1.575$	$c_{13} = 7.10$	

**Cinnabar** ( $\text{HgS}$ ); 32  
 $N_o = 2.83$ ,  $N_e = 3.15$  for  $\lambda = 0.694 \mu\text{m}$   
 $N_o = 2.70$ ,  $N_e = 2.99$  for  $\lambda = 1.06 \mu\text{m}$   
 $N_o = 2.60$ ,  $N_e = 2.87$  for  $\lambda = 10.6 \mu\text{m}$   
 $\chi_{11} = 2.4 \cdot 10^{-7}$  CGSE units

**Copper chloride** ( $\text{CuCl}$ );  $\bar{4}3m$   
For  $\lambda = 0.535 \mu\text{m}$ ,  $N = 1.996$ ;  $r_{41} = 18.3 \cdot 10^{-8}$  CGSE units

## Corundum (see ruby)

Deuterated (DKDP)  $\text{KH}_2\text{PO}_4$ ;  $\bar{4}2m$   
 For  $\lambda = 0.546 \mu\text{m}$ ,  $N_0 = 1.47$ ,  $N_e = 1.51$

$d$ , $10^{-8}$ CGSE units	$s$ , $10^{-12}$ CGSE units	$c$ , $10^{10}$ CGSE units	$\epsilon$	$\alpha$ , $10^{-6} \text{ K}^{-1}$
$d_{14} = 4.2$	$s_{11} = 1.65$	$c_{11} = 86.8$	$\epsilon_1 = \epsilon_2 = 4.6$	$\alpha_1 = \alpha_2 = 36$
$d_{36} = 69.6$	$s_{12} = -0.4$	$c_{12} = 40.2$	$\epsilon_3 = 21.8$	$\alpha_3 = 41.1$
	$s_{13} = -0.75$	$c_{13} = 47.6$		
	$s_{33} = 2.0$	$c_{23} = 85.7$		
	$s_{44} = 7.9$	$c_{44} = 12.7$		
	$s_{66} = 16.6$	$c_{66} = 6.0$		

## DKDP (see KDP)

EDT, ethylene diamine tartrate ( $\text{C}_6\text{H}_{14}\text{H}_2\text{O}_6$ ); 2  
 $\rho = 1.538 \text{ g/cm}^3$

$d$ , $10^{-4}$ CGSE units	$s$ , $10^{-12}$ CGSE units	$\alpha$ , $10^{-6} \text{ K}^{-1}$
$d_{11} = -30.4$	$s_{11} = 3.34$	$\alpha_1 = 0$
$d_{16} = -36.6$	$s_{12} = -0.3$	$\alpha_2 = 20.3$
$d_{21} = 30.3$	$s_{13} = -3.0$	$\alpha_3 = 80.0$
$d_{22} = 6.6$	$s_{15} = -1.7$	$\alpha_5 = -32$
$d_{23} = -34$	$s_{22} = 3.65$	
$d_{25} = -53.8$	$s_{23} = -1.8$	
$d_{31} = -50.9$		
$d_{36} = -55.1$	$s_{46} = 0.38$	
	$s_{55} = 11.6$	
	$s_{66} = 19.1$	

Fluoride ( $\text{CaF}_2$ );  $m3m$ 

$\rho = 3.18 \text{ g/cm}^3$ ,  $T_{\text{melt}} = 1360 \text{ }^\circ\text{C}$ .  
 For  $\lambda = 0.589 \mu\text{m}$ ,  $N = 1.43384$ .

$\pi_{11} = -0.29 \cdot 10^{-11}$  CGSE units,  $\pi_{12} = 1.16 \cdot 10^{-11}$  CGSE units,  $\pi_{44} = 0.698 \cdot 10^{-11}$  CGSE units.

Gallium arsenide (GaAs);  $\bar{4}3m$ 

$\rho = 5.316 \text{ g/cm}^3$ ,  $T_{\text{melt}} = 1238 \text{ }^\circ\text{C}$ .

For  $\lambda = 0.546 \mu\text{m}$ ,  $N = 3.15$ ,  $r_{11} = 12.5 \cdot 10^{-8}$  CGSE units  
 For  $\lambda = 0.8-12 \mu\text{m}$ ,  $N = 3.42$ ,  $r_{11} = 3.6 \cdot 10^{-8}$  CGSE units,  
 $s_{11} = 12.64 \cdot 10^{-12}$  CGSE units,  $c_{11} = 1.19 \cdot 10^{10}$  CGSE units  
 $s_{44} = 18.60 \cdot 10^{-12}$  CGSE units,  $c_{44} = 0.54 \cdot 10^{10}$  CGSE units,  
 $s_{12} = 4.23 \cdot 10^{-12}$  CGSE units,  $c_{12} = 0.59 \cdot 10^{10}$  CGSE units.

Gallium phosphide (GaP);  $\bar{4}3m$ 

For  $\lambda = 0.540 \mu\text{m}$ ,  $N = 3.495$ ,  $r_{41} = 1.5 \cdot 10^{-8}$  CGSE units

**Germanium (Ge);  $m3m$**   
 $\rho = 5.327 \text{ g/cm}^3$ ,  $T_{\text{melt}} = 936 \text{ }^{\circ}\text{C}$

$s, 10^{-12} \text{ CGSE}$ units	$c, 10^{+11} \text{ CGSE}$ units	$\Pi_{ij}, 10^{-12} \text{ CGSE}$ units		$\rho, \text{ ohm} \cdot \text{cm}$	
		$n\text{-Ge}$	$p\text{-Ge}$	$n\text{-Ge}$	$p\text{-Ge}$
$s_{11} = 0.979$	$c_{11} = 13.114$	$\Pi_{11} = 4.7$	$\Pi_{11} = -3.7$	9.9	1.1
$s_{12} = -0.267$	$c_{12} = 4.924$	$\Pi_{12} = -5.0$	$\Pi_{12} = 3.2$		
$s_{44} = 1.497$	$c_{44} = 6.816$	$\Pi_{44} = -137.9$	$\Pi_{44} = 96.7$		

**Graphite (C);  $6/mmm$**   
 $\rho = 2.21 \text{ g/cm}^3$ ,  $T_{\text{melt}} = 3800\text{-}3900 \text{ }^{\circ}\text{C}$   
 $\alpha_1 = \alpha_2 = 1.5 \cdot 10^{-6} \text{ K}^{-1}$ ,  $\alpha_3 = 28.2 \cdot 10^{-6} \text{ K}^{-1}$

**Greenockite**, see cadmium sulphide

**Gypsum ( $\text{CaCO}_3$ );  $mmm$**   
 $N_g = 1.532$ ,  $N_m = 1.527$ ,  $N_p = 1.522$

**Indium antimonide (InSb);  $\overline{4}3m$**   
 $\rho = 5.75 \text{ g/cm}^3$ ,  $T_{\text{melt}} = 523 \text{ }^{\circ}\text{C}$

$s, 10^{-12} \text{ CGSE}$ units	$c, 10^{+11} \text{ CGSE}$ units	$\Pi, 10^{-18}$ CGSE units	$\rho,$ $\text{ohm} \cdot \text{cm}$
$s_{11} = 2.42$	$c_{11} = 6.72$	$\Pi_{11} = -70$	0.54
$s_{12} = -0.855$	$c_{12} = 3.07$	$\Pi_{12} = -115$	
$s_{44} = 3.3$	$c_{44} = 3.02$	$\Pi_{44} = 300$	

**KDP**, see Potassium dihydrophosphate

**Lead telluride ( $\text{PbTe}$ );  $m3m$**   
 $\rho = 8.16 \text{ g/cm}^3$ ,  $T_{\text{melt}} = 917 \text{ }^{\circ}\text{C}$

$s, 10^{-12} \text{ CGSE}$ units	$\Pi, 10^{-12} \text{ CGSE}$ units		$\rho, \text{ ohm} \cdot \text{cm}$ (carrier con- centration $3 \cdot 10^{18} \text{ cm}^{-3}$ )	
	$n\text{-PbTe}$	$p\text{-PbTe}$	$n\text{-PbTe}$	$p\text{-PbTe}$
$s_{11} = 0.947$	$\Pi_{11} = 20$	$\Pi_{11} = 35$	1-3	1-3
$s_{12} = -0.073$	$\Pi_{12} = 25$	$\Pi_{12} = 40$		
$s_{44} = 7.63$	$\Pi_{44} = -107$	$\Pi_{44} = 185$		

**Lithium iodate ( $\text{LiIO}_3$ );  $6$**   
 $\rho = 4.5 \text{ g/cm}^3$ ,  $T_{\text{melt}} = 420 \text{ }^{\circ}\text{C}$   
For  $\lambda = 1060 \text{ \AA}$ ;  $N_o = 1.86$ ,  $N_e = 1.72$

**Lithium niobate (LiNbO<sub>3</sub>); 3m**  
**Ferroelectric,  $T_C = 1160^\circ\text{C}$ ,  $T_{\text{melt}} = 1253^\circ\text{C}$ ,  $\rho = 4.7 \text{ g/cm}^3$**   
 $\epsilon_1 = \epsilon_2 = 99.5$ ,  $\epsilon_3 = 38.5$ .  
 For  $\lambda = 0.106 \mu\text{m}$ ,  $N_o = 2.2336$ ,  $N_e = 2.1567$ .  
 For  $\lambda = 0.530 \mu\text{m}$ ,  $N_o = 2.3225$ ,  $N_e = 2.3212$   
 $r_{22} = 0.1 \cdot 10^{-8}$  CGSE units,  $c_{11} = 204 \cdot 10^{10}$  CGSE units,  $c_{12} = 53 \cdot 10^{10}$  CGSE units  
 $r_{13} = 0.25 \cdot 10^{-8}$  CGSE units,  $c_{33} = 242 \cdot 10^{10}$  CGSE units,  $c_{13} = 75$  CGSE units  
 $r_{33} = 0.9 \cdot 10^{-8}$  CGSE units,  $c_{44} = 74 \cdot 10^{10}$  CGSE units,  $c_{14} = 9$  CGSE units  
 $r_{51} = 0.9 \cdot 10^{-8}$  CGSE units,  $c_{66} = 64 \cdot 10^{10}$  CGSE units,  
 $\chi_{22} = 3.8 \cdot 10^{-8}$  CGSE units,  $\chi_{31} = 6.1 \cdot 10^{-8}$  CGSE units  
 $\chi_{33} = 49.8 \cdot 10^{-8}$  CGSE units  
 $[g_{mnk}]$ , in  $10^{-22} \text{ N}^{-1} \text{ V}^{-1} \text{ m}^3$ :

$$\begin{array}{ll} g_{111} = -6.23, & g_{241} = -2.46 \\ g_{131} = -9.48 & g_{341} = -2.89 \\ g_{141} = 15.14 & g_{441} = -21.00 \\ g_{221} = 0.58 & g_{153} = 1.14 \end{array}$$

$d_{22} = 0.63 \cdot 10^{-6}$  CGSE units,  $d_{31} = -0.33 \cdot 10^{-7}$  CGSE units  
 $d_{15} = 2.04 \cdot 10^{-6}$  CGSE units,  $d_{33} = 1.6 \cdot 10^{-4}$  CGSE units  
 For  $\lambda = 0.630 \mu\text{m}$ ,  $N_c = 2.20$   
 $p_{31} = 0.178$ ,  $p_{13} = 0.092$ ,  $p_{33} = 0.088$ ,  
 $p_{41} = 0.155$ ,  $p_{31} = 0.036$ ,  $p_{13} = 0.072$

**Lithium sulphate (Li<sub>2</sub>SO<sub>4</sub>·H<sub>2</sub>O); 2**  
 $\rho = 2.06 \text{ g/cm}^3$ ,  $\gamma_2 = 30$  CGSE units

$d$ , $10^{-8}$ CGSE units	$s$ , $10^{-12}$ CGSE units	$\epsilon$
$d_{14} = 14.0$	$s_{11} = 2.39$	$\epsilon_1^t = 5.6$
$d_{16} = 12.5$	$s_{22} = 2.13$	$\epsilon_2^t = 6.5$
$d_{21} = 11.6$	$s_{33} = 2.31$	$\epsilon_3^t = 10.3$
$d_{22} = 45.0$	$s_{41} = 3.69$	$\epsilon_5^t = 0.07$
$d_{23} = -5.5$	$s_{55} = 4.1$	
$d_{25} = 16.5$		$\epsilon_{12}^t = 0.95$
$d_{34} = 26.4$		$\epsilon_{13}^t = -0.5$
$d_{36} = 10.0$		$\epsilon_{23}^t = 0.36$
		$\epsilon_{25}^t = 0.71$
		$\epsilon_{35}^t = -1.2$
		$\epsilon_{46}^t = 0.05$
		$\epsilon_{56}^t = 0.41$
		$\epsilon_{66}^t = 7.40$

**Lithium tantalate (LiTaO<sub>3</sub>); 3m**  
**Ferroelectric,  $T_C = 630^\circ\text{C}$**   
 $\rho = 7.58 \text{ g/cm}^3$ ,  $\gamma_3 = 75$  CGSE units,  $\sigma_3 = 10^{-11} \text{ ohm}^{-1} \cdot \text{cm}^{-1}$ ,  $\epsilon_3 = 80$ .  
 For  $\lambda = 0.633 \mu\text{m}$ ,  $N_o = 2.176$ ,  $N_e = 2.180$   
 $r_{13} = 21 \cdot 10^{-8}$  CGSE units,  $r_{33} = 90.8 \cdot 10^{-8}$  CGSE units,  
 $r_{31} = 60 \cdot 10^{-8}$  CGSE units,  $r_{22} = 3 \cdot 10^{-8}$  CGSE units

**Potassium alum (KAl[SO<sub>4</sub>]<sub>2</sub>·12H<sub>2</sub>O); m3**  
 $\pi_{11} = 3.7 \cdot 10^{-11}$  CGSE units,  $\pi_{13} = 8.5 \cdot 10^{-11}$  CGSE units,  
 $\pi_{12} = 9.1 \cdot 10^{-11}$  CGSE units,  $\pi_{14} = -0.65 \cdot 10^{-12}$  CGSE units

**Potassium bromide (KBr); m3m**  
 $\rho = 2.75 \text{ g/cm}^3$ ,  $T_{\text{melt}} = 730^\circ\text{C}$

$c_{11} = 3.46 \cdot 10^{11}$  CGSE units,  
 $c_{12} = 0.58 \cdot 10^{11}$  CGSE units,  
 $c_{44} = 0.505 \cdot 10^{11}$  CGSE units

**Potassium chloride (KCl);  $m3m$**   
 $\rho = 1.98 \text{ g/cm}^3$ ,  $T_{\text{melt}} = 776 \text{ }^{\circ}\text{C}$

$c_{11} = 3.980 \cdot 10^{11}$  CGSE units,  $s_{11} = 2.62 \cdot 10^{-12}$  CGSE units,  
 $c_{44} = 0.625 \cdot 10^{11}$  CGSE units,  $s_{44} = 16.0 \cdot 10^{-12}$  CGSE units,  
 $c_{12} = 0.620 \cdot 10^{11}$  CGSE units,  $s_{12} = 0.35 \cdot 10^{-12}$  CGSE units

**Potassium dihydropophosphate (KDP) ( $\text{KH}_2\text{PO}_4$ );  $\bar{4}2m$**

Ferroelectric,  $T_C = 151 \text{ }^{\circ}\text{C}$ . At the Curie point,  $P^* = 10^4$  CGSE units.

$\varepsilon_3 = 7 \cdot 10^4$ ,  $\gamma_3 = 1500$  CGSE units,  $\rho = 2.338 \text{ g/cm}^3$ ,

$T_{\text{melt}} = 254 \text{ }^{\circ}\text{C}$ ,  $\epsilon_p = 0.1 \text{ cal} \cdot \text{g}^{-1} \text{K}^{-1}$ .

For  $\lambda = 0.546 \mu\text{m}$ ,  $N_o = 1.511$ ,  $N_e = 1.469$ .

$r_{41} = 25 \cdot 10^{-8}$  CGSE units,  $r_{63} = -30 \cdot 10^{-8}$  CGSE units.

For  $\lambda = 0.535 \mu\text{m}$ ,  $\Pi_{66} = 0.5 \cdot 10^{-12}$  CGSE units

$\chi_{14} = 0.59 \cdot 10^{-8}$  CGSE units,  $\chi_{36} = 0.62 \cdot 10^{-8}$  CGSE units

**Potassium niobate-tantalate (KTN,  $\text{KTa, Nb}_{1-x}\text{O}_3$ )**

Ferroelectric,  $T_C = 10 \text{ }^{\circ}\text{C}$ . Symmetry:  $4mm$  below  $T_C$ ,  $m3m$  above  $T_C$ .

For  $\lambda = 0.633 \mu\text{m}$ ,  $N_o = 2.318$ ,  $N_e = 2.277$  (in tetragonal phase).

$r_{33}(n_1/n_3)r_{13} = 15 \cdot 10^{-6}$  CGSE units,  $r_{42} = 24 \cdot 10^{-6}$  CGSE units,

$R_{11} - R_{12} = 9.67 \cdot 10^{-12}$  CGSE units.

**Potassium tartrate ( $\text{C}_4\text{H}_4\text{O}_6$ ); 2**

$\rho = 1.988 \text{ g/cm}^3$ ,  $\gamma_2 = -4.9$  CGSE units.

$d, 10^{-8}$ CGSE units	$s, 10^{-12}$ CGSE units	$\epsilon$	$\alpha, 10^{-8} \text{ K}^{-1}$
$d_{14} = -25.0$	$s_{11} = +2.24$ $s_{33} = +3.86$	$\epsilon_1 = 6.44$	$\alpha_1 = +12.0$
$d_{16} = +6.5$	$s_{12} = -0.08$ $s_{34} = +0.90$	$\epsilon_2 = 5.80$	$\alpha_2 = 44.8$
$d_{21} = -2.2$	$s_{13} = -1.64$ $s_{44} = +11.90$	$\epsilon_3 = 6.49$	$\alpha_3 = 32.0$
$d_{22} = 8.5$	$s_{15} = -0.64$ $s_{46} = 0.57$	$\epsilon_5 = 0.005$	$\alpha_5 = -12.0$
$d_{23} = -10.4$	$s_{22} = +3.37$ $s_{55} = 8.15$		
$d_{25} = -22.5$	$s_{23} = -1.05$ $s_{66} = 10.41$		
$d_{34} = +29.4$	$s_{35} = -0.57$		
$d_{36} = -66.0$			

**Quartz ( $\text{SiO}_2$ )**

Symmetry of low-temperature phase 32, of high-temperature phase 622.

$\rho = 2.648 \text{ g/cm}^3$ ,  $T_{\text{melt}} = 1700 \text{ }^{\circ}\text{C}$ .

For  $\lambda = 0.589 \mu\text{m}$ ,  $N_o = 1.544$ ,  $N_e = 1.553$ .

For  $\lambda = 0.530 \mu\text{m}$ ,  $N_o = 1.5468$ ,  $N_e = 1.5559$ .

For  $\lambda = 1.06 \mu\text{m}$ ,  $N_o = 1.5340$ ,  $N_e = 1.5428$ .

For  $\lambda = 0.510 \mu\text{m}$  (in right-handed quartz):  $g_{11} = -5.82$ ,  $g_{33} = +12.96$ ,

$\epsilon_p = 0.177 \text{ cal} \cdot \text{g}^{-1} \text{K}^{-1}$ ,  $\rho_1 = \rho_2 = 200 \cdot 10^{14} \text{ ohm} \cdot \text{cm}$ ,  $\rho_3 = 1 \cdot 10^{14} \text{ ohm} \cdot \text{cm}$ .

For  $\lambda = 0.546 \mu\text{m}$ ,  $r_{11} = 0.59 \cdot 10^{-8}$  CGSE units,  $r_{41} = 1.4 \cdot 10^{-8}$  CGSE units.

For  $\lambda = 1.06 \mu\text{m}$ ,  $\chi = 1.2 \cdot 10^{-8}$  CGSE units

$d, 10^{-8}$ CGSE units	$s, 10^{-14}$ CGSE units	$c, 10^{10}$ CGSE units	$\epsilon$	$\alpha, 10^{-6} \text{ K}^{-1}$
$d_{14} = -6.76$	$s_{11} = 127.9$	$c_{11} = 86.05$	$\epsilon_1 = \epsilon_2 = 4.5$	$\alpha_1 = \alpha_2 = 13.4$
$d_{36} = +2.56$	$s_{12} = -15.35$	$c_{12} = 4.85$	$\epsilon_3 = 4.6$	$\alpha_3 = 7.8$
	$s_{13} = -11.0$	$c_{13} = 10.45$		
	$s_{14} = -44.6$	$c_{14} = 18.25$		
	$s_{33} = 95.6$	$c_{33} = 107.1$		
	$s_{44} = 197.8$	$c_{44} = 58.65$		
	$s_{66} = 286.5$	$c_{66} = 40.5$		

Temperature coefficient of elastic compliances of quartz at 25 °C  
 $s_{ij}(T) = s_{ij}(T_0) [1 + T_{s_{ij}}^{(1)}(T - T_0) + T_{s_{ij}}^{(2)}(T - T_0)]$

$ij$	$T^{(1)}, 10^6 \text{ }^{\circ}\text{C}^{-1}$	$T^{(2)}, 10^9 \text{ }^{\circ}\text{C}^{-1}$
11	15.5	85.3
33	140	247
12	-1370	21 385
13	-166	-718
44	210	262
66	-145	-85
14	134	93

Resorcine ( $\text{C}_6\text{H}_4(\text{OH})_2$ ); mm  
 $\rho = 1.272 \text{ g/cm}^3$ ,  $T_{\text{melt}} \approx 100 \text{ }^{\circ}\text{C}$

$d, 10^{-8}$ CGSE units	$s, 10^{-12}$ CGSE units	$c, 10^{10}$ CGSE units	$\epsilon$
$d_{15} = 53.9$	$s_{11} = 19$	$c_{11} = 10.3$	$\epsilon_1 = 3.51$
$d_{31} = -12.4$	$s_{22} = 10.6$	$c_{22} = 14.4$	$\epsilon_2 = 4.14$
$d_{33} = 16.8$	$s_{33} = 15$	$c_{33} = 12.9$	$\epsilon_3 = 3.54$
$d_{24} = 55.3$	$s_{44} = 30.7$	$c_{44} = 3.3$	
$d_{32} = -12.8$	$s_{55} = 23$	$c_{55} = 4.4$	
	$s_{66} = 25$	$c_{66} = 4.0$	
	$s_{12} = -4$	$c_{12} = 6.2$	
	$s_{13} = -3.4$	$c_{13} = 7.4$	
	$s_{23} = -8.8$	$c_{23} = 6.9$	

Rochelle salt ( $\text{NaKC}_4\text{H}_4\text{O}_6 \cdot 4\text{H}_2\text{O}$ )  
 Ferroelectric with two Curie points: lower point at  $-18 \text{ }^{\circ}\text{C}$  and upper point at  $24 \text{ }^{\circ}\text{C}$ . Symmetry is 2 in the range  $(-18) \text{--}(+24) \text{ }^{\circ}\text{C}$  (ferroelectric phase), and

symmetry of paraelectric phase is 222. In the neighbourhood of the upper Curie point,  $\gamma_1 = 200$  CGSE points.

$\rho = 1.77 \text{ g/cm}^3$ ,  $T_{\text{melt}} = 55^\circ\text{C}$ . For  $\lambda = 0.546 \mu\text{m}$ ,  $N_g = 1.4954$ ,  $N_m = 1.4920$ ,  $N_p = 1.4900$

$P^s = 7.5 \cdot 10^2$  CGSE units,  $g_{14} = 6.7 \cdot 10^{-7}$  CGSE units,  
 $p_{44} = 8.9 \cdot 10^{-3}$  CGSE units,  $m_{41} = 0.224 \cdot 10^{-7}$  CGSE units

$d, g, 10^{-8}$ CGSE units	$s, 10^{-12}$ CGSE units	$c, 10^{10}$ CGSE units	$\epsilon$	$\alpha, 10^{-6} \text{ K}^{-1}$
$d_{14} = 1150$	$s_{11} = 5.2$	$c_{11} = 40$	$\epsilon_1^t = 480$	$\alpha_1 = 58.3$
$d_{25} = -160$	$s_{12} = -2.1$	$c_{12} = -30$	$\epsilon_2^t = 12$	$\alpha_2 = 35.5$
$d_{36} = 35$	$s_{13} = -2.0$	$c_{13} = -40$	$\epsilon_3^t = 10$	$\alpha_3 = -136.1$
$g_{14} = 31$	$s_{22} = 3.4$	$c_{22} = 50$	$\epsilon_1^r = 220$	
$g_{25} = -170$	$s_{23} = -1.3$	$c_{23} = -30$	$\epsilon_2^r = 11$	
$g_{36} = 44$	$s_{33} = 3.2$	$c_{33} = 60$	$\epsilon_3^r = 9.8$	
	$s_{44} = 20$	$c_{44} = 10$		
	$s_{55} = 32$	$c_{55} = 3$		
	$s_{66} = 10$	$c_{66} = 10$		

Rock salt (NaCl);  $m3m$

$\rho = 2.2 \text{ g/cm}^3$ ,  $T_{\text{melt}} = 804^\circ\text{C}$ .

For  $\lambda = 0.589 \mu\text{m}$ ,  $N = 1.51$ .

$\pi_{11} = 0.25 \cdot 10^{11}$  CGSE units,  $R_{11} = 2.7 \cdot 10^{12}$  CGSE units,  
 $\pi_{12} = 1.46 \cdot 10^{-11}$  CGSE units,  $R_{12} = -1.35 \cdot 10^{-12}$  CGSE units,  
 $\pi_{14} = -0.85 \cdot 10^{-11}$  CGSE units,  $R_{44} = 0.9 \cdot 10^{-12}$  CGSE units.

Rubidium dihydroposphate, RDP ( $\text{RbH}_2\text{PO}_4$ );  $\bar{4}2m$

For  $\lambda = 0.547 \mu\text{m}$ ,  $N_o = 1.609$ ,  $N_e = 1.479$ ;  $\pi_{66} = 10.5 \cdot 10^{-12}$  CGSE units.

Ruby ( $\alpha\text{-Al}_2\text{O}_3$ );  $\bar{3}m$  (corundum crystals red-coloured by chromium dopant)

$\rho = 3.98 \text{ g/cm}^3$ ,  $T_{\text{melt}} = 2030^\circ\text{C}$

For  $\lambda = 0.589 \mu\text{m}$ ,  $N_o = 1.768$ ,  $N_e = 1.759$ .

$s, 10^{-12}$ CGSE units	$c, 10^{11}$ CGSE units	$\epsilon [1]$	$\alpha, 10^{-6} \text{ K}^{-1}$
$s_{11} = 0.2353$	$c_{11} = 49.68$	$\epsilon_1 = \epsilon_2 = 8.6$	$\alpha_1 = \alpha_2 = 5.0$
$s_{33} = 0.2170$	$c_{33} = 49.81$	$\epsilon_3 = 10.55$	$\alpha_3 = 6.66$
$s_{44} = 0.6940$	$c_{44} = 14.74$		
$s_{12} = -0.0716$	$c_{12} = 16.36$		
$s_{13} = -0.0364$	$c_{13} = 11.09$		
$s_{14} = -0.0489$	$c_{14} = -2.35$		

Rutile ( $\text{TiO}_2$ );  $4/mmm$

$\rho = 4.26 \text{ g/cm}^3$ ,  $T_{\text{melt}} = 1820^\circ\text{C}$ ,  $\epsilon_1 = 86$ ,  $\epsilon_3 = 170$ .

For  $\lambda = 0.630 \mu\text{m}$ ,  $N_o = 2.600$ ,  $N_e = 2.890$ .

Silicon (Si);  $m3m$

$\rho = 2.328 \text{ g/cm}^3$ ,  $T_{\text{melt}} = 1410^\circ\text{C}$ ,  $c_p = 0.181 \text{ cal}\cdot\text{g}^{-1}\text{ K}^{-1}$ ,  $\epsilon = 12$ .

Sodium chlorate ( $\text{NaClO}_3$ );  $23$

$\rho = 2.49 \text{ g/cm}^3$ ,  $\epsilon = 5.75$ ,  $\alpha = 43.4 \cdot 10^{-8} \text{ K}^{-1}$

$s, 10^{-12}$ CGSE units	$c, 10^{10}$ CGSE units	$\Pi_{ij}, 10^{-12}$ CGSE units		$\rho, \text{ohm}\cdot\text{cm}$	
		$n\text{-Si}$	$p\text{-Si}$	$n\text{-Si}$	$p\text{-Si}$
$s_{11} = 0.768$	$c_{11} = 16.57$	$\Pi_{11} = -102.2$	$\Pi_{11} = 6.5$	11.7	78
$s_{12} = -0.214$	$c_{12} = 6.39$	$\Pi_{12} = 58.4$	$\Pi_{12} = -1.1$		
$s_{44} = 1.256 [1]$	$c_{14} = 7.96$	$\Pi_{44} = -13.6$	$\Pi_{44} = 138.1$		

$d_{14} = 6.1 \cdot 10^{-8}$  CGSE units,  $s_{11} = 23.35 \cdot 10^{-13}$  CGSE units,  
 $s_{12} = -5.15 \cdot 10^{-13}$  CGSE units,  $s_{44} = 85.4 \cdot 10^{-13}$  CGSE units

**Sodium chloride**, see rock salt

**Sphalerite**, see zinc sulphide

**Strontium titanate** ( $\text{SrTiO}_3$ );  $m3m$

Ferroelectric,  $T_C = 240^\circ\text{C}$ ,  $R_{11} - R_{12} = 0.065$  CGSE units

**Tourmaline**;  $3m$

$\rho \approx 2.90\text{-}3.25 \text{ g/cm}^3$ ,  $T_{\text{melt}} = 1102^\circ\text{C}$

$N_o = 1.59$ ,  $N_e = 1.43$ ;  $c_p = 0.2 \text{ cal}\cdot\text{g}^{-1} \text{ K}^{-1}$ ,  $\gamma_3 = 1.3$  CGSE units

$d, 10^{-8}$ CGSE units	$s, 10^{-12}$ CGSE units	$c, 10^{10}$ CGSE units	$\epsilon$	$\alpha, 10^{-6} \text{ K}^{-1}$
$d_{15} = 10.9$	$s_{11} = 0.385$	$c_{11} = 272$	$\epsilon_1 = \epsilon_2 = 8.2$	$\alpha_1 = \alpha_2 = 3.6$
$d_{22} = 1.0$	$s_{12} = 0.048$	$c_{12} = 40$	$\epsilon_3 = 7.5$	$\alpha_3 = -8.8$
$d_{31} = 1.03$	$s_{13} = 0.071$	$c_{13} = 35$		
$d_{33} = 5.5$	$s_{33} = 0.636$	$c_{33} = 165$		
	$s_{44} = 154$	$c_{44} = 65$		
	$s_{14} = 0.045$	$d_{14} = -6.8$		

**Triglycin sulphate**, TGS

Ferroelectric,  $T_C = 49^\circ\text{C}$

Symmetry of ferroelectric phase 2, symmetry of paraelectric phase  $2/m$ . Near the Curie point  $\gamma_2 = 500$  CGSE units,  $\epsilon_2 = 200$ .

**Wurtzite**, see zinc sulphide

**Yttrium-iron garnet**,  $\text{YIG}$  ( $\text{Y}_3\text{Fe}_5\text{O}_{12}$ );  $m3m$

$\rho = 5.17 \text{ g/cm}^3$

For  $\lambda = 1.15 \mu\text{m}$ ,  $N = 2.22$

$p_{11} = 0.325$ ,  $p_{12} = 0.073$ ,  $p_{44} = 0.041$

**Zinc sulphide** ( $\text{ZnS}$ ):

(i) **Sphalerite** (cubic  $\text{ZnS}$ );  $\overline{43}m$

$\rho = 4.102 \text{ g/cm}^3$ ,  $N = 2.37$ .

For  $\lambda = 0.546 \mu\text{m}$ ,  $\epsilon = 8.37$ ,  $d_{14} = 9.54 \cdot 10^{-8}$  CGSE units,  $s_{11} = 18.39 \cdot 10^{-13}$  CGSE units,  $s_{12} = -7.07 \cdot 10^{-12}$  CGSE units,  $s_{44} = 21.69 \cdot 10^{-13}$  CGSE units.

For  $\lambda = 0.546 \mu\text{m}$ ,  $r_{41} = 5.0 \cdot 10^{-8}$  CGSE units

(ii) **Wurtzite** (hexagonal  $\text{ZnS}$ );  $6mm$

$d_{11} = 8.6 \cdot 10^{-8}$  CGSE units.

**Table 15**  
**Units of Physical Quantities and Conversion Factors for the Corresponding Units in the SI and CGSE Systems**

Quantity	Symbol	System of units	Unit			Conversion factor
			dimension	name	abbreviation	
Density	$\rho$	SI CGSE	$\text{kg} \cdot \text{m}^{-3}$ $\text{g} \cdot \text{cm}^{-3}$	kilogram per cubic metre gram per cubic centimetre	$\text{kg/m}^3$ $\text{g/cm}^3$	$1 \text{ g/cm}^3 = 10^3 \text{ kg/m}^3$
Temperature	$T$	SI CGSE	$\text{K}$ $^{\circ}\text{C}$	kelvin degree Celsius	$\text{K}$ $^{\circ}\text{C}$	$T [\text{K}] = T [^{\circ}\text{C}] + 273.15$
Entropy	$S$	SI CGSE	$\text{kg} \cdot \text{m}^2 \cdot \text{s}^{-2} \cdot \text{K}^{-1}$ $\text{g} \cdot \text{cm}^2 \cdot \text{s}^{-2} \cdot \text{K}^{-1}$	joule per kelvin calorie per kelvin	$\text{J/K}$ $\text{cal/K}$	$1 \text{ cal/K} = 4.19 \text{ J/K}$
Heat capacity	$C$	SI CGSE	$\text{kg} \cdot \text{m}^2 \cdot \text{s}^{-2} \cdot \text{K}^{-1}$ $\text{g} \cdot \text{cm}^2 \cdot \text{s}^{-2} \cdot \text{K}^{-1}$	joule per kelvin calorie per kelvin	$\text{J/K}$ $\text{cal/K}$	$1 \text{ cal/K} = 4.19 \text{ J/K}$
Electric charge	$Q$	SI CGSE	$\text{A} \cdot \text{s}$ $\text{g}^{1/2} \cdot \text{cm}^{3/2} \cdot \text{s}^{-1}$	coulomb or ampere-second CGSE unit	$\text{C}$ , $\text{A} \cdot \text{s}$ CGSE unit	$1 \text{ CGSE unit of charge} = (1/3) \cdot 10^{-9} \text{ C}$
Electric potential difference (voltage)	$\varphi$	SI CGSE	$\text{kg} \cdot \text{m}^2 \cdot \text{s}^{-3} \cdot \text{A}^{-1}$ $\text{g}^{1/2} \cdot \text{cm}^{1/2} \cdot \text{s}^{-1}$	volt	CGSE unit $\text{V}$	$1 \text{ CGSE unit of voltage} = 300 \text{ V}$
Force	$F$	SI CGSE	$\text{kg} \cdot \text{m} \cdot \text{s}^{-2}$ $\text{g} \cdot \text{cm} \cdot \text{s}^{-2}$	newton dyne	$\text{N}$ $\text{dyne}$	$1 \text{ dyne} = 10^{-5} \text{ N}$

Table 15 (cont'd)

Quantity	Symbol	System of units	Unit			Conversion factor
			dimension	name	abbreviation	
Displacement under deformation	$u$	SI CGSE	$\text{m}$ $\text{cm}$	metre centimetre	$\text{m}$ $\text{cm}$	$1 \text{ cm} = 10^{-2} \text{ m}$
Strength of electric field	$E$	SI CGSE	$\text{kg} \cdot \text{m} \cdot \text{s}^{-3} \cdot \text{A}^{-1}$ $\text{g}^{1/2} \cdot \text{cm}^{-1/2} \cdot \text{s}^{-1}$	volt per metre CGSE unit	$\text{V/m}$	$1 \text{ CGSE unit} = 3 \cdot 10^4 \text{ V/m}$
Electric induction	$D$	SI CGSE	$\text{m}^{-2} \cdot \text{s} \cdot \text{A}$ $\text{g}^{1/2} \cdot \text{cm}^{-1/2} \cdot \text{s}^{-1}$	coulomb per square metre CGSE unit	$\text{C/m}^2$	$1 \text{ CGSE unit} = \frac{1}{4\pi 3} \times 10^{-5} \text{ C/m}^2$
Electric polarization	$P$	SI CGSE	$\text{m}^{-2} \cdot \text{s} \cdot \text{A}$ $\text{g}^{1/2} \cdot \text{cm}^{-1/2} \cdot \text{s}^{-1}$	coulomb per square metre CGSE unit	$\text{C/m}^2$	$1 \text{ CGSE unit} = \frac{1}{4\pi 3} \cdot 10^{-5} \text{ C/m}^2$
Pyroelectric coefficients	$\gamma_i$	SI CGSE	$\text{m}^{-2} \cdot \text{s} \cdot \text{A} \cdot \text{K}^{-1}$ $\text{g}^{1/2} \cdot \text{cm}^{-1/2} \cdot \text{s}^{-1} \cdot \text{K}^{-1}$	coulomb per square metre per kelvin CGSE unit	$\text{C}/(\text{m}^2 \cdot \text{K})$	$1 \text{ CGSE unit} = \frac{1}{4\pi 3} \cdot 10^{-5} \text{ C}/(\text{m}^2 \cdot \text{K})$
Electrocaloric coefficients	$q_i$	SI CGSE	$\text{kg}^{-1} \cdot \text{m}^{-1} \cdot \text{s} \cdot \text{A} \cdot \text{K}$ $\text{g}^{1/2} \cdot \text{cm}^{1/2} \cdot \text{s} \cdot \text{K}$	kelvin-metre per volt CGSE unit	$\text{K} \cdot \text{m}/\text{V}$	$1 \text{ CGSE unit} = \frac{1}{3} \cdot 10^{-4} \text{ K} \cdot \text{m}/\text{V}$

Table 15 (cont'd)

Quantity	Symbol	System of units		Unit		Conversion factor
		SI	CGSE	dimension	name	
Mechanical stress	$t_{ij}$	SI	$\text{kg} \cdot \text{m}^{-1} \cdot \text{s}^{-2}$	newton per square metre	$\text{N/m}^2$	$1 \text{ dyne/cm}^2 = 0.1 \text{ N/m}^2$
		CGSE	$\text{g} \cdot \text{cm}^{-1} \cdot \text{s}^{-2}$	dyne per square centimetre	$\text{dyne/cm}^2$	
Mechanical strain	$r_{ij}$	SI	—	metre per metre centimetre per centimetre	$\text{m/m}$	$1 \text{ cm/cm}$
	CGSE	—	—	—	—	
Thermal expansion	$\alpha_{ij}$	SI	$\text{K}^{-1}$	kelvin to power minus one	$\text{K}^{-1}$	$1$
	CGSE	$\text{K}^{-1}$	—	—	—	
Dielectric permittivity	$\varepsilon_{ij}$	SI	$\text{kg}^{-1} \cdot \text{m}^{-3} \cdot \text{s}^4 \cdot \text{A}^2$	farad per metre CGSE unit	$\text{F/m}$	$1 \text{ CGSE unit} = \frac{1}{4\pi g} 10^{-9} \text{ F/m}$
	CGSE	—	—	—	—	
Dielectric impermeability	$\eta_{ij}$	SI	$\text{kg} \cdot \text{m}^3 \cdot \text{s}^{-4} \cdot \text{A}^{-2}$	metre per farad CGSE unit	$\text{m/F}$	$1 \text{ CGSE unit} = 36\pi \cdot 10^8 \text{ m/F}$
	CGSE	—	—	—	—	
Magnetic permeability	$\mu_{ij}$	SI	$\text{kg} \cdot \text{m} \cdot \text{s}^{-2} \cdot \text{A}^{-2}$	henry per metre CGSE unit	$\text{H/m}$	$1 \text{ CGSE unit} = \frac{1}{8} \cdot 10^{-6} \text{ H/m}$
	CGSE	$\text{cm}^{-2} \cdot \text{s}^{-2}$	—	—	—	
Electric conductivity	$\sigma_{ij}$	SI	$\text{kg}^{-1} \cdot \text{m}^{-3} \cdot \text{s}^3 \cdot \text{A}^2$	siemens per metre CGSE unit	$\text{S/m}$	$1 \text{ CGSE unit} = \frac{1}{9} \cdot 10^{-9} \text{ S/m}$
	CGSE	$\text{s}^{-1}$	—	—	—	

Table 15 (cont'd)

Quantity	Symbol	System of units	System of units	dimension	name	Unit	abbreviation	Conversion factor
Electric resistivity	$\rho_{ij}$	SI CGSE	kg·m <sup>3</sup> ·s <sup>-3</sup> ·A <sup>-2</sup> s	ohm·metre	CGSE unit	ohm·m	1 CGSE unit = 9.10 <sup>-9</sup> ohm·m	
Piezoelectric coefficients	$d_{ijk}$	SI CGSE	kg <sup>-1</sup> ·m <sup>-1</sup> ·s <sup>3</sup> ·A g <sup>-1/2</sup> ·cm <sup>1/2</sup> ·s	coulomb per newton	CGSE unit	C/N	1 CGSE unit = $\frac{1}{3} \cdot 10^{-4}$ C/N	
	$e_{ijk}$	SI CGSE	m <sup>-2</sup> ·s·A g <sup>-1/2</sup> ·cm <sup>-1/2</sup> ·s <sup>-1</sup>	coulomb per square metre	CGSE unit	C/m <sup>2</sup>	1 CGSE unit = $\frac{1}{3} \cdot 10^{-5}$ C/m <sup>2</sup>	
	$g_{ijk}$	SI CGSE	m <sup>2</sup> ·s <sup>-1</sup> ·A <sup>-1</sup> g <sup>-1/2</sup> ·cm <sup>1/2</sup> ·s	square metre per coulomb	CGSE unit	m <sup>2</sup> /C	1 CGSE unit = 3.10 <sup>6</sup> m <sup>2</sup> /C	
	$h_{ijk}$	SI CGSE	kg·m·s <sup>-3</sup> ·A <sup>-1</sup> g <sup>1/2</sup> ·cm <sup>-1/2</sup> ·s <sup>-1</sup>	newton per coulomb	CGSE unit	N/C	1 CGSE unit = 3.10 <sup>4</sup> N/C	
Coefficients of linear electrooptic effect	$r_{ijk}$	SI CGSE	m <sup>2</sup> ·s <sup>-1</sup> ·A <sup>-1</sup> g <sup>-1/2</sup> ·cm <sup>1/2</sup> ·s	square metre per coulomb	CGSE unit	m <sup>2</sup> /C	1 CGSE unit = 3.10 <sup>6</sup> m <sup>2</sup> /C	
Nonlinear dielectric susceptibility	$\chi$	SI CGSE	kg·m·s <sup>-3</sup> ·A <sup>-1</sup> g <sup>1/2</sup> ·cm <sup>-1/2</sup> ·s <sup>-1</sup>	square metre per volt	CGSE unit	m <sup>2</sup> /V	1 CGSE unit = $\frac{1}{300}$ m <sup>2</sup> /V	

Table 15 (cont'd)

Quantity	Symbol	System of units	Units			Conversion factor
			dimension	name	abbreviation	
Elastic compliances	$s_{ijkl}$	SI CGSE	$\text{kg}^{-1} \cdot \text{m} \cdot \text{s}^2$ $\text{g}^{-1} \cdot \text{cm} \cdot \text{s}^2$	square metre per newton square centimetre per dyne	$\text{m}^2/\text{N}$ $\text{cm}^2/\text{dyne}$	$1 \text{ cm}^2/\text{dyne} = 10 \text{ m}^2/\text{N}$
Elastic stiffnesses	$c_{ijkl}$	SI CGSE	$\text{kg} \cdot \text{m}^{-1} \cdot \text{s}^{-2}$ $\text{g} \cdot \text{cm}^{-1} \cdot \text{s}^{-2}$	newton per square metre dyne per square centimetre	$\text{N/m}^2$ $\text{dyne/cm}^2$	$1 \text{ dyne/cm}^2 = 0.1 \text{ N/m}^2$
Coefficients of piezooptic effect	$\pi_{ijkl}$	SI CGSE	$\text{kg}^{-1} \cdot \text{m} \cdot \text{s}^2$ $\text{g}^{-1} \cdot \text{cm} \cdot \text{s}^2$	square metre per newton CGSE unit	$\text{m}^2/\text{N}$	$1 \text{ CGSE unit} = 10 \text{ m}^2/\text{N}$
Coefficients of elastooptic effect	$p_{ijkl}$	SI CGSE	—	—	—	—
Coefficients of piezoresistance effect	$\Pi_{ijkl}$	SI CGSE	$\text{kg} \cdot \text{m}^4 \cdot \text{s}^{-4} \cdot \text{A}^{-4}$ $\text{g}^{-1} \cdot \text{cm} \cdot \text{s}^{-4}$	kilogram-metre to power seven per Coulomb to power four CGSE unit	$\text{kg} \cdot \text{m}^7/\text{C}^4$	$1 \text{ CGSE unit} = 81 \cdot 10^{19} \text{ kg} \cdot \text{m}^7/\text{C}^4$

Table 16

## Tensors of Physical Properties of Crystals Mentioned in the Book

Equation number, page number	Property or coefficients	Basic equation	General relations between components
<b>I. Rank One Tensors Relating a Scalar and a Vector</b>			
(3.2), 00	Pyroelectric effect	$\Delta P_i = \gamma_i \Delta T$	
(3.4), 00	Electrocaloric effect	$\Delta T = q_i \Delta E_i$	
	Polarization under hydrostatic pressure	$P_i = -d_{ijk} t$	
<b>II. Rank Two Tensors Relating Two Vectors</b>			
00, 000	Dielectric permittivity	$D_i = \epsilon_{ij} E_j$	Symmetric tensor
(9.1), 000	Dielectric impermeability (polarization constant)	$E_i = \eta_{ij} D_j$	Same
00	Dielectric susceptibility	$p_i = \chi_0 \chi_{ij} E_j$	Same
00	Magnetic permeability	$B_i = \mu_{ij} H_j$	Same
	Magnetic susceptibility	$J_i = \mu_0 \psi_{ij} H_j$	Same
(4.1), 00	Electric conductivity	$j_i = \sigma_{ik} E_k$	Same
00	Heat conductivity	$q_i = -\lambda_{ij} \frac{dT}{dx_j}$	Same
<b>III. Rank Two Tensors Relating a Scalar and a Rank Two Tensor</b>			
(5.20), 000	Thermal expansion	$r_{ij} = \alpha_{ij} \Delta T$	Symmetric tensor
000	Thermoelastic stress	$t_{ij} = -\alpha'_{ij} \Delta T$	Same
(7.16), 000	Strain under hydrostatic compression	$r_{ij} = -s_{ijk} t$	Same
<b>IV. Rank Two Tensors Relating a Scalar and a Rank Two Tensor</b>			
(6.1), 00	Direct piezoelectric effect	$p_i = d_{ijk} t_{jk}$	$d_{ijk} = d_{ikj}$
(6.2), 00	Same	$p_i = l_{ijk} r_{jk}$	$l_{ijk} = l_{ikj}$
(6.3), 00	Same	$E_i = -g_{ijk} t_{jk}$	$g_{ijk} = g_{ikj}$
(6.4), 00	Same	$E_i = -h_{ijk} r_{jk}$	$h_{ijk} = h_{ikj}$
(6.16), 00	Inverse piezoelectric effect	$r_{jk} = d_{ijk} E_i$	
(6.17), 00	Same	$r_{jk} = g_{ijk} p_i$	
(6.18), 00	Same	$t_{jk} = -l_{ijk} E_i$	
(6.19), 00	Same	$t_{jk} = -h_{ijk} p_i$	
(11.1), 000	Electrooptic effect	$\Delta \eta_{ij} = r_{ijk} E_k$	$r_{ijk} = r_{jik}$
(11.2),		$\Delta \eta_{ij} = m_{ijk} P_k$	$m_{ijk} = m_{jik}$

Table 16 (cont'd)

Equation number, page number	Property or coefficients	Basic equation	General relations between components
V. Rank Four Tensors Relating Two Rank Two Tensors			
(7.1), 000	Elastic compliances	$r_{ij} = s_{ijkl}t_{kl}$	$s_{ijkl} = s_{ijkl} = s_{ijlk} = s_{klij}$
(7.2), 000	Elastic stiffnesses	$t_{ij} = c_{ijhl}r_{kl}$	$c_{ijkl} = c_{ijhl} = c_{ijlk} = c_{klij}$
(10.4), 000	Elastooptic constants	$\Delta\eta_{ij} = p_{ijhl}r_{kl}$	$p_{ijkl} = p_{jihl} = p_{ijlh}$
(10.3), 000	Piezooptic constants	$\Delta\eta_{ij} = \pi_{ijhl}t_{kl}$	$\pi_{ijhl} = \pi_{jikl} = \pi_{ijlk}$
(8.5), 000	Piezoresistive constants	$E_i = \rho_{ik}^0 (\delta_{kl} + \Pi_{klmn}t_{mn}) j_l$	$\Pi_{klmn} = \Pi_{lkmn} = \Pi_{klmn} = \Pi_{lknm}$
(8.6), 000	Elastoresistive constants	$E_i = \rho_{ik}^0 (\delta_{kl} + m_{klpg}r_{pg}) j_l$	$m_{klmn} = m_{lkmn} = m_{klnm} = m_{lknm}$
(6.25), 000	Electrostriction constants	$r_{ij} = R_{ijmn}E_mE_n$	$R_{ijmn} = R_{ijmn} = R_{jimn} = R_{jimn}$
(6.26), 000		$r_{ij} = Q_{ijmn}P_mP_n$	$Q_{ijmn} = Q_{ijnm} = Q_{jimn} = Q_{jinm}$
(6.27), 000		$t_{ij} = G_{ijmn}P_mP_n$	$G_{ijmn} = G_{ijnm} = G_{jimn} = G_{jinm}$
		$t_{ij} = H_{ijmn}E_mE_n$	$H_{ijmn} = H_{ijnm} = H_{jimn} = H_{jinm}$
VI. Rank Five Tensor Relating a Vector and a Rank Four Tensor			
(13.20), 000	Elastoelectric constants	$\Delta c_{ijkl} = g_{mijkl}E_m$	$g_{mijkl} = g_{mjikl} = g_{mijlk} = -g_{mklij}$
VII. Rank Two Axial Tensor Relating a Pseudoscalar to Direction			
(13.5), 000	Optical activity (gyration tensor)	$G = g_{ijli}l_j$	Symmetric tensor
Tensors Mentioned in the Book and not Describing Properties of Crystals			
00	Stress		Symmetric tensor
(5.11), 00	Strain together with rotation	$l_{ij} = \frac{\partial u_i}{\partial x_j}$	$[l_{ij}]$ is not symmetric
(5.12), 00	Strain together with rotation	$l_{ij} = r_{ij} + \omega_{ij}$	$[r_{ij}]$ is not symmetric $[\omega_{ij}]$ is not symmetric

